



universität  
wien

# DISSERTATION

Titel der Dissertation

„Microscopic analysis of the effects of post-translational modifications on protein structure, dynamics and aggregation by molecular dynamics simulations“

verfasst von

**Drazen Petrov**

angestrebter akademischer Grad

**Doctor of Philosophy (PhD)**

Wien, 2013

Studienkennzahl lt. Studienblatt: A 094 490

Dissertationsgebiet lt. Studienblatt: Molekulare Biologie

Betreut von: Dr. Bojan Zagrovic, A.B.



This cumulative dissertation is based on the following publications:

Petrov, D.,\* Margreitter, C.,\* Grandits, M., Oostenbrink, C. & Zagrovic, B. (2013). A systematic framework for molecular dynamics simulations of protein post-translational modifications. *PLoS Comput. Biol.* **9** (7), e1003154. (Chapter I)      *\*joint first authors*

Margreitter, C.,\* Petrov, D.\* & Zagrovic, B. (2013). Vienna-PTM web server: a toolkit for MD simulations of protein post-translational modifications. *Nucleic Acids Res.* **41** (Web Server issue), W422-6. (Chapter II)      *\*joint first authors*

Petrov, D. & Zagrovic, B. (2011). Microscopic analysis of protein oxidative damage: effect of carbonylation on structure, dynamics, and aggregability of villin headpiece. *J. Am. Chem. Soc.* **133** (18), 7016-7024. (Chapter III)

Petrov, D. & Zagrovic, B. (2013). Are current atomistic force fields accurate enough to study proteins in crowded environments? To be submitted to *Proc. Natl. Acad. Sci. U.S.A.* (Chapter IV)

Petrov, D., Daura, X. & Zagrovic, B. (2013). Effect of oxidative damage on the stability and dimerization of superoxide dismutase 1. To be submitted to *PLoS Comput. Biol.* (Chapter V)

The author's contribution to each publication is clearly stated at the beginning of each corresponding chapter.



## ABSTRACT

From enzymatic activation and cell-cycle control to transcription and translation regulation, post-translational modifications (PTMs) of proteins play a key role in numerous cellular processes by directly affecting protein structure, dynamics and interaction networks. However, despite the importance of understanding how PTMs affect protein properties and behaviour at the atomic level, suitable molecular dynamics (MD) simulation tools and parameters for treating PTMs have never been developed in a systematic fashion. Here, we generate and validate force field parameters (GROMOS 45a3 and 54a7) needed to run MD simulations of PTMs and develop an automated online tool for introducing PTMs into native proteins for over 250 different types of modifications. What is more, we characterize PTMs and compare them against the 20 canonical amino acids in terms of their physico-chemical properties by using thermodynamic integration (TI), molecular hydrophobicity potential and other computational approaches.

As an example of a non-enzymatic PTM, we study metal-catalyzed carbonylation, one of the most dominant mechanisms of oxidative damage to proteins. Notably, highly carbonylated proteins have been observed in potentially cytotoxic aggregates present in late-onset diseases including neurodegenerative diseases, cancer and diabetes. However, the effects of carbonylation on protein stability, dynamics and aggregation at the microscopic level are still poorly understood. Here, we perform extensive MD simulations of carbonylated villin headpiece domain accompanied by bioinformatic analysis of its aggregation propensity. Our results suggest that high concentrations of carbonylation, far above typical cellular levels are required for protein destabilization and unfolding, while aggregation propensity can drastically increase even upon a single “carbonylation mutation”. Additionally, we obtain high-resolution insight into the aggregation process of native and carbonylated villin headpiece and discover that several widely-used classical MD force fields appear to be significantly biased towards protein aggregation. Finally, we use MD and TI to study the impact of oxidative stress on protein stability and protein-protein interactions in the case of SOD1 homo-dimer whose destabilization is believed to be involved in amyotrophic lateral sclerosis.



## ZUSAMMENFASSUNG

Eine Vielzahl von physiologischen Prozessen wird von posttranslationalen Modifikationen (PTMs) gesteuert, welche ihren Einfluss über eine Veränderung der Proteinstruktur, -dynamik und -interaktionsnetzwerken ausüben. Darunter fallen unter anderem die Kontrolle des Zellzyklus, die Regulierung von Transkription und Translation sowie die Steuerung der Aktivität vieler Enzyme. Trotz der vielen Bereiche in denen PTMs eine wichtige Rolle spielen fehlen angemessene Werkzeuge und Parameter für molekulardynamische (MD) Simulationen um ihre Auswirkungen auf Proteine genauer verstehen zu können. In dieser Arbeit generieren und validieren wir die notwendigen "Force-Field" Parameter (GROMOS 45a3 und 54a7) um MD Simulationen mit PTMs durchführen zu können. Zusätzlich präsentieren wir ein automatisiertes „online-tool“ welches erlaubt native Proteine mit über 250 verschiedenen PTMs zu versehen. Außerdem werden die PTMs charakterisiert und anschließend mit den 20 kanonischen Aminosäuren mittels Thermodynamischer Integration (TI), molekularem hydrophobischen Potential und anderen Computer-basierten Methoden verglichen.

Als ein Beispiel für nicht-enzymatische posttranslationale Modifikationen, wir untersuchen metall-katalysierte Carbonylierung, eine der häufigsten Formen von oxidativem Schaden von Proteinen. Proteine mit hohem Carbonylierungsgrad bilden zellschädigende Aggregate die häufig in Spätformen von neurodegenerativen Krankheiten, Krebs und Diabetes beobachtet werden. Dennoch sind die Effekte der Carbonylierung auf Proteinstabilität, -dynamik und Aggregation auf mikroskopischem Level noch immer schlecht verstanden. Hier führen wir umfangreiche MD Simulationen mit Carbonylierter „villin headpiece domain“ durch und analysieren anschließend das Aggregationsverhalten. Unsere Daten weisen darauf hin, dass erst ein überdurchschnittlich hoher, weit über zellulären Levels liegender, Carbonylierungsgrad zu einer Destabilisierung des Proteins und seiner Entfaltung führt, wohingegen die Aggregationswahrscheinlichkeit schon mit einer einzigen Carbonylierungsmutation drastisch steigen kann. Außerdem bekommen wir detaillierte Einsicht in den Aggregationsprozess von nativer und carbonylierter „villin headpiece domain“ und entdecken, dass einige weit verbreitete klassische MD-Kraftfelder scheinen in Richtung zur Aggregation erheblich beeinflusst zu sein. Schlussendlich verwenden wir MD und TI um den Einfluss von oxidativem Stress auf Proteinstabilität und Protein-Protein

Interaktion im Fall des SOD1 Homo-Dimers dessen Destabilisierung wahrscheinlich eine entscheidende Rolle in amyotrophischer Lateralsklerose zu spielt, zu untersuchen.



## TABLE OF CONTENTS

Preamble	11
Chapter I - A systematic framework for molecular dynamics simulations of protein post-translational modifications	25
Chapter II - Vienna-PTM web server: a toolkit for MD simulations of protein post-translational modifications	171
Chapter III - Microscopic analysis of protein oxidative damage: effect of carbonylation on structure, dynamics, and aggregability of villin headpiece	195
Chapter IV - Are current atomistic force fields accurate enough to study proteins in crowded environments?	227
Chapter V - Effect of oxidative damage on the stability and dimerization of superoxide dismutase 1	253
Concluding discussion	271
Acknowledgements	283
Curriculum vitae	287



## Preamble

Proteins carry out a vast array of vital biological functions in living cells ranging from DNA replication and transcription to translation and cell-cycle control to catalysis of metabolic reactions and signal transduction. Importantly, proteomes, i.e., inventories of synthesized proteins, are typically a few orders of magnitude more complex than their cognate genomes.<sup>1-3</sup> For example, there are more than 1 million distinct protein species in humans, significantly outnumbering the 20-25 thousand human genes known.<sup>1,4,5</sup> The expansion of genome coding capabilities is facilitated by two principal mechanisms: 1) alternative splicing at the transcriptional level generating multiple mRNAs from a single DNA template,<sup>6-8</sup> and 2) protein post-translational modifications (PTMs),<sup>3,5,9</sup> the focus of this thesis. More than 400 chemically different types of modifications of amino-acid side chains and the backbone have been identified to date with over 70000 individual PTMs occurring in more than 20000 proteins.<sup>10,11</sup> Importantly, these chemical alterations of polypeptides play a key role in different cellular processes, ranging from enzymatic activation to transcription and translation regulation to disease development and aging.<sup>5,12-17</sup> Notably, enzymes dedicated to such modifications account for approximately 5% of cellular protein content in higher eukaryotes.<sup>5</sup> For example, kinases, which predominantly catalyze phosphorylation of serine, threonine and tyrosine residues and are one of the largest and most important classes of PTM enzymes, actively participate in various regulatory mechanisms with a direct impact on enzyme activation and inhibition, signal transduction pathways and networks, cellular response to external stimuli, cell cycle, tumor suppression, etc.<sup>18-21</sup> Other prominent examples of addition of small functional groups to proteins such as acetylation, methylation, S-nitrosylation and hydroxylation control a large number of biological functions and processes, including cellular metabolism and signaling, gene expression and epigenetic regulation, transport and translocation of biomolecules, protein life-time and turnover and stabilization of structural proteins.<sup>22-29</sup> Remarkably, hydroxyproline, mainly implicated in the formation of collagen fibrils, is more abundant than seven individual canonical amino acids, comprising roughly 4% of all amino acids found in animal tissue.<sup>26</sup> Moreover, enzyme-mediated transfer of larger moieties such as peptides (e.g., ubiquitin and SUMO), cofactors (e.g., biotin, flavins and hemes), lipid anchors (e.g., prenylation, palmitoylation and myristoylation) and carbohydrate chains (glycosylation), targets proteins to degradation by proteasome machinery and relocation to cell membranes, modulates their function and

activity, and is implicated in quality control by aiding and regulating protein folding/refolding and secretion.<sup>5,30-34</sup> Furthermore, a large body of proteins is subjected to simultaneous modifications at multiple sites by different types of reactions, often affecting biological outcome in a combinatorial fashion.<sup>5,17,35</sup> Most notably, interplay of tandem modifications, methylations, acetylations and phosphorylations among others, from a pool of more than 50 experimentally identified PTM sites (generating  $>10^{20}$  possible states) in human histones influences both activation and silencing of gene translation, including different counteracting modifications at the same residue (e.g., acetylation and methylation of LYS9 in the histone H3 protein are prevalently associated with opposite effects on gene expression).<sup>11,35,36</sup> What is more, a battery of enzymes designated for removal of introduced modifications control intensity and duration of propagated signals and effects, with only a small subset of PTMs being irreversible and lacking such regulatory mechanisms.<sup>5,37,38</sup>

In addition to enzymatic PTMs, proteins undergo uncontrolled covalent modifications triggered by reactive oxygen species (ROS) and reactive nitrogen species (RNS), including metal-catalyzed carbonylation, oxidation and nitration of aromatic amino-acid residues, oxidation of sulfur-containing residues and the protein backbone, or even protein fragmentation due to backbone breakage.<sup>12,39,40</sup> Protein non-enzymatic modifications may lead to cytotoxicity via impaired biological function and interactions, aggregation and misfolding.<sup>40-43</sup> Importantly, oxidative damage to proteins is associated with aging and age-related disorders such as neurodegenerative diseases, cancer, and diabetes.<sup>12,40,44,45</sup> While oxidized proteins are targeted for degradation, they can escape the ubiquitin-proteasome or other proteolytic pathways and accumulate in cells.<sup>43,46,47</sup> Markedly, late-onset pathologies are characterized by formation of insoluble aggregates typically comprised of highly oxidized proteins.<sup>48-51</sup> Furthermore, antioxidant enzymes (e.g., superoxide dismutase family) and small molecules (e.g., glutathione) scavenge free radicals (ROS and RNS), thus protecting the proteasome integrity, an important factor in preventing cellular senescence and aging.<sup>52-55</sup> Notably, irreversible metal-catalyzed carbonylation is one of the most prominent and the most studied biomarkers of oxidative damage and aging, whose level exponentially increases in the last third of the life-span in different species, ranging from houseflies to humans.<sup>56-58</sup> However, it is still largely unclear whether oxidative modifications to proteins

are a direct cause or only a consequence and useful reporter of aging.<sup>45,53,59</sup> Moreover, in addition to proteins, different biomolecules and cellular components are also affected by ROS and RNS, including DNA and lipid membranes.<sup>52,53,60</sup> In general, mounting evidence has linked oxidative stress and aging through different mechanisms: malfunctioning mitochondria coupled with increased production of ROS and RNS, impaired antioxidant protection, DNA damage, defective protein function and interactions, and protein aggregation in combination with compromised proteolytic machinery.<sup>44,52,53,60-63</sup> However, despite the widely-accepted notion that oxidative stress is a source of damage that accumulates with time and facilitates aging, several beneficial aspects of reactions involving free radicals in biological processes have also been reported, including cell signaling and even life-span prolongation.<sup>53,64-66</sup>

By directly affecting physico-chemical properties of target amino-acid, PTMs carry out their functions through modulation of protein structure, dynamics and interaction networks. However, despite their utmost relevance in different biological contexts, effects of PTMs at the microscopic level remain poorly understood. While experimental methods typically obtain time- and ensemble-averaged data and are limited in the number of measurable observables, molecular dynamics (MD) simulations provide high-resolution insight into biomolecular properties and behavior, and are in principle an ideally suited tool for addressing this problem.<sup>67-69</sup> In particular, MD simulations involve numerical solution of Newton's equation of motion for a system of particles, given an empirical potential energy function defining interactions in the system. Importantly, in MD, positions and velocities of simulated particles, i.e., microscopic states of the system, can be determined with femtosecond temporal and sub-femtometer spatial resolution. In this way, such simulations can access distributions and time series of any definable physical quantity, which can then be linked to macroscopic thermodynamic and kinetic properties of the system through ensemble averaging. Even though the interactions that govern atomic and molecular motions are of quantum nature, they are in MD approximated by a force field, i.e., a set of classical potential energy terms in combination with associated parameters, typically derived by fitting atomic or molecular properties of small molecules against calculated quantum-mechanical or experimentally measured data. For instance, the functional form (exemplified in equation 1) of a widely-used GROMOS force field,<sup>70-72</sup> also employed in this

thesis, is separated into bonded terms related to interactions between covalently linked atoms and non-bonded (non-covalent) terms describing van der Waals and electrostatic interactions. Specifically, bonded interactions are divided into contributions from covalent bond stretching, bond-angle bending, and improper and torsional dihedral angle terms, mimicked by different types of harmonic-like potentials and trigonometric functions, and corresponding parameters (highlighted in red, equation 1): the force constants  $K_b$ ,  $K_\theta$  and  $K_\xi$ , and the equilibrium values  $b_0$ ,  $\theta_0$  and  $\xi_0$  of the bond, the bond angle and the improper dihedral angle terms, respectively, with  $K_\phi$ ,  $\delta$  and  $m$  being the force constant, the phase shift and the multiplicity of the torsional dihedral angle term. On the other hand, interactions of non-bonded atom pairs in the GROMOS force field are described by the Lennard-Jones potential (van der Waals contribution) defined by the depth of the potential well  $\epsilon$  (highlighted in red) and the distance at which the potential is zero  $\sigma$  (related to the distance at which the potential reaches its minimum, highlighted in red), and by the Coulomb potential (electrostatic contribution from charged species) defined by the atomic partial charges  $q$  (highlighted in red). In the equation,  $b$ ,  $\theta$ ,  $\xi$ ,  $\phi$  and  $r$  represent the actual values of the bond length, the bond angle, the improper and torsional dihedral angles, and the distance between non-bonded atom pair, respectively,  $i$  and  $j$  are the summation indices,  $\epsilon_0$  is the dielectric permittivity of vacuum and  $\epsilon_1$  is the relative permittivity of the solvent, and  $RF$  stands for a reaction field contribution to electrostatic interactions.

$$E_{pot} = \sum_{bonds} \frac{K_{b,i}}{4} (b_i^2 - b_{i,0}^2)^2 + \sum_{angles} \frac{K_{\theta,i}}{2} (\cos \theta_i - \cos \theta_{i,0})^2 + \sum_{impropers} \frac{K_{\xi,i}}{2} (\xi_i - \xi_{i,0})^2 + \sum_{dihedrals} \frac{K_{\phi,i}}{2} [1 + \cos \delta_i \cos(m_i \phi_i)] + \sum_{atom\ pairs} \left( 4\epsilon_{i,j} \left[ \left( \frac{\sigma_{i,j}}{r_{i,j}} \right)^{12} - \left( \frac{\sigma_{i,j}}{r_{i,j}} \right)^6 \right] + \frac{q_i q_j}{4\pi\epsilon_0\epsilon_1 r_{i,j}} + RF_{i,j} \right) \quad (1)$$

In general, atomic force fields (e.g., GROMOS,<sup>72</sup> AMBER,<sup>73</sup> CHARMM<sup>74</sup> and OPLS<sup>75</sup>) have a very similar form of the interaction function, yet, despite their aim to accurately describe biomolecular systems, do markedly differ in parameter values due to alternative parameterization strategies.<sup>72-75</sup> These approximations and discrepancies notwithstanding, MD simulations have been successfully applied to study biomolecular systems, proteins in particular.<sup>67,68,76,77</sup> Various kinetic and thermodynamic aspects of protein folding have been examined in detail, including folding rates, pathways and intermediate states,

conformational entropy, protein stability and unfolding-refolding under denaturing conditions.<sup>77-89</sup> Additionally, dynamics, partial folding and conformational states of intrinsically disordered proteins have been evaluated through extensive sampling of their free energy landscape by MD simulations.<sup>90-92</sup> Furthermore, protein interactions with different biomolecules such as small chemicals, other peptides and proteins, nucleic acids and lipid membranes have been extensively investigated. In particular, MD has been used to study protein-ligand interactions and binding affinities in the context of allosteric regulation, enzymatic functions and underlying mechanisms, and even rational drug and enzyme design,<sup>93-101</sup> together with protein aggregation, DNA-protein complex formation, and membrane transport and permeation.<sup>102-108</sup> What is more, MD simulations are often combined with experimental methods to achieve better understanding of specific phenomena, improve structure refinement (e.g., X-ray crystallography), explore artifacts and limitations of experimental methods, but also to test and validate force field accuracy.<sup>109-115</sup> Taken together, these studies highlight the power of the MD method to probe microscopic-level dynamics of a wide range of biological processes that are not directly accessible to experimentalists. Importantly, with rapid progress in computer capabilities and advances in software development,<sup>76,116,117</sup> the range of applicability of MD simulations is expected to grow in the years to come, with ever-increasing system sizes and time scales.

As explained above, a large number of different PTMs have been discovered and linked to various essential biological processes. Most studies have focused on identification of modified proteins and target sites or impact of PTMs on gross cellular function, often providing very little detail about the underlying molecular mechanisms. On the other hand, microscopic effects of several PTM-mediated processes have been examined, including MD studies typically focusing on a single modification or in the best case a few modification types for a small subset of proteins.<sup>118-123</sup> However, despite the great importance of understanding how PTMs affect proteins at the atomistic level and the power of the MD method to provide such high-resolution insight, simulations of post-translationally modified proteins lag significantly behind the studies of unmodified, native proteins. This is, arguably, first and foremost due to a general deficiency of suitable computational tools and force field parameters for treating PTMs. To fill this gap, the first principal aim of this thesis has been



to provide a comprehensive, user-friendly platform for studying PTMs using MD simulations by systematic parameterization of a large set of PTMs and development of supporting MD-related modeling tools. Second, using these tools, we have explored the effects of non-enzymatic oxidative modifications on protein structure, dynamics and aggregation, and their potential implications in disease development and aging.

## OUTLINE

Despite the wide-spread role and biological importance of PTMs, a systematic framework for treating post-translationally modified proteins by MD simulations has never been developed. In **Chapter I**, we present novel force field parameters for more than 250 different types of enzymatic and non-enzymatic PTMs that have been derived in the context of GROMOS 45a3 and 54a7 parameter sets and cover nearly the complete space of known PTMs. Moreover, these parameters have been validated by reproducing experimentally measured hydration free energies, an important thermodynamic property related to hydrophobicity, for a set of small molecules chemically related to PTMs. Using the reported parameters, physico-chemical properties of modified amino acids were quantified and compared with their canonical counterparts. As a complement to this work, in **Chapter II** we present the Vienna-PTM web server, a publically available tool for automated introduction of desired PTMs to protein 3D structures with subsequent structure optimization via energy-minimization. Vienna-PTM also serves as a repository of the developed parameters described in Chapter I, providing a comprehensive platform for preparing, running and analyzing MD simulations of modified proteins.

Metal-catalyzed carbonylation is one of the most important oxidative modifications of proteins associated with late-onset diseases and aging. In **Chapter III**, we discuss MD simulations used to study the effects of carbonylation on structure and dynamics of the villin headpiece domain, a structurally well-characterized actin-binding polypeptide. Moreover, changes in local hydrophobicity upon carbonylation and their impact on protein aggregation propensity are examined. The relationship between protein aggregation and carbonylation is further investigated in **Chapter IV**. In particular, we performed and analyzed an exhaustive set of MD simulations of the native and carbonylated villin

headpiece domain under various conditions, including different protein and ion concentrations, electrostatics treatments and force fields. In addition to providing direct insight into villin self-association mechanism, these simulations were used to test the limitations of current force fields to accurately describe protein-protein interactions and protein behavior in biologically relevant crowded environments.

Finally, in **Chapter V**, by utilizing MD simulations in combination with the thermodynamic integration approach, we explore how different oxidative modifications affect folding and dimerization free energies of superoxide dismutase 1, a key homo-dimeric antioxidant enzyme in humans linked with amyotrophic lateral sclerosis, a devastating age-related disease. We also discuss potential advances and applications of free energy calculation methods.

## REFERENCES

1. Jensen, O. N. Modification-specific proteomics: Characterization of post-translational modifications by mass spectrometry. *Curr. Opin. Chem. Biol.* **8**, 33-41 (2004).
2. Walsh, C. T. Posttranslational modification of proteins: expanding nature's inventory. Roberts and Company Publishers, Englewood, Colorado, 2006.
3. Kamath, K. S., Vasavada, M. S. & Srivastava, S. Proteomic databases and tools to decipher post-translational modifications. *J Proteomics* **75**, 127-144 (2011).
4. Collins, F. S., Lander, E. S., Rogers, J., Waterston, R. H. & Int Human Genome Sequencing, C. Finishing the euchromatic sequence of the human genome. *Nature* **431**, 931-945 (2004).
5. Walsh, C. T., Garneau-Tsodikova, S. & Gatto, G. J., Jr. Protein posttranslational modifications: the chemistry of proteome diversifications. *Angew. Chem. Int. Ed.* **44**, 7342-7372 (2005).
6. Maniatis, T. & Tasic, B. Alternative pre-mRNA splicing and proteome expansion in metazoans. *Nature* **418**, 236-243 (2002).
7. Black, D. L. Mechanisms of alternative pre-messenger RNA splicing. *Annu. Rev. Biochem.* **72**, 291-336 (2003).
8. Matlin, A. J., Clark, F. & Smith, C. W. J. Understanding alternative splicing: Towards a cellular code. *Nat. Rev. Mol. Cell Biol.* **6**, 386-398 (2005).
9. Mann, M. & Jensen, O. N. Proteomic analysis of post-translational modifications. *Nat. Biotechnol.* **21**, 255-261 (2003).
10. Lee, T. Y. *et al.* dbPTM: an information repository of protein post-translational modification. *Nucleic Acids Res.* **34**, D622-D627 (2006).
11. UniProt, C. Reorganizing the protein space at the Universal Protein Resource (UniProt). *Nucleic Acids Res.* **40**, D71-D75 (2012).
12. Levine, R. L. & Stadtman, E. R. Oxidative modification of proteins during aging. *Exp. Gerontol.* **36**, 1495-1502 (2001).
13. Kwon, S. J., Choi, E. Y., Choi, Y. J., Ahn, J. H. & Park, O. K. Proteomics studies of post-translational modifications in plants. *J. Exp. Bot.* **57**, 1547-1551 (2006).
14. Walsh, G. & Jefferis, R. Post-translational modifications in the context of therapeutic proteins. *Nat. Biotechnol.* **24**, 1241-1252 (2006).
15. Sims, R. J., III & Reinberg, D. Is there a code embedded in proteins that is based on post-translational modifications? *Nat. Rev. Mol. Cell Biol.* **9**, 815-820 (2008).
16. Nussinov, R., Tsai, C.-J., Xin, F. & Radivojac, P. Allosteric post-translational modification codes. *Trends Biochem. Sci.* **37**, 447-455 (2012).
17. Lothrop, A. P., Torres, M. P. & Fuchs, S. M. Deciphering post-translational modification codes. *FEBS Lett.* **587**, 1247-1257 (2013).
18. Seger, R. & Krebs, E. G. The MAPK signaling cascade. *FASEB J.* **9**, 726-735 (1995).
19. Ashcroft, M., Kubbutat, M. H. G. & Vousden, K. H. Regulation of p53 function and stability by phosphorylation. *Mol. Cell. Biol.* **19**, 1751-1758 (1999).
20. Cohen, P. The role of protein phosphorylation in human health and disease. *Eur. J. Biochem.* **268**, 5001-5010 (2001).
21. Ciesla, J., Fraczyk, T. & Rode, W. Phosphorylation of basic amino acid residues in proteins: important but easily missed. *Acta Biochim. Pol.* **58**, 137-147 (2011).

22. Kivirikki, K. & Prockop, D. J. Enzymatic hydroxylation of proline and lysine in procollagen. *Proc. Natl. Acad. Sci. U.S.A.* **57**, 782-8 (1967).
23. Martinez-Ruiz, A. & Lamas, S. S-nitrosylation: a potential new paradigm in signal transduction. *Cardiovasc. Res.* **62**, 43-52 (2004).
24. Paik, W. K., Paik, D. C. & Kim, S. Historical review: the field of protein methylation. *Trends Biochem. Sci.* **32**, 146-152 (2007).
25. Bedford, M. T. & Clarke, S. G. Protein arginine methylation in mammals: Who, what, and why. *Mol. Cell* **33**, 1-13 (2009).
26. Gorres, K. L. & Raines, R. T. Prolyl 4-hydroxylase. *Crit. Rev. Biochem. Mol. Biol.* **45**, 106-124 (2010).
27. Hwang, C.-S., Shemorry, A. & Varshavsky, A. N-terminal acetylation of cellular proteins creates specific degradation signals. *Science* **327**, 973-977 (2010).
28. Zhao, S. *et al.* Regulation of Cellular Metabolism by Protein Lysine Acetylation. *Science* **327**, 1000-1004 (2010).
29. Anand, P. & Stamler, J. S. Enzymatic mechanisms regulating protein S-nitrosylation: implications in health and disease. *J. Mol. Med.* **90**, 233-244 (2012).
30. Spiro, R. G. Protein glycosylation: nature, distribution, enzymatic formation, and disease implications of glycopeptide bonds. *Glycobiology* **12**, 43R-56R (2002).
31. Jitrapakdee, S. & Wallace, J. C. The biotin enzyme family: Conserved structural motifs and domain rearrangements. *Curr. Protein Pept. Sci.* **4**, 217-229 (2003).
32. Resh, M. D. Membrane targeting of lipid modified signal transduction proteins. *Subcell. Biochem.* **37**, 217-232 (2004).
33. Ikeda, F. & Dikic, I. Atypical ubiquitin chains: new molecular signals - 'Protein modifications: Beyond the usual suspects' review series. *EMBO Rep.* **9**, 536-542 (2008).
34. Komander, D. The emerging complexity of protein ubiquitination. *Biochem. Soc. Trans.* **37**, 937-953 (2009).
35. Latham, J. A. & Dent, S. Y. Cross-regulation of histone modifications. *Nat. Struct. Mol. Biol.* **14**, 1017-1024 (2007).
36. van Rossum, B., Fischle, W. & Selenko, P. Asymmetrically modified nucleosomes expand the histone code. *Nat. Struct. Mol. Biol.* **19**, 1064-1066 (2012).
37. Jackson, M. D. & Denu, J. M. Molecular reactions of protein phosphatases - Insights from structure and chemistry. *Chem. Rev.* **101**, 2313-2340 (2001).
38. Grozinger, C. M. & Schreiber, S. L. Deacetylase enzymes: Biological functions and the use of small-molecule inhibitors. *Chem. Biol.* **9**, 3-16 (2002).
39. Davies, K. J. A., Delsignore, M. E. & Lin, S. W. Protein damage and degradation by oxygen radicals. II. Modification of amino-acids. *J. Biol. Chem.* **262**, 9902-9907 (1987).
40. Berlett, B. S. & Stadtman, E. R. Protein oxidation in aging, disease, and oxidative stress. *J. Biol. Chem.* **272**, 20313-20316 (1997).
41. Davies, K. J. A. & Delsignore, M. E. Protein damage and degradation by oxygen radicals. III. Modification of secondary and tertiary structure. *J. Biol. Chem.* **262**, 9908-9913 (1987).
42. Linton, S., Davies, M. J. & Dean, R. T. Protein oxidation and ageing. *Exp. Gerontol.* **36**, 1503-1518 (2001).
43. Squier, T. C. Oxidative stress and protein aggregation during biological aging. *Exp. Gerontol.* **36**, 1539-1550 (2001).
44. Sohal, R. S. Role of oxidative stress and protein oxidation in the aging process. *Free Radic. Biol. Med.* **33**, 37-44 (2002).

45. Garcia-Garcia, A. *et al.* Biomarkers of Protein Oxidation in Human Disease. *Curr. Mol. Med.* **12**, 681-697 (2012).
46. Davies, K. J. Degradation of oxidized proteins by the 20S proteasome. *Biochimie* **83**, 301-310 (2001).
47. Grune, T., Jung, T., Merker, K. & Davies, K. J. Decreased proteolysis caused by protein aggregates, inclusion bodies, plaques, lipofuscin, ceroid, and 'aggresomes' during oxidative stress, aging, and disease. *Int. J. Biochem. Cell Biol.* **36**, 2519-2530 (2004).
48. Ross, C. A. & Poirier, M. A. Protein aggregation and neurodegenerative disease. *Nat. Med.* **10**, S10-S17 (2004).
49. Choi, J. *et al.* Oxidative modifications and aggregation of Cu,Zn-superoxide dismutase associated with Alzheimer and Parkinson diseases. *J. Biol. Chem.* **280**, 11648-11655 (2005).
50. Chiti, F. & Dobson, C. M. Protein misfolding, functional amyloid, and human disease. *Annu. Rev. Biochem.* **75**, 333-366 (2006).
51. Dalle-Donne, I., Rossi, R., Colombo, R., Giustarini, D. & Milzani, A. Biomarkers of oxidative damage in human disease. *Clin. Chem.* **52**, 601-623 (2006).
52. Finkel, T. & Holbrook, N. J. Oxidants, oxidative stress and the biology of ageing. *Nature* **408**, 239-247 (2000).
53. Valko, M. *et al.* Free radicals and antioxidants in normal physiological functions and human disease. *Int. J. Biochem. Cell Biol.* **39**, 44-84 (2007).
54. Perez, V. I. *et al.* Protein stability and resistance to oxidative stress are determinants of longevity in the longest-living rodent, the naked mole-rat. *Proc. Natl. Acad. Sci. U.S.A.* **106**, 3059-3064 (2009).
55. Krisko, A. & Radman, M. Protein damage and death by radiation in *Escherichia coli* and *Deinococcus radiodurans*. *Proc. Natl. Acad. Sci. U.S.A.* **107**, 14373-14377 (2010).
56. Levine, R. L. Carbonyl modified proteins in cellular regulation, aging, and disease. *Free Radic. Biol. Med.* **32**, 790-796 (2002).
57. Nystrom, T. Role of oxidative carbonylation in protein quality control and senescence. *EMBO J.* **24**, 1311-1317 (2005).
58. Dalle-Donne, I. *et al.* Protein carbonylation, cellular dysfunction, and disease progression. *J. Cell. Mol. Med.* **10**, 389-406 (2006).
59. Andersen, J. K. Oxidative stress in neurodegeneration: cause or consequence? *Nat. Med.* **10**, S18-S25 (2004).
60. Kregel, K. C. & Zhang, H. J. An integrated view of oxidative stress in aging: Basic mechanisms, functional effects, and pathological considerations. *Am. J. Physiol. Regul. Integr. Comp. Physiol.* **292**, R18-R36 (2007).
61. Cooke, M. S., Evans, M. D., Dizdaroglu, M. & Lunec, J. Oxidative DNA damage: mechanisms, mutation, and disease. *FASEB J.* **17**, 1195-1214 (2003).
62. Kirkwood, T. B. L. Understanding the odd science of aging. *Cell* **120**, 437-447 (2005).
63. Lin, M. T. & Beal, M. F. Mitochondrial dysfunction and oxidative stress in neurodegenerative diseases. *Nature* **443**, 787-795 (2006).
64. Sohal, R. S., Agarwal, S., Dubey, A. & Orr, W. C. Protein oxidative damage is associated with life expectancy of houseflies. *Proc. Natl. Acad. Sci. U.S.A.* **90**, 7255-7259 (1993).
65. Gems, D. & Partridge, L. Stress-response hormesis and aging: "That which does not kill us makes us stronger". *Cell Metab.* **7**, 200-203 (2008).
66. Cai, Z. & Yan, L. J. Protein oxidative modifications: Beneficial roles in disease and health. *Journal of biochemical and pharmacological research* **1**, 15-26 (2013).

67. Karplus, M. & McCammon, J. A. Molecular dynamics simulations of biomolecules. *Nat. Struct. Biol.* **9**, 646-652 (2002).
68. van Gunsteren, W. F. *et al.* Biomolecular modeling: Goals, problems, perspectives. *Angew. Chem. Int. Ed.* **45**, 4064-4092 (2006).
69. Kruschel, D. & Zagrovic, B. Conformational averaging in structural biology: issues, challenges and computational solutions. *Mol Biosyst* **5**, 1606-1616 (2009).
70. Schuler, L., Daura, X. & van Gunsteren, W. An improved GROMOS96 force field for aliphatic hydrocarbons in the condensed phase. *J. Comput. Chem.* **22**, 1205-1218 (2001).
71. Oostenbrink, C., Villa, A., Mark, A. E. & van Gunsteren, W. F. A biomolecular force field based on the free enthalpy of hydration and solvation: the GROMOS force-field parameter sets 53A5 and 53A6. *J. Comput. Chem.* **25**, 1656-1676 (2004).
72. Schmid, N. *et al.* Definition and testing of the GROMOS force-field versions 54A7 and 54B7. *Eur. Biophys. J.* **40**, 843-856 (2011).
73. Lindorff-Larsen, K. *et al.* Improved side-chain torsion potentials for the Amber ff99SB protein force field. *Proteins* **78**, 1950-1958 (2010).
74. Chen, J. H., Im, W. P. & Brooks, C. L. Balancing solvation and intramolecular interactions: Toward a consistent generalized born force field. *J. Am. Chem. Soc.* **128**, 3728-3736 (2006).
75. Kaminski, G. A., Friesner, R. A., Tirado-Rives, J. & Jorgensen, W. L. Evaluation and reparametrization of the OPLS-AA force field for proteins via comparison with accurate quantum chemical calculations on peptides. *J Phys Chem B* **105**, 6474-6487 (2001).
76. Schlick, T., Collepardo-Guevara, R., Halvorsen, L. A., Jung, S. & Xiao, X. Biomolecular modeling and simulation: a field coming of age. *Q. Rev. Biophys.* **44**, 191-228 (2011).
77. Best, R. B. Atomistic molecular simulations of protein folding. *Curr. Opin. Struct. Biol.* **22**, 52-61 (2012).
78. Duan, Y. & Kollman, P. A. Pathways to a protein folding intermediate observed in a 1-microsecond simulation in aqueous solution. *Science* **282**, 740-744 (1998).
79. Daura, X., van Gunsteren, W. F. & Mark, A. E. Folding-unfolding thermodynamics of a beta-heptapeptide from equilibrium simulations. *Proteins* **34**, 269-280 (1999).
80. Schafer, H., Mark, A. E. & van Gunsteren, W. F. Absolute entropies from molecular dynamics simulation trajectories. *J Chem Phys* **113**, 7809-7817 (2000).
81. Snow, C. D., Nguyen, N., Pande, V. S. & Gruebele, M. Absolute comparison of simulated and experimental protein-folding dynamics. *Nature* **420**, 102-106 (2002).
82. Zagrovic, B., Snow, C. D., Shirts, M. R. & Pande, V. S. Simulation of folding of a small alpha-helical protein in atomistic detail using worldwide-distributed computing. *J. Mol. Biol.* **323**, 927-937 (2002).
83. Pande, V. S. *et al.* Atomistic protein folding simulations on the submillisecond time scale using worldwide distributed computing. *Biopolymers* **68**, 91-109 (2003).
84. Muff, S. & Caflisch, A. Kinetic analysis of molecular dynamics simulations reveals changes in the denatured state and switch of folding pathways upon single-point mutation of a beta-sheet miniprotein. *Proteins* **70**, 1185-1195 (2008).
85. Baron, R., Huenenberger, P. H. & McCammon, J. A. Absolute single-molecule entropies from quasi-harmonic analysis of microsecond molecular dynamics: Correction terms and convergence properties. *J. Chem. Theory. Comput.* **5**, 3150-3160 (2009).
86. Lin, Z., Kornfeld, J., Maechler, M. & van Gunsteren, W. F. Prediction of folding equilibria of differently substituted peptides using one-step perturbation. *J. Am. Chem. Soc.* **132**, 7276-7278 (2010).
87. Seeliger, D. & de Groot, B. L. Protein thermostability calculations using alchemical free energy simulations. *Biophys. J.* **98**, 2309-2316 (2010).

88. Shaw, D. E. *et al.* Atomic-level characterization of the structural dynamics of proteins. *Science* **330**, 341-346 (2010).
89. Lindorff-Larsen, K., Piana, S., Dror, R. O. & Shaw, D. E. How fast-folding proteins fold. *Science* **334**, 517-520 (2011).
90. Cino, E. A., Wong-ekkabut, J., Karttunen, M. & Choy, W.-Y. Microsecond molecular dynamics simulations of intrinsically disordered proteins involved in the oxidative stress response. *PLoS ONE* **6**, e27371 (2011).
91. Phillips, J. L., Colvin, M. E. & Newsam, S. Validating clustering of molecular dynamics simulations using polymer models. *BMC Bioinformatics* **12** (2011).
92. Lindorff-Larsen, K., Trbovic, N., Maragakis, P., Piana, S. & Shaw, D. E. Structure and dynamics of an unfolded protein examined by molecular dynamics simulation. *J. Am. Chem. Soc.* **134**, 3787-3791 (2012).
93. Piana, S., Carloni, P. & Parrinello, M. Role of conformational fluctuations in the enzymatic reaction of HIV-1 protease. *J. Mol. Biol.* **319**, 567-583 (2002).
94. Liang, S. *et al.* Exploring the molecular design of protein interaction sites with molecular dynamics simulations and free energy calculations. *Biochemistry* **48**, 399-414 (2009).
95. Chodera, J. D. *et al.* Alchemical free energy methods for drug discovery: Progress and challenges. *Curr. Opin. Struct. Biol.* **21**, 150-160 (2011).
96. Durrant, J. D. & McCammon, J. A. Molecular dynamics simulations and drug discovery. *BMC Biol.* **9** (2011).
97. Grant, B. J. *et al.* Novel allosteric sites on Ras for lead generation. *PLoS ONE* **6** (2011).
98. Huang, D. & Caflisch, A. The free energy landscape of small molecule unbinding. *PLoS Comp. Biol.* **7** (2011).
99. de Ruiter, A. & Oostenbrink, C. Free energy calculations of protein-ligand interactions. *Curr. Opin. Chem. Biol.* **15**, 547-552 (2011).
100. Privett, H. K. *et al.* Iterative approach to computational enzyme design. *Proc. Natl. Acad. Sci. U.S.A.* **109**, 3790-3795 (2012).
101. Shuai Liu *et al.* Lead Optimization Mapper: Automating free energy calculations for lead optimization. *In preparation*.
102. Gsponer, J., Haberthur, U. & Caflisch, A. The role of side-chain interactions in the early steps of aggregation: Molecular dynamics simulations of an amyloid-forming peptide from the yeast prion Sup35. *Proc. Natl. Acad. Sci. U.S.A.* **100**, 5154-5159 (2003).
103. Noskov, S. Y., Berneche, S. & Roux, B. Control of ion selectivity in potassium channels by electrostatic and dynamic properties of carbonyl ligands. *Nature* **431**, 830-834 (2004).
104. Ma, B. & Nussinov, R. Simulations as analytical tools to understand protein aggregation and predict amyloid conformation. *Curr. Opin. Chem. Biol.* **10**, 445-452 (2006).
105. Pan, Y. & Nussinov, R. Structural basis for p53 binding-induced DNA bending. *J. Biol. Chem.* **282**, 691-699 (2007).
106. MacKerell, A. D., Jr. & Nilsson, L. Molecular dynamics simulations of nucleic acid-protein complexes. *Curr. Opin. Struct. Biol.* **18**, 194-199 (2008).
107. Khalili-Araghi, F. *et al.* Molecular dynamics simulations of membrane channels and transporters. *Curr. Opin. Struct. Biol.* **19**, 128-137 (2009).
108. Chen, R. & Mark, A. E. The effect of membrane curvature on the conformation of antimicrobial peptides: Implications for binding and the mechanism of action. *Eur. Biophys. J.* **40**, 545-553 (2011).

109. Gros, P., van Gunsteren, W. F. & Hol, W. G. J. Inclusion of thermal motion in crystallographic structures by restrained molecular-dynamics. *Science* **249**, 1149-1152 (1990).
110. Soares, T. A., Daura, X., Oostenbrink, C., Smith, L. J. & van Gunsteren, W. F. Validation of the GROMOS force-field parameter set 45A3 against nuclear magnetic resonance data of hen egg lysozyme. *J. Biomol. NMR* **30**, 407-422 (2004).
111. Zagrovic, B. & van Gunsteren, W. F. Comparing atomistic simulation data with the NMR experiment: How much can NOEs actually tell us? *Proteins* **63**, 210-218 (2006).
112. van Gunsteren, W. F., Dolenc, J. & Mark, A. E. Molecular simulation as an aid to experimentalists. *Curr. Opin. Struct. Biol.* **18**, 149-153 (2008).
113. Kuzmanic, A., Kruschel, D., van Gunsteren, W. F., Pannu, N. S. & Zagrovic, B. Dynamics may significantly influence the estimation of interatomic distances in biomolecular X-ray structures. *J. Mol. Biol.* **411**, 286-297 (2011).
114. Lindorff-Larsen, K. *et al.* Systematic validation of protein force fields against experimental data. *PLoS ONE* **7** (2012).
115. Nygaard, R. *et al.* The Dynamic Process of beta(2)-Adrenergic Receptor Activation. *Cell* **152**, 532-542 (2013).
116. Shaw, D. E. *et al.* Anton, a special-purpose machine for molecular dynamics simulation. *Commun ACM* **51**, 91-97 (2008).
117. Pronk, S. *et al.* GROMACS 4.5: a high-throughput and highly parallel open source molecular simulation toolkit. *Bioinformatics* **29**, 845-854 (2013).
118. Volkman, B. F., Lipson, D., Wemmer, D. E. & Kern, D. Two-state allosteric behavior in a single-domain signaling protein. *Science* **291**, 2429-2433 (2001).
119. Bottomley, M. J. Structures of protein domains that create or recognize histone modifications. *EMBO Rep.* **5**, 464-469 (2004).
120. Grauffel, C., Stote, R. H. & Dejaegere, A. Force field parameters for the simulation of modified histone tails. *J. Comput. Chem.* **31**, 2434-2451 (2010).
121. Polyansky, A. A. & Zagrovic, B. Protein electrostatic properties predefining the level of surface hydrophobicity change upon phosphorylation. *J Phys Chem Lett* **3**, 973-976 (2012).
122. Potoyan, D. A. & Papoian, G. A. Regulation of the H4 tail binding and folding landscapes via lys-16 acetylation. *Proc. Natl. Acad. Sci. U.S.A.* **109**, 17857-17862 (2012).
123. Seeliger, D. *et al.* Quantitative assessment of protein interaction with methyl-lysine analogues by hybrid computational and experimental approaches. *ACS Chem. Biol.* **7**, 150-154 (2012).



# Chapter I

## A systematic framework for molecular dynamics simulations of protein post-translational modifications

Petrov, D.,\* Margreitter, C.,\* Grandits, M., Oostenbrink, C. & Zagrovic, B. (2013). *PLoS Comput. Biol.* **9** (7), e1003154.

\*The authors contribute equally to this work.

DP, CM and BZ conceived and designed the experiments. DP, CM, MG, CO and BZ performed the experiments. DP, CO and BZ analyzed the data. DP, CM, MG, CO and BZ wrote the paper.

**ABSTRACT**

By directly affecting structure, dynamics and interaction networks of their targets, post-translational modifications (PTMs) of proteins play a key role in different cellular processes ranging from enzymatic activation to regulation of signal transduction to cell-cycle control. Despite the great importance of understanding how PTMs affect proteins at the atomistic level, a systematic framework for treating post-translationally modified amino acids by molecular dynamics (MD) simulations, a premier high-resolution computational biology tool, has never been developed. Here, we report and validate force field parameters (GROMOS 45a3 and 54a7) required to run and analyze MD simulations of more than 250 different types of enzymatic and non-enzymatic PTMs. The newly developed GROMOS 54a7 parameters in particular exhibit near chemical accuracy in matching experimentally measured hydration free energies (RMSE = 4.2 kJ/mol over the validation set). Using this tool, we quantitatively show that the majority of PTMs greatly alter the hydrophobicity and other physico-chemical properties of target amino acids, with the extent of change in many cases being comparable to the complete range spanned by native amino acids.

**AUTHOR SUMMARY**

Post-translational modifications, i.e., chemical changes of protein amino acids, play a key role in different cellular processes, ranging from enzymatic activation to transcription and translation regulation to disease development and aging. However, our understanding of their effects on protein structure, dynamics and interaction networks at the atomistic level is still largely incomplete. In particular, molecular dynamics simulations, despite their power to provide a high-resolution insight into biomolecular function and underlying mechanisms, have been limited to unmodified, native proteins due to a surprising deficiency of suitable tools and systematically developed parameters for treating modified proteins. To fill this gap, we develop and validate force field parameters, an essential part of the molecular dynamics method, for more than 250 different types of enzymatic and non-enzymatic post-translational modifications. Additionally, using this tool, we quantitatively show that microscopic properties of target amino acids, such as hydrophobicity, are greatly affected by the majority of modifications. The parameters presented in this study greatly expand the range of applicability of computational methods, and in particular molecular dynamics

simulations, to a large set of new systems with utmost biological and biomedical importance.

## INTRODUCTION

Proteins in the cell continually get covalently modified in different post-translational, enzyme-controlled reactions.<sup>1-3</sup> Additionally, protein modifications frequently arise in a non-controlled fashion as well, mainly as a consequence of oxidative stress.<sup>4</sup> While enzymatic post-translational modifications (PTMs) play important regulatory roles in a large number of different cellular processes, non-enzymatic PTMs are predominantly linked with protein damage and are involved in age-related diseases such as neurodegenerative disorders, diabetes and cancer.<sup>2,4-7</sup> Despite the general importance of PTMs in different biological contexts, their effect on protein structure, dynamics and interaction networks at the atomistic level remains poorly understood. In particular, molecular dynamics (MD) simulations, a widely used high-resolution computational method for studying biomolecular properties and behavior,<sup>8-10</sup> have been limited to unmodified, native proteins due to a surprising deficiency of suitable tools and systematically developed parameters for treating PTMs, with only sporadic exceptions.<sup>11-16</sup>

MD simulations capture atomic and molecular motions based on Newton's equation of motion and an empirical potential energy function that defines interactions between simulated particles. The latter is defined by a force field, i.e., a self-consistent set of physically realistic equations and semi-empirical parameters describing all interactions in a given system. Force-field parameters are typically obtained by fitting atomic or molecular properties of small molecules against calculated quantum-mechanical or experimentally measured data. As the applied parameterization strategies often differ from each other, considerably different parameter values have been derived in many cases.<sup>17-20</sup> Here, we develop force field parameters for over 250 different types of enzymatic and non-enzymatic modifications of amino-acid side chains as well as protein termini within the context of GROMOS 45a3<sup>19</sup> and 54a7<sup>21,22</sup> force fields (Table S1). We choose GROMOS force fields because of their widespread usage, high accuracy in reproducing experimental results and general transferability of parameters when it comes to identical chemical groups in different compounds<sup>21</sup> (e.g., from the hydroxyl group of tyrosine to the hydroxyl group of 7-hydroxytryptophan). The functional form of a typical force field is exemplified in equation 1 for GROMOS class force fields,

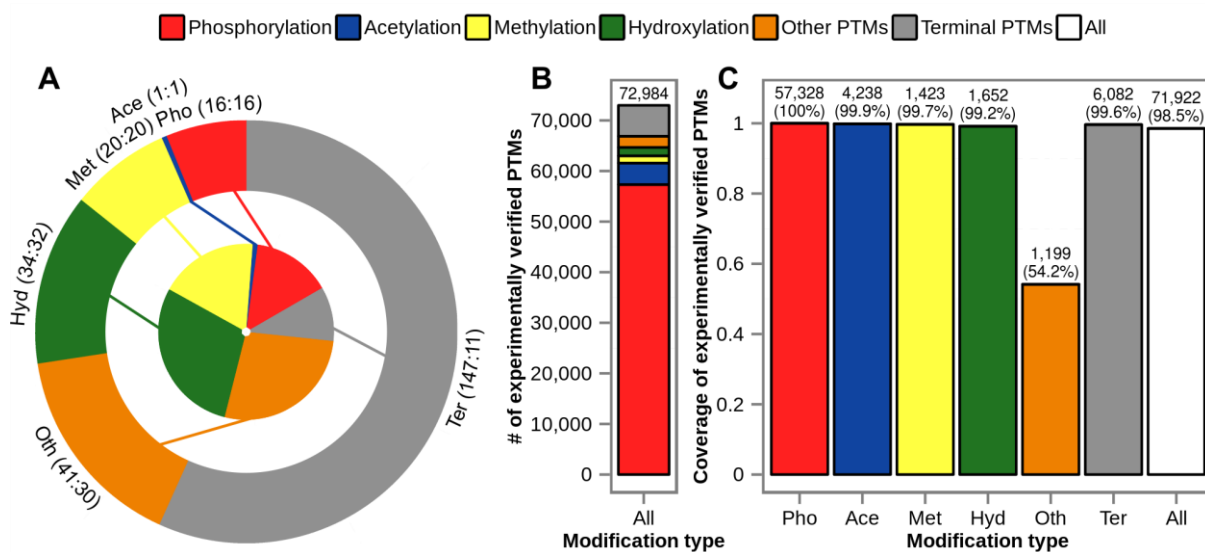
$$E_{pot} = \sum_{bonds} \frac{K_{b,i}}{4} (b_i^2 - \mathbf{b}_{i,0}^2)^2 + \sum_{angles} \frac{K_{\theta,i}}{2} (\cos \theta_i - \cos \theta_{i,0})^2 + \sum_{impropers} \frac{K_{\xi,i}}{2} (\xi_i - \xi_{i,0})^2 + \sum_{dihedrals} \frac{K_{\phi,i}}{2} [1 + \cos \delta_i \cos(\mathbf{m}_i \phi_i)] + \sum_{atom\ pairs} \left( 4\epsilon_{ij} \left[ \left( \frac{\sigma_{ij}}{r_{ij}} \right)^{12} - \left( \frac{\sigma_{ij}}{r_{ij}} \right)^6 \right] + \frac{q_i q_j}{4\pi\epsilon_0\epsilon_1 r_{ij}} + RF_{i,j} \right), \quad (1)$$

with parameters highlighted using boldface letters and RF representing a reaction field contribution to the electrostatic interactions. The non-bonded interaction terms in the GROMOS force field are primarily parameterized against thermodynamic data of small molecules, either in the pure liquid state, or in aqueous or nonpolar solution. Therefore, we validate the obtained parameters by reproducing experimental hydration free energies (HFEs), a measure of hydrophobicity and arguably one of the most important amino-acid properties with implications in protein folding, ligand binding or protein-lipid interactions. Finally, we analyze physico-chemical properties related to hydrophobicity of all parameterized PTMs according to their type and compare them against the 20 canonical amino acids.

## RESULTS

### Parameterization of PTMs

One of the principal objectives in our parameterization has been the coverage of experimentally known PTMs, which is as complete as possible. Following an exhaustive literature search and analysis of an online PTM database PTMdb,<sup>23</sup> we have compiled a diverse list of enzymatic and non-enzymatic PTMs, including phosphorylation, methylation, acetylation, hydroxylation, carboxylation, carbonylation, nitration, deamidation and many others (Figure 1a, Table S1), covering a total of 259 distinct PTM reactions or 110 non-redundant post-translationally modified amino acids and protein termini. The lower number in the latter case reflects the fact that different PTM reactions can lead to the same modified product (e.g., glutamic semialdehyde is a product of both arginine and proline carbonylation). We have generated GROMOS 45a3 (Dataset S1) and 54a7 (Dataset S2) force field parameters for the non-redundant set of compounds by either direct transfer or analogy to already parameterized compounds including amino acids, nitrogenous bases and other small molecules or completely novel parameterization (see Methods for more details).



**Figure 1. Summary of the number and coverage of parameterized PTMs.** a) the number of parameterized PTMs by type (outer annulus) together with the number of parameterized non-redundant compounds by type (inner circle), labeled accordingly (number of PTMs: number of compounds); b) the number of experimentally verified PTMs by type annotated in the UniProt database (total of 72,984); c) coverage of experimentally verified PTMs shown as percentages with the values and the number of covered modifications displayed (top of bars). Color code: phosphorylation-red, acetylation-blue, methylation-yellow, hydroxylation-green, other PTMs-orange, terminal PTMs-gray and all-white.

How well do the obtained parameters cover the space of biologically relevant PTMs? To address this question, we have analyzed PTMs that have been experimentally verified (72,984) and annotated as such in the UniProt database<sup>24</sup> (21,411 protein entries, Dataset S3). Phosphorylation is by-far the most abundant modification type in the UniProt database (78.5% of all UniProt PTMs), followed by acetylation, hydroxylation and methylation (Figure 1b). Note that terminal PTMs account for a sizable fraction of all annotated modification at 8.3%. Strikingly, the parameterized compounds reported herein match every annotated phosphorylation modification, 99.9% of acetylation, 99.2% of hydroxylation and 99.7% of methylation modifications, for a grand-total coverage of 98.5% of all PTMs reported in UniProt (Figure 1c). Concerning PTMs that are not covered by our parameters, they are all extremely rare, each accounting for less than 0.5% of all UniProt PTMs. Finally, we provide parameters for 33 PTMs (Table S1), mostly non-enzymatic ones, that have to date not been reported in UniProt.

## Validation against experimental HFEs

HFE, a free energy difference between a compound solvated in water and the same compound in the gas phase, is an experimentally measurable property related to hydrophobicity, and it has been originally used to re-parameterize the GROMOS force field in 2004.<sup>21</sup> A proper description of functional groups in the hydrated phase is of crucial importance for virtually all relevant biomolecular processes, so we have used the same thermodynamic quantity to validate the parameters obtained in the present study. To the best of our knowledge, experimental HFEs are available for the exact side chain analogs of 13 parameterized PTMs only and we have therefore in the validation set also included compounds, which are chemically related to PTM side chains for which no experimental HFEs were available, for a total of 26 different molecules (only a single representative compound was included for each group of PTMs involving the same chemical moiety, Table 1). Note that the additional compounds related to PTM side chains have been parameterized in the same way as the relevant PTMs.

**Table 1.** HFEs of the molecules in the validation set: comparison between experimental and calculated values using the GROMOS 54a7 parameter set.

Compound	HFE (kJ/mol)	
	experimental	ffG54a7
<b>Validation set. PTM-side-chain analogs</b>		
N-butylacetamide	-39.0	-37.9
<i>o</i> -cresol	-24.6	-24.8
<i>m</i> -cresol	-23.0	-28.2
2-methyl-2-propanol	-18.7	-15.1
2-methyl-1-propanol	-18.8	-18.6
propan-2-ol	-19.8	-16.1
N-methylacetamine	-41.9	-38.0
methylpropanoate	-12.3	-5.8
methylacetate	-13.1	-8.7
dimethylsulfide	-6.7	-9.1
butanal	-13.3	-10.8
propanal	-14.4	-11.8

butane	8.7	9.5
<b>Validation set. Compounds similar to PTM-side-chain analogs</b>		
diethylamine	-17.0	-11.7
trimethylamine	-13.4	-4.7
ethene	5.4	13.8
bromobenzene	-6.1	-8.6
aniline	-23.0	-25.8
acetophenone	-19.2	-16.3
N-methylformamide	-41.9	-39.5
chlorophenol	-19.0	-22.8
*2-nitrophenol	-19.2	-33.8
nitrobenzene	-17.2	-15.6
acetone	-16.1	-8.5
dimethylsulfoxide	-42.3	-39.4
methylsulfonylmethane	-42.2	-41.9
<b>RMSE</b>	-	<b>4.2</b>
<b>Additional compounds</b>		
#2-nitrophenol	-19.2	-17.4
3-nitrophenol	-40.3	-43.0
4-nitrophenol	-44.5	-44.2
4-methylimidazole (N $\delta$ -H)	-42.9	-46.7
4-methylimidazole (N $\epsilon$ -H)		-62.0
1-methylimidazole (N $\delta$ -H)	-35.2	-25.2
1-methylimidazole (N $\epsilon$ -H)		-34.5

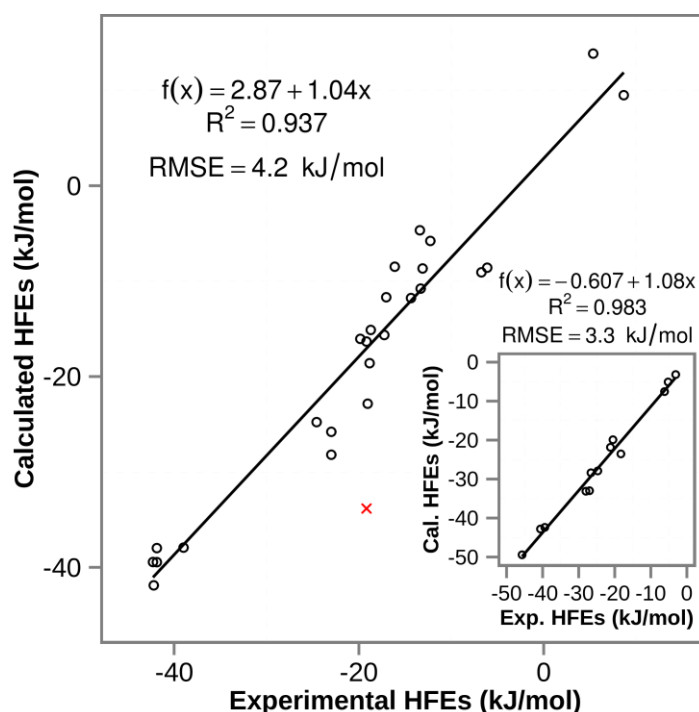
The outlier 2-nitrophenol described by: \*parameters used for other nitro-containing compounds, and #parameters derived to match the experimental HFE.

Experimental HFEs are taken from refs.<sup>21,48-50</sup>

We have used MD simulations and the thermodynamic integration (TI) approach<sup>25</sup> (see *Methods* for more details) to calculate the HFEs for neutral forms small-molecule analogs of the canonical amino-acid side chains and for the compounds in the validation set using both the 45a3 (Table S2) and 54a7 (Table 1) parameter sets of the GROMOS force field. As a consequence of the parameterization strategy behind them, the canonical amino acids



exhibit an excellent agreement with experimental HFEs when it comes to the 54a7 parameter set, with a root-mean-square error (RMSE) of 3.3 kJ/mol (RT = 2.5 kJ/mol at room temperature) and an almost perfect correlation with experimental HFEs (correlation coefficient  $R^2 = 0.98$ ) (Figure 2). Remarkably, the newly generated GROMOS 54a7 force field parameters of PTM-related compounds exhibit a nearly equal level of matching of experimental HFEs with an RMSE of 4.2 kJ/mol (Table 1) and a correlation coefficient  $R^2$  of 0.94 (Figure 2) over 25 different compounds, excluding a single outlier, 2-nitrophenol (Figure 2, red X symbol). This compound, containing nitro and hydroxyl groups attached to a benzene ring, deviates from the experimental value by 14.6 kJ/mol.



**Figure 2. Experimental vs. calculated HFEs of compounds from the validation set (GROMOS 54a7).** Correlation is captured by the regression line, its parameters, Pearson correlation coefficient and overall RMSE, with the outlier 2-nitrophenol in red (X symbol). The same comparison for canonical amino acids is shown in the inset. Note that error bars of calculated HFEs are comparable to the size of the symbols, with the average standard error of 0.4 kJ/mol.

Considering the outlier 2-nitrophenol in more detail, additional calculations have shown that *p*-cresol (a tyrosine side-chain analog), *o*-cresol, *m*-cresol and nitrobenzene, compounds containing either a hydroxyl group or a nitro group attached to a benzene ring, agree well with experimental HFEs with an overall RMSE of 2.7 kJ/mol only. This suggests

that, although parameters of individual groups do reproduce experimental HFEs, the agreement with experiment may significantly worsen if they appear in combination. In order to test this, we have calculated HFEs of 3- and 4-nitrophenol and compared them against experimental values. Interestingly, the calculated HFEs of both compounds match experimental values (Table 1) suggesting either that these groups exert a specific influence on each other only in 2-nitrophenol or that the experimentally measured HFE may simply not be reliable for this compound. To account for the former possibility, we have derived a set of parameters *de novo* for 2-nitrophenol that closely match its experimental HFE with an absolute value of the deviation of 1.8 kJ/mol (Table 1). Note that we report both versions of nitrotyrosine (Table S1), a cognate PTM to 2-nitrophenol.

Finally, we have also excluded 4-methylimidazole (a histidine side-chain analog) and 1-methylimidazole from the HFE analysis of the canonical amino acids and PTMs, respectively, even though experimental HFEs are available for both compounds. Since histidine exists in two tautomeric states, described by different parameters, the calculated HFE depends on the choice of the state used for calculations, with one matching the experimental HFE and the other varying by approximately 20 kJ/mol (Table 1). Consequently, the same problem exists for 1'- and 3'-methylhistidine, whose parameters are based on those of histidine, where one tautomer matches while the other deviates from the experimental HFE (Table 1).

In contrast to GROMOS 54a7, the 45a3 parameter set does not reproduce experimental HFEs well (Table S2 and Figure S1). Namely, the slope of 0.79 and the offset of 3.8 kJ/mol of the regression line suggest that the calculated HFEs are largely overestimated (RMSE = 10.8 kJ/mol) for the amino-acid side chain analogs, as observed previously.<sup>21</sup> The same effect persists for the PTM compounds, with a RMSE from experimental HFEs of 15 kJ/mol (Figure S1). As the GROMOS 45a3 parameter set was not parameterized to match experimental HFEs for polar compounds, such level of deviation was to be expected.

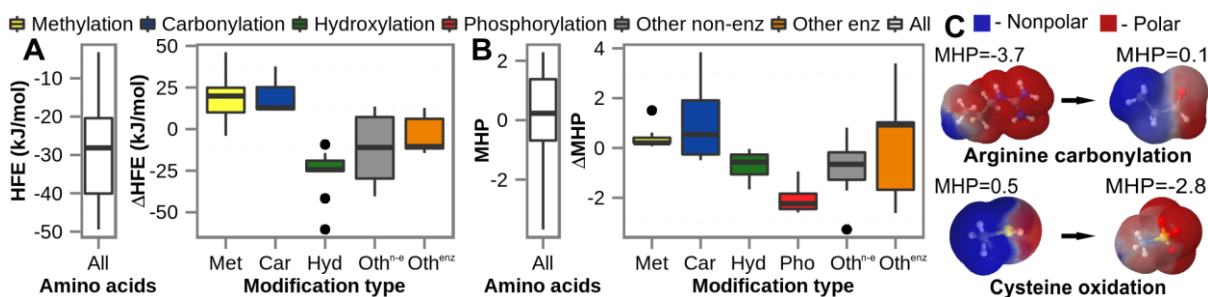
Due to a lack of pertinent experimental data, seven parameterized PTMs (carboxyllysine, homocitrulline, citrulline, S-carbamoyl-cysteine, S-nitrosocysteine, 2-oxo-histidine and pyruvic acid) have remained unrepresented in the validation set, and therefore unverified in terms of reproducing experimental HFEs. To further assess the quality of the parameters for these compounds, we have compared them to those obtained by the Automated Topology

Builder,<sup>26</sup> a widely used online service for automated parameterization of small molecules compatible with the GROMOS 54a7 force field. While manually curated approaches are arguably superior to automated ones, it is reassuring to see that the two sets of parameters match closely. For example, we have observed close agreement between the sets of partial charges obtained using the two methods for these seven compounds, with a Pearson correlation coefficient  $R$  of 0.93 and an overall RMSD of  $0.2 e^-$ .

### **Comparison of physico-chemical properties of PTMs and canonical amino acids**

As an application of the newly developed PTM parameters, we focus on the changes in several key physico-chemical properties of amino acids introduced by PTMs. Interestingly, the majority of post-translationally modified amino acids are larger in size than their native counterparts, with more than 85% of PTMs increasing the molecular weight and more than 80% of PTMs increasing the solvent accessible surface area (SASA) of the affected residues (Table S3) as calculated on energy-minimized (using the GROMOS 54a7 parameter set) configurations of PTMs and canonical amino acids. What is more, PTMs introduce significant changes in the electrostatic properties of target residues as illustrated in the case of net charge and dipole moment (Table S3). For example, 42% of all PTMs studied here undergo a charge change of  $1 e^-$  or more in absolute value, with 88% of such changes resulting in a more negatively charged species. Moreover, the average absolute value of the change in dipole moment upon PTM equals 1.7 Debye, which is comparable in magnitude to the average dipole moment of 2.7 Debye or its standard deviation of 1.9 Debye as calculated in both cases over all unmodified residues using GROMOS 54a7 parameters and energy-minimized configurations. Finally, given the general importance of hydrophobicity in various biological processes, it is critical to understand in a quantitative manner how PTMs modulate the hydrophobicity of target amino acids. To address this question, we have used TI and GROMOS 54a7 parameters to calculate HFEs of all parameterized PTMs in neutral protonation states, since the available experimental data is insufficient for such an analysis. Our results show that methylation and carbonylation modifications increase HFEs on average by 18.6 kJ/mol and 20.5 kJ/mol, respectively, while hydroxylation modifications exhibit an opposite effect and decrease HFEs by on average 25.1 kJ/mol (Figure 3a). These changes are extremely relevant if one considers the fact that the two central quartiles of the

distribution of HFEs for canonical amino acids span the range from approximately -40 kJ/mol to -20 kJ/mol (Figure 3a). Furthermore, the most extreme cases, i.e., symmetric dimethylation of arginine ( $\Delta\text{HFE} = 46.2$  kJ/mol) and di-hydroxylation of phenylalanine ( $\Delta\text{HFE} = -60.3$  kJ/mol) are comparable in absolute values to the total span of the canonical amino acid HFEs (-49.4 kJ/mol to -3.2 kJ/mol, Figure 3a). In other words, the effect of some PTMs on the HFEs of target amino acids is as large as the difference which would arise by mutating the most hydrophobic to the most hydrophilic canonical amino acid or vice versa. While some of these effects agree well with what one would qualitatively expect, for a number of PTMs our results are the first to provide a quantitative framework for such an analysis.



**Figure 3. Hydrophobicity-related properties of PTMs compared to canonical amino acids.** a) hydration free energies (HFEs) and b) molecular hydrophobicity potentials (MHPs). Distributions calculated of HFEs and MHPs of the canonical amino acids are captured using white boxes on the left side of both a) and b) panels. The distributions of HFE and MHP changes upon different types of PTMs are shown in colored boxes sorted according to the median of the underlying distributions. The distributions are shown using the box-and-whisker plotting method. Color code: methylation-yellow, carbonylation-blue, hydroxylation-green, phosphorylation-red, other enzymatic modifications-gray, other non-enzymatic modification-orange and all-white; c) change in surface MHP upon arginine carbonylation and cysteine oxidation, modifications with the most positive and the most negative MHP change, respectively. Note that we have not taken N-acetylglucosamine into account for the HFE and MHP analysis, since glycosylation modifications predominantly result in carbohydrate chains attached to target residues, while we provide parameters for this carbohydrate only as the first one in a typical chain.

As both calculation and experimental measurement of HFEs are limited to neutral compounds only, the above analysis does not take into account charged modifications such as phosphorylation. To address this, we have used the molecular hydrophobicity potential (MHP)<sup>27</sup> approach to estimate hydrophobicity of all parameterized PTMs using their protonation states at physiological pH. MHP values are semi-empirical estimates of  $\log P$ , a

given compound's partition coefficient between water and the non-polar solvent octanol and are widely used in computational drug design.<sup>28,29</sup> Similarly to the HFEs analysis, MHP calculations show that carbonylation and methylation are hydrophobicity-increasing modifications (Figure 3b), in contrast to phosphorylation and hydroxylation, which are hydrophilicity-increasing modifications. Finally, this analysis shows that PTMs can drastically change hydrophobic/hydrophilic properties of affected residues, e.g., arginine carbonylation shifts a highly hydrophilic to a highly hydrophobic residue, while cysteine oxidation does exactly the opposite (Figure 3c). By changing the chemical nature of affected residues, PTMs frequently completely alter their physico-chemical properties such as hydrophobicity, a feature with potentially far-reaching biological implications.<sup>11,12,30</sup>

## DISCUSSION

Despite the importance of understanding PTMs at the molecular level, MD simulations of post-translationally modified proteins lag significantly behind the studies of unmodified proteins, and this seems primarily due to a general lack of suitable computational tools and simulation parameters for treating PTMs. This study is to the best of our knowledge the first-ever effort to develop force-field parameters for the large majority of known PTMs in a systematic fashion. We have generated GROMOS force field (45a3 and 54a7) parameters for over 250 different enzymatic and non-enzymatic PTMs, spanning a wide range of modification types with a close to complete coverage of experimentally verified PTMs (Figure 1). Since GROMOS 54a7 force field parameters were fitted to reproduce experimental HFEs, we have tested the quality of the PTM parameters, obtained by manually curating the parameters of different groups mostly in analogy to canonical amino acids, by comparing the calculated HFEs against the experimental values. The newly generated parameters compatible with the GROMOS 54a7 parameter set reproduce experimental HFEs almost equally well as the original ones (Table 1 and Figure 2). Overall, only a few parameterized PTMs have not been directly validated against experimental HFEs due to a lack of experimentally available data. In those cases, however, good matching with the parameters obtained using an orthogonal, fully automated approach<sup>26</sup> lends support to the general validity of the reported parameters. However, one should emphasize that the full range of validity of the presented parameters could and should be delineated only by

directly comparing MD simulations of different post-translationally modified proteins in biologically relevant contexts with relevant experimental data.

To date, PTMs in MD simulations have been treated in separate studies using different procedures and force fields, typically focusing on a single modification at a time.<sup>11,13,16</sup> Additionally, there are some available tools for automated generation of parameters (e.g., the AMBER<sup>31</sup> feature *antechamber* and online tools SwissParam<sup>32</sup>, PRODRG<sup>33</sup>, ATB<sup>26</sup> and *q4md-forcefieldtools*<sup>34</sup>), however, envisioned for small molecules rather than protein PTMs. The parameters reported herein have comparative advantage over these sources along three principal directions. First, we provide exclusively human curated and validated PTM force-field parameters, which are mutually fully consistent as well as being consistent with canonical amino acids. Second, we provide PTM parameters in both GROMOS<sup>35</sup> and GROMACS<sup>36</sup> format, widely used MD simulation packages (supporting GROMOS version 11 and GROMACS versions 3.x and newer), suitable for immediate simulation of modified proteins without any additional work required. This should be contrasted with the above tools that provide parameters for isolated compounds only. Finally, in combination with a publicly available online tool for introducing PTMs of choice to a user-supplied protein 3D structure (Vienna-PTM server, <http://vienna-ptm.univie.ac.at>),<sup>37</sup> we provide a comprehensive, user-friendly toolkit for studying PTMs using MD simulations.

During their lifecycle in the cell, almost all proteins undergo one or more different PTMs affecting their structure, dynamics and interaction networks and, subsequently, their function through direct alteration of chemical and physico-chemical properties of target residues (Figure 3). The force field parameters presented here, together with the Vienna-PTM webserver, provide a systematic framework required to study the effects of PTMs using MD simulations. As a first step in this direction, we have here compared the hydrophobicity-related variables (HFEs and MFP values) of native and modified amino acids and quantitatively showed that PTMs can have an extremely strong, biologically significant effect in this context. It has already been documented that some PTMs exert their biological effect through a general modification of the hydrophobicity of their targets. For example, lysine trimethylation is known to directly affect the binding of retinoic acid receptors, which regulate genes involved in growth, differentiation and apoptosis, to their partners via an

increase in site-specific hydrophobicity.<sup>38</sup> Moreover, acetylated and methylated lysine residues in histones, i.e., some of the key components of the histone code, are recognized by the hydrophobic binding pockets of bromo- and chromo-domains based on the difference in hydrophobicity between the modified and unmodified lysines.<sup>39</sup> Furthermore, we have recently shown that carbonylation, which affects lysine, arginine, proline and threonine residues, drastically increases local propensity for aggregation in proteins by affecting the hydrophobicity of the modified sites.<sup>11</sup> While other, more specific effects of PTMs on the structure, dynamics and interaction profile of target proteins are certainly important, a major change in hydrophobicity, net charge, isoelectric point or any other general physico-chemical property caused by a PTM at a given site could certainly have major biological repercussions. We believe that our present study will provide a solid foundation for exploring such timely and important issues in the future. However, this is only one possible application of the PTM force-field parameters reported herein. From direct MD simulations to biomolecular structure refinement to computational free energy estimation and drug design, these parameters expand the range of MD methodology to a large class of biomolecular systems of paramount importance. It is our hope that this advance will play a catalytic role in bringing together realistic cell biology, dominated by PTMs, and the quantitative, reductionist power of structural biology and chemistry, as embodied in the MD method, and help shed light on a broad spectrum of important biological questions at the microscopic level.

## **METHODS**

### **Parameterization of PTMs**

One of the aims of the GROMOS force fields is to allow for the transfer of parameters between chemically similar groups in different compounds. Accordingly, we have derived GROMOS 45a3 and 54a7 force field parameters describing 110 post-translationally modified amino acids and protein termini (Table S1) by either novel parameterization or direct transfer from or analogy to already parameterized compounds including amino acids, nitrogenous bases and other small molecules according to the following principles and rationales.

**General principles:**

- Parameters were directly transferred from chemically identical groups (e.g., from the hydroxyl group of tyrosine to the hydroxyl group of 7-hydroxytryptophan) if such exist among parameterized compounds. If not, parameters were either directly transferred or inferred by analogy to the chemically most similar parameterized compound.
- Partial charges were assigned to add up to an integer net charge for every charge group, primarily by adjusting partial charges of less exposed atoms (e.g., the phosphorus atom of phospho-residues), while keeping them intact for terminal, more exposed atoms to affect interactions with other compounds as little as possible.

**Modification type-specific principles:**

- 1) PHOSPHORYLATION: Parameters directly transferred from phosphate and hydroxyl groups of nucleotides (e.g., ATP). The partial charge on the phosphorus atom fixed to get an integral net charge of a parameterized compound (dependent on the protonation state). The rest of a parameterized compound left unchanged. Additionally, analogy to the ester group reported by Chandrasekhar and others<sup>40</sup> used for phosphoaspartate.
- 2) METHYLATION: Parameters directly transferred or derived by analogy to different methyl-containing groups depending on the net charge and chemical context as follows:
  - a. directly transferred or derived by analogy from amines reported by Oostenbrink and others<sup>41</sup> for methylated lysine and histidine residues,
  - b. directly transferred or derived by analogy from nucleotides (e.g., ATP), arginine and amines reported by Oostenbrink and others<sup>41</sup> for methylated arginine residues,
  - c. derived by analogy to the peptide bond and the cognate native residues for methyl-asparagine and methyl-glutamine,
  - d. directly transferred from the ester group reported by Chandrasekhar and others<sup>40</sup> for aspartate methyl ester and glutamate methyl ester,



- e. directly transferred from methionine for S-methylcysteine.
- 3) ACETYLATION: Parameters derived by analogy to the peptide bond and the carboxamide group (e.g., glutamine).
  - 4) HYDROXYLATION: Parameters directly transferred from the hydroxyl group of threonine or tyrosine, if attached to an aliphatic or aromatic carbon atom, respectively.
  - 5) CARBOXYLATION: Parameters directly transferred from the carboxyl group (e.g., glutamate).
  - 6) SULFATION: Parameters derived by analogy to the phosphate group of nucleotides (e.g., adenosine).
  - 7) DEHYDRATION: Parameters directly transferred from aliphatic carbon atoms using a bond type with a shorter equilibrium distance to mimic the properties of the double bond.
  - 8) BROMIDATION: Parameters directly transferred from 8-bromo-guanosine triphosphate reported by Hritz and Oostenbrink.<sup>42</sup>
  - 9) S-NYTROSILATION: The oxygen atom parameters directly transferred for the carbonyl group (e.g., the peptide bond), with the nitrogen and sulfur atom partial charges fixed to add up to 0 net charge.
  - 10) CITRULLINATION: Parameters derived by analogy to the peptide bond and the carboxamide group (e.g., glutamine).
  - 11) ALLYSINE FORMATION: The oxygen atom parameters directly transferred for the carbonyl group (e.g., glutamine), with the carbon and hydrogen atom derived by analogy to the aldehyde group reported by Dolenc and others.<sup>43</sup>
  - 12) GLYCOSYLATION: Parameters directly transferred from the peptide bond and monosaccharide molecules (e.g., glucose).
  - 13) CARBONYLATION: The oxygen atom parameters directly transferred for the carbonyl group (e.g., glutamine), with the carbon and hydrogen atom derived by analogy to the aldehyde group reported by Dolenc and others.<sup>43</sup>
  - 14) OXIDATION: Parameters directly transferred from different oxygen-containing groups depending on the net charge and chemical context:

- a. from the carbonyl group (e.g., glutamine) and the phosphate group of nucleotides (e.g., adenosine) for methionine sulfoxide and methionine sulfone, respectively, with the partial charge of the sulphur atom fixed to get 0 net charge for oxidative modifications of methionine,
- b. from the carboxyl group (e.g., glutamate) for cysteine oxidation modifications,
- c. from the carbonyl group (e.g., glutamine) for the remaining oxidation modifications.

15) NITRATION: The oxygen atom parameters directly transferred from different oxygen-containing groups, with the nitrogen and carbon atoms partial charges adjusted to add up to an integer net charge, depending on the protonation state and chemical context; or derived *de novo* to match the experimental HFE of 2-nitrophenol:

- a. from the base-linked oxygen atom of the phosphate group of nucleotides (e.g., adenosine) for the protonated forms of nitrotyrosine and nitrotryptophan,
- b. derived *de novo* to match the HFE of 2-nitrophenol for the protonated form of nitrotyrosine,
- c. from the base-linked oxygen atom of the phosphate group of nucleotides (e.g., adenosine) and the carboxyl group (e.g., glutamate) for the nitro and carboxyl groups, respectively, of the deprotonated form of nitrotyrosine.

16) KYNURENINE FORMATION: Parameters directly transferred from the carbonyl group (e.g., glutamine), the peptide bond and the amine group of the deprotonated arginine, with the carbon and hydrogen atom derived by analogy to the aldehyde group reported by Dolenc and others<sup>43</sup> for formyl-kynurenine.

17) CHLORINATION: Parameters directly transferred from chloroform.

18) CARBAMYLATION: Parameters directly transferred from the peptide bond, carboxyl group (e.g., glutamate) and the carboxamide group (e.g., glutamine).

19) NORLEUCINE: Parameters directly transferred from aliphatic carbon atoms.

20) N-TERMINAL METHYLATION: Parameters directly transferred from lysine methylation.

21) N-TERMINAL ACETYLATION: Parameters directly transferred from lysine acetylation.

- 22) N-TERMINAL PYRROLIDONE FORMATION: Parameters directly transferred from proline oxidation.
- 23) N-TERMINAL FORMYLATION: Parameters directly transferred from the peptide bond with the carbon and hydrogen atoms derived by analogy to the aldehyde group reported by Dolenc and others.<sup>43</sup>
- 24) N-TERMINAL PYRUVATE FORMATION: Parameters directly transferred from the carbonyl group (e.g., glutamine), with a bond type of a shorter equilibrium distance used between the carbonyl carbon atoms to account for the double bond effect.
- 25) C-TERMINAL AMIDATION: Parameters directly transferred from the carboxamide group of e.g., glutamine.
- 26) C-TERMINAL METHYLATION: Parameters directly transferred from the ester group reported by Chandrasekhar and others.<sup>40</sup>

We include detailed descriptions of parameter choices as comments in Dataset S1 and Dataset S2.

### **Molecular dynamics simulations and thermodynamic integration setup**

We have used the thermodynamic integration approach,<sup>25</sup> a widely used computational method based on MD simulations, to calculate hydration free energies (HFEs) of neutral forms of small-molecule analogs of 14 amino-acid side chains (the same set as in Oostenbrink et al.<sup>21</sup>), compounds from the validation set and side chain analogs of all parameterized PTMs with a charge neutral protonation state. Non-bonded (van der Waals and Coulomb) interactions, coupled to a parameter  $\lambda$ , were scaled down to zero in a stepwise manner in vacuum and water. Free energy changes of these processes were calculated as the integral of the ensemble average of the derivative of the total Hamiltonian of the system with respect to  $\lambda$ , over the interval from  $\lambda = 0$  to  $\lambda = 1$ . For vacuum calculations, three independent simulations, each 5 ns long, were run at 21 equally spaced  $\lambda$ -points with the temperature kept at 500 K and additional random kicks introduced by Langevin dynamics integration method,<sup>44</sup> in order to avoid convergence problems due to inefficient sampling of the conformational space. Water simulations were run in five independent copies, each 0.5 ns long, at 21 equally spaced  $\lambda$ -points, together with 10 additional  $\lambda$ -points placed in the regions of the least smoothness of the integrated curve,

using SPC explicit water,<sup>45</sup> a reaction field electrostatic scheme with a cutoff of  $r_c = 1.4$  nm and the dielectric constant of  $\epsilon_{rf} = 65$  and a Berendsen thermostat and barostat keeping the temperature and pressure at 300 K ( $\tau_T = 0.05$  ps) and 1 bar ( $\tau_p = 1$  ps and compressibility =  $4.5 \times 10^{-5}$  bar<sup>-1</sup>).<sup>46</sup> A soft-core formalism<sup>47</sup> was used to avoid singularities of the potential energy. The aforementioned integrals were evaluated by the generalized Simpson's rule for non-equidistant nodes using the averages over the independent simulations at each  $\lambda$ -point. HFEs were calculated as the difference between the change in free energy upon the removal of non-bonded interactions calculated in vacuum and calculated in water.

## FUNDING

This work was supported in part by the Austrian Science Fund FWF (START grant Y 514-B11 to BZ, <http://www.fwf.ac.at/>), the Vienna Science and Technology fund (WWFF grant number LS08-QM03 to CO, <http://www.wwtf.at/>), and European Research Council (ERC Starting Independent grants 279408 to BZ and 260408 to CO <http://erc.europa.eu/>). The funders had no role in study design, data collection and analysis, decision to publish, or preparation of the manuscript.

## ACKNOWLEDGEMENTS

We thank A. Polyansky for help with MHP calculations and members of the Laboratory of Computational Biophysics at MFPL for useful advice and critical reading of the manuscript.

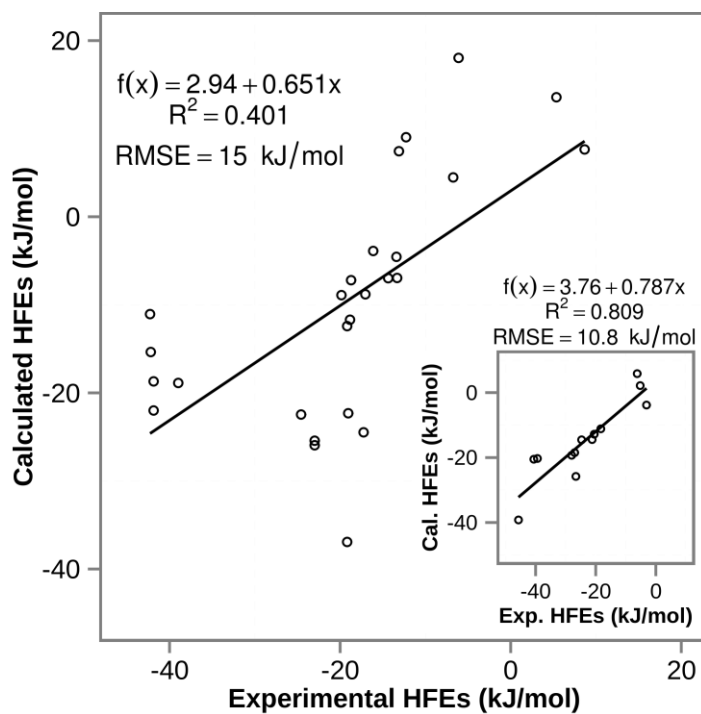
## REFERENCES

1. Mann, M. & Jensen, O. N. Proteomic analysis of post-translational modifications. *Nat. Biotechnol.* **21**, 255-261 (2003).
2. Walsh, C. T., Garneau-Tsodikova, S. & Gatto, G. J., Jr. Protein posttranslational modifications: the chemistry of proteome diversifications. *Angew. Chem. Int. Ed.* **44**, 7342-7372 (2005).
3. Bartova, E., Krejci, J., Harnicarova, A., Galiova, G. & Kozubek, S. Histone modifications and nuclear architecture: A review. *J. Histochem. Cytochem.* **56**, 711-721 (2008).
4. Berlett, B. S. & Stadtman, E. R. Protein oxidation in aging, disease, and oxidative stress. *J. Biol. Chem.* **272**, 20313-20316 (1997).
5. Nystrom, T. Role of oxidative carbonylation in protein quality control and senescence. *EMBO J.* **24**, 1311-1317 (2005).
6. Deribe, Y. L., Pawson, T. & Dikic, I. Post-translational modifications in signal integration. *Nat. Struct. Mol. Biol.* **17**, 666-672 (2010).
7. van Rossum, B., Fischle, W. & Selenko, P. Asymmetrically modified nucleosomes expand the histone code. *Nat. Struct. Mol. Biol.* **19**, 1064-1066 (2012).
8. van Gunsteren, W. F. *et al.* Biomolecular modeling: Goals, problems, perspectives. *Angew. Chem. Int. Ed.* **45**, 4064-4092 (2006).
9. Kruschel, D. & Zagrovic, B. Conformational averaging in structural biology: issues, challenges and computational solutions. *Mol Biosyst* **5**, 1606-1616 (2009).
10. Best, R. B. Atomistic molecular simulations of protein folding. *Curr. Opin. Struct. Biol.* **22**, 52-61 (2012).
11. Petrov, D. & Zagrovic, B. Microscopic analysis of protein oxidative damage: Effect of carbonylation on structure, dynamics, and aggregability of villin headpiece. *J. Am. Chem. Soc.* **133**, 7016-7024 (2011).
12. Polyansky, A. A. & Zagrovic, B. Protein Electrostatic Properties Predefining the Level of Surface Hydrophobicity Change upon Phosphorylation. *J Phys Chem Lett* **3**, 973-976 (2012).
13. Potoyan, D. A. & Papoian, G. A. Regulation of the H4 tail binding and folding landscapes via Lys-16 acetylation. *Proc. Natl. Acad. Sci. U.S.A.* **109**, 17857-17862 (2012).
14. Olausson, B. E. S. *et al.* Molecular dynamics simulations reveal specific interactions of post-translational palmitoyl modifications with rhodopsin in membranes. *J. Am. Chem. Soc.* **134**, 4324-4331 (2012).
15. Marlowe, A. E., Singh, A. & Yingling, Y. G. The effect of point mutations on structure and mechanical properties of collagen-like fibril: A molecular dynamics study. *Mater Sci Eng C Mater Biol Appl* **32**, 2583-2588 (2012).
16. Seeliger, D. *et al.* Quantitative assessment of protein interaction with methyl-lysine analogues by hybrid computational and experimental approaches. *ACS Chem. Biol.* **7**, 150-154 (2012).
17. Jorgensen, W. L., Maxwell, D. S. & TiradoRives, J. Development and testing of the OPLS all-atom force field on conformational energetics and properties of organic liquids. *J. Am. Chem. Soc.* **118**, 11225-11236 (1996).
18. MacKerell, A. D. *et al.* All-atom empirical potential for molecular modeling and dynamics studies of proteins. *J Phys Chem B* **102**, 3586-3616 (1998).
19. Schuler, L. D., Daura, X. & van Gunsteren, W. F. An improved GROMOS96 force field for aliphatic hydrocarbons in the condensed phase. *J. Comput. Chem.* **22**, 1205-1218 (2001).
20. Duan, Y. *et al.* A point-charge force field for molecular mechanics simulations of proteins based on condensed-phase quantum mechanical calculations. *J. Comput. Chem.* **24**, 1999-2012 (2003).

21. Oostenbrink, C., Villa, A., Mark, A. E. & van Gunsteren, W. F. A biomolecular force field based on the free enthalpy of hydration and solvation: the GROMOS force-field parameter sets 53A5 and 53A6. *J. Comput. Chem.* **25**, 1656-1676 (2004).
22. Schmid, N. *et al.* Definition and testing of the GROMOS force-field versions 54A7 and 54B7. *Eur. Biophys. J.* **40**, 843-856 (2011).
23. Lee, T. Y. *et al.* dbPTM: an information repository of protein post-translational modification. *Nucleic Acids Res.* **34**, D622-D627 (2006).
24. UniProt, C. Reorganizing the protein space at the Universal Protein Resource (UniProt). *Nucleic Acids Res.* **40**, D71-D75 (2012).
25. Beveridge, D. L. & DiCapua, F. M. Free energy via molecular simulation: applications to chemical and biomolecular systems. *Annu. Rev. Biophys. Biophys. Chem.* **18**, 431-492 (1989).
26. Malde, A. K. *et al.* An Automated Force Field Topology Builder (ATB) and Repository: Version 1.0. *J. Chem. Theory. Comput.* **7**, 4026-4037 (2011).
27. Efremov, R. G. *et al.* Molecular lipophilicity in protein modeling and drug design. *Curr. Med. Chem.* **14**, 393-415 (2007).
28. Polyansky, A. A., Chugunov, A. O., Vassilevski, A. A., Grishin, E. V. & Efremov, R. G. Recent Advances in Computational Modeling of alpha-Helical Membrane-Active Peptides. *Curr. Protein Peptide Sci.* **13**, 644-657 (2012).
29. Vistoli, G. *et al.* Predicting the physicochemical profile of diastereoisomeric histidine-containing dipeptides by property space analysis. *Chirality* **24**, 566-576 (2012).
30. Hlevnjak, M., Zitkovic, G. & Zagrovic, B. Hydrophilicity matching - A potential prerequisite for the formation of protein-protein complexes in the cell. *PLoS ONE* **5(6)** (2010).
31. Case, D. A. *et al.* AMBER 12. University of California, San Francisco, 2012.
32. Zoete, V., Cuendet, M. A., Grosdidier, A. & Michielin, O. SwissParam: A fast force field generation tool for small organic molecules. *J. Comput. Chem.* **32**, 2359-2368 (2011).
33. Schuttelkopf, A. W. & van Aalten, D. M. F. PRODRG: a tool for high-throughput crystallography of protein-ligand complexes. *Acta Crystallogr. Sect. D. Biol. Crystallogr.* **60**, 1355-1363 (2004).
34. Vanquelef, E. *et al.* RED Server: a web service for deriving RESP and ESP charges and building force field libraries for new molecules and molecular fragments. *Nucleic Acids Res.* **39**, W511-W517 (2011).
35. Schmid, N., Christ, C. D., Christen, M., Eichenberger, A. P. & van Gunsteren, W. F. Architecture, implementation and parallelisation of the GROMOS software for biomolecular simulation. *Comput. Phys. Commun.* **183**, 890-903 (2012).
36. Lindahl, E., Hess, B. & van der Spoel, D. GROMACS 3.0: a package for molecular simulation and trajectory analysis. *J Mol Model* **7**, 306-317 (2001).
37. Margreitter, C., Petrov, D. & Zagrovic, B. Vienna-PTM web server: A toolkit for MD simulations of protein post-translational modifications. *Nucleic Acids Res.* (2013).
38. Huq, M. D. M., Tsai, N. P., Khan, S. A. & Wei, L. N. Lysine trimethylation of retinoic acid receptor-alpha - A novel means to regulate receptor function. *Mol Cell Proteomics* **6**, 677-688 (2007).
39. Bottomley, M. J. Structures of protein domains that create or recognize histone modifications. *EMBO Rep.* **5**, 464-469 (2004).
40. Chandrasekhar, I., Oostenbrink, C. & van Gunsteren, W. F. Simulating the physiological phase of hydrated DPPC bilayers: The ester moiety. *Soft Mater* **2**, 27-45 (2004).
41. Oostenbrink, C., Juchli, D. & van Gunsteren, W. F. Amine hydration: A united-atom force-field solution. *Chemphyschem* **6**, 1800-1804 (2005).

42. Hritz, J. & Oostenbrink, C. Efficient free energy calculations for compounds with multiple stable conformations separated by high energy barriers. *J Phys Chem B* **113**, 12711-12720 (2009).
43. Dolenc, J., Oostenbrink, C., Koller, J. & van Gunsteren, W. F. Molecular dynamics simulations and free energy calculations of netropsin and distamycin binding to an AAAAA DNA binding site. *Nucleic Acids Res.* **33**, 725-733 (2005).
44. Brunger, A., Brooks, C. L. & Karplus, M. Stochastic boundary-conditions for molecular-dynamics simulations of ST2 water. *Chem. Phys. Lett.* **105**, 495-500 (1984).
45. Berendsen, H. J. C., Postma, J. P. M., van Gunsteren, W. F. & Hermans, J. in *Intermolecular Forces* (ed B. Pullman) 331-342 (Reidel, Dordrecht, 1981).
46. Berendsen, H. J. C., Postma, J. P. M., van Gunsteren, W. F., Dinola, A. & Haak, J. R. Molecular-dynamics with coupling to an external bath. *J Chem Phys* **81**, 3684-3690 (1984).
47. Beutler, T. C., Mark, A. E., Vanschaik, R. C., Gerber, P. R. & van Gunsteren, W. F. Avoiding singularities and numerical instabilities in free-energy calculations based on molecular simulations. *Chem. Phys. Lett.* **222**, 529-539 (1994).
48. Gallicchio, E., Zhang, L. Y. & Levy, R. M. The SGB/NP hydration free energy model based on the surface generalized born solvent reaction field and novel nonpolar hydration free energy estimators. *J. Comput. Chem.* **23**, 517-529 (2002).
49. Rizzo, R. C., Aynechi, T., Case, D. A. & Kuntz, I. D. Estimation of absolute free energies of hydration using continuum methods: Accuracy of partial, charge models and optimization of nonpolar contributions. *J. Chem. Theory. Comput.* **2**, 128-139 (2006).
50. Sulea, T., Wanapun, D., Dennis, S. & Purisima, E. O. Prediction of SAMPL-1 hydration free energies using a continuum electrostatics-dispersion model. *J Phys Chem B* **113**, 4511-4520 (2009).

## Appendices to Chapter I



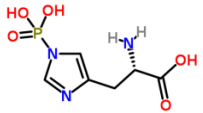
**Figure S1. Experimental vs. calculated HFES of compounds from the validation set (GROMOS 45a3).** Correlation is captured by the regression line, its parameters, Pearson correlation coefficient and overall RMSE. The same comparison for canonical amino acids is shown in the inset. Note that error bars of calculated HFES are comparable to the size of the symbols, with the average standard error of 0.4 kJ/mol.



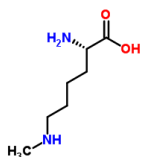
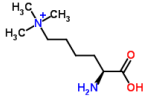
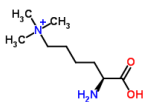
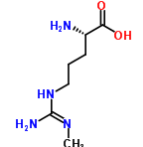
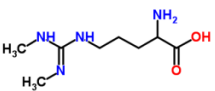
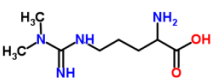
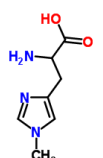
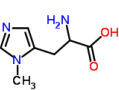
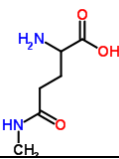
**Table S1. Parameterized post-translational modifications with the 3-letter code, chemical names and structures.** If two protonation states are possible, the one with higher occupancy at the physiologic pH is highlighted in bold. Note that modifications marked with: 1) \* were already parameterized in GROMOS force field, 2) # have to date not been reported in UNIPROT, 3) + no prolines included and 4) <sup>HFE</sup> parameters derived to match the experimental HFE.

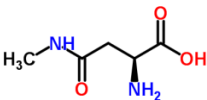
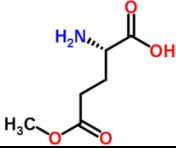
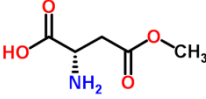
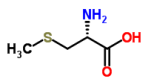
### ENZYMATIC

# PTM	AA	code	chemical	structure	
<b>Phosphorylation</b>					
1	1	SER	S1P	phosphoserine (-1)	
2	2		<b>S2P</b>	phosphoserine (-2)	
3	3	THR	T1P	phosphothreonine (-1)	
4	4		<b>T2P</b>	phosphothreonine (-2)	
5	5	TYR	Y1P	phosphotyrosine (-1)	
6	6		<b>Y2P</b>	phosphotyrosine (-2)	
7	7	ASP	D1P	phosphoaspartate (-1)	
8	8		<b>D2P</b>	phosphoaspartate (-2)	
9	9	LYS	K1P <sup>#</sup>	phospholysine (-1)	
10	10		<b>K2P<sup>#</sup></b>	phospholysine (-2)	
11	11	ARG	R0P <sup>#</sup>	phosphoarginine (0)	
12	12		<b>R1P<sup>#</sup></b>	phosphoarginine (-1)	
13	13	HIS	H11	1-phosphohistidine (-1)	
14	14		<b>H12</b>	1-phosphohistidine (-2)	

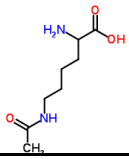
15	15	HIS	H31	3-phosphohistidine (-1)	
16	16		<b>H32</b>	3-phosphohistidine (-2)	

### Methylation

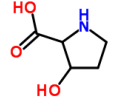
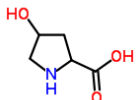
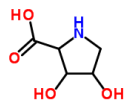
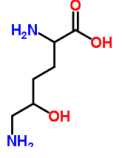
17	17	LYS	KMN	N6-methyllysine (0)	
18	18		<b>KMC</b>	N6-methyllysine (+1)	
19	19	LYS	K2M	N6,N6-dimethyllysine (0)	
20	20		<b>K2C</b>	N6,N6-dimethyllysine (+1)	
21	21	LYS	K3C	N6,N6,N6-trimethyllysine	
22	22	ARG	RMN	omega-N-methylarginine (0)	
23	23		<b>RMC</b>	omega-N-methylarginine (+1)	
24	24	ARG	RSM	symmetric-dimethylarginine (0)	
25	25		<b>RMS</b>	symmetric-dimethylarginine (+1)	
26	26	ARG	RAM	asymmetric-dimethylarginine (0)	
27	27		<b>RMA</b>	asymmetric-dimethylarginine (+1)	
28	28	HIS	<b>H1M</b>	1-methylhistidine (0)	
29	29		H1C	1-methylhistidine (+1)	
30	30	HIS	<b>H3M</b>	3-methylhistidine (0)	
31	31		H3C	3-methylhistidine (+1)	
32	32	GLN	QME	N5-methylglutamine	

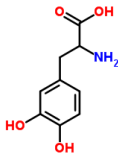
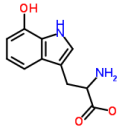
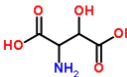
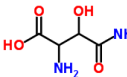
33	33	ASN	NME	N4-methylasparagine	
34	34	GLU	EME	glutamate methyl ester	
35	35	ASP	DMA <sup>#</sup>	aspartate methyl ester	
36	36	CYS	CYM	S-methylcysteine	

**Acetylation**

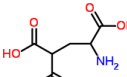
37	37	LYS	KAC	N6-acetyllysine	
----	----	-----	-----	-----------------	---

**Hydroxylation**

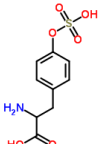
38	38	PRO	PH3	3-hydroxyproline (R)	
39	39		P3H	3-hydroxyproline (S)	
40	1*	PRO	HYP	4-hydroxyproline (R)	
41	40		HY2	4-hydroxyproline (S)	
42	41	PRO	PHH	3,4-dihydroxyproline	
43	42	LYS	KH5	5-hydroxylysine (0,R)	
44	43		K5H	5-hydroxylysine (0,S)	
45	44		KPH	5-hydroxylysine (+1,R)	
46	45		KHP	5-hydroxylysine (+1,S)	

47	46	TYR	HTY	3,4-dihydroxyphenylalanine	
48	47	TRP	W7H	7-hydroxytryptophan	
49	48	ASP	DH3	3-hydroxyaspartate (-1,R)	
50	49		D3H	3-hydroxyaspartate (-1,S)	
51	50		DN3	3-hydroxyaspartate (0,R)	
52	51		D3N	3-hydroxyaspartate (0,S)	
53	52	ASN	N3H	3-hydroxyasparagine (R)	
54	53		NH3	3-hydroxyasparagine (S)	


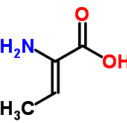
### Carboxylation

55	54	GLU	ECA	4-carboxyglutamate (-2)	
56	55		ECN	4-carboxyglutamate (-1)	

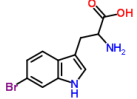
### Sulfation

57	56	TYR	YSU	sulfotyrosine	
----	----	-----	-----	---------------	---

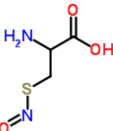
### Dehydration

58	57	SER	SDH	dehydroalanine	
59	58	THR	TDH	2,3-didehydrobutyryne	

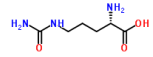
**Bromidation**

60	59	TRP	WBR	6-bromotryptophan	
----	----	-----	-----	-------------------	---

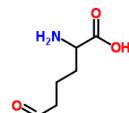
**S-nitrosylation**

61	60	CYS	CSN	S-nitrosocysteine	
----	----	-----	-----	-------------------	---

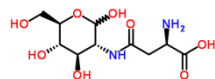
**Citrullination**

62	61	ARG	RCI	citrulline	
----	----	-----	-----	------------	---

**Allysine formation (the same as carbonylation)**

63	62	LYS	KAL	allysine (aminoadipic semialdehyde)	
----	----	-----	-----	-------------------------------------	---

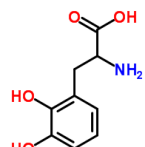
**Glycosylation**


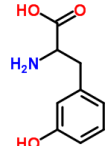
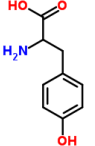
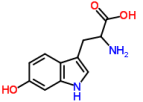
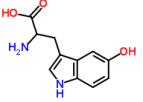

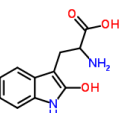
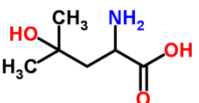
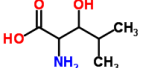
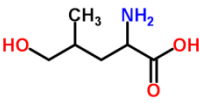
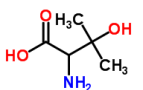
64	63	ASN	NNG	N-acetylglucosamine (N4-linked to ASN)	
----	----	-----	-----	--	---


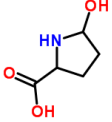
**NONENZYMATIC**

# PTM	AA	Code	chemical	structure
-------	----	------	----------	-----------

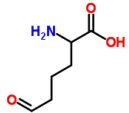
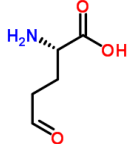
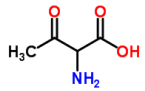
**Hydroxylation**

65	64	PHE	F23 <sup>#</sup>	2,3-dihydroxyphenylalanine	
----	----	-----	------------------	----------------------------	---

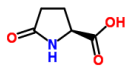
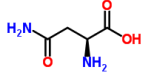
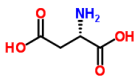
66	65	PHE	F2H <sup>#</sup>	2-hydroxyphenylalanine	
67	66	PHE	F3H <sup>#</sup>	3-hydroxyphenylalanine	
68	2*	PHE	TYR <sup>#</sup>	tyrosine	
69	67	TRP	W6H <sup>#</sup>	6-hydroxytryptophan	
70	68	TRP	W5H <sup>#</sup>	5-hydroxytryptophan	
71	69	TRP	W4H <sup>#</sup>	4-hydroxytryptophan	
72	70	TRP	W2H <sup>#</sup>	2-hydroxytryptophan	
73	71	LEU	L3H <sup>#</sup>	3-hydroxyleucine (R)	
74	72		LH3 <sup>#</sup>	3-hydroxyleucine (S)	
75	73	LEU	L4H <sup>#</sup>	4-hydroxyleucine	
76	74	LEU	L5H <sup>#</sup>	5-hydroxyleucine (R)	
77	75		LH5 <sup>#</sup>	5-hydroxyleucine (S)	
78	76	VAL	V3H	3-hydroxyvaline	

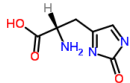
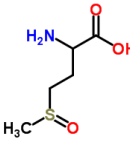
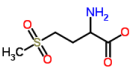
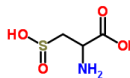
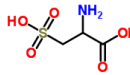
79	77	CYS	CYH	cysteine sulfenic acid	
80	78	PRO	PH5 <sup>#</sup>	5-hydroxyproline (R)	
81	79		P5H <sup>#</sup>	5-hydroxyproline (S)	

**Carbonylation**

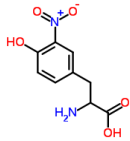
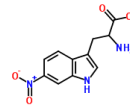
63	62	LYS	KAL	allysine (aminoadipic semialdehyde)	
82	80	PRO	GSA <sup>#</sup>	glutamic semialdehyde	
83		ARG			
84	81	THR	TOX <sup>#</sup>	2-amino-3-ketobutyric acid	

**Oxidation**

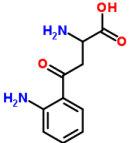
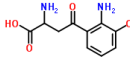
85	82	PRO	PGA <sup>#</sup>	pyroglutamic acid	
86	3*	HIS	ASN	asparagine	
87	4*	HIS	ASP	aspartic acid (-1)	
88	5*		ASPH	aspartic acid (0)	

89	83	HIS	H2X <sup>#</sup>	2-oxo-histidine	
90	84	MET	MSX	methionine sulfoxide (R)	
91	85		MXS	methionine sulfoxide (S)	
92	86	MET	MES	methionine sulfone	
93	87	CYS	CSA	cysteine sulfinic acid	
94	88	CYS	CSE <sup>#</sup>	cysteic acid	


### Nitration

95	89	TYR	YNI	3-nitrotyrosine (-1)	
96	90		YNN <sup>HFE</sup>	3-nitrotyrosine (0)	
			YNB	3-nitrotyrosine (0)	
97	91	TRP	WNI <sup>#</sup>	6-nitrotryptophan	

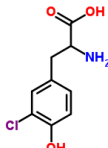
### Kynurenine formation

98	92	TRP	WKY <sup>#</sup>	kynurenine	
99	93	TRP	WKH <sup>#</sup>	3-hydroxykynurenine	

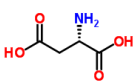
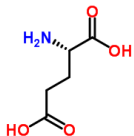


100	94	TRP	WKF <sup>#</sup>	formylkynurenine	
-----	----	-----	------------------	------------------	---

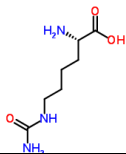
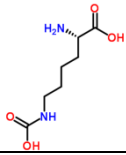
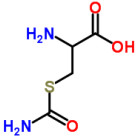
**Chlorination**

101	95	TYR	YCH <sup>#</sup>	chlorotyrosine	
-----	----	-----	------------------	----------------	---

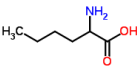
**Deamidation**

102	4*	ASN	ASP	aspartic acid (-1)	
103	5*		ASPH	aspartic acid (0)	
104	6*	GLN	GLU	glutamic acid (-1)	
105	7*		GLUH	glutamic acid (0)	

**Carbamylation**

106	96	LYS	KAM <sup>#</sup>	homocitrulline	
107	97	LYS	KCA	carboxyllysine (+1)	
108	98		KCN	carboxyllysine (0)	
109	99	CYS	CAM <sup>#</sup>	S-carbamoylcysteine	

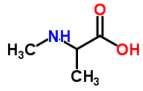
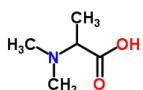
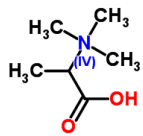
**Norleucine**

110	100	LEU	LNO <sup>#</sup>	norleucine	
111		LYS			
112		MET			

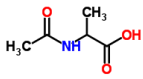
## N-TERMINAL

# PTM	AA	Code	chemical	structure
-------	----	------	----------	-----------

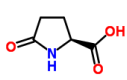
## Methylation

113-132	101	all	1NM	N-methyl-AA (0)	
133-152	102		1NM+	N-methyl-AA (+1)	
153-171	103	all <sup>+</sup>	2NM	N,N-dimethyl-AA (0)	
172-191	104		2NM+	N,N-dimethyl-AA (+1)	
193-210	105	all <sup>+</sup>	3NM+	N,N,N-trimethyl-AA	

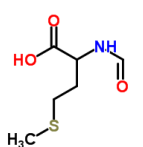
## Acetylation

211-230	106	all	NAC	N-acetyl-AA	
---------	-----	-----	-----	-------------	---

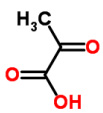
## Pyrrolidone formation

231	81	GLN	PGA	pyroglutamic acid	
232		GLU			

## Formylation

233	107	MET	FOR	N-formylmethionine	
-----	-----	-----	-----	--------------------	---


## Pyruvate formation

234	108	SER	PYA	pyruvic acid	
235		CYS			
236		VAL			


## C-TERMINAL

# PTM	AA	Code	chemical	structure
-------	----	------	----------	-----------

## Amidation

237-256	109	all	AMD	AA-amide	
---------	-----	-----	-----	----------	---

## Methylation

257	110	CYS	CME	AA-methyl ester	
258		LEU			
259		LYS			

**Table S2.** HFEs of the molecules in the validation set, comparison between the experimental and calculated values using the GROMOS 45a3 parameter set.

Compound	HFE (kJ/mol)	
	experimental	ffG45a3
<b>Validation set. PTM-side-chain analogs</b>		
N-butylacetamide	-39.0	-18.9
<i>o</i> -cresol	-24.6	-22.5
<i>m</i> -cresol	-23.0	-25.9
2-methyl-2-propanol	-18.7	-7.2
2-methyl-1-propanol	-18.8	-11.7
propan-2-ol	-19.8	-8.9
N-methylacetamine	-41.9	-18.7
methylpropanoate	-12.3	9.0
methylacetate	-13.1	7.4
dimethylsulfide	-6.7	4.5
butanal	-13.3	-7.0
propanal	-14.4	-7.0
butane	8.7	7.6
<b>Validation set. Compounds similar to PTM-side-chain analogs</b>		
diethylamine	-17.0	-8.8
trimethylamine	-13.4	-4.6
ethene	5.4	13.6
bromobenzene	-6.1	18.0
aniline	-23.0	-25.4
acetophenone	-19.2	-12.4
N-methylformamide	-41.9	-22.0
chlorophenol	-19.0	-22.3
2-nitrophenol	-19.2	-36.9
nitrobenzene	-17.2	-24.5
acetone	-16.1	-3.9
dimethylsulfoxide	-42.3	-11.1
methylsulfonylmethane	-42.2	-15.4
<b>RMSE</b>	-	<b>15.0</b>

**Table S3. Comparison of physico-chemical properties of PTMs and canonical amino acids.** Molecular weight (MW), solvent accessible surface area (SASA), net charge and dipole moment (DM) shown for PTMs and cognate amino acids in parentheses.

PTM (AA)	chemical	MW (u)	SASA (nm <sup>2</sup> )	net charge	DM (D)
S1P (SER)	phosphoserine (-1)	110.0 (31.0)	1.88 (1.20)	-1 (0)	N/A (2.30)
S2P (SER)	phosphoserine (-2)	109.0 (31.0)	1.93 (1.20)	-2 (0)	N/A (2.30)
T1P (THR)	phosphothreonine (-1)	124.0 (45.1)	2.12 (1.41)	-1 (0)	N/A (2.23)
T2P (THR)	phosphothreonine (-2)	123.0 (45.1)	2.15 (1.41)	-2 (0)	N/A (2.23)
Y1P (TYR)	phosphotyrosine (-1)	186.1 (107.1)	2.81 (2.41)	-1 (0)	N/A (2.06)
Y2P (TYR)	phosphotyrosine (-2)	185.1 (107.1)	2.73 (2.41)	-2 (0)	N/A (2.06)
D1P (ASP)	phosphoaspartate (-1)	138.0 (58.0)	2.23 (1.57)	-1 (-1)	N/A (N/A)
D2P (ASP)	phosphoaspartate (-2)	137.0 (58.0)	2.17 (1.57)	-2 (-1)	N/A (N/A)
K1P (LYS)	phospholysine (-1)	151.1 (73.1)	2.59 (1.92)	-1 (1)	N/A (N/A)
K2P (LYS)	phospholysine (-2)	150.1 (73.1)	2.54 (1.92)	-2 (1)	N/A (N/A)
R0P (ARG)	phosphoarginine (0)	180.1 (101.2)	2.82 (2.21)	0 (1)	14.65 (N/A)
R1P (ARG)	phosphoarginine (-1)	179.1 (101.2)	2.73 (2.21)	-1 (1)	N/A (N/A)
H11 (HIS)	1-phosphohistidine (-1)	160.1 (81.1)	2.36 (1.91)	-1 (0)	N/A (6.43)
H12 (HIS)	1-phosphohistidine (-2)	159.1 (81.1)	2.39 (1.91)	-2 (0)	N/A (6.43)
H31 (HIS)	3-phosphohistidine (-1)	160.1 (81.1)	2.51 (1.91)	-1 (0)	N/A (6.43)
H32 (HIS)	3-phosphohistidine (-2)	159.1 (81.1)	2.53 (1.91)	-2 (0)	N/A (6.43)
KMN (LYS)	N6-methyllysine (0)	86.2 (73.1)	2.40 (1.92)	0 (1)	1.84 (N/A)
KMC (LYS)	N6-methyllysine (+1)	87.2 (73.1)	2.26 (1.92)	1 (1)	N/A (N/A)
K2M (LYS)	N6,N6-dimethyllysine (0)	100.2 (73.1)	2.72 (1.92)	0 (1)	1.58 (N/A)
K2C (LYS)	N6,N6-dimethyllysine (+1)	101.2 (73.1)	2.45 (1.92)	1 (1)	N/A (N/A)
K3C (LYS)	N6,N6,N6-trimethyllysine	115.2 (73.1)	2.68 (1.92)	1 (1)	N/A (N/A)
RMN (ARG)	omega-N-methylarginine (0)	114.2 (101.2)	2.38 (2.21)	0 (1)	2.78 (N/A)
RMC (ARG)	omega-N-methylarginine (+1)	115.2 (101.2)	2.43 (2.21)	1 (1)	N/A (N/A)
RSM (ARG)	symmetric-dimethylarginine (0)	128.2 (101.2)	2.80 (2.21)	0 (1)	0.94 (N/A)
RMS (ARG)	symmetric-dimethylarginine (+1)	129.2 (101.2)	2.69 (2.21)	1 (1)	N/A (N/A)
RAM (ARG)	asymmetric-dimethylarginine (0)	128.2 (101.2)	2.62 (2.21)	0 (1)	3.55 (N/A)
RMA (ARG)	asymmetric-dimethylarginine (+1)	129.2 (101.2)	2.69 (2.21)	1 (1)	N/A (N/A)
H1M (HIS)	1-methylhistidine (0)	95.1 (81.1)	2.24 (1.91)	0 (0)	6.10 (6.43)
H1C (HIS)	1-methylhistidine (+1)	96.1 (81.1)	2.19 (1.91)	1 (0)	N/A (6.43)
H3M (HIS)	3-methylhistidine (0)	95.1 (81.1)	2.32 (1.91)	0 (0)	4.33 (6.43)
H3C (HIS)	3-methylhistidine (+1)	96.1 (81.1)	2.01 (1.91)	1 (0)	N/A (6.43)
QME (GLN)	N5-methylglutamine	86.1 (72.1)	2.07 (1.80)	0 (0)	2.28 (4.94)
NME (ASN)	N4-methylasparagine	72.1 (58.1)	1.97 (1.56)	0 (0)	4.14 (4.90)
EME (GLU)	glutamate methyl ester	87.1 (72.1)	1.99 (1.79)	0 (-1)	5.27 (N/A)
DMA (ASP)	aspartate methyl ester	73.1 (58.0)	1.80 (1.57)	0 (-1)	5.31 (N/A)
CYM (CYS)	S-methylcysteine	61.1 (47.1)	1.65 (1.41)	0 (0)	2.74 (1.84)
KAC (LYS)	N6-acetyllysine	114.2 (73.1)	2.67 (1.92)	0 (1)	4.12 (N/A)
PH3 (PRO)	3-hydroxyproline (R)	58.1 (42.1)	1.61 (1.59)	0 (0)	2.32 (N/A)
P3H (PRO)	3-hydroxyproline (S)	58.1 (42.1)	1.64 (1.59)	0 (0)	2.27 (N/A)

HYP (PRO)	4-hydroxyproline (R)	58.1 (42.1)	1.77 (1.59)	0 (0)	2.14 (N/A)
HY2 (PRO)	4-hydroxyproline (S)	58.1 (42.1)	1.67 (1.59)	0 (0)	2.20 (N/A)
PHH (PRO)	3,4-dihydroxyproline	74.1 (42.1)	1.76 (1.59)	0 (0)	3.66 (N/A)
KH5 (LYS)	5-hydroxylysine (0,R)	88.1 (73.1)	2.03 (1.92)	0 (1)	3.62 (N/A)
K5H (LYS)	5-hydroxylysine (0,S)	88.1 (73.1)	2.17 (1.92)	0 (1)	5.86 (N/A)
KPH (LYS)	5-hydroxylysine (+1,R)	89.1 (73.1)	2.05 (1.92)	1 (1)	N/A (N/A)
KHP (LYS)	5-hydroxylysine (+1,S)	89.1 (73.1)	2.03 (1.92)	1 (1)	N/A (N/A)
HTY (TYR)	3,4-dihydroxyphenylalanine	123.1 (107.1)	2.29 (2.41)	0 (0)	3.97 (2.06)
W7H (TRP)	7-hydroxytryptophan	146.2 (130.2)	2.70 (2.63)	0 (0)	3.19 (3.65)
DH3 (ASP)	3-hydroxyaspartate (-1,R)	74.0 (58.0)	1.52 (1.57)	-1 (-1)	N/A (N/A)
D3H (ASP)	3-hydroxyaspartate (-1,S)	74.0 (58.0)	1.57 (1.57)	-1 (-1)	N/A (N/A)
DN3 (ASP)	3-hydroxyaspartate (0,R)	75.0 (58.0)	1.61 (1.57)	0 (-1)	0.58 (N/A)
D3N (ASP)	3-hydroxyaspartate (0,S)	75.0 (58.0)	1.56 (1.57)	0 (-1)	3.79 (N/A)
N3H (ASN)	3-hydroxyasparagine (R)	74.1 (58.1)	1.71 (1.56)	0 (0)	3.34 (4.90)
NH3 (ASN)	3-hydroxyasparagine (S)	74.1 (58.1)	1.84 (1.56)	0 (0)	6.30 (4.90)
ECA (GLU)	4-carboxyglutamate (-2)	115.1 (72.1)	2.06 (1.79)	-2 (-1)	N/A (N/A)
ECN (GLU)	4-carboxyglutamate (-1)	116.1 (72.1)	2.20 (1.79)	-1 (-1)	N/A (N/A)
YSU (TYR)	sulfotyrosine	186.2 (107.1)	2.66 (2.41)	-1 (0)	N/A (2.06)
SDH (SER)	dehydroalanine	14.0 (31.0)	1.06 (1.20)	0 (0)	0.00 (2.30)
TDH (THR)	2,3-didehydrobutyrine	28.1 (45.1)	1.39 (1.41)	0 (0)	0.00 (2.23)
WBR (TRP)	6-bromotryptophan	209.1 (130.2)	2.88 (2.63)	0 (0)	3.16 (3.65)
CSN (CYS)	S-nitrosocysteine	76.1 (47.1)	1.71 (1.41)	0 (0)	3.15 (1.84)
RCI (ARG)	citrulline	101.1 (101.2)	2.22 (2.21)	0 (1)	5.21 (N/A)
KAL (LYS)	allysine (aminoadipic semialdehyde)	71.1 (73.1)	2.04 (1.92)	0 (1)	2.96 (N/A)
NNG (ASN)	N-acetylglucosamine	261.3 (58.1)	3.73 (1.56)	0 (0)	9.10 (4.90)
F23 (PHE)	2,3-dihydroxyphenylalanine	123.1 (91.1)	2.29 (2.28)	0 (0)	4.55 (0.74)
F2H (PHE)	2-hydroxyphenylalanine	107.1 (91.1)	2.13 (2.28)	0 (0)	3.11 (0.74)
F3H (PHE)	3-hydroxyphenylalanine	107.1 (91.1)	2.08 (2.28)	0 (0)	2.73 (0.74)
TYR (PHE)	tyrosine	107.1 (91.1)	2.41 (2.28)	0 (0)	2.06 (0.74)
W6H (TRP)	6-hydroxytryptophan	146.2 (130.2)	2.75 (2.63)	0 (0)	1.32 (3.65)
W5H (TRP)	5-hydroxytryptophan	146.2 (130.2)	2.71 (2.63)	0 (0)	3.46 (3.65)
W4H (TRP)	4-hydroxytryptophan	146.2 (130.2)	2.71 (2.63)	0 (0)	4.88 (3.65)
W2H (TRP)	2-hydroxytryptophan	146.2 (130.2)	2.73 (2.63)	0 (0)	5.19 (3.65)
L3H (LEU)	3-hydroxyleucine (R)	73.1 (57.1)	1.96 (1.88)	0 (0)	2.23 (0.00)
LH3 (LEU)	3-hydroxyleucine (S)	73.1 (57.1)	1.86 (1.88)	0 (0)	2.25 (0.00)
L4H (LEU)	4-hydroxyleucine	73.1 (57.1)	1.92 (1.88)	0 (0)	2.19 (0.00)
L5H (LEU)	5-hydroxyleucine (R)	73.1 (57.1)	1.98 (1.88)	0 (0)	2.17 (0.00)
LH5 (LEU)	5-hydroxyleucine (S)	73.1 (57.1)	2.01 (1.88)	0 (0)	2.19 (0.00)
V3H (VAL)	3-hydroxyvaline	59.1 (43.1)	1.70 (1.55)	0 (0)	2.30 (0.00)
CYH (CYS)	cysteine sulfenic acid	63.1 (47.1)	1.62 (1.41)	0 (0)	2.38 (1.84)
PH5 (PRO)	5-hydroxyproline (R)	58.1 (42.1)	1.69 (1.59)	0 (0)	2.21 (N/A)
P5H (PRO)	5-hydroxyproline (S)	58.1 (42.1)	1.79 (1.59)	0 (0)	2.17 (N/A)
GSA (PRO)	glutamic semialdehyde	57.1 (42.1)	1.64 (1.59)	0 (0)	2.95 (N/A)
GSA (ARG)	glutamic semialdehyde	57.1 (101.2)	1.64 (2.21)	0 (1)	2.95 (N/A)

TOX (THR)	2-amino-3-ketobutyric acid	43.0 (45.1)	1.40 (1.41)	0 (0)	2.66 (2.23)
PGA (PRO)	pyroglutamic acid	56.1 (42.1)	1.74 (1.59)	0 (0)	2.65 (N/A)
ASN (HIS)	asparagine	58.1 (81.1)	1.56 (1.91)	0 (0)	4.90 (6.43)
ASP (HIS)	aspartic acid (-1)	58.0 (81.1)	1.57 (1.91)	-1 (0)	N/A (6.43)
H2X (HIS)	2-oxo-histidine	95.1 (81.1)	2.00 (1.91)	0 (0)	9.64 (6.43)
MSX (MET)	methionine sulfoxide (R)	91.2 (75.2)	2.02 (1.94)	0 (0)	4.27 (2.62)
MXS (MET)	methionine sulfoxide (S)	91.2 (75.2)	2.11 (1.94)	0 (0)	4.23 (2.62)
MES (MET)	methionine sulfone	107.2 (75.2)	2.14 (1.94)	0 (0)	6.80 (2.62)
CSA (CYS)	cysteine sulfinic acid	78.1 (47.1)	1.69 (1.41)	-1 (0)	N/A (1.84)
CSE (CYS)	cysteic acid	94.1 (47.1)	1.80 (1.41)	-1 (0)	N/A (1.84)
YNI (TYR)	3-nitrotyrosine (-1)	151.1 (107.1)	2.61 (2.41)	-1 (0)	N/A (2.06)
YNN (TYR)	3-nitrotyrosine (0)	152.1 (107.1)	2.62 (2.41)	0 (0)	5.44 (2.06)
YNB (TYR)	3-nitrotyrosine (0)	152.1 (107.1)	2.62 (2.41)	0 (0)	3.83 (2.06)
WNI (TRP)	6-nitrotryptophan	175.2 (130.2)	3.06 (2.63)	0 (0)	3.08 (3.65)
WKY (TRP)	kynurenine	134.2 (130.2)	2.60 (2.63)	0 (0)	4.16 (3.65)
WKH (TRP)	3-hydroxykynurenine	150.2 (130.2)	2.66 (2.63)	0 (0)	2.78 (3.65)
WKF (TRP)	formylkynurenine	162.2 (130.2)	2.98 (2.63)	0 (0)	3.03 (3.65)
YCH (TYR)	chlorotyrosine	141.6 (107.1)	2.44 (2.41)	0 (0)	3.43 (2.06)
ASP (ASN)	aspartic acid (-1)	58.0 (58.1)	1.57 (1.56)	-1 (0)	N/A (4.90)
GLU (GLN)	glutamic acid (-1)	72.1 (72.1)	1.79 (1.80)	-1 (0)	N/A (4.94)
KAM (LYS)	homocitruline	115.2 (73.1)	2.46 (1.92)	0 (1)	5.24 (N/A)
KCA (LYS)	carboxyllysine (+1)	115.1 (73.1)	2.48 (1.92)	-1 (1)	N/A (N/A)
KCN (LYS)	carboxyllysine (0)	116.1 (73.1)	2.49 (1.92)	0 (1)	3.63 (N/A)
CAM (CYS)	S-carbamoylcysteine	90.1 (47.1)	1.99 (1.41)	0 (0)	4.81 (1.84)
LNO (LEU)	norleucine	57.1 (57.1)	1.88 (1.88)	0 (0)	0.00 (0.00)
LNO (LYS)	norleucine	57.1 (73.1)	1.88 (1.92)	0 (1)	0.00 (N/A)
LNO (MET)	norleucine	57.1 (75.2)	1.88 (1.94)	0 (0)	0.00 (2.62)

## Dataset S1. Force field parameters for the GROMOS force field 45A3 parameter set

```

; This file contains extended force field parameters for the GROMOS force field 45A3
parameters set
; GROMACS 4.5.x format - files: aminoacids.rtp, aminoacids.n.tdb, aminoacids.c.tdb
and aminoacids.hdb
; Authors: Drazen Petrov, Christian Margreitter, Melanie Grandits, Chris Oostenbrink
& Bojan Zagrovic
; Parameter files in GROMACS 4.3.x and 4.4.x, and GROMOS formats available at
http://vienna-ptm.univie.ac.at/

; aminoacids.rtp file (backbone and side chain parameters)

[ bondedtypes ]
; bonds angles dihedrals impropers
2 2 1 2

; phosphoserine (-1)
[S1P]
[ atoms ]
N N -0.28000 0
H H 0.28000 0
CA CH1 0.00000 1
CB CH2 0.15000 2 ; from the carbon atom attached to the phosphate group of
nucleotides (e.g., ATP)
OG OA -0.36000 2 ; from the phosphate group of nucleotides (e.g., ATP)
PD P 0.63000 2 ; to add up to -1 net charge
OE1 OM -0.63500 2 ; from the phosphate group of nucleotides (e.g., ATP)
OE2 OM -0.63500 2 ; from the phosphate group of nucleotides (e.g., ATP)
OE3 OA -0.54800 2 ; from the hydroxyl group of nucleotides (e.g., ATP)
HE3 H 0.39800 2 ; from the hydroxyl group of nucleotides (e.g., ATP)
C C 0.380 3
O O -0.380 3
[ bonds ]
N H gb_2
N CA gb_20
CA C gb_26
C O gb_4
C +N gb_9
CA CB gb_26
CB OG gb_17
OG PD gb_27
PD OE1 gb_23
PD OE2 gb_23
PD OE3 gb_27
OE3 HE3 gb_1
[ exclusions ]
; ai aj
OE1 HE3
OE2 HE3
OG HE3
[ angles ]
; ai aj ak gromos type
-C N H ga_31
H N CA ga_17
-C N CA ga_30
N CA C ga_12
CA C +N ga_18
CA C O ga_29
O C +N ga_32
N CA CB ga_12
C CA CB ga_12
CA CB OG ga_12
CB OG PD ga_25
OG PD OE1 ga_13
OG PD OE2 ga_13
OG PD OE3 ga_13
OE1 PD OE2 ga_13
OE1 PD OE3 ga_13
OE2 PD OE3 ga_13
[ impropers ]
; ai aj ak al gromos type
N -C CA H gi_1
C CA +N O gi_1
CA N C CB gi_2
[ dihedrals ]
; ai aj ak al gromos type
-C A -C N CA gd_4
-C N CA C gd_19
N CA C +N gd_20
N CA CB OG gd_17
CA CB OG PD gd_12
CB OG PD OE1 gd_9
CB OG PD OE1 gd_11

; phosphothreonine (-1)
[T1P]
[ atoms ]
N N -0.28000 0
H H 0.28000 0
CA CH1 0.00000 1
CB CH1 0.15000 2 ; from the carbon atom attached to the phosphate group of
nucleotides (e.g., ATP)
OG1 OA -0.36000 2 ; from the phosphate group of nucleotides (e.g., ATP)
PD P 0.63000 2 ; to add up to -1 net charge
OE1 OM -0.63500 2 ; from the phosphate group of nucleotides (e.g., ATP)
OE2 OM -0.63500 2 ; from the phosphate group of nucleotides (e.g., ATP)
OE3 OA -0.54800 2 ; from the hydroxyl group of nucleotides (e.g., ATP)
HE3 H 0.39800 2 ; from the hydroxyl group of nucleotides (e.g., ATP)
CG2 CH3 0.00000 3
C C 0.380 4
O O -0.380 4
[ bonds ]
N H gb_2
N CA gb_20
CA C gb_26
C O gb_4
C +N gb_9
CA CB gb_26
CB OG1 gb_17
CB CG2 gb_26
OG1 PD gb_27
PD OE1 gb_23
PD OE2 gb_23
PD OE3 gb_27

```



```

OE3 HE3 gb_1
[exclusions]
; ai aj
OE1 HE3
OE2 HE3
OG1 HE3
[angles]
; ai aj ak gromos type
-C N H ga_31
H N CA ga_17
-C N CA ga_30
N CA C ga_12
CA C +N ga_18
CA C O ga_29
O C +N ga_32
N CA CB ga_12
C CA CB ga_12
CA CB OG1 ga_12
CA CB CG2 ga_14
OG1 CB CG2 ga_14
CB OG1 PD ga_25
OG1 PD OE1 ga_13
OG1 PD OE2 ga_13
OG1 PD OE3 ga_4
OE1 PD OE2 ga_28
OE1 PD OE3 ga_13
OE2 PD OE3 ga_13
PD OE3 HE3 ga_11
[impropers]
; ai aj ak al gromos type
N -C CA H gi_1
C CA +N O gi_1
CA N C CB gi_2
CB OG1 CG2 CA gi_2
[dihedrals]
; ai aj ak al gromos type
-C A -C N CA gd_4
-C N CA C gd_19
N CA C +N gd_20
N CA CB OG1 gd_17
CA CB OG1 PD gd_12
CB OG1 PD OE1 gd_9
OG1 PD OE3 HE3 gd_11

; phosphothreonine (-2)
[T2P]
[atoms]
N N -0.28000 0
H H 0.28000 0
CA CH1 0.00000 1
CB CH1 0.15000 2; from the carbon atom attached to the phosphate group of
nucleotides (e.g., ATP)
OG1 OA -0.36000 2; from the phosphate group of nucleotides (e.g., ATP)
PD P 0.11500 2; to add up to -2 net charge
OE1 OM -0.63500 2; from the phosphate group of nucleotides (e.g., ATP)
OE2 OM -0.63500 2; from the phosphate group of nucleotides (e.g., ATP)
OE3 OM -0.63500 2; from the phosphate group of nucleotides (e.g., ATP)
CG2 CH3 0.00000 3
C C 0.380 4
O O -0.380 4
[bonds]
N H gb_2
N CA gb_20
CA C gb_26
C O gb_4
C +N gb_9
CA CB gb_26
CB OG1 gb_17
CB CG2 gb_26
OG1 PD gb_27
PD OE1 gb_23
PD OE2 gb_23
PD OE3 gb_23
[angles]
; ai aj ak gromos type
-C N H ga_31
H N CA ga_17
-C N CA ga_30
N CA C ga_12
CA C +N ga_18
CA C O ga_29
O C +N ga_32
N CA CB ga_12
C CA CB ga_12
CA CB OG1 ga_12
CA CB CG2 ga_14
OG1 CB CG2 ga_14
CB OG1 PD ga_25
OG1 PD OE1 ga_13
OG1 PD OE2 ga_13
OG1 PD OE3 ga_13

OE1 PD OE2 ga_13
OE1 PD OE3 ga_13
OE2 PD OE3 ga_13
CB OG1 PD OE1 gd_9
CB OG1 PD OE1 gd_11

; phosphotyrosine (-1)
[Y1P]
[atoms]
N N -0.28000 0
H H 0.28000 0
CA CH1 0.00000 1
CB CH2 0.00000 1
CG C 0.00000 1
CD1 C -0.10000 2
HD1 HC 0.10000 2
CD2 C -0.10000 3
HD2 HC 0.10000 3
CE1 C -0.10000 4
HE1 HC 0.10000 4
CE2 C -0.10000 5
HE2 HC 0.10000 5
CZ C 0.15000 6; from the carbon atom attached to the phosphate group of
nucleotides (e.g., ATP)
OH OA -0.36000 6; from the phosphate group of nucleotides (e.g., ATP)
PT P 0.63000 6; to add up to -1 net charge
OI1 OM -0.63500 6; from the phosphate group of nucleotides (e.g., ATP)
OI2 OM -0.63500 6; from the phosphate group of nucleotides (e.g., ATP)
OI3 OA -0.54800 6; from the hydroxyl group of nucleotides (e.g., ATP)
HI3 H 0.39800 6; from the hydroxyl group of nucleotides (e.g., ATP)
C C 0.380 7
O O -0.380 7
[bonds]
N H gb_2
N CA gb_20
CA C gb_26
C O gb_4
C +N gb_9
CA CB gb_26
CB CG gb_26
CG CD1 gb_15
CG CD2 gb_15
CD1 HD1 gb_3
CD1 CE1 gb_15
CD2 HD2 gb_3
CD2 CE2 gb_15
CE1 HE1 gb_3
CE1 CZ gb_15
CE2 HE2 gb_3
CE2 CZ gb_15
CZ OH gb_12
OH PT gb_27
PT OI1 gb_23
PT OI2 gb_23
PT OI3 gb_27
OI3 HI3 gb_1
[exclusions]
; ai aj
CB HD1
CB HD2
CB CE1
CB CE2
CG HE1
CG HE2
CG CZ
CD1 HD2
CD1 CE2
CD1 OH
HD1 CD2
HD1 HE1
HD1 CZ
CD2 CE1
CD2 OH
HD2 HE2
HD2 CZ
CE1 HE2
HE1 CE2
HE1 OH
HE2 OH
OH HI3

```

```

O11 HI3
O12 HI3
[ angles ]
; ai aj ak gromos type
-C N H ga_31
H N CA ga_17
-C N CA ga_30
N CA C ga_12
CA C +N ga_18
CA C O ga_29
O C +N ga_32
N CA CB ga_12
C CA CB ga_12
CA CB CG ga_14
CB CG CD1 ga_26
CB CG CD2 ga_26
CD1 CG CD2 ga_26
CG CD1 HD1 ga_24
HD1 CD1 CE1 ga_24
CG CD1 CE1 ga_26
CG CD2 HD2 ga_24
HD2 CD2 CE2 ga_24
CG CD2 CE2 ga_26
CD1 CE1 HE1 ga_24
HE1 CE1 CZ ga_24
CD1 CE1 CZ ga_26
CD2 CE2 HE2 ga_24
HE2 CE2 CZ ga_24
CD2 CE2 CZ ga_26
CE1 CZ CE2 ga_26
CE1 CZ OH ga_26
CE2 CZ OH ga_26
CZ OH PT ga_25
OH PT O11 ga_13
OH PT O12 ga_13
OH PT O13 ga_4
O11 PT O12 ga_28
O11 PT O13 ga_13
O12 PT O13 ga_13
HI3 O13 PT ga_11
[ impropers ]
; ai aj ak al gromos type
N -C CA H gi_1
C CA +N O gi_1
CA N C CB gi_2
CG CD1 CD2 CB gi_1
CD2 CG CD1 CE1 gi_1
CD1 CG CD2 CE2 gi_1
CG CD1 CE1 CZ gi_1
CG CD2 CE2 CZ gi_1
CD1 CE1 CZ CE2 gi_1
CD2 CE2 CZ CE1 gi_1
CD1 CG CE1 HD1 gi_1
CD2 CG CE2 HD2 gi_1
CE1 CZ CD1 HE1 gi_1
CE2 CZ CD2 HE2 gi_1
CZ CE1 CE2 OH gi_1
[ dihedrals ]
; ai aj ak al gromos type
-CA -C N CA gd_4
-C N CA C gd_19
N CA C +N gd_20
N CA CB CG gd_17
CA CB CG CD1 gd_20
CE1 CZ OH PT gd_2
CZ OH PT O13 gd_9
CZ OH PT O13 gd_11
OH PT O13 HI3 gd_9
OH PT O13 HI3 gd_11
; phosphotyrosine (-2)
[Y2P]
[ atoms ]
N N -0.28000 0
H H 0.28000 0
CA CH1 0.00000 1
CB CH2 0.00000 1
CG C 0.00000 1
CD1 C -0.10000 2
HD1 HC 0.10000 2
CD2 C -0.10000 3
HD2 HC 0.10000 3
CE1 C -0.10000 4
HE1 HC 0.10000 4
CE2 C -0.10000 5
HE2 HC 0.10000 5
CZ C 0.15000 6 ; from the carbon atom attached to the phosphate group of
nucleotides (e.g., ATP)
OH OA -0.36000 6 ; from the phosphate group of nucleotides (e.g., ATP)
PT P 0.11500 6 ; to add up to -2 net charge
O11 OM -0.63500 6 ; from the phosphate group of nucleotides (e.g., ATP)
O12 OM -0.63500 6 ; from the phosphate group of nucleotides (e.g., ATP)
O13 OM -0.63500 6 ; from the phosphate group of nucleotides (e.g., ATP)
C C 0.380 7
O O -0.380 7
[ bonds ]
N H gb_2
N CA gb_20
CA C gb_26
C O gb_4
C +N gb_9
CA CB gb_26
CB CG gb_26
CG CD1 gb_15
CG CD2 gb_15
CD1 HD1 gb_3
CD1 CE1 gb_15
CD2 HD2 gb_3
CD2 CE2 gb_15
CE1 HE1 gb_3
CE1 CZ gb_15
CE2 HE2 gb_3
CE2 CZ gb_15
CZ OH gb_12
OH PT gb_27
PT O11 gb_23
PT O12 gb_23
PT O13 gb_23
[ exclusions ]
; ai aj
CB HD1
CB HD2
CB CE1
CB CE2
CG HE1
CG HE2
CG CZ
CD1 HD2
CD1 CE2
CD1 OH
HD1 CD2
HD1 HE1
HD1 CZ
CD2 CE1
CD2 OH
HD2 HE2
HD2 CZ
CE1 HE2
HE1 CE2
HE1 OH
HE2 OH
[ angles ]
; ai aj ak gromos type
-C N H ga_31
H N CA ga_17
-C N CA ga_30
N CA C ga_12
CA C +N ga_18
CA C O ga_29
O C +N ga_32
N CA CB ga_12
C CA CB ga_12
CA CB CG ga_14
CB CG CD1 ga_26
CB CG CD2 ga_26
CD1 CG CD2 ga_26
CG CD1 HD1 ga_24
HD1 CD1 CE1 ga_24
CG CD1 CE1 ga_26
CG CD2 HD2 ga_24
HD2 CD2 CE2 ga_24
CG CD2 CE2 ga_26
CD1 CE1 HE1 ga_24
HE1 CE1 CZ ga_24
CD1 CE1 CZ ga_26
CD2 CE2 HE2 ga_24
HE2 CE2 CZ ga_24
CD2 CE2 CZ ga_26
CE1 CZ CE2 ga_26
CE1 CZ OH ga_26
CE2 CZ OH ga_26
CZ OH PT ga_25
OH PT O11 ga_13
OH PT O12 ga_13
OH PT O13 ga_4
O11 PT O12 ga_13
O11 PT O13 ga_13
O12 PT O13 ga_13
[ impropers ]
; ai aj ak al gromos type
N -C CA H gi_1
C CA +N O gi_1
CA N C CB gi_2
CG CD1 CD2 CB gi_1
CD2 CG CD1 CE1 gi_1
CD1 CG CD2 CE2 gi_1
CG CD1 CE1 CZ gi_1
CG CD2 CE2 CZ gi_1
CD1 CE1 CZ CE2 gi_1
CD2 CE2 CZ CE1 gi_1
CD1 CG CE1 HD1 gi_1
CD2 CG CE2 HD2 gi_1
CE1 CZ CD1 HE1 gi_1
CE2 CZ CD2 HE2 gi_1
CZ CE1 CE2 OH gi_1

```

```

CG CD1 CE1 CZ gi_1
CG CD2 CE2 CZ gi_1
CD1 CE1 CZ CE2 gi_1
CD2 CE2 CZ CE1 gi_1
CD1 CG CE1 HD1 gi_1
CD2 CG CE2 HD2 gi_1
CE1 CZ CD1 HE1 gi_1
CE2 CZ CD2 HE2 gi_1
CZ CE1 CE2 OH gi_1
[ dihedrals ]
; ai aj ak al gromos type
-C A -C N CA gd_4
-C N CA C gd_19
N CA C +N gd_20
N CA CB CG gd_17
CA CB CG CD1 gd_20
CE1 CZ OH PT gd_2
CZ OH PT OI1 gd_9
CZ OH PT OI1 gd_11

; phosphoaspartate (-1)
[ D1P ]
[ atoms ]
N N -0.28000 0
H H 0.28000 0
CA CH1 0.00000 1
CB CH2 0.00000 1
CG C 0.53000 2; to add up to -1 net charge
OD1 O -0.38000 2; from the carbonyl oxygen (of e.g., the peptide bond)
OD2 OA -0.36000 2; from the phosphate group of nucleotides (e.g., ATP)
PE P 0.63000 2; from the phosphate group (of e.g., S1P)
OZ1 OM -0.63500 2; from the phosphate group of nucleotides (e.g., ATP)
OZ2 OM -0.63500 2; from the phosphate group of nucleotides (e.g., ATP)
OZ3 OA -0.54800 2; from the hydroxyl group of nucleotides (e.g., ATP)
HZ3 H 0.39800 2; from the hydroxyl group of nucleotides (e.g., ATP)
C C 0.380 3
O O -0.380 3
[ bonds ]
N H gb_2
N CA gb_20
CA C gb_26
C O gb_4
C +N gb_9
CA CB gb_26
CB CG gb_26
CG OD1 gb_4
CG OD2 gb_12
OD2 PE gb_27
PE OZ1 gb_23
PE OZ2 gb_23
PE OZ3 gb_27
OZ3 HZ3 gb_1
[ exclusions ]
; ai aj
OZ1 HZ3
OZ2 HZ3
OD2 HZ3
[ angles ]
; ai aj ak gromos type
-C N H ga_31
H N CA ga_17
-C N CA ga_30
N CA C ga_12
CA C +N ga_18
CA C O ga_29
O C +N ga_32
N CA CB ga_12
C CA CB ga_12
CA CB CG ga_14
CB CG OD1 ga_21
CB CG OD2 ga_18
OD1 CG OD2 ga_32
CG OD2 PE ga_25
OD2 PE OZ1 ga_13
OD2 PE OZ2 ga_13
OD2 PE OZ3 ga_13
OZ1 PE OZ2 ga_13
OZ1 PE OZ3 ga_13
OZ2 PE OZ3 ga_13
[ impropers ]
; ai aj ak al gromos type
N -C CA H gi_1
C CA +N O gi_1
CA N C CB gi_2
CG OD1 OD2 CB gi_1
[ dihedrals ]
; ai aj ak al gromos type
-C A -C N CA gd_4
-C N CA C gd_19
N CA C +N gd_20
N CA CB CG gd_17
CA CB CG OD2 gd_20
CB CG OD2 PE gd_3
CG OD2 PE OZ1 gd_9
CG OD2 PE OZ1 gd_11

; phosphoaspartate (-2)
[ D2P ]
[ atoms ]
N N -0.28000 0
H H 0.28000 0
CA CH1 0.00000 1
CB CH2 0.00000 1
CG C 0.53000 2; to add up to -2 net charge
OD1 O -0.38000 2; from the carbonyl oxygen (of e.g., the peptide bond)
OD2 OA -0.36000 2; from the phosphate group of nucleotides (e.g., ATP)
PE P 0.11500 2; from the phosphate group (of e.g., S2P)
OZ1 OM -0.63500 2; from the phosphate group of nucleotides (e.g., ATP)
OZ2 OM -0.63500 2; from the phosphate group of nucleotides (e.g., ATP)
OZ3 OM -0.63500 2; from the phosphate group of nucleotides (e.g., ATP)
C C 0.380 3
O O -0.380 3
[ bonds ]
N H gb_2
N CA gb_20
CA C gb_26
C O gb_4
C +N gb_9
CA CB gb_26
CB CG gb_26
CG OD1 gb_4
CG OD2 gb_12
OD2 PE gb_27
PE OZ1 gb_23
PE OZ2 gb_23
PE OZ3 gb_23
[ angles ]
; ai aj ak gromos type
-C N H ga_31
H N CA ga_17
-C N CA ga_30
N CA C ga_12
CA C +N ga_18
CA C O ga_29
O C +N ga_32
N CA CB ga_12
C CA CB ga_12
CA CB CG ga_14
CB CG OD1 ga_21
CB CG OD2 ga_18
OD1 CG OD2 ga_32
CG OD2 PE ga_25
OD2 PE OZ1 ga_13
OD2 PE OZ2 ga_13
OD2 PE OZ3 ga_13
OZ1 PE OZ2 ga_13
OZ1 PE OZ3 ga_13
OZ2 PE OZ3 ga_13
[ impropers ]
; ai aj ak al gromos type
N -C CA H gi_1
C CA +N O gi_1
CA N C CB gi_2
CG OD1 OD2 CB gi_1
[ dihedrals ]
; ai aj ak al gromos type
-C A -C N CA gd_4
-C N CA C gd_19
N CA C +N gd_20
N CA CB CG gd_17
CA CB CG OD2 gd_20
CB CG OD2 PE gd_3
CG OD2 PE OZ1 gd_9
CG OD2 PE OZ1 gd_11

; phospholysine (-1)
[ K1P ]
[ atoms ]
N N -0.28000 0
H H 0.28000 0
CA CH1 0.00000 1
CB CH2 0.00000 1
CG CH2 0.00000 2
CD CH2 0.00000 2
CE CH2 0.00000 3
NZ NE -0.28000 4; from NE of ARGN
HZ H 0.28000 4; from HE of ARGN
PH P 0.42000 5; to add up to -1 net charge
OI1 OM -0.63500 5; from the phosphate group of nucleotides (e.g., ATP)
OI2 OM -0.63500 5; from the phosphate group of nucleotides (e.g., ATP)
OI3 OA -0.54800 5; from the hydroxyl group of nucleotides (e.g., ATP)
HI3 H 0.39800 5; from the hydroxyl group of nucleotides (e.g., ATP)
C C 0.380 6

```

```

O O -0.380 6
[ bonds ]
N H gb_2
N CA gb_20
CA C gb_26
C O gb_4
C +N gb_9
CA CB gb_26
CB CG gb_26
CG CD gb_26
CD CE gb_26
CE NZ gb_20
NZ HZ gb_2
NZ PH gb_23
PH OI1 gb_23
PH OI2 gb_23
PH OI3 gb_27
OI3 HI3 gb_1
[ exclusions ]
; ai aj
OI1 HI3
OI2 HI3
NZ HI3
HZ OI1
HZ OI2
HZ OI3
[ angles ]
; ai aj ak gromos type
-C N H ga_31
H N CA ga_17
-C N CA ga_30
N CA C ga_12
CA C +N ga_18
CA C O ga_29
O C +N ga_32
N CA CB ga_12
C CA CB ga_12
CA CB CG ga_14
CB CG CD ga_14
CG CD CE ga_14
CD CE NZ ga_14
CE NZ HZ ga_19
HZ NZ PH ga_22
CE NZ PH ga_32
NZ PH OI1 ga_13
NZ PH OI2 ga_13
NZ PH OI3 ga_13
OI1 PH OI2 ga_13
OI1 PH OI3 ga_13
OI2 PH OI3 ga_13
[ impropers ]
; ai aj ak al gromos type
N -C CA H gi_1
C CA +N O gi_1
CA N C CB gi_2
NZ CE PH HZ gi_1
[ dihedrals ]
; ai aj ak al gromos type
-CA -C N CA gd_4
-C N CA C gd_19
N CA C +N gd_20
N CA CB CG gd_17
CA CB CG CD gd_17
CB CG CD CE gd_17
CG CD CE NZ gd_17
CD CE NZ PH gd_19
CE NZ PH OI3 gd_19
NZ PH OI3 HI3 gd_9
NZ PH OI3 HI3 gd_11
; phospholysine (-2)
[ K2P ]
[ atoms ]
N N -0.28000 0
H H 0.28000 0
CA CH1 0.00000 1
CB CH2 0.00000 1
CG CH2 0.00000 2
CD CH2 0.00000 2
CE CH2 0.00000 3
NZ NE -0.28000 4; from NE of ARGN
HZ H 0.28000 4; from HE of ARGN
PH P -0.09500 5; to add up to -2 net charge
OI1 OM -0.63500 5; from the phosphate group of nucleotides (e.g., ATP)
OI2 OM -0.63500 5; from the phosphate group of nucleotides (e.g., ATP)
OI3 OM -0.63500 5; from the phosphate group of nucleotides (e.g., ATP)
C C 0.380 6
O O -0.380 6
[ bonds ]
N H gb_2
N CA gb_20
CA C gb_26
C O gb_4
C +N gb_9
CA CB gb_26
CB CG gb_26
CG CD gb_26
CD NE gb_20
C O gb_4
C +N gb_9
CA CB gb_26
CB CG gb_26
CG CD gb_26
CD NE gb_20
[ exclusions ]
; ai aj
HZ OI1
HZ OI2
HZ OI3
[ angles ]
; ai aj ak gromos type
-C N H ga_31
H N CA ga_17
-C N CA ga_30
N CA C ga_12
CA C +N ga_18
CA C O ga_29
O C +N ga_32
N CA CB ga_12
C CA CB ga_12
CA CB CG ga_14
CB CG CD ga_14
CG CD CE ga_14
CD CE NZ ga_14
CE NZ HZ ga_19
HZ NZ PH ga_22
CE NZ PH ga_32
NZ PH OI1 ga_13
NZ PH OI2 ga_13
NZ PH OI3 ga_13
OI1 PH OI2 ga_13
OI1 PH OI3 ga_13
OI2 PH OI3 ga_13
[ impropers ]
; ai aj ak al gromos type
N -C CA H gi_1
C CA +N O gi_1
CA N C CB gi_2
NZ CE PH HZ gi_1
[ dihedrals ]
; ai aj ak al gromos type
-CA -C N CA gd_4
-C N CA C gd_19
N CA C +N gd_20
N CA CB CG gd_17
CA CB CG CD gd_17
CB CG CD CE gd_17
CG CD CE NZ gd_17
CD CE NZ PH gd_19
CE NZ PH OI1 gd_19
; phosphoarginine (0)
[ ROP ]
[ atoms ]
N N -0.28000 0
H H 0.28000 0
CA CH1 0.00000 1
CB CH2 0.00000 1
CG CH2 0.00000 1
CD CH2 0.09000 2
NE NE -0.11000 2
HE H 0.24000 2
CZ C 0.43000 2; to add up to 1 net charge
NH1 NZ -0.26000 2
HH11 H 0.24000 2
HH12 H 0.24000 2
NH2 NE -0.11000 2; from NE nitrogen atom of ARG
HH2 H 0.24000 2; from terminal hydrogen atoms of ARG
PT P 0.42000 3; to add up to -1 net charge
OI1 OM -0.63500 3; from the phosphate group of nucleotides (e.g., ATP)
OI2 OM -0.63500 3; from the phosphate group of nucleotides (e.g., ATP)
OI3 OA -0.54800 3; from the hydroxyl group of nucleotides (e.g., ATP)
HI3 H 0.39800 3; from the hydroxyl group of nucleotides (e.g., ATP)
C C 0.380 4
O O -0.380 4
[ bonds ]
N H gb_2
N CA gb_20
CA C gb_26
C O gb_4
C +N gb_9
CA CB gb_26
CB CG gb_26
CG CD gb_26
CD NE gb_20

```

```

NE HE gb_2
NE CZ gb_10
CZ NH1 gb_10
CZ NH2 gb_10
NH1 HH11 gb_2
NH1 HH12 gb_2
NH2 HH2 gb_2
NH2 PT gb_23
PT OI1 gb_23
PT OI2 gb_23
PT OI3 gb_27
OI3 HI3 gb_1
[exclusions ]
; ai aj
HH2 OI1
HH2 OI2
HH2 OI3
HI3 OI1
HI3 OI2
HI3 NH2
[angles ]
; ai aj ak gromos type
-C N H ga_31
H N CA ga_17
-C N CA ga_30
N CA C ga_12
CA C +N ga_18
CA C O ga_29
O C +N ga_32
N CA CB ga_12
C CA CB ga_12
CA CB CG ga_14
CB CG CD ga_14
CG CD NE ga_12
CD NE HE ga_19
HE NE CZ ga_22
CD NE CZ ga_32
NE CZ NH1 ga_27
NE CZ NH2 ga_27
NH1 CZ NH2 ga_27
CZ NH1 HH11 ga_22
CZ NH1 HH12 ga_22
HH11 NH1 HH12 ga_23
CZ NH2 HH2 ga_22
HH2 NH2 PT ga_19
CZ NH2 PT ga_32
NH2 PT OI1 ga_13
NH2 PT OI2 ga_13
NH2 PT OI3 ga_4
OI1 PT OI2 ga_28
OI1 PT OI3 ga_13
OI2 PT OI3 ga_13
PT OI3 HI3 ga_11
[impropers ]
; ai aj ak al gromos type
N -C CA H gi_1
C CA +N O gi_1
CA N C CB gi_2
NE CD CZ HE gi_1
CZ NH1 NH2 NE gi_1
NH1 HH11 HH12 CZ gi_1
NH2 CZ PT HH2 gi_1
[dihedrals ]
; ai aj ak al gromos type
-CA -C N CA gd_4
-C N CA C gd_19
N CA C +N gd_20
N CA CB CG gd_17
CA CB CG CD gd_17
CB CG CD NE gd_17
CG CD NE CZ gd_19
CD NE CZ NH2 gd_4
NE CZ NH1 HH11 gd_4
NE CZ NH2 PT gd_4
CZ NH2 PT OI3 gd_19
NH2 PT OI3 HI3 gd_9
NH2 PT OI3 HI3 gd_11
; phosphoarginine (-1)
[R1P ]
[atoms ]
N N -0.28000 0
H H 0.28000 0
CA CH1 0.00000 1
CB CH2 0.00000 1
CG CH2 0.00000 1
CD CH2 0.09000 2
NE NE -0.11000 2
HE H 0.24000 2
CZ C 0.43000 2 ; to add up to 1 net charge
NH1 NZ -0.26000 2
HH11 H 0.24000 2
HH12 H 0.24000 2
NH2 NE -0.11000 2 ; from NE nitrogen atom of ARG
HH2 H 0.24000 2 ; from terminal hydrogen atoms of ARG
PT P -0.09500 3 ; to add up to -2 net charge
OI1 OM -0.63500 3 ; from the phosphate group of nucleotides (e.g., ATP)
OI2 OM -0.63500 3 ; from the phosphate group of nucleotides (e.g., ATP)
OI3 OM -0.63500 3 ; from the phosphate group of nucleotides (e.g., ATP)
C C 0.380 4
O O -0.380 4
[bonds ]
N H gb_2
N CA gb_20
CA C gb_26
C O gb_4
C +N gb_9
CA CB gb_26
CB CG gb_26
CG CD gb_26
CD NE gb_20
NE HE gb_2
NE CZ gb_10
CZ NH1 gb_10
CZ NH2 gb_10
NH1 HH11 gb_2
NH1 HH12 gb_2
NH2 HH2 gb_2
NH2 PT gb_23
PT OI1 gb_23
PT OI2 gb_23
PT OI3 gb_23
[exclusions ]
; ai aj
HH2 OI1
HH2 OI2
HH2 OI3
[angles ]
; ai aj ak gromos type
-C N H ga_31
H N CA ga_17
-C N CA ga_30
N CA C ga_12
CA C +N ga_18
CA C O ga_29
O C +N ga_32
N CA CB ga_12
C CA CB ga_12
CA CB CG ga_14
CB CG CD ga_14
CG CD NE ga_12
CD NE HE ga_19
HE NE CZ ga_22
CD NE CZ ga_32
NE CZ NH1 ga_27
NE CZ NH2 ga_27
NH1 CZ NH2 ga_27
CZ NH1 HH11 ga_22
CZ NH1 HH12 ga_22
HH11 NH1 HH12 ga_23
CZ NH2 HH2 ga_22
HH2 NH2 PT ga_19
CZ NH2 PT ga_32
NH2 PT OI1 ga_13
NH2 PT OI2 ga_13
NH2 PT OI3 ga_4
OI1 PT OI2 ga_28
OI1 PT OI3 ga_13
OI2 PT OI3 ga_13
PT OI3 HI3 ga_11
[impropers ]
; ai aj ak al gromos type
N -C CA H gi_1
C CA +N O gi_1
CA N C CB gi_2
NE CD CZ HE gi_1
CZ NH1 NH2 NE gi_1
NH1 HH11 HH12 CZ gi_1
NH2 CZ PT HH2 gi_1
[dihedrals ]
; ai aj ak al gromos type
-CA -C N CA gd_4
-C N CA C gd_19
N CA C +N gd_20
N CA CB CG gd_17
CA CB CG CD gd_17
CB CG CD NE gd_17
CG CD NE CZ gd_19
CD NE CZ NH2 gd_4
NE CZ NH1 HH11 gd_4
NE CZ NH2 PT gd_4
CZ NH2 PT OI3 gd_19
NH2 PT OI3 HI3 gd_9
NH2 PT OI3 HI3 gd_11
; ai aj ak al gromos type
-CA -C N CA gd_4
-C N CA C gd_19
N CA C +N gd_20
N CA CB CG gd_17
CA CB CG CD gd_17
CB CG CD NE gd_17
CG CD NE CZ gd_19
CD NE CZ NH2 gd_4
NE CZ NH1 HH11 gd_4
NE CZ NH2 PT gd_4
CZ NH2 PT OI1 gd_19
; 1-phosphohistidine (-1)
[H11 ]
[atoms ]
N N -0.28000 0

```

```

H H 0.28000 0
CA CH1 0.00000 1
CB CH2 0.00000 1
CG C 0.29000 2
ND1 NR -0.58000 2
CE1 CR1 0.29000 2
CD2 CR1 0.00000 3
NE2 NR 0.00000 3
PZ P 0.42000 4 ; to add up to -1 net charge
OH1 OM -0.63500 4 ; from the phosphate group of nucleotides (e.g., ATP)
OH2 OM -0.63500 4 ; from the phosphate group of nucleotides (e.g., ATP)
OH3 OA -0.54800 4 ; from the hydroxyl group of nucleotides (e.g., ATP)
HH3 H 0.39800 4 ; from the hydroxyl group of nucleotides (e.g., ATP)
C C 0.380 5
O O -0.380 5
[ bonds ]
N H gb_2
N CA gb_20
CA C gb_26
C O gb_4
C +N gb_9
CA CB gb_26
CB CG gb_26
CG ND1 gb_9
CG CD2 gb_9
ND1 CE1 gb_9
CD2 NE2 gb_9
CE1 NE2 gb_9
NE2 PZ gb_23
PZ OH1 gb_23
PZ OH2 gb_23
PZ OH3 gb_27
OH3 HH3 gb_1
[ exclusions ]
; ai aj
CB CE1
CB NE2
PZ CD2
PZ NE2
HH3 NE2
HH3 OH1
HH3 OH2
[ angles ]
; ai aj ak gromos type
-C N H ga_31
H N CA ga_17
-C N CA ga_30
N CA C ga_12
CA C +N ga_18
CA C O ga_29
O C +N ga_32
N CA CB ga_12
C CA CB ga_12
CA CB CG ga_14
CB CG ND1 ga_36
CB CG CD2 ga_36
ND1 CG CD2 ga_6
CG ND1 CE1 ga_6
CG CD2 NE2 ga_6
ND1 CE1 NE2 ga_6
CD2 NE2 CE1 ga_6
CD2 NE2 PZ ga_36
CE1 NE2 PZ ga_36
NE2 PZ OH1 ga_13
NE2 PZ OH2 ga_13
NE2 PZ OH3 ga_4
OH1 PZ OH2 ga_28
OH1 PZ OH3 ga_13
OH2 PZ OH3 ga_13
PZ OH3 HH3 ga_11
[ impropers ]
; ai aj ak al gromos type
N -C CA H gi_1
C CA +N O gi_1
CA N C CB gi_2
CG ND1 CD2 CB gi_1
CD2 CG ND1 CE1 gi_1
ND1 CG CD2 NE2 gi_1
CG ND1 CE1 NE2 gi_1
CG CD2 NE2 CE1 gi_1
CD2 NE2 CE1 ND1 gi_1
NE2 CD2 CE1 PZ gi_1
[ dihedrals ]
; ai aj ak al gromos type
-C -C N CA gd_4
-C N CA C gd_19
N CA C +N gd_20
N CA CB CG gd_17
CA CB CG ND1 gd_20
CD2 NE2 PZ OH3 gd_19
NE2 PZ OH3 HH3 gd_9
NE2 PZ OH3 HH3 gd_11
; 1-phosphohistidine (-2)
[ H12 ]
[ atoms ]
N N -0.28000 0
H H 0.28000 0
CA CH1 0.00000 1
CB CH2 0.00000 1
CG C 0.29000 2
ND1 NR -0.58000 2
CE1 CR1 0.29000 2
CD2 CR1 0.00000 3
NE2 NR 0.00000 3
PZ P -0.09500 4 ; to add up to -2 net charge
OH1 OM -0.63500 4 ; from the phosphate group of nucleotides (e.g., ATP)
OH2 OM -0.63500 4 ; from the phosphate group of nucleotides (e.g., ATP)
OH3 OM -0.63500 4 ; from the phosphate group of nucleotides (e.g., ATP)
C C 0.380 5
O O -0.380 5
[ bonds ]
N H gb_2
N CA gb_20
CA C gb_26
C O gb_4
C +N gb_9
CA CB gb_26
CB CG gb_26
CG ND1 gb_9
CG CD2 gb_9
ND1 CE1 gb_9
CD2 NE2 gb_9
CE1 NE2 gb_9
NE2 PZ gb_23
PZ OH1 gb_23
PZ OH2 gb_23
PZ OH3 gb_23
[ exclusions ]
; ai aj
CB CE1
CB NE2
PZ CD2
PZ NE2
[ angles ]
; ai aj ak gromos type
-C N H ga_31
H N CA ga_17
-C N CA ga_30
N CA C ga_12
CA C +N ga_18
CA C O ga_29
O C +N ga_32
N CA CB ga_12
C CA CB ga_12
CA CB CG ga_14
CB CG ND1 ga_36
CB CG CD2 ga_36
ND1 CG CD2 ga_6
CG ND1 CE1 ga_6
CG CD2 NE2 ga_6
ND1 CE1 NE2 ga_6
CD2 NE2 CE1 ga_6
CD2 NE2 PZ ga_36
CE1 NE2 PZ ga_36
NE2 PZ OH1 ga_13
NE2 PZ OH2 ga_13
NE2 PZ OH3 ga_13
OH1 PZ OH2 ga_13
OH1 PZ OH3 ga_13
OH2 PZ OH3 ga_13
[ impropers ]
; ai aj ak al gromos type
N -C CA H gi_1
C CA +N O gi_1
CA N C CB gi_2
CG ND1 CD2 CB gi_1
CD2 CG ND1 CE1 gi_1
ND1 CG CD2 NE2 gi_1
CG ND1 CE1 NE2 gi_1
CG CD2 NE2 CE1 gi_1
CD2 NE2 CE1 ND1 gi_1
NE2 CD2 CE1 PZ gi_1
[ dihedrals ]
; ai aj ak al gromos type
-C -C N CA gd_4
-C N CA C gd_19
N CA C +N gd_20
N CA CB CG gd_17
CA CB CG ND1 gd_20
CD2 NE2 PZ OH1 gd_19
; 3-phosphohistidine (-1)
[ H31 ]
[ atoms ]
N N -0.28000 0

```

```

H H 0.28000 0
CA CH1 0.00000 1
CB CH2 0.00000 1
CG C 0.00000 2
ND1 NR 0.00000 2
CD2 CR1 0.29000 3
CE1 CR1 0.29000 3
NE2 NR -0.58000 3
PE3 P 0.42000 4 ; to add up to -1 net charge
OZ1 OM -0.63500 4 ; from the phosphate group of nucleotides (e.g., ATP)
OZ2 OM -0.63500 4 ; from the phosphate group of nucleotides (e.g., ATP)
OZ3 OA -0.54800 4 ; from the hydroxyl group of nucleotides (e.g., ATP)
HZ3 H 0.39800 4 ; from the hydroxyl group of nucleotides (e.g., ATP)
C C 0.380 5
O O -0.380 5
[ bonds ]
N H gb_2
N CA gb_20
CA C gb_26
C O gb_4
C +N gb_9
CA CB gb_26
CB CG gb_26
CG ND1 gb_9
CG CD2 gb_9
ND1 CE1 gb_9
ND1 PE3 gb_23
CD2 NE2 gb_9
CE1 NE2 gb_9
PE3 OZ1 gb_23
PE3 OZ2 gb_23
PE3 OZ3 gb_27
OZ3 HZ3 gb_1
[ exclusions ]
; ai aj
CB CE1
CB NE2
CB PE3
PE3 CD2
PE3 NE2
HZ3 ND1
HZ3 OZ1
HZ3 OZ2
[ angles ]
; ai aj ak gromos type
-C N H ga_31
H N CA ga_17
-C N CA ga_30
N CA C ga_12
CA C +N ga_18
CA C O ga_29
O C +N ga_32
N CA CB ga_12
C CA CB ga_12
CA CB CG ga_14
CB CG ND1 ga_36
CB CG CD2 ga_36
ND1 CG CD2 ga_6
CG ND1 CE1 ga_6
CG ND1 PE3 ga_36
CE1 ND1 PE3 ga_36
CG CD2 NE2 ga_6
ND1 CE1 NE2 ga_6
CD2 NE2 CE1 ga_6
ND1 PE3 OZ1 ga_13
ND1 PE3 OZ2 ga_13
ND1 PE3 OZ3 ga_4
OZ1 PE3 OZ2 ga_28
OZ1 PE3 OZ3 ga_13
OZ2 PE3 OZ3 ga_13
PE3 OZ3 HZ3 ga_11
[ impropers ]
; ai aj ak al gromos type
N -C CA H gi_1
C CA +N O gi_1
CA N C CB gi_2
CG ND1 CD2 CB gi_1
CD2 CG ND1 CE1 gi_1
ND1 CG CD2 NE2 gi_1
CG ND1 CE1 NE2 gi_1
CG CD2 NE2 CE1 gi_1
CD2 NE2 CE1 ND1 gi_1
ND1 CG CE1 PE3 gi_1
[ dihedrals ]
; ai aj ak al gromos type
-CA -C N CA gd_4
-C N CA C gd_19
N CA C +N gd_20
N CA CB CG gd_17
CA CB CG ND1 gd_20
CG ND1 PE3 OZ3 gd_19
ND1 PE3 OZ3 HZ3 gd_9
ND1 PE3 OZ3 HZ3 gd_11
; 3-phosphohistidine (-2)
[ H32 ]
[ atoms ]
N N -0.28000 0
H H 0.28000 0
CA CH1 0.00000 1
CB CH2 0.00000 1
CG C 0.00000 2
ND1 NR 0.00000 2
CD2 CR1 0.29000 3
CE1 CR1 0.29000 3
NE2 NR -0.58000 3
PE3 P -0.09500 4 ; to add up to -2 net charge
OZ1 OM -0.63500 4 ; from the phosphate group of nucleotides (e.g., ATP)
OZ2 OM -0.63500 4 ; from the phosphate group of nucleotides (e.g., ATP)
OZ3 OM -0.63500 4 ; from the phosphate group of nucleotides (e.g., ATP)
C C 0.380 5
O O -0.380 5
[ bonds ]
N H gb_2
N CA gb_20
CA C gb_26
C O gb_4
C +N gb_9
CA CB gb_26
CB CG gb_26
CG ND1 gb_9
CG CD2 gb_9
ND1 CE1 gb_9
ND1 PE3 gb_23
CD2 NE2 gb_9
CE1 NE2 gb_9
PE3 OZ1 gb_23
PE3 OZ2 gb_23
PE3 OZ3 gb_23
[ exclusions ]
; ai aj
CB CE1
CB NE2
CB PE3
PE3 CD2
PE3 NE2
[ angles ]
; ai aj ak gromos type
-C N H ga_31
H N CA ga_17
-C N CA ga_30
N CA C ga_12
CA C +N ga_18
CA C O ga_29
O C +N ga_32
N CA CB ga_12
C CA CB ga_12
CA CB CG ga_14
CB CG ND1 ga_36
CB CG CD2 ga_36
ND1 CG CD2 ga_6
CG ND1 CE1 ga_6
CG CD2 NE2 ga_6
ND1 CE1 NE2 ga_6
CD2 NE2 CE1 ga_6
ND1 PE3 OZ1 ga_13
ND1 PE3 OZ2 ga_13
ND1 PE3 OZ3 ga_13
OZ1 PE3 OZ2 ga_13
OZ2 PE3 OZ3 ga_13
OZ1 PE3 OZ3 ga_13
[ impropers ]
; ai aj ak al gromos type
N -C CA H gi_1
C CA +N O gi_1
CA N C CB gi_2
CG ND1 CD2 CB gi_1
CD2 CG ND1 CE1 gi_1
ND1 CG CD2 NE2 gi_1
CG ND1 CE1 NE2 gi_1
CG CD2 NE2 CE1 gi_1
CD2 NE2 CE1 ND1 gi_1
ND1 CG CE1 PE3 gi_1
[ dihedrals ]
; ai aj ak al gromos type
-CA -C N CA gd_4
-C N CA C gd_19
N CA C +N gd_20
N CA CB CG gd_17
CA CB CG ND1 gd_20
CG ND1 PE3 OZ1 gd_19
; N6-methyllysine (0)
[ KMN ]

```

```

[ atoms ]
  N N -0.28000 0
  H H 0.28000 0
  CA CH1 0.00000 1
  CB CH2 0.00000 1
  CG CH2 0.00000 2
  CD CH2 0.00000 2
  CE CH2 0.21000 3 ; from trimethylamine reported by Oostenbrink et al. DOI:
10.1002/cphc.200400542
  NZ NT -0.83000 3 ; from NZ of LYS
  HZ H 0.41000 3 ; derived from terminal hydrogen atoms of LYS
  CH CH3 0.21000 3 ; from trimethylamine reported by Oostenbrink et al. DOI:
10.1002/cphc.200400542
  C C 0.380 4
  O O -0.380 4
[ bonds ]
  N H gb_2
  N CA gb_20
  CA C gb_26
  C O gb_4
  C +N gb_9
  CA CB gb_26
  CB CG gb_26
  CG CD gb_26
  CD CE gb_26
  CE NZ gb_20
  NZ HZ gb_2
  NZ CH gb_20
[ angles ]
; ai aj ak gromos type
-C N H ga_31
H N CA ga_17
-C N CA ga_30
N CA C ga_12
CA C +N ga_18
CA C O ga_29
O C +N ga_32
N CA CB ga_12
C CA CB ga_12
CA CB CG ga_14
CB CG CD ga_14
CG CD CE ga_14
CD CE NZ ga_14
CE NZ HZ ga_10
HZ NZ CH ga_10
CE NZ CH ga_12
[ impropers ]
; ai aj ak al gromos type
N -C CA H gi_1
C CA +N O gi_1
CA N C CB gi_2
[ dihedrals ]
; ai aj ak al gromos type
-C -C N CA gd_4
-C N CA C gd_19
N CA C +N gd_20
N CA CB CG gd_17
CA CB CG CD gd_17
CB CG CD CE gd_17
CG CD CE NZ gd_17
CD CE NZ CH gd_14

; N6-methyllysine (+1)
[KMC]
[ atoms ]
  N N -0.28000 0
  H H 0.28000 0
  CA CH1 0.00000 1
  CB CH2 0.00000 1
  CG CH2 0.00000 2
  CD CH2 0.00000 2
  CE CH2 0.20000 3 ; derived by analogy to methyl groups of amines reported
by Oostenbrink et al. DOI: 10.1002/cphc.200400542
  NZ NL 0.10400 3 ; to add up to +1 net charge
  HZ1 H 0.24800 3
  HZ2 H 0.24800 3
  CH CH3 0.20000 3 ; derived by analogy to methyl groups of amines reported
by Oostenbrink et al. DOI: 10.1002/cphc.200400542
  C C 0.380 4
  O O -0.380 4
[ bonds ]
  N H gb_2
  N CA gb_20
  CA C gb_26
  C O gb_4
  C +N gb_9
  CA CB gb_26
  CB CG gb_26
  CG CD gb_26
  CD CE gb_26
  CE NZ gb_20
  NZ CH1 gb_20
  NZ CH2 gb_20
[ angles ]
; ai aj ak gromos type
-C N H ga_31
H N CA ga_17
-C N CA ga_30
N CA C ga_12
CA C +N ga_18
CA C O ga_29
O C +N ga_32
N CA CB ga_12
C CA CB ga_12
CA CB CG ga_14
CB CG CD ga_14
CG CD CE ga_14
CD CE NZ ga_14
CE NZ CH1 ga_12
CE NZ CH2 ga_12
CH1 NZ CH2 ga_12
[ impropers ]
; ai aj ak al gromos type
N -C CA H gi_1
C CA +N O gi_1
CA N C CB gi_2
[ dihedrals ]
; ai aj ak al gromos type
-C -C N CA gd_4
-C N CA C gd_19
N CA C +N gd_20
N CA CB CG gd_17
CA CB CG CD gd_17
CB CG CD CE gd_17
CG CD CE NZ gd_17
CD CE NZ CH gd_14

; N6,N6-dimethyllysine (0)
[K2M]
[ atoms ]
  N N -0.28000 0
  H H 0.28000 0
  CA CH1 0.00000 1
  CB CH2 0.00000 1
  CG CH2 0.00000 2
  CD CH2 0.00000 2
  CE CH2 0.21000 3 ; from trimethylamine reported by Oostenbrink et al. DOI:
10.1002/cphc.200400542
  NZ NT -0.63000 3 ; from trimethylamine reported by Oostenbrink et al. DOI:
10.1002/cphc.200400542
  CH1 CH3 0.21000 3 ; from trimethylamine reported by Oostenbrink et al. DOI:
10.1002/cphc.200400542
  CH2 CH3 0.21000 3 ; from trimethylamine reported by Oostenbrink et al. DOI:
10.1002/cphc.200400542
  C C 0.380 4
  O O -0.380 4
[ bonds ]
  N H gb_2
  N CA gb_20
  CA C gb_26
  C O gb_4
  C +N gb_9
  CA CB gb_26
  CB CG gb_26
  CG CD gb_26
  CD CE gb_26
  CE NZ gb_20
  NZ CH1 gb_20
  NZ CH2 gb_20
[ angles ]
; ai aj ak gromos type
-C N H ga_31
H N CA ga_17
-C N CA ga_30
N CA C ga_12
CA C +N ga_18
CA C O ga_29
O C +N ga_32
N CA CB ga_12
C CA CB ga_12
CA CB CG ga_14
CB CG CD ga_14
CG CD CE ga_14
CD CE NZ ga_14
CE NZ CH1 ga_12
CE NZ CH2 ga_12
CH1 NZ CH2 ga_12
[ impropers ]
; ai aj ak al gromos type
N -C CA H gi_1
C CA +N O gi_1
CA N C CB gi_2

```



```

[ dihedrals ]
; ai aj ak al gromos type
-C A N CA gd_4
-C N CA C gd_19
N CA C +N gd_20
N CA CB CG gd_17
CA CB CG CD gd_17
CB CG CD CE gd_17
CG CD CE NZ gd_17
CD CE NZ CH1 gd_14

; N6,N6-dimethyllysine (+1)
[ K2C ]
[ atoms ]
N N -0.28000 0
H H 0.28000 0
CA CH1 0.00000 1
CB CH2 0.00000 1
CG CH2 0.00000 2
CD CH2 0.00000 2
CE CH2 0.20000 3 ; derived by analogy to methyl groups of amines reported
by Oostenbrink et al. DOI: 10.1002/cphc.200400542
NZ NL 0.15200 3 ; to add up to +1 net charge
HZ H 0.24800 3
CH1 CH3 0.20000 3 ; derived by analogy to methyl groups of amines reported
by Oostenbrink et al. DOI: 10.1002/cphc.200400542
CH2 CH3 0.20000 3 ; derived by analogy to methyl groups of amines reported
by Oostenbrink et al. DOI: 10.1002/cphc.200400542
C C 0.380 4
O O -0.380 4
[ bonds ]
N H gb_2
N CA gb_20
CA C gb_26
C O gb_4
C +N gb_9
CA CB gb_26
CB CG gb_26
CG CD gb_26
CD CE gb_26
CE NZ gb_20
NZ HZ gb_2
NZ CH1 gb_20
NZ CH2 gb_20
[ angles ]
; ai aj ak gromos type
-C N H ga_31
H N CA ga_17
-C N CA ga_30
N CA C ga_12
CA C +N ga_18
CA C O ga_29
O C +N ga_32
N CA CB ga_12
C CA CB ga_12
CA CB CG ga_14
CB CG CD ga_14
CG CD CE ga_14
CD CE NZ ga_14
CE NZ CH1 ga_12
CE NZ CH2 ga_12
CE NZ CH3 ga_12
CH1 NZ CH2 ga_12
CH1 NZ CH3 ga_12
CH2 NZ CH3 ga_12
[ impropers ]
; ai aj ak al gromos type
N -C CA H gi_1
C CA +N O gi_1
CA N C CB gi_2
[ dihedrals ]
; ai aj ak al gromos type
-C A N CA gd_4
-C N CA C gd_19
N CA C +N gd_20
N CA CB CG gd_17
CA CB CG CD gd_17
CB CG CD CE gd_17
CG CD CE NZ gd_17
CD CE NZ CH1 gd_14

; omega-N-methylarginine (0)
[ RMN ]
[ atoms ]
N N -0.28000 0
H H 0.28000 0
CA CH1 0.00000 1
CB CH2 0.00000 1
CG CH2 0.00000 2
CD CH2 0.00000 2
NE NE -0.28000 3
HE H 0.28000 3
CZ C 0.18000 4 ; 0.36 charge divided between CZ and CT to add up to 0 net
charge, similar to methyl groups of other methylation residues and also used in other
building blocks (e.g., TMP)
NH1 NE -0.36000 4 ; from ring nitrogen atoms of nucleotides (e.g., ATP)
CT CH3 0.18000 4 ; 0.36 charge divided between CZ and CT to add up to 0 net
charge, similar to methyl groups of other methylation residues and also used in other
building blocks (e.g., TMP)
NH2 NZ -0.83000 5
HH21 H 0.41500 5
HH22 H 0.41500 5
C C 0.380 6
O O -0.380 6
[ bonds ]
N H gb_2
N CA gb_20
CA C gb_26
C O gb_4
C +N gb_9
CA CB gb_26
CB CG gb_26
CG CD gb_26
CD NE gb_20
NE HE gb_2

```

```

NE CZ gb_10
CZ NH1 gb_10
CZ NH2 gb_10
NH1 CT gb_20
NH2 HH21 gb_2
NH2 HH22 gb_2
[ angles ]
; ai aj ak gromos type
-C N H ga_31
H N CA ga_17
-C N CA ga_30
N CA C ga_12
CA C +N ga_18
CA C O ga_29
O C +N ga_32
N CA CB ga_12
C CA CB ga_12
CA CB CG ga_14
CB CG CD ga_14
CG CD NE ga_12
CD NE HE ga_19
HE NE CZ ga_22
CD NE CZ ga_32
NE CZ NH1 ga_27
NE CZ NH2 ga_27
NH1 CZ NH2 ga_27
CZ NH1 CT ga_26
CZ NH2 HH21 ga_22
CZ NH2 HH22 ga_22
HH21 NH2 HH22 ga_23
[ impropers ]
; ai aj ak al gromos type
N -C CA H gi_1
C CA +N O gi_1
CA N C CB gi_2
NE CD CZ HE gi_1
CZ NH1 NH2 NE gi_1
NH2 HH21 HH22 CZ gi_1
[ dihedrals ]
; ai aj ak al gromos type
-C -C N CA gd_4
-C N CA C gd_19
N CA C +N gd_20
N CA CB CG gd_17
CA CB CG CD gd_17
CB CG CD NE gd_17
CG CD NE CZ gd_19
CD NE CZ NH1 gd_4
NE CZ NH1 HH11 gd_4
NE CZ NH2 CT gd_4

; omega-N-methylarginine (+1)
[RMC]
[ atoms ]
N N -0.28000 0
H H 0.28000 0
CA CH1 0.00000 1
CB CH2 0.00000 1
CG CH2 0.00000 1
CD CH2 0.09000 2
NE NE -0.11000 2
HE H 0.24000 2
CZ C 0.34000 2
NH1 NZ -0.26000 2
HH11 H 0.24000 2
HH12 H 0.24000 2
NH2 NZ -0.11000 2 ; from NE atom of ARG
HH2 H 0.24000 2
CT CH3 0.09000 2 ; from CD atom of ARG
C C 0.380 3
O O -0.380 3
[ bonds ]
N H gb_2
N CA gb_20
CA C gb_26
C O gb_4
C +N gb_9
CA CB gb_26
CB CG gb_26
CG CD gb_26
CD NE gb_20
NE HE gb_2
NE CZ gb_10
CZ NH1 gb_10
CZ NH2 gb_10
NH1 HH11 gb_2
NH1 HH12 gb_2
NH2 HH2 gb_2
NH2 CT gb_20
[ angles ]
; ai aj ak gromos type
-C N H ga_31
H N CA ga_17
-C N CA ga_30
N CA C ga_12
CA C +N ga_18
CA C O ga_29
O C +N ga_32
N CA CB ga_12
C CA CB ga_12
CA CB CG ga_14
CB CG CD ga_14
CG CD NE ga_12
CD NE HE ga_19
HE NE CZ ga_22
CD NE CZ ga_32
NE CZ NH1 ga_27
NE CZ NH2 ga_27
NH1 CZ NH2 ga_27
CZ NH1 HH11 ga_22
CZ NH1 HH12 ga_22
HH11 NH1 HH12 ga_23
CZ NH2 HH2 ga_22
HH2 NH2 CT ga_19
CZ NH2 CT ga_32
[ impropers ]
; ai aj ak al gromos type
N -C CA H gi_1
C CA +N O gi_1
CA N C CB gi_2
NE CD CZ HE gi_1
CZ NH1 NH2 NE gi_1
NH1 HH11 HH12 CZ gi_1
NH2 HH2 CT CZ gi_1
[ dihedrals ]
; ai aj ak al gromos type
-C -C N CA gd_4
-C N CA C gd_19
N CA C +N gd_20
N CA CB CG gd_17
CA CB CG CD gd_17
CB CG CD NE gd_17
CG CD NE CZ gd_19
CD NE CZ NH1 gd_4
NE CZ NH1 HH11 gd_4
NE CZ NH2 CT gd_4

; symmetric-dimethylarginine (0)
[RSM]
[ atoms ]
N N -0.28000 0
H H 0.28000 0
CA CH1 0.00000 1
CB CH2 0.00000 1
CG CH2 0.00000 2
CD CH2 0.00000 2
NE NE -0.28000 3
HE H 0.28000 3
CZ C 0.18000 4 ; 0.36 charge divided between CZ and CT1 to add up to 0 net
charge, similar to methyl groups of other methylation residues and also used in other
building blocks (e.g., TMP)
NH1 NE -0.36000 4 ; from ring nitrogen atoms of nucleotides (e.g., ATP)
CT1 CH3 0.18000 4 ; 0.36 charge divided between CZ and CT1 to add up to 0
net charge, similar to methyl groups of other methylation residues and also used in
other building blocks (e.g., TMP)
NH2 NE -0.28000 5 ; from NE atom of ARGN
HH2 H 0.28000 5 ; from HE atom of ARGN
CT2 CH3 0.00000 6 ; from CD atom of ARGN
C C 0.380 7
O O -0.380 7
[ bonds ]
N H gb_2
N CA gb_20
CA C gb_26
C O gb_4
C +N gb_9
CA CB gb_26
CB CG gb_26
CG CD gb_26
CD NE gb_20
NE HE gb_2
NE CZ gb_10
CZ NH1 gb_10
CZ NH2 gb_10
NH1 CT1 gb_20
NH2 HH2 gb_2
NH2 CT2 gb_20
[ angles ]
; ai aj ak gromos type
-C N H ga_31
H N CA ga_17
-C N CA ga_30
N CA C ga_12
CA C +N ga_18
CA C O ga_29
O C +N ga_32

```

```

N CA CB ga_12
C CA CB ga_12
CA CB CG ga_14
CB CG CD ga_14
CG CD NE ga_12
CD NE HE ga_19
HE NE CZ ga_22
CD NE CZ ga_32
NE CZ NH1 ga_27
NE CZ NH2 ga_27
NH1 CZ NH2 ga_27
CZ NH1 CT1 ga_26
CZ NH2 HH2 ga_22
HH2 NH2 CT2 ga_19
CZ NH2 CT2 ga_32
[impropers]
; ai aj ak al gromos type
N -C CA H gi_1
C CA +N O gi_1
CA N C CB gi_2
NE CD CZ HE gi_1
CZ NH1 NH2 NE gi_1
NH2 HH2 CT2 CZ gi_1
[dihedrals]
; ai aj ak al gromos type
-CA -C N CA gd_4
-C N CA C gd_19
N CA C +N gd_20
N CA CB CG gd_17
CA CB CG CD gd_17
CB CG CD NE gd_17
CG CD NE CZ gd_19
CD NE CZ NH1 gd_4
NE CZ NH1 CT1 gd_4
NE CZ NH2 CT2 gd_4

; symmetric-dimethylarginine (+1)
[RMS]
[atoms]
N N -0.28000 0
H H 0.28000 0
CA CH1 0.00000 1
CB CH2 0.00000 1
CG CH2 0.00000 1
CD CH2 0.09000 2
NE NE -0.11000 2
HE H 0.24000 2
CZ C 0.34000 2
NH1 NZ -0.11000 2 ; from NE atom of ARG
HH1 H 0.24000 2
CT1 CH3 0.09000 2 ; from CD atom of ARG
NH2 NZ -0.11000 2 ; from NE atom of ARG
HH2 H 0.24000 2
CT2 CH3 0.09000 2 ; from CD atom of ARG
C C 0.380 3
O O -0.380 3
[bonds]
N H gb_2
N CA gb_20
CA C gb_26
C O gb_4
C +N gb_9
CA CB gb_26
CB CG gb_26
CG CD gb_26
CD NE gb_20
NE HE gb_2
NE CZ gb_10
CZ NH1 gb_10
CZ NH2 gb_10
NH1 HH1 gb_2
NH1 CT1 gb_20
NH2 HH2 gb_2
NH2 CT2 gb_20
[angles]
; ai aj ak gromos type
-C N H ga_31
H N CA ga_17
-C N CA ga_30
N CA C ga_12
CA C +N ga_18
CA C O ga_29
O C +N ga_32
N CA CB ga_12
C CA CB ga_12
CA CB CG ga_14
CB CG CD ga_14
CG CD NE ga_12
CD NE HE ga_19
HE NE CZ ga_22
CD NE CZ ga_32
NE CZ NH1 ga_27
NE CZ NH2 ga_27
NH1 CZ NH2 ga_27
CZ NH1 HH1 ga_22
CZ NH2 CT1 ga_27
CZ NH2 CT2 ga_27
CT1 NH2 CT2 ga_27

NH1 CZ NH2 ga_27
CZ NH1 HH1 ga_22
CZ NH2 CT1 ga_27
CZ NH2 CT2 ga_27
CT1 NH2 CT2 ga_27

[impropers]
; ai aj ak al gromos type
N -C CA H gi_1
C CA +N O gi_1
CA N C CB gi_2
NE CD CZ HE gi_1
CZ NH1 NH2 NE gi_1
NH1 HH1 CT1 CZ gi_1
NH2 HH2 CT2 CZ gi_1
[dihedrals]
; ai aj ak al gromos type
-CA -C N CA gd_4
-C N CA C gd_19
N CA C +N gd_20
N CA CB CG gd_17
CA CB CG CD gd_17
CB CG CD NE gd_17
CG CD NE CZ gd_19
CD NE CZ NH1 gd_4
NE CZ NH1 CT1 gd_4
NE CZ NH2 CT2 gd_4

; asymmetric-dimethylarginine (0)
[RAM]
[atoms]
N N -0.28000 0
H H 0.28000 0
CA CH1 0.00000 1
CB CH2 0.00000 1
CG CH2 0.00000 2
CD CH2 0.00000 2
NE NE -0.28000 3
HE H 0.28000 3
CZ C 0.15000 4
NH1 NE -0.54800 4
HH1 H 0.39800 4
NH2 NZ -0.20000 5 ; from ring nitrogen atoms of nucleotides (e.g., ATP)
CT1 CH3 0.10000 5 ; 0.2 charge divided between CT1 and CT2 to add up to 0
net charge, also similar to methyl groups of methyl-arginine modifications and used
for ring carbons in nucleotides (e.g., DCYT)
CT2 CH3 0.10000 5 ; 0.2 charge divided between CT1 and CT2 to add up to 0
net charge, also similar to methyl groups of methyl-arginine modifications and used
for ring carbons in nucleotides (e.g., DCYT)
C C 0.380 6
O O -0.380 6
[bonds]
N H gb_2
N CA gb_20
CA C gb_26
C O gb_4
C +N gb_9
CA CB gb_26
CB CG gb_26
CG CD gb_26
CD NE gb_20
NE HE gb_2
NE CZ gb_10
CZ NH1 gb_10
CZ NH2 gb_10
NH1 HH1 gb_2
NH2 CT1 gb_20
NH2 CT2 gb_20
[angles]
; ai aj ak gromos type
-C N H ga_31
H N CA ga_17
-C N CA ga_30
N CA C ga_12
CA C +N ga_18
CA C O ga_29
O C +N ga_32
N CA CB ga_12
C CA CB ga_12
CA CB CG ga_14
CB CG CD ga_14
CG CD NE ga_12
CD NE HE ga_19
HE NE CZ ga_22
CD NE CZ ga_32
NE CZ NH1 ga_27
NE CZ NH2 ga_27
NH1 CZ NH2 ga_27
CZ NH1 HH1 ga_22
CZ NH2 CT1 ga_27
CZ NH2 CT2 ga_27
CT1 NH2 CT2 ga_27

```

```

[impropers]
; ai aj ak al gromos type
N -C CA H gi_1
C CA +N O gi_1
CA N C CB gi_2
NE CD CZ HE gi_1
CZ NH1 NH2 NE gi_1
NH2 CT1 CT2 CZ gi_1
[ dihedrals ]
; ai aj ak al gromos type
-C A -C N CA gd_4
-C N CA C gd_19
N CA C +N gd_20
N CA CB CG gd_17
CA CB CG CD gd_17
CB CG CD NE gd_17
CG CD NE CZ gd_19
CD NE CZ NH1 gd_4
NE CZ NH1 HH1 gd_4
NE CZ NH2 CT1 gd_4

; asymmetric-dimethylarginine (+1)
[RMA]
[ atoms ]
N N -0.28000 0
H H 0.28000 0
CA CH1 0.00000 1
CB CH2 0.00000 1
CG CH2 0.00000 1
CD CH2 0.09000 2
NE NE -0.11000 2
HE H 0.24000 2
CZ C 0.43000 2; from CZ of R1P
NH1 NZ -0.26000 2
HH11 H 0.24000 2
HH12 H 0.24000 2
NH2 NZ -0.05000 2; to add up to +1 net charge, also used for nitrogen atoms
in histidine building blocks
CT1 CH3 0.09000 2; from CD atom of ARG
CT2 CH3 0.09000 2; from CD atom of ARG
C C 0.380 3
O O -0.380 3
[ bonds ]
N H gb_2
N CA gb_20
CA C gb_26
C O gb_4
C +N gb_9
CA CB gb_26
CB CG gb_26
CG CD gb_26
CD NE gb_20
NE HE gb_2
NE CZ gb_10
CZ NH1 gb_10
CZ NH2 gb_10
NH1 HH11 gb_2
NH1 HH12 gb_2
NH2 CT1 gb_20
NH2 CT2 gb_20
[ angles ]
; ai aj ak gromos type
-C N H ga_31
H N CA ga_17
-C N CA ga_30
N CA C ga_12
CA C +N ga_18
CA C O ga_29
O C +N ga_32
N CA CB ga_12
C CA CB ga_12
CA CB CG ga_14
CB CG ND1 ga_36
CB CG CD2 ga_36
ND1 CG CD2 ga_6
CG ND1 CE1 ga_6
CG CD2 NE2 ga_6
ND1 CE1 NE2 ga_6
CD2 NE2 CE1 ga_6
CD2 NE2 CZ ga_36
CE1 NE2 CZ ga_36
[impropers]
; ai aj ak al gromos type
N -C CA H gi_1
C CA +N O gi_1
CA N C CB gi_2
CG ND1 CD2 CB gi_1
CD2 CG ND1 CE1 gi_1
ND1 CG CD2 NE2 gi_1
CG ND1 CE1 NE2 gi_1
CG CD2 NE2 CE1 gi_1
CD2 NE2 CE1 ND1 gi_1
NE2 CD2 CE1 CZ gi_1
[ dihedrals ]
; ai aj ak al gromos type
-C A -C N CA gd_4
-C N CA C gd_19
N CA C +N gd_20
N CA CB CG gd_17
CA CB CG ND1 gd_20

; 1-methylhistidine (0)
[H1M]
[ atoms ]
N N -0.28000 0
H H 0.28000 0
CA CH1 0.00000 1
CB CH2 0.00000 1
CG C 0.13000 2
ND1 NR -0.58000 2
CD2 CR1 0.00000 2
CE1 CR1 0.26000 2
NE2 NR 0.00000 2
CZ CH3 0.19000 2; from HE2 in HISB
C C 0.380 3
O O -0.380 3
[ bonds ]
N H gb_2
N CA gb_20
CA C gb_26
C O gb_4
C +N gb_9
CA CB gb_26
CB CG gb_26
CG ND1 gb_9
CG CD2 gb_9
ND1 CE1 gb_9
CD2 NE2 gb_9
CE1 NE2 gb_9
NE2 CZ gb_21
[ exclusions ]
; ai aj
CB CE1
CB NE2
CG CZ
ND1 CZ
[ angles ]
; ai aj ak gromos type
-C N H ga_31
H N CA ga_17
-C N CA ga_30
N CA C ga_12
CA C +N ga_18
CA C O ga_29
O C +N ga_32
N CA CB ga_12
C CA CB ga_12
CA CB CG ga_14
CB CG ND1 ga_36
CB CG CD2 ga_36
ND1 CG CD2 ga_6
CG ND1 CE1 ga_6
CG CD2 NE2 ga_6
ND1 CE1 NE2 ga_6
CD2 NE2 CE1 ga_6
CD2 NE2 CZ ga_36
CE1 NE2 CZ ga_36
[impropers]
; ai aj ak al gromos type
N -C CA H gi_1
C CA +N O gi_1
CA N C CB gi_2
CG ND1 CD2 CB gi_1
CD2 CG ND1 CE1 gi_1
ND1 CG CD2 NE2 gi_1
CG ND1 CE1 NE2 gi_1
CG CD2 NE2 CE1 gi_1
CD2 NE2 CE1 ND1 gi_1
NE2 CD2 CE1 CZ gi_1
[ dihedrals ]
; ai aj ak al gromos type
-C A -C N CA gd_4
-C N CA C gd_19
N CA C +N gd_20
N CA CB CG gd_17
CA CB CG ND1 gd_20

; 1-methylhistidine (+1)
[H1C]

```

```

[atoms]
N N -0.28000 0
H H 0.28000 0
CA CH1 0.00000 1
CB CH2 0.00000 1
CG C -0.05000 2
ND1 NR 0.38000 2
HD1 H 0.30000 2
CD2 CR1 0.00000 2
CE1 CR1 -0.14000 2
NE2 NR 0.31000 2
CZ CH3 0.20000 2 ; derived by analogy to methyl groups of amines reported
by Oostenbrink et al. DOI: 10.1002/cphc.200400542
C C 0.380 3
O O -0.380 3
[bonds]
N H gb_2
N CA gb_20
CA C gb_26
C O gb_4
C +N gb_9
CA CB gb_26
CB CG gb_26
CG ND1 gb_9
CG CD2 gb_9
ND1 HD1 gb_2
ND1 CE1 gb_9
CD2 NE2 gb_9
CE1 NE2 gb_9
NE2 CZ gb_21
[exclusions]
; ai aj
CB HD1
CB CE1
CB NE2
CG CZ
ND1 CZ
HD1 CD2
HD1 NE2
[angles]
; ai aj ak gromos type
-C N H ga_31
H N CA ga_17
-C N CA ga_30
N CA C ga_12
CA C +N ga_18
CA C O ga_29
O C +N ga_32
N CA CB ga_12
C CA CB ga_12
CA CB CG ga_14
CB CG ND1 ga_36
CB CG CD2 ga_36
ND1 CG CD2 ga_6
CG ND1 CE3 ga_36
CG ND1 CE1 ga_6
CE3 ND1 CE1 ga_36
CG CD2 NE2 ga_6
ND1 CE1 NE2 ga_6
CD2 NE2 CE1 ga_6
[impropers]
; ai aj ak al gromos type
N -C CA H gi_1
C CA +N O gi_1
CA N C CB gi_2
CG ND1 CD2 CB gi_1
CD2 CG ND1 CE1 gi_1
ND1 CG CD2 NE2 gi_1
CG ND1 CE1 NE2 gi_1
CG CD2 NE2 CE1 gi_1
CD2 NE2 CE1 ND1 gi_1
ND1 CG CE1 HD1 gi_1
NE2 CD2 CE1 CZ gi_1
[dihedrals]
; ai aj ak al gromos type
-C -C N CA gd_4
-C N CA C gd_19
N CA C +N gd_20
N CA CB CG gd_17
CA CB CG ND1 gd_20
; 3-methylhistidine (0)
[H3M]
[atoms]
N N -0.28000 0
H H 0.28000 0
CA CH1 0.00000 1
CB CH2 0.00000 1
CG C -0.05000 2
ND1 NR 0.38000 2
CD2 CR1 0.00000 2
CE1 CR1 -0.14000 2
CE3 CH3 0.20000 2 ; derived by analogy to methyl groups of amines reported
by Oostenbrink et al. DOI: 10.1002/cphc.200400542
NE2 NR 0.31000 2
HE2 H 0.30000 2
C C 0.380 3
O O -0.380 3
[bonds]
N H gb_2
N CA gb_20
CA C gb_26
C O gb_4
C +N gb_9
CA CB gb_26
CB CG gb_26
CG ND1 gb_9
CE1 CR1 0.26000 2
CE3 CH3 0.19000 2 ; from HD1 in HISA
NE2 NR -0.58000 2
C C 0.380 3
O O -0.380 3
[exclusions]
; ai aj
CB CE3
CB CE1
CB NE2
CE3 CD2
CE3 NE2
[angles]
; ai aj ak gromos type
-C N H ga_31
H N CA ga_17
-C N CA ga_30
N CA C ga_12
CA C +N ga_18
CA C O ga_29
O C +N ga_32
N CA CB ga_12
C CA CB ga_12
CA CB CG ga_14
CB CG ND1 ga_36
CB CG CD2 ga_36
ND1 CG CD2 ga_6
CG ND1 CE3 ga_36
CG ND1 CE1 ga_6
CE3 ND1 CE1 ga_36
CG CD2 NE2 ga_6
ND1 CE1 NE2 ga_6
CD2 NE2 CE1 ga_6
[impropers]
; ai aj ak al gromos type
N -C CA H gi_1
C CA +N O gi_1
CA N C CB gi_2
CG ND1 CD2 CB gi_1
CD2 CG ND1 CE1 gi_1
ND1 CG CD2 NE2 gi_1
CG ND1 CE1 NE2 gi_1
CG CD2 NE2 CE1 gi_1
CD2 NE2 CE1 ND1 gi_1
ND1 CG CE1 CE3 gi_1
[dihedrals]
; ai aj ak al gromos type
-C -C N CA gd_4
-C N CA C gd_19
N CA C +N gd_20
N CA CB CG gd_17
CA CB CG ND1 gd_20
; 3-methylhistidine (+1)
[H3C]
[atoms]
N N -0.28000 0
H H 0.28000 0
CA CH1 0.00000 1
CB CH2 0.00000 1
CG C -0.05000 2
ND1 NR 0.38000 2
CD2 CR1 0.00000 2
CE1 CR1 -0.14000 2
CE3 CH3 0.20000 2 ; derived by analogy to methyl groups of amines reported
by Oostenbrink et al. DOI: 10.1002/cphc.200400542
NE2 NR 0.31000 2
HE2 H 0.30000 2
C C 0.380 3
O O -0.380 3
[bonds]
N H gb_2
N CA gb_20
CA C gb_26
C O gb_4
C +N gb_9
CA CB gb_26
CB CG gb_26
CG ND1 gb_9

```

```

CG CD2 gb_9
ND1 CE3 gb_21
ND1 CE1 gb_9
CD2 NE2 gb_9
CE1 NE2 gb_9
NE2 HE2 gb_2
[exclusions ]
; ai aj
CB CE3
CB CE1
CB NE2
CG HE2
ND1 HE2
CE3 CD2
CE3 NE2
[angles ]
; ai aj ak gromos type
-C N H ga_31
H N CA ga_17
-C N CA ga_30
N CA C ga_12
CA C +N ga_18
CA C O ga_29
O C +N ga_32
N CA CB ga_12
C CA CB ga_12
CA CB CG ga_14
CB CG ND1 ga_36
CB CG CD2 ga_36
ND1 CG CD2 ga_6
CG ND1 CE3 ga_36
CG ND1 CE1 ga_6
CE3 ND1 CE1 ga_36
CG CD2 NE2 ga_6
ND1 CE1 NE2 ga_6
CD2 NE2 CE1 ga_6
CD2 NE2 HE2 ga_35
CE1 NE2 HE2 ga_35
[impropers ]
; ai aj ak al gromos type
N -C CA H gi_1
C CA +N O gi_1
CA N C CB gi_2
CG ND1 CD2 CB gi_1
CD2 CG ND1 CE1 gi_1
ND1 CG CD2 NE2 gi_1
CG ND1 CE1 NE2 gi_1
CG CD2 NE2 CE1 gi_1
CD2 NE2 CE1 ND1 gi_1
ND1 CG CE1 CE3 gi_1
NE2 CD2 CE1 HE2 gi_1
[dihedrals ]
; ai aj ak al gromos type
-CA -C N CA gd_4
-C N CA C gd_19
N CA C +N gd_20
N CA CB CG gd_17
CA CB CG ND1 gd_20

; N5-methylglutamine
[QME ]
[atoms ]
N N -0.28000 0
H H 0.28000 0
CA CH1 0.00000 1
CB CH2 0.00000 1
CG CH2 0.10000 2 ; by analogy to the aldehyde group reported by Dolenc et
al. DOI: 10.1093/nar/gki195
CD C 0.28000 2 ; by analogy to the aldehyde group reported by Dolenc et al.
DOI: 10.1093/nar/gki195
OE1 O -0.38000 2
NE2 N -0.28000 3 ; from the peptide bond
HE2 H 0.28000 3 ; from the peptide bond
CZ CH3 0.00000 4
C C 0.380 5
O O -0.380 5
[bonds ]
N H gb_2
N CA gb_20
CA C gb_26
C O gb_4
C +N gb_9
CA CB gb_26
CB CG gb_26
CG CD gb_26
CD OE1 gb_4
CD NE2 gb_9
NE2 HE2 gb_2
NE2 CZ gb_20
[angles ]
; ai aj ak gromos type
-C N H ga_31
H N CA ga_17
-C N CA ga_30
N CA C ga_12
CA C +N ga_18
CA C O ga_29
O C +N ga_32
N CA CB ga_12
C CA CB ga_12
CA CB CG ga_14
CB CG OD1 ga_29
CB CG ND2 ga_18
OD1 CG ND2 ga_32
CG ND2 HD2 ga_31
HD2 ND2 CE ga_17
CG ND2 CE ga_30
[impropers ]
; ai aj ak al gromos type
N -C CA H gi_1
C CA +N O gi_1
CA N C CB gi_2
CG OD1 ND2 CB gi_1
ND2 CE CG HD2 gi_1
[dihedrals ]
; ai aj ak al gromos type
-CA -C N CA gd_4
-C N CA C gd_19
N CA C +N gd_20
N CA CB CG gd_17
CA CB CG ND2 gd_20
CB CG ND2 CE gd_4

-C N CA ga_30
N CA C ga_12
CA C +N ga_18
CA C O ga_29
O C +N ga_32
N CA CB ga_12
C CA CB ga_12
CA CB CG ga_14
CB CG CD ga_14
CG CD OE1 ga_29
CG CD NE2 ga_18
OE1 CD NE2 ga_32
CD NE2 HE2 ga_31
HE2 NE2 CZ ga_17
CD NE2 CZ ga_30
[impropers ]
; ai aj ak al gromos type
N -C CA H gi_1
C CA +N O gi_1
CA N C CB gi_2
CD OE1 NE2 CG gi_1
NE2 CZ CD HE2 gi_1
[dihedrals ]
; ai aj ak al gromos type
-CA -C N CA gd_4
-C N CA C gd_19
N CA C +N gd_20
N CA CB CG gd_17
CA CB CG ND2 gd_20
CG CD NE2 CZ gd_4

; N4-methylasparagine
[NME ]
[atoms ]
N N -0.28000 0
H H 0.28000 0
CA CH1 0.00000 1
CB CH2 0.10000 2 ; by analogy to the aldehyde group reported by Dolenc et
al. DOI: 10.1093/nar/gki195
CG C 0.28000 2 ; by analogy to the aldehyde group reported by Dolenc et al.
DOI: 10.1093/nar/gki195
OD1 O -0.38000 2
ND2 N -0.28000 3 ; from the peptide bond
HD2 H 0.28000 3 ; from the peptide bond
CE CH3 0.00000 4
C C 0.380 5
O O -0.380 5
[bonds ]
N H gb_2
N CA gb_20
CA C gb_26
C O gb_4
C +N gb_9
CA CB gb_26
CB CG gb_26
CG OD1 gb_4
CG ND2 gb_9
ND2 HD2 gb_2
ND2 CE gb_20
[angles ]
; ai aj ak gromos type
-C N H ga_31
H N CA ga_17
-C N CA ga_30
N CA C ga_12
CA C +N ga_18
CA C O ga_29
O C +N ga_32
N CA CB ga_12
C CA CB ga_12
CA CB CG ga_14
CB CG OD1 ga_29
CB CG ND2 ga_18
OD1 CG ND2 ga_32
CG ND2 HD2 ga_31
HD2 ND2 CE ga_17
CG ND2 CE ga_30
[impropers ]
; ai aj ak al gromos type
N -C CA H gi_1
C CA +N O gi_1
CA N C CB gi_2
CG OD1 ND2 CB gi_1
ND2 CE CG HD2 gi_1
[dihedrals ]
; ai aj ak al gromos type
-CA -C N CA gd_4
-C N CA C gd_19
N CA C +N gd_20
N CA CB CG gd_17
CA CB CG ND2 gd_20
CB CG ND2 CE gd_4

```

```

; glutamate methyl ester
[ EME ]
[ atoms ]
N N -0.28000 0
H H 0.28000 0
CA CH1 0.00000 1
CB CH2 0.00000 1
CG CH2 0.00000 1
CD C 0.56000 2; from the carbonyl group (of e.g., GLU) with the partial
charge increased by 0.18 - see the comment of CZ atom
OE1 O -0.38000 2; from the carbonyl group (of e.g., GLU)
OE2 OA -0.36000 2; from the ring oxygen atom of nucleotides (e.g., ATP)
CZ CH3 0.18000 2; 0.36 charge divided between CD and CZ to add up to 0 net
charge, similar to methyl groups of other methylation residues and also used in other
building blocks (e.g., TMP)
C C 0.380 3
O O -0.380 3
[ bonds ]
N H gb_2
N CA gb_20
CA C gb_26
C O gb_4
C +N gb_9
CA CB gb_26
CB CG gb_26
CG CD gb_26
CD OE1 gb_4
CD OE2 gb_12
OE2 CZ gb_17
[ angles ]
; ai aj ak al gromos type
-C N H ga_31
H N CA ga_17
-C N CA ga_30
N CA C ga_12
CA C +N ga_18
CA C O ga_29
O C +N ga_32
N CA CB ga_12
C CA CB ga_12
CA CB CG ga_14
CB CG CD ga_14
CG CD OE1 ga_29
CG CD OE2 ga_18
OE1 CD OE2 ga_32
CD OE2 CZ ga_11
[ impropers ]
; ai aj ak al gromos type
N -C CA H gi_1
C CA +N O gi_1
CA N C CB gi_2
CD OE1 OE2 CG gi_1
[ dihedrals ]
; ai aj ak al gromos type
-C -C N CA gd_4
-C N CA C gd_19
N CA C +N gd_20
N CA CB CG gd_17
CA CB CG CD gd_17
CB CG CD OE2 gd_20
CG CD OE2 CZ gd_3
; aspartate methyl ester
[ DMA ]
[ atoms ]
N N -0.28000 0
H H 0.28000 0
CA CH1 0.00000 1
CB CH2 0.00000 1
CG C 0.56000 2; from the carbonyl group (of e.g., GLU) with the partial
charge increased by 0.18 - see the comment of CE atom
OD1 O -0.38000 2; from the carbonyl group (of e.g., GLU)
OD2 OA -0.36000 2; from the ring oxygen atom of nucleotides (e.g., ATP)
CE CH3 0.18000 2; 0.36 charge divided between CG and CE to add up to 0 net
charge, similar to methyl groups of other methylation residues and also used in other
building blocks (e.g., TMP)
C C 0.380 3
O O -0.380 3
[ bonds ]
N H gb_2
N CA gb_20
CA C gb_26
C O gb_4
C +N gb_9
CA CB gb_26
CB CG gb_26
CG OD1 gb_4
CG OD2 gb_12
OD2 CE gb_17
[ angles ]
; ai aj ak gromos type
-C N H ga_31
H N CA ga_17
-C N CA ga_30
N CA C ga_12
CA C +N ga_18
CA C O ga_29
O C +N ga_32
N CA CB ga_12
C CA CB ga_12
CA CB CG ga_14
CB CG CD ga_14
CG CD OE1 ga_29
CG CD OE2 ga_18
OE1 CD OE2 ga_32
CD OE2 CZ ga_11
[ impropers ]
; ai aj ak al gromos type
N -C CA H gi_1
C CA +N O gi_1
CA N C CB gi_2
CD OE1 OE2 CG gi_1
[ dihedrals ]
; ai aj ak al gromos type
-C -C N CA gd_4
-C N CA C gd_19
N CA C +N gd_20
N CA CB CG gd_17
CA CB CG CD gd_17
CB CG CD OE2 gd_20
CG CD OE2 CZ gd_3
; N6-acetylysine
[ KAC ]
[ atoms ]
N N -0.28000 0
H H 0.28000 0
CA CH1 0.00000 1
CB CH2 0.00000 1
CG CH2 0.00000 2
CD CH2 0.00000 2
CE CH2 0.00000 3
NZ N -0.28000 4; from the peptide bond
HZ H 0.28000 4; from the peptide bond
CH C 0.28000 5; by analogy to the aldehyde group reported by Dolenc et al.
DOI: 10.1093/nar/gki195
OI2 O -0.38000 5; from the carbonyl group (of e.g., GLN)
CI1 CH3 0.10000 5; by analogy to the aldehyde group reported by Dolenc et
al. DOI: 10.1093/nar/gki195
C C 0.380 6
O O -0.380 6
H N CA ga_17
-C N CA ga_30
N CA C ga_12
CA C +N ga_18
CA C O ga_29
O C +N ga_32
N CA CB ga_12
C CA CB ga_12
CA CB CG ga_14
CB CG OD1 ga_29
CB CG OD2 ga_18
OD1 CG OD2 ga_32
CG OD2 CE ga_11
[ impropers ]
; ai aj ak al gromos type
N -C CA H gi_1
C CA +N O gi_1
CA N C CB gi_2
CG OD1 OD2 CB gi_1
[ dihedrals ]
; ai aj ak al gromos type
-C -C N CA gd_4
-C N CA C gd_19
N CA C +N gd_20
N CA CB CG gd_17
CA CB CG OD2 gd_20
CB CG OD2 CE gd_3
; S-methylcysteine
[ CYM ]
[ atoms ]
N N -0.28000 0
H H 0.28000 0
CA CH1 0.00000 1
CB CH2 0.00000 1; from MET
SG S 0.00000 2; from MET
CD CH3 0.00000 2; from MET
C C 0.380 3
O O -0.380 3
[ bonds ]
N H gb_2
N CA gb_20
CA C gb_26
C O gb_4
C +N gb_9
CA CB gb_26
CB SG gb_30
SG CD gb_29
[ angles ]
; ai aj ak gromos type
-C N H ga_31
H N CA ga_17
-C N CA ga_30
N CA C ga_12
CA C +N ga_18
CA C O ga_29
O C +N ga_32
N CA CB ga_12
C CA CB ga_12
CA CB SG ga_15
CB SG CD ga_3
[ impropers ]
; ai aj ak al gromos type
N -C CA H gi_1
C CA +N O gi_1
CA N C CB gi_2
[ dihedrals ]
; ai aj ak al gromos type
-C -C N CA gd_4
-C N CA C gd_19
N CA C +N gd_20
N CA CB SG gd_17
CA CB SG CD gd_13

```

```

[ bonds ]
N H gb_2
N CA gb_20
CA C gb_26
C O gb_4
C +N gb_9
CA CB gb_26
CB CG gb_26
CG CD gb_26
CD CE gb_26
CE NZ gb_20
NZ HZ gb_2
NZ CH gb_9
CH OI2 gb_4
CH CI1 gb_26
[ angles ]
; ai aj ak gromos type
-C N H ga_31
H N CA ga_17
-C N CA ga_30
N CA C ga_12
CA C +N ga_18
CA C O ga_29
O C +N ga_32
N CA CB ga_12
C CA CB ga_12
CA CB CG ga_14
CB CG CD ga_14
CG CD CE ga_14
CD CE NZ ga_14
CE NZ HZ ga_17
HZ NZ CH ga_31
CE NZ CH ga_30
NZ CH OI2 ga_32
NZ CH CI1 ga_18
OI2 CH CI1 ga_29
[ impropers ]
; ai aj ak al gromos type
N -C CA H gi_1
C CA +N O gi_1
CA N C CB gi_2
NZ CH CE HZ gi_1
CH CI1 NZ OI2 gi_1
[ dihedrals ]
; ai aj ak al gromos type
-C A -C N CA gd_4
-C N CA C gd_19
N CA C +N gd_20
N CA CB CG gd_17
CA CB CG CD gd_17
CB CG CD CE gd_17
CG CD CE NZ gd_17
CD CE NZ CH gd_19
CE NZ CH CI1 gd_4

; 3-hydroxyproline (R)
[ PH3 ]
[ atoms ]
N N 0.00000 0
CA CH1 0.00000 1
CB CH1 0.15000 2; from the hydroxyl group of THR
OG1 OA -0.54800 2; from the hydroxyl group of THR
HG1 H 0.39800 2; from the hydroxyl group of THR
CG2 CH2 0.00000 3
CD CH2 0.00000 3
C C 0.380 4
O O -0.380 4
[ bonds ]
N CA gb_20
CA C gb_26
C O gb_4
C +N gb_9
CA CB gb_26
CB OG1 gb_17
OG1 HG1 gb_1
CB CG2 gb_26
CG2 CD gb_26
CD N gb_20
[ angles ]
; ai aj ak gromos type
-C N CA ga_30
N CA C ga_12
CA C +N ga_18
CA C O ga_29
O C +N ga_32
N CA CB ga_12
C CA CB ga_12
CA CB OG1 ga_12
CA CB CG2 ga_12
CB OG1 HG1 ga_11
OG1 CB CG2 ga_12
CB CG2 CD ga_12
CG2 CD N ga_12
CD N CA ga_20
-C N CD ga_30
[ impropers ]
; ai aj ak al gromos type
N -C CA CD gi_1
C CA +N O gi_1
CA N C CB gi_2
CB CA CG2 OG1 gi_2
[ dihedrals ]
; ai aj ak al gromos type
-C A -C N CA gd_4
-C N CA C gd_19
N CA C +N gd_20
N CA CB CG2 gd_17
CA CB OG1 HG1 gd_12
CA CB CG2 CD gd_17
CB CG2 CD N gd_17
CG2 CD N CA gd_19

; 4-hydroxyproline (S)
[ HY2 ]
[ atoms ]
N N 0.00000 0
CA CH1 0.00000 1
CB CH2 0.00000 1
CG CH1 0.15000 2; from the hydroxyl group of THR
OD1 OA -0.54800 2; from the hydroxyl group of THR
HD1 H 0.39800 2; from the hydroxyl group of THR
CD2 CH2 0.00000 3
C C 0.380 4
O O -0.380 4
[ bonds ]
N CA gb_20
CA C gb_26
C O gb_4
C +N gb_9

```



```

CA CB gb_26
CB CG gb_26
CG OD1 gb_17
OD1 HD1 gb_1
CG CD2 gb_26
CD2 N gb_20
[angles]
; ai aj ak gromos type
-C N CA ga_30
N CA C ga_12
CA C +N ga_18
CA C O ga_29
O C +N ga_32
N CA CB ga_12
C CA CB ga_12
CA CB CG ga_12
CB CG OD1 ga_12
CB CG CD2 ga_12
CG OD1 HD1 ga_11
OD1 CG CD2 ga_12
CG CD2 N ga_12
CD2 N CA ga_20
-C N CD2 ga_30
[impropers]
; ai aj ak al gromos type
N -C CA CD2 gi_1
C CA +N O gi_1
CA N C CB gi_2
CG CB CD2 OD1 gi_2
[dihedrals]
; ai aj ak al gromos type
-C -C N CA gd_4
-C N CA C gd_19
N CA C +N gd_20
N CA CB CG gd_17
CA CB CG CD2 gd_17
CB CG OD1 HD1 gd_12
CB CG CD2 N gd_17
CG CD2 N CA gd_19
; 3,4-dihydroxyproline
[PHH]
[atoms]
N N 0.00000 0
CA CH1 0.00000 1
CB CH1 0.15000 2 ; from the hydroxyl group of THR
OG1 OA -0.54800 2 ; from the hydroxyl group of THR
HG1 H 0.39800 2 ; from the hydroxyl group of THR
CG2 CH1 0.15000 3 ; from the hydroxyl group of THR
OD1 OA -0.54800 3 ; from the hydroxyl group of THR
HD1 H 0.39800 3 ; from the hydroxyl group of THR
CD2 CH2 0.00000 4
C C 0.380 5
O O -0.380 5
[bonds]
N CA gb_20
CA C gb_26
C O gb_4
C +N gb_9
CA CB gb_26
CB OG1 gb_17
OG1 HG1 gb_1
CB CG2 gb_26
CG2 OD1 gb_17
OD1 HD1 gb_1
CG2 CD2 gb_26
CD2 N gb_20
[angles]
; ai aj ak gromos type
-C N CA ga_30
N CA C ga_12
CA C +N ga_18
CA C O ga_29
O C +N ga_32
N CA CB ga_12
C CA CB ga_12
CA CB CG ga_14
CB CG CD ga_14
CG CD OE1 ga_12
CG CD CE2 ga_12
OE1 CD CE2 ga_12
CD OE1 HE1 ga_11
CD CE2 NZ ga_14
CE2 NZ HZ1 ga_10
CE2 NZ HZ2 ga_10
HZ1 NZ HZ2 ga_9
[impropers]
; ai aj ak al gromos type
N -C CA H gi_1
C CA +N O gi_1
CA N C CB gi_2
CD CE2 OE1 CG gi_2
[dihedrals]
; ai aj ak al gromos type
-C -C N CA gd_4
-C N CA C gd_19
N CA C +N gd_20
N CA CB CG gd_17
CA CB CG CD gd_17
CB CG CD CE2 gd_17
CG CD OE1 HE1 gd_12
CG CD CE2 NZ gd_17
CD CE2 NZ HZ1 gd_14
; 5-hydroxylysine (0,5)
[K5H]
[atoms]
N N -0.28000 0
H H 0.28000 0
CA CH1 0.00000 1
CB CH2 0.00000 1
CG CH2 0.00000 2
CD CH1 0.15000 3 ; from the hydroxyl group of THR
CG2 CB CD2 OD1 gi_2
[dihedrals]
; ai aj ak al gromos type
-C -C N CA gd_4
-C N CA C gd_19
N CA C +N gd_20
N CA CB CG2 gd_17
CA CB OG1 HG1 gd_12
CA CB CG2 CD2 gd_17
CB CG2 OD1 HD1 gd_12
CB CG2 CD2 N gd_17
CG2 CD2 N CA gd_19
; 5-hydroxylysine (0,R)
[KH5]
[atoms]
N N -0.28000 0
H H 0.28000 0
CA CH1 0.00000 1
CB CH2 0.00000 1
CG CH2 0.00000 2
CD CH1 0.15000 3 ; from the hydroxyl group of THR
OE1 OA -0.54800 3 ; from the hydroxyl group of THR
HE1 H 0.39800 3 ; from the hydroxyl group of THR
CE2 CH2 0.00000 4
NZ NT -0.83000 5
HZ1 H 0.41500 5
HZ2 H 0.41500 5
C C 0.380 6
O O -0.380 6
[bonds]
N H gb_2
N CA gb_20
CA C gb_26
C O gb_4
C +N gb_9
CA CB gb_26
CB CG gb_26
CG CD gb_26
CD OE1 gb_17
CD CE2 gb_26
OE1 HE1 gb_1
CE2 NZ gb_20
NZ HZ1 gb_2
NZ HZ2 gb_2
[angles]
; ai aj ak gromos type
-C N H ga_31
H N CA ga_17
-C N CA ga_30
N CA C ga_12
CA C +N ga_18
CA C O ga_29
O C +N ga_32
N CA CB ga_12
C CA CB ga_12
CA CB CG ga_14
CB CG CD ga_14
CG CD OE1 ga_12
CG CD CE2 ga_12
OE1 CD CE2 ga_12
CD OE1 HE1 ga_11
CD CE2 NZ ga_14
CE2 NZ HZ1 ga_10
CE2 NZ HZ2 ga_10
HZ1 NZ HZ2 ga_9
[impropers]
; ai aj ak al gromos type
N -C CA H gi_1
C CA +N O gi_1
CA N C CB gi_2
CD CE2 OE1 CG gi_2
[dihedrals]
; ai aj ak al gromos type
-C -C N CA gd_4
-C N CA C gd_19
N CA C +N gd_20
N CA CB CG gd_17
CA CB CG CD gd_17
CB CG CD CE2 gd_17
CG CD OE1 HE1 gd_12
CG CD CE2 NZ gd_17
CD CE2 NZ HZ1 gd_14
; 5-hydroxylysine (0,S)
[K5H]
[atoms]
N N -0.28000 0
H H 0.28000 0
CA CH1 0.00000 1
CB CH2 0.00000 1
CG CH2 0.00000 2
CD CH1 0.15000 3 ; from the hydroxyl group of THR

```

```

OE1 OA -0.54800 3 ; from the hydroxyl group of THR
HE1 H 0.39800 3 ; from the hydroxyl group of THR
CE2 CH2 0.00000 4
NZ NT -0.83000 5
HZ1 H 0.41500 5
HZ2 H 0.41500 5
C C 0.380 6
O O -0.380 6
[ bonds ]
N H gb_2
N CA gb_20
CA C gb_26
C O gb_4
C +N gb_9
CA CB gb_26
CB CG gb_26
CG CD gb_26
CD OE1 gb_17
CD CE2 gb_26
OE1 HE1 gb_1
CE2 NZ gb_20
NZ HZ1 gb_2
NZ HZ2 gb_2
[ angles ]
; ai aj ak gromos type
-C N H ga_31
H N CA ga_17
-C N CA ga_30
N CA C ga_12
CA C +N ga_18
CA C O ga_29
O C +N ga_32
N CA CB ga_12
C CA CB ga_12
CA CB CG ga_14
CB CG CD ga_14
CG CD OE1 ga_12
CG CD CE2 ga_12
OE1 CD CE2 ga_12
CD OE1 HE1 ga_11
CD CE2 NZ ga_14
CE2 NZ HZ1 ga_10
CE2 NZ HZ2 ga_10
CE2 NZ HZ3 ga_10
HZ1 NZ HZ2 ga_9
HZ1 NZ HZ3 ga_9
HZ2 NZ HZ3 ga_9
[ impropers ]
; ai aj ak al gromos type
N -C CA H gi_1
C CA +N O gi_1
CA N C CB gi_2
CD OE1 CE2 CG gi_2
[ dihedrals ]
; ai aj ak al gromos type
-CA -C N CA gd_4
-C N CA C gd_19
N CA C +N gd_20
N CA CB CG gd_17
CA CB CG CD gd_17
CB CG CD CE2 gd_17
CG CD OE1 HE1 gd_12
CG CD CE2 NZ gd_17
CD CE2 NZ HZ1 gd_14
; 5-hydroxylysine (+1,R)
[ KPH ]
[ atoms ]
N N -0.28000 0
H H 0.28000 0
CA CH1 0.00000 1
CB CH2 0.00000 1
CG CH2 0.00000 2
CD CH1 0.15000 3 ; from the hydroxyl group of THR
OE1 OA -0.54800 3 ; from the hydroxyl group of THR
HE1 H 0.39800 3 ; from the hydroxyl group of THR
CE2 CH2 0.12700 4
NZ NL 0.12900 4
HZ1 H 0.24800 4
HZ2 H 0.24800 4
HZ3 H 0.24800 4
C C 0.380 5
O O -0.380 5
[ bonds ]
N H gb_2
N CA gb_20
CA C gb_26
C O gb_4
C +N gb_9
CA CB gb_26
CB CG gb_26
CG CD gb_26
CD OE1 gb_17
CD CE2 gb_26
OE1 HE1 gb_1
CE2 NZ gb_20
NZ HZ1 gb_2
NZ HZ2 gb_2
NZ HZ3 gb_2
[ angles ]
; ai aj ak gromos type
-C N H ga_31
H N CA ga_17
-C N CA ga_30
N CA C ga_12
CA C +N ga_18
CA C O ga_29
O C +N ga_32
N CA CB ga_12
C CA CB ga_12
CA CB CG ga_14
CB CG CD ga_14
CG CD OE1 ga_12
CG CD CE2 ga_12
OE1 CD CE2 ga_12
CD OE1 HE1 ga_11
CD CE2 NZ ga_14
CE2 NZ HZ1 ga_10
CE2 NZ HZ2 ga_10
CE2 NZ HZ3 ga_10
HZ1 NZ HZ2 ga_9
HZ1 NZ HZ3 ga_9
HZ2 NZ HZ3 ga_9
[ impropers ]
; ai aj ak al gromos type
N -C CA H gi_1
C CA +N O gi_1
CA N C CB gi_2
CD CE2 OE1 CG gi_2
[ dihedrals ]
; ai aj ak al gromos type
-CA -C N CA gd_4
-C N CA C gd_19
N CA C +N gd_20
N CA CB CG gd_17
CA CB CG CD gd_17
CB CG CD CE2 gd_17
CG CD OE1 HE1 gd_12
CG CD CE2 NZ gd_17
CD CE2 NZ HZ1 gd_14
; 5-hydroxylysine (+1,S)
[ KHP ]
[ atoms ]
N N -0.28000 0
H H 0.28000 0
CA CH1 0.00000 1
CB CH2 0.00000 1
CG CH2 0.00000 2
CD CH1 0.15000 3 ; from the hydroxyl group of THR
OE1 OA -0.54800 3 ; from the hydroxyl group of THR
HE1 H 0.39800 3 ; from the hydroxyl group of THR
CE2 CH2 0.12700 4
NZ NL 0.12900 4
HZ1 H 0.24800 4
HZ2 H 0.24800 4
HZ3 H 0.24800 4
C C 0.380 5
O O -0.380 5
[ bonds ]
N H gb_2
N CA gb_20
CA C gb_26
C O gb_4
C +N gb_9
CA CB gb_26
CB CG gb_26
CG CD gb_26
CD OE1 gb_17
CD CE2 gb_26
OE1 HE1 gb_1
CE2 NZ gb_20
NZ HZ1 gb_2
NZ HZ2 gb_2
NZ HZ3 gb_2
[ angles ]
; ai aj ak gromos type
-C N H ga_31
H N CA ga_17
-C N CA ga_30
N CA C ga_12
CA C +N ga_18
CA C O ga_29
O C +N ga_32
N CA CB ga_12
C CA CB ga_12
CA CB CG ga_14
CB CG CD ga_14
CG CD OE1 ga_12
CG CD CE2 ga_12
OE1 CD CE2 ga_12
CD OE1 HE1 ga_11
CD CE2 NZ ga_14
CE2 NZ HZ1 ga_10
CE2 NZ HZ2 ga_10
CE2 NZ HZ3 ga_10
HZ1 NZ HZ2 ga_9
HZ1 NZ HZ3 ga_9
HZ2 NZ HZ3 ga_9

```

```

CG CD CE2 ga_12
OE1 CD CE2 ga_12
CD OE1 HE1 ga_11
CD CE2 NZ ga_14
CE2 NZ HZ1 ga_10
CE2 NZ HZ2 ga_10
CE2 NZ HZ3 ga_10
HZ1 NZ HZ2 ga_9
HZ1 NZ HZ3 ga_9
HZ2 NZ HZ3 ga_9
[impropers]
; ai aj ak al gromos type
N -C CA H gi_1
C CA +N O gi_1
CA N C CB gi_2
CD OE1 CE2 CG gi_2
[dihedrals]
; ai aj ak al gromos type
-C -C N CA gd_4
-C N CA C gd_19
N CA C +N gd_20
N CA CB CG gd_17
CA CB CG CD gd_17
CB CG CD CE2 gd_17
CG CD OE1 HE1 gd_17
CG CD CE2 NZ gd_17
CD CE2 NZ HZ1 gd_14

; 3,4-dihydroxyphenylalanine
[HTY]
[atoms]
N N -0.28000 0
H H 0.28000 0
CA CH1 0.00000 1
CB CH2 0.00000 1
CG C 0.00000 1
CD1 C -0.10000 2
HD1 HC 0.10000 2
CD2 C -0.10000 3
HD2 HC 0.10000 3
CE1 C 0.15000 4 ; from the hydroxyl group of TYR
OZ1 OA -0.54800 4 ; from the hydroxyl group of TYR
HZ1 H 0.39800 4 ; from the hydroxyl group of TYR
CE2 C -0.10000 5
HE2 HC 0.10000 5
CZ2 C 0.15000 6 ; from the hydroxyl group of TYR
OH OA -0.54800 6 ; from the hydroxyl group of TYR
HH H 0.39800 6 ; from the hydroxyl group of TYR
C C 0.380 7
O O -0.380 7
[bonds]
N H gb_2
N CA gb_20
CA C gb_26
C O gb_4
C +N gb_9
CA CB gb_26
CB CG gb_26
CG CD1 gb_15
CG CD2 gb_15
CD1 HD1 gb_3
CD1 CE1 gb_15
CD2 HD2 gb_3
CD2 CE2 gb_15
CE1 CZ2 gb_15
CE1 OZ1 gb_12
OZ1 HZ1 gb_1
CE2 HE2 gb_3
CE2 CZ2 gb_15
CZ2 OH gb_12
OH HH gb_1
[exclusions]
; ai aj
CB HD1
CB HD2
CB CE1
CB CE2
CG OZ1
CG HE2
CG CZ2
CD1 HD2
CD1 CE2
CD1 OH
HD1 CD2
HD1 OZ1
HD1 CZ2
CD2 CE1
CD2 OH
HD2 HE2
HD2 CZ2
CE1 HE2
OZ1 CE2
OZ1 OH
HE2 OH
HH OZ1
HH HZ1
HZ1 OH
[angles]
; ai aj ak gromos type
-C N H ga_31
H N CA ga_17
-C N CA ga_30
N CA C ga_12
CA C +N ga_18
CA C O ga_29
O C +N ga_32
N CA CB ga_12
C CA CB ga_12
CA CB CG ga_14
CB CG CD1 ga_26
CB CG CD2 ga_26
CD1 CG CD2 ga_26
CG CD1 HD1 ga_24
HD1 CD1 CE1 ga_24
CG CD1 CE1 ga_26
CG CD2 HD2 ga_24
HD2 CD2 CE2 ga_24
CG CD2 CE2 ga_26
CD1 CE1 OZ1 ga_26
CD1 CE1 CZ2 ga_26
OZ1 CE1 CZ2 ga_26
CE1 OZ1 HZ1 ga_11
CD2 CE2 HE2 ga_24
HE2 CE2 CZ2 ga_24
CD2 CE2 CZ2 ga_26
CE1 CZ2 CE2 ga_26
CE1 CZ2 OH ga_26
CE2 CZ2 OH ga_26
CZ2 OH HH ga_11
[impropers]
; ai aj ak al gromos type
N -C CA H gi_1
C CA +N O gi_1
CA N C CB gi_2
CG CD1 CD2 CB gi_1
CD2 CG CD1 CE1 gi_1
CD1 CG CD2 CE2 gi_1
CG CD1 CE1 CZ2 gi_1
CG CD2 CE2 CZ2 gi_1
CD1 CE1 CZ2 CE2 gi_1
CD2 CE2 CZ2 CE1 gi_1
CD1 CG CE1 HD1 gi_1
CD2 CG CE2 HD2 gi_1
CE1 CZ2 CD1 OZ1 gi_1
CE2 CZ2 CD2 HE2 gi_1
CZ2 CE1 CE2 OH gi_1
[dihedrals]
; ai aj ak al gromos type
-C -C N CA gd_4
-C N CA C gd_19
N CA C +N gd_20
N CA CB CG gd_17
CA CB CG CD1 gd_20
CD1 CE1 OZ1 HZ1 gd_2
CE1 CZ2 OH HH gd_2

; 7-hydroxytryptophan
[W7H]
[atoms]
N N -0.28000 0
H H 0.28000 0
CA CH1 0.00000 1
CB CH2 0.00000 1
CG C -0.14000 2
CD1 C -0.10000 2
HD1 HC 0.10000 2
CD2 C 0.00000 2
NE1 NR -0.05000 2
HE1 H 0.19000 2
CE2 C 0.00000 2
CE3 C -0.10000 3
HE3 HC 0.10000 3
CZ2 C 0.15000 4 ; from the hydroxyl group of TYR
OH2 OA -0.54800 4 ; from the hydroxyl group of TYR
HH2 H 0.39800 4 ; from the hydroxyl group of TYR
CZ3 C -0.10000 5
HZ3 HC 0.10000 5
CH3 C -0.10000 6
HH3 HC 0.10000 6
C C 0.380 7
O O -0.380 7
[bonds]
N H gb_2
N CA gb_20
CA C gb_26
C O gb_4

```

```

C +N gb_9
CA CB gb_26
CB CG gb_26
CG CD1 gb_9
CG CD2 gb_15
CD1 HD1 gb_3
CD1 NE1 gb_9
CD2 CE2 gb_15
CD2 CE3 gb_15
NE1 HE1 gb_2
NE1 CE2 gb_9
CE2 CZ2 gb_15
CE3 HE3 gb_3
CE3 CZ3 gb_15
CZ2 OH2 gb_12
CZ2 CH3 gb_15
CZ3 HZ3 gb_3
CZ3 CH3 gb_15
OH2 HH2 gb_1
CH3 HH3 gb_3
[ exclusions ]
; ai aj
CB HD1
CB NE1
CB CE2
CB CE3
CG HE1
CG HE3
CG CZ2
CG CZ3
CD1 CE3
CD1 CZ2
HD1 CD2
HD1 HE1
HD1 CE2
CD2 HE1
CD2 HZ3
CD2 OH2
CD2 CH3
NE1 CE3
NE1 OH2
NE1 CH3
HE1 CZ2
CE2 HE3
CE2 CZ3
CE2 HH3
CE3 CZ2
CE3 HH3
HE3 HZ3
HE3 CH3
CZ2 HZ3
CZ3 OH2
HZ3 HH3
OH2 HH3
[ angles ]
; ai aj ak gromos type
-C N H ga_31
H N CA ga_17
-C N CA ga_30
N CA C ga_12
CA C +N ga_18
CA C O ga_29
O C +N ga_32
N CA CB ga_12
C CA CB ga_12
CA CB CG ga_14
CB CG CD1 ga_36
CB CG CD2 ga_36
CD1 CG CD2 ga_6
CG CD1 HD1 ga_35
HD1 CD1 NE1 ga_35
CG CD1 NE1 ga_6
CG CD2 CE2 ga_6
CD1 NE1 CE2 ga_6
CD1 NE1 HE1 ga_35
HE1 NE1 CE2 ga_35
NE1 CE2 CD2 ga_6
CG CD2 CE3 ga_38
NE1 CE2 CZ2 ga_38
CD2 CE2 CZ2 ga_26
CE2 CD2 CE3 ga_26
CD2 CE3 HE3 ga_24
HE3 CE3 CZ3 ga_24
CD2 CE3 CZ3 ga_26
CE2 CZ2 OH2 ga_26
CE2 CZ2 CH3 ga_26
OH2 CZ2 CH3 ga_26
CE3 CZ3 HZ3 ga_24
HZ3 CZ3 CH3 ga_24
CE3 CZ3 CH3 ga_26
CZ2 OH2 HH2 ga_11
CZ2 CH3 HH3 ga_24
HH3 CH3 CZ3 ga_24

CZ2 CH3 CZ3 ga_26
[ impropers ]
; ai aj ak al gromos type
N -C CA H gi_1
C CA +N O gi_1
CA N C CB gi_2
CG CD1 CD2 CB gi_1
CD2 CG CD1 NE1 gi_1
CD1 CG CD2 CE2 gi_1
CG CD1 NE1 CE2 gi_1
CG CD2 CE2 NE1 gi_1
CD1 NE1 CE2 CD2 gi_1
CD1 CG NE1 HD1 gi_1
NE1 CD1 CE2 HE1 gi_1
CD2 CE2 CE3 CG gi_1
CE2 CD2 CZ2 NE1 gi_1
CE3 CD2 CE2 CZ2 gi_1
CD2 CE2 CZ2 CH3 gi_1
CE2 CD2 CE3 CZ3 gi_1
CE2 CZ2 CH3 CZ3 gi_1
CD2 CE3 CZ3 CH3 gi_1
CE3 CZ3 CH3 CZ2 gi_1
CE3 CD2 CZ3 HE3 gi_1
CZ2 CE2 CH3 OH2 gi_1
CZ3 CE3 CH3 HZ3 gi_1
CH3 CZ2 CZ3 HH3 gi_1
[ dihedrals ]
; ai aj ak al gromos type
-CA -C N CA gd_4
-C N CA C gd_19
N CA C +N gd_20
N CA CB CG gd_17
CA CB CG CD2 gd_20
CE2 CZ2 OH2 HH2 gd_2

; 3-hydroxyaspartate (-1,R)
[ DH3 ]
[ atoms ]
N N -0.28000 0
H H 0.28000 0
CA CH1 0.00000 1
CB CH1 0.15000 2 ; from the hydroxyl group of THR
OG1 OA -0.54800 2 ; from the hydroxyl group of THR
HG1 H 0.39800 2 ; from the hydroxyl group of THR
CG2 C 0.27000 3
OD1 OM -0.63500 3
OD2 OM -0.63500 3
C C 0.380 4
O O -0.380 4
[ bonds ]
N H gb_2
N CA gb_20
CA C gb_26
C O gb_4
C +N gb_9
CA CB gb_26
CB OG1 gb_17
CB CG2 gb_26
OG1 HG1 gb_1
CG2 OD1 gb_5
CG2 OD2 gb_5
[ angles ]
; ai aj ak gromos type
-C N H ga_31
H N CA ga_17
-C N CA ga_30
N CA C ga_12
CA C +N ga_18
CA C O ga_29
O C +N ga_32
N CA CB ga_12
C CA CB ga_12
CA CB CG ga_14
CA CB CD1 ga_36
CB CG CD2 ga_36
CD1 CG CD2 ga_6
CG CD1 HD1 ga_35
HD1 CD1 NE1 ga_35
CG CD1 NE1 ga_6
CG CD2 CE2 ga_6
CD1 NE1 CE2 ga_6
CD1 NE1 HE1 ga_35
HE1 NE1 CE2 ga_35
NE1 CE2 CD2 ga_6
CG CD2 CE3 ga_38
NE1 CE2 CZ2 ga_38
CD2 CE2 CZ2 ga_26
CE2 CD2 CE3 ga_26
CD2 CE3 HE3 ga_24
HE3 CE3 CZ3 ga_24
CD2 CE3 CZ3 ga_26
CE2 CZ2 OH2 ga_26
CE2 CZ2 CH3 ga_26
OH2 CZ2 CH3 ga_26
CE3 CZ3 HZ3 ga_24
HZ3 CZ3 CH3 ga_24
CE3 CZ3 CH3 ga_26
CZ2 OH2 HH2 ga_11
CZ2 CH3 HH3 ga_24
HH3 CH3 CZ3 ga_24

[ impropers ]
; ai aj ak al gromos type
N -C CA H gi_1
C CA +N O gi_1
CA N C CB gi_2
CB CG2 OG1 CA gi_2
CG2 OD1 OD2 CB gi_1
[ dihedrals ]
; ai aj ak al gromos type
-CA -C N CA gd_4
-C N CA C gd_19
N CA C +N gd_20
N CA CB CG2 gd_17
CA CB OG1 HG1 gd_12

```

```

CA CB CG2 OD1 gd_20
; 3-hydroxyaspartate (-1,S)
[D3H]
[atoms]
N N -0.28000 0
H H 0.28000 0
CA CH1 0.00000 1
CB CH1 0.15000 2; from the hydroxyl group of THR
OG1 OA -0.54800 2; from the hydroxyl group of THR
HG1 H 0.39800 2; from the hydroxyl group of THR
CG2 C 0.27000 3
OD1 OM -0.63500 3
OD2 OM -0.63500 3
C C 0.380 4
O O -0.380 4
[bonds]
N H gb_2
N CA gb_20
CA C gb_26
C O gb_4
C +N gb_9
CA CB gb_26
CB OG1 gb_17
CB CG2 gb_26
OG1 HG1 gb_1
CG2 OD1 gb_5
CG2 OD2 gb_5
[angles]
; ai aj ak gromos type
-C N H ga_31
H N CA ga_17
-C N CA ga_30
N CA C ga_12
CA C +N ga_18
CA C O ga_29
O C +N ga_32
N CA CB ga_12
C CA CB ga_12
CA CB OG1 ga_12
CA CB CG2 ga_12
OG1 CB CG2 ga_12
CB OG1 HG1 ga_11
CB CG2 OD1 ga_21
CB CG2 OD2 ga_21
OD1 CG2 OD2 ga_37
[impropers]
; ai aj ak al gromos type
N -C CA H gi_1
C CA +N O gi_1
CA N C CB gi_2
CB OG1 CG2 CA gi_2
CG2 OD1 OD2 CB gi_1
[dihedrals]
; ai aj ak al gromos type
-CA -C N CA gd_4
-C N CA C gd_19
N CA C +N gd_20
N CA CB CG2 gd_17
CA CB OG1 HG1 gd_12
CA CB CG2 OD2 gd_20
CB CG2 OD2 HD2 gd_3
; 3-hydroxyaspartate (0,S)
[D3N]
[atoms]
N N -0.28000 0
H H 0.28000 0
CA CH1 0.00000 1
CB CH1 0.15000 2; from the hydroxyl group of THR
OG1 OA -0.54800 2; from the hydroxyl group of THR
HG1 H 0.39800 2; from the hydroxyl group of THR
CG2 C 0.53000 3
OD1 O -0.38000 3
OD2 OA -0.54800 3
HD2 H 0.39800 3
C C 0.380 4
O O -0.380 4
[bonds]
N H gb_2
N CA gb_20
CA C gb_26
C O gb_4
C +N gb_9
CA CB gb_26
CB OG1 gb_17
CB CG2 gb_26
OG1 HG1 gb_1
CG2 OD1 gb_4
CG2 OD2 gb_12
OD2 HD2 gb_1
[angles]
; ai aj ak gromos type
-C N H ga_31
H N CA ga_17
-C N CA ga_30
N CA C ga_12
CA C +N ga_18
CA C O ga_29
O C +N ga_32
N CA CB ga_12
C CA CB ga_12
CA CB OG1 ga_12
CA CB CG2 ga_12
OG1 CB CG2 ga_12
CB OG1 HG1 ga_11
CB CG2 OD1 ga_29
CB CG2 OD2 ga_18
OD1 CG2 OD2 ga_32
CG2 OD2 HD2 ga_11
[impropers]
; ai aj ak al gromos type
N -C CA H gi_1
C CA +N O gi_1
CA N C CB gi_2
CB OG1 CG2 CA gi_2
CG2 OD1 OD2 CB gi_1
[dihedrals]
; ai aj ak al gromos type
-CA -C N CA gd_4
-C N CA C gd_19
N CA C +N gd_20
N CA CB CG2 gd_17
CA CB OG1 HG1 gd_12
CA CB CG2 OD1 gd_20
; 3-hydroxyaspartate (0,R)
[DN3]
[atoms]
N N -0.28000 0
H H 0.28000 0
CA CH1 0.00000 1
CB CH1 0.15000 2; from the hydroxyl group of THR
OG1 OA -0.54800 2; from the hydroxyl group of THR
HG1 H 0.39800 2; from the hydroxyl group of THR
CG2 C 0.53000 3
OD1 O -0.38000 3
OD2 OA -0.54800 3
HD2 H 0.39800 3
C C 0.380 4
O O -0.380 4
[bonds]
N H gb_2
N CA gb_20
CA C gb_26
C O gb_4
C +N gb_9
CA CB gb_26
CB OG1 gb_17
CB CG2 gb_26
OG1 HG1 gb_1
CG2 OD1 gb_4
CG2 OD2 gb_12
OD2 HD2 gb_1
[angles]
; ai aj ak gromos type
-C N H ga_31
H N CA ga_17
-C N CA ga_30
N CA C ga_12
CA C +N ga_18
CA C O ga_29
O C +N ga_32
N CA CB ga_12
C CA CB ga_12
CA CB OG1 ga_12
CA CB CG2 ga_12
OG1 CB CG2 ga_12
CB OG1 HG1 ga_11
CB CG2 OD1 ga_29
CB CG2 OD2 ga_18
OD1 CG2 OD2 ga_32
CG2 OD2 HD2 ga_11
[impropers]
; ai aj ak al gromos type
N -C CA H gi_1
C CA +N O gi_1
CA N C CB gi_2
CB OG1 CG2 CA gi_2
CG2 OD1 OD2 CB gi_1
[dihedrals]
; ai aj ak al gromos type
-CA -C N CA gd_4
-C N CA C gd_19
N CA C +N gd_20
N CA CB CG2 gd_17

```

```

CA CB OG1 HG1 gd_12
CA CB CG2 OD2 gd_20
CB CG2 OD2 HD2 gd_3

;3-hydroxyasparagine (R)
[N3H]
[atoms]
  N N -0.28000 0
  H H 0.28000 0
  CA CH1 0.00000 1
  CB CH1 0.15000 2; from the hydroxyl group of THR
  OG1 OA -0.54800 2; from the hydroxyl group of THR
  HG1 H 0.39800 2; from the hydroxyl group of THR
  CG2 C 0.38000 3
  OD1 O -0.38000 3
  ND2 NT -0.83000 4
  HD21 H 0.41500 4
  HD22 H 0.41500 4
  C C 0.380 5
  O O -0.380 5
[bonds]
  N H gb_2
  N CA gb_20
  CA C gb_26
  C O gb_4
  C +N gb_9
  CA CB gb_26
  CB OG1 gb_17
  CB CG2 gb_26
  OG1 HG1 gb_1
  CG2 OD1 gb_4
  CG2 ND2 gb_8
  ND2 HD21 gb_2
  ND2 HD22 gb_2
[angles]
; ai aj ak gromos type
-C N H ga_31
H N CA ga_17
-C N CA ga_30
N CA C ga_12
CA C +N ga_18
CA C O ga_29
O C +N ga_32
N CA CB ga_12
C CA CB ga_12
CA CB CG2 ga_12
CA CB OG1 ga_12
OG1 CB CG2 ga_12
CB OG1 HG1 ga_11
CB CG2 OD1 ga_29
CB CG2 ND2 ga_18
OD1 CG2 ND2 ga_32
CG2 ND2 HD21 ga_22
CG2 ND2 HD22 ga_22
HD21 ND2 HD22 ga_23
[impropers]
; ai aj ak al gromos type
N -C CA H gi_1
C CA +N O gi_1
CA N C CB gi_2
CB OG1 CG2 CA gi_2
CG2 OD1 ND2 CB gi_1
ND2 HD21 HD22 CG2 gi_1
[dihedrals]
; ai aj ak al gromos type
-CA -C N CA gd_4
-C N CA C gd_19
N CA C +N gd_20
N CA CB CG2 gd_17
CA CB OG1 HG1 gd_12
CA CB CG2 ND2 gd_20
CB CG2 ND2 HD21 gd_4

;4-carboxylglutamate (-2)
[ECA]
[atoms]
  N N -0.28000 0
  H H 0.28000 0
  CA CH1 0.00000 1
  CB CH2 0.00000 1
  CG CH1 0.00000 1
  CD1 C 0.27000 2
  OE1 OM -0.63500 2
  OE2 OM -0.63500 2
  CD2 C 0.27000 3; from GLU
  OE3 OM -0.63500 3; from GLU
  OE4 OM -0.63500 3; from GLU
  C C 0.380 4
  O O -0.380 4
[bonds]
  N H gb_2
  N CA gb_20
  CA C gb_26
  C O gb_4
  C +N gb_9
  CA CB gb_26
  CB CG gb_26
  CG CD1 gb_26
  CD1 OE1 gb_5
  CD1 OE2 gb_5
  CG CD2 gb_26
  CD2 OE3 gb_5
  CD2 OE4 gb_5
[angles]
; ai aj ak gromos type
-C N H ga_31
H N CA ga_17
-C N CA ga_30
N CA C ga_12
CA C +N ga_18
CA C O ga_29
O C +N ga_32
N CA CB ga_12
C CA CB ga_12
CA CB CG ga_14
CB CG CD1 ga_12
CB CG CD2 ga_12

;3-hydroxyasparagine (S)
[NH3]
[atoms]
  N N -0.28000 0
  H H 0.28000 0
  CA CH1 0.00000 1
  CB CH1 0.15000 2; from the hydroxyl group of THR
  OG1 OA -0.54800 2; from the hydroxyl group of THR
  HG1 H 0.39800 2; from the hydroxyl group of THR
  CG2 C 0.38000 3
  OD1 O -0.38000 3
  ND2 NT -0.83000 4
  HD21 H 0.41500 4
  HD22 H 0.41500 4
  C C 0.380 5
  O O -0.380 5
[bonds]
  N H gb_2
  N CA gb_20
  CA C gb_26

```

```

CD1 CG CD2 ga_12
CG CD1 OE1 ga_21
CG CD1 OE2 ga_21
OE1 CD1 OE2 ga_37
CG CD2 OE3 ga_21
CG CD2 OE4 ga_21
OE3 CD2 OE4 ga_37
[impropers]
; ai aj ak al gromos type
N -C CA H gi_1
C CA +N O gi_1
CA N C CB gi_2
CG CD1 CD2 CB gi_2
CD1 OE1 OE2 CG gi_1
CD2 OE3 OE4 CG gi_1
[dihedrals]
; ai aj ak al gromos type
-CA -C N CA gd_4
-C N CA C gd_19
N CA C +N gd_20
N CA CB CG gd_17
CA CB CG CD1 gd_17
CB CG CD1 OE2 gd_20
CB CG CD2 OE4 gd_20

; 4-carboxyglutamate (-1)
[ECN]
[atoms]
N N -0.28000 0
H H 0.28000 0
CA CH1 0.00000 1
CB CH2 0.00000 1
CG CH1 0.00000 1
CD1 C 0.53000 2; from GLUH
OE1 O -0.38000 2; from GLUH
OE2 OA -0.54800 2; from GLUH
HE2 H 0.39800 2; from GLUH
CD2 C 0.27000 3
OE3 OM -0.63500 3
OE4 OM -0.63500 3
C C 0.380 4
O O -0.380 4
[bonds]
N H gb_2
N CA gb_20
CA C gb_26
C O gb_4
C +N gb_9
CA CB gb_26
CB CG gb_26
CG CD1 gb_26
CD1 OE1 gb_4
CD1 OE2 gb_12
OE2 HE2 gb_1
CG CD2 gb_26
CD2 OE3 gb_5
CD2 OE4 gb_5
[angles]
; ai aj ak gromos type
-C N H ga_31
H N CA ga_17
-C N CA ga_30
N CA C ga_12
CA C +N ga_18
CA C O ga_29
O C +N ga_32
N CA CB ga_12
C CA CB ga_12
CA CB CG ga_14
CB CG CD1 ga_12
CB CG CD2 ga_12
CD1 CG CD2 ga_12
CG CD1 OE1 ga_29
CG CD1 OE2 ga_18
OE1 CD1 OE2 ga_32
CD1 OE2 HE2 ga_11
CG CD2 OE3 ga_21
CG CD2 OE4 ga_21
OE3 CD2 OE4 ga_37
[impropers]
; ai aj ak al gromos type
N -C CA H gi_1
C CA +N O gi_1
CA N C CB gi_2
CG CD1 CD2 CB gi_2
CD1 OE1 OE2 CG gi_1
CD2 OE3 OE4 CG gi_1
[dihedrals]
; ai aj ak al gromos type
-CA -C N CA gd_4
-C N CA C gd_19
N CA C +N gd_20
N CA CB CG gd_17
CA CB CG CD1 gd_17
CB CG CD1 OE2 gd_20
CB CG CD2 OE4 gd_20

CA CB CG CD1 gd_17
CB CG CD1 OE2 gd_20
CG CD1 OE2 HE2 gd_3
CB CG CD2 OE4 gd_20

; sulfotyrosine
[YSU]
[atoms]
N N -0.28000 0
H H 0.28000 0
CA CH1 0.00000 1
CB CH2 0.00000 1
CG C 0.00000 1
CD1 C -0.10000 2
HD1 HC 0.10000 2
CD2 C -0.10000 3
HD2 HC 0.10000 3
CE1 C -0.10000 4
HE1 HC 0.10000 4
CE2 C -0.10000 5
HE2 HC 0.10000 5
CZ C 0.15000 6; from the carbon atom attached to the phosphate group of
nucleotides (e.g., ATP)
OH OA -0.36000 6; from the phosphate group of nucleotides (e.g., ATP)
ST S 1.11500 6; to add up to -1 net charge
OI1 OM -0.63500 6; from the phosphate group of nucleotides (e.g., ATP)
OI2 OM -0.63500 6; from the phosphate group of nucleotides (e.g., ATP)
OI3 OM -0.63500 6; from the phosphate group of nucleotides (e.g., ATP)
C C 0.380 7
O O -0.380 7
[bonds]
N H gb_2
N CA gb_20
CA C gb_26
C O gb_4
C +N gb_9
CA CB gb_26
CB CG gb_26
CG CD1 gb_15
CG CD2 gb_15
CD1 HD1 gb_3
CD1 CE1 gb_15
CD2 HD2 gb_3
CD2 CE2 gb_15
CE1 HE1 gb_3
CE1 CZ gb_15
CE2 HE2 gb_3
CE2 CZ gb_15
CZ OH gb_12
OH ST gb_24
ST OI1 gb_24
ST OI2 gb_24
ST OI3 gb_24
[exclusions]
; ai aj
CB HD1
CB HD2
CB CE1
CB CE2
CG HE1
CG HE2
CG CZ
CD1 HD2
CD1 CE2
CD1 OH
HD1 CD2
HD1 HE1
HD1 CZ
CD2 CE1
CD2 OH
HD2 HE2
HD2 CZ
CE1 HE2
HE1 CE2
HE1 OH
HE2 OH
[angles]
; ai aj ak gromos type
-C N H ga_31
H N CA ga_17
-C N CA ga_30
N CA C ga_12
CA C +N ga_18
CA C O ga_29
O C +N ga_32
N CA CB ga_12
C CA CB ga_12
CA CB CG ga_14
CB CG CD1 ga_12
CB CG CD2 ga_12
CD1 CG CD2 ga_12
CG CD1 OE1 ga_29
CG CD1 OE2 ga_18
OE1 CD1 OE2 ga_32
CD1 OE2 HE2 ga_11
CG CD2 OE3 ga_21
CG CD2 OE4 ga_21
OE3 CD2 OE4 ga_37
[impropers]
; ai aj ak al gromos type
N -C CA H gi_1
C CA +N O gi_1
CA N C CB gi_2
CG CD1 CD2 CB gi_2
CD1 OE1 OE2 CG gi_1
CD2 OE3 OE4 CG gi_1
[dihedrals]
; ai aj ak al gromos type
-CA -C N CA gd_4
-C N CA C gd_19
N CA C +N gd_20
N CA CB CG gd_17
CA CB CG CD1 gd_17
CB CG CD1 OE2 gd_20
CB CG CD2 OE4 gd_20

```

```

CG CD1 CE1 ga_26
CG CD2 HD2 ga_24
HD2 CD2 CE2 ga_24
CG CD2 CE2 ga_26
CD1 CE1 HE1 ga_24
HE1 CE1 CZ ga_24
CD1 CE1 CZ ga_26
CD2 CE2 HE2 ga_24
HE2 CE2 CZ ga_24
CD2 CE2 CZ ga_26
CE1 CZ CE2 ga_26
CE1 CZ OH ga_26
CE2 CZ OH ga_26
CZ OH ST ga_11
OH ST OI1 ga_12
OH ST OI2 ga_12
OH ST OI3 ga_12
OI1 ST OI2 ga_12
OI1 ST OI3 ga_12
OI2 ST OI3 ga_12
[impropers]
; ai aj ak al gromos type
N -C CA H gi_1
C CA +N O gi_1
CA N C CB gi_2
CG CD1 CD2 CB gi_1
CD2 CG CD1 CE1 gi_1
CD1 CG CD2 CE2 gi_1
CG CD1 CE1 CZ gi_1
CG CD2 CE2 CZ gi_1
CD1 CE1 CZ CE2 gi_1
CD2 CE2 CZ CE1 gi_1
CD1 CG CE1 HD1 gi_1
CD2 CG CE2 HD2 gi_1
CE1 CZ CD1 HE1 gi_1
CE2 CZ CD2 HE2 gi_1
CZ CE1 CE2 OH gi_1
[dihedrals]
; ai aj ak al gromos type
-C A -C N CA gd_4
-C N CA C gd_19
N CA C +N gd_20
N CA CB CG gd_17
CA CB CG CD1 gd_20
CE1 CZ OH ST gd_2
CZ OH ST OI1 gd_20
; dehydroalanine
[SDH]
[atoms]
N N -0.28000 0
H H 0.28000 0
CA CH0 0.00000 1; from aliphatic carbon atoms
CB CH2 0.00000 1; from aliphatic carbon atoms
C C 0.380 2
O O -0.380 2
[bonds]
N H gb_2
N CA gb_20
CA C gb_26
C O gb_4
C +N gb_9
CA CB gb_9 ; a shorter bond type to mimic double bond properties
[angles]
; ai aj ak gromos type
-C N H ga_31
H N CA ga_17
-C N CA ga_30
N CA C ga_26
CA C +N ga_18
CA C O ga_29
O C +N ga_32
N CA CB ga_26
C CA CB ga_26
[impropers]
; ai aj ak al gromos type
N -C CA H gi_1
C CA +N O gi_1
CA N C CB gi_1
[dihedrals]
; ai aj ak al gromos type
-C A -C N CA gd_4
-C N CA C gd_19
N CA C +N gd_20
N CA CB CG gd_17
; 2,3-dihydrobutyrine
[TDH]
[atoms]
N N -0.28000 0
H H 0.28000 0
CA CH0 0.00000 1; from aliphatic carbon atoms
CB CH1 0.00000 2; from aliphatic carbon atoms
CG CH3 0.00000 2
C C 0.380 3
O O -0.380 3
[bonds]
N H gb_2
N CA gb_20
CA C gb_26
C O gb_4
C +N gb_9
CA CB gb_9 ; a shorter bond type to mimic double bond properties
[angles]
; ai aj ak gromos type
-C N H ga_31
H N CA ga_17
-C N CA ga_30
N CA C ga_26
CA C +N ga_18
CA C O ga_29
O C +N ga_32
N CA CB ga_26
C CA CB ga_26
[impropers]
; ai aj ak al gromos type
N -C CA H gi_1
C CA +N O gi_1
CA N C CB gi_1
[dihedrals]
; ai aj ak al gromos type
-C A -C N CA gd_4
-C N CA C gd_19
N CA C +N gd_20
N CA CB CG gd_17
; 6-bromotryptophan
[WBR]
[atoms]
N N -0.28000 0
H H 0.28000 0
CA CH1 0.00000 1
CB CH2 0.00000 1
CG C -0.14000 2
CD1 C -0.10000 2
HD1 HC 0.10000 2
CD2 C 0.00000 2
NE1 NR -0.05000 2
HE1 H 0.19000 2
CE2 C 0.00000 2
CE3 C -0.10000 3
HE3 HC 0.10000 3
CZ2 C -0.10000 4
HZ2 HC 0.10000 4
CZ3 C -0.10000 5
HZ3 HC 0.10000 5
CH2 C 0.05500 6; from 8-bromo-guanosine reported by Hritz and
Oostenbrink. DOI:10.1021/jp902968m
BRT BR -0.05500 6; from 8-bromo-guanosine reported by Hritz and
Oostenbrink. DOI:10.1021/jp902968m
C C 0.380 7
O O -0.380 7
[bonds]
N H gb_2
N CA gb_20
CA C gb_26
C O gb_4
C +N gb_9
CA CB gb_26
CB CG gb_26
CG CD1 gb_9
CG CD2 gb_15
CD1 HD1 gb_3
CD1 NE1 gb_9
CD2 CE2 gb_15
CD2 CE3 gb_15
NE1 HE1 gb_2
NE1 CE2 gb_9
CE2 CZ2 gb_15
CE3 HE3 gb_3
CE3 CZ3 gb_15
CZ2 HZ2 gb_3
CZ2 CH2 gb_15
CZ3 HZ3 gb_3
CZ3 CH2 gb_15
CH2 BRT gb_39
[exclusions]
; ai aj
CB HD1
CB NE1
CB CE2
CB CE3
CG HE1
CG HE3
CG CZ2

```





```

N CA C ga_12
CA C +N ga_18
CA C O ga_29
O C +N ga_32
N CA CB ga_12
C CA CB ga_12
CA CB CG ga_14
CB CG CD ga_14
CG CD NE ga_12
CD NE HE ga_17
HE NE CZ ga_31
CD NE CZ ga_30
NE CZ OH1 ga_21
NE CZ NH2 ga_29
OH1 CZ NH2 ga_21
CZ NH2 HH21 ga_22
CZ NH2 HH22 ga_22
HH21 NH2 HH22 ga_23
[ impropers ]
; ai aj ak al gromos type
N -C CA H gi_1
C CA +N O gi_1
CA N C CB gi_2
NE CD CZ HE gi_1
CZ OH1 NH2 NE gi_1
NH2 HH21 HH22 CZ gi_1
[ dihedrals ]
; ai aj ak al gromos type
-CA -C N CA gd_4
-C N CA C gd_19
N CA C +N gd_20
N CA CB CG gd_17
CA CB CG CD gd_17
CB CG CD NE gd_17
CG CD NE CZ gd_19
CD NE CZ NH2 gd_4
NE CZ NH2 HH21 gd_4

; allysine (aminoadipic semialdehyde)
[ KAL ]
[ atoms ]
N N -0.28000 0
H H 0.28000 0
CA CH1 0.00000 1
CB CH2 0.00000 1
CG CH2 0.00000 2
CD CH2 0.00000 2
CE C 0.28000 3 ; by analogy to the aldehyde group reported by Dolenc et al.
DOI: 10.1093/nar/gki195
OZ O -0.38000 3 ; from the carbonyl group (of e.g., GLN)
HE HC 0.10000 3 ; by analogy to the aldehyde group reported by Dolenc et al.
DOI: 10.1093/nar/gki195
C C 0.380 4
O O -0.380 4
[ bonds ]
N H gb_2
N CA gb_20
CA C gb_26
C O gb_4
C +N gb_9
CA CB gb_26
CB CG gb_26
CG CD gb_26
CD CE gb_26
CE HE gb_3
CE OZ gb_4
[ angles ]
; ai aj ak gromos type
-C N H ga_31
H N CA ga_17
-C N CA ga_30
N CA C ga_12
CA C +N ga_18
CA C O ga_29
O C +N ga_32
N CA CB ga_12
C CA CB ga_12
CA CB CG ga_14
CB CG CD ga_14
CG CD CE ga_14
CD CE HE ga_24
HE CE OZ ga_24
CD CE OZ ga_26
[ impropers ]
; ai aj ak al gromos type
N -C CA H gi_1
C CA +N O gi_1
CA N C CB gi_2
CE OZ CD HE gi_1
[ dihedrals ]
; ai aj ak al gromos type
-CA -C N CA gd_4
-C N CA C gd_19
N CA C +N gd_20
N CA CB CG gd_17
CA CB CG CD gd_17
CB CG CD NE gd_17
CG CD NE CZ gd_19
CD NE CZ NH2 gd_4
NE CZ NH2 HH21 gd_4

N CA C +N gd_20
N CA CB CG gd_17
CA CB CG CD gd_17
CB CG CD CE gd_17
CG CD CE OZ gd_20
; N-acetylglucosamine (N4-linked to ASN)
[ NNG ]
[ atoms ]
N N -0.28000 0
H H 0.28000 0
CA CH1 0.00000 1
CB CH2 0.00000 1
CG C 0.38000 2
OD1 O -0.38000 2
ND2 N -0.28000 3
HD2 H 0.28000 3
C1 CH1 0.18000 4 ; 0.36 charge divided between C1 and C5 to add up to 0 net
charge, also used in other building blocks (e.g., TMP)
O5 OA -0.36000 4 ; from carbohydrates (e.g., GALB)
C5 CH1 0.18000 4 ; 0.36 charge divided between C1 and C5 to add up to 0 net
charge, also used in other building blocks (e.g., TMP)
C6 CH2 0.15000 5 ; from carbohydrates (e.g., GALB)
O6 OA -0.54800 5 ; from carbohydrates (e.g., GALB)
HO6 H 0.39800 5 ; from carbohydrates (e.g., GALB)
C2 CH1 0.00000 6 ; from aliphatic carbon atoms
C4 CH1 0.15000 7 ; from carbohydrates (e.g., GALB)
O4 OA -0.54800 7 ; from carbohydrates (e.g., GALB)
HO4 H 0.39800 7 ; from carbohydrates (e.g., GALB)
C3 CH1 0.15000 8 ; from carbohydrates (e.g., GALB)
O3 OA -0.54800 8 ; from carbohydrates (e.g., GALB)
HO3 H 0.39800 8 ; from carbohydrates (e.g., GALB)
N2 N -0.28000 9 ; from the peptide bond
HN2 H 0.28000 9 ; from the peptide bond
C7 C 0.28000 10 ; by analogy to the aldehyde group reported by Dolenc et al.
DOI: 10.1093/nar/gki195
O7 O -0.38000 10 ; from the carbonyl group (of e.g., GLN)
C8 CH3 0.10000 10 ; by analogy to the aldehyde group reported by Dolenc et
al. DOI: 10.1093/nar/gki195
C C 0.380 11
O O -0.380 11
[ bonds ]
N H gb_2
N CA gb_20
CA C gb_26
C O gb_4
C +N gb_9
CA CB gb_26
CB CG gb_26
CG OD1 gb_4
CG ND2 gb_9
ND2 HD2 gb_2
ND2 C1 gb_20
C1 O5 gb_19
O5 C5 gb_19
C5 C6 gb_25
C6 O6 gb_19
O6 HO6 gb_1
C5 C4 gb_25
C4 O4 gb_19
O4 HO4 gb_1
C4 C3 gb_25
C3 O3 gb_19
O3 HO3 gb_1
C3 C2 gb_25
C2 C1 gb_25
C2 N2 gb_20
N2 HN2 gb_2
N2 C7 gb_9
C7 O7 gb_4
C7 C8 gb_26
[ angles ]
; ai aj ak gromos type
-C N H ga_31
H N CA ga_17
-C N CA ga_30
N CA C ga_12
CA C +N ga_18
CA C O ga_29
O C +N ga_32
N CA CB ga_12
C CA CB ga_12
CA CB CG ga_14
CB CG CD ga_14
CG CD CE ga_14
CD CE HE ga_24
HE CE OZ ga_24
CD CE OZ ga_26
[ impropers ]
; ai aj ak al gromos type
N -C CA H gi_1
C CA +N O gi_1
CA N C CB gi_2
CE OZ CD HE gi_1
[ dihedrals ]
; ai aj ak al gromos type
-CA -C N CA gd_4
-C N CA C gd_19
N CA C +N gd_20
N CA CB CG gd_17
CA CB CG CD gd_17
CB CG CD NE gd_17
CG CD NE CZ gd_19
CD NE CZ NH2 gd_4
NE CZ NH2 HH21 gd_4

```

```

O5 C5 C6 ga_8
O5 C5 C4 ga_8
C6 C5 C4 ga_7
C5 C6 O6 ga_8
C6 O6 HO6 ga_11
C5 C4 O4 ga_8
C5 C4 C3 ga_7
O4 C4 C3 ga_8
C4 O4 HO4 ga_11
C4 C3 O3 ga_8
C4 C3 C2 ga_7
C2 C3 O3 ga_8
C3 O3 HO3 ga_11
C3 C2 C1 ga_7
C3 C2 N2 ga_8
C1 C2 N2 ga_8
C2 N2 HN2 ga_17
C2 N2 C7 ga_30
HN2 N2 C7 ga_31
N2 C7 O7 ga_32
N2 C7 C8 ga_18
O7 C7 C8 ga_29
[impropers]
; ai aj ak al gromos type
N -C CA H gi_1
C CA +N O gi_1
CA N C CB gi_2
CG OD1 ND2 CB gi_1
ND2 CG C1 HD2 gi_1
C1 O5 ND2 C2 gi_2
C5 O5 C6 C4 gi_2
C2 N2 C3 C1 gi_2
C3 O3 C2 C4 gi_2
C4 C3 O4 C5 gi_2
N2 C7 C2 HN2 gi_1
C7 C8 N2 O7 gi_1
[dihedrals]
; ai aj ak al gromos type
-C CA N CA gd_4
-C N CA C gd_19
N CA C +N gd_20
N CA CB CG gd_17
CA CB CG ND2 gd_20
CB CG ND2 C1 gd_4
CG ND2 C1 O5 gd_19
ND2 C1 C2 C3 gd_17
ND2 C1 C2 C3 gd_7
O5 C1 C2 C3 gd_7
O5 C1 C2 N2 gd_8
ND2 C1 C2 N2 gd_8
C1 C2 N2 C7 gd_19
C2 N2 C7 C8 gd_4
C1 C2 C3 C4 gd_17
C1 C2 C3 O3 gd_7
N2 C2 C3 C4 gd_7
N2 C2 C3 O3 gd_8
C2 C3 O3 HO3 gd_12
C2 C3 C4 C5 gd_17
C2 C3 C4 O4 gd_7
O3 C3 C4 C5 gd_7
O3 C3 C4 O4 gd_8
C3 C4 O4 HO4 gd_12
C2 C1 O5 C5 gd_14
C1 O5 C5 C4 gd_14
C4 C5 C6 O6 gd_17
C4 C5 C6 O6 gd_7
O5 C5 C6 O6 gd_8
C5 C6 O6 HO6 gd_12
C6 C5 C4 C3 gd_17
O5 C5 C4 C3 gd_7
C6 C5 C4 O4 gd_7
O5 C5 C4 O4 gd_8
; 2,3-dihydroxyphenylalanine
[F23]
[atoms]
N N -0.28000 0
H H 0.28000 0
CA CH1 0.00000 1
CB CH2 0.00000 1
CG C 0.00000 1
CD1 C 0.15000 2 ; from the hydroxyl group of TYR
OE3 OA -0.54800 2 ; from the hydroxyl group of TYR
HE3 H 0.39800 2 ; from the hydroxyl group of TYR
CD2 C -0.10000 3
HD2 HC 0.10000 3
CE1 C 0.15000 4 ; from the hydroxyl group of TYR
OZ1 OA -0.54800 4 ; from the hydroxyl group of TYR
HZ1 H 0.39800 4 ; from the hydroxyl group of TYR
CE2 C -0.10000 5
HE2 HC 0.10000 5
CZ2 C -0.10000 6
HZ2 HC 0.10000 6
C C 0.380 7
O O -0.380 7
[bonds]
N H gb_2
N CA gb_20
CA C gb_26
C O gb_4
C +N gb_9
CA CB gb_26
CB CG gb_26
CG CD1 gb_15
CG CD2 gb_15
CD1 CE1 gb_15
CD1 OE3 gb_12
OE3 HE3 gb_1
CD2 HD2 gb_3
CD2 CE2 gb_15
CE1 CZ2 gb_15
CE1 OZ1 gb_12
OZ1 HZ1 gb_1
CE2 HE2 gb_3
CE2 CZ2 gb_15
CZ2 HZ2 gb_3
[exclusions]
; ai aj
CB HD2
CB CE1
CB CE2
CB OE3
CG OZ1
CG HE2
CG CZ2
CD1 HD2
CD1 CE2
CD1 HZ2
CD2 CE1
CD2 OE3
CD2 HZ2
HD2 HE2
HD2 CZ2
CE1 HE2
CE2 OZ1
HE2 HZ2
OE3 CZ2
OE3 OZ1
HZ2 OZ1
OE3 HZ1
HE3 OZ1
HE3 HZ1
[angles]
; ai aj ak gromos type
-C N H ga_31
H N CA ga_17
-C N CA ga_30
N CA C ga_12
CA C +N ga_18
CA C O ga_29
O C +N ga_32
N CA CB ga_12
C CA CB ga_12
CA CB CG ga_14
CB CG CD1 ga_26
CB CG CD2 ga_26
CD1 CG CD2 ga_26
CG CD1 CE1 ga_26
CG CD1 OE3 ga_26
CE1 CD1 OE3 ga_26
CG CD2 HD2 ga_24
HD2 CD2 CE2 ga_24
CG CD2 CE2 ga_26
CD1 CE1 CZ2 ga_26
CD1 CE1 OZ1 ga_26
CZ2 CE1 OZ1 ga_26
CD2 CE2 HE2 ga_24
HE2 CE2 CZ2 ga_24
CD2 CE2 CZ2 ga_26
CD1 OE3 HE3 ga_11
CE1 CZ2 HZ2 ga_24
CE2 CZ2 HZ2 ga_24
CE1 CZ2 CE2 ga_26
CE1 OZ1 HZ1 ga_11
[impropers]
; ai aj ak al gromos type
N -C CA H gi_1
C CA +N O gi_1
CA N C CB gi_2
CG CD1 CD2 CB gi_1
CD2 CG CD1 CE1 gi_1
CD1 CG CD2 CE2 gi_1
CG CD1 CE1 CZ2 gi_1
CG CD2 CE2 CZ2 gi_1
CD1 CE1 CZ2 CE2 gi_1
CD2 CE2 CZ2 CE1 gi_1

```

```

CD1 CG CE1 OE3 gi_1
CD2 CG CE2 HD2 gi_1
CE1 CZ2 CD1 OZ1 gi_1
CE2 CZ2 CD2 HE2 gi_1
CZ2 CE1 CE2 HZ2 gi_1
[ dihedrals ]
; ai aj ak al gromos type
-C A -C N CA gd_4
-C N CA C gd_19
N CA C +N gd_20
N CA CB CG gd_17
CA CB CG CD1 gd_20
CG CD1 OE3 HE3 gd_2
CD1 CE1 OZ1 HZ1 gd_2

; 2-hydroxyphenylalanine
[F2H]
[ atoms ]
N N -0.28000 0
H H 0.28000 0
CA CH1 0.00000 1
CB CH2 0.00000 1
CG C 0.00000 1
CD1 C 0.15000 2; from the hydroxyl group of TYR
OE3 OA -0.54800 2; from the hydroxyl group of TYR
HE3 H 0.39800 2; from the hydroxyl group of TYR
CD2 C -0.10000 3
HD2 HC 0.10000 3
CE1 C -0.10000 4
HE1 HC 0.10000 4
CE2 C -0.10000 5
HE2 HC 0.10000 5
CZ C -0.10000 6
HZ HC 0.10000 6
C C 0.380 7
O O -0.380 7
[ bonds ]
N H gb_2
N CA gb_20
CA C gb_26
C O gb_4
C +N gb_9
CA CB gb_26
CB CG gb_26
CG CD1 gb_15
CG CD2 gb_15
CD1 OE3 gb_12
CD1 CE1 gb_15
CD2 HD2 gb_3
CD2 CE2 gb_15
CE1 HE1 gb_3
CE1 CZ gb_15
CE2 HE2 gb_3
CE2 CZ gb_15
OE3 HE3 gb_1
CZ HZ gb_3
[ exclusions ]
; ai aj
CB HD2
CB CE1
CB CE2
CB OE3
CG HE1
CG HE2
CG CZ
CD1 HD2
CD1 CE2
CD1 HZ
CD2 OE3
CD2 CE1
CD2 HZ
HD2 HE2
HD2 CZ
CE1 HE2
HE1 CE2
HE1 OE3
HE1 HZ
HE2 HZ
OE3 CZ
[ angles ]
; ai aj ak gromos type
-C N H ga_31
H N CA ga_17
-C N CA ga_30
N CA C ga_12
CA C +N ga_18
CA C O ga_29
O C +N ga_32
N CA CB ga_12
C CA CB ga_12
CA CB CG ga_14
CB CG CD1 ga_26
CB CG CD2 ga_26

CD1 CG CD2 ga_26
CG CD1 CE1 ga_26
CG CD1 OE3 ga_26
CE1 CD1 OE3 ga_26
CG CD2 HD2 ga_24
HD2 CD2 CE2 ga_24
CG CD2 CE2 ga_26
CD1 CE1 HE1 ga_24
HE1 CE1 CZ ga_24
CD1 CE1 CZ ga_26
CD2 CE2 HE2 ga_24
HE2 CE2 CZ ga_24
CD2 CE2 CZ ga_26
CD1 OE3 HE3 ga_11
CE1 CZ HZ ga_24
CE2 CZ HZ ga_24
CE1 CZ CE2 ga_26
[ impropers ]
; ai aj ak al gromos type
N -C CA H gi_1
C CA +N O gi_1
CA N C CB gi_2
CG CD1 CD2 CB gi_1
CD2 CG CD1 CE1 gi_1
CD1 CG CD2 CE2 gi_1
CG CD1 CE1 CZ gi_1
CG CD2 CE2 CZ gi_1
CD1 CE1 CZ CE2 gi_1
CD2 CE2 CZ CE1 gi_1
CD1 CG CE1 OE3 gi_1
CD2 CG CE2 HD2 gi_1
CE1 CZ CD1 HE1 gi_1
CE2 CZ CD2 HE2 gi_1
CZ CE1 CE2 HZ gi_1
[ dihedrals ]
; ai aj ak al gromos type
-C A -C N CA gd_4
-C N CA C gd_19
N CA C +N gd_20
N CA CB CG gd_17
CA CB CG CD1 gd_20
CG CD1 OE3 HE3 gd_2

; 3-hydroxyphenylalanine
[F3H]
[ atoms ]
N N -0.28000 0
H H 0.28000 0
CA CH1 0.00000 1
CB CH2 0.00000 1
CG C 0.00000 1
CD1 C -0.10000 2
HD1 HC 0.10000 2
CD2 C -0.10000 3
HD2 HC 0.10000 3
CE1 C 0.15000 4; from the hydroxyl group of TYR
OZ1 OA -0.54800 4; from the hydroxyl group of TYR
HZ1 H 0.39800 4; from the hydroxyl group of TYR
CE2 C -0.10000 5
HE2 HC 0.10000 5
CZ2 C -0.10000 6
HZ2 HC 0.10000 6
C C 0.380 7
O O -0.380 7
[ bonds ]
N H gb_2
N CA gb_20
CA C gb_26
C O gb_4
C +N gb_9
CA CB gb_26
CB CG gb_26
CG CD1 gb_15
CG CD2 gb_15
CD1 HD1 gb_3
CD1 CE1 gb_15
CD2 HD2 gb_3
CD2 CE2 gb_15
CE1 CZ2 gb_15
CE1 OZ1 gb_12
CE2 HE2 gb_3
CE2 CZ2 gb_15
CZ2 HZ2 gb_3
OZ1 HZ1 gb_1
[ exclusions ]
; ai aj
CB HD1
CB HD2
CB CE1
CB CE2
CG HE2
CG CZ2
CG OZ1

```

```

CD1 HD2
CD1 CE2
CD1 HZ2
HD1 CD2
HD1 CZ2
HD1 OZ1
CD2 CE1
CD2 HZ2
HD2 HE2
HD2 CZ2
CE1 HE2
CE2 OZ1
HE2 HZ2
HZ2 OZ1
[angles]
; ai aj ak gromos type
-C N H ga_31
H N CA ga_17
-C N CA ga_30
N CA C ga_12
CA C +N ga_18
CA C O ga_29
O C +N ga_32
N CA CB ga_12
C CA CB ga_12
CA CB CG ga_14
CB CG CD1 ga_26
CB CG CD2 ga_26
CD1 CG CD2 ga_26
CG CD1 HD1 ga_24
HD1 CD1 CE1 ga_24
CG CD1 CE1 ga_26
CG CD2 HD2 ga_24
HD2 CD2 CE2 ga_24
CG CD2 CE2 ga_26
CD1 CE1 CZ2 ga_26
CD1 CE1 OZ1 ga_26
CZ2 CE1 OZ1 ga_26
CD2 CE2 HE2 ga_24
HE2 CE2 CZ2 ga_24
CD2 CE2 CZ2 ga_26
CE1 CZ2 HZ2 ga_24
CE2 CZ2 HZ2 ga_24
CE1 CZ2 CE2 ga_26
CE1 OZ1 HZ1 ga_11
[impropers]
; ai aj ak al gromos type
N -C CA H gi_1
C CA +N O gi_1
CA N C CB gi_2
CG CD1 CD2 CB gi_1
CD2 CG CD1 CE1 gi_1
CD1 CG CD2 CE2 gi_1
CG CD1 CE1 CZ2 gi_1
CG CD2 CE2 CZ2 gi_1
CD1 CE1 CZ2 CE2 gi_1
CD2 CE2 CZ2 CE1 gi_1
CD1 CG CE1 HD1 gi_1
CD2 CG CE2 HD2 gi_1
CE1 CZ2 CD1 OZ1 gi_1
CE2 CZ2 CD2 HE2 gi_1
CZ2 CE1 CE2 HZ2 gi_1
[dihedrals]
; ai aj ak al gromos type
-C -C N CA gd_4
-C N CA C gd_19
N CA C +N gd_20
N CA CB CG gd_17
CA CB CG CD1 gd_20
CD1 CE1 OZ1 HZ1 gd_2

; 6-hydroxytryptophan
[W6H]
[atoms]
N N -0.28000 0
H H 0.28000 0
CA CH1 0.00000 1
CB CH2 0.00000 1
CG C -0.14000 2
CD1 C -0.10000 2
HD1 HC 0.10000 2
CD2 C 0.00000 2
NE1 NR -0.05000 2
HE1 H 0.19000 2
CE2 C 0.00000 2
CE3 C -0.10000 3
HE3 HC 0.10000 3
CZ2 C -0.10000 4
HZ2 HC 0.10000 4
CZ3 C -0.10000 5
HZ3 HC 0.10000 5
CH2 C 0.15000 6 ; from the hydroxyl group of TYR
OI OA -0.54800 6 ; from the hydroxyl group of TYR

HI H 0.39800 6 ; from the hydroxyl group of TYR
C C 0.380 7
O O -0.380 7
[bonds]
N H gb_2
N CA gb_20
CA C gb_26
C O gb_4
C +N gb_9
CA CB gb_26
CB CG gb_26
CG CD1 gb_9
CG CD2 gb_15
CD1 HD1 gb_3
CD1 NE1 gb_9
CD2 CE2 gb_15
CD2 CE3 gb_15
NE1 HE1 gb_2
NE1 CE2 gb_9
CE2 CZ2 gb_15
CE3 HE3 gb_3
CE3 CZ3 gb_15
CZ2 HZ2 gb_3
CZ2 CH2 gb_15
CZ3 HZ3 gb_3
CZ3 CH2 gb_15
CH2 OI gb_12
OI HI gb_1
[exclusions]
; ai aj
CB HD1
CB NE1
CB CE2
CB CE3
CG HE1
CG HE3
CG CZ2
CG CZ3
CD1 CE3
CD1 CZ2
HD1 CD2
HD1 HE1
HD1 CE2
CD2 HE1
CD2 HZ2
CD2 HZ3
CD2 CH2
NE1 CE3
NE1 HZ2
NE1 CH2
HE1 CZ2
CE2 HE3
CE2 CZ3
CE2 OI
CE3 CZ2
CE3 OI
HE3 HZ3
HE3 CH2
CZ2 HZ3
HZ2 CZ3
HZ2 OI
HZ3 OI
[angles]
; ai aj ak gromos type
-C N H ga_31
H N CA ga_17
-C N CA ga_30
N CA C ga_12
CA C +N ga_18
CA C O ga_29
O C +N ga_32
N CA CB ga_12
C CA CB ga_12
CA CB CG ga_14
CB CG CD1 ga_36
CB CG CD2 ga_36
CD1 CG CD2 ga_6
CG CD1 HD1 ga_35
HD1 CD1 NE1 ga_35
CG CD1 NE1 ga_6
CG CD2 CE2 ga_6
CD1 NE1 CE2 ga_6
CD1 NE1 HE1 ga_35
HE1 NE1 CE2 ga_35
NE1 CE2 CD2 ga_6
CG CD2 CE3 ga_38
NE1 CE2 CZ2 ga_38
CD2 CE2 CZ2 ga_26
CE2 CD2 CE3 ga_26
CD2 CE3 HE3 ga_24
HE3 CE3 CZ3 ga_24
CD2 CE3 CZ3 ga_26
CE2 CZ2 HZ2 ga_24

```

```

H22 C22 CH2 ga_24
CE2 C22 CH2 ga_26
CE3 C23 HZ3 ga_24
HZ3 C23 CH2 ga_24
CE3 C23 CH2 ga_26
C22 CH2 C23 ga_26
C22 CH2 OI ga_26
C23 CH2 OI ga_26
CH2 OI HI ga_11
[ impropers ]
; ai aj ak al gromos type
N -C CA H gi_1
C CA +N O gi_1
CA N C CB gi_2
CG CD1 CD2 CB gi_1
CD2 CG CD1 NE1 gi_1
CD1 CG CD2 CE2 gi_1
CG CD1 NE1 CE2 gi_1
CG CD2 CE2 NE1 gi_1
CD1 NE1 CE2 CD2 gi_1
CD1 CG NE1 HD1 gi_1
NE1 CD1 CE2 HE1 gi_1
CD2 CE2 CE3 CG gi_1
CE2 CD2 C22 NE1 gi_1
CE3 CD2 CE2 C22 gi_1
CD2 CE2 C22 CH2 gi_1
CE2 CD2 CE3 C23 gi_1
CE2 C22 CH2 C23 gi_1
CD2 CE3 C23 CH2 gi_1
CE3 C23 CH2 C22 gi_1
CE3 CD2 C23 HE3 gi_1
C22 CE2 CH2 HZ2 gi_1
C23 CE3 CH2 HZ3 gi_1
CH2 C22 C23 OI gi_1
[ dihedrals ]
; ai aj ak al gromos type
-CA -C N CA gd_4
-C N CA C gd_19
N CA C +N gd_20
N CA CB CG gd_17
CA CB CG CD2 gd_20
C22 CH2 OI HI gd_2

; 5-hydroxytryptophan
[ WSH ]
[ atoms ]
N N -0.28000 0
H H 0.28000 0
CA CH1 0.00000 1
CB CH2 0.00000 1
CG C -0.14000 2
CD1 C -0.10000 2
HD1 HC 0.10000 2
CD2 C 0.00000 2
NE1 NR -0.05000 2
HE1 H 0.19000 2
CE2 C 0.00000 2
CE3 C -0.10000 3
HE3 HC 0.10000 3
C22 C -0.10000 4
H22 HC 0.10000 4
C23 C 0.15000 5 ; from the hydroxyl group of TYR
OH3 OA -0.54800 5 ; from the hydroxyl group of TYR
HH3 H 0.39800 5 ; from the hydroxyl group of TYR
CH2 C -0.10000 6
HH2 HC 0.10000 6
C C 0.380 7
O O -0.380 7
[ bonds ]
N H gb_2
N CA gb_20
CA C gb_26
C O gb_4
C +N gb_9
CA CB gb_26
CB CG gb_26
CG CD1 gb_9
CG CD2 gb_15
CD1 HD1 gb_3
CD1 NE1 gb_9
CD2 CE2 gb_15
CD2 CE3 gb_15
NE1 HE1 gb_2
NE1 CE2 gb_9
CE2 C22 gb_15
CE3 HE3 gb_3
CE3 C23 gb_15
C22 HZ2 gb_3
C22 CH2 gb_15
C23 CH2 gb_15
C23 OH3 gb_12
CH2 HH2 gb_3
OH3 HH3 gb_1

[ exclusions ]
; ai aj
CB HD1
CB NE1
CB CE2
CB CE3
CG HE1
CG HE3
CG C22
CG C23
CD1 CE3
CD1 C22
HD1 CD2
HD1 HE1
HD1 CE2
CD2 HE1
CD2 HZ2
CD2 OH3
CD2 CH2
NE1 CE3
NE1 HZ2
NE1 CH2
HE1 C22
CE2 HE3
CE2 C23
CE2 HH2
CE3 C22
CE3 HH2
HE3 OH3
HE3 CH2
C22 OH3
H22 C23
H22 HH2
OH3 HH2
[ angles ]
; ai aj ak gromos type
-C N H ga_31
H N CA ga_17
-C N CA ga_30
N CA C ga_12
CA C +N ga_18
CA C O ga_29
O C +N ga_32
N CA CB ga_12
C CA CB ga_12
CA CB CG ga_14
CB CG CD1 ga_36
CB CG CD2 ga_36
CD1 CG CD2 ga_6
CG CD1 HD1 ga_35
HD1 CD1 NE1 ga_35
CG CD1 NE1 ga_6
CG CD2 CE2 ga_6
CD1 NE1 CE2 ga_6
CD1 NE1 HE1 ga_35
HE1 NE1 CE2 ga_35
NE1 CE2 CD2 ga_6
CG CD2 CE3 ga_38
NE1 CE2 C22 ga_38
CD2 CE2 C22 ga_26
CE2 CD2 CE3 ga_26
CD2 CE3 HE3 ga_24
HE3 CE3 C23 ga_24
CD2 CE3 C23 ga_26
CE2 C22 HZ2 ga_24
H22 C22 CH2 ga_24
CE2 C22 CH2 ga_26
CE3 C23 OH3 ga_26
CH2 C23 OH3 ga_26
C23 OH3 HH3 ga_11
CE3 C23 CH2 ga_26
C22 CH2 HH2 ga_24
HH2 CH2 C23 ga_24
C22 CH2 C23 ga_26
[ impropers ]
; ai aj ak al gromos type
N -C CA H gi_1
C CA +N O gi_1
CA N C CB gi_2
CG CD1 CD2 CB gi_1
CD2 CG CD1 NE1 gi_1
CD1 CG CD2 CE2 gi_1
CG CD1 NE1 CE2 gi_1
CG CD2 CE2 NE1 gi_1
CD1 NE1 CE2 CD2 gi_1
CD1 CG NE1 HD1 gi_1
NE1 CD1 CE2 HE1 gi_1
CD2 CE2 CE3 CG gi_1
CE2 CD2 C22 NE1 gi_1
CE3 CD2 CE2 C22 gi_1
CD2 CE2 C22 CH2 gi_1
CE2 CD2 CE3 C23 gi_1
CE2 C22 CH2 C23 gi_1
CD2 CE3 C23 CH2 gi_1
CE3 C23 CH2 C22 gi_1
CE3 CD2 C23 HE3 gi_1
C22 CE2 CH2 HZ2 gi_1
C23 CE3 CH2 HZ3 gi_1
CH2 C22 C23 OI gi_1

```

```

CD2 CE3 CZ3 CH2 gi_1
CE3 CZ3 CH2 CZ2 gi_1
CE3 CD2 CZ3 HE3 gi_1
CZ2 CE2 CH2 HZ2 gi_1
CZ3 CE3 CH2 OH3 gi_1
CH2 CZ2 CZ3 HH2 gi_1
[ dihedrals ]
; ai aj ak al gromos type
-C A -C N CA gd_4
-C N CA C gd_19
N CA C +N gd_20
N CA CB CG gd_17
CA CB CG CD2 gd_20
CE3 CZ3 OH3 HH3 gd_2

; 4-hydroxytryptophan
[W4H]
[ atoms ]
N N -0.28000 0
H H 0.28000 0
CA CH1 0.00000 1
CB CH2 0.00000 1
CG C -0.14000 2
CD1 C -0.10000 2
HD1 HC 0.10000 2
CD2 C 0.00000 2
NE1 NR -0.05000 2
HE1 H 0.19000 2
CE2 C 0.00000 2
CE3 C 0.15000 3 ; from the hydroxyl group of TYR
OZ4 OA -0.54800 3 ; from the hydroxyl group of TYR
HZ4 H 0.39800 3 ; from the hydroxyl group of TYR
CZ2 C -0.10000 4
HZ2 HC 0.10000 4
CZ3 C -0.10000 5
HZ3 HC 0.10000 5
CH2 C -0.10000 6
HH2 HC 0.10000 6
C C 0.380 7
O O -0.380 7
[ bonds ]
N H gb_2
N CA gb_20
CA C gb_26
C O gb_4
C +N gb_9
CA CB gb_26
CB CG gb_26
CG CD1 gb_9
CG CD2 gb_15
CD1 HD1 gb_3
CD1 NE1 gb_9
CD2 CE2 gb_15
CD2 CE3 gb_15
NE1 HE1 gb_2
NE1 CE2 gb_9
CE2 CZ2 gb_15
CE3 OZ4 gb_12
CE3 CZ3 gb_15
CZ2 HZ2 gb_3
CZ2 CH2 gb_15
CZ3 HZ3 gb_3
CZ3 CH2 gb_15
OZ4 HZ4 gb_1
CH2 HH2 gb_3
[ exclusions ]
; ai aj
CB HD1
CB NE1
CB CE2
CB CE3
CG HE1
CG CZ2
CG CZ3
CG OZ4
CD1 CE3
CD1 CZ2
HD1 CD2
HD1 HE1
HD1 CE2
CD2 HE1
CD2 HZ2
CD2 HZ3
CD2 CH2
NE1 CE3
NE1 HZ2
NE1 CH2
HE1 CZ2
CE2 CZ3
CE2 HH2
CE2 OZ4
CE3 CZ2
CE3 HH2

CZ2 HZ3
HZ2 CZ3
HZ2 HH2
HZ3 OZ4
HZ3 HH2
OZ4 CH2
[ angles ]
; ai aj ak gromos type
-C N H ga_31
H N CA ga_17
-C N CA ga_30
N CA C ga_12
CA C +N ga_18
CA C O ga_29
O C +N ga_32
N CA CB ga_12
C CA CB ga_12
CA CB CG ga_14
CB CG CD1 ga_36
CB CG CD2 ga_36
CD1 CG CD2 ga_6
CG CD1 HD1 ga_35
HD1 CD1 NE1 ga_35
CG CD1 NE1 ga_6
CG CD2 CE2 ga_6
CD1 NE1 CE2 ga_6
CD1 NE1 HE1 ga_35
HE1 NE1 CE2 ga_35
NE1 CE2 CD2 ga_6
CG CD2 CE3 ga_38
NE1 CE2 CZ2 ga_38
CD2 CE2 CZ2 ga_26
CE2 CD2 CE3 ga_26
CD2 CE3 CZ3 ga_26
CD2 CE3 OZ4 ga_26
CZ3 CE3 OZ4 ga_26
CE2 CZ2 HZ2 ga_24
HZ2 CZ2 CH2 ga_24
CE2 CZ2 CH2 ga_26
CE3 CZ3 HZ3 ga_24
HZ3 CZ3 CH2 ga_24
CE3 CZ3 CH2 ga_26
CE3 OZ4 HZ4 ga_11
CZ2 CH2 HH2 ga_24
HH2 CH2 CZ3 ga_24
CZ2 CH2 CZ3 ga_26
[ impropers ]
; ai aj ak al gromos type
N -C CA H gi_1
C CA +N O gi_1
CA N C CB gi_2
CG CD1 CD2 CB gi_1
CD2 CG CD1 NE1 gi_1
CD1 CG CD2 CE2 gi_1
CG CD1 NE1 CE2 gi_1
CG CD2 CE2 NE1 gi_1
CD1 NE1 CE2 CD2 gi_1
CD1 CG NE1 HD1 gi_1
NE1 CD1 CE2 HE1 gi_1
CD2 CE2 CE3 CG gi_1
CE2 CD2 CZ2 NE1 gi_1
CE3 CD2 CE2 CZ2 gi_1
CD2 CE2 CZ2 CH2 gi_1
CE2 CD2 CE3 CZ3 gi_1
CE2 CZ2 CH2 CZ3 gi_1
CD2 CE3 CZ3 CH2 gi_1
CE3 CZ3 CH2 CZ2 gi_1
CE3 CD2 CZ3 OZ4 gi_1
CZ2 CE2 CH2 HZ2 gi_1
CZ3 CE3 CH2 HZ3 gi_1
CH2 CZ2 CZ3 HH2 gi_1
[ dihedrals ]
; ai aj ak al gromos type
-C A -C N CA gd_4
-C N CA C gd_19
N CA C +N gd_20
N CA CB CG gd_17
CA CB CG CD2 gd_20
CD2 CE3 OZ4 HZ4 gd_2

; 2-hydroxytryptophan
[W2H]
[ atoms ]
N N -0.28000 0
H H 0.28000 0
CA CH1 0.00000 1
CB CH2 0.00000 1
CG C -0.14000 2
CD1 C 0.15000 2 ; from the hydroxyl group of TYR
OE4 OA -0.54800 2 ; from the hydroxyl group of TYR
HE4 H 0.39800 2 ; from the hydroxyl group of TYR
CD2 C 0.00000 2
NE1 NR -0.05000 2

```

```

HE1 H 0.19000 2
CE2 C 0.00000 2
CE3 C -0.10000 3
HE3 HC 0.10000 3
CZ2 C -0.10000 4
H22 HC 0.10000 4
CZ3 C -0.10000 5
HZ3 HC 0.10000 5
CH2 C -0.10000 6
HH2 HC 0.10000 6
C C 0.380 7
O O -0.380 7
[ bonds ]
N H gb_2
N CA gb_20
CA C gb_26
C O gb_4
C +N gb_9
CA CB gb_26
CB CG gb_26
CG CD1 gb_9
CG CD2 gb_15
CD1 OE4 gb_12
CD1 NE1 gb_9
CD2 CE2 gb_15
CD2 CE3 gb_15
NE1 HE1 gb_2
NE1 CE2 gb_9
CE2 CZ2 gb_15
CE3 HE3 gb_3
CE3 CZ3 gb_15
OE4 HE4 gb_1
CZ2 HZ2 gb_3
CZ2 CH2 gb_15
CZ3 HZ3 gb_3
CZ3 CH2 gb_15
CH2 HH2 gb_3
[ exclusions ]
; ai aj
CB NE1
CB CE2
CB CE3
CB OE4
CG HE1
CG HE3
CG CZ2
CG CZ3
CD1 CE3
CD1 CZ2
CD2 HE1
CD2 OE4
CD2 HZ2
CD2 HZ3
CD2 CH2
NE1 CE3
NE1 HE4
NE1 HZ2
NE1 CH2
HE1 OE4
HE1 CZ2
CE2 HE3
CE2 OE4
CE2 CZ3
CE2 HH2
CE3 CZ2
CE3 HH2
HE3 HZ3
HE3 CH2
CZ2 HZ3
H22 CZ3
H22 HH2
HZ3 HH2
[ angles ]
; ai aj ak gromos type
-C N H ga_31
H N CA ga_17
-C N CA ga_30
N CA C ga_12
CA C +N ga_18
CA C O ga_29
O C +N ga_32
N CA CB ga_12
C CA CB ga_12
CA CB CG ga_14
CB CG CD1 ga_36
CB CG CD2 ga_36
CD1 CG CD2 ga_6
CG CD1 NE1 ga_6
CG CD1 OE4 ga_36
NE1 CD1 OE4 ga_36
CG CD2 CE2 ga_6
CD1 NE1 CE2 ga_6
CD1 NE1 HE1 ga_35
HE1 NE1 CE2 ga_35
NE1 CE2 CD2 ga_6
CG CD2 CE3 ga_38
NE1 CE2 CZ2 ga_38
CD2 CE2 CZ2 ga_26
CE2 CD2 CE3 ga_26
CD2 CE3 HE3 ga_24
HE3 CE3 CZ3 ga_24
CD2 CE3 CZ3 ga_26
CD1 OE4 HE4 ga_11
CE2 CZ2 HZ2 ga_24
H22 CZ2 CH2 ga_24
CE2 CZ2 CH2 ga_26
CE3 CZ3 HZ3 ga_24
HZ3 CZ3 CH2 ga_24
CE3 CZ3 CH2 ga_26
CZ2 CH2 HH2 ga_24
HH2 CH2 CZ3 ga_24
CZ2 CH2 CZ3 ga_26
[ impropers ]
; ai aj ak al gromos type
N -C CA H gi_1
C CA +N O gi_1
CA N C CB gi_2
CG CD1 CD2 CB gi_1
CD2 CG CD1 NE1 gi_1
CD1 CG CD2 CE2 gi_1
CG CD1 NE1 CE2 gi_1
CG CD2 CE2 NE1 gi_1
CD1 NE1 CE2 CD2 gi_1
CD1 CG NE1 OE4 gi_1
NE1 CD1 CE2 HE1 gi_1
CD2 CE2 CE3 CG gi_1
CE2 CD2 CZ2 NE1 gi_1
CE3 CD2 CE2 CZ2 gi_1
CD2 CE2 CZ2 CH2 gi_1
CE2 CD2 CE3 CZ3 gi_1
CE2 CZ2 CH2 CZ3 gi_1
CD2 CE3 CZ3 CH2 gi_1
CE3 CZ3 CH2 CZ2 gi_1
CE3 CD2 CZ3 HE3 gi_1
CZ2 CE2 CH2 HZ2 gi_1
CZ3 CE3 CH2 HZ3 gi_1
CH2 CZ2 CZ3 HH2 gi_1
[ dihedrals ]
; ai aj ak al gromos type
-C -C N CA gd_4
-C N CA C gd_19
N CA C +N gd_20
N CA CB CG gd_17
CA CB CG CD2 gd_20
CG CD1 OE4 HE4 gd_2
; 3-hydroxyleucine (R)
[ L3H ]
[ atoms ]
N N -0.28000 0
H H 0.28000 0
CA CH1 0.00000 1
CB CH1 0.15000 2; from the hydroxyl group of THR
OG1 OA -0.54800 2; from the hydroxyl group of THR
HG1 H 0.39800 2; from the hydroxyl group of THR
CG2 CH1 0.00000 3
CD1 CH3 0.00000 3
CD2 CH3 0.00000 3
C C 0.380 4
O O -0.380 4
[ bonds ]
N H gb_2
N CA gb_20
CA C gb_26
C O gb_4
C +N gb_9
CA CB gb_26
CB CG2 gb_26
CB OG1 gb_17
OG1 HG1 gb_1
CG2 CD1 gb_26
CG2 CD2 gb_26
[ angles ]
; ai aj ak gromos type
-C N H ga_31
H N CA ga_17
-C N CA ga_30
N CA C ga_12
CA C O ga_29
O C +N ga_32
N CA CB ga_12
C CA CB ga_12
CA CB CG ga_14
CB CG CD1 ga_36
CB CG CD2 ga_36
CD1 CG CD2 ga_6
CG CD1 NE1 ga_6
CG CD1 OE4 ga_36
NE1 CD1 OE4 ga_36
CG CD2 CE2 ga_6
CD1 NE1 CE2 ga_6
OG1 CB CG2 ga_12

```



```

CB CG2 CD1 ga_14
CB CG2 CD2 ga_14
CD1 CG2 CD2 ga_14
CB OG1 HG1 ga_11
[impropers]
; ai aj ak al gromos type
N -C CA H gi_1
C CA +N O gi_1
CA N C CB gi_2
CB OG1 CG2 CA gi_2
CG2 CD2 CD1 CB gi_2
[dihedrals]
; ai aj ak al gromos type
-C -C N CA gd_4
-C N CA C gd_19
N CA C +N gd_20
N CA CB CG2 gd_17
CA CB OG1 HG1 gd_12
CA CB CG2 CD1 gd_17

; 3-hydroxyleucine (S)
[LH3]
[atoms]
N N -0.28000 0
H H 0.28000 0
CA CH1 0.00000 1
CB CH1 0.15000 2; from the hydroxyl group of THR
OG1 OA -0.54800 2; from the hydroxyl group of THR
HG1 H 0.39800 2; from the hydroxyl group of THR
CG2 CH1 0.00000 3
CD1 CH3 0.00000 3
CD2 CH3 0.00000 3
C C 0.380 4
O O -0.380 4
[bonds]
N H gb_2
N CA gb_20
CA C gb_26
C O gb_4
C +N gb_9
CA CB gb_26
CB CG2 gb_26
CB OG1 gb_17
OG1 HG1 gb_1
CG2 CD1 gb_26
CG2 CD2 gb_26
[angles]
; ai aj ak gromos type
-C N H ga_31
H N CA ga_17
-C N CA ga_30
N CA C ga_12
CA C +N ga_18
CA C O ga_29
O C +N ga_32
N CA CB ga_12
C CA CB ga_12
CA CB CG ga_14
CB CG CD1 ga_12
CB CG CD2 ga_12
CB CG OD3 ga_12
CD1 CG CD2 ga_12
CD1 CG OD3 ga_12
CD2 CG OD3 ga_12
CG OD3 HD3 ga_11
[impropers]
; ai aj ak al gromos type
N -C CA H gi_1
C CA +N O gi_1
CA N C CB gi_2
[dihedrals]
; ai aj ak al gromos type
-C -C N CA gd_4
-C N CA C gd_19
N CA C +N gd_20
N CA CB CG gd_17
CA CB CG OD3 gd_17
CB CG OD3 HD3 gd_12

; 5-hydroxyleucine (R)
[L5H]
[atoms]
N N -0.28000 0
H H 0.28000 0
CA CH1 0.00000 1
CB CH2 0.00000 1
CG CH1 0.00000 2
CD1 CH3 0.00000 2
CD2 CH2 0.15000 3; from the hydroxyl group of THR
OE OA -0.54800 3; from the hydroxyl group of THR
HE H 0.39800 3; from the hydroxyl group of THR
C C 0.380 4
O O -0.380 4
[bonds]
N H gb_2
N CA gb_20
CA C gb_26
C O gb_4
C +N gb_9
CA CB gb_26
CB CG gb_26
CG CD1 gb_26
CG CD2 gb_26
CD2 OE gb_17
OE HE gb_1
[angles]
; ai aj ak gromos type
-C N H ga_31
H N CA ga_17
-C N CA ga_30
N CA C ga_12
CA C +N ga_18
CA C O ga_29
O C +N ga_32
N CA CB ga_12
C CA CB ga_12
CA CB CG ga_14
CB CG CD1 ga_14
CB CG CD2 ga_14
CD1 CG CD2 ga_14
CG CD2 OE ga_12
CD2 OE HE ga_11
[impropers]
; ai aj ak al gromos type
N -C CA H gi_1
C CA +N O gi_1
CA N C CB gi_2
[impropers]
; ai aj ak al gromos type
N -C CA H gi_1
C CA +N O gi_1
CA N C CB gi_2
CB CG2 OG1 CA gi_2
CG2 CD2 CD1 CB gi_2
[dihedrals]
; ai aj ak al gromos type
-C -C N CA gd_4
-C N CA C gd_19
N CA C +N gd_20
N CA CB CG2 gd_17
CA CB OG1 HG1 gd_12
CA CB CG2 CD1 gd_17

; 4-hydroxyleucine
[L4H]
[atoms]
N N -0.28000 0
H H 0.28000 0
CA CH1 0.00000 1
CB CH2 0.00000 1
CG CH0 0.15000 2; from the hydroxyl group of THR
OD3 OA -0.54800 2; from the hydroxyl group of THR
HD3 H 0.39800 2; from the hydroxyl group of THR
CD1 CH3 0.00000 3
CD2 CH3 0.00000 4
C C 0.380 5
O O -0.380 5
[impropers]
; ai aj ak al gromos type
N -C CA H gi_1
C CA +N O gi_1
CA N C CB gi_2
[impropers]
; ai aj ak al gromos type
N -C CA H gi_1
C CA +N O gi_1
CA N C CB gi_2

```

```

CA N C CB gi_2
CG CD2 CD1 CB gi_2
[dihedrals]
; ai aj ak al gromos type
-CA -C N CA gd_4
-C N CA C gd_19
N CA C +N gd_20
N CA CB CG gd_17
CA CB CG CD2 gd_17
CB CG CD2 OE gd_17
CG CD2 OE HE gd_12

; 5-hydroxyleucine (S)
[LH5]
[atoms]
N N -0.28000 0
H H 0.28000 0
CA CH1 0.00000 1
CB CH2 0.00000 1
CG CH1 0.00000 2
CD1 CH3 0.00000 2
CD2 CH2 0.15000 3; from the hydroxyl group of THR
OE OA -0.54800 3; from the hydroxyl group of THR
HE H 0.39800 3; from the hydroxyl group of THR
C C 0.380 4
O O -0.380 4
[bonds]
N H gb_2
N CA gb_20
CA C gb_26
C O gb_4
C +N gb_9
CA CB gb_26
CB CG gb_26
CG CD1 gb_26
CG CD2 gb_26
CD2 OE gb_17
OE HE gb_1
[angles]
; ai aj ak gromos type
-C N H ga_31
H N CA ga_17
-C N CA ga_30
N CA C ga_12
CA C +N ga_18
CA C O ga_29
O C +N ga_32
N CA CB ga_12
C CA CB ga_12
CA CB CG ga_14
CB CG CD1 ga_14
CB CG CD2 ga_14
CD1 CG CD2 ga_14
CG CD2 OE ga_12
CD2 OE HE ga_11
[impropers]
; ai aj ak al gromos type
N -C CA H gi_1
C CA +N O gi_1
CA N C CB gi_2
CG CD1 CD2 CB gi_2
[dihedrals]
; ai aj ak al gromos type
-CA -C N CA gd_4
-C N CA C gd_19
N CA C +N gd_20
N CA CB OG3 gd_17
CA CB OG3 HG3 gd_12

; 3-hydroxyvaline
[V3H]
[atoms]
N N -0.28000 0
H H 0.28000 0
CA CH1 0.00000 1
CB CH0 0.15000 2; from the hydroxyl group of THR
OG3 OA -0.54800 2; from the hydroxyl group of THR
HG3 H 0.39800 2; from the hydroxyl group of THR
CG1 CH3 0.00000 3
CG2 CH3 0.00000 4
C C 0.380 5
O O -0.380 5
[bonds]
N H gb_2
N CA gb_20
CA C gb_26
C O gb_4
C +N gb_9
CA CB gb_26
CB CG1 gb_26
CB CG2 gb_26

CB OG3 gb_17
OG3 HG3 gb_1
[angles]
; ai aj ak gromos type
-C N H ga_31
H N CA ga_17
-C N CA ga_30
N CA C ga_12
CA C +N ga_18
CA C O ga_29
O C +N ga_32
N CA CB ga_12
C CA CB ga_12
CA CB CG ga_14
CB CG CD1 ga_14
CB CG CD2 ga_14
CD1 CG CD2 ga_14
CG CD2 OE ga_12
OD HD gb_1
[impropers]
; ai aj ak al gromos type
N -C CA H gi_1
C CA +N O gi_1
CA N C CB gi_2
[dihedrals]
; ai aj ak al gromos type
-CA -C N CA gd_4
-C N CA C gd_19
N CA C +N gd_20
N CA CB OG3 gd_17
CA CB OG3 HG3 gd_12

; cysteine sulfenic acid
[CYH]
[atoms]
N N -0.28000 0
H H 0.28000 0
CA CH1 0.00000 1
CB CH2 0.00000 1
SG S 0.15000 2; from the hydroxyl group of THR
OD OA -0.54800 2; from the hydroxyl group of THR
HD H 0.39800 2; from the hydroxyl group of THR
C C 0.380 3
O O -0.380 3
[bonds]
N H gb_2
N CA gb_20
CA C gb_26
C O gb_4
C +N gb_9
CA CB gb_26
CB SG gb_30
SG OD gb_27
OD HD gb_1
[angles]
; ai aj ak gromos type
-C N H ga_31
H N CA ga_17
-C N CA ga_30
N CA C ga_12
CA C +N ga_18
CA C O ga_29
O C +N ga_32
N CA CB ga_12
CA CB SG ga_15
CB SG OD ga_12
SG OD HD ga_11
[impropers]
; ai aj ak al gromos type
N -C CA H gi_1
C CA +N O gi_1
CA N C CB gi_2
[dihedrals]
; ai aj ak al gromos type
-CA -C N CA gd_4
-C N CA C gd_19
N CA C +N gd_20
N CA CB SG gd_17
CA CB SG OD gd_13
CB SG OD HD gd_12

; 5-hydroxyproline (R)
[PH5]
[atoms]
N N 0.00000 0
CA CH1 0.00000 1
CB CH2 0.00000 1
CG CH2 0.00000 2
CD CH1 0.15000 3; from the hydroxyl group of THR
OE OA -0.54800 3; from the hydroxyl group of THR
HE H 0.39800 3; from the hydroxyl group of THR

```

```

C C 0.380 4
O O -0.380 4
[ bonds ]
N CA gb_20
CA C gb_26
C O gb_4
C +N gb_9
CA CB gb_26
CB CG gb_26
CG CD gb_26
CD OE gb_17
OE HE gb_1
CD N gb_20
[ exclusions ]
; ai aj
N HE
[ angles ]
; ai aj ak gromos type
-C N CA ga_30
N CA C ga_12
CA C +N ga_18
CA C O ga_29
O C +N ga_32
N CA CB ga_12
C CA CB ga_12
CA CB CG ga_12
CB CG CD ga_12
CG CD OE ga_12
CG CD N ga_12
OE CD N ga_12
CD OE HE ga_11
CD N CA ga_20
-C N CD ga_30
[ impropers ]
; ai aj ak al gromos type
N -C CA CD gi_1
C CA +N O gi_1
CA N C CB gi_2
CD CG N OE gi_2
[ dihedrals ]
; ai aj ak al gromos type
-C -C N CA gd_4
-C N CA C gd_19
N CA C +N gd_20
N CA CB CG gd_17
CA CB CG CD gd_17
CB CG CD N gd_17
CG CD OE HE gd_12
CG CD N CA gd_19
; 5-hydroxyproline (S)
[ P5H ]
[ atoms ]
N N 0.00000 0
CA CH1 0.00000 1
CB CH2 0.00000 1
CG CH2 0.00000 2
CD CH1 0.15000 3 ; from the hydroxyl group of THR
OE OA -0.54800 3 ; from the hydroxyl group of THR
HE H 0.39800 3 ; from the hydroxyl group of THR
C C 0.380 4
O O -0.380 4
[ bonds ]
N CA gb_20
CA C gb_26
C O gb_4
C +N gb_9
CA CB gb_26
CB CG gb_26
CG CD gb_26
CD OE gb_17
OE HE gb_1
CD N gb_20
[ exclusions ]
; ai aj
N HE
[ angles ]
; ai aj ak gromos type
-C N CA ga_30
N CA C ga_12
CA C +N ga_18
CA C O ga_29
O C +N ga_32
N CA CB ga_12
C CA CB ga_12
CA CB CG ga_12
CB CG CD ga_12
CG CD OE ga_12
CG CD N ga_12
OE CD N ga_12
CD OE HE ga_11
CD N CA ga_20
-C N CD ga_30
[ impropers ]
; ai aj ak al gromos type
N -C CA CD gi_1
C CA +N O gi_1
CA N C CB gi_2
CD CG N OE gi_2
[ dihedrals ]
; ai aj ak al gromos type
-C -C N CA gd_4
-C N CA C gd_19
N CA C +N gd_20
N CA CB CG gd_17
CA CB CG CD gd_17
CB CG CD N gd_17
CG CD OE HE gd_12
CG CD N CA gd_19
; glutamic semialdehyde
[ GSA ]
[ atoms ]
N N -0.28000 0
H H 0.28000 0
CA CH1 0.00000 1
CB CH2 0.00000 1
CG CH2 0.00000 1
CD C 0.28000 2 ; by analogy to the aldehyde group reported by Dolenc et al.
DOI: 10.1093/nar/gki195
HD HC 0.10000 2 ; by analogy to the aldehyde group reported by Dolenc et
al. DOI: 10.1093/nar/gki195
OE O -0.38000 2 ; from the carbonyl group (of e.g., GLN)
C C 0.380 3
O O -0.380 3
[ bonds ]
N H gb_2
N CA gb_20
CA C gb_26
C O gb_4
C +N gb_9
CA CB gb_26
CB CG gb_26
CG CD gb_26
CD HD gb_3
CD OE gb_4
[ angles ]
; ai aj ak gromos type
-C N H ga_31
H N CA ga_17
-C N CA ga_30
N CA C ga_12
CA C +N ga_18
CA C O ga_29
O C +N ga_32
N CA CB ga_12
C CA CB ga_12
CA CB CG ga_14
CB CG CD ga_14
CG CD HD ga_24
HD CD OE ga_24
CG CD OE ga_26
[ impropers ]
; ai aj ak al gromos type
N -C CA H gi_1
C CA +N O gi_1
CA N C CB gi_2
CD OE CG HD gi_1
[ dihedrals ]
; ai aj ak al gromos type
-C -C N CA gd_4
-C N CA C gd_19
N CA C +N gd_20
N CA CB CG gd_17
CA CB CG CD gd_17
CB CG CD OE gd_20
; 2-amino-3-ketobutyric acid
[ TOX ]
[ atoms ]
N N -0.28000 0
H H 0.28000 0
CA CH1 0.00000 1
CB C 0.38000 2 ; from the carbonyl group (of e.g., GLN)
OG1 O -0.38000 2 ; from the carbonyl group (of e.g., GLN)
CG2 CH3 0.00000 3
C C 0.380 4
O O -0.380 4
[ bonds ]
N H gb_2
N CA gb_20
CA C gb_26
C O gb_4
C +N gb_9
CA CB gb_26
CB OG1 gb_4

```

```

CB CG2 gb_26
[ angles ]
; ai aj ak gromos type
-C N H ga_31
H N CA ga_17
-C N CA ga_30
N CA C ga_12
CA C +N ga_18
CA C O ga_29
O C +N ga_32
N CA CB ga_12
C CA CB ga_12
CA CB OG1 ga_26
CA CB CG2 ga_26
OG1 CB CG2 ga_26
[ impropers ]
; ai aj ak al gromos type
N -C CA H gi_1
C CA +N O gi_1
CA N C CB gi_2
CB OG1 CG2 CA gi_1
[ dihedrals ]
; ai aj ak al gromos type
-C A -C N CA gd_4
-C N CA C gd_19
N CA C +N gd_20
N CA CB OG1 gd_20

; pyroglutamic acid
[ PGA ]
[ atoms ]
N N 0.00000 0
CA CH1 0.00000 1
CB CH2 0.00000 1
CG CH2 0.00000 2
CD C 0.38000 3 ; from the carbonyl group (of e.g., GLN)
OE O -0.38000 3 ; from the carbonyl group (of e.g., GLN)
C C 0.380 4
O O -0.380 4
[ bonds ]
N CA gb_20
CA C gb_26
C O gb_4
C +N gb_9
CA CB gb_26
CB CG gb_26
CG CD gb_26
CD OE gb_4
CD N gb_9
[ angles ]
; ai aj ak gromos type
-C N CA ga_30
N CA C ga_12
CA C +N ga_18
CA C O ga_29
O C +N ga_32
N CA CB ga_12
C CA CB ga_12
CA CB CG ga_12
CB CG CD ga_12
CG CD N ga_18
CG CD OE ga_29
N CD OE ga_32
CD N CA ga_20
-C N CD ga_30
[ impropers ]
; ai aj ak al gromos type
N -C CA CD gi_1
C CA +N O gi_1
CA N C CB gi_2
CG ND1 CD2 CB gi_1
CD2 CG ND1 CE1 gi_1
ND1 CG CD2 NE2 gi_1
ND1 CG CE1 HD1 gi_1
CG ND1 CE1 NE2 gi_1
CG CD2 NE2 CE1 gi_1
CD2 NE2 CE1 ND1 gi_1
CE1 OZ NE2 ND1 gi_1
NE2 CD2 CE1 HE2 gi_1
[ dihedrals ]
; ai aj ak al gromos type
-C A -C N CA gd_4
-C N CA C gd_19
N CA C +N gd_20
N CA CB CG gd_17
CA CB CG CD gd_17
CB CG CD N gd_20
CG CD N CA gd_4

; 2-oxo-histidine
[ H2X ]
[ atoms ]
N N -0.28000 0
H H 0.28000 0
CA CH1 0.00000 1
CB CH2 0.00000 1
CG C 0.00000 2
ND1 NR -0.28000 3
HD1 H 0.28000 3
CD2 CR1 0.00000 4
NE2 NR -0.28000 5

HE2 H 0.28000 5
CE1 C 0.38000 6 ; from the carbonyl group (of e.g., GLN)
OZ O -0.38000 6 ; from the carbonyl group (of e.g., GLN)
C C 0.380 7
O O -0.380 7
[ bonds ]
N H gb_2
N CA gb_20
CA C gb_26
C O gb_4
C +N gb_9
CA CB gb_26
CB CG gb_26
CG ND1 gb_9
CG CD2 gb_9
ND1 HD1 gb_2
ND1 CE1 gb_9
CD2 NE2 gb_9
CE1 NE2 gb_9
CE1 OZ gb_4
NE2 HE2 gb_2
[ exclusions ]
; ai aj
CB HD1
CB CE1
CB NE2
CG HE2
CG OZ
HD1 CD2
HD1 NE2
HD1 OZ
ND1 HE2
CD2 OZ
HE2 OZ
[ angles ]
; ai aj ak gromos type
-C N H ga_31
H N CA ga_17
-C N CA ga_30
N CA C ga_12
CA C +N ga_18
CA C O ga_29
O C +N ga_32
N CA CB ga_12
C CA CB ga_12
CA CB CG ga_14
CB CG ND1 ga_36
CB CG CD2 ga_36
ND1 CG CD2 ga_6
CG ND1 HD1 ga_35
CG ND1 CE1 ga_6
HD1 ND1 CE1 ga_35
CG CD2 NE2 ga_6
ND1 CE1 NE2 ga_6
ND1 CE1 OZ ga_36
NE2 CE1 OZ ga_36
CD2 NE2 CE1 ga_6
CD2 NE2 HE2 ga_35
CE1 NE2 HE2 ga_35
[ impropers ]
; ai aj ak al gromos type
N -C CA H gi_1
C CA +N O gi_1
CA N C CB gi_2
CG ND1 CD2 CB gi_1
CD2 CG ND1 CE1 gi_1
ND1 CG CD2 NE2 gi_1
ND1 CG CE1 HD1 gi_1
CG ND1 CE1 NE2 gi_1
CG CD2 NE2 CE1 gi_1
CD2 NE2 CE1 ND1 gi_1
CE1 OZ NE2 ND1 gi_1
NE2 CD2 CE1 HE2 gi_1
[ dihedrals ]
; ai aj ak al gromos type
-C A -C N CA gd_4
-C N CA C gd_19
N CA C +N gd_20
N CA CB CG gd_17
N CA C +N gd_20
N CA CB CG gd_17
CA CB CG ND1 gd_20

; methionine sulfoxide (R)
[ MSX ]
[ atoms ]
N N -0.28000 0
H H 0.28000 0
CA CH1 0.00000 1
CB CH2 0.00000 1
CG CH2 0.00000 1
SD S 0.38000 2 ; to add up to 0 net charge
OE2 O -0.38000 2 ; from the carbonyl group (e.g., GLN)
CE1 CH3 0.00000 3
C C 0.380 4

```



```

CA C +N ga_18
CA C O ga_29
O C +N ga_32
N CA CB ga_12
C CA CB ga_12
CA CB SG ga_15
CB SG OD1 ga_5
OD1 SG OD2 ga_5
CB SG OD2 ga_5
[ impropers ]
; ai aj ak al gromos type
N -C CA H gi_1
C CA +N O gi_1
CA N C CB gi_2
SG CB OD1 OD2 gi_2
[ dihedrals ]
; ai aj ak al gromos type
-CA -C N CA gd_4
-C N CA C gd_19
N CA C +N gd_20
N CA CB SG gd_17
CA CB SG OD1 gd_13

; cysteine acid
[CSE]
[ atoms ]
N N -0.28000 0
H H 0.28000 0
CA CH1 0.00000 1
CB CH2 0.15000 2 ; from the carbon atom attached to the phosphate group of
nucleotides (e.g., ATP)
SG S 0.75500 2 ; to add up to -1 net charge
OD1 OM -0.63500 2 ; from the phosphate group of nucleotides (e.g., ATP)
OD2 OM -0.63500 2 ; from the phosphate group of nucleotides (e.g., ATP)
OD3 OM -0.63500 2 ; from the phosphate group of nucleotides (e.g., ATP)
C C 0.380 3
O O -0.380 3
[ bonds ]
N H gb_2
N CA gb_20
CA C gb_26
C O gb_4
C +N gb_9
CA CB gb_26
CB SG gb_30
SG OD1 gb_24
SG OD2 gb_24
SG OD3 gb_24
[ angles ]
; ai aj ak gromos type
-C N H ga_31
H N CA ga_17
-C N CA ga_30
N CA C ga_12
CA C +N ga_18
CA C O ga_29
O C +N ga_32
N CA CB ga_12
C CA CB ga_12
CA CB SG ga_15
CB SG OD1 ga_12
OD1 SG OD2 ga_12
CB SG OD2 ga_12
CB SG OD3 ga_12
OD1 SG OD3 ga_12
OD2 SG OD3 ga_12
[ impropers ]
; ai aj ak al gromos type
N -C CA H gi_1
C CA +N O gi_1
CA N C CB gi_2
[ dihedrals ]
; ai aj ak al gromos type
-CA -C N CA gd_4
-C N CA C gd_19
N CA C +N gd_20
N CA CB SG gd_17
CA CB SG OD1 gd_13

; 3-nitrotyrosine (-1)
[YNI]
[ atoms ]
N N -0.28000 0
H H 0.28000 0
CA CH1 0.00000 1
CB CH2 0.00000 1
CG C 0.00000 1
CD1 C -0.10000 2
HD1 HC 0.10000 2
CD2 C -0.10000 3
HD2 HC 0.10000 3
CE1 C 0.10000 4 ; to add up to -1 net charge
NZ1 NR 0.05500 4 ; to add up to -1 net charge

OH1 O -0.36000 4 ; from the phosphate group of nucleotides (e.g., ATP)
OH2 O -0.36000 4 ; from the phosphate group of nucleotides (e.g., ATP)
CZ2 C 0.20000 4 ; to add up to -1 net charge
OH3 OM -0.63500 4 ; from the carboxyl group (of e.g., GLU)
CE2 C -0.10000 5
HE2 HC 0.10000 5
C C 0.380 6
O O -0.380 6
[ bonds ]
N H gb_2
N CA gb_20
CA C gb_26
C O gb_4
C +N gb_9
CA CB gb_26
CB CG gb_26
CG CD1 gb_15
CG CD2 gb_15
CD1 HD1 gb_3
CD1 CE1 gb_15
CD2 HD2 gb_3
CD2 CE2 gb_15
CE1 NZ1 gb_11
NZ1 OH1 gb_5
NZ1 OH2 gb_5
CE1 CZ2 gb_15
CE2 HE2 gb_3
CE2 CZ2 gb_15
CZ2 OH3 gb_12
[ exclusions ]
; ai aj
CB HD1
CB HD2
CB CE1
CB CE2
CG HE2
CG NZ1
CG CZ2
CD1 HD2
CD1 CE2
CD1 OH3
HD1 CD2
HD1 NZ1
HD1 CZ2
CD2 CE1
CD2 OH3
HD2 HE2
HD2 CZ2
CE1 HE2
HE2 OH3
NZ1 CE2
NZ1 OH3
[ angles ]
; ai aj ak gromos type
-C N H ga_31
H N CA ga_17
-C N CA ga_30
N CA C ga_12
CA C +N ga_18
CA C O ga_29
O C +N ga_32
N CA CB ga_12
C CA CB ga_12
CA CB SG ga_15
CB CG CD1 ga_26
CB CG CD2 ga_26
CD1 CG CD2 ga_26
CG CD1 HD1 ga_24
HD1 CD1 CE1 ga_24
CG CD1 CE1 ga_26
CG CD2 HD2 ga_24
HD2 CD2 CE2 ga_24
CG CD2 CE2 ga_26
CD1 CE1 NZ1 ga_26
CD1 CE1 CZ2 ga_26
NZ1 CE1 CZ2 ga_26
CE1 NZ1 OH1 ga_26
CE1 NZ1 OH2 ga_26
OH1 NZ1 OH2 ga_26
CD2 CE2 HE2 ga_24
HE2 CE2 CZ2 ga_24
CD2 CE2 CZ2 ga_26
CE1 CZ2 CE2 ga_26
CE1 CZ2 OH3 ga_26
CE2 CZ2 OH3 ga_26
[ impropers ]
; ai aj ak al gromos type
N -C CA H gi_1
C CA +N O gi_1
CA N C CB gi_2
CG CD1 CD2 CB gi_1
CD2 CG CD1 CE1 gi_1
CD1 CG CD2 CE2 gi_1

```

```

CG CD1 CE1 C22 gi_1
CG CD2 CE2 C22 gi_1
CD1 CE1 C22 CE2 gi_1
CD2 CE2 C22 CE1 gi_1
CD1 CG CE1 HD1 gi_1
CD2 CG CE2 HD2 gi_1
CE1 C22 CD1 NZ1 gi_1
CE2 C22 CD2 HE2 gi_1
C22 CE1 CE2 OH3 gi_1
NZ1 CE1 OH1 OH2 gi_1
[ dihedrals ]
; ai aj ak al gromos type
-CA -C N CA gd_4
-C N CA C gd_19
N CA C +N gd_20
N CA CB CG gd_17
CA CB CG CD1 gd_20
CE1 C22 OH3 HH3 gd_2
CD1 CE1 NZ1 OH1 gd_4

; 3-nitrotyrosine (0)
[ YNN ]
[ atoms ]
N N -0.28000 0
H H 0.28000 0
CA CH1 0.00000 1
CB CH2 0.00000 1
CG C 0.00000 1
CD1 C -0.10000 2
HD1 HC 0.10000 2
CD2 C -0.10000 3
HD2 HC 0.10000 3
CE1 C 0.10000 4 ; newly developed parameters tp match the experimental
HFE
NZ1 NR 0.30000 4 ; newly developed parameters tp match the experimental
HFE
OH1 O -0.20000 4 ; newly developed parameters tp match the experimental
HFE
OH2 O -0.20000 4 ; newly developed parameters tp match the experimental
HFE
CE2 C -0.10000 5
HE2 HC 0.10000 5
C22 C 0.05000 6 ; newly developed parameters tp match the experimental
HFE
OH3 OA -0.36000 6 ; newly developed parameters tp match the experimental
HFE
HH3 H 0.31000 6 ; newly developed parameters tp match the experimental
HFE
C C 0.380 7
O O -0.380 7
[ bonds ]
N H gb_2
N CA gb_20
CA C gb_26
C O gb_4
C +N gb_9
CA CB gb_26
CB CG gb_26
CG CD1 gb_15
CG CD2 gb_15
CD1 HD1 gb_3
CD1 CE1 gb_15
CD2 HD2 gb_3
CD2 CE2 gb_15
CE1 NZ1 gb_11
NZ1 OH1 gb_5
NZ1 OH2 gb_5
CE1 C22 gb_15
CE2 HE2 gb_3
CE2 C22 gb_15
C22 OH3 gb_12
OH3 HH3 gb_1
[ exclusions ]
; ai aj
CB HD1
CB HD2
CB CE1
CB CE2
CG HE2
CG NZ1
CG C22
CD1 HD2
CD1 CE2
CD1 OH3
HD1 CD2
HD1 NZ1
HD1 C22
CD2 CE1
CD2 OH3
HD2 HE2
HD2 C22
CE1 HE2
HE2 OH3

NZ1 CE2
NZ1 OH3
[ angles ]
; ai aj ak gromos type
-C N H ga_31
H N CA ga_17
-C N CA ga_30
N CA C ga_12
CA C +N ga_18
CA C O ga_29
O C +N ga_32
N CA CB ga_12
C CA CB ga_12
CA CB CG ga_14
CB CG CD1 ga_26
CB CG CD2 ga_26
CD1 CG CD2 ga_26
CG CD1 HD1 ga_24
HD1 CD1 CE1 ga_24
CG CD1 CE1 ga_26
CG CD2 HD2 ga_24
HD2 CD2 CE2 ga_24
CG CD2 CE2 ga_26
CD1 CE1 NZ1 ga_26
CD1 CE1 C22 ga_26
NZ1 CE1 C22 ga_26
CE1 NZ1 OH1 ga_26
CE1 NZ1 OH2 ga_26
OH1 NZ1 OH2 ga_26
CD2 CE2 HE2 ga_24
HE2 CE2 C22 ga_24
CD2 CE2 C22 ga_26
CE1 C22 CE2 ga_26
CE1 C22 OH3 ga_26
CE2 C22 OH3 ga_26
C22 OH3 HH3 ga_11
[ impropers ]
; ai aj ak al gromos type
N -C CA H gi_1
C CA +N O gi_1
CA N C CB gi_2
CG CD1 CD2 CB gi_1
CD2 CG CD1 CE1 gi_1
CD1 CG CD2 CE2 gi_1
CG CD1 CE1 C22 gi_1
CG CD2 CE2 C22 gi_1
CD1 CE1 C22 CE2 gi_1
CD2 CE2 C22 CE1 gi_1
CD1 CG CE1 HD1 gi_1
CD2 CG CE2 HD2 gi_1
CE1 C22 CD1 NZ1 gi_1
CE2 C22 CD2 HE2 gi_1
C22 CE1 CE2 OH3 gi_1
NZ1 CE1 OH1 OH2 gi_1
[ dihedrals ]
; ai aj ak al gromos type
-CA -C N CA gd_4
-C N CA C gd_19
N CA C +N gd_20
N CA CB CG gd_17
CA CB CG CD1 gd_20
CE1 C22 OH3 HH3 gd_2
CD1 CE1 NZ1 OH1 gd_4

; 3-nitrotyrosine (0)
[ YNB ]
[ atoms ]
N N -0.28000 0
H H 0.28000 0
CA CH1 0.00000 1
CB CH2 0.00000 1
CG C 0.00000 1
CD1 C -0.10000 2
HD1 HC 0.10000 2
CD2 C -0.10000 3
HD2 HC 0.10000 3
CE1 C 0.10000 4 ; to add up to 0 net charge
NZ1 NR 0.62000 4 ; to add up to 0 net charge
OH1 O -0.36000 4 ; from the phosphate group of nucleotides (e.g., ATP)
OH2 O -0.36000 4 ; from the phosphate group of nucleotides (e.g., ATP)
CE2 C -0.10000 5
HE2 HC 0.10000 5
C22 C 0.15000 6
OH3 OA -0.54800 6
HH3 H 0.39800 6
C C 0.380 7
O O -0.380 7
[ bonds ]
N H gb_2
N CA gb_20
CA C gb_26
C O gb_4
C +N gb_9

```

```

CA CB gb_26
CB CG gb_26
CG CD1 gb_15
CG CD2 gb_15
CD1 HD1 gb_3
CD1 CE1 gb_15
CD2 HD2 gb_3
CD2 CE2 gb_15
CE1 NZ1 gb_11
NZ1 OH1 gb_5
NZ1 OH2 gb_5
CE1 CZ2 gb_15
CE2 HE2 gb_3
CE2 CZ2 gb_15
CZ2 OH3 gb_12
OH3 HH3 gb_1
[ exclusions ]
; ai aj
CB HD1
CB HD2
CB CE1
CB CE2
CG HE2
CG NZ1
CG CZ2
CD1 HD2
CD1 CE2
CD1 OH3
HD1 CD2
HD1 NZ1
HD1 CZ2
CD2 CE1
CD2 OH3
HD2 HE2
HD2 CZ2
CE1 HE2
HE2 OH3
NZ1 CE2
NZ1 OH3
[ angles ]
; ai aj ak gromos type
-C N H ga_31
H N CA ga_17
-C N CA ga_30
N CA C ga_12
CA C +N ga_18
CA C O ga_29
O C +N ga_32
N CA CB ga_12
C CA CB ga_12
CA CB CG ga_14
CB CG CD1 ga_26
CB CG CD2 ga_26
CD1 CG CD2 ga_26
CG CD1 HD1 ga_24
HD1 CD1 CE1 ga_24
CG CD1 CE1 ga_26
CG CD2 HD2 ga_24
HD2 CD2 CE2 ga_24
CG CD2 CE2 ga_26
CD1 CE1 NZ1 ga_26
CD1 CE1 CZ2 ga_26
NZ1 CE1 CZ2 ga_26
CE1 NZ1 OH1 ga_26
CE1 NZ1 OH2 ga_26
OH1 NZ1 OH2 ga_26
CD2 CE2 HE2 ga_24
HE2 CE2 CZ2 ga_24
CD2 CE2 CZ2 ga_26
CE1 CZ2 CE2 ga_26
CE1 CZ2 OH3 ga_26
CE2 CZ2 OH3 ga_26
CZ2 OH3 HH3 ga_11
[ impropers ]
; ai aj ak al gromos type
N -C CA H gi_1
C CA +N O gi_1
CA N C CB gi_2
CG CD1 CD2 CB gi_1
CD2 CG CD1 CE1 gi_1
CD1 CG CD2 CE2 gi_1
CG CD1 CE1 CZ2 gi_1
CG CD2 CE2 CZ2 gi_1
CD1 CE1 CZ2 CE2 gi_1
CD2 CE2 CZ2 CE1 gi_1
CD1 CG CE1 HD1 gi_1
CD2 CG CE2 HD2 gi_1
CE1 CZ2 CD1 NZ1 gi_1
CE2 CZ2 CD2 HE2 gi_1
CZ2 CE1 CE2 OH3 gi_1
NZ1 CE1 OH1 OH2 gi_1
[ dihedrals ]
; ai aj ak al gromos type
-C N CA gd_4
-C N CA C gd_19
N CA C +N gd_20
N CA CB CG gd_17
CA CB CG CD1 gd_20
CE1 CZ2 OH3 HH3 gd_2
CD1 CE1 NZ1 OH1 gd_4
; 6-nitrotryptophan
[ WNI ]
[ atoms ]
N N -0.28000 0
H H 0.28000 0
CA CH1 0.00000 1
CB CH2 0.00000 1
CG C -0.14000 2
CD1 C -0.10000 2
HD1 HC 0.10000 2
CD2 C 0.00000 2
NE1 NR -0.05000 2
HE1 H 0.19000 2
CE2 C 0.00000 2
CE3 C -0.10000 3
HE3 HC 0.10000 3
CZ2 C -0.10000 4
HZ2 HC 0.10000 4
CZ3 C -0.10000 5
HZ3 HC 0.10000 5
CH2 C 0.10000 6 ; to add up to 0 net charge
NT NR 0.62000 6 ; to add up to 0 net charge
O11 O -0.36000 6 ; from the phosphate group of nucleotides (e.g., ATP)
O12 O -0.36000 6 ; from the phosphate group of nucleotides (e.g., ATP)
C C 0.380 7
O O -0.380 7
[ bonds ]
N H gb_2
N CA gb_20
CA C gb_26
C O gb_4
C +N gb_9
CA CB gb_26
CB CG gb_26
CG CD1 gb_9
CG CD2 gb_15
CD1 HD1 gb_3
CD1 NE1 gb_9
CD2 CE2 gb_15
CD2 CE3 gb_15
NE1 HE1 gb_2
NE1 CE2 gb_9
CE2 CZ2 gb_15
CE3 HE3 gb_3
CE3 CZ3 gb_15
CZ2 HZ2 gb_3
CZ2 CH2 gb_15
CZ3 HZ3 gb_3
CZ3 CH2 gb_15
CH2 NT gb_11
NT O11 gb_5
NT O12 gb_5
[ exclusions ]
; ai aj
CB HD1
CB NE1
CB CE2
CB CE3
CG HE1
CG HE3
CG CZ2
CG CZ3
CD1 CE3
CD1 CZ2
HD1 CD2
HD1 HE1
HD1 CE2
CD2 HE1
CD2 HZ2
CD2 HZ3
NE1 CE3
NE1 HZ2
NE1 CH2
HE1 CZ2
CE2 HE3
CE2 CZ3
CE2 NT
CE3 CZ2
CE3 NT
HE3 HZ3
HE3 CH2
CZ2 HZ3
HZ2 CZ3
HZ2 NT

```



```

HZ3 NT
[angles]
; ai aj ak gromos type
-C N H ga_31
H N CA ga_17
-C N CA ga_30
N CA C ga_12
CA C +N ga_18
CA C O ga_29
O C +N ga_32
N CA CB ga_12
C CA CB ga_12
CA CB CG ga_14
CB CG CD1 ga_36
CB CG CD2 ga_36
CD1 CG CD2 ga_6
CG CD1 HD1 ga_35
HD1 CD1 NE1 ga_35
CG CD1 NE1 ga_6
CG CD2 CE2 ga_6
CD1 NE1 CE2 ga_6
CD1 NE1 HE1 ga_35
HE1 NE1 CE2 ga_35
NE1 CE2 CD2 ga_6
CG CD2 CE3 ga_38
NE1 CE2 CZ2 ga_38
CD2 CE2 CZ2 ga_26
CE2 CD2 CE3 ga_26
CD2 CE3 HE3 ga_24
HE3 CE3 CZ3 ga_24
CD2 CE3 CZ3 ga_26
CE2 CZ2 HZ2 ga_24
HZ2 CZ2 CH2 ga_24
CE2 CZ2 CH2 ga_26
CE3 CZ3 HZ3 ga_24
HZ3 CZ3 CH2 ga_24
CE3 CZ3 CH2 ga_26
CZ2 CH2 CZ3 ga_26
CZ2 CH2 NT ga_26
CZ3 CH2 NT ga_26
CH2 NT OI1 ga_26
CH2 NT OI2 ga_26
OI1 NT OI2 ga_26
[impropers]
; ai aj ak al gromos type
N -C CA H gi_1
C CA +N O gi_1
CA N C CB gi_2
CG CD1 CD2 CB gi_1
CD2 CG CD1 NE1 gi_1
CD1 CG CD2 CE2 gi_1
CG CD1 NE1 CE2 gi_1
CG CD2 CE2 NE1 gi_1
CD1 NE1 CE2 CD2 gi_1
CD1 CG NE1 HD1 gi_1
NE1 CD1 CE2 HE1 gi_1
CD2 CE2 CE3 CG gi_1
CE2 CD2 CZ2 NE1 gi_1
CE3 CD2 CE2 CZ2 gi_1
CD2 CE2 CZ2 CH2 gi_1
CE2 CD2 CE3 CZ3 gi_1
CE2 CZ2 CH2 CZ3 gi_1
CD2 CE3 CZ3 CH2 gi_1
CE3 CZ3 CH2 CZ2 gi_1
CE3 CD2 CZ3 HE3 gi_1
CZ2 CE2 CH2 HZ2 gi_1
CZ3 CE3 CH2 HZ3 gi_1
CH2 CZ2 CZ3 NT gi_1
NT OI1 OI2 CH2 gi_1
[dihedrals]
; ai aj ak al gromos type
-CA -C N CA gd_4
-C N CA C gd_19
N CA C +N gd_20
N CA CB CG gd_17
CA CB CG CD2 gd_20
CZ2 CH2 NT OI1 gd_4

; kynurenine
[WKY]
[atoms]
N N -0.28000 0
H H 0.28000 0
CA CH1 0.00000 1
CB CH2 0.00000 1
CG C 0.38000 2
OD1 O -0.38000 2
CD2 C 0.00000 3
CE1 C 0.00000 3
NZ1 NT -0.83000 4; from ARGN
HZ11 H 0.41500 4; from ARGN
HZ12 H 0.41500 4; from ARGN
CE2 C -0.10000 5
HE2 HC 0.10000 5
CZ2 C -0.10000 6
HZ2 HC 0.10000 6
CZ3 C -0.10000 7
HZ3 HC 0.10000 7
CH C -0.10000 8
HH HC 0.10000 8
C C 0.380 9
O O -0.380 9
[bonds]
N H gb_2
N CA gb_20
CA C gb_26
C O gb_4
C +N gb_9
CA CB gb_26
CB CG gb_26
CG OD1 gb_4
CG CD2 gb_22
CD2 CE1 gb_15
CD2 CE2 gb_15
CE1 NZ1 gb_8
CE1 CZ2 gb_15
CE2 HE2 gb_3
CE2 CZ3 gb_15
NZ1 HZ11 gb_2
NZ1 HZ12 gb_2
CZ2 HZ2 gb_3
CZ2 CH gb_15
CZ3 HZ3 gb_3
CZ3 CH gb_15
CH HH gb_3
[exclusions]
; ai aj
CB CE1
CB CE2
CG NZ1
CG HE2
CG CZ2
CG CZ3
CD2 HZ11
CD2 HZ12
CD2 HZ2
CD2 HZ3
CD2 CH
CE1 HE2
CE1 CZ3
CE1 HH
CE2 CZ2
CE2 HH
HE2 HZ3
HE2 CH
NZ1 CE2
NZ1 HZ2
NZ1 CH
HZ11 CZ2
HZ12 CZ2
CZ2 HZ3
HZ2 CZ3
HZ2 HH
HZ3 HH
[angles]
; ai aj ak gromos type
-C N H ga_31
H N CA ga_17
-C N CA ga_30
N CA C ga_12
CA C +N ga_18
CA C O ga_29
O C +N ga_32
N CA CB ga_12
C CA CB ga_12
CA CB CG ga_14
CB CG OD1 ga_26
CB CG CD2 ga_26
OD1 CG CD2 ga_26
CG CD2 CE1 ga_26
CG CD2 CE2 ga_26
CE1 CD2 CE2 ga_26
CD2 CE1 NZ1 ga_26
CD2 CE1 CZ2 ga_26
NZ1 CE1 CZ2 ga_26
CD2 CE2 HE2 ga_24
HE2 CE2 CZ3 ga_24
CD2 CE2 CZ3 ga_26
CE1 NZ1 HZ11 ga_22
CE1 NZ1 HZ12 ga_22
HZ11 NZ1 HZ12 ga_23
CE1 CZ2 HZ2 ga_24
HZ2 CZ2 CH ga_24
CE1 CZ2 CH ga_26
CE2 CZ3 HZ3 ga_24
HZ3 CZ3 CH ga_24

```

```

CE2 CZ3 CH ga_26
CZ2 CH HH ga_24
CZ3 CH HH ga_24
CZ2 CH CZ3 ga_26
[impropers]
; ai aj ak al gromos type
  N -C CA H gi_1
  C CA +N O gi_1
  CA N C CB gi_2
  CG CD2 OD1 CB gi_1
  CD2 CE1 CE2 CG gi_1
  CE2 CD2 CE1 CZ2 gi_1
  CE1 CD2 CE2 CZ3 gi_1
  CD2 CE1 CZ2 CH gi_1
  CD2 CE2 CZ3 CH gi_1
  CE1 CZ2 CH CZ3 gi_1
  CE2 CZ3 CH CZ2 gi_1
  CE1 CD2 CZ2 NZ1 gi_1
  CE2 CD2 CZ3 HE2 gi_1
  NZ1 HZ11 HZ12 CE1 gi_1
  CZ2 CH CE1 HZ2 gi_1
  CZ3 CH CE2 HZ3 gi_1
  CH CZ2 CZ3 HH gi_1
[dihedrals]
; ai aj ak al gromos type
-CA -C N CA gd_4
-C N CA C gd_19
N CA C +N gd_20
N CA CB CG gd_17
CA CB CG CD2 gd_20
CB CG CD2 CE1 gd_1
CD2 CE1 NZ1 HZ11 gd_4

; 3-hydroxykynurenine
[WKH]
[atoms]
  N N -0.28000 0
  H H 0.28000 0
  CA CH1 0.00000 1
  CB CH2 0.00000 1
  CG C 0.38000 2
  OD1 O -0.38000 2
  CD2 C 0.00000 3
  CE1 C 0.00000 3
  NZ1 NT -0.83000 4; from ARGN
  HZ11 H 0.41500 4; from ARGN
  HZ12 H 0.41500 4; from ARGN
  CE2 C -0.10000 5
  HE2 HC 0.10000 5
  CZ2 C 0.15000 6; from the hydroxyl group of TYR
  OH1 OA -0.54800 6; from the hydroxyl group of TYR
  HH1 H 0.39800 6; from the hydroxyl group of TYR
  CZ3 C -0.10000 7
  HZ3 HC 0.10000 7
  CH2 C -0.10000 8
  HH2 HC 0.10000 8
  C C 0.380 9
  O O -0.380 9
[bonds]
  N H gb_2
  N CA gb_20
  CA C gb_26
  C O gb_4
  C +N gb_9
  CA CB gb_26
  CB CG gb_26
  CG OD1 gb_4
  CG CD2 gb_22
  CD2 CE1 gb_15
  CD2 CE2 gb_15
  CE1 NZ1 gb_8
  CE1 CZ2 gb_15
  CE2 HE2 gb_3
  CE2 CZ3 gb_15
  NZ1 HZ11 gb_2
  NZ1 HZ12 gb_2
  CZ2 OH1 gb_12
  CZ2 CH2 gb_15
  CZ3 HZ3 gb_3
  CZ3 CH2 gb_15
  OH1 HH1 gb_1
  CH2 HH2 gb_3
[exclusions]
; ai aj
  CB CE1
  CB CE2
  CG HE2
  CG NZ1
  CG CZ2
  CG CZ3
  CD2 HZ11
  CD2 HZ12
  CD2 HZ3
  CD2 OH1
  CD2 CH2
  CE1 HE2
  CE1 CZ3
  CE1 HH1
  CE1 HH2
  CE2 CZ2
  CE2 HH2
  HE2 HZ3
  HE2 CH2
  NZ1 CE2
  NZ1 OH1
  NZ1 HH1
  NZ1 CH2
  HZ11 CZ2
  HZ11 OH1
  HZ12 CZ2
  HZ12 OH1
  CZ2 HZ3
  HZ3 HH2
  OH1 CZ3
  OH1 HH2
  HH1 CH2
[angles]
; ai aj ak gromos type
-C N H ga_31
H N CA ga_17
-C N CA ga_30
N CA C ga_12
CA C +N ga_18
CA C O ga_29
O C +N ga_32
N CA CB ga_12
C CA CB ga_12
CA CB CG ga_14
CB CG OD1 ga_26
CB CG CD2 ga_26
OD1 CG CD2 ga_26
CG CD2 CE1 ga_26
CG CD2 CE2 ga_26
CE1 CD2 CE2 ga_26
CD2 CE1 NZ1 ga_26
CD2 CE1 CZ2 ga_26
NZ1 CE1 CZ2 ga_26
CD2 CE2 HE2 ga_24
HE2 CE2 CZ3 ga_24
CD2 CE2 CZ3 ga_26
CE1 NZ1 HZ11 ga_22
CE1 NZ1 HZ12 ga_22
HZ11 NZ1 HZ12 ga_23
CE1 CZ2 OH1 ga_26
CE1 CZ2 CH2 ga_26
OH1 CZ2 CH2 ga_26
CE2 CZ3 HZ3 ga_24
HZ3 CZ3 CH2 ga_24
CE2 CZ3 CH2 ga_26
CZ2 OH1 HH1 ga_11
CZ2 CH2 HH2 ga_24
CZ3 CH2 HH2 ga_24
CZ2 CH2 CZ3 ga_26
[impropers]
; ai aj ak al gromos type
  N -C CA H gi_1
  C CA +N O gi_1
  CA N C CB gi_2
  CG CD2 OD1 CB gi_1
  CD2 CE1 CE2 CG gi_1
  CE2 CD2 CE1 CZ2 gi_1
  CE1 CD2 CE2 CZ3 gi_1
  CD2 CE1 CZ2 CH2 gi_1
  CD2 CE2 CZ3 CH2 gi_1
  CE1 CZ2 CH2 CZ3 gi_1
  CE2 CZ3 CH2 CZ2 gi_1
  CE1 CD2 CZ2 NZ1 gi_1
  CE2 CD2 CZ3 HE2 gi_1
  NZ1 HZ11 HZ12 CE1 gi_1
  CZ2 CH2 CE1 OH1 gi_1
  CZ3 CH2 CE2 HZ3 gi_1
  CH2 CZ2 CZ3 HH2 gi_1
[dihedrals]
; ai aj ak al gromos type
-CA -C N CA gd_4
-C N CA C gd_19
N CA C +N gd_20
N CA CB CG gd_17
CA CB CG CD2 gd_20
CB CG CD2 CE1 gd_1
CD2 CE1 NZ1 HZ11 gd_4
CE1 CZ2 OH1 HH1 gd_2

; formyl-kynurenine
[WKF]
[atoms]

```

```

N N -0.28000 0
H H 0.28000 0
CA CH1 0.00000 1
CB CH2 0.00000 1
CG C 0.38000 2
OD1 O -0.38000 2
CD2 C 0.00000 3
CE1 C 0.00000 3
NZ1 N -0.28000 4 ; from the peptide bond
HZ1 H 0.28000 4 ; from the peptide bond
CH1 C 0.28000 5 ; by analogy to the aldehyde group reported by Dolenc et al.
DOI: 10.1093/nar/gki195
HH1 HC 0.10000 5 ; by analogy to the aldehyde group reported by Dolenc et al. DOI: 10.1093/nar/gki195
OI O -0.38000 5 ; from the carbonyl group (of e.g., GLN)
CE2 C -0.10000 6
HE2 HC 0.10000 6
CZ2 C -0.10000 7
HZ2 HC 0.10000 7
CZ3 C -0.10000 8
HZ3 HC 0.10000 8
CH2 C -0.10000 9
HH2 HC 0.10000 9
C C 0.380 10
O O -0.380 10
[ bonds ]
N H gb_2
N CA gb_20
CA C gb_26
C O gb_4
C +N gb_9
CA CB gb_26
CB CG gb_26
CG OD1 gb_4
CG CD2 gb_22
CD2 CE1 gb_15
CD2 CE2 gb_15
CE1 NZ1 gb_8
CE1 CZ2 gb_15
CE2 HE2 gb_3
CE2 CZ3 gb_15
NZ1 HZ1 gb_2
NZ1 CH1 gb_9
CZ2 HZ2 gb_3
CZ2 CH2 gb_15
CZ3 HZ3 gb_3
CZ3 CH2 gb_15
CH1 HH1 gb_3
CH1 OI gb_4
CH2 HH2 gb_3
[ exclusions ]
; ai aj
CB CE1
CB CE2
CG NZ1
CG HE2
CG CZ2
CG CZ3
CD2 HZ1
CD2 HZ2
CD2 HZ3
CD2 CH2
CE1 HE2
CE1 CZ3
CE1 HH2
CE2 CZ2
CE2 HH2
HE2 HZ3
HE2 CH2
NZ1 CE2
NZ1 HZ2
NZ1 CH2
HZ1 CZ2
CZ2 HZ3
HZ2 CZ3
HZ2 HH2
HZ3 HH2
[ angles ]
; ai aj ak gromos type
-C N H ga_31
H N CA ga_17
-C N CA ga_30
N CA C ga_12
CA C +N ga_18
CA C O ga_29
O C +N ga_32
N CA CB ga_12
C CA CB ga_12
CA CB CG ga_14
CB CG OD1 ga_26
CB CG CD2 ga_26
OD1 CG CD2 ga_26
CG CD2 CE1 ga_26
CG CD2 CE2 ga_26
CE1 CD2 CE2 ga_26
CD2 CE1 NZ1 ga_26
NZ1 CE1 CZ2 ga_26
CD2 CE2 HE2 ga_24
HE2 CE2 CZ3 ga_24
CD2 CE2 CZ3 ga_26
CE1 NZ1 HZ1 ga_17
HZ1 NZ1 CH1 ga_31
CE1 NZ1 CH1 ga_30
CE1 CZ2 HZ2 ga_24
HZ2 CZ2 CH2 ga_24
CE1 CZ2 CH2 ga_26
CE2 CZ3 HZ3 ga_24
HZ3 CZ3 CH2 ga_24
CE2 CZ3 CH2 ga_26
NZ1 CH1 HH1 ga_18
HH1 CH1 OI ga_29
NZ1 CH1 OI ga_32
CZ2 CH2 HH2 ga_24
CZ3 CH2 HH2 ga_24
CZ2 CH2 CZ3 ga_26
[ impropers ]
; ai aj ak al gromos type
N -C CA H gi_1
C CA +N O gi_1
CA N C CB gi_2
CG CD2 OD1 CB gi_1
CD2 CE1 CE2 CG gi_1
CE2 CD2 CE1 CZ2 gi_1
CE1 CD2 CE2 CZ3 gi_1
CD2 CE1 CZ2 CH2 gi_1
CD2 CE2 CZ3 CH2 gi_1
CE1 CZ2 CH2 CZ3 gi_1
CE2 CZ3 CH2 CZ2 gi_1
CE1 CD2 CZ2 NZ1 gi_1
CE2 CD2 CZ3 HE2 gi_1
NZ1 CH1 CE1 HZ1 gi_1
CZ2 CH2 CE1 HZ2 gi_1
CZ3 CH2 CE2 HZ3 gi_1
CH1 OI NZ1 HH1 gi_1
CH2 CZ2 CZ3 HH2 gi_1
[ dihedrals ]
; ai aj ak al gromos type
-CA -C N CA gd_4
-C N CA C gd_19
N CA C +N gd_20
N CA CB CG gd_17
CA CB CG CD2 gd_20
CB CG CD2 CE1 gd_1
CD2 CE1 NZ1 CH1 gd_4
CE1 NZ1 CH1 OI gd_4
; chlorotyrosine
[ YCH ]
[ atoms ]
N N -0.28000 0
H H 0.28000 0
CA CH1 0.00000 1
CB CH2 0.00000 1
CG C 0.00000 1
CD1 C -0.10000 2
HD1 HC 0.10000 2
CD2 C -0.10000 3
HD2 HC 0.10000 3
CE1 C 0.08700 4 ; from CHCL3
CLZ1 CL -0.08700 4 ; from CHCL3
CE2 C -0.10000 5
HE2 HC 0.10000 5
CZ2 C 0.15000 6
OH OA -0.54800 6
HH H 0.39800 6
C C 0.380 7
O O -0.380 7
[ bonds ]
N H gb_2
N CA gb_20
CA C gb_26
C O gb_4
C +N gb_9
CA CB gb_26
CB CG gb_26
CG CD1 gb_15
CG CD2 gb_15
CD1 HD1 gb_3
CD1 CE1 gb_15
CD2 HD2 gb_3
CD2 CE2 gb_15
CE1 CLZ1 gb_37
CE1 CZ2 gb_15
CE2 HE2 gb_3
CE2 CZ2 gb_15

```

```

CZ2 OH gb_12
OH HH gb_1
[ exclusions ]
; ai aj
CB HD1
CB HD2
CB CE1
CB CE2
CG HE2
CG CLZ1
CG CZ2
CD1 HD2
CD1 CE2
CD1 OH
HD1 CD2
HD1 CLZ1
HD1 CZ2
CD2 CE1
CD2 OH
HD2 HE2
HD2 CZ2
CE1 HE2
HE2 OH
CLZ1 CE2
CLZ1 OH
[ angles ]
; ai aj ak gromos type
-C N H ga_31
H N CA ga_17
-C N CA ga_30
N CA C ga_12
CA C +N ga_18
CA C O ga_29
O C +N ga_32
N CA CB ga_12
C CA CB ga_12
CA CB CG ga_14
CB CG CD1 ga_26
CB CG CD2 ga_26
CD1 CG CD2 ga_26
CG CD1 HD1 ga_24
HD1 CD1 CE1 ga_24
CG CD1 CE1 ga_26
CG CD2 HD2 ga_24
HD2 CD2 CE2 ga_24
CG CD2 CE2 ga_26
CD1 CE1 CLZ1 ga_26
CD1 CE1 CZ2 ga_26
CLZ1 CE1 CZ2 ga_26
CD2 CE2 HE2 ga_24
HE2 CE2 CZ2 ga_24
CD2 CE2 CZ2 ga_26
CE1 CZ2 CE2 ga_26
CE1 CZ2 OH ga_26
CE2 CZ2 OH ga_26
CZ2 OH HH ga_11
[ impropers ]
; ai aj ak al gromos type
N -C CA H gi_1
C CA +N O gi_1
CA N C CB gi_2
CG CD1 CD2 CB gi_1
CD2 CG CD1 CE1 gi_1
CD1 CG CD2 CE2 gi_1
CG CD1 CE1 CZ2 gi_1
CG CD2 CE2 CZ2 gi_1
CD1 CE1 CZ2 CE2 gi_1
CD2 CE2 CZ2 CE1 gi_1
CD1 CG CE1 HD1 gi_1
CD2 CG CE2 HD2 gi_1
CE1 CZ2 CD1 CLZ1 gi_1
CE2 CZ2 CD2 HE2 gi_1
CZ2 CE1 CE2 OH gi_1
[ dihedrals ]
; ai aj ak al gromos type
-CA -C N CA gd_4
-C N CA C gd_19
N CA C +N gd_20
N CA CB CG gd_17
CA CB CG CD gd_17
CG CG CD CE gd_17
CG CD CE NZ gd_17
CD CE NZ CH gd_19
CE NZ CH NI2 gd_4
NZ CH NI2 HI21 gd_4
; carboxyllysine (-1)
[ KCA ]
[ atoms ]
N N -0.28000 0
H H 0.28000 0
CA CH1 0.00000 1
CB CH2 0.00000 1
CG CH2 0.00000 2
CD CH2 0.00000 2
CE CH2 0.00000 2
NZ N -0.28000 4 ; from the peptide bond
HZ H 0.28000 4 ; from the peptide bond
CH C 0.27000 5 ; from the carboxyl group (of e.g., GLU)
OI1 OM -0.63500 5 ; from the carboxyl group (of e.g., GLU)
OI2 OM -0.63500 5 ; from the carboxyl group (of e.g., GLU)
C C 0.380 6
O O -0.380 6
[ bonds ]
N H gb_2
N CA gb_20
CA C gb_26
C O gb_4
C +N gb_9
CA CB gb_26
CB CG gb_26
CG CD gb_26
CD CE gb_26
CE NZ gb_20
NZ HZ gb_2
NZ CH gb_9
CH OI1 gb_4
CH NI2 gb_8
NI2 HI21 gb_2
NI2 HI22 gb_2
[ angles ]
; ai aj ak gromos type
-C N H ga_31
H N CA ga_17
-C N CA ga_30
N CA C ga_12
CA C +N ga_18
CA C O ga_29
O C +N ga_32
N CA CB ga_12
C CA CB ga_12
CA CB CG ga_14
CB CG CD ga_14
CG CD CE ga_14
CD CE NZ ga_14
CE NZ HZ ga_17
CE NZ CH ga_30
HZ NZ CH ga_31
NZ CH OI1 ga_29
NZ CH NI2 ga_21
OI1 CH NI2 ga_29
CH NI2 HI21 ga_22
CH NI2 HI22 ga_22
HI21 NI2 HI22 ga_23
[ impropers ]
; ai aj ak al gromos type
N -C CA H gi_1
C CA +N O gi_1
CA N C CB gi_2
NZ CH CE HZ gi_1
CH NI2 OI1 NZ gi_1
NI2 HI21 HI22 CH gi_1
[ dihedrals ]
; ai aj ak al gromos type
-CA -C N CA gd_4
-C N CA C gd_19
N CA C +N gd_20
N CA CB CG gd_17
CA CB CG CD gd_17
CG CG CD CE gd_17
CG CD CE NZ gd_17
CD CE NZ CH gd_19
CE NZ CH NI2 gd_4
NZ CH NI2 HI21 gd_4
; carboxyllysine (-1)
[ KCA ]
[ atoms ]
N N -0.28000 0
H H 0.28000 0
CA CH1 0.00000 1
CB CH2 0.00000 1
CG CH2 0.00000 2
CD CH2 0.00000 2
CE CH2 0.00000 2
NZ N -0.28000 4 ; from the peptide bond
HZ H 0.28000 4 ; from the peptide bond
CH C 0.27000 5 ; from the carboxyl group (of e.g., GLU)
OI1 OM -0.63500 5 ; from the carboxyl group (of e.g., GLU)
OI2 OM -0.63500 5 ; from the carboxyl group (of e.g., GLU)
C C 0.380 6
O O -0.380 6
[ bonds ]
N H gb_2
N CA gb_20
CA C gb_26
C O gb_4
C +N gb_9

```

```

CA CB gb_26
CB CG gb_26
CG CD gb_26
CD CE gb_26
CE NZ gb_20
NZ HZ gb_2
NZ CH gb_9
CH OI1 gb_5
CH OI2 gb_5
[angles]
; ai aj ak gromos type
-C N H ga_31
H N CA ga_17
-C N CA ga_30
N CA C ga_12
CA C +N ga_18
CA C O ga_29
O C +N ga_32
N CA CB ga_12
C CA CB ga_12
CA CB CG ga_14
CB CG CD ga_14
CG CD CE ga_14
CD CE NZ ga_14
CE NZ HZ ga_17
CE NZ CH ga_30
HZ NZ CH ga_31
NZ CH OI1 ga_21
NZ CH OI2 ga_21
OI1 CH OI2 ga_37
[impropers]
; ai aj ak al gromos type
N -C CA H gi_1
C CA +N O gi_1
CA N C CB gi_2
NZ CH CE HZ gi_1
CH NZ OI1 OI2 gi_1
[dihedrals]
; ai aj ak al gromos type
-CA -C N CA gd_4
-C N CA C gd_19
N CA C +N gd_20
N CA CB CG gd_17
CA CB CG CD gd_17
CB CG CD CE gd_17
CG CD CE NZ gd_17
CD CE NZ CH gd_19
CE NZ CH OI2 gd_4
NZ CH OI2 HI2 gd_3
; S-carbamoyl-cysteine
[CAM]
[atoms]
N N -0.28000 0
H H 0.28000 0
CA CH1 0.00000 1
CB CH2 0.00000 1
SG S 0.00000 1
CD C 0.38000 2; from ASN/GLN
OE1 O -0.38000 2; from ASN/GLN
NE2 NT -0.83000 3; from ASN/GLN
HE21 H 0.41500 3; from ASN/GLN
HE22 H 0.41500 3; from ASN/GLN
C C 0.380 4
O O -0.380 4
[atoms]
N H gb_2
N CA gb_20
CA C gb_26
C O gb_4
C +N gb_9
CA CB gb_26
CB SG gb_30
SG CD gb_30
CD OE1 gb_4
CD NE2 gb_8
NE2 HE21 gb_2
NE2 HE22 gb_2
[angles]
; ai aj ak gromos type
-C N H ga_31
H N CA ga_17
-C N CA ga_30
N CA C ga_12
CA C +N ga_18
CA C O ga_29
O C +N ga_32
N CA CB ga_12
CA CB SG ga_15
CB SG CD ga_3
SG CD OE1 ga_29
SG CD NE2 ga_18
OE1 CD NE2 ga_32
CD NE2 HE21 ga_22
CD NE2 HE22 ga_22
HE21 NE2 HE22 ga_23
[impropers]
; ai aj ak al gromos type
N -C CA H gi_1
C CA +N O gi_1
CA N C CB gi_2
CD NE2 OE1 SG gi_1
NE2 CD HE21 HE22 gi_1
[dihedrals]
; ai aj ak al gromos type
-CA -C N CA gd_4
-C N CA C gd_19
N CA C +N gd_20
N CA CB SG gd_17
CA CB SG CD gd_13

```

```

CB SG CD NE2 gd_20
SG CD NE2 HE21 gd_4

; norleucine
[LNO]
[atoms]
N N -0.28000 0
H H 0.28000 0
CA CH1 0.00000 1
CB CH2 0.00000 1; from aliphatic carbon atoms
CG CH2 0.00000 1; from aliphatic carbon atoms
CD CH2 0.00000 2; from aliphatic carbon atoms
CE CH3 0.00000 2; from aliphatic carbon atoms
C C 0.380 3
O O -0.380 3
[bonds]
N H gb_2
N CA gb_20
CA C gb_26
C O gb_4
C +N gb_9
CA CB gb_26
CB CG gb_26
CG CD gb_26
CD CE gb_26
[angles]
; ai aj ak gromos type
-C N H ga_31
H N CA ga_17
-C N CA ga_30
N CA C ga_12
CA C +N ga_18
CA C O ga_29
O C +N ga_32
N CA CB ga_12
C CA CB ga_12
CA CB CG ga_14
CB CG CD ga_14
CG CD CE ga_14
[impropers]
; ai aj ak al gromos type
N -C CA H gi_1
C CA +N O gi_1
CA N C CB gi_2
[dihedrals]
; ai aj ak al gromos type
-CA -C N CA gd_4
-C N CA C gd_19
N CA C +N gd_20
N CA CB CG gd_17
CA CB CG CD gd_17
CB CG CD CE gd_17

; pyruvic acid (N-terminal modification)
[PYA]
[atoms]
CA C 0.380 0; from the carbonyl group (of e.g., GLN)
OB2 O -0.380 0; from the carbonyl group (of e.g., GLN)
CB1 CH3 0.00000 1; from aliphatic carbon atoms
C C 0.380 2
O O -0.380 2
[bonds]
CA C gb_22; shorter bond type to account for double bond effect
CA OB2 gb_4
C O gb_4
C +N gb_9
CA CB1 gb_26
[angles]
; ai aj ak gromos type
CA C +N ga_18
CA C O ga_29
O C +N ga_32
C CA CB1 ga_26
C CA OB2 ga_26
OB2 CA CB1 ga_26
[impropers]
; ai aj ak al gromos type
C CA +N O gi_1
CA OB2 C CB1 gi_1
[dihedrals]
; ai aj ak al gromos type
CB1 CA C +N gd_4

; aminoacids.n.tdb file (N-terminal parameters)

; N-methyl-AA (0)
[1NM]
[replace]
N NT 14.0067 -0.83
; from NZ of LYS

CA CH1 13.019 0.210 0
; from trimethylamine reported by Oostenbrink et al. DOI:
10.1002/cphc.200400542
[add]
1 1 H1 N CA C
H 1.008 0.410
; derived from terminal hydrogen atoms of LYS
1 4 CN1 N CA C
CH3 15.035 0.210
; from trimethylamine reported by Oostenbrink et al. DOI:
10.1002/cphc.200400542
[delete]
H
[bonds]
N H1 gb_2
N CN1 gb_20
[angles]
CN1 N H1 ga_10
CA N H1 ga_10
CA N CN1 ga_12
[dihedrals]
CN1 N CA C gd_14

; N-methyl-glycine (0)
[GLY-1NM]
[replace]
N NT 14.0067 -0.83
; from NZ of LYS
CA CH2 14.027 0.210 0
; from trimethylamine reported by Oostenbrink et al. DOI:
10.1002/cphc.200400542
[add]
1 1 H1 N CA C
H 1.008 0.410
; derived from terminal hydrogen atoms of LYS
1 4 CN1 N CA C
CH3 15.035 0.210
; from trimethylamine reported by Oostenbrink et al. DOI:
10.1002/cphc.200400542
[delete]
H
[bonds]
N H1 gb_2
N CN1 gb_20
[angles]
CN1 N H1 ga_10
CA N H1 ga_10
CA N CN1 ga_12
[dihedrals]
CN1 N CA C gd_14

; N-methyl-proline (0)
[PRO-1NM]
[replace]
N NT 14.0067 -0.63
; from trimethylamine reported by Oostenbrink et al. DOI:
10.1002/cphc.200400542
CA CH1 13.019 0.210 0
; from trimethylamine reported by Oostenbrink et al. DOI:
10.1002/cphc.200400542
CD CH2 14.027 0.210 0
; from trimethylamine reported by Oostenbrink et al. DOI:
10.1002/cphc.200400542
[add]
1 4 CN1 N CA C
CH3 15.035 0.210
; from trimethylamine reported by Oostenbrink et al. DOI:
10.1002/cphc.200400542
[bonds]
N CN1 gb_20
[angles]
CA N CN1 ga_12
CD N CN1 ga_12
[dihedrals]
CN1 N CA C gd_14

; N-methyl-AA (+1)
[1NM+]
[replace]
N NL 14.0067 0.104
; to add up to +1 net charge
CA CH1 13.019 0.200 0
; derived by analogy to methyl groups of amines reported by
Oostenbrink et al. DOI: 10.1002/cphc.200400542
[add]
2 4 H N CA C
H 1.008 0.248
1 1 CN1 N CA C
CH3 15.035 0.200
; derived by analogy to methyl groups of amines reported by
Oostenbrink et al. DOI: 10.1002/cphc.200400542
[delete]
H

```

```

[ bonds ]
N      H1      gb_2
N      H2      gb_2
N      CN1     gb_20
[ angles ]
H1     N      H2      ga_9
H2     N      CN1     ga_10
CN1    N      H1      ga_10
CA     N      H1      ga_10
CA     N      H2      ga_10
CA     N      CN1     ga_12
[ dihedrals ]
CN1    N      CA      C      gd_14

; N-methyl-glycine (+1)
[ GLY-1NM+ ]
[ replace ]
N      NL      14.0067 0.104          ; to add up to +1 net
charge
CA     CH2     14.027 0.200          0          ; derived by analogy to
methyl groups of amines reported by Oostenbrink et al. DOI:
10.1002/cphc.200400542
[ add ]
2      4      H      N      CA      C
H      1.008 0.248
1      1      CN1     N      CA      C
CH3    15.035 0.200          ; derived by analogy to
methyl groups of amines reported by Oostenbrink et al. DOI:
10.1002/cphc.200400542
[ delete ]
H
[ bonds ]
N      H1      gb_2
N      H2      gb_2
N      CN1     gb_20
[ angles ]
H1     N      H2      ga_9
H2     N      CN1     ga_10
CN1    N      H1      ga_10
CA     N      H1      ga_10
CA     N      H2      ga_10
CA     N      CN1     ga_12
[ dihedrals ]
CN1    N      CA      C      gd_14

; N-methyl-proline (+1)
[ PRO-1NM+ ]
[ replace ]
N      NL      14.0067 0.152          ; to add up to +1 net
charge
CA     CH1     13.019 0.200          0          ; derived by analogy to
methyl groups of amines reported by Oostenbrink et al. DOI:
10.1002/cphc.200400542
CD     CH2     14.027 0.200          0          ; derived by analogy to
methyl groups of amines reported by Oostenbrink et al. DOI:
10.1002/cphc.200400542
[ add ]
1      4      H      N      CA      C
H      1.008 0.248
1      1      CN1     N      CA      C
CH3    15.035 0.200          ; derived by analogy to
methyl groups of amines reported by Oostenbrink et al. DOI:
10.1002/cphc.200400542
[ bonds ]
N      H      gb_2
N      CN1     gb_20
[ angles ]
H      N      CD      ga_10
CD     N      CN1     ga_12
CN1    N      H      ga_10
CA     N      H      ga_10
CA     N      CD      ga_12
CA     N      CN1     ga_12
[ dihedrals ]
CN1    N      CA      C      gd_14

; N,N-dimethyl-AA (0)
[ 2NM ]
[ replace ]
N      NT      14.0067 -0.63          ; from trimethylamine reported by Oostenbrink et al. DOI:
10.1002/cphc.200400542
CA     CH1     13.019 0.210          0          ; from trimethylamine reported by Oostenbrink et al. DOI:
10.1002/cphc.200400542
[ add ]
2      4      CN      N      CA      C
CH3    15.035 0.210          ; from trimethylamine reported by Oostenbrink et al. DOI:
10.1002/cphc.200400542
[ delete ]
H
[ bonds ]
N      H1      gb_2
N      CN1     gb_20
N      CN2     gb_20
[ angles ]
CN1    N      H1      ga_10
CN1    N      CN2     ga_12
CN2    N      H1      ga_10
CA     N      H1      ga_10
CA     N      CN2     ga_12
CA     N      CN1     ga_12
[ dihedrals ]
CN1    N      CA      C      gd_14

; N,N-dimethyl-glycine (+1)
[ GLY-2NM+ ]
[ replace ]
N      NL      14.0067 0.152          ; to add up to +1 net
charge
CA     CH2     14.027 0.200          0          ; derived by analogy to
methyl groups of amines reported by Oostenbrink et al. DOI:
10.1002/cphc.200400542
[ add ]
1      1      H1      N      CA      C
H      1.008 0.248
2      4      CN      N      CA      C
CH3    15.035 0.200          ; derived by analogy to
methyl groups of amines reported by Oostenbrink et al. DOI:
10.1002/cphc.200400542
[ delete ]
H
[ bonds ]
N      H1      gb_2
N      CN1     gb_20
N      CN2     gb_20
[ angles ]
CN1    N      H1      ga_10
CN1    N      CN2     ga_12
CN2    N      H1      ga_10
CA     N      H1      ga_10
CA     N      CN2     ga_12
CA     N      CN1     ga_12
[ dihedrals ]
CN1    N      CA      C      gd_14

; N,N-dimethyl-glycine (0)
[ GLY-2NM ]
[ replace ]
N      NT      14.0067 -0.63          ; from trimethylamine reported by Oostenbrink et al. DOI:
10.1002/cphc.200400542
CA     CH2     14.027 0.210          0          ; from trimethylamine reported by Oostenbrink et al. DOI:
10.1002/cphc.200400542
[ add ]
2      4      CN      N      CA      C
CH3    15.035 0.210          ; from trimethylamine reported by Oostenbrink et al. DOI:
10.1002/cphc.200400542
[ delete ]
H
[ bonds ]
N      H1      gb_2
N      CN1     gb_20
N      CN2     gb_20
[ angles ]
CN1    N      H1      ga_10
CN1    N      CN2     ga_12
CN2    N      H1      ga_10
CA     N      H1      ga_10
CA     N      CN2     ga_12
CA     N      CN1     ga_12
[ dihedrals ]
CN1    N      CA      C      gd_14

```

; N,N-dimethyl-proline (+1)  
 [ PRO-2NM+ ]  
 [ replace ]  
 N NL 14.0067 0.200 ; to add up to +1 net charge  
 CA CH1 13.019 0.200 0 ; derived by analogy to methyl groups of amines reported by Oostenbrink et al. DOI: 10.1002/cphc.200400542  
 CD CH2 14.027 0.200 0 ; derived by analogy to methyl groups of amines reported by Oostenbrink et al. DOI: 10.1002/cphc.200400542  
 [ add ]  
 2 4 CN N CA C  
 CH3 15.035 0.200 ; derived by analogy to methyl groups of amines reported by Oostenbrink et al. DOI: 10.1002/cphc.200400542  
 [ bonds ]  
 N CN1 gb\_20  
 N CN2 gb\_20  
 [ angles ]  
 CN1 N CD ga\_12  
 CN1 N CN2 ga\_12  
 CN2 N CD ga\_12  
 CA N CN2 ga\_12  
 CA N CN1 ga\_12  
 [ dihedrals ]  
 CN1 N CA C gd\_14

; N,N,N-trimethyl-AA (+1)  
 [ 3NM+ ]  
 [ replace ]  
 N NL 14.0067 0.200 ; to add up to +1 net charge  
 CA CH1 13.019 0.200 0 ; derived by analogy to methyl groups of amines reported by Oostenbrink et al. DOI: 10.1002/cphc.200400542  
 [ add ]  
 3 4 CN N CA C  
 CH3 15.035 0.200 ; derived by analogy to methyl groups of amines reported by Oostenbrink et al. DOI: 10.1002/cphc.200400542  
 [ delete ]  
 H  
 [ bonds ]  
 N CN1 gb\_20  
 N CN2 gb\_20  
 N CN3 gb\_20  
 [ angles ]  
 CN1 N CN3 ga\_12  
 CN1 N CN2 ga\_12  
 CN2 N CN3 ga\_12  
 CA N CN3 ga\_12  
 CA N CN2 ga\_12  
 CA N CN1 ga\_12  
 [ dihedrals ]  
 CN1 N CA C gd\_14

; N,N,N-trimethyl-glycine (+1)  
 [ GLY-3NM+ ]  
 [ replace ]  
 N NL 14.0067 0.200 ; to add up to +1 net charge  
 CA CH2 14.027 0.200 0 ; derived by analogy to methyl groups of amines reported by Oostenbrink et al. DOI: 10.1002/cphc.200400542  
 [ add ]  
 3 4 CN N CA C  
 CH3 15.035 0.200 ; derived by analogy to methyl groups of amines reported by Oostenbrink et al. DOI: 10.1002/cphc.200400542  
 [ delete ]  
 H  
 [ bonds ]  
 N CN1 gb\_20  
 N CN2 gb\_20  
 N CN3 gb\_20  
 [ angles ]  
 CN1 N CN3 ga\_12  
 CN1 N CN2 ga\_12  
 CN2 N CN3 ga\_12  
 CA N CN3 ga\_12  
 CA N CN2 ga\_12  
 CA N CN1 ga\_12  
 [ dihedrals ]  
 CN1 N CA C gd\_14

; N-acetyl-AA  
 [ NAC ]  
 [ add ]  
 1 2 H N C CA  
 H 1.008 0.2800 ; from the peptide bond

1 1 CN1 N C CA  
 C 12.011 0.2800 ; by analogy to the aldehyde group reported by Dolenc et al. DOI: 10.1093/nar/gki195  
 1 2 ON2 N CA C  
 O 15.9994 -0.3800 ; from the carbonyl group (of e.g., GLU)  
 1 2 CN2 N C CA  
 CH3 15.035 0.1000 ; by analogy to the aldehyde group reported by Dolenc et al. DOI: 10.1093/nar/gki195  
 [ bonds ]  
 N H gb\_2  
 N CN1 gb\_9  
 CN1 ON2 gb\_4  
 CN1 CN2 gb\_26  
 [ angles ]  
 CA N H ga\_17  
 CN1 N H ga\_31  
 CN1 N CA ga\_30  
 N CN1 ON2 ga\_32  
 N CN1 CN2 ga\_18  
 CN2 CN1 ON2 ga\_29  
 [ impropers ]  
 N CN1 CA H gi\_1  
 CN1 CN2 N ON2 gi\_1  
 [ dihedrals ]  
 CN2 CN1 N CA gd\_4  
 CN1 N CA C gd\_19

; N-acetyl-proline  
 [ PRO-NAC ]  
 [ add ]  
 1 1 CN1 N C CA  
 C 12.011 0.3800 ; from the carbonyl group (of e.g., GLU)  
 1 2 ON2 N CA C  
 O 15.9994 -0.2800 ; by analogy to the aldehyde group reported by Dolenc et al. DOI: 10.1093/nar/gki195  
 1 2 CN2 N C CA  
 CH3 15.035 0.1000 ; by analogy to the aldehyde group reported by Dolenc et al. DOI: 10.1093/nar/gki195  
 [ bonds ]  
 N CN1 gb\_9  
 CN1 ON2 gb\_4  
 CN1 CN2 gb\_26  
 [ angles ]  
 CN1 N CD ga\_30  
 CN1 N CA ga\_30  
 N CN1 ON2 ga\_32  
 N CN1 CN2 ga\_18  
 CN2 CN1 ON2 ga\_29  
 [ impropers ]  
 N CN1 CA CD gi\_1  
 CN1 CN2 N ON2 gi\_1  
 [ dihedrals ]  
 CN2 CN1 N CA gd\_4  
 CN1 N CA C gd\_19

; pyroglutamic acid  
 [ PGA-NH ]  
 [ replace ]  
 N N 14.0067 -0.28  
 [ add ]  
 1 1 H N CA CD  
 H 1.008 0.28  
 [ bonds ]  
 N H gb\_2  
 [ angles ]  
 CA N H ga\_30  
 CD N H ga\_30  
 [ impropers ]  
 N CA CD H gi\_1  
 [ dihedrals ]  
 CD N CA C gd\_19

; N-formylmethionine  
 [ MET-FOR ]  
 [ add ]  
 1 2 H N C CA  
 H 1.008 0.28 ; from the peptide bond  
 1 1 CN1 N C CA  
 C 12.011 0.2800 ; by analogy to the aldehyde group reported by Dolenc et al. DOI: 10.1093/nar/gki195  
 1 2 ON2 N CA C  
 O 15.9994 -0.3800 ; from the carbonyl group (of e.g., GLU)  
 1 2 HN1 N C CA



```

H          1.008      0.1
; by analogy to the aldehyde group reported by Dolenc et al. DOI:
10.1093/nar/gki195
[ bonds ]
N          H          gb_2
N          CN1       gb_9
CN1       ON2       gb_4
CN1       HN1       gb_3
[ angles ]
CA        N          H          ga_17
CA        N          CN1      ga_30
H         N          CN1      ga_31
N         CN1       ON2      ga_32
N         CN1       HN1      ga_18
ON2      CN1       HN1      ga_29
[ impropers ]
N         CN1       CA        H          gi_1
CN1      N         ON2      HN1      gi_1
[ dihedrals ]
ON2      CN1       N         CA        gd_4
CN1      N         CA        C         gd_19

; aminoacids.c.tdb file (C-terminal parameters)

; AA-amide
[ AMD ]
[ add ]
1         2         NC1       C         CA        N
          NT        14.00670  -0.8300  ; from ASN/GLN
1         1         HC11      C         O         N
          H         1.008      0.4150
          ; from ASN/GLN
1         1         HC12      C         N         O
          H         1.008      0.4150
          ; from ASN/GLN
[ bonds ]
C         NC1       gb_8
NC1      HC11      gb_2
NC1      HC12      gb_2
[ angles ]
O         C         NC1       ga_32
CA        C         O         ga_29
CA        C         NC1       ga_18
C         NC1      HC11      ga_22
C         NC1      HC12      ga_22
HC11     NC1      HC12      ga_23
[ impropers ]
C         CA        O         NC1       gi_1
NC1      C         HC11      HC12      gi_1
[ dihedrals ]
N         CA        C         NC1       gd_20
CA        C         NC1      HC11      gd_4

; AA-methyl ester
[ CME ]
[ replace ]
C         C         12.011     0.56
          ; from the carbonyl group (of e.g., GLU) with the partial charge
          increased by 0.18 - see the comment of CC2 atom
O         OA        15.9994   -0.36
          ; from the ring oxygen atom of nucleotides (e.g., ATP)
[ add ]
1         2         OC1       C         CA        N
          O         15.9994   -0.38
          ; from the carbonyl group (of e.g., GLU)
1         2         CC2       O         C         CA
          CH3      15.035     0.18
          ; 0.36 charge divided between CG and CE to add up to 0 net charge,
          similar to methyl groups of other methylation residues and also used in other
          building blocks (e.g., TMP)
[ bonds ]
C         O         gb_12
C         OC1      gb_4
O         CC2      gb_17
[ angles ]
O         C         OC1       ga_32
C         O         CC2      ga_11
CA        C         O         ga_18
CA        C         OC1      ga_29
[ dihedrals ]
N         CA        C         O         gd_20
CA        C         O         CC2      gd_3
[ impropers ]
C         CA        OC1      O         gi_1

; aminoacids.hdb file (hydrogen database)

; phosphoserine (-1)
S1P 2
1         1         H          N          -C         CA
1         2         HE3       OE3       PD         OG

; phosphoserine (-2)
S2P 1
1         1         H          N          -C         CA
          ; phosphothreonine (-1)
T1P 2
1         1         H          N          -C         CA
1         2         HE3       OE3       PD         OG1
          ; phosphothreonine (-2)
T2P 1
1         1         H          N          -C         CA
          ; phosphotyrosine (-1)
Y1P 6
1         1         H          N          -C         CA
1         1         HD1       CD1       CG         CE1
1         1         HD2       CD2       CG         CE2
1         1         HE1       CE1       CD1       CZ
1         1         HE2       CE2       CD2       CZ
1         2         HI3       OI3       PT         OH
          ; phosphotyrosine (-2)
Y2P 5
1         1         H          N          -C         CA
1         1         HD1       CD1       CG         CE1
1         1         HD2       CD2       CG         CE2
1         1         HE1       CE1       CD1       CZ
1         1         HE2       CE2       CD2       CZ
          ; phosphoaspartate (-1)
D1P 2
1         1         H          N          -C         CA
1         2         HZ3       OZ3       PE         OD2
          ; phosphoaspartate (-2)
D2P 1
1         1         H          N          -C         CA
          ; phospholysine (-1)
K1P 3
1         1         H          N          -C         CA
1         1         HZ       NZ       PH         CE
1         2         HI3       OI3       PH         NZ
          ; phospholysine (-2)
K2P 2
1         1         H          N          -C         CA
1         1         HZ       NZ       PH         CE
          ; phosphoarginine (0)
R0P 5
1         1         H          N          -C         CA
1         1         HE       NE       CD         CZ
2         3         HH1      NH1      CZ         NE
1         1         HH2      NH2      PT         CZ
1         2         HI3       OI3       PT         NH2
          ; phosphoarginine (-1)
R1P 4
1         1         H          N          -C         CA
1         1         HE       NE       CD         CZ
2         3         HH1      NH1      CZ         NE
1         1         HH2      NH2      PT         CZ
          ; 1-phosphohistidine (-1)
H11 2
1         1         H          N          -C         CA
1         2         HH3      OH3      PZ         NE2
          ; 1-phosphohistidine (-2)
H12 1
1         1         H          N          -C         CA
          ; 3-phosphohistidine (-1)
H31 2
1         1         H          N          -C         CA
1         2         HZ3      OZ3      PE3        ND1
          ; 3-phosphohistidine (-2)
H32 1
1         1         H          N          -C         CA
          ; N6-methyllysine (0)
KMN 2
1         1         H          N          -C         CA
1         2         HZ       NZ       CE         CD
          ; N6-methyllysine (+1)
KMC 2
1         1         H          N          -C         CA
2         4         HZ       NZ       CE         CD
          ; N6,N6-dimethyllysine (0)
K2M 1
1         1         H          N          -C         CA
          ; N6,N6-dimethyllysine (+1)
K2C 2
1         1         H          N          -C         CA
1         2         HZ       NZ       CE         CD
          ; N6,N6,N6-trimethyllysine
K3C 1
1         1         H          N          -C         CA
          ; omega-N-methylarginine (0)
RMN 3
1         1         H          N          -C         CA
1         1         HE       NE       CD         CZ
2         3         HH2      NH2      CZ         NE
          ; omega-N-methylarginine (+1)
RMC 4

```

1	1	H	N	-C	CA	; 3,4-dihydroxyphenylalanine					
1	1	HE	NE	CD	CZ	HTY 6					
2	3	HH1	NH1	CZ	NE	1	1	H	N	-C	CA
1	1	HH2	NH2	CT	CZ	1	1	HD1	CD1	CG	CE1
; symmetric-dimethylarginine (0)						1	1	HD2	CD2	CG	CE2
RSM 3						1	2	HZ1	OZ1	CE1	CD1
1	1	H	N	-C	CA	1	1	HE2	CE2	CD2	CZ2
1	1	HE	NE	CD	CZ	1	2	HH	OH	CZ2	CE1
1	1	HH2	NH2	CT2	CZ	; 7-hydroxytryptophan					
; symmetric-dimethylarginine (+1)						W7H 7					
RMS 4						1	1	H	N	-C	CA
1	1	H	N	-C	CA	1	1	HD1	CD1	CG	NE1
1	1	HE	NE	CD	CZ	1	1	HE1	NE1	CD1	CE2
1	1	HH1	NH1	CT1	CZ	1	1	HE3	CE3	CD2	CZ3
1	1	HH2	NH2	CT2	CZ	1	1	HZ3	CZ3	CE3	CH3
; asymmetric-dimethylarginine (0)						1	1	HH3	CH3	CZ3	CZ2
RAM 3						1	2	HH2	OH2	CZ2	CE2
1	1	H	N	-C	CA	; 3-hydroxyaspartate (-1,R)					
1	1	HE	NE	CD	CZ	DH3 2					
1	2	HH1	NH1	CZ	NE	1	1	H	N	-C	CA
; asymmetric-dimethylarginine (+1)						1	2	HG1	OG1	CB	CA
RMA 3						; 3-hydroxyaspartate (-1,S)					
1	1	H	N	-C	CA	D3H 2					
1	1	HE	NE	CD	CZ	1	1	H	N	-C	CA
2	3	HH1	NH1	CZ	NE	1	2	HG1	OG1	CB	CA
; 1-methylhistidine (0)						; 3-hydroxyaspartate (0,R)					
H1M 1						DN3 3					
1	1	H	N	-C	CA	1	1	H	N	-C	CA
; 1-methylhistidine (+1)						1	2	HG1	OG1	CB	CA
H1C 2						1	2	HD2	OD2	CG2	CB
1	1	H	N	-C	CA	; 3-hydroxyaspartate (0,S)					
1	1	HD1	ND1	CG	CE1	D3N 3					
; 3-methylhistidine (0)						1	1	H	N	-C	CA
H3M 1						1	2	HG1	OG1	CB	CA
1	1	H	N	-C	CA	1	2	HD2	OD2	CG2	CB
; 3-methylhistidine (+1)						; 3-hydroxyasparagine (R)					
H3C 2						N3H 3					
1	1	H	N	-C	CA	1	1	H	N	-C	CA
1	1	HE2	NE2	CE1	CD2	1	2	HG1	OG1	CB	CA
; N5-methylglutamine						2	3	HD2	ND2	CG2	CB
QME 2						; 3-hydroxyasparagine (S)					
1	1	H	N	-C	CA	NH3 3					
1	1	HE2	NE2	CZ	CD	1	1	H	N	-C	CA
; N4-methylasparagine						1	2	HG1	OG1	CB	CA
NME 2						2	3	HD2	ND2	CG2	CB
1	1	H	N	-C	CA	; 4-carboxyglutamate (-2)					
1	1	HD2	ND2	CE	CG	ECA 1					
; glutamate methyl ester						1	1	H	N	-C	CA
EME 1						; 4-carboxyglutamate (-1)					
1	1	H	N	-C	CA	ECN 2					
; aspartate methyl ester						1	1	H	N	-C	CA
DMA 1						1	2	HE2	OE2	CD1	CG
1	1	H	N	-C	CA	; sulfotyrosine					
; 5-methylcysteine						YSU 5					
CYM 1						1	1	H	N	-C	CA
1	1	H	N	-C	CA	1	1	HD1	CD1	CG	CE1
; N6-acetyllysine						1	1	HD2	CD2	CG	CE2
KAC 2						1	1	HE1	CE1	CD1	CZ
1	1	H	N	-C	CA	1	1	HE2	CE2	CD2	CZ
1	1	HZ	NZ	CE	CH	; dehydroalanine					
; 3-hydroxyproline (R)						SDH 1					
PH3 1						1	1	H	N	-C	CA
1	2	HG1	OG1	CB	CA	; 2,3-didehydrobutyryne					
; 3-hydroxyproline (S)						TDH 1					
P3H 1						1	1	H	N	-C	CA
1	2	HG1	OG1	CB	CA	; 6-bromotryptophan					
; 4-hydroxyproline (S)						WBR 6					
HY2 1						1	1	H	N	-C	CA
1	2	HD1	OD1	CG	CB	1	1	HD1	CD1	CG	NE1
; 3,4-dihydroxyproline						1	1	HE1	NE1	CD1	CE2
PHH 2						1	1	HE3	CE3	CD2	CZ3
1	2	HG1	OG1	CB	CA	1	1	HZ3	CZ3	CE3	CH2
1	2	HD1	OD1	CG2	CB	1	1	HZ2	CZ2	CE2	CH2
; 5-hydroxylysine (0,R)						; S-nitrosocysteine					
KH5 3						CSN 1					
1	1	H	N	-C	CA	1	1	H	N	-C	CA
1	2	HE1	OE1	CD	CB	; citrulline					
2	4	HZ	NZ	CE2	CD	RCl 3					
; 5-hydroxylysine (0,S)						1	1	H	N	-C	CA
KSH 3						1	1	HE	NE	CD	CZ
1	1	H	N	-C	CA	2	3	HH2	NH2	CZ	NE
1	2	HE1	OE1	CD	CB	; allysine (amino adipic semialdehyde)					
2	4	HZ	NZ	CE2	CD	KAL 2					
; 5-hydroxylysine (+1,R)						1	1	H	N	-C	CA
KPH 3						1	1	HE	CE	OZ	CD
1	1	H	N	-C	CA	; N-acetylglucosamine (N4-linked to ASN)					
1	2	HE1	OE1	CD	CB	NNG 6					
3	4	HZ	NZ	CE2	CD	1	1	H	N	-C	CA
; 5-hydroxylysine (+1,S)						1	1	HD2	ND2	CG	C1
KHP 3						1	1	HN2	N2	C7	C2
1	1	H	N	-C	CA	1	2	HO3	O3	C3	C2
1	2	HE1	OE1	CD	CB	1	2	HO4	O4	C4	C3
3	4	HZ	NZ	CE2	CD	1	2	HO6	O6	C6	C5

; 2,3-dihydroxyphenylalanine						1	2	HE	OE	CD	CG
F23	6					; glutamic semialdehyde					
1	1	H	N	-C	CA	GSA 2					
1	2	HE3	OE3	CD1	CG	1	1	H	N	-C	CA
1	1	HD2	CD2	CG	CE2	1	1	HD	CD	OE	CG
1	2	HZ1	OZ1	CE1	CD1	; 2-amino-3-ketobutyric acid					
1	1	HE2	CE2	CD2	CZ2	TOX	1				
1	1	HZ2	CZ2	CE1	CE2	1	1	H	N	-C	CA
; 2-hydroxyphenylalanine						; 2-oxo-histidine					
F2H	6					H2X 3					
1	1	H	N	-C	CA	1	1	H	N	-C	CA
1	2	HE3	OE3	CD1	CG	1	1	HD1	ND1	CG	CE1
1	1	HD2	CD2	CG	CE2	1	1	HE2	NE2	CE1	CD2
1	1	HE1	CE1	CD1	CZ	; methionine sulfoxide (R)					
1	1	HE2	CE2	CD2	CZ	MSX	1				
1	1	HZ	CZ	CE1	CE2	1	1	H	N	-C	CA
; 3-hydroxyphenylalanine						; methionine sulfoxide (S)					
F3H	6					MXS 1					
1	1	H	N	-C	CA	1	1	H	N	-C	CA
1	1	HD1	CD1	CG	CE1	; methionine sulfone					
1	1	HD2	CD2	CG	CE2	MES	1				
1	2	HZ1	OZ1	CE1	CD1	1	1	H	N	-C	CA
1	1	HE2	CE2	CD2	CZ2	; cysteine sulfinic acid					
1	1	HZ2	CZ2	CE1	CE2	CSA	1				
; 6-hydroxytryptophan						; cysteic acid					
W6H	7					CSE 1					
1	1	H	N	-C	CA	1	1	H	N	-C	CA
1	1	HD1	CD1	CG	NE1	; 3-nitrotyrosine (-1)					
1	1	HE1	NE1	CD1	CE2	YNI	4				
1	1	HE3	CE3	CD2	CZ3	1	1	H	N	-C	CA
1	1	HZ3	CZ3	CE3	CH2	1	1	HD1	CD1	CG	CE1
1	2	HI	OI	CH2	CZ2	1	1	HD2	CD2	CG	CE2
1	1	HZ2	CZ2	CE2	CH2	1	1	HE2	CE2	CD2	CZ2
; 5-hydroxytryptophan						; 3-nitrotyrosine (0)					
W5H	7					YNN 5					
1	1	H	N	-C	CA	1	1	H	N	-C	CA
1	1	HD1	CD1	CG	NE1	1	1	HD1	CD1	CG	CE1
1	1	HE1	NE1	CD1	CE2	1	1	HD2	CD2	CG	CE2
1	1	HE3	CE3	CD2	CZ3	1	1	HE2	CE2	CD2	CZ2
1	2	HH3	OH3	CZ3	CE2	1	1	HE2	CE2	CD2	CZ2
1	1	HH2	CH2	CZ3	CZ2	1	2	HH3	OH3	CZ2	CE1
1	1	HZ2	CZ2	CE2	CH2	; 3-nitrotyrosine (0)					
; 4-hydroxytryptophan						YNB 5					
W4H	7										
1	1	H	N	-C	CA	1	1	H	N	-C	CA
1	1	HD1	CD1	CG	NE1	1	1	HD1	CD1	CG	CE1
1	1	HE1	NE1	CD1	CE2	1	1	HD2	CD2	CG	CE2
1	2	HZ4	OZ4	CE3	CD2	1	1	HE2	CE2	CD2	CZ2
1	1	HZ3	CZ3	CE3	CH2	1	2	HH3	OH3	CZ2	CE1
1	1	HH2	CH2	CZ3	CZ2	; 6-nitrotryptophan					
1	1	HZ2	CZ2	CE2	CH2	WNI	6				
; 2-hydroxytryptophan						; kynurenine					
W2H	7					WKY 6					
1	1	H	N	-C	CA	1	1	H	N	-C	CA
1	2	HE4	OE4	CD1	CG	1	1	HE2	CE2	CD2	CZ3
1	1	HE1	NE1	CD1	CE2	1	1	HZ1	NZ1	CE1	CD2
1	1	HE3	CE3	CD2	CZ3	1	1	HZ2	CZ2	CE1	CH
1	1	HZ3	CZ3	CE3	CH2	1	1	HZ3	CZ3	CE2	CH
1	1	HH2	CH2	CZ3	CZ2	1	1	HZ3	CZ3	CE2	CH
1	1	HZ2	CZ2	CE2	CH2	1	1	HH	CH	CZ2	CZ3
; 3-hydroxytryptophan						; 3-hydroxykynurenine					
L3H	2					WKH 6					
1	1	H	N	-C	CA	1	1	H	N	-C	CA
1	2	HG1	OG1	CB	CA	1	1	HE2	CE2	CD2	CZ3
; 3-hydroxytryptophan						; 3-hydroxykynurenine					
LH3	2					WKH 6					
1	1	H	N	-C	CA	1	1	HE2	CE2	CD2	CZ3
1	2	HG1	OG1	CB	CA	1	1	HZ1	NZ1	CE1	CD2
; 4-hydroxytryptophan						; 3-hydroxykynurenine					
L4H	2					WKH 6					
1	1	H	N	-C	CA	1	1	HZ3	CZ3	CE2	CH2
1	2	HD3	OD3	CG	CB	1	2	HH1	OH1	CZ2	CE1
1	1	H	N	-C	CA	1	1	HH2	CH2	CZ2	CZ3
; 5-hydroxytryptophan						; formyl-kynurenine					
L5H	2					WKF 7					
1	1	H	N	-C	CA	1	1	H	N	-C	CA
1	2	HE	OE	CD2	CG	1	1	HE2	CE2	CD2	CZ3
; 5-hydroxytryptophan						; formyl-kynurenine					
LH5	2					WKF 7					
1	1	H	N	-C	CA	1	1	HZ1	NZ1	CE1	CH1
1	2	HE	OE	CD2	CG	1	1	HZ2	CZ2	CE1	CH2
1	1	H	N	-C	CA	1	1	HZ3	CZ3	CE2	CH2
1	2	HE	OE	CD2	CG	1	1	HH1	CH1	NZ1	OI
1	1	H	N	-C	CA	1	1	HH2	CH2	CZ2	CZ3
; 3-hydroxyvaline						; chlorotyrosine					
V3H	2					YCH 5					
1	1	H	N	-C	CA	1	1	H	N	-C	CA
1	2	HG3	OG3	CB	CA	1	1	HD1	CD1	CG	CE1
; cysteine sulfenic acid						; chlorotyrosine					
CYH	2					YCH 5					
1	1	H	N	-C	CA	1	1	HD2	CD2	CG	CE2
1	2	HD	OD	SG	CB	1	1	HE2	CE2	CD2	CZ2
; 5-hydroxyproline (R)						; homocitrulline					
PH5	1					KAM 3					
1	2	HE	OE	CD	CG	1	1	H	N	-C	CA
; 5-hydroxyproline (S)						; homocitrulline					
P5H	1					KAM 3					
1	1	H	N	-C	CA	1	1	HZ	NZ	CH	CE
1	2	HD	OD	SG	CB	1	1	HZ	NZ	CH	CE
1	1	H	N	-C	CA	2	4	HI2	NI2	CH	NZ

```

; carboxyllysine (-1)
KCA 2
1 1 H N -C CA
1 1 HZ NZ CH CE
; carboxyllysine (0)
KCN 3
1 1 H N -C CA
1 1 HZ NZ CH CE
1 2 HI2 OI2 CH NZ

; S-carbamoyl-cysteine
CAM 2
1 1 H N -C CA
2 3 HE2 NE2 CD SG
; norleucine
LNO 1
1 1 H N -C CA

```

## Dataset S2. Force field parameters for the GROMOS force field 54A7 parameter set.

```

; This file contains extended force field parameters for the GROMOS force field 54A7
parameters set
; GROMACS 4.5.x format - files: aminoacids.rtp, aminoacids.n.tdb, aminoacids.c.tdb
and aminoacids.hdb
; Authors: Drazen Petrov, Christian Margreitter, Melanie Grandits, Chris Oostenbrink
& Bojan Zagrovic
; Parameter files in GROMACS 4.3.x and 4.4.x, and GROMOS formats available at
http://vienna-ptm.univie.ac.at/

; aminoacids.rtp file (backbone and side chain parameters)

[ bondedtypes ]
; bonds angles dihedrals impropers
2 2 1 2

; phosphoserine (-1)
[S1P]
[ atoms ]
N N -0.31000 0
H H 0.31000 0
CA CH1 0.00000 1
CB CH2 0.15000 2; from the carbon atom attached to the phosphate group of
nucleotides (e.g., ATP)
OG OA -0.36000 2; from the phosphate group of nucleotides (e.g., ATP)
PD P 0.63000 2; to add up to -1 net charge
OE1 OM -0.63500 2; from the phosphate group of nucleotides (e.g., ATP)
OE2 OM -0.63500 2; from the phosphate group of nucleotides (e.g., ATP)
OE3 OA -0.54800 2; from the hydroxyl group of nucleotides (e.g., ATP)
HE3 H 0.39800 2; from the hydroxyl group of nucleotides (e.g., ATP)
C C 0.450 3
O O -0.450 3
[ bonds ]
N H gb_2
N CA gb_21
CA CB gb_27
CA C gb_27
CB OG gb_18
OG PD gb_28
PD OE1 gb_24
PD OE2 gb_24
PD OE3 gb_28
OE3 HE3 gb_1
C O gb_5
C +N gb_10
[ exclusions ]
; ai aj
OE1 HE3
OE2 HE3
OG HE3
[ angles ]
; ai aj ak gromos type
-C N H ga_32
-C N CA ga_31
H N CA ga_18
N CA CB ga_13
N CA C ga_13
CB CA C ga_13
CA CB OG ga_13
CB OG PD ga_26
OG PD OE1 ga_14
OG PD OE2 ga_14
OG PD OE3 ga_14
OE1 PD OE2 ga_14
OE1 PD OE3 ga_14
OE2 PD OE3 ga_14
PD OE3 HE3 ga_12
CA C O ga_30
CA C +N ga_19
O C +N ga_33
[ impropers ]
; ai aj ak al gromos type
N -C CA H gi_1
CA N C CB gi_2
C CA +N O gi_1
[ dihedrals ]
; ai aj ak al gromos type
-C N CA C gd_14
-C N CA C gd_44
-C N CA C gd_43
N CA CB OG gd_34
N CA C +N gd_45
N CA C +N gd_42
CA CB OG PD gd_23
CB OG PD OE3 gd_19
CB OG PD OE3 gd_22
OG PD OE3 HE3 gd_19
OG PD OE3 HE3 gd_22

; phosphoserine (-2)
[S2P]
[ atoms ]
N N -0.31000 0
H H 0.31000 0
CA CH1 0.00000 1
CB CH2 0.15000 2; from the carbon atom attached to the phosphate group of
nucleotides (e.g., ATP)
OG OA -0.36000 2; from the phosphate group of nucleotides (e.g., ATP)
PD P 0.11500 2; to add up to -2 net charge
OE1 OM -0.63500 2; from the phosphate group of nucleotides (e.g., ATP)
OE2 OM -0.63500 2; from the phosphate group of nucleotides (e.g., ATP)
OE3 OM -0.63500 2; from the phosphate group of nucleotides (e.g., ATP)
C C 0.450 3
O O -0.450 3
[ bonds ]
N H gb_2
N CA gb_21
CA CB gb_27
CA C gb_27
CB OG gb_18
OG PD gb_28
PD OE1 gb_24
PD OE2 gb_24
PD OE3 gb_24
C O gb_5
C +N gb_10
[ angles ]
; ai aj ak gromos type
-C N H ga_32
-C N CA ga_31
H N CA ga_18
N CA CB ga_13
N CA C ga_13
CB CA C ga_13
CA CB OG ga_13
CB OG PD ga_26
OG PD OE1 ga_14
OG PD OE2 ga_14
OG PD OE3 ga_14
OE1 PD OE2 ga_14
OE1 PD OE3 ga_14
OE2 PD OE3 ga_14
CA C O ga_30
CA C +N ga_19
O C +N ga_33
[ impropers ]
; ai aj ak al gromos type
N -C CA H gi_1
CA N C CB gi_2
C CA +N O gi_1
[ dihedrals ]
; ai aj ak al gromos type
-C -C N CA gd_14
-C N CA C gd_44
-C N CA C gd_43
N CA CB OG gd_34
N CA C +N gd_45
N CA C +N gd_42
CA CB OG PD gd_23
CB OG PD OE1 gd_19
CB OG PD OE1 gd_22

; phosphothreonine (-1)
[T1P]

```

```

[atoms]
N N -0.31000 0
H H 0.31000 0
CA CH1 0.00000 1
CB CH1 0.15000 2; from the carbon atom attached to the phosphate group of
nucleotides (e.g., ATP)
OG1 OA -0.36000 2; from the phosphate group of nucleotides (e.g., ATP)
PD P 0.63000 2; to add up to -1 net charge
OE1 OM -0.63500 2; from the phosphate group of nucleotides (e.g., ATP)
OE2 OM -0.63500 2; from the phosphate group of nucleotides (e.g., ATP)
OE3 OA -0.54800 2; from the hydroxyl group of nucleotides (e.g., ATP)
HE3 H 0.39800 2; from the hydroxyl group of nucleotides (e.g., ATP)
CG2 CH3 0.00000 3
C C 0.450 4
O O -0.450 4
[bonds]
N H gb_2
N CA gb_21
CA CB gb_27
CA C gb_27
CB OG1 gb_18
CB CG2 gb_27
OG1 PD gb_28
PD OE1 gb_24
PD OE2 gb_24
PD OE3 gb_28
OE3 HE3 gb_1
C O gb_5
C +N gb_10
[exclusions]
; ai aj
OE1 HE3
OE2 HE3
OG1 HE3
[angles]
; ai aj ak gromos type
-C N H ga_32
-C N CA ga_31
H N CA ga_18
N CA CB ga_13
N CA C ga_13
CB CA C ga_13
CA CB OG1 ga_13
CA CB CG2 ga_15
OG1 CB CG2 ga_15
CB OG1 PD ga_26
OG1 PD OE1 ga_14
OG1 PD OE2 ga_14
OG1 PD OE3 ga_5
OE1 PD OE2 ga_29
OE1 PD OE3 ga_14
OE2 PD OE3 ga_14
PD OE3 HE3 ga_12
CA C O ga_30
CA C +N ga_19
O C +N ga_33
[impropers]
; ai aj ak al gromos type
N -C CA H gi_1
CA N C CB gi_2
CB OG1 CG2 CA gi_2
C CA +N O gi_1
[dihedrals]
; ai aj ak al gromos type
-C -C N CA gd_14
-C N CA C gd_44
-C N CA C gd_43
N CA CB OG1 gd_34
N CA C +N gd_45
N CA C +N gd_42
CA CB OG1 PD gd_23
CB OG1 PD OE3 gd_19
CB OG1 PD OE1 gd_22
; phosphothreonine (-2)
[T2P]
[atoms]
N N -0.31000 0
H H 0.31000 0
CA CH1 0.00000 1
CB CH1 0.15000 2; from the carbon atom attached to the phosphate group of
nucleotides (e.g., ATP)
OG1 OA -0.36000 2; from the phosphate group of nucleotides (e.g., ATP)
PD P 0.11500 2; to add up to -2 net charge
OE1 OM -0.63500 2; from the phosphate group of nucleotides (e.g., ATP)
OE2 OM -0.63500 2; from the phosphate group of nucleotides (e.g., ATP)
OE3 OM -0.63500 2; from the phosphate group of nucleotides (e.g., ATP)
CG2 CH3 0.00000 3
C C 0.450 4
O O -0.450 4
[bonds]
N H gb_2
N CA gb_21
CA CB gb_27
CA C gb_27
CB CG gb_27
CG CD1 gb_16
CG CD2 gb_16
CD1 HD1 gb_3
CD1 CE1 gb_16
CD2 HD2 gb_3
CD2 CE2 gb_16
CE1 HE1 gb_3
CE1 CZ gb_16
CE2 HE2 gb_3
CE2 CZ gb_16
N H gb_2
N CA gb_21
CA CB gb_27
CA C gb_27
CB OG1 gb_18
CB CG2 gb_27
OG1 PD gb_28
PD OE1 gb_24
PD OE2 gb_24
PD OE3 gb_28
C O gb_5
C +N gb_10
[angles]
; ai aj ak gromos type
-C N H ga_32
-C N CA ga_31
H N CA ga_18
N CA CB ga_13
N CA C ga_13
CB CA C ga_13
CA CB OG1 ga_13
CA CB CG2 ga_15
OG1 CB CG2 ga_15
OG1 CB CG2 ga_15
CB OG1 PD ga_26
OG1 PD OE1 ga_14
OG1 PD OE2 ga_14
OG1 PD OE3 ga_14
OE1 PD OE2 ga_14
OE1 PD OE3 ga_14
OE2 PD OE3 ga_14
OE2 PD OE3 ga_14
CA C O ga_30
CA C +N ga_19
O C +N ga_33
[impropers]
; ai aj ak al gromos type
N -C CA H gi_1
CA N C CB gi_2
CB OG1 CG2 CA gi_2
C CA +N O gi_1
[dihedrals]
; ai aj ak al gromos type
-C -C N CA gd_14
-C N CA C gd_44
-C N CA C gd_43
N CA CB OG1 gd_34
N CA C +N gd_45
N CA C +N gd_42
CA CB OG1 PD gd_23
CB OG1 PD OE1 gd_19
CB OG1 PD OE1 gd_22
; phosphotyrosine (-1)
[Y1P]
[atoms]
N N -0.31000 0
H H 0.31000 0
CA CH1 0.00000 1
CB CH2 0.00000 1
CG C 0.00000 1
CD1 C -0.14000 2
HD1 HC 0.14000 2
CD2 C -0.14000 3
HD2 HC 0.14000 3
CE1 C -0.14000 4
HE1 HC 0.14000 4
CE2 C -0.14000 5
HE2 HC 0.14000 5
CZ C 0.15000 6; from the carbon atom attached to the phosphate group of
nucleotides (e.g., ATP)
OH OA -0.36000 6; from the phosphate group of nucleotides (e.g., ATP)
PT P 0.63000 6; to add up to -1 net charge
OI1 OM -0.63500 6; from the phosphate group of nucleotides (e.g., ATP)
OI2 OM -0.63500 6; from the phosphate group of nucleotides (e.g., ATP)
OI3 OA -0.54800 6; from the hydroxyl group of nucleotides (e.g., ATP)
HI3 H 0.39800 6; from the hydroxyl group of nucleotides (e.g., ATP)
C C 0.450 7
O O -0.450 7
[bonds]
N H gb_2
N CA gb_21
CA CB gb_27
CA C gb_27
CB CG gb_27
CG CD1 gb_16
CG CD2 gb_16
CD1 HD1 gb_3
CD1 CE1 gb_16
CD2 HD2 gb_3
CD2 CE2 gb_16
CE1 HE1 gb_3
CE1 CZ gb_16
CE2 HE2 gb_3
CE2 CZ gb_16

```

```

CZ OH gb_13
OH PT gb_28
PT OI1 gb_24
PT OI2 gb_24
PT OI3 gb_28
OI3 HI3 gb_1
C O gb_5
C +N gb_10
[ exclusions ]
; ai aj
CB HD1
CB HD2
CB CE1
CB CE2
CG HE1
CG HE2
CG CZ
CD1 HD2
CD1 CE2
CD1 OH
HD1 CD2
HD1 HE1
HD1 CZ
CD2 CE1
CD2 OH
HD2 HE2
HD2 CZ
CE1 HE2
HE1 CE2
HE1 OH
HE2 OH
OH HI3
OI1 HI3
OI2 HI3
[ angles ]
; ai aj ak gromos type
-C N H ga_32
-C N CA ga_31
H N CA ga_18
N CA CB ga_13
N CA C ga_13
CB CA C ga_13
CA CB CG ga_15
CB CG CD1 ga_27
CB CG CD2 ga_27
CD1 CG CD2 ga_27
CG CD1 HD1 ga_25
CG CD1 CE1 ga_27
HD1 CD1 CE1 ga_25
CG CD2 HD2 ga_25
CG CD2 CE2 ga_27
HD2 CD2 CE2 ga_25
CD1 CE1 HE1 ga_25
CD1 CE1 CZ ga_27
HE1 CE1 CZ ga_25
CD2 CE2 HE2 ga_25
CD2 CE2 CZ ga_27
HE2 CE2 CZ ga_25
CE1 CZ CE2 ga_27
CE1 CZ OH ga_27
CE2 CZ OH ga_27
CZ OH PT ga_26
OH PT OI1 ga_14
OH PT OI2 ga_14
OH PT OI3 ga_5
OI1 PT OI2 ga_29
OI1 PT OI3 ga_14
OI2 PT OI3 ga_14
PT OI3 HI3 ga_12
CA C O ga_30
CA C +N ga_19
O C +N ga_33
[ impropers ]
; ai aj ak al gromos type
N -C CA H gi_1
CA N C CB gi_2
CG CD1 CD2 CB gi_1
CG CD1 CE1 CZ gi_1
CG CD2 CE2 CZ gi_1
CD1 CG CD2 CE2 gi_1
CD1 CG CE1 HD1 gi_1
CD1 CE1 CZ CE2 gi_1
CD2 CG CD1 CE1 gi_1
CD2 CG CE2 HD2 gi_1
CD2 CE2 CZ CE1 gi_1
HE1 CD1 CZ CE1 gi_1
HE2 CD2 CZ CE2 gi_1
CZ CE1 CE2 OH gi_1
C CA +N O gi_1
[ dihedrals ]
; ai aj ak al gromos type
-C -C N CA gd_14
-C N CA C gd_44
-C N CA C gd_43
N CA CB CG gd_34
N CA C +N gd_45
N CA C +N gd_42
CA CB CG CD1 gd_40
CE1 CZ OH PT gd_11
CZ OH PT OI3 gd_19
CZ OH PT OI3 gd_22
OH PT OI3 HI3 gd_19
OH PT OI3 HI3 gd_22
; phosphotyrosine (-2)
[ Y2P ]
[ atoms ]
N N -0.31000 0
H H 0.31000 0
CA CH1 0.00000 1
CB CH2 0.00000 1
CG C 0.00000 1
CD1 C -0.14000 2
HD1 HC 0.14000 2
CD2 C -0.14000 3
HD2 HC 0.14000 3
CE1 C -0.14000 4
HE1 HC 0.14000 4
CE2 C -0.14000 5
HE2 HC 0.14000 5
CZ C 0.15000 6 ; from the carbon atom attached to the phosphate group of
nucleotides (e.g., ATP)
OH OA -0.36000 6 ; from the phosphate group of nucleotides (e.g., ATP)
PT P 0.11500 6 ; to add up to -2 net charge
OI1 OM -0.63500 6 ; from the phosphate group of nucleotides (e.g., ATP)
OI2 OM -0.63500 6 ; from the phosphate group of nucleotides (e.g., ATP)
OI3 OM -0.63500 6 ; from the phosphate group of nucleotides (e.g., ATP)
C C 0.450 7
O O -0.450 7
[ bonds ]
N H gb_2
N CA gb_21
CA CB gb_27
CA C gb_27
CB CG gb_27
CG CD1 gb_16
CG CD2 gb_16
CD1 HD1 gb_3
CD1 CE1 gb_16
CD2 HD2 gb_3
CD2 CE2 gb_16
CE1 HE1 gb_3
CE1 CZ gb_16
CE2 HE2 gb_3
CE2 CZ gb_16
CZ OH gb_13
OH PT gb_28
PT OI1 gb_24
PT OI2 gb_24
PT OI3 gb_24
C O gb_5
C +N gb_10
[ exclusions ]
; ai aj
CB HD1
CB HD2
CB CE1
CB CE2
CG HE1
CG HE2
CG CZ
CD1 HD2
CD1 CE2
CD1 OH
HD1 CD2
HD1 HE1
HD1 CZ
CD2 CE1
CD2 OH
HD2 HE2
HD2 CZ
CE1 HE2
HE1 CE2
HE1 OH
HE2 OH
OH HI3
OI1 HI3
OI2 HI3
[ angles ]
; ai aj ak gromos type
-C N H ga_32
-C N CA ga_31
H N CA ga_18
N CA CB ga_13
N CA C ga_13
CB CA C ga_13
CA CB CG ga_15
CB CG CD1 ga_27
CB CG CD2 ga_27
CD1 CG CD2 ga_27
CG CD1 HD1 ga_25
CG CD1 CE1 ga_27
HD1 CD1 CE1 ga_25
CG CD2 HD2 ga_25
CG CD2 CE2 ga_27
HD2 CD2 CE2 ga_25
CD1 CE1 HE1 ga_25
CD1 CE1 CZ ga_27
HE1 CE1 CZ ga_25
CD2 CE2 HE2 ga_25
CD2 CE2 CZ ga_27
HE2 CE2 CZ ga_25
CE1 CZ CE2 ga_27
CE1 CZ OH ga_27
CE2 CZ OH ga_27
CZ OH PT ga_26
OH PT OI1 ga_14
OH PT OI2 ga_14
OH PT OI3 ga_5
OI1 PT OI2 ga_29
OI1 PT OI3 ga_14
OI2 PT OI3 ga_14
PT OI3 HI3 ga_12
CA C O ga_30
CA C +N ga_19
O C +N ga_33
[ impropers ]
; ai aj ak al gromos type
N -C CA H gi_1
CA N C CB gi_2
CG CD1 CD2 CB gi_1
CG CD1 CE1 CZ gi_1
CG CD2 CE2 CZ gi_1
CD1 CG CD2 CE2 gi_1
CD1 CG CE1 HD1 gi_1
CD1 CE1 CZ CE2 gi_1
CD2 CG CD1 CE1 gi_1
CD2 CG CE2 HD2 gi_1
CD2 CE2 CZ CE1 gi_1
HE1 CD1 CZ CE1 gi_1
HE2 CD2 CZ CE2 gi_1
CZ CE1 CE2 OH gi_1
C CA +N O gi_1
[ dihedrals ]
; ai aj ak al gromos type
-C -C N CA gd_14
-C N CA C gd_44

```

```

CD1 CG CD2 ga_27
CG CD1 HD1 ga_25
CG CD1 CE1 ga_27
HD1 CD1 CE1 ga_25
CG CD2 HD2 ga_25
CG CD2 CE2 ga_27
HD2 CD2 CE2 ga_25
CD1 CE1 HE1 ga_25
CD1 CE1 CZ ga_27
HE1 CE1 CZ ga_25
CD2 CE2 HE2 ga_25
CD2 CE2 CZ ga_27
HE2 CE2 CZ ga_25
CE1 CZ CE2 ga_27
CE1 CZ OH ga_27
CE2 CZ OH ga_27
CZ OH PT ga_26
OH PT OI1 ga_14
OH PT OI2 ga_14
OH PT OI3 ga_14
OI1 PT OI2 ga_14
OI1 PT OI3 ga_14
OI2 PT OI3 ga_14
CA C O ga_30
CA C +N ga_19
O C +N ga_33
[impropers]
; ai aj ak al gromos type
N -C CA H gi_1
CA N C CB gi_2
CG CD1 CD2 CB gi_1
CG CD1 CE1 CZ gi_1
CG CD2 CE2 CZ gi_1
CD1 CG CD2 CE2 gi_1
CD1 CG CE1 HD1 gi_1
CD1 CE1 CZ CE2 gi_1
CD2 CG CD1 CE1 gi_1
CD2 CG CE2 HD2 gi_1
CD2 CE2 CZ CE1 gi_1
HE1 CD1 CZ CE1 gi_1
HE2 CD2 CZ CE2 gi_1
CZ CE1 CE2 OH gi_1
C CA +N O gi_1
[dihedrals]
; ai aj ak al gromos type
-C A -C N CA gd_14
-C N CA C gd_44
-C N CA C gd_43
N CA CB CG gd_34
N CA C +N gd_45
N CA C +N gd_42
CA CB CG CD1 gd_40
CE1 CZ OH PT gd_11
CZ OH PT OI1 gd_19
CZ OH PT OI1 gd_22
; phosphoaspartate (-1)
[D1P]
[atoms]
N N -0.31000 0
H H 0.31000 0
CA CH1 0.00000 1
CB CH2 0.00000 1
CG C 0.30900 2; to add up to -1 net charge
OD1 O -0.45000 2; from the carbonyl oxygen (of e.g., the peptide bond)
OD2 OE -0.06900 2; from the ester oxygen reported by Horta et al. DOI:
10.1021/ct1006407
PE P 0.63000 2; from the phosphate group (of e.g., S1P)
OZ1 OM -0.63500 2; from the phosphate group of nucleotides (e.g., ATP)
OZ2 OM -0.63500 2; from the phosphate group of nucleotides (e.g., ATP)
OZ3 OA -0.54800 2; from the hydroxyl group of nucleotides (e.g., ATP)
HZ3 H 0.39800 2; from the hydroxyl group of nucleotides (e.g., ATP)
C C 0.450 3
O O -0.450 3
[bonds]
N H gb_2
N CA gb_21
CA CB gb_27
CA C gb_27
CB CG gb_27
CG OD1 gb_5
CG OD2 gb_13
OD2 PE gb_28
PE OZ1 gb_24
PE OZ2 gb_24
PE OZ3 gb_28
OZ3 HZ3 gb_1
C O gb_5
C +N gb_10
[exclusions]
; ai aj
OD2 HZ3
OZ1 HZ3
OZ2 HZ3
[angles]
; ai aj ak gromos type
-C N H ga_32
-C N CA ga_31
H N CA ga_18
N CA CB ga_13
N CA C ga_13
CB CA C ga_13
CA CB CG ga_15
CB CG OD1 ga_30
CB CG OD2 ga_19
OD1 CG OD2 ga_33
CG OD2 PE ga_26
OD2 PE OZ1 ga_14
OD2 PE OZ2 ga_14
OD2 PE OZ3 ga_5
OZ1 PE OZ2 ga_29
OZ1 PE OZ3 ga_14
OZ2 PE OZ3 ga_14
PE OZ3 HZ3 ga_12
CA C O ga_30
CA C +N ga_19
O C +N ga_33
[impropers]
; ai aj ak al gromos type
N -C CA H gi_1
CA N C CB gi_2
CG OD1 OD2 CB gi_1
C CA +N O gi_1
[dihedrals]
; ai aj ak al gromos type
-C A -C N CA gd_14
-C N CA C gd_44
-C N CA C gd_43
N CA CB CG gd_34
N CA C +N gd_45
N CA C +N gd_42
CA CB CG OD2 gd_40
CB CG OD2 PE gd_12
CG OD2 PE OZ3 gd_19
CG OD2 PE OZ3 gd_22
OD2 PE OZ3 HZ3 gd_19
OD2 PE OZ3 HZ3 gd_22
; phosphoaspartate (-2)
[D2P]
[atoms]
N N -0.31000 0
H H 0.31000 0
CA CH1 0.00000 1
CB CH2 0.00000 1
CG C 0.30900 2; to add up to -2 net charge
OD1 O -0.45000 2; from the carbonyl oxygen (of e.g., the peptide bond)
OD2 OE -0.06900 2; from the ester oxygen reported by Horta et al. DOI:
10.1021/ct1006407
PE P 0.11500 2; from the phosphate group (of e.g., S2P)
OZ1 OM -0.63500 2; from the phosphate group of nucleotides (e.g., ATP)
OZ2 OM -0.63500 2; from the phosphate group of nucleotides (e.g., ATP)
OZ3 OM -0.63500 2; from the phosphate group of nucleotides (e.g., ATP)
C C 0.450 3
O O -0.450 3
[bonds]
N H gb_2
N CA gb_21
CA CB gb_27
CA C gb_27
CB CG gb_27
CG OD1 gb_5
CG OD2 gb_13
OD2 PE gb_28
PE OZ1 gb_24
PE OZ2 gb_24
PE OZ3 gb_24
C O gb_5
C +N gb_10
[angles]
; ai aj ak gromos type
-C N H ga_32
-C N CA ga_31
H N CA ga_18
N CA CB ga_13
N CA C ga_13
CB CA C ga_13
CA CB CG ga_15
CB CG OD1 ga_30
CB CG OD2 ga_19
OD1 CG OD2 ga_33
CG OD2 PE ga_26
OD2 PE OZ1 ga_14
OD2 PE OZ2 ga_14
OD2 PE OZ3 ga_14
OZ1 PE OZ2 ga_14

```

```

OZ1 PE OZ3 ga_14
OZ2 PE OZ3 ga_14
CA C O ga_30
CA C +N ga_19
O C +N ga_33
[impropers]
; ai aj ak al gromos type
N -C CA H gi_1
CA N C CB gi_2
CG OD1 OD2 CB gi_1
C CA +N O gi_1
[dihedrals]
; ai aj ak al gromos type
-C A -C N CA gd_14
-C N CA C gd_44
-C N CA C gd_43
N CA CB CG gd_34
N CA C +N gd_45
N CA C +N gd_42
CA CB CG OD2 gd_40
CB CG OD2 PE gd_12
CG OD2 PE OZ1 gd_19
CG OD2 PE OZ1 gd_22

;phospholysine (-1)
[K1P]
[atoms]
N N -0.31000 0
H H 0.31000 0
CA CH1 0.00000 1
CB CH2 0.00000 1
CG CH2 0.00000 2
CD CH2 0.00000 2
CE CH2 0.00000 3
NZ NE -0.31000 4; from NE of ARGN
HZ H 0.31000 4; from HE of ARGN
PH P 0.42000 5; to add up to -1 net charge
O11 OM -0.63500 5; from the phosphate group of nucleotides (e.g., ATP)
O12 OM -0.63500 5; from the phosphate group of nucleotides (e.g., ATP)
O13 OA -0.54800 5; from the hydroxyl group of nucleotides (e.g., ATP)
HI3 H 0.39800 5; from the hydroxyl group of nucleotides (e.g., ATP)
C C 0.450 6
O O -0.450 6
[bonds]
N H gb_2
N CA gb_21
CA CB gb_27
CA C gb_27
CB CG gb_27
CG CD gb_27
CD CE gb_27
CE NZ gb_21
NZ HZ gb_2
NZ PH gb_24
PH O11 gb_24
PH O12 gb_24
PH O13 gb_28
O13 HI3 gb_1
C O gb_5
C +N gb_10
[exclusions]
; ai aj
HZ O11
HZ O12
HZ O13
NZ HI3
O11 HI3
O12 HI3
[angles]
; ai aj ak gromos type
-C N H ga_32
-C N CA ga_31
H N CA ga_18
N CA CB ga_13
N CA C ga_13
CB CA C ga_13
CA CB CG ga_15
CB CG CD ga_15
CG CD CE ga_15
CD CE NZ ga_15
CE NZ HZ ga_20
HZ NZ PH ga_23
CE NZ PH ga_33
NZ PH O11 ga_14
NZ PH O12 ga_14
O11 PH O12 ga_14
O11 PH O13 ga_14
O12 PH O13 ga_14
HI3 O13 PH ga_12
CA C O ga_30
CA C +N ga_19
O C +N ga_33

[impropers]
; ai aj ak al gromos type
N -C CA H gi_1
CA N C CB gi_2
C CA +N O gi_1
[dihedrals]
; ai aj ak al gromos type
-C A -C N CA gd_14
-C N CA C gd_44
-C N CA C gd_43
N CA CB CG gd_34
N CA C +N gd_45
N CA C +N gd_42
CA CB CG CD gd_34
CB CG CD CE gd_34
CG CD CE NZ gd_34
CD CE NZ PH gd_39
CE NZ PH O13 gd_39
NZ PH O13 HI3 gd_19
NZ PH O13 HI3 gd_22

;phospholysine (-2)
[K2P]
[atoms]
N N -0.31000 0
H H 0.31000 0
CA CH1 0.00000 1
CB CH2 0.00000 1
CG CH2 0.00000 2
CD CH2 0.00000 2
CE CH2 0.00000 3
NZ NE -0.31000 4; from NE of ARGN
HZ H 0.31000 4; from HE of ARGN
PH P -0.09500 5; to add up to -2 net charge
O11 OM -0.63500 5; from the phosphate group of nucleotides (e.g., ATP)
O12 OM -0.63500 5; from the phosphate group of nucleotides (e.g., ATP)
O13 OM -0.63500 5; from the phosphate group of nucleotides (e.g., ATP)
C C 0.450 6
O O -0.450 6
[bonds]
N H gb_2
N CA gb_21
CA CB gb_27
CA C gb_27
CB CG gb_27
CG CD gb_27
CD CE gb_27
CE NZ gb_21
NZ HZ gb_2
NZ PH gb_24
PH O11 gb_24
PH O12 gb_24
PH O13 gb_24
C O gb_5
C +N gb_10
[exclusions]
; ai aj
HZ O11
HZ O12
HZ O13
[angles]
; ai aj ak gromos type
-C N H ga_32
-C N CA ga_31
H N CA ga_18
N CA CB ga_13
N CA C ga_13
CB CA C ga_13
CA CB CG ga_15
CB CG CD ga_15
CG CD CE ga_15
CD CE NZ ga_15
CE NZ HZ ga_20
HZ NZ PH ga_23
CE NZ PH ga_33
NZ PH O11 ga_14
NZ PH O12 ga_14
O11 PH O12 ga_14
O11 PH O13 ga_14
O12 PH O13 ga_14
CA C O ga_30
CA C +N ga_19
O C +N ga_33
[impropers]
; ai aj ak al gromos type
N -C CA H gi_1
CA N C CB gi_2
C CA +N O gi_1
[dihedrals]
; ai aj ak al gromos type
-C A -C N CA gd_14
-C N CA C gd_44

```



```

-C N CA C gd_43
N CA CB CG gd_34
N CA C +N gd_45
N CA C +N gd_42
CA CB CG CD gd_34
CB CG CD CE gd_34
CG CD CE NZ gd_34
CD CE NZ PH gd_39
CE NZ PH OI1 gd_39

; phosphoarginine (0)
[ ROP ]
[ atoms ]
N N -0.31000 0
H H 0.31000 0
CA CH1 0.00000 1
CB CH2 0.00000 1
CG CH2 0.00000 1
CD CH2 0.09000 2
NE NE -0.11000 2
HE H 0.24000 2
CZ C 0.43000 2; to add up to 1 net charge
NH1 NZ -0.26000 2
HH11 H 0.24000 2
HH12 H 0.24000 2
NH2 NE -0.11000 2; from NE nitrogen atom of ARG
HH2 H 0.24000 2; from terminal hydrogen atoms of ARG
PT P 0.42000 3; to add up to -1 net charge
OI1 OM -0.63500 3; from the phosphate group of nucleotides (e.g., ATP)
OI2 OM -0.63500 3; from the phosphate group of nucleotides (e.g., ATP)
OI3 OA -0.54800 3; from the hydroxyl group of nucleotides (e.g., ATP)
HI3 H 0.39800 3; from the hydroxyl group of nucleotides (e.g., ATP)
C C 0.450 4
O O -0.450 4
[ bonds ]
N H gb_2
N CA gb_21
CA CB gb_27
CA C gb_27
CB CG gb_27
CG CD gb_27
CD NE gb_21
NE HE gb_2
NE CZ gb_11
CZ NH1 gb_11
CZ NH2 gb_11
NH1 HH11 gb_2
NH1 HH12 gb_2
NH2 HH2 gb_2
NH2 PT gb_24
PT OI1 gb_24
PT OI2 gb_24
PT OI3 gb_28
OI3 HI3 gb_1
C O gb_5
C +N gb_10
[ exclusions ]
; ai aj
HH2 OI1
HH2 OI2
HH2 OI3
NH2 HI3
OI1 HI3
OI2 HI3
[ angles ]
; ai aj ak gromos type
-C N H ga_32
-C N CA ga_31
H N CA ga_18
N CA CB ga_13
N CA C ga_13
CB CA C ga_13
CA CB CG ga_15
CB CG CD ga_15
CG CD NE ga_13
CD NE HE ga_20
CD NE CZ ga_33
HE NE CZ ga_23
NE CZ NH1 ga_28
NE CZ NH2 ga_28
NH1 CZ NH2 ga_28
CZ NH1 HH11 ga_23
CZ NH1 HH12 ga_23
HH11 NH1 HH12 ga_24
CZ NH2 HH2 ga_23
HH2 NH2 PT ga_20
CZ NH2 PT ga_33
NH2 PT OI1 ga_14
NH2 PT OI2 ga_14
NH2 PT OI3 ga_5
OI1 PT OI2 ga_29
OI1 PT OI3 ga_14
OI2 PT OI3 ga_14

PT OI3 HI3 ga_12
CA C O ga_30
CA C +N ga_19
O C +N ga_33
[ impropers ]
; ai aj ak al gromos type
N -C CA H gi_1
CA N C CB gi_2
NE CD CZ HE gi_1
CZ NH1 NH2 NE gi_1
NH1 HH11 HH12 CZ gi_1
NH2 PT CZ HH2 gi_1
C CA +N O gi_1
[ dihedrals ]
; ai aj ak al gromos type
-C -C N CA gd_14
-C N CA C gd_44
-C N CA C gd_43
N CA CB CG gd_34
N CA C +N gd_45
N CA C +N gd_42
CA CB CG CD gd_34
CB CG CD NE gd_34
CG CD NE CZ gd_39
CD NE CZ NH2 gd_14
NE CZ NH1 HH11 gd_14
NE CZ NH2 PT gd_14
CZ NH2 PT OI3 gd_39
NH2 PT OI3 HI3 gd_19
NH2 PT OI3 HI3 gd_22

; phosphoarginine (-1)
[ R1P ]
[ atoms ]
N N -0.31000 0
H H 0.31000 0
CA CH1 0.00000 1
CB CH2 0.00000 1
CG CH2 0.00000 1
CD CH2 0.09000 2
NE NE -0.11000 2
HE H 0.24000 2
CZ C 0.43000 2; to add up to 1 net charge
NH1 NZ -0.26000 2
HH11 H 0.24000 2
HH12 H 0.24000 2
NH2 NE -0.11000 2; from NE nitrogen atom of ARG
HH2 H 0.24000 2; from terminal hydrogen atoms of ARG
PT P -0.09500 3; to add up to -2 net charge
OI1 OM -0.63500 3; from the phosphate group of nucleotides (e.g., ATP)
OI2 OM -0.63500 3; from the phosphate group of nucleotides (e.g., ATP)
OI3 OM -0.63500 3; from the phosphate group of nucleotides (e.g., ATP)
C C 0.450 4
O O -0.450 4
[ bonds ]
N H gb_2
N CA gb_21
CA CB gb_27
CA C gb_27
CB CG gb_27
CG CD gb_27
CD NE gb_21
NE HE gb_2
NE CZ gb_11
CZ NH1 gb_11
CZ NH2 gb_11
NH1 HH11 gb_2
NH1 HH12 gb_2
NH2 HH2 gb_2
NH2 PT gb_24
PT OI1 gb_24
PT OI2 gb_24
PT OI3 gb_24
C O gb_5
C +N gb_10
[ exclusions ]
; ai aj
HH2 OI1
HH2 OI2
HH2 OI3
[ angles ]
; ai aj ak gromos type
-C N H ga_32
-C N CA ga_31
H N CA ga_18
N CA CB ga_13
N CA C ga_13
CB CA C ga_13
CA CB CG ga_15
CB CG CD ga_15
CG CD NE ga_13
CD NE HE ga_20
CD NE CZ ga_33
HE NE CZ ga_23
NE CZ NH1 ga_28
NE CZ NH2 ga_28
NH1 CZ NH2 ga_28
CZ NH1 HH11 ga_23
CZ NH1 HH12 ga_23
HH11 NH1 HH12 ga_24
CZ NH2 HH2 ga_23
HH2 NH2 PT ga_20
CZ NH2 PT ga_33
NH2 PT OI1 ga_14
NH2 PT OI2 ga_14
NH2 PT OI3 ga_5
OI1 PT OI2 ga_29
OI1 PT OI3 ga_14
OI2 PT OI3 ga_14

```

```

HE NE CZ ga_23
NE CZ NH1 ga_28
NE CZ NH2 ga_28
NH1 CZ NH2 ga_28
CZ NH1 HH11 ga_23
CZ NH1 HH12 ga_23
HH11 NH1 HH12 ga_24
CZ NH2 HH2 ga_23
HH2 NH2 PT ga_20
CZ NH2 PT ga_33
NH2 PT OI1 ga_14
NH2 PT OI2 ga_14
NH2 PT OI3 ga_14
OI1 PT OI2 ga_14
OI1 PT OI3 ga_14
OI2 PT OI3 ga_14
CA C O ga_30
CA C +N ga_19
O C +N ga_33
[impropers]
; ai aj ak al gromos type
N -C CA H gi_1
CA N C CB gi_2
NE CD CZ HE gi_1
CZ NH1 NH2 NE gi_1
NH1 HH11 HH12 CZ gi_1
NH2 PT CZ HH2 gi_1
C CA +N O gi_1
[dihedrals]
; ai aj ak al gromos type
-CA -C N CA gd_14
-C N CA C gd_44
-C N CA C gd_43
N CA CB CG gd_34
N CA C +N gd_45
N CA C +N gd_42
CA CB CG CD gd_34
CB CG CD NE gd_34
CG CD NE CZ gd_39
CD NE CZ NH2 gd_14
NE CZ NH1 HH11 gd_14
NE CZ NH2 PT gd_14
CZ NH2 PT OI1 gd_39

;1-phosphohistidine (-1)
[H11]
[atoms]
N N -0.31000 0
H H 0.31000 0
CA CH1 0.00000 1
CB CH2 0.00000 1
CG C 0.00000 2
ND1 NR -0.54000 2
CD2 C 0.13000 2
HD2 HC 0.14000 2
CE1 C 0.13000 2
HE1 HC 0.14000 2
NE2 NR 0.00000 2
PZ P 0.42000 3 ; to add up to -1 net charge
OH1 OM -0.63500 3 ; from the phosphate group of nucleotides (e.g., ATP)
OH2 OM -0.63500 3 ; from the phosphate group of nucleotides (e.g., ATP)
OH3 OA -0.54800 3 ; from the hydroxyl group of nucleotides (e.g., ATP)
HH3 H 0.39800 3 ; from the hydroxyl group of nucleotides (e.g., ATP)
C C 0.450 4
O O -0.450 4
[bonds]
N H gb_2
N CA gb_21
CA CB gb_27
CA C gb_27
CB CG gb_27
CG ND1 gb_10
CG CD2 gb_10
ND1 CE1 gb_10
CD2 HD2 gb_3
CD2 NE2 gb_10
CE1 HE1 gb_3
CE1 NE2 gb_10
NE2 PZ gb_24
PZ OH1 gb_24
PZ OH2 gb_24
PZ OH3 gb_28
OH3 HH3 gb_1
C O gb_5
C +N gb_10
[exclusions]
; ai aj
CB HD2
CB CE1
CB NE2
CG HE1
CG PZ
ND1 HD2

ND1 PZ
CD2 HE1
HD2 CE1
HD2 PZ
HE1 PZ
HH3 NE2
HH3 OH1
HH3 OH2
[angles]
; ai aj ak gromos type
-C N H ga_32
-C N CA ga_31
H N CA ga_18
N CA CB ga_13
N CA C ga_13
CB CA C ga_13
CA CB CG ga_15
CB CG ND1 ga_37
CB CG CD2 ga_37
ND1 CG CD2 ga_7
CG ND1 CE1 ga_7
CG CD2 HD2 ga_36
CG CD2 NE2 ga_7
HD2 CD2 NE2 ga_36
ND1 CE1 HE1 ga_36
ND1 CE1 NE2 ga_7
HE1 CE1 NE2 ga_36
CD2 NE2 CE1 ga_7
CD2 NE2 PZ ga_37
CE1 NE2 PZ ga_37
NE2 PZ OH1 ga_14
NE2 PZ OH2 ga_14
NE2 PZ OH3 ga_5
OH1 PZ OH2 ga_29
OH1 PZ OH3 ga_14
OH2 PZ OH3 ga_14
PZ OH3 HH3 ga_12
CA C O ga_30
CA C +N ga_19
O C +N ga_33
[impropers]
; ai aj ak al gromos type
N -C CA H gi_1
CA N C CB gi_2
CG ND1 CD2 CB gi_1
CG ND1 CE1 NE2 gi_1
CG CD2 NE2 CE1 gi_1
ND1 CG CD2 NE2 gi_1
ND1 CE1 NE2 CD2 gi_1
CD2 CG ND1 CE1 gi_1
CD2 CG NE2 HD2 gi_1
CE1 ND1 NE2 HE1 gi_1
NE2 CD2 CE1 PZ gi_1
C CA +N O gi_1
[dihedrals]
; ai aj ak al gromos type
-CA -C N CA gd_14
-C N CA C gd_44
-C N CA C gd_43
N CA CB CG gd_34
N CA C +N gd_45
N CA C +N gd_42
CA CB CG ND1 gd_40
CD2 NE2 PZ OH3 gd_19
CD2 NE2 PZ OH3 gd_22
NE2 PZ OH3 HH3 gd_19
NE2 PZ OH3 HH3 gd_22

;1-phosphohistidine (-2)
[H12]
[atoms]
N N -0.31000 0
H H 0.31000 0
CA CH1 0.00000 1
CB CH2 0.00000 1
CG C 0.00000 2
ND1 NR -0.54000 2
CD2 C 0.13000 2
HD2 HC 0.14000 2
CE1 C 0.13000 2
HE1 HC 0.14000 2
NE2 NR 0.00000 2
PZ P -0.09500 3 ; to add up to -2 net charge
OH1 OM -0.63500 3 ; from the phosphate group of nucleotides (e.g., ATP)
OH2 OM -0.63500 3 ; from the phosphate group of nucleotides (e.g., ATP)
OH3 OM -0.63500 3 ; from the phosphate group of nucleotides (e.g., ATP)
C C 0.450 4
O O -0.450 4
[bonds]
N H gb_2
N CA gb_21
CA CB gb_27
CA C gb_27

```

```

CB CG gb_27
CG ND1 gb_10
CG CD2 gb_10
ND1 CE1 gb_10
CD2 HD2 gb_3
CD2 NE2 gb_10
CE1 HE1 gb_3
CE1 NE2 gb_10
NE2 PZ gb_24
PZ OH1 gb_24
PZ OH2 gb_24
PZ OH3 gb_24
C O gb_5
C +N gb_10
[exclusions]
; ai aj
CB HD2
CB CE1
CB NE2
CG HE1
CG PZ
ND1 HD2
ND1 PZ
CD2 HE1
HD2 CE1
HD2 PZ
HE1 PZ
[angles]
; ai aj ak gromos type
-C N H ga_32
-C N CA ga_31
H N CA ga_18
N CA CB ga_13
N CA C ga_13
CB CA C ga_13
CA CB CG ga_15
CB CG ND1 ga_37
CB CG CD2 ga_37
ND1 CG CD2 ga_7
CG ND1 CE1 ga_7
CG CD2 HD2 ga_36
CG CD2 NE2 ga_7
HD2 CD2 NE2 ga_36
ND1 CE1 HE1 ga_36
ND1 CE1 NE2 ga_7
HE1 CE1 NE2 ga_36
CD2 NE2 CE1 ga_7
CD2 NE2 PZ ga_37
CE1 NE2 PZ ga_37
NE2 PZ OH1 ga_14
NE2 PZ OH2 ga_14
NE2 PZ OH3 ga_14
OH1 PZ OH2 ga_14
OH1 PZ OH3 ga_14
OH2 PZ OH3 ga_14
CA C O ga_30
CA C +N ga_19
O C +N ga_33
[impropers]
; ai aj ak al gromos type
N -C CA H gi_1
CA N C CB gi_2
CG ND1 CD2 CB gi_1
CG ND1 CE1 NE2 gi_1
CG CD2 NE2 CE1 gi_1
ND1 CG CD2 NE2 gi_1
ND1 CE1 NE2 CD2 gi_1
CD2 CG ND1 CE1 gi_1
CD2 CG NE2 HD2 gi_1
CE1 ND1 NE2 HE1 gi_1
NE2 CD2 CE1 PZ gi_1
C CA +N O gi_1
[dihedrals]
; ai aj ak al gromos type
-C -C N CA gd_14
-C N CA C gd_44
-C N CA C gd_43
N CA CB CG gd_34
N CA C +N gd_45
N CA C +N gd_42
CA CB CG ND1 gd_40
CD2 NE2 PZ OH1 gd_19
CD2 NE2 PZ OH1 gd_22
; 3-phosphohistidine (-1)
[H31]
[atoms]
N N -0.31000 0
H H 0.31000 0
CA CH1 0.00000 1
CB CH2 0.00000 1
CG C 0.00000 2
ND1 NR 0.00000 2
CD2 C 0.13000 3
HD2 HC 0.14000 3
CE1 C 0.13000 3
HE1 HC 0.14000 3
NE2 NR -0.54000 3
PE3 P 0.42000 4; to add up to -1 net charge
OZ1 OM -0.63500 4; from the phosphate group of nucleotides (e.g., ATP)
OZ2 OM -0.63500 4; from the phosphate group of nucleotides (e.g., ATP)
OZ3 OA -0.54800 4; from the hydroxyl group of nucleotides (e.g., ATP)
HZ3 H 0.39800 4; from the hydroxyl group of nucleotides (e.g., ATP)
C C 0.450 5
O O -0.450 5
[bonds]
N H gb_2
N CA gb_21
CA CB gb_27
CA C gb_27
CB CG gb_27
CG ND1 gb_10
CG CD2 gb_10
ND1 CE1 gb_10
ND1 PE3 gb_24
CD2 HD2 gb_3
CD2 NE2 gb_10
CE1 HE1 gb_3
CE1 NE2 gb_10
PE3 OZ1 gb_24
PE3 OZ2 gb_24
PE3 OZ3 gb_28
OZ3 HZ3 gb_1
C O gb_5
C +N gb_10
[exclusions]
; ai aj
CB PE3
CB HD2
CB CE1
CB NE2
CG HE1
ND1 HD2
PE3 CD2
PE3 HE1
PE3 NE2
CD2 HE1
HD2 CE1
HZ3 ND1
HZ3 OZ1
HZ3 OZ2
[angles]
; ai aj ak gromos type
-C N H ga_32
-C N CA ga_31
H N CA ga_18
N CA CB ga_13
N CA C ga_13
CB CA C ga_13
CA CB CG ga_15
CB CG ND1 ga_37
CB CG CD2 ga_37
ND1 CG CD2 ga_7
CG ND1 CE1 ga_7
CG CD2 HD2 ga_36
CG CD2 NE2 ga_7
HD2 CD2 NE2 ga_36
ND1 CE1 HE1 ga_36
ND1 CE1 NE2 ga_7
HE1 CE1 NE2 ga_36
CD2 NE2 CE1 ga_7
ND1 PE3 OZ1 ga_14
ND1 PE3 OZ2 ga_14
ND1 PE3 OZ3 ga_5
OZ1 PE3 OZ2 ga_29
OZ1 PE3 OZ3 ga_14
OZ2 PE3 OZ3 ga_14
PE3 OZ3 HZ3 ga_12
CA C O ga_30
CA C +N ga_19
O C +N ga_33
[impropers]
; ai aj ak al gromos type
N -C CA H gi_1
CA N C CB gi_2
CG ND1 CD2 CB gi_1
CG ND1 CE1 NE2 gi_1
CG CD2 NE2 CE1 gi_1
ND1 CG CD2 NE2 gi_1
ND1 CE1 NE2 CD2 gi_1
CD2 CG ND1 CE1 gi_1
CD2 CG NE2 HD2 gi_1
CE1 ND1 NE2 HE1 gi_1
NE2 CD2 CE1 PZ gi_1
C CA +N O gi_1

```

```

C CA +N O gi_1
[ dihedrals ]
; ai aj ak al gromos type
-C -C N CA gd_14
-C N CA C gd_44
-C N CA C gd_43
N CA CB CG gd_34
N CA C +N gd_45
N CA C +N gd_42
CA CB CG ND1 gd_40
CG ND1 PE3 OZ3 gd_19
CG ND1 PE3 OZ3 gd_22
ND1 PE3 OZ3 HZ3 gd_19
ND1 PE3 OZ3 HZ3 gd_22

; 3-phosphohistidine (-2)
[ H32 ]
[ atoms ]
N N -0.31000 0
H H 0.31000 0
CA CH1 0.00000 1
CB CH2 0.00000 1
CG C 0.00000 2
ND1 NR 0.00000 2
CD2 C 0.13000 3
HD2 HC 0.14000 3
CE1 C 0.13000 3
HE1 HC 0.14000 3
NE2 NR -0.54000 3
PE3 P -0.09500 4 ; to add up to -2 net charge
OZ1 OM -0.63500 4 ; from the phosphate group of nucleotides (e.g., ATP)
OZ2 OM -0.63500 4 ; from the phosphate group of nucleotides (e.g., ATP)
OZ3 OM -0.63500 4 ; from the phosphate group of nucleotides (e.g., ATP)
C C 0.450 5
O O -0.450 5
[ bonds ]
N H gb_2
N CA gb_21
CA CB gb_27
CA C gb_27
CB CG gb_27
CG ND1 gb_10
CG CD2 gb_10
ND1 CE1 gb_10
ND1 PE3 gb_24
CD2 HD2 gb_3
CD2 NE2 gb_10
CE1 HE1 gb_3
CE1 NE2 gb_10
PE3 OZ1 gb_24
PE3 OZ2 gb_24
PE3 OZ3 gb_24
C O gb_5
C +N gb_10
[ exclusions ]
; ai aj
CB PE3
CB HD2
CB CE1
CB NE2
CG HE1
ND1 HD2
PE3 CD2
PE3 HE1
PE3 NE2
CD2 HE1
HD2 CE1
[ angles ]
; ai aj ak gromos type
-C N H ga_32
-C N CA ga_31
H N CA ga_18
N CA CB ga_13
N CA C ga_13
CB CA C ga_13
CA CB CG ga_15
CB CG ND1 ga_37
CB CG CD2 ga_37
ND1 CG CD2 ga_7
CG ND1 CE1 ga_7
CG ND1 PE3 ga_37
CE1 ND1 PE3 ga_37
CG CD2 HD2 ga_36
CG CD2 NE2 ga_7
HD2 CD2 NE2 ga_36
ND1 CE1 HE1 ga_36
ND1 CE1 NE2 ga_7
HE1 CE1 NE2 ga_36
CD2 NE2 CE1 ga_7
ND1 PE3 OZ1 ga_14
ND1 PE3 OZ2 ga_14
ND1 PE3 OZ3 ga_14
OZ1 PE3 OZ2 ga_14

```

```

OZ1 PE3 OZ3 ga_14
OZ2 PE3 OZ3 ga_14
CA C O ga_30
CA C +N ga_19
O C +N ga_33
[ impropers ]
; ai aj ak al gromos type
N -C CA H gi_1
CA N C CB gi_2
CG ND1 CD2 CB gi_1
CG ND1 CE1 NE2 gi_1
CG CD2 NE2 CE1 gi_1
ND1 CG CD2 NE2 gi_1
ND1 CE1 NE2 CD2 gi_1
CD2 CG ND1 CE1 gi_1
CD2 CG NE2 HD2 gi_1
CE1 ND1 NE2 HE1 gi_1
ND1 CG CE1 PE3 gi_1
C CA +N O gi_1
[ dihedrals ]
; ai aj ak al gromos type
-C -C N CA gd_14
-C N CA C gd_44
-C N CA C gd_43
N CA CB CG gd_34
N CA C +N gd_45
N CA C +N gd_42
CA CB CG ND1 gd_40
CG ND1 PE3 OZ1 gd_19
CG ND1 PE3 OZ1 gd_22

; N6-methyllysine (0)
[ KMN ]
[ atoms ]
N N -0.31000 0
H H 0.31000 0
CA CH1 0.00000 1
CB CH2 0.00000 1
CG CH2 0.00000 2
CD CH2 0.00000 2
CE CH2 0.22000 3 ; from dimethylamine reported by Oostenbrink et al. DOI:
10.1002/cphc.200400542
NZ NT -0.88000 3 ; from dimethylamine reported by Oostenbrink et al. DOI:
10.1002/cphc.200400542
HZ H 0.44000 3 ; from dimethylamine reported by Oostenbrink et al. DOI:
10.1002/cphc.200400542
CH CH3 0.22000 3 ; from dimethylamine reported by Oostenbrink et al. DOI:
10.1002/cphc.200400542
C C 0.450 4
O O -0.450 4
[ bonds ]
N H gb_2
N CA gb_21
CA CB gb_27
CA C gb_27
CB CG gb_27
CG CD gb_27
CD CE gb_27
CE NZ gb_21
NZ HZ gb_2
NZ CH gb_21
C O gb_5
C +N gb_10
[ angles ]
; ai aj ak gromos type
-C N H ga_32
-C N CA ga_31
H N CA ga_18
N CA CB ga_13
N CA C ga_13
CB CA C ga_13
CA CB CG ga_15
CB CG CD ga_15
CG CD CE ga_15
CD CE NZ ga_15
CE NZ HZ ga_11
HZ NZ CH ga_11
CE NZ CH ga_13
CA C O ga_30
CA C +N ga_19
O C +N ga_33
[ impropers ]
; ai aj ak al gromos type
N -C CA H gi_1
CA N C CB gi_2
C CA +N O gi_1
[ dihedrals ]
; ai aj ak al gromos type
-C -C N CA gd_14
-C N CA C gd_44
-C N CA C gd_43
N CA CB CG gd_34
N CA C +N gd_45

```

```

N CA C +N gd_42
CA CB CG CD gd_34
CB CG CD CE gd_34
CG CD CE NZ gd_34
CD CE NZ CH gd_29

; N6-methyllysine (+1)
[KMC]
[atoms]
N N -0.31000 0
H H 0.31000 0
CA CH1 0.00000 1
CB CH2 0.00000 1
CG CH2 0.00000 2
CD CH2 0.00000 2
CE CH2 0.20000 3 ; derived by analogy to methyl groups of amines reported
by Oostenbrink et al. DOI: 10.1002/cphc.200400542
NZ NL 0.10400 3 ; to add up to +1 net charge
HZ1 H 0.24800 3
HZ2 H 0.24800 3
CH CH3 0.20000 3 ; derived by analogy to methyl groups of amines reported
by Oostenbrink et al. DOI: 10.1002/cphc.200400542
C C 0.450 4
O O -0.450 4
[bonds]
N H gb_2
N CA gb_21
CA CB gb_27
CA C gb_27
CB CG gb_27
CG CD gb_27
CD CE gb_27
CE NZ gb_21
NZ HZ1 gb_2
NZ HZ2 gb_2
NZ CH gb_21
C O gb_5
C +N gb_10
[angles]
; ai aj ak gromos type
-C N H ga_32
-C N CA ga_31
H N CA ga_18
N CA CB ga_13
N CA C ga_13
CB CA C ga_13
CA CB CG ga_15
CB CG CD ga_15
CG CD CE ga_15
CD CE NZ ga_15
CE NZ HZ1 ga_11
CE NZ HZ2 ga_11
HZ1 NZ HZ2 ga_10
HZ1 NZ CH ga_11
HZ2 NZ CH ga_11
CE NZ CH ga_13
CA C O ga_30
CA C +N ga_19
O C +N ga_33
[impropers]
; ai aj ak al gromos type
N -C CA H gi_1
CA N C CB gi_2
C CA +N O gi_1
[dihedrals]
; ai aj ak al gromos type
-C CA -C N CA gd_14
-C N CA C gd_44
-C N CA C gd_43
N CA CB CG gd_34
N CA C +N gd_45
N CA C +N gd_42
CA CB CG CD gd_34
CB CG CD CE gd_34
CG CD CE NZ gd_34
CD CE NZ CH gd_29

; N6,N6-dimethyllysine (0)
[K2M]
[atoms]
N N -0.31000 0
H H 0.31000 0
CA CH1 0.00000 1
CB CH2 0.00000 1
CG CH2 0.00000 2
CD CH2 0.00000 2
CE CH2 0.21000 3 ; from trimethylamine reported by Oostenbrink et al. DOI:
10.1002/cphc.200400542
NZ NT -0.63000 3 ; from trimethylamine reported by Oostenbrink et al. DOI:
10.1002/cphc.200400542
CH1 CH3 0.21000 3 ; from trimethylamine reported by Oostenbrink et al. DOI:
10.1002/cphc.200400542
CH2 CH3 0.21000 3 ; from trimethylamine reported by Oostenbrink et al. DOI:
10.1002/cphc.200400542
C C 0.450 4
O O -0.450 4
[bonds]
N H gb_2
N CA gb_21
CA CB gb_27
CA C gb_27
CB CG gb_27
CG CD gb_27
CD CE gb_27
CE NZ gb_21
NZ HZ gb_2
NZ CH1 gb_21
NZ CH2 gb_21
C O gb_5
C +N gb_10
[angles]
; ai aj ak gromos type
-C N H ga_32
-C N CA ga_31
H N CA ga_18
N CA CB ga_13
CB CA C ga_13
CA CB CG ga_15
CB CG CD ga_15
CG CD CE ga_15
CD CE NZ ga_15
CE NZ CH1 ga_13
CE NZ CH2 ga_13
CH1 NZ CH2 ga_13
CA C O ga_30
CA C +N ga_19
O C +N ga_33
[impropers]
; ai aj ak al gromos type
N -C CA H gi_1
CA N C CB gi_2
C CA +N O gi_1
[dihedrals]
; ai aj ak al gromos type
-C CA -C N CA gd_14
-C N CA C gd_44
-C N CA C gd_43
N CA CB CG gd_34
N CA C +N gd_45
N CA C +N gd_42
CA CB CG CD gd_34
CB CG CD CE gd_34
CG CD CE NZ gd_34
CD CE NZ CH1 gd_29

```

```

CB CA C ga_13
CA CB CG ga_15
CB CG CD ga_15
CG CD CE ga_15
CD CE NZ ga_15
CE NZ HZ ga_11
CH1 NZ HZ ga_11
CH2 NZ HZ ga_11
CE NZ CH1 ga_13
CE NZ CH2 ga_13
CH1 NZ CH2 ga_13
CA C O ga_30
CA C +N ga_19
O C +N ga_33
[ impropers ]
; ai aj ak al gromos type
N -C CA H gi_1
CA N C CB gi_2
C CA +N O gi_1
[ dihedrals ]
; ai aj ak al gromos type
-C -C N CA gd_14
-C N CA C gd_44
-C N CA C gd_43
N CA CB CG gd_34
N CA C +N gd_45
N CA C +N gd_42
CA CB CG CD gd_34
CB CG CD CE gd_34
CG CD CE NZ gd_34
CD CE NZ CH1 gd_29

; N6,N6,N6-trimethyllysine
[ K3C ]
[ atoms ]
N N -0.31000 0
H H 0.31000 0
CA CH1 0.00000 1
CB CH2 0.00000 1
CG CH2 0.00000 2
CD CH2 0.00000 2
CE CH2 0.20000 3; derived by analogy to methyl groups of amines reported
by Oostenbrink et al. DOI: 10.1002/cphc.200400542
NZ NL 0.20000 3; to add up to +1 net charge
CH1 CH3 0.20000 3; derived by analogy to methyl groups of amines reported
by Oostenbrink et al. DOI: 10.1002/cphc.200400542
CH2 CH3 0.20000 3; derived by analogy to methyl groups of amines reported
by Oostenbrink et al. DOI: 10.1002/cphc.200400542
CH3 CH3 0.20000 3; derived by analogy to methyl groups of amines reported
by Oostenbrink et al. DOI: 10.1002/cphc.200400542
C C 0.450 4
O O -0.450 4
[ bonds ]
N H gb_2
N CA gb_21
CA CB gb_27
CA C gb_27
CB CG gb_27
CG CD gb_27
CD CE gb_27
CE NZ gb_21
NZ CH1 gb_21
NZ CH2 gb_21
NZ CH3 gb_21
C O gb_5
C +N gb_10
[ angles ]
; ai aj ak gromos type
-C N H ga_32
-C N CA ga_31
H N CA ga_18
N CA CB ga_13
N CA C ga_13
CB CA C ga_13
CA CB CG ga_15
CB CG CD ga_15
CG CD NE ga_13
CD NE HE ga_20
CD NE CZ ga_33
HE NE CZ ga_23
NE CZ NH1 ga_28
NE CZ NH2 ga_28
NH1 CZ NH2 ga_28
CZ NH1 CT ga_27
CZ NH2 HH21 ga_23
CZ NH2 HH22 ga_23
HH21 NH2 HH22 ga_24
CA C O ga_30
CA C +N ga_19
O C +N ga_33
[ impropers ]
; ai aj ak al gromos type
N -C CA H gi_1
CA N C CB gi_2
NE CD CZ HE gi_1
CZ NH1 NH2 NE gi_1
NH2 HH21 HH22 CZ gi_1
C CA +N O gi_1
[ dihedrals ]
; ai aj ak al gromos type
N -C CA H gi_1
CA N C CB gi_2
C CA +N O gi_1
[ dihedrals ]
; ai aj ak al gromos type
N N -0.31000 0
H H 0.31000 0
CA CH1 0.00000 1
CB CH2 0.00000 1
CG CH2 0.00000 2
CD CH2 0.00000 2
NE NE -0.31000 3
HE H 0.31000 3
CZ C 0.18000 4; 0.36 charge divided between CZ and CT to add up to 0 net
charge, similar to methyl groups of other methylation residues and also used in other
building blocks (e.g., TMP)
NH1 NE -0.36000 4; from ring nitrogen atoms of nucleotides (e.g., ATP)
CT CH3 0.18000 4; 0.36 charge divided between CZ and CT to add up to 0 net
charge, similar to methyl groups of other methylation residues and also used in other
building blocks (e.g., TMP)
NH2 NZ -0.88000 5
HH21 H 0.44000 5
HH22 H 0.44000 5
C C 0.450 6
O O -0.450 6
[ bonds ]
N H gb_2
N CA gb_21
CA CB gb_27
CA C gb_27
CB CG gb_27
CG CD gb_27
CD NE gb_21
NE HE gb_2
NE CZ gb_11
CZ NH1 gb_11
CZ NH2 gb_11
NH1 CT gb_21
NH2 HH21 gb_2
NH2 HH22 gb_2
C O gb_5
C +N gb_10
[ angles ]
; ai aj ak gromos type
-C N H ga_32
-C N CA ga_31
H N CA ga_18
N CA CB ga_13
N CA C ga_13
CB CA C ga_13
CA CB CG ga_15
CB CG CD ga_15
CG CD NE ga_13
CD NE HE ga_20
CD NE CZ ga_33
HE NE CZ ga_23
NE CZ NH1 ga_28
NE CZ NH2 ga_28
NH1 CZ NH2 ga_28
CZ NH1 CT ga_27
CZ NH2 HH21 ga_23
CZ NH2 HH22 ga_23
HH21 NH2 HH22 ga_24
CA C O ga_30
CA C +N ga_19
O C +N ga_33
[ impropers ]
; ai aj ak al gromos type
N -C CA H gi_1
CA N C CB gi_2
NE CD CZ HE gi_1
CZ NH1 NH2 NE gi_1
NH2 HH21 HH22 CZ gi_1
C CA +N O gi_1
[ dihedrals ]
; ai aj ak al gromos type
-C -C N CA gd_14
-C N CA C gd_44
-C N CA C gd_43
N CA CB CG gd_34
N CA C +N gd_45
N CA C +N gd_42
CA CB CG CD gd_34
CB CG CD CE gd_34
CG CD CE NZ gd_34
CD CE NZ CH1 gd_29

```

```

CB CG CD NE gd_34
CG CD NE CZ gd_39
CD NE CZ NH1 gd_14
NE CZ NH1 CT gd_14
NE CZ NH2 HH21 gd_14

; omega-N-methylarginine (+1)
[RMC]
[atoms]
N N -0.31000 0
H H 0.31000 0
CA CH1 0.00000 1
CB CH2 0.00000 1
CG CH2 0.00000 1
CD CH2 0.09000 2
NE NE -0.11000 2
HE H 0.24000 2
CZ C 0.34000 2
NH1 NZ -0.26000 2
HH11 H 0.24000 2
HH12 H 0.24000 2
NH2 NZ -0.11000 2 ; from NE atom of ARG
HH2 H 0.24000 2
CT CH3 0.09000 2 ; from CD atom of ARG
C C 0.450 3
O O -0.450 3
[bonds]
N H gb_2
N CA gb_21
CA CB gb_27
CA C gb_27
CB CG gb_27
CG CD gb_27
CD NE gb_21
NE HE gb_2
NE CZ gb_11
CZ NH1 gb_11
CZ NH2 gb_11
NH1 HH11 gb_2
NH1 HH12 gb_2
NH2 HH2 gb_2
NH2 CT gb_21
C O gb_5
C +N gb_10
[angles]
; ai aj ak gromos type
-C N H ga_32
-C N CA ga_31
H N CA ga_18
N CA CB ga_13
N CA C ga_13
CB CA C ga_13
CA CB CG ga_15
CB CG CD ga_15
CG CD NE ga_13
CD NE HE ga_20
CD NE CZ ga_33
HE NE CZ ga_23
NE CZ NH1 ga_28
NE CZ NH2 ga_28
NH1 CZ NH2 ga_28
CZ NH1 CT1 ga_27
CZ NH2 HH2 ga_23
HH2 NH2 CT2 ga_20
CZ NH2 CT2 ga_33
CA C O ga_30
CA C +N ga_19
O C +N ga_33
[impropers]
; ai aj ak al gromos type
N -C CA H gi_1
CA N C CB gi_2
NE CD CZ HE gi_1
CZ NH1 NH2 NE gi_1
NH1 HH11 HH12 CZ gi_1
NH2 HH2 CT CZ gi_1
C CA +N O gi_1
[dihedrals]
; ai aj ak al gromos type
-C -C N CA gd_14
-C N CA C gd_44
-C N CA C gd_43
N CA CB CG gd_34
N CA C +N gd_45
N CA C +N gd_42
CA CB CG CD gd_34
CB CG CD NE gd_34
CG CD NE CZ gd_39
CD NE CZ NH1 gd_14
NE CZ NH1 CT1 gd_14
NE CZ NH2 CT2 gd_14

; symmetric-dimethylarginine (0)
[RSM]
[atoms]
N N -0.31000 0
H H 0.31000 0
CA CH1 0.00000 1
CB CH2 0.00000 1
CG CH2 0.00000 2
CD CH2 0.00000 2
NE NE -0.31000 3
HE H 0.31000 3
CZ C 0.18000 4 ; 0.36 charge divided between CZ and CT1 to add up to 0 net
charge, similar to methyl groups of other methylation residues and also used in other
building blocks (e.g., TMP)
NH1 NE -0.36000 4 ; from ring nitrogen atoms of nucleotides (e.g., ATP)
CT1 CH3 0.18000 4 ; 0.36 charge divided between CZ and CT1 to add up to 0
net charge, similar to methyl groups of other methylation residues and also used in
other building blocks (e.g., TMP)
NH2 NE -0.31000 5 ; from NE atom of ARGN
HH2 H 0.31000 5 ; from HE atom of ARGN
CT2 CH3 0.00000 6 ; from CD atom of ARGN
C C 0.450 7
O O -0.450 7
[bonds]
N H gb_2
N CA gb_21
CA CB gb_27
CA C gb_27
CB CG gb_27
CG CD gb_27
CD NE gb_21
NE HE gb_2
NE CZ gb_11
CZ NH1 gb_11
CZ NH2 gb_11
NH1 CT1 gb_21
NH2 HH2 gb_2
NH2 CT2 gb_21
C O gb_5
C +N gb_10
[angles]
; ai aj ak gromos type
-C N H ga_32
-C N CA ga_31
H N CA ga_18
N CA CB ga_13
N CA C ga_13
CB CA C ga_13
CA CB CG ga_15
CB CG CD ga_15
CG CD NE ga_13
CD NE HE ga_20
CD NE CZ ga_33
HE NE CZ ga_23
NE CZ NH1 ga_28
NE CZ NH2 ga_28
NH1 CZ NH2 ga_28
CZ NH1 CT1 ga_27
CZ NH2 HH2 ga_23
HH2 NH2 CT2 ga_20
CZ NH2 CT2 ga_33
CA C O ga_30
CA C +N ga_19
O C +N ga_33
[impropers]
; ai aj ak al gromos type
N -C CA H gi_1
CA N C CB gi_2
NE CD CZ HE gi_1
CZ NH1 NH2 NE gi_1
NH2 HH2 CT2 CZ gi_1
C CA +N O gi_1
[dihedrals]
; ai aj ak al gromos type
-C -C N CA gd_14
-C N CA C gd_44
-C N CA C gd_43
N CA CB CG gd_34
N CA C +N gd_45
N CA C +N gd_42
CA CB CG CD gd_34
CB CG CD NE gd_34
CG CD NE CZ gd_39
CD NE CZ NH1 gd_14
NE CZ NH1 CT1 gd_14
NE CZ NH2 CT2 gd_14

; symmetric-dimethylarginine (+1)
[RMS]
[atoms]
N N -0.31000 0
H H 0.31000 0

```

```

CA CH1 0.00000 1
CB CH2 0.00000 1
CG CH2 0.00000 1
CD CH2 0.09000 2
NE NE -0.11000 2
HE H 0.24000 2
CZ C 0.34000 2
NH1 NZ -0.11000 2 ; from NE atom of ARG
HH1 H 0.24000 2
CT1 CH3 0.09000 2 ; from CD atom of ARG
NH2 NZ -0.11000 2 ; from NE atom of ARG
HH2 H 0.24000 2
CT2 CH3 0.09000 2 ; from CD atom of ARG
C C 0.450 3
O O -0.450 3
[ bonds ]
N H gb_2
N CA gb_21
CA CB gb_27
CA C gb_27
CB CG gb_27
CG CD gb_27
CD NE gb_21
NE HE gb_2
NE CZ gb_11
CZ NH1 gb_11
CZ NH2 gb_11
NH1 HH1 gb_2
NH1 CT1 gb_21
NH2 HH2 gb_2
NH2 CT2 gb_21
C O gb_5
C +N gb_10
[ angles ]
; ai aj ak gromos type
-C N H ga_32
-C N CA ga_31
H N CA ga_18
N CA CB ga_13
N CA C ga_13
CB CA C ga_13
CA CB CG ga_15
CB CG CD ga_15
CG CD NE ga_13
CD NE HE ga_20
CD NE CZ ga_33
HE NE CZ ga_23
NE CZ NH1 ga_28
NE CZ NH2 ga_28
NH1 CZ NH2 ga_28
CZ NH1 HH1 ga_23
CZ NH2 CT1 ga_28
CZ NH2 CT2 ga_28
CT1 NH2 CT2 ga_28
CA C O ga_30
CA C +N ga_19
O C +N ga_33
[ impropers ]
; ai aj ak al gromos type
N -C CA H gi_1
CA N C CB gi_2
NE CD CZ HE gi_1
CZ NH1 NH2 NE gi_1
NH1 HH1 CT1 CZ gi_1
NH2 HH2 CT2 CZ gi_1
C CA +N O gi_1
[ dihedrals ]
; ai aj ak al gromos type
-C -C N CA gd_14
-C N CA C gd_44
-C N CA C gd_43
N CA CB CG gd_34
N CA C +N gd_45
N CA C +N gd_42
CA CB CG CD gd_34
CB CG CD NE gd_34
CG CD NE CZ gd_39
CD NE CZ NH1 gd_14
NE CZ NH1 CT1 gd_14
NE CZ NH2 CT2 gd_14
; asymmetric-dimethylarginine (0)
[ RAM ]
[ atoms ]
N N -0.31000 0
H H 0.31000 0
CA CH1 0.00000 1
CB CH2 0.00000 1
CG CH2 0.00000 1
CD CH2 0.09000 2
NE NE -0.11000 2
HE H 0.24000 2
CZ C 0.43000 2 ; from CZ of R1P
NH1 NZ -0.26000 2
HH11 H 0.24000 2
HH12 H 0.24000 2
HE H 0.31000 3
CZ C 0.26600 4
NH1 NE -0.67400 4
HH1 H 0.40800 4
NH2 NZ -0.20000 5 ; from ring nitrogen atoms of nucleotides (e.g., ATP)
CT1 CH3 0.10000 5 ; 0.2 charge divided between CT1 and CT2 to add up to 0
net charge, also similar to methyl groups of methyl-arginine modifications and used
for ring carbons in nucleotides (e.g., DCYT)
CT2 CH3 0.10000 5 ; 0.2 charge divided between CT1 and CT2 to add up to 0
net charge, also similar to methyl groups of methyl-arginine modifications and used
for ring carbons in nucleotides (e.g., DCT)
C C 0.450 6
O O -0.450 6
[ bonds ]
N H gb_2
N CA gb_21
CA CB gb_27
CA C gb_27
CB CG gb_27
CG CD gb_27
CD NE gb_21
NE HE gb_2
NE CZ gb_11
CZ NH1 gb_11
CZ NH2 gb_11
NH1 HH1 gb_2
NH2 CT1 gb_21
NH2 CT2 gb_21
C O gb_5
C +N gb_10
[ angles ]
; ai aj ak gromos type
-C N H ga_32
-C N CA ga_31
H N CA ga_18
N CA CB ga_13
N CA C ga_13
CB CA C ga_13
CA CB CG ga_15
CB CG CD ga_15
CG CD NE ga_13
CD NE HE ga_20
CD NE CZ ga_33
HE NE CZ ga_23
NE CZ NH1 ga_28
NE CZ NH2 ga_28
NH1 CZ NH2 ga_28
CZ NH1 HH1 ga_23
CZ NH2 CT1 ga_28
CZ NH2 CT2 ga_28
CT1 NH2 CT2 ga_28
CA C O ga_30
CA C +N ga_19
O C +N ga_33
[ impropers ]
; ai aj ak al gromos type
N -C CA H gi_1
CA N C CB gi_2
NE CD CZ HE gi_1
CZ NH1 NH2 NE gi_1
NH2 CT1 CT2 CZ gi_1
C CA +N O gi_1
[ dihedrals ]
; ai aj ak al gromos type
-C -C N CA gd_14
-C N CA C gd_44
-C N CA C gd_43
N CA CB CG gd_34
N CA C +N gd_45
N CA C +N gd_42
CA CB CG CD gd_34
CB CG CD NE gd_34
CG CD NE CZ gd_39
CD NE CZ NH1 gd_14
NE CZ NH1 HH1 gd_14
NE CZ NH2 CT1 gd_14
; asymmetric-dimethylarginine (+1)
[ RMA ]
[ atoms ]
N N -0.31000 0
H H 0.31000 0
CA CH1 0.00000 1
CB CH2 0.00000 1
CG CH2 0.00000 1
CD CH2 0.09000 2
NE NE -0.11000 2
HE H 0.24000 2
CZ C 0.43000 2 ; from CZ of R1P
NH1 NZ -0.26000 2
HH11 H 0.24000 2
HH12 H 0.24000 2

```



NH2 NZ -0.05000 2 ; to add up to +1 net charge, also used for nitrogen atoms

in histidine building blocks

CT1 CH3 0.09000 2 ; from CD atom of ARG

CT2 CH3 0.09000 2 ; from CD atom of ARG

C C 0.450 3

O O -0.450 3

[ bonds ]

N H gb\_2

N CA gb\_21

CA CB gb\_27

CA C gb\_27

CB CG gb\_27

CG CD gb\_27

CD NE gb\_21

NE HE gb\_2

NE CZ gb\_11

CZ NH1 gb\_11

CZ NH2 gb\_11

NH1 HH11 gb\_2

NH1 HH12 gb\_2

NH2 CT1 gb\_21

NH2 CT2 gb\_21

C O gb\_5

C +N gb\_10

[ angles ]

; ai aj ak gromos type

-C N H ga\_32

-C N CA ga\_31

H N CA ga\_18

N CA CB ga\_13

N CA C ga\_13

CB CA C ga\_13

CA CB CG ga\_15

CB CG CD ga\_15

CG CD NE ga\_13

CD NE HE ga\_20

CD NE CZ ga\_33

HE NE CZ ga\_23

NE CZ NH1 ga\_28

NE CZ NH2 ga\_28

NH1 CZ NH2 ga\_28

CZ NH1 HH11 ga\_23

CZ NH1 HH12 ga\_23

HH11 NH1 HH12 ga\_24

CZ NH2 CT1 ga\_28

CZ NH2 CT2 ga\_28

CT1 NH2 CT2 ga\_28

CA C O ga\_30

CA C +N ga\_19

O C +N ga\_33

[ impropers ]

; ai aj ak al gromos type

N -C CA H gi\_1

CA N C CB gi\_2

NE CD CZ HE gi\_1

CZ NH1 NH2 NE gi\_1

NH1 HH11 HH12 CZ gi\_1

NH2 CT1 CT2 CZ gi\_1

C CA +N O gi\_1

[ dihedrals ]

; ai aj ak al gromos type

-CA -C N CA gd\_14

-C N CA C gd\_44

-C N CA C gd\_43

N CA CB CG gd\_34

N CA C +N gd\_45

N CA C +N gd\_42

CA CB CG CD gd\_34

CB CG CD NE gd\_34

CG CD NE CZ gd\_39

CD NE CZ NH1 gd\_14

NE CZ NH1 HH11 gd\_14

NE CZ NH2 CT1 gd\_14

; 1-methylhistidine (0)

[ H1M ]

[ atoms ]

N N -0.31000 0

H H 0.31000 0

CA CH1 0.00000 1

CB CH2 0.00000 1

CG C 0.00000 2

ND1 NR -0.54000 2

CD2 C 0.00000 2

HD2 HC 0.14000 2

CE1 C 0.09000 2 ; to add up to 0 net charge, also from CD atom of ARG

HE1 HC 0.14000 2

NE2 NR -0.05000 2

CZ CH3 0.22000 2 ; from the methyl groups of dimethylamine reported by

Oostenbrink et al. DOI: 10.1002/cphc.200400542

C C 0.450 3

O O -0.450 3

[ bonds ]

N H gb\_2

N CA gb\_21

CA CB gb\_27

CA C gb\_27

CB CG gb\_27

CG ND1 gb\_10

CG CD2 gb\_10

ND1 CE1 gb\_10

CD2 HD2 gb\_3

CD2 NE2 gb\_10

CE1 HE1 gb\_3

CE1 NE2 gb\_10

NE2 CZ gb\_22

C O gb\_5

C +N gb\_10

[ exclusions ]

; ai aj

CB HD2

CB CE1

CB NE2

CG HE1

CG CZ

ND1 HD2

ND1 CZ

CD2 HE1

HD2 CE1

HD2 CZ

HE1 CZ

[ angles ]

; ai aj ak gromos type

-C N H ga\_32

-C N CA ga\_31

H N CA ga\_18

N CA CB ga\_13

N CA C ga\_13

CB CA C ga\_13

CA CB CG ga\_15

CB CG ND1 ga\_37

CB CG CD2 ga\_37

ND1 CG CD2 ga\_7

CG ND1 CE1 ga\_7

CG CD2 HD2 ga\_36

CG CD2 NE2 ga\_7

HD2 CD2 NE2 ga\_36

ND1 CE1 HE1 ga\_36

ND1 CE1 NE2 ga\_7

HE1 CE1 NE2 ga\_36

CD2 NE2 CE1 ga\_7

CD2 NE2 CZ ga\_37

CE1 NE2 CZ ga\_37

CA C O ga\_30

CA C +N ga\_19

O C +N ga\_33

[ impropers ]

; ai aj ak al gromos type

N -C CA H gi\_1

CA N C CB gi\_2

CG ND1 CD2 CB gi\_1

CG ND1 CE1 NE2 gi\_1

CG CD2 NE2 CE1 gi\_1

ND1 CG CD2 NE2 gi\_1

ND1 CE1 NE2 CD2 gi\_1

CD2 CG ND1 CE1 gi\_1

CD2 CG NE2 HD2 gi\_1

CE1 ND1 NE2 HE1 gi\_1

NE2 CD2 CE1 CZ gi\_1

C CA +N O gi\_1

[ dihedrals ]

; ai aj ak al gromos type

-CA -C N CA gd\_14

-C N CA C gd\_44

-C N CA C gd\_43

N CA CB CG gd\_34

N CA C +N gd\_45

N CA C +N gd\_42

CA CB CG ND1 gd\_40

; 1-methylhistidine (+1)

[ H1C ]

[ atoms ]

N N -0.31000 0

H H 0.31000 0

CA CH1 0.00000 1

CB CH2 0.00000 1

CG C -0.05000 2

ND1 NR 0.38000 2

HD1 H 0.30000 2

CD2 C -0.10000 2

HD2 HC 0.10000 2

CE1 C -0.24000 2 ; to add up to +1 net charge

HE1 HC 0.10000 2

NE2 NR 0.31000 2

CZ CH3 0.20000 2 ; derived by analogy to methyl groups of amines reported by Oostenbrink et al. DOI: 10.1002/cphc.200400542

C C 0.450 3  
O O -0.450 3

[ bonds ]

N H gb\_2  
N CA gb\_21  
CA CB gb\_27  
CA C gb\_27  
CB CG gb\_27  
CG ND1 gb\_10  
CG CD2 gb\_10  
ND1 HD1 gb\_2  
ND1 CE1 gb\_10  
CD2 HD2 gb\_3  
CD2 NE2 gb\_10  
CE1 HE1 gb\_3  
CE1 NE2 gb\_10  
NE2 CZ gb\_22  
C O gb\_5  
C +N gb\_10

[ exclusions ]

; ai aj

CB HD1  
CB HD2  
CB CE1  
CB NE2  
CG HE1  
CG CZ  
ND1 HD2  
ND1 CZ  
HD1 CD2  
HD1 HE1  
HD1 NE2  
CD2 HE1  
HD2 CE1  
HD2 CZ  
HE1 CZ

[ angles ]

; ai aj ak gromos type

-C N H ga\_32  
-C N CA ga\_31  
H N CA ga\_18  
N CA CB ga\_13  
N CA C ga\_13  
CB CA C ga\_13  
CA CB CG ga\_15  
CB CG ND1 ga\_37  
CB CG CD2 ga\_37  
ND1 CG CD2 ga\_7  
CG ND1 HD1 ga\_36  
CG ND1 CE1 ga\_7  
HD1 ND1 CE1 ga\_36  
CG CD2 HD2 ga\_36  
CG CD2 NE2 ga\_7  
HD2 CD2 NE2 ga\_36  
ND1 CE1 HE1 ga\_36  
ND1 CE1 NE2 ga\_7  
HE1 CE1 NE2 ga\_36  
CD2 NE2 CE1 ga\_7  
CD2 NE2 CZ ga\_37  
CE1 NE2 CZ ga\_37  
CA C O ga\_30  
CA C +N ga\_19  
O C +N ga\_33

[ impropers ]

; ai aj ak al gromos type

N -C CA H gi\_1  
CA N C CB gi\_2  
CG ND1 CD2 CB gi\_1  
CG ND1 CE1 NE2 gi\_1  
CG CD2 NE2 CE1 gi\_1  
ND1 CG CD2 NE2 gi\_1  
ND1 CG CE1 HD1 gi\_1  
ND1 CE1 NE2 CD2 gi\_1  
CD2 CG ND1 CE1 gi\_1  
CD2 CG NE2 HD2 gi\_1  
CE1 ND1 NE2 HE1 gi\_1  
NE2 CD2 CE1 CZ gi\_1  
C CA +N O gi\_1

[ dihedrals ]

; ai aj ak al gromos type

-CA -C N CA gd\_14  
-C N CA C gd\_44  
-C N CA C gd\_43  
N CA CB CG gd\_34  
N CA C +N gd\_45  
N CA C +N gd\_42  
CA CB CG ND1 gd\_40

; 3-methylhistidine (0)

[ H3M ]

[ atoms ]

N N -0.31000 0

H H 0.31000 0

CA CH1 0.00000 1

CB CH2 0.00000 1

CG C 0.00000 2

ND1 NR -0.05000 2

CD2 C 0.00000 2

HD2 HC 0.14000 2

CE1 C 0.09000 2 ; to add up to 0 net charge

CE3 CH3 0.22000 2 ; from the methyl groups of dimethylamine reported by

Oostenbrink et al. DOI: 10.1002/cphc.200400542

HE1 HC 0.14000 2

NE2 NR -0.54000 2

C C 0.450 3

O O -0.450 3

[ bonds ]

N H gb\_2

N CA gb\_21

CA CB gb\_27

CA C gb\_27

CB CG gb\_27

CG ND1 gb\_10

CG CD2 gb\_10

ND1 CE3 gb\_22

ND1 CE1 gb\_10

CD2 HD2 gb\_3

CD2 NE2 gb\_10

CE1 HE1 gb\_3

CE1 NE2 gb\_10

C O gb\_5

C +N gb\_10

[ exclusions ]

; ai aj

CB CE3

CB HD2

CB CE1

CB NE2

CG HE1

ND1 HD2

CE3 CD2

CE3 HE1

CE3 NE2

CD2 HE1

HD2 CE1

[ angles ]

; ai aj ak gromos type

-C N H ga\_32  
-C N CA ga\_31  
H N CA ga\_18  
N CA CB ga\_13  
N CA C ga\_13  
CB CA C ga\_13  
CA CB CG ga\_15  
CB CG ND1 ga\_37  
CB CG CD2 ga\_37  
ND1 CG CD2 ga\_7  
CG ND1 CE3 ga\_37  
CG ND1 CE1 ga\_7  
CE3 ND1 CE1 ga\_37  
CG CD2 HD2 ga\_36  
CG CD2 NE2 ga\_7  
HD2 CD2 NE2 ga\_36  
ND1 CE1 HE1 ga\_36  
ND1 CE1 NE2 ga\_7  
HE1 CE1 NE2 ga\_36  
CD2 NE2 CE1 ga\_7  
CA C O ga\_30  
CA C +N ga\_19  
O C +N ga\_33

[ impropers ]

; ai aj ak al gromos type

N -C CA H gi\_1  
CA N C CB gi\_2  
CG ND1 CD2 CB gi\_1  
CG ND1 CE1 NE2 gi\_1  
CG CD2 NE2 CE1 gi\_1  
ND1 CG CD2 NE2 gi\_1  
ND1 CG CE1 CE3 gi\_1  
ND1 CE1 NE2 CD2 gi\_1  
CD2 CG ND1 CE1 gi\_1  
CD2 CG NE2 HD2 gi\_1  
CE1 ND1 NE2 HE1 gi\_1  
C CA +N O gi\_1

[ dihedrals ]

; ai aj ak al gromos type

-CA -C N CA gd\_14  
-C N CA C gd\_44  
-C N CA C gd\_43  
N CA CB CG gd\_34  
N CA C +N gd\_45  
N CA C +N gd\_42  
CA CB CG ND1 gd\_40

```

; 3-methylhistidine (+1)
[H3C]
[atoms]
  N N -0.31000 0
  H H 0.31000 0
  CA CH1 0.00000 1
  CB CH2 0.00000 1
  CG C -0.05000 2
  ND1 NR 0.38000 2
  CE3 CH3 0.20000 2; derived by analogy to methyl groups of amines reported
by Oostenbrink et al. DOI: 10.1002/cphc.200400542
  CD2 C -0.10000 2
  HD2 HC 0.10000 2
  CE1 C -0.24000 2; to add up to +1 net charge
  HE1 HC 0.10000 2
  NE2 NR 0.31000 2
  HE2 H 0.30000 2
  C C 0.450 3
  O O -0.450 3
[bonds]
  N H gb_2
  N CA gb_21
  CA CB gb_27
  CA C gb_27
  CB CG gb_27
  CG ND1 gb_10
  CG CD2 gb_10
  ND1 CE3 gb_22
  ND1 CE1 gb_10
  CD2 HD2 gb_3
  CD2 NE2 gb_10
  CE1 HE1 gb_3
  CE1 NE2 gb_10
  NE2 HE2 gb_2
  C O gb_5
  C +N gb_10
[exclusions]
; ai aj
  CB CE3
  CB HD2
  CB CE1
  CB NE2
  CG HE1
  CG HE2
  ND1 HD2
  ND1 HE2
  CE3 CD2
  CE3 HE1
  CE3 NE2
  CD2 HE1
  HD2 CE1
  HD2 HE2
  HE1 HE2
[angles]
; ai aj ak gromos type
  -C N H ga_32
  -C N CA ga_31
  H N CA ga_18
  N CA CB ga_13
  N CA C ga_13
  CB CA C ga_13
  CB CA C ga_13
  CA CB CG ga_15
  CA CB CG ga_15
  CB CG ND1 ga_37
  CB CG CD2 ga_37
  ND1 CG CD2 ga_7
  CG ND1 CE3 ga_37
  CG ND1 CE1 ga_7
  CE3 ND1 CE1 ga_37
  CG CD2 HD2 ga_36
  CG CD2 NE2 ga_7
  HD2 CD2 NE2 ga_36
  ND1 CE1 HE1 ga_36
  ND1 CE1 NE2 ga_7
  HE1 CE1 NE2 ga_36
  CD2 NE2 CE1 ga_7
  CD2 NE2 HE2 ga_36
  CE1 NE2 HE2 ga_36
  CA C O ga_30
  CA C +N ga_19
  O C +N ga_33
[impropers]
; ai aj ak al gromos type
  N -C CA H gi_1
  CA N C CB gi_2
  CG ND1 CD2 CB gi_1
  CG ND1 CE1 NE2 gi_1
  CG CD2 NE2 CE1 gi_1
  ND1 CG CD2 NE2 gi_1
  ND1 CG CE1 CE3 gi_1
  ND1 CE1 NE2 CD2 gi_1
  CD2 CG ND1 CE1 gi_1
  CD2 CG NE2 HD2 gi_1
  CE1 ND1 NE2 HE1 gi_1
  NE2 CD2 CE1 HE2 gi_1
  C CA +N O gi_1
[dihedrals]
; ai aj ak al gromos type
  -CA -C N CA gd_14
  -C N CA C gd_44
  -C N CA C gd_43
  N CA CB CG gd_34
  N CA C +N gd_45
  N CA C +N gd_42
  CA CB CG ND1 gd_40
; N5-methylglutamine
[QME]
[atoms]
  N N -0.31000 0
  H H 0.31000 0
  CA CH1 0.00000 1
  CB CH2 0.00000 1
  CG CH2 0.10000 2; by analogy to the aldehyde group reported by Dolenc et
al. DOI: 10.1093/nar/gki195
  CD C 0.19000 2; by analogy to GLN, the peptide bond and the aldehyde
group reported by Dolenc et al. DOI: 10.1093/nar/gki195
  OE1 O -0.45000 2
  NE2 N -0.15000 2; by analogy to GLN and the peptide bond
  HE2 H 0.31000 2; from the hydrogen atom of the peptide bond
  CZ CH3 0.00000 3
  C C 0.450 4
  O O -0.450 4
[bonds]
  N H gb_2
  N CA gb_21
  CA CB gb_27
  CA C gb_27
  CB CG gb_27
  CG CD gb_27
  CD OE1 gb_5
  CD NE2 gb_9
  NE2 HE2 gb_2
  NE2 CZ gb_21
  C O gb_5
  C +N gb_10
[angles]
; ai aj ak gromos type
  -C N H ga_32
  -C N CA ga_31
  H N CA ga_18
  N CA CB ga_13
  N CA C ga_13
  CB CA C ga_13
  CA CB CG ga_15
  CB CG CD ga_15
  CG CD OE1 ga_30
  CG CD NE2 ga_19
  OE1 CD NE2 ga_33
  CD NE2 HE2 ga_32
  HE2 NE2 CZ ga_18
  CD NE2 CZ ga_31
  CA C O ga_30
  CA C +N ga_19
  O C +N ga_33
[impropers]
; ai aj ak al gromos type
  N -C CA H gi_1
  CA N C CB gi_2
  CD OE1 NE2 CG gi_1
  NE2 CZ CD HE2 gi_1
  C CA +N O gi_1
[dihedrals]
; ai aj ak al gromos type
  -CA -C N CA gd_14
  -C N CA C gd_44
  -C N CA C gd_43
  N CA CB CG gd_34
  N CA C +N gd_45
  N CA C +N gd_42
  CA CB CG CD gd_34
  CB CG CD NE2 gd_40
  CG CD NE2 CZ gd_14
; N4-methylasparagine
[NME]
[atoms]
  N N -0.31000 0
  H H 0.31000 0
  CA CH1 0.00000 1
  CB CH2 0.10000 2; by analogy to the aldehyde group reported by Dolenc et
al. DOI: 10.1093/nar/gki195
  CG C 0.19000 2; by analogy to ASN, the peptide bond and the aldehyde
group reported by Dolenc et al. DOI: 10.1093/nar/gki195
  OD1 O -0.45000 2
  ND2 N -0.15000 2; by analogy to ASN and the peptide bond
  HD2 H 0.31000 2; from the hydrogen of the peptide bond

```

```

CE CH3 0.00000 3
C C 0.450 4
O O -0.450 4
[ bonds ]
N H gb_2
N CA gb_21
CA CB gb_27
CA C gb_27
CB CG gb_27
CG OD1 gb_5
CG ND2 gb_9
ND2 HD2 gb_2
ND2 CE gb_21
C O gb_5
C +N gb_10
[ angles ]
; ai aj ak al gromos type
-C N H ga_32
-C N CA ga_31
H N CA ga_18
N CA CB ga_13
N CA C ga_13
CB CA C ga_13
CA CB CG ga_15
CB CG OD1 ga_30
CB CG ND2 ga_19
OD1 CG ND2 ga_33
CG ND2 HD2 ga_32
HD2 ND2 CE ga_18
CG ND2 CE ga_31
CA C O ga_30
CA C +N ga_19
O C +N ga_33
[ impropers ]
; ai aj ak al gromos type
N -C CA H gi_1
CA N C CB gi_2
CG OD1 ND2 CB gi_1
ND2 CE CG HD2 gi_1
C CA +N O gi_1
[ dihedrals ]
; ai aj ak al gromos type
-CA -C N CA gd_14
-C N CA C gd_44
-C N CA C gd_43
N CA CB CG gd_34
N CA C +N gd_45
N CA C +N gd_42
CA CB CG CD gd_34
CB CG CD OE2 gd_40
CG CD OE2 CZ gd_12

; aspartate methyl ester
[ DMA ]
[ atoms ]
N N -0.31000 0
H H 0.31000 0
CA CH1 0.00000 1
CB CH2 0.00000 1
CG C 0.25300 2; from the ester group reported by Chandrasekhar et al. DOI:
10.1081/smts-120030764
OD1 O -0.45000 2; from the ester group reported by Chandrasekhar et al.
DOI: 10.1081/smts-120030764
OD2 OE -0.06900 2; from the ester group reported by Chandrasekhar et al.
DOI: 10.1081/smts-120030764
CE CH3 0.26600 2; from the ester group reported by Chandrasekhar et al.
DOI: 10.1081/smts-120030764
C C 0.450 3
O O -0.450 3
[ bonds ]
N H gb_2
N CA gb_21
CA CB gb_27
CA C gb_27
CB CG gb_27
CG OD1 gb_5
CG OD2 gb_13
OD2 CE gb_18
C O gb_5
C +N gb_10
[ angles ]
; ai aj ak al gromos type
-C N H ga_32
-C N CA ga_31
H N CA ga_18
N CA CB ga_13
N CA C ga_13
CB CA C ga_13
CA CB CG ga_15
CB CG OD1 ga_30
CB CG OD2 ga_19
OD1 CG OD2 ga_33
CG OD2 CE ga_22
CA C O ga_30
CA C +N ga_19
O C +N ga_33
[ impropers ]
; ai aj ak al gromos type
N -C CA H gi_1
CA N C CB gi_2
CG OD1 OD2 CB gi_1
C CA +N O gi_1
[ dihedrals ]
; ai aj ak al gromos type
-CA -C N CA gd_14
-C N CA C gd_44
-C N CA C gd_43
N CA CB CG gd_34
N CA C +N gd_45
N CA C +N gd_42
CA CB CG OD2 gd_40
CB CG OD2 CE gd_12

; S-methylcysteine
[ CYM ]
[ atoms ]
N N -0.31000 0
H H 0.31000 0
CA CH1 0.00000 1
CB CH2 0.24100 2; from MET
SG S -0.48200 2; from MET
CD CH3 0.24100 2; from MET

```

```

C C 0.450 3
O O -0.450 3
[ bonds ]
N H gb_2
N CA gb_21
CA CB gb_27
CA C gb_27
CB SG gb_32
SG CD gb_31
C O gb_5
C +N gb_10
[ angles ]
; ai aj ak gromos type
-C N H ga_32
-C N CA ga_31
H N CA ga_18
N CA CB ga_13
N CA C ga_13
CB CA C ga_13
CA CB SG ga_16
CB SG CD ga_4
CA C O ga_30
CA C +N ga_19
O C +N ga_33
[ impropers ]
; ai aj ak al gromos type
N -C CA H gi_1
CA N C CB gi_2
C CA +N O gi_1
[ dihedrals ]
; ai aj ak al gromos type
-C -C N CA gd_14
-C N CA C gd_44
-C N CA C gd_43
N CA CB CG gd_34
N CA C +N gd_45
N CA C +N gd_42
CA CB CG CD gd_34
CB CG CD CE gd_34
CG CD CE NZ gd_34
CD CE NZ CH gd_39
CE NZ CH C11 gd_14

; 3-hydroxyproline (R)
[ PH3 ]
[ atoms ]
N N 0.00000 0
CA CH1 0.00000 1
CB CH1 0.26600 2; from the hydroxyl group of THR
OG1 OA -0.67400 2; from the hydroxyl group of THR
HG1 H 0.40800 2; from the hydroxyl group of THR
CG2 CH2R 0.00000 3
CD CH2R 0.00000 3
C C 0.450 4
O O -0.450 4
[ bonds ]
N CA gb_21
N CD gb_21
CA CB gb_27
CA C gb_27
CB OG1 gb_18
CB CG2 gb_27
OG1 HG1 gb_1
CG2 CD gb_27
C O gb_5
C +N gb_10
[ angles ]
; ai aj ak gromos type
-C N CA ga_31
-C N CD ga_31
CA N CD ga_21
N CA CB ga_13
N CA C ga_13
CB CA C ga_13
CA CB OG1 ga_13
CA CB CG2 ga_13
OG1 CB CG2 ga_13
CB OG1 HG1 ga_12
CB CG2 CD ga_13
N CD CG2 ga_13
CA C O ga_30
CA C +N ga_19
O C +N ga_33
[ impropers ]
; ai aj ak al gromos type
N -C CA CD gi_1
CA N C CB gi_2
CB CG2 CA OG1 gi_2
C CA +N O gi_1
[ dihedrals ]
; ai aj ak al gromos type
-C -C N CA gd_14
-C N CA C gd_44
-C N CA C gd_43
CA N CD CG2 gd_39
N CA CB CG2 gd_34
N CA C +N gd_45
N CA C +N gd_42
CA CB OG1 HG1 gd_23
CA CB CG2 CD gd_34
CB CG2 CD N gd_34

; 3-hydroxyproline (S)
[ P3H ]
[ atoms ]
N N 0.00000 0
CA CH1 0.00000 1
CB CH1 0.26600 2; from the hydroxyl group of THR
OG1 OA -0.67400 2; from the hydroxyl group of THR
HG1 H 0.40800 2; from the hydroxyl group of THR
CG2 CH2R 0.00000 3
CD CH2R 0.00000 3
C C 0.450 4
O O -0.450 4

```

```

[ bonds ]
N CA gb_21
N CD gb_21
CA CB gb_27
CA C gb_27
CB OG1 gb_18
CB CG2 gb_27
OG1 HG1 gb_1
CG2 CD gb_27
C O gb_5
C +N gb_10
[ angles ]
; ai aj ak gromos type
-C N CA ga_31
-C N CD ga_31
CA N CD ga_21
N CA CB ga_13
N CA C ga_13
CB CA C ga_13
CA CB OG1 ga_13
CA CB CG2 ga_13
OG1 CB CG2 ga_13
CB OG1 HG1 ga_12
CB CG2 CD ga_13
N CD CG2 ga_13
CA C O ga_30
CA C +N ga_19
O C +N ga_33
[ impropers ]
; ai aj ak al gromos type
N -C CA CD gi_1
CA N C CB gi_2
CB CA CG2 OG1 gi_2
C CA +N O gi_1
[ dihedrals ]
; ai aj ak al gromos type
-C CA CD gi_1
CA N C CB gi_2
CB CA CG2 OG1 gi_2
C CA +N O gi_1
; 4-hydroxyproline (S)
[ HY2 ]
[ atoms ]
N N 0.00000 0
CA CH1 0.00000 1
CB CH2R 0.00000 1
CG CH1 0.26600 2 ; from the hydroxyl group of THR
OD1 OA -0.67400 2 ; from the hydroxyl group of THR
HD1 H 0.40800 2 ; from the hydroxyl group of THR
CD2 CH2R 0.00000 3
C C 0.450 4
O O -0.450 4
[ bonds ]
N CA gb_21
N CD2 gb_21
CA CB gb_27
CA C gb_27
CB CG gb_27
CG OD1 gb_18
CG CD2 gb_27
OD1 HD1 gb_1
C O gb_5
C +N gb_10
[ angles ]
; ai aj ak gromos type
-C N CA ga_31
-C N CD2 ga_31
CA N CD2 ga_21
N CA CB ga_13
N CA C ga_13
CB CA C ga_13
CA CB OG1 ga_13
CA CB CG2 ga_13
OG1 CB CG2 ga_13
CB OG1 HG1 ga_12
CB CG2 OD1 ga_13
CB CG2 CD2 ga_13
OD1 CG2 CD2 ga_13
CG2 OD1 HD1 ga_12
N CD2 CG2 ga_13
CA C O ga_30
CA C +N ga_19
O C +N ga_33
[ impropers ]
; ai aj ak al gromos type
N -C CA CD2 gi_1
CA N C CB gi_2
CB CA CG2 OG1 gi_2
CG2 CB CD2 OD1 gi_2
C CA +N O gi_1
[ dihedrals ]
; ai aj ak al gromos type
-C CA CD2 gi_1
CA N C CB gi_2
CB CA CG2 OG1 gi_2
CG2 CB CD2 OD1 gi_2
C CA +N O gi_1
; 5-hydroxylysine (O,R)
[ KH5 ]
[ atoms ]
N N -0.31000 0
H H 0.31000 0
CA CH1 0.00000 1
CB CH2 0.00000 1
CG CH2 0.00000 2
CD CH1 0.26600 3 ; from the hydroxyl group of THR
OE1 OA -0.67400 3 ; from the hydroxyl group of THR
HE1 H 0.40800 3 ; from the hydroxyl group of THR
CE2 CH2 -0.24000 4
[ dihedrals ]
; ai aj ak al gromos type
-C CA CD2 gi_1
CA N C CB gi_2
CB CA CG2 OG1 gi_2
CG2 CB CD2 OD1 gi_2
C CA +N O gi_1
; 3,4-dihydroxyproline
[ PHH ]
[ atoms ]
N N 0.00000 0
CA CH1 0.00000 1
CB CH1 0.26600 2 ; from the hydroxyl group of THR
OG1 OA -0.67400 2 ; from the hydroxyl group of THR
HG1 H 0.40800 2 ; from the hydroxyl group of THR
CG2 CH1 0.26600 3 ; from the hydroxyl group of THR
OD1 OA -0.67400 3 ; from the hydroxyl group of THR
HD1 H 0.40800 3 ; from the hydroxyl group of THR
CD2 CH2R 0.00000 4
C C 0.450 5
O O -0.450 5
[ bonds ]
N CA gb_21
N CD2 gb_21
CA CB gb_27
CA C gb_27
CB OG1 gb_18
CB CG2 gb_27
OG1 HG1 gb_1
CG2 OD1 gb_18
CG2 CD2 gb_27
OD1 HD1 gb_1
C O gb_5
C +N gb_10
[ angles ]
; ai aj ak gromos type
-C N CA ga_31
-C N CD2 ga_31
CA N CD2 ga_21
N CA CB ga_13
N CA C ga_13
CB CA C ga_13
CA CB OG1 ga_13
CA CB CG2 ga_13
OG1 CB CG2 ga_13
CB OG1 HG1 ga_12
CB CG2 OD1 ga_13
CB CG2 CD2 ga_13
OD1 CG2 CD2 ga_13
CG2 OD1 HD1 ga_12
N CD2 CG2 ga_13
CA C O ga_30
CA C +N ga_19
O C +N ga_33
[ impropers ]
; ai aj ak al gromos type
N -C CA CD2 gi_1
CA N C CB gi_2
CB CA CG2 OG1 gi_2
CG2 CB CD2 OD1 gi_2
C CA +N O gi_1
[ dihedrals ]
; ai aj ak al gromos type
-C CA CD2 gi_1
CA N C CB gi_2
CB CA CG2 OG1 gi_2
CG2 CB CD2 OD1 gi_2
C CA +N O gi_1

```

```

NZ NT -0.64000 4
HZ1 H 0.44000 4
HZ2 H 0.44000 4
C C 0.450 5
O O -0.450 5
[ bonds ]
N H gb_2
N CA gb_21
CA CB gb_27
CA C gb_27
CB CG gb_27
CG CD gb_27
CD OE1 gb_18
CD CE2 gb_27
OE1 HE1 gb_1
CE2 NZ gb_21
NZ HZ1 gb_2
NZ HZ2 gb_2
C O gb_5
C +N gb_10
[ angles ]
; ai aj ak gromos type
-C N H ga_32
-C N CA ga_31
H N CA ga_18
N CA CB ga_13
N CA C ga_13
CB CA C ga_13
CA CB CG ga_15
CB CG CD ga_15
CG CD OE1 ga_13
CG CD CE2 ga_13
OE1 CD CE2 ga_13
CD OE1 HE1 ga_12
CD CE2 NZ ga_15
CE2 NZ HZ1 ga_11
CE2 NZ HZ2 ga_11
HZ1 NZ HZ2 ga_10
CA C O ga_30
CA C +N ga_19
O C +N ga_33
[ impropers ]
; ai aj ak al gromos type
N -C CA H gi_1
CA N C CB gi_2
CD CE2 OE1 CG gi_2
C CA +N O gi_1
[ dihedrals ]
; ai aj ak al gromos type
-CA -C N CA gd_14
-C N CA C gd_44
-C N CA C gd_43
N CA CB CG gd_34
N CA C +N gd_45
N CA C +N gd_42
CA CB CG CD gd_34
CB CG CD CE2 gd_34
CG CD OE1 HE1 gd_23
CG CD CE2 NZ gd_34
CD CE2 NZ HZ1 gd_29
; 5-hydroxylysine (0,5)
[ K5H ]
[ atoms ]
N N -0.31000 0
H H 0.31000 0
CA CH1 0.00000 1
CB CH2 0.00000 1
CG CH2 0.00000 2
CD CH1 0.26600 3 ; from the hydroxyl group of THR
OE1 OA -0.67400 3 ; from the hydroxyl group of THR
HE1 H 0.40800 3 ; from the hydroxyl group of THR
CE2 CH2 -0.24000 4
NZ NT -0.64000 4
HZ1 H 0.44000 4
HZ2 H 0.44000 4
C C 0.450 5
O O -0.450 5
[ bonds ]
N H gb_2
N CA gb_21
CA CB gb_27
CA C gb_27
CB CG gb_27
CG CD gb_27
CD OE1 gb_18
CD CE2 gb_27
OE1 HE1 gb_1
CE2 NZ gb_21
NZ HZ1 gb_2
NZ HZ2 gb_2
NZ HZ3 gb_2
C O gb_5
C +N gb_10
[ angles ]
; ai aj ak gromos type
-C N H ga_32
-C N CA ga_31
H N CA ga_18
N CA CB ga_13
N CA C ga_13
CB CA C ga_13
CA CB CG ga_15
CB CG CD ga_15
CG CD OE1 ga_13
CG CD CE2 ga_13
OE1 CD CE2 ga_13
CD OE1 HE1 ga_12
CD CE2 NZ ga_15
CE2 NZ HZ1 ga_11
CE2 NZ HZ2 ga_11
CE2 NZ HZ3 ga_11
[ angles ]
; ai aj ak gromos type
-C N H ga_32
-C N CA ga_31
H N CA ga_18
N CA CB ga_13
N CA C ga_13
CB CA C ga_13
CA CB CG ga_15
CB CG CD ga_15
CG CD OE1 ga_13
CG CD CE2 ga_13
OE1 CD CE2 ga_13
CD OE1 HE1 ga_12
CD CE2 NZ ga_15
CE2 NZ HZ1 ga_11
CE2 NZ HZ2 ga_11
CE2 NZ HZ3 ga_11
[ impropers ]
; ai aj ak al gromos type
N -C CA H gi_1
CA N C CB gi_2
CD CE2 OE1 CG gi_2
C CA +N O gi_1
[ dihedrals ]
; ai aj ak al gromos type
-CA -C N CA gd_14
-C N CA C gd_44
-C N CA C gd_43
N CA CB CG gd_34
N CA C +N gd_45
N CA C +N gd_42
CA CB CG CD gd_34
CB CG CD CE2 gd_34
CG CD OE1 HE1 gd_23
CG CD CE2 NZ gd_34
CD CE2 NZ HZ1 gd_29
; 5-hydroxylysine (+1,R)
[ KPH ]
[ atoms ]
N N -0.31000 0
H H 0.31000 0
CA CH1 0.00000 1
CB CH2 0.00000 1
CG CH2 0.00000 2
CD CH1 0.26600 3 ; from the hydroxyl group of THR
OE1 OA -0.67400 3 ; from the hydroxyl group of THR
HE1 H 0.40800 3 ; from the hydroxyl group of THR
CE2 CH2 0.12700 4
NZ NL 0.12900 4
HZ1 H 0.24800 4
HZ2 H 0.24800 4
HZ3 H 0.24800 4
C C 0.450 5
O O -0.450 5
[ bonds ]
N H gb_2
N CA gb_21
CA CB gb_27
CA C gb_27
CB CG gb_27
CG CD gb_27
CD OE1 gb_18
CD CE2 gb_27
OE1 HE1 gb_1
CE2 NZ gb_21
NZ HZ1 gb_2
NZ HZ2 gb_2
NZ HZ3 gb_2
C O gb_5
C +N gb_10
[ angles ]
; ai aj ak gromos type
-C N H ga_32
-C N CA ga_31
H N CA ga_18
N CA CB ga_13
N CA C ga_13
CB CA C ga_13
CA CB CG ga_15
CB CG CD ga_15
CG CD OE1 ga_13
CG CD CE2 ga_13
OE1 CD CE2 ga_13
CD OE1 HE1 ga_12
CD CE2 NZ ga_15
CE2 NZ HZ1 ga_11
CE2 NZ HZ2 ga_11
CE2 NZ HZ3 ga_11

```

```

H21 NZ H22 ga_10
H21 NZ H23 ga_10
H22 NZ H23 ga_10
CA C O ga_30
CA C +N ga_19
O C +N ga_33
[ impropers ]
; ai aj ak al gromos type
N -C CA H gi_1
CA N C CB gi_2
CD CE2 OE1 CG gi_2
C CA +N O gi_1
[ dihedrals ]
; ai aj ak al gromos type
-CA -C N CA gd_14
-C N CA C gd_44
-C N CA C gd_43
N CA CB CG gd_34
N CA C +N gd_45
N CA C +N gd_42
CA CB CG CD gd_34
CB CG CD CE2 gd_34
CG CD OE1 HE1 gd_23
CG CD CE2 NZ gd_34
CD CE2 NZ HZ1 gd_29

; 5-hydroxylysine (+1,S)
[ KHP ]
[ atoms ]
N N -0.31000 0
H H 0.31000 0
CA CH1 0.00000 1
CB CH2 0.00000 1
CG CH2 0.00000 2
CD CH1 0.26600 3 ; from the hydroxyl group of THR
OE1 OA -0.67400 3 ; from the hydroxyl group of THR
HE1 H 0.40800 3 ; from the hydroxyl group of THR
CE2 CH2 0.12700 4
NZ NL 0.12900 4
H21 H 0.24800 4
H22 H 0.24800 4
H23 H 0.24800 4
C C 0.450 5
O O -0.450 5
[ bonds ]
N H gb_2
N CA gb_21
CA CB gb_27
CA C gb_27
CB CG gb_27
CG CD gb_27
CD OE1 gb_18
CD CE2 gb_27
OE1 HE1 gb_1
CE2 NZ gb_21
NZ HZ1 gb_2
NZ HZ2 gb_2
NZ HZ3 gb_2
C O gb_5
C +N gb_10
[ angles ]
; ai aj ak gromos type
-C N H ga_32
-C N CA ga_31
H N CA ga_18
N CA CB ga_13
N CA C ga_13
CB CA C ga_13
CA CB CG ga_15
CB CG CD ga_15
CG CD OE1 ga_13
CG CD CE2 ga_13
OE1 CD CE2 ga_13
CD OE1 HE1 ga_12
CD CE2 NZ ga_15
CE2 NZ HZ1 ga_11
CE2 NZ HZ2 ga_11
CE2 NZ HZ3 ga_11
H21 NZ H22 ga_10
H21 NZ H23 ga_10
H22 NZ H23 ga_10
CA C O ga_30
CA C +N ga_19
O C +N ga_33
[ impropers ]
; ai aj ak al gromos type
N -C CA H gi_1
CA N C CB gi_2
CD OE1 CE2 CG gi_2
C CA +N O gi_1
[ dihedrals ]
; ai aj ak al gromos type
-CA -C N CA gd_14
-C N CA C gd_44
-C N CA C gd_43
N CA CB CG gd_34
N CA C +N gd_45
N CA C +N gd_42
CA CB CG CD gd_34
CB CG CD CE2 gd_34
CG CD OE1 HE1 gd_23
CG CD CE2 NZ gd_34
CD CE2 NZ HZ1 gd_29

; 3,4-dihydroxyphenylalanine
[ HTY ]
[ atoms ]
N N -0.31000 0
H H 0.31000 0
CA CH1 0.00000 1
CB CH2 0.00000 1
CG C 0.00000 1
CD1 C -0.14000 2
HD1 HC 0.14000 2
CD2 C -0.14000 3
HD2 HC 0.14000 3
CE1 C 0.20300 4 ; from the hydroxyl group of TYR
OZ1 OA -0.61100 4 ; from the hydroxyl group of TYR
H21 H 0.40800 4 ; from the hydroxyl group of TYR
CE2 C -0.14000 5
HE2 HC 0.14000 5
CZ2 C 0.20300 6 ; from the hydroxyl group of TYR
OH OA -0.61100 6 ; from the hydroxyl group of TYR
HH H 0.40800 6 ; from the hydroxyl group of TYR
C C 0.450 7
O O -0.450 7
[ bonds ]
N H gb_2
N CA gb_21
CA CB gb_27
CA C gb_27
CB CG gb_27
CG CD1 gb_16
CG CD2 gb_16
CD1 HD1 gb_3
CD1 CE1 gb_16
CD2 HD2 gb_3
CD2 CE2 gb_16
CE1 OZ1 gb_13
CE1 CZ2 gb_16
OZ1 HZ1 gb_1
CE2 HE2 gb_3
CE2 CZ2 gb_16
CZ2 OH gb_13
OH HH gb_1
C O gb_5
C +N gb_10
[ exclusions ]
; ai aj
CB HD1
CB HD2
CB CE1
CB CE2
CG OZ1
CG HE2
CG CZ2
CD1 HD2
CD1 CE2
CD1 OH
HD1 CD2
HD1 OZ1
HD1 CZ2
CD2 CE1
CD2 OH
HD2 HE2
HD2 CZ2
CE1 HE2
OZ1 CE2
OZ1 OH
HE2 OH
HH OZ1
HH HZ1
HZ1 OH
[ angles ]
; ai aj ak gromos type
-C N H ga_32
-C N CA ga_31
H N CA ga_18
N CA CB ga_13
N CA C ga_13
CB CA C ga_13
CA CB CG ga_15
CB CG CD ga_15
CG CD OE1 ga_13
CG CD CE2 ga_13
OE1 CD CE2 ga_13
CD OE1 HE1 ga_12
CD CE2 NZ ga_15
CE2 NZ HZ1 ga_11
CE2 NZ HZ2 ga_11
CE2 NZ HZ3 ga_11
H21 NZ H22 ga_10
H21 NZ H23 ga_10
H22 NZ H23 ga_10
CA C O ga_30
CA C +N ga_19
O C +N ga_33
[ impropers ]
; ai aj ak al gromos type
N -C CA H gi_1
CA N C CB gi_2
CD OE1 CE2 CG gi_2
C CA +N O gi_1
[ dihedrals ]
; ai aj ak al gromos type
-CA -C N CA gd_14

```



```

CG CD1 CE1 ga_27
HD1 CD1 CE1 ga_25
CG CD2 HD2 ga_25
CG CD2 CE2 ga_27
HD2 CD2 CE2 ga_25
CD1 CE1 OZ1 ga_27
CD1 CE1 CZ2 ga_27
OZ1 CE1 CZ2 ga_27
CE1 OZ1 HZ1 ga_12
CD2 CE2 HE2 ga_25
CD2 CE2 CZ2 ga_27
HE2 CE2 CZ2 ga_25
CE1 CZ2 CE2 ga_27
CE1 CZ2 OH ga_27
CE2 CZ2 OH ga_27
CZ2 OH HH ga_12
CA C O ga_30
CA C +N ga_19
O C +N ga_33
[impropers]
; ai aj ak al gromos type
N -C CA H gi_1
CA N C CB gi_2
CG CD1 CD2 CB gi_1
CG CD1 CE1 CZ2 gi_1
CG CD2 CE2 CZ2 gi_1
CD1 CG CD2 CE2 gi_1
CD1 CG CE1 HD1 gi_1
CD1 CE1 CZ2 CE2 gi_1
CD2 CG CD1 CE1 gi_1
CD2 CG CE2 HD2 gi_1
CD2 CE2 CZ2 CE1 gi_1
CE1 CZ2 CD1 OZ1 gi_1
HE2 CD2 CZ2 CE2 gi_1
CZ2 CE1 CE2 OH gi_1
C CA +N O gi_1
[dihedrals]
; ai aj ak al gromos type
-C -C N CA gd_14
-C N CA C gd_44
-C N CA C gd_43
N CA CB CG gd_34
N CA C +N gd_45
N CA C +N gd_42
CA CB CG CD1 gd_40
CD1 CE1 OZ1 HZ1 gd_11
CE1 CZ2 OH HH gd_11

; 7-hydroxytryptophan
[W7H]
[atoms]
N N -0.31000 0
H H 0.31000 0
CA CH1 0.00000 1
CB CH2 0.00000 1
CG C -0.21000 2
CD1 C -0.14000 2
HD1 HC 0.14000 2
CD2 C 0.00000 2
NE1 NR -0.10000 2
HE1 H 0.31000 2
CE2 C 0.00000 2
CE3 C -0.14000 3
HE3 HC 0.14000 3
CZ2 C 0.20300 4 ; from the hydroxyl group of TYR
OH2 OA -0.61100 4 ; from the hydroxyl group of TYR
HH2 H 0.40800 4 ; from the hydroxyl group of TYR
CZ3 C -0.14000 5
HZ3 HC 0.14000 5
CH3 C -0.14000 6
HH3 HC 0.14000 6
C C 0.450 7
O O -0.450 7
[bonds]
N H gb_2
N CA gb_21
CA CB gb_27
CA C gb_27
CB CG gb_27
CG CD1 gb_10
CG CD2 gb_16
CD1 HD1 gb_3
CD1 NE1 gb_10
CD2 CE2 gb_16
CD2 CE3 gb_16
NE1 HE1 gb_2
NE1 CE2 gb_10
CE2 CZ2 gb_16
CE3 HE3 gb_3
CE3 CZ3 gb_16
CZ2 OH2 gb_13
OH2 HH2 gb_1
CZ2 CH3 gb_16

CZ3 HZ3 gb_3
CZ3 CH3 gb_16
CH3 HH3 gb_3
C O gb_5
C +N gb_10
[exclusions]
; ai aj
CB HD1
CB NE1
CB CE2
CB CE3
CG HE1
CG HE3
CG CZ2
CG CZ3
CD1 CE3
CD1 CZ2
HD1 CD2
HD1 HE1
HD1 CE2
CD2 HE1
CD2 OH2
CD2 HZ3
CD2 CH3
NE1 CE3
NE1 OH2
NE1 CH3
HE1 CZ2
CE2 HE3
CE2 CZ3
CE2 HH3
CE3 CZ2
CE3 HH3
HE3 HZ3
HE3 CH3
CZ2 HZ3
OH2 CZ3
OH2 HH3
HZ3 HH3
[angles]
; ai aj ak gromos type
-C N H ga_32
-C N CA ga_31
H N CA ga_18
N CA CB ga_13
N CA C ga_13
CB CA C ga_13
CA CB CG ga_15
CB CG CD1 ga_37
CB CG CD2 ga_37
CD1 CG CD2 ga_7
CG CD1 HD1 ga_36
CG CD1 NE1 ga_7
HD1 CD1 NE1 ga_36
CG CD2 CE2 ga_7
CG CD2 CE3 ga_39
CE2 CD2 CE3 ga_27
CD1 NE1 HE1 ga_36
CD1 NE1 CE2 ga_7
HE1 NE1 CE2 ga_36
CD2 CE2 NE1 ga_7
CD2 CE2 CZ2 ga_27
NE1 CE2 CZ2 ga_39
CD2 CE3 HE3 ga_25
CD2 CE3 CZ3 ga_27
HE3 CE3 CZ3 ga_25
CE2 CZ2 OH2 ga_27
CE2 CZ2 CH3 ga_27
OH2 CZ2 CH3 ga_27
HH2 OH2 CZ2 ga_12
CE3 CZ3 HZ3 ga_25
CE3 CZ3 CH3 ga_27
HZ3 CZ3 CH3 ga_25
CZ2 CH3 CZ3 ga_27
CZ2 CH3 HH3 ga_25
CZ3 CH3 HH3 ga_25
CA C O ga_30
CA C +N ga_19
O C +N ga_33
[impropers]
; ai aj ak al gromos type
N -C CA H gi_1
CA N C CB gi_2
CG CD1 CD2 CB gi_1
CG CD1 NE1 CE2 gi_1
CG CD2 CE2 NE1 gi_1
CD1 CG CD2 CE2 gi_1
CD1 CG NE1 HD1 gi_1
CD1 NE1 CE2 CD2 gi_1
CD2 CG CD1 NE1 gi_1
CD2 CE2 CE3 CG gi_1
CD2 CE2 CZ2 CH3 gi_1
CD2 CE3 CZ3 CH3 gi_1

```

```

NE1 CD1 CE2 HE1 gi_1
CE2 CD2 CE3 CZ3 gi_1
CE2 CD2 CZ2 NE1 gi_1
CE2 CZ2 CH3 CZ3 gi_1
CE3 CD2 CE2 CZ2 gi_1
CE3 CD2 CZ3 HE3 gi_1
CE3 CZ3 CH3 CZ2 gi_1
CZ2 CE2 CH3 OH2 gi_1
CZ3 CE3 CH3 HZ3 gi_1
CH3 CZ2 CZ3 HH3 gi_1
C CA +N O gi_1
[ dihedrals ]
; ai aj ak al gromos type
-CA -C N CA gd_14
-C N CA C gd_44
-C N CA C gd_43
N CA CB CG gd_34
N CA C +N gd_45
N CA C +N gd_42
CA CB CG CD2 gd_40
CE2 CZ2 OH2 HH2 gd_11

; 3-hydroxyaspartate (-1,R)
[ DH3 ]
[ atoms ]
N N -0.31000 0
H H 0.31000 0
CA CH1 0.00000 1
CB CH1 0.26600 2; from the hydroxyl group of THR
OG1 OA -0.67400 2; from the hydroxyl group of THR
HG1 H 0.40800 2; from the hydroxyl group of THR
CG2 C 0.27000 3
OD1 OM -0.63500 3
OD2 OM -0.63500 3
C C 0.450 4
O O -0.450 4
[ bonds ]
N H gb_2
N CA gb_21
CA CB gb_27
CA C gb_27
CB OG1 gb_18
CB CG2 gb_27
OG1 HG1 gb_1
CG2 OD1 gb_6
CG2 OD2 gb_6
C O gb_5
C +N gb_10
[ angles ]
; ai aj ak gromos type
-C N H ga_32
-C N CA ga_31
H N CA ga_18
N CA CB ga_13
N CA C ga_13
CB CA C ga_13
CA CB OG1 ga_13
CA CB CG2 ga_13
OG1 CB CG2 ga_13
CB OG1 HG1 ga_12
CB CG2 OD1 ga_22
CB CG2 OD2 ga_22
OD1 CG2 OD2 ga_38
CA C O ga_30
CA C +N ga_19
O C +N ga_33
[ impropers ]
; ai aj ak al gromos type
N -C CA H gi_1
CA N C CB gi_2
CB OG1 CG2 CA gi_2
CG2 OD1 OD2 CB gi_1
C CA +N O gi_1
[ dihedrals ]
; ai aj ak al gromos type
-CA -C N CA gd_14
-C N CA C gd_44
-C N CA C gd_43
N CA CB CG2 gd_34
N CA C +N gd_45
N CA C +N gd_42
CA CB OG1 HG1 gd_23
CA CB CG2 OD1 gd_40

; 3-hydroxyaspartate (0,R)
[ DN3 ]
[ atoms ]
N N -0.31000 0
H H 0.31000 0
CA CH1 0.00000 1
CB CH1 0.26600 2; from the hydroxyl group of THR
OG1 OA -0.67400 2; from the hydroxyl group of THR
HG1 H 0.40800 2; from the hydroxyl group of THR
CG2 C 0.33000 3
OD1 O -0.45000 3
OD2 OA -0.28800 3
HD2 H 0.40800 3
C C 0.450 4
O O -0.450 4
[ bonds ]
N H gb_2
N CA gb_21
CA CB gb_27
CA C gb_27
CB OG1 gb_18
CB CG2 gb_27
OG1 HG1 gb_1
CG2 OD1 gb_5
CG2 OD2 gb_13
OD2 HD2 gb_1
C O gb_5
C +N gb_10
[ angles ]
; ai aj ak gromos type
-C N H ga_32
-C N CA ga_31
H N CA ga_18
N CA CB ga_13
N CA C ga_13
CB CA C ga_13
CA CB OG1 ga_13
CA CB CG2 ga_13
OG1 CB CG2 ga_13
CB OG1 HG1 ga_12

```

```

CB CG2 OD1 ga_30
CB CG2 OD2 ga_19
OD1 CG2 OD2 ga_33
CG2 OD2 HD2 ga_12
CA C O ga_30
CA C +N ga_19
O C +N ga_33
[impropers]
; ai aj ak al gromos type
N -C CA H gi_1
CA N C CB gi_2
CB CG2 OG1 CA gi_2
CG2 OD1 OD2 CB gi_1
C CA +N O gi_1
[dihedrals]
; ai aj ak al gromos type
-C -C N CA gd_14
-C N CA C gd_44
-C N CA C gd_43
N CA CB CG2 gd_34
N CA C +N gd_45
N CA C +N gd_42
CA CB OG1 HG1 gd_23
CA CB CG2 OD2 gd_40
CB CG2 OD2 HD2 gd_12

```

```
; 3-hydroxyaspartate (0,S)
```

```
[D3N]
```

```
[atoms]
```

```

N N -0.31000 0
H H 0.31000 0
CA CH1 0.00000 1
CB CH1 0.26600 2; from the hydroxyl group of THR
OG1 OA -0.67400 2; from the hydroxyl group of THR
HG1 H 0.40800 2; from the hydroxyl group of THR
CG2 C 0.33000 3
OD1 O -0.45000 3
OD2 OA -0.28800 3
HD2 H 0.40800 3
C C 0.450 4
O O -0.450 4

```

```
[bonds]
```

```

N H gb_2
N CA gb_21
CA CB gb_27
CA C gb_27
CB OG1 gb_18
CB CG2 gb_27
OG1 HG1 gb_1
CG2 OD1 gb_5
CG2 OD2 gb_13
OD2 HD2 gb_1
C O gb_5
C +N gb_10

```

```
[angles]
```

```
; ai aj ak gromos type
```

```

-C N H ga_32
-C N CA ga_31
H N CA ga_18
N CA CB ga_13
N CA C ga_13
CB CA C ga_13
CA CB OG1 ga_13
CA CB CG2 ga_13
OG1 CB CG2 ga_13
CB OG1 HG1 ga_12
CB CG2 OD1 ga_30
CB CG2 OD2 ga_19
OD1 CG2 OD2 ga_33
CG2 OD2 HD2 ga_12
CA C O ga_30
CA C +N ga_19
O C +N ga_33

```

```
[impropers]
```

```
; ai aj ak al gromos type
```

```

N -C CA H gi_1
CA N C CB gi_2
CB OG1 CG2 CA gi_2
CG2 OD1 OD2 CB gi_1
C CA +N O gi_1
[dihedrals]
; ai aj ak al gromos type
-C -C N CA gd_14
-C N CA C gd_44
-C N CA C gd_43
N CA CB CG2 gd_34
N CA C +N gd_45
N CA C +N gd_42
CA CB OG1 HG1 gd_23
CA CB CG2 OD2 gd_40
CB CG2 OD2 HD2 gd_12

```

```
; 3-hydroxyasparagine (R)
```

```
[N3H]
```

```
[atoms]
```

```

N N -0.31000 0
H H 0.31000 0
CA CH1 0.00000 1
CB CH1 0.26600 2; from the hydroxyl group of THR
OG1 OA -0.67400 2; from the hydroxyl group of THR
HG1 H 0.40800 2; from the hydroxyl group of THR
CG2 C 0.29000 3
OD1 O -0.45000 3
ND2 NT -0.72000 3
HD21 H 0.44000 3
HD22 H 0.44000 3
C C 0.450 4
O O -0.450 4

```

```
[bonds]
```

```

N H gb_2
N CA gb_21
CA CB gb_27
CA C gb_27
CB OG1 gb_18
CB CG2 gb_27
OG1 HG1 gb_1
CG2 OD1 gb_5
CG2 ND2 gb_9
ND2 HD21 gb_2
ND2 HD22 gb_2
C O gb_5
C +N gb_10

```

```
[angles]
```

```
; ai aj ak gromos type
```

```

-C N H ga_32
-C N CA ga_31
H N CA ga_18
N CA CB ga_13
N CA C ga_13
CB CA C ga_13
CA CB OG1 ga_13
CA CB CG2 ga_13
OG1 CB CG2 ga_13
CB OG1 HG1 ga_12
CB CG2 OD1 ga_30
CB CG2 ND2 ga_19
OD1 CG2 ND2 ga_33
CG2 ND2 HD21 ga_23
CG2 ND2 HD22 ga_23
HD21 ND2 HD22 ga_24
CA C O ga_30
CA C +N ga_19
O C +N ga_33

```

```
[impropers]
```

```
; ai aj ak al gromos type
```

```

N -C CA H gi_1
CA N C CB gi_2
CB CG2 OG1 CA gi_2
CG2 OD1 ND2 CB gi_1
ND2 HD21 HD22 CG2 gi_1
C CA +N O gi_1

```

```
[dihedrals]
```

```
; ai aj ak al gromos type
```

```

-C -C N CA gd_14
-C N CA C gd_44
-C N CA C gd_43
N CA CB CG2 gd_34
N CA C +N gd_45
N CA C +N gd_42
CA CB OG1 HG1 gd_23
CA CB CG2 ND2 gd_40
CB CG2 ND2 HD21 gd_14

```

```
; 3-hydroxyasparagine (S)
```

```
[NH3]
```

```
[atoms]
```

```

N N -0.31000 0
H H 0.31000 0
CA CH1 0.00000 1
CB CH1 0.26600 2; from the hydroxyl group of THR
OG1 OA -0.67400 2; from the hydroxyl group of THR
HG1 H 0.40800 2; from the hydroxyl group of THR
CG2 C 0.29000 3
OD1 O -0.45000 3
ND2 NT -0.72000 3
HD21 H 0.44000 3
HD22 H 0.44000 3
C C 0.450 4
O O -0.450 4

```

```
[bonds]
```

```

N H gb_2
N CA gb_21
CA CB gb_27
CA C gb_27
CB OG1 gb_18

```

```

CB CG2 gb_27
OG1 HG1 gb_1
CG2 OD1 gb_5
CG2 ND2 gb_9
ND2 HD21 gb_2
ND2 HD22 gb_2
C O gb_5
C +N gb_10
[angles]
; ai aj ak gromos type
-C N H ga_32
-C N CA ga_31
H N CA ga_18
N CA CB ga_13
N CA C ga_13
CB CA C ga_13
CA CB OG1 ga_13
CA CB CG2 ga_13
OG1 CB CG2 ga_13
CB OG1 HG1 ga_12
CB CG2 OD1 ga_30
CB CG2 ND2 ga_19
OD1 CG2 ND2 ga_33
CG2 ND2 HD21 ga_23
CG2 ND2 HD22 ga_23
HD21 ND2 HD22 ga_24
CA C O ga_30
CA C +N ga_19
O C +N ga_33
[impropers]
; ai aj ak al gromos type
N -C CA H gi_1
CA N C CB gi_2
CB OG1 CG2 CA gi_2
CG2 OD1 ND2 CB gi_1
ND2 HD21 HD22 CG2 gi_1
C CA +N O gi_1
[dihedrals]
; ai aj ak al gromos type
-CA -C N CA gd_14
-C N CA C gd_44
-C N CA C gd_43
N CA CB CG2 gd_34
N CA C +N gd_45
N CA C +N gd_42
CA CB OG1 HG1 gd_23
CA CB CG2 ND2 gd_40
CB CG2 ND2 HD21 gd_14
;4-carboxylglutamate (-2)
[ECA]
[atoms]
N N -0.31000 0
H H 0.31000 0
CA CH1 0.00000 1
CB CH2 0.00000 1
CG CH1 0.00000 1
CD1 C 0.27000 2
OE1 OM -0.63500 2
OE2 OM -0.63500 2
CD2 C 0.27000 3; from GLU
OE3 OM -0.63500 3; from GLU
OE4 OM -0.63500 3; from GLU
C C 0.450 4
O O -0.450 4
[bonds]
N H gb_2
N CA gb_21
CA CB gb_27
CA C gb_27
CB CG gb_27
CG CD1 gb_27
CD1 OE1 gb_6
CD1 OE2 gb_6
CG CD2 gb_27
CD2 OE3 gb_6
CD2 OE4 gb_6
C O gb_5
C +N gb_10
[angles]
; ai aj ak gromos type
-C N H ga_32
-C N CA ga_31
H N CA ga_18
N CA CB ga_13
N CA C ga_13
CB CA C ga_13
CA CB CG ga_15
CB CG CD1 ga_13
CB CG CD2 ga_13
CD1 CG CD2 ga_13
CG CD1 OE1 ga_30
CG CD1 OE2 ga_19
OE1 CD1 OE2 ga_33
CD1 OE2 HE2 ga_12
CG CD2 OE3 ga_22
CG CD2 OE4 ga_22
OE3 CD2 OE4 ga_38
CA C O ga_30
CA C +N ga_19
O C +N ga_33
[impropers]
; ai aj ak al gromos type
N -C CA H gi_1
CA N C CB gi_2
CG CD1 CD2 CB gi_2
CD1 OE1 OE2 CG gi_1
CD2 OE3 OE4 CG gi_1
C CA +N O gi_1
[dihedrals]
; ai aj ak al gromos type
-CA -C N CA gd_14
-C N CA C gd_44
-C N CA C gd_43
N CA CB CG gd_34
N CA C +N gd_45
N CA C +N gd_42
CA CB CG CD1 gd_34
CB CG CD1 OE2 gd_40
CB CG CD2 OE4 gd_40
;4-carboxylglutamate (-1)
[ECN]
[atoms]
N N -0.31000 0
H H 0.31000 0
CA CH1 0.00000 1
CB CH2 0.00000 1
CG CH1 0.00000 1
CD1 C 0.33000 2; from GLUH
OE1 O -0.45000 2; from GLUH
OE2 OA -0.28800 2; from GLUH
HE2 H 0.40800 2; from GLUH
CD2 C 0.27000 3
OE3 OM -0.63500 3
OE4 OM -0.63500 3
C C 0.450 4
O O -0.450 4
[bonds]
N H gb_2
N CA gb_21
CA CB gb_27
CA C gb_27
CB CG gb_27
CG CD1 gb_27
CD1 OE1 gb_5
CD1 OE2 gb_13
OE2 HE2 gb_1
CG CD2 gb_27
CD2 OE3 gb_6
CD2 OE4 gb_6
C O gb_5
C +N gb_10
[angles]
; ai aj ak gromos type
-C N H ga_32
-C N CA ga_31
H N CA ga_18
N CA CB ga_13
N CA C ga_13
CB CA C ga_13
CA CB CG ga_15
CB CG CD1 ga_13
CB CG CD2 ga_13
CD1 CG CD2 ga_13
CG CD1 OE1 ga_30
CG CD1 OE2 ga_19
OE1 CD1 OE2 ga_33
CD1 OE2 HE2 ga_12
CG CD2 OE3 ga_22
CG CD2 OE4 ga_22
OE3 CD2 OE4 ga_38
CA C O ga_30
CA C +N ga_19
O C +N ga_33
[impropers]
; ai aj ak al gromos type
N -C CA H gi_1
CA N C CB gi_2
CG CD1 CD2 CB gi_2
CD1 OE1 OE2 CG gi_1
CD2 OE3 OE4 CG gi_1
C CA +N O gi_1
[dihedrals]
; ai aj ak al gromos type
-CA -C N CA gd_14
-C N CA C gd_44

```

```

-C N CA C gd_43
N CA CB CG gd_34
N CA C +N gd_45
N CA C +N gd_42
CA CB CG CD1 gd_34
CB CG CD1 OE2 gd_40
CG CD1 OE2 HE2 gd_12
CB CG CD2 OE4 gd_40

; sulfotyrosine
[YSU]
[atoms]
N N -0.31000 0
H H 0.31000 0
CA CH1 0.00000 1
CB CH2 0.00000 1
CG C 0.00000 1
CD1 C -0.14000 2
HD1 HC 0.14000 2
CD2 C -0.14000 3
HD2 HC 0.14000 3
CE1 C -0.14000 4
HE1 HC 0.14000 4
CE2 C -0.14000 5
HE2 HC 0.14000 5
CZ C 0.15000 6; from the carbon atom attached to the phosphate group of
nucleotides (e.g., ATP)
OH OA -0.36000 6; from the phosphate group of nucleotides (e.g., ATP)
ST S 1.11500 6; to add up to -1 net charge
O11 OM -0.63500 6; from the phosphate group of nucleotides (e.g., ATP)
O12 OM -0.63500 6; from the phosphate group of nucleotides (e.g., ATP)
O13 OM -0.63500 6; from the phosphate group of nucleotides (e.g., ATP)
C C 0.450 7
O O -0.450 7
[bonds]
N H gb_2
N CA gb_21
CA CB gb_27
CA C gb_27
CB CG gb_27
CG CD1 gb_16
CG CD2 gb_16
CD1 HD1 gb_3
CD1 CE1 gb_16
CD2 HD2 gb_3
CD2 CE2 gb_16
CE1 HE1 gb_3
CE1 CZ gb_16
CE2 HE2 gb_3
CE2 CZ gb_16
CZ OH gb_13
OH ST gb_25
ST OI1 gb_25
ST OI2 gb_25
ST OI3 gb_25
C O gb_5
C +N gb_10
[exclusions]
; ai aj
CB HD1
CB HD2
CB CE1
CB CE2
CG HE1
CG HE2
CG CZ
CD1 HD2
CD1 CE2
CD1 OH
HD1 CD2
HD1 HE1
HD1 CZ
CD2 CE1
CD2 OH
HD2 HE2
HD2 CZ
CE1 HE2
HE1 CE2
HE1 OH
HE2 OH
[angles]
; ai aj ak gromos type
-C N H ga_32
-C N CA ga_31
H N CA ga_18
N CA CB ga_13
N CA C ga_13
CB CA C ga_13
CA CB CG ga_15
CB CG CD1 ga_27
CB CG CD2 ga_27
CD1 CG CD2 ga_27
CG CD1 HD1 ga_25
CG CD1 CE1 ga_27
HD1 CD1 CE1 ga_25
CG CD2 HD2 ga_25
CG CD2 CE2 ga_27
HD2 CD2 CE2 ga_25
CD1 CE1 HE1 ga_25
CD1 CE1 CZ ga_27
HE1 CE1 CZ ga_25
CD2 CE2 HE2 ga_25
CD2 CE2 CZ ga_27
HE2 CE2 CZ ga_25
CE1 CZ CE2 ga_27
CE1 CZ OH ga_27
CE2 CZ OH ga_27
CZ OH ST ga_12
OH ST OI1 ga_13
OH ST OI2 ga_13
OH ST OI3 ga_13
OI1 ST OI2 ga_13
OI1 ST OI3 ga_13
OI2 ST OI3 ga_13
CA C O ga_30
CA C +N ga_19
O C +N ga_33
[impropers]
; ai aj ak al gromos type
N -C CA H gi_1
CA N C CB gi_2
CG CD1 CD2 CB gi_1
CG CD1 CE1 CZ gi_1
CG CD2 CE2 CZ gi_1
CD1 CG CD2 CE2 gi_1
CD1 CG CE1 HD1 gi_1
CD1 CE1 CZ CE2 gi_1
CD2 CG CD1 CE1 gi_1
CD2 CG CE2 HD2 gi_1
CD2 CE2 CZ CE1 gi_1
HE1 CD1 CZ CE1 gi_1
HE2 CD2 CZ CE2 gi_1
CZ CE1 CE2 OH gi_1
C CA +N O gi_1
[dihedrals]
; ai aj ak al gromos type
-CA -C N CA gd_14
-C N CA C gd_44
-C N CA C gd_43
N CA CB CG gd_34
N CA C +N gd_45
N CA C +N gd_42
CA CB CG CD1 gd_40
CE1 CZ OH ST gd_11
CZ OH ST OI1 gd_40

; dehydroalanine
[SDH]
[atoms]
N N -0.31000 0
H H 0.31000 0
CA CH0 0.00000 1; from aliphatic carbon atoms
CB CH2 0.00000 1; from aliphatic carbon atoms
C C 0.450 2
O O -0.450 2
[bonds]
N H gb_2
N CA gb_21
CA CB gb_10 ; a shorter bond type to mimic double bond properties
CA C gb_27
C O gb_5
C +N gb_10
[angles]
; ai aj ak gromos type
-C N H ga_32
-C N CA ga_31
H N CA ga_18
N CA CB ga_27
N CA C ga_27
CB CA C ga_27
CA C O ga_30
CA C +N ga_19
O C +N ga_33
[impropers]
; ai aj ak al gromos type
N -C CA H gi_1
CA N C CB gi_1
C CA +N O gi_1
[dihedrals]
; ai aj ak al gromos type
-CA -C N CA gd_14
-C N CA C gd_44
-C N CA C gd_43
N CA C +N gd_45
N CA C +N gd_42

```

```

; 2,3-didehydrobutyrine
[TDH]
[atoms]
N N -0.31000 0
H H 0.31000 0
CA CH0 0.00000 1; from aliphatic carbon atoms
CB CH1 0.00000 1; from aliphatic carbon atoms
CG CH3 0.00000 2
C C 0.450 3
O O -0.450 3
[bonds]
N H gb_2
N CA gb_21
CA CB gb_10 ; a shorter bond type to mimic double bond properties
CA C gb_27
CB CG gb_27
C O gb_5
C +N gb_10
[angles]
; ai aj ak gromos type
-C N H ga_32
-C N CA ga_31
H N CA ga_18
N CA CB ga_27
N CA C ga_27
CB CA C ga_27
CA CB CG ga_27
CA C O ga_30
CA C +N ga_19
O C +N ga_33
[impropers]
; ai aj ak al gromos type
N -C CA H gi_1
CA N C CB gi_1
C CA +N O gi_1
[dihedrals]
; ai aj ak al gromos type
-CA -C N CA gd_14
-C N CA C gd_44
-C N CA C gd_43
N CA CB CG gd_14
N CA C +N gd_45
N CA C +N gd_42

; 6-bromotryptophan
[WBR]
[atoms]
N N -0.31000 0
H H 0.31000 0
CA CH1 0.00000 1
CB CH2 0.00000 1
CG C -0.21000 2
CD1 C -0.14000 2
HD1 HC 0.14000 2
CD2 C 0.00000 2
NE1 NR -0.10000 2
HE1 H 0.31000 2
CE2 C 0.00000 2
CE3 C -0.14000 3
HE3 HC 0.14000 3
CZ2 C -0.14000 4
HZ2 HC 0.14000 4
CZ3 C -0.14000 5
HZ3 HC 0.14000 5
CH2 C 0.05500 6; from 8-bromo-guanosine reported by Hritz and
Oostenbrink. DOI:10.1021/jp902968m
BRT BR -0.05500 6; from 8-bromo-guanosine reported by Hritz and
Oostenbrink. DOI:10.1021/jp902968m
C C 0.450 7
O O -0.450 7
[bonds]
N H gb_2
N CA gb_21
CA CB gb_27
CA C gb_27
CB CG gb_27
CG CD1 gb_10
CG CD2 gb_16
CD1 HD1 gb_3
CD1 NE1 gb_10
CD2 CE2 gb_16
CD2 CE3 gb_16
NE1 HE1 gb_2
NE1 CE2 gb_10
CE2 CZ2 gb_16
CE3 HE3 gb_3
CE3 CZ3 gb_16
CZ2 HZ2 gb_3
CZ2 CH2 gb_16
CZ3 HZ3 gb_3
CZ3 CH2 gb_16
CH2 BRT gb_42

C O gb_5
C +N gb_10
[exclusions]
; ai aj
CB HD1
CB NE1
CB CE2
CB CE3
CG HE1
CG HE3
CG CZ2
CG CZ3
CD1 CE3
CD1 CZ2
HD1 CD2
HD1 HE1
HD1 CE2
CD2 HE1
CD2 HZ2
CD2 HZ3
CD2 CH2
NE1 CE3
NE1 HZ2
NE1 CH2
HE1 CZ2
CE2 HE3
CE2 CZ3
CE2 BRT
CE3 CZ2
CE3 BRT
HE3 HZ3
HE3 CH2
CZ2 HZ3
HZ2 CZ3
HZ2 BRT
HZ3 BRT
[angles]
; ai aj ak gromos type
-C N H ga_32
-C N CA ga_31
H N CA ga_18
N CA CB ga_13
N CA C ga_13
CB CA C ga_13
CA CB CG ga_15
CB CG CD1 ga_37
CB CG CD2 ga_37
CD1 CG CD2 ga_7
CG CD1 HD1 ga_36
CG CD1 NE1 ga_7
HD1 CD1 NE1 ga_36
CG CD2 CE2 ga_7
CG CD2 CE3 ga_39
CE2 CD2 CE3 ga_27
CD1 NE1 HE1 ga_36
CD1 NE1 CE2 ga_7
HE1 NE1 CE2 ga_36
CD2 CE2 NE1 ga_7
CD2 CE2 CZ2 ga_27
NE1 CE2 CZ2 ga_39
CD2 CE3 HE3 ga_25
CD2 CE3 CZ3 ga_27
HE3 CE3 CZ3 ga_25
CE2 CZ2 HZ2 ga_25
CE2 CZ2 CH2 ga_27
HZ2 CZ2 CH2 ga_25
CE3 CZ3 HZ3 ga_25
CE3 CZ3 CH2 ga_27
HZ3 CZ3 CH2 ga_25
CZ2 CH2 CZ3 ga_27
CZ2 CH2 BRT ga_27
CZ3 CH2 BRT ga_27
CA C O ga_30
CA C +N ga_19
O C +N ga_33
[impropers]
; ai aj ak al gromos type
N -C CA H gi_1
CA N C CB gi_2
CG CD1 CD2 CB gi_1
CG CD1 NE1 CE2 gi_1
CG CD2 CE2 NE1 gi_1
CD1 CG CD2 CE2 gi_1
CD1 CG NE1 HD1 gi_1
CD1 NE1 CE2 CD2 gi_1
CD2 CG CD1 NE1 gi_1
CD2 CE2 CE3 CG gi_1
CD2 CE2 CZ2 CH2 gi_1
CD2 CE3 CZ3 CH2 gi_1
NE1 CD1 CE2 HE1 gi_1
CE2 CD2 CE3 CZ3 gi_1
CE2 CD2 CZ2 NE1 gi_1
CE2 CZ2 CH2 CZ3 gi_1

```

```

CE3 CD2 CE2 CZ2 gi_1
CE3 CD2 CZ3 HE3 gi_1
CE3 CZ3 CH2 CZ2 gi_1
CZ2 CE2 CH2 HZ2 gi_1
CZ3 CE3 CH2 HZ3 gi_1
CH2 CZ2 CZ3 BRT gi_1
C CA +N O gi_1
[ dihedrals ]
; ai aj ak al gromos type
-C A -C N CA gd_14
-C N CA C gd_44
-C N CA C gd_43
N CA CB CG gd_34
N CA C +N gd_45
N CA C +N gd_42
CA CB CG CD2 gd_40

; S-nitrosocysteine
[ CSN ]
[ atoms ]
N N -0.31000 0
H H 0.31000 0
CA CH1 0.00000 1
CB CH2 0.00000 1
SG S 0.10000 2; to add up to 0 net charge
ND NR 0.35000 2; to add up to 0 net charge
OE O -0.45000 2; from the carbonyl group (of e.g., the peptide bond)
C C 0.450 3
O O -0.450 3
[ bonds ]
N H gb_2
N CA gb_21
CA CB gb_27
CA C gb_27
CB SG gb_32
SG ND gb_31 ; from MET
ND OE gb_5 ; from the carbonyl group (of e.g., the peptide bond)
C O gb_5
C +N gb_10
[ angles ]
; ai aj ak gromos type
-C N H ga_32
-C N CA ga_31
H N CA ga_18
N CA CB ga_13
N CA C ga_13
CB CA C ga_13
CA CB SG ga_16
CB SG ND ga_6
SG ND OE ga_26
CA C O ga_30
CA C +N ga_19
O C +N ga_33
[ impropers ]
; ai aj ak al gromos type
N -C CA H gi_1
CA N C CB gi_2
NE CD CZ HE gi_1
CZ OH1 NH2 NE gi_1
NH2 HH21 HH22 CZ gi_1
C CA +N O gi_1
[ dihedrals ]
; ai aj ak al gromos type
-C A -C N CA gd_14
-C N CA C gd_44
-C N CA C gd_43
N CA CB CG gd_34
N CA C +N gd_45
N CA C +N gd_42
CA CB CG CD gd_34
CB CG CD NE gd_34
CG CD NE CZ gd_39
CD NE CZ NH2 gd_14
NE CZ NH2 HH21 gd_14

; allysine (aminoadipic semialdehyde)
[ KAL ]
[ atoms ]
N N -0.31000 0
H H 0.31000 0
CA CH1 0.00000 1
CB CH2 0.00000 1
CG CH2 0.00000 2
CD CH2 0.00000 2
CE C 0.35000 3; by analogy to the aldehyde group reported by Dolenc et al.
DOI: 10.1093/nar/gki195
HE HC 0.10000 3; by analogy to the aldehyde group reported by Dolenc et al.
DOI: 10.1093/nar/gki195
OZ O -0.45000 3; from the carbonyl group (of e.g., GLN)
C C 0.450 4
O O -0.450 4
[ bonds ]
N H gb_2
N CA gb_21
CA CB gb_27
CA C gb_27
CB CG gb_27
CG CD gb_27
CD CE gb_27
CE HE gb_3
CE OZ gb_5
C O gb_5
C +N gb_10
[ angles ]
; ai aj ak gromos type
-C N H ga_32
-C N CA ga_31
H N CA ga_18
N CA CB ga_13
N CA C ga_13
CB CA C ga_13
CA CB CG ga_15
CB CG CD ga_15
CG CD NE ga_13
CD NE HE ga_18
CD NE CZ ga_31
HE NE CZ ga_32
NE CZ OH1 ga_30
NE CZ NH2 ga_22
OH1 CZ NH2 ga_30
CZ NH2 HH21 ga_23
CZ NH2 HH22 ga_23
HH21 NH2 HH22 ga_24
CA C O ga_30
CA C +N ga_19
O C +N ga_33
[ impropers ]
; ai aj ak al gromos type
N -C CA H gi_1
CA N C CB gi_2
NE CD CZ HE gi_1
CZ OH1 NH2 NE gi_1
NH2 HH21 HH22 CZ gi_1
C CA +N O gi_1
[ dihedrals ]
; ai aj ak al gromos type
-C A -C N CA gd_14
-C N CA C gd_44
-C N CA C gd_43
N CA CB CG gd_34
N CA C +N gd_45
N CA C +N gd_42
CA CB CG CD gd_34
CB CG CD NE gd_34
CG CD NE CZ gd_39
CD NE CZ NH2 gd_14
NE CZ NH2 HH21 gd_14

; citrulline
[ RCI ]
[ atoms ]
N N -0.31000 0
H H 0.31000 0
CA CH1 0.00000 1
CB CH2 0.00000 1
CG CH2 0.00000 2
CD CH2 0.00000 2
NE N -0.31000 3
HE H 0.31000 3
CZ C 0.29000 4; from ASN/GLN
OH1 O -0.45000 4; from ASN/GLN
NH2 NT -0.72000 4; from ASN/GLN
HH21 H 0.44000 4; from ASN/GLN
HH22 H 0.44000 4; from ASN/GLN
C C 0.450 5
O O -0.450 5
[ bonds ]
N H gb_2
N CA gb_21
CA CB gb_27
CA C gb_27
CB CG gb_27

```

```

CG CD CE ga_15
CD CE HE ga_25
CD CE OZ ga_27
HE CE OZ ga_25
CA C O ga_30
CA C +N ga_19
O C +N ga_33
[ impropers ]
; ai aj ak al gromos type
N -C CA H gi_1
CA N C CB gi_2
C CA +N O gi_1
CE OZ CD HE gi_1
[ dihedrals ]
; ai aj ak al gromos type
-CA -C N CA gd_14
-C N CA C gd_44
-C N CA C gd_43
N CA CB CG gd_34
N CA C +N gd_45
N CA C +N gd_42
CA CB CG CD gd_34
CB CG CD CE gd_34
CG CD CE OZ gd_40

; N-acetylglucosamine (N4-linked to ASN)
[ NNG ]
[ atoms ]
N N -0.31000 0
H H 0.31000 0
CA CH1 0.00000 1
CB CH2 0.00000 1
CG C 0.45000 2; from the peptide bond
OD1 O -0.45000 2; from the peptide bond
ND2 N -0.31000 3; from the peptide bond
HD2 H 0.31000 3; from the peptide bond
C1 CH1 0.24000 4; 0.48 charge divided between C1 and C5 to add up to 0 net
charge
O5 OA -0.48000 4; from carbohydrates (e.g., GALB)
C5 CH1 0.24000 4; 0.48 charge divided between C1 and C5 to add up to 0 net
charge
C6 CH2 0.23200 5; from carbohydrates (e.g., GALB)
O6 OA -0.64200 5; from carbohydrates (e.g., GALB)
HO6 H 0.41000 5; from carbohydrates (e.g., GALB)
C2 CH1 0.00000 6; from aliphatic carbon atoms
C4 CH1 0.23200 7; from carbohydrates (e.g., GALB)
O4 OA -0.64200 7; from carbohydrates (e.g., GALB)
HO4 H 0.41000 7; from carbohydrates (e.g., GALB)
C3 CH1 0.23200 8; from carbohydrates (e.g., GALB)
O3 OA -0.64200 8; from carbohydrates (e.g., GALB)
HO3 H 0.41000 8; from carbohydrates (e.g., GALB)
N2 N -0.15000 9; by analogy to ASN/GLN and the peptide bond
HN2 H 0.31000 9; from the hydrogen of the peptide bond
C7 C 0.19000 9; by analogy to ASN/GLN, the peptide bond and the aldehyde
group reported by Dolenc et al. DOI: 10.1093/nar/gki195
O7 O -0.45000 9; from the carbonyl group (of e.g., GLN)
C8 CH3 0.10000 9; by analogy to the aldehyde group reported by Dolenc et
al. DOI: 10.1093/nar/gki195
C C 0.450 10
O O -0.450 10
[ bonds ]
N H gb_2
N CA gb_21
CA CB gb_27
CA C gb_27
CB CG gb_27
CG OD1 gb_5
CG ND2 gb_9
ND2 HD2 gb_2
ND2 C1 gb_21
C4 C3 gb_26
C4 C5 gb_26
C4 O4 gb_20
O4 HO4 gb_1
C3 O3 gb_20
C3 C2 gb_26
O3 HO3 gb_1
C2 C1 gb_26
C2 N2 gb_21
N2 HN2 gb_2
N2 C7 gb_9
C7 O7 gb_5
C7 C8 gb_27
C6 O6 gb_20
C6 C5 gb_26
O6 HO6 gb_1
C5 O5 gb_20
O5 C1 gb_20
C O gb_5
C +N gb_10
[ angles ]
; ai aj ak gromos type
-C N H ga_32
-C N CA ga_31
H N CA ga_18
N CA CB ga_13
N CA C ga_13
CB CA C ga_13
CA CB CG ga_15
CB CG OD1 ga_30
CB CG ND2 ga_19
OD1 CG ND2 ga_33
CG ND2 HD2 ga_18
CG ND2 C1 ga_31
HD2 ND2 C1 ga_32
ND2 C1 C2 ga_9
ND2 C1 O5 ga_9
C2 C1 O5 ga_9
C3 C2 N2 ga_9
C3 C2 C1 ga_8
N2 C2 C1 ga_9
C2 N2 HN2 ga_18
C2 N2 C7 ga_31
HN2 N2 C7 ga_32
N2 C7 O7 ga_33
N2 C7 C8 ga_19
O7 C7 C8 ga_30
C4 C3 O3 ga_9
C4 C3 C2 ga_8
O3 C3 C2 ga_9
C3 O3 HO3 ga_12
C5 C4 O4 ga_9
C5 C4 C3 ga_8
O4 C4 C3 ga_9
C4 O4 HO4 ga_12
C4 C5 C6 ga_8
C4 C5 O5 ga_9
C6 C5 O5 ga_9
O6 C6 C5 ga_9
C6 O6 HO6 ga_12
C5 O5 C1 ga_10
CA C O ga_30
CA C +N ga_19
O C +N ga_33
[ impropers ]
; ai aj ak al gromos type
N -C CA H gi_1
CA N C CB gi_2
CG OD1 ND2 CB gi_1
ND2 CG C1 HD2 gi_1
C1 O5 ND2 C2 gi_2
C5 O5 C6 C4 gi_2
C2 N2 C3 C1 gi_2
C3 O3 C2 C4 gi_2
C4 C3 O4 C5 gi_2
N2 C7 C2 HN2 gi_1
C7 C8 N2 O7 gi_1
C CA +N O gi_1
[ dihedrals ]
; ai aj ak al gromos type
-CA -C N CA gd_14
-C N CA C gd_44
-C N CA C gd_43
N CA CB CG gd_34
N CA C +N gd_45
N CA C +N gd_42
CA CB CG ND2 gd_40
CB CG ND2 C1 gd_14
CG ND2 C1 O5 gd_39
C1 C2 N2 C7 gd_39
C2 N2 C7 C8 gd_14
C3 C2 C1 O5 gd_17
C3 C2 C1 ND2 gd_17
C3 C2 C1 ND2 gd_34
N2 C2 C1 ND2 gd_18
N2 C2 C1 O5 gd_18
C2 C3 O3 HO3 gd_30
C4 C3 C2 N2 gd_17
C4 C3 C2 C1 gd_34
O3 C3 C2 N2 gd_18
O3 C3 C2 C1 gd_17
C3 C4 O4 HO4 gd_30
C5 C4 C3 O3 gd_17
C5 C4 C3 C2 gd_34
O4 C4 C3 O2 gd_18
O4 C4 C3 C2 gd_17
O4 C4 C5 C6 gd_17
C3 C4 C5 C6 gd_34
C3 C4 C5 O5 gd_17
O4 C4 C5 O5 gd_18
C5 C6 O6 HO6 gd_30
O6 C6 C5 C4 gd_1
O6 C6 C5 O5 gd_3
O6 C6 C5 O5 gd_35
C4 C5 O5 C1 gd_29
C5 O5 C1 C2 gd_29

```



; 2,3-dihydroxyphenylalanine

[ F23 ]

[ atoms ]

```

N N -0.31000 0
H H 0.31000 0
CA CH1 0.00000 1
CB CH2 0.00000 1
CG C 0.00000 1
CD1 C 0.20300 2 ; from the hydroxyl group of TYR
OE3 OA -0.61100 2 ; from the hydroxyl group of TYR
HE3 H 0.40800 2 ; from the hydroxyl group of TYR
CD2 C -0.14000 3
HD2 HC 0.14000 3
CE1 C 0.20300 4 ; from the hydroxyl group of TYR
OZ1 OA -0.61100 4 ; from the hydroxyl group of TYR
HZ1 H 0.40800 4 ; from the hydroxyl group of TYR
CE2 C -0.14000 5
HE2 HC 0.14000 5
CZ2 C -0.14000 6
HZ2 HC 0.14000 6
C C 0.450 7
O O -0.450 7

```

[ bonds ]

```

N H gb_2
N CA gb_21
CA CB gb_27
CA C gb_27
CB CG gb_27
CG CD1 gb_16
CG CD2 gb_16
CD1 OE3 gb_13
CD1 CE1 gb_16
CD2 HD2 gb_3
CD2 CE2 gb_16
CE1 OZ1 gb_13
CE1 CZ2 gb_16
CE2 HE2 gb_3
CE2 CZ2 gb_16
OE3 HE3 gb_1
CZ2 HZ2 gb_3
OZ1 HZ1 gb_1
C O gb_5
C +N gb_10

```

[ exclusions ]

; ai aj

```

CB HD2
CB CE1
CB CE2
CB OE3
CG HE2
CG OZ1
CG CZ2
CD1 HD2
CD1 CE2
CD1 HZ2
CD2 CE1
CD2 OE3
CD2 HZ2
HD2 HE2
HD2 CZ2
CE1 HE2
CE2 OZ1
HE2 HZ2
OE3 CZ2
OE3 OZ1
HZ2 OZ1
OE3 HZ1
HE3 OZ1
HE3 HZ1

```

[ angles ]

; ai aj ak gromos type

```

-C N H ga_32
-C N CA ga_31
H N CA ga_18
N CA CB ga_13
N CA C ga_13
CB CA C ga_13
CA CB CG ga_15
CB CG CD1 ga_27
CB CG CD2 ga_27
CD1 CG CD2 ga_27
CG CD1 CE1 ga_27
CG CD1 OE3 ga_27
CE1 CD1 OE3 ga_27
CG CD2 HD2 ga_25
CG CD2 CE2 ga_27
HD2 CD2 CE2 ga_25
CD1 CE1 CZ2 ga_27
CD1 CE1 OZ1 ga_27
CZ2 CE1 OZ1 ga_27
CD2 CE2 HE2 ga_25
CD2 CE2 CZ2 ga_27

```

```

HE2 CE2 CZ2 ga_25
CD1 OE3 HE3 ga_12
CE1 CZ2 CE2 ga_27
CE1 CZ2 HZ2 ga_25
CE2 CZ2 HZ2 ga_25
CE1 OZ1 HZ1 ga_12
CA C O ga_30
CA C +N ga_19
O C +N ga_33

```

[ impropers ]

; ai aj ak al gromos type

```

N -C CA H gi_1
CA N C CB gi_2
CG CD1 CD2 CB gi_1
CG CD1 CE1 CZ2 gi_1
CG CD2 CE2 CZ2 gi_1
CD1 CG CD2 CE2 gi_1
CD1 CG CE1 OE3 gi_1
CD1 CE1 CZ2 CE2 gi_1
CD2 CG CD1 CE1 gi_1
CD2 CG CE2 HD2 gi_1
CD2 CE2 CZ2 CE1 gi_1
OZ1 CD1 CZ2 CE1 gi_1
HE2 CD2 CZ2 CE2 gi_1
CZ2 CE1 CE2 HZ2 gi_1
C CA +N O gi_1

```

[ dihedrals ]

; ai aj ak al gromos type

```

-C -C N CA gd_14
-C N CA C gd_44
-C N CA C gd_43
N CA CB CG gd_34
N CA C +N gd_45
N CA C +N gd_42
CA CB CG CD1 gd_40
CG CD1 OE3 HE3 gd_11
CD1 CE1 OZ1 HZ1 gd_11

```

; 2-hydroxyphenylalanine

[ F2H ]

[ atoms ]

```

N N -0.31000 0
H H 0.31000 0
CA CH1 0.00000 1
CB CH2 0.00000 1
CG C 0.00000 1
CD1 C 0.20300 2 ; from the hydroxyl group of TYR
OE3 OA -0.61100 2 ; from the hydroxyl group of TYR
HE3 H 0.40800 2 ; from the hydroxyl group of TYR
CD2 C -0.14000 3
HD2 HC 0.14000 3
CE1 C -0.14000 4
HE1 HC 0.14000 4
CE2 C -0.14000 5
HE2 HC 0.14000 5
CZ C -0.14000 6
HZ HC 0.14000 6
C C 0.450 7
O O -0.450 7

```

[ bonds ]

```

N H gb_2
N CA gb_21
CA CB gb_27
CA C gb_27
CB CG gb_27
CG CD1 gb_16
CG CD2 gb_16
CD1 OE3 gb_13
CD1 CE1 gb_16
CD2 HD2 gb_3
CD2 CE2 gb_16
CE1 HE1 gb_3
CE1 CZ gb_16
CE2 HE2 gb_3
CE2 CZ gb_16
OE3 HE3 gb_1
CZ HZ gb_3
C O gb_5
C +N gb_10

```

[ exclusions ]

; ai aj

```

CB HD2
CB CE1
CB CE2
CG HE1
CG HE2
CB OE3
CG CZ
CD1 HD2
CD1 CE2
CD1 HZ
CD2 CE1
CD2 OE3

```

```

CD2 HZ
HD2 HE2
HD2 CZ
CE1 HE2
HE1 CE2
HE1 OE3
HE1 HZ
HE2 HZ
OE3 CZ
[angles]
; ai aj ak gromos type
-C N H ga_32
-C N CA ga_31
H N CA ga_18
N CA CB ga_13
N CA C ga_13
CB CA C ga_13
CA CB CG ga_15
CB CG CD1 ga_27
CB CG CD2 ga_27
CD1 CG CD2 ga_27
CG CD1 CE1 ga_27
CG CD1 OE3 ga_27
CE1 CD1 OE3 ga_27
CG CD2 HD2 ga_25
CG CD2 CE2 ga_27
HD2 CD2 CE2 ga_25
CD1 CE1 HE1 ga_25
CD1 CE1 CZ ga_27
HE1 CE1 CZ ga_25
CD2 CE2 HE2 ga_25
CD2 CE2 CZ ga_27
HE2 CE2 CZ ga_25
CD1 OE3 HE3 ga_12
CE1 CZ CE2 ga_27
CE1 CZ HZ ga_25
CE2 CZ HZ ga_25
CA C O ga_30
CA C +N ga_19
O C +N ga_33
[impropers]
; ai aj ak al gromos type
N -C CA H gi_1
CA N C CB gi_2
CG CD1 CD2 CB gi_1
CG CD1 CE1 CZ gi_1
CG CD2 CE2 CZ gi_1
CD1 CG CD2 CE2 gi_1
CD1 CG CE1 OE3 gi_1
CD1 CE1 CZ CE2 gi_1
CD2 CG CD1 CE1 gi_1
CD2 CG CE2 HD2 gi_1
CD2 CE2 CZ CE1 gi_1
HE1 CD1 CZ CE1 gi_1
HE2 CD2 CZ CE2 gi_1
CZ CE1 CE2 HZ gi_1
C CA +N O gi_1
[dihedrals]
; ai aj ak al gromos type
-CA -C N CA gd_14
-C N CA C gd_44
-C N CA C gd_43
N CA CB CG gd_34
N CA C +N gd_45
N CA C +N gd_42
CA CB CG CD1 gd_40
CG CD1 OE3 HE3 gd_11
; 3-hydroxyphenylalanine
[F3H]
[atoms]
N N -0.31000 0
H H 0.31000 0
CA CH1 0.00000 1
CB CH2 0.00000 1
CG C 0.00000 1
CD1 C -0.14000 2
HD1 HC 0.14000 2
CD2 C -0.14000 3
HD2 HC 0.14000 3
CE1 C 0.20300 4 ; from the hydroxyl group of TYR
OZ1 OA -0.61100 4 ; from the hydroxyl group of TYR
HZ1 H 0.40800 4 ; from the hydroxyl group of TYR
CE2 C -0.14000 5
HE2 HC 0.14000 5
CZ2 C -0.14000 6
HZ2 HC 0.14000 6
C C 0.450 7
O O -0.450 7
[bonds]
N H gb_2
N CA gb_21
CA CB gb_27
CA C gb_27
CB CG gb_27
CG CD1 gb_16
CG CD2 gb_16
CD1 HD1 gb_3
CD1 CE1 gb_16
CD2 HD2 gb_3
CD2 CE2 gb_16
CE1 OZ1 gb_13
CE1 CZ2 gb_16
CE2 HE2 gb_3
CE2 CZ2 gb_16
CZ2 HZ2 gb_3
OZ1 HZ1 gb_1
C O gb_5
C +N gb_10
[exclusions]
; ai aj
CB HD1
CB HD2
CB CE1
CB CE2
CG HE2
CG CZ2
CG OZ1
CD1 HD2
CD1 CE2
CD1 HZ2
HD1 CD2
HD1 CZ2
HD1 OZ1
CD2 CE1
CD2 HZ2
HD2 HE2
HD2 CZ2
CE1 HE2
CE2 OZ1
HE2 HZ2
HZ2 OZ1
[angles]
; ai aj ak gromos type
-C N H ga_32
-C N CA ga_31
H N CA ga_18
N CA CB ga_13
N CA C ga_13
CB CA C ga_13
CA CB CG ga_15
CB CG CD1 ga_27
CB CG CD2 ga_27
CD1 CG HD1 ga_25
CG CD1 CE1 ga_27
HD1 CD1 CE1 ga_25
CG CD2 HD2 ga_25
CG CD2 CE2 ga_27
HD2 CD2 CE2 ga_25
CD1 CE1 OZ1 ga_27
CZ2 CE1 OZ1 ga_27
CD2 CE2 HE2 ga_25
CD2 CE2 CZ2 ga_27
HE2 CE2 CZ2 ga_25
CE1 CZ2 CE2 ga_27
CE1 CZ2 HZ2 ga_25
CE2 CZ2 HZ2 ga_25
CE1 OZ1 HZ1 ga_12
CA C O ga_30
CA C +N ga_19
O C +N ga_33
[impropers]
; ai aj ak al gromos type
N -C CA H gi_1
CA N C CB gi_2
CG CD1 CD2 CB gi_1
CG CD1 CE1 CZ gi_1
CG CD2 CE2 CZ gi_1
CD1 CG CD2 CE2 gi_1
CD1 CG CE1 OE3 gi_1
CD1 CE1 CZ CE2 gi_1
CD2 CG CD1 CE1 gi_1
CD2 CG CE2 HD2 gi_1
CD2 CE2 CZ CE1 gi_1
HE1 CD1 CZ CE1 gi_1
HE2 CD2 CZ CE2 gi_1
CZ CE1 CE2 HZ gi_1
C CA +N O gi_1
[dihedrals]
; ai aj ak al gromos type
-CA -C N CA gd_14
-C N CA C gd_44
-C N CA C gd_43
N CA CB CG gd_34
N CA C +N gd_45
N CA C +N gd_42
CA CB CG CD1 gd_40
CG CD1 OE3 HE3 gd_11

```

```

N CA C +N gd_45
N CA C +N gd_42
CA CB CG CD1 gd_40
CD1 CE1 OZ1 HZ1 gd_11

; 6-hydroxytryptophan
[W6H]
[atoms]
N N -0.31000 0
H H 0.31000 0
CA CH1 0.00000 1
CB CH2 0.00000 1
CG C -0.21000 2
CD1 C -0.14000 2
HD1 HC 0.14000 2
CD2 C 0.00000 2
NE1 NR -0.10000 2
HE1 H 0.31000 2
CE2 C 0.00000 2
CE3 C -0.14000 3
HE3 HC 0.14000 3
CZ2 C -0.14000 4
HZ2 HC 0.14000 4
CZ3 C -0.14000 5
HZ3 HC 0.14000 5
CH2 C 0.20300 6 ; from the hydroxyl group of TYR
OI OA -0.61100 6 ; from the hydroxyl group of TYR
HI H 0.40800 6 ; from the hydroxyl group of TYR
C C 0.450 7
O O -0.450 7
[bonds]
N H gb_2
N CA gb_21
CA CB gb_27
CA C gb_27
CB CG gb_27
CG CD1 gb_10
CG CD2 gb_16
CD1 HD1 gb_3
CD1 NE1 gb_10
CD2 CE2 gb_16
CD2 CE3 gb_16
NE1 HE1 gb_2
NE1 CE2 gb_10
CE2 CZ2 gb_16
CE3 HE3 gb_3
CE3 CZ3 gb_16
CZ2 HZ2 gb_3
CZ2 CH2 gb_16
CZ3 HZ3 gb_3
CZ3 CH2 gb_16
CH2 OI gb_13
OI HI gb_1
C O gb_5
C +N gb_10
[exclusions]
; ai aj
CB HD1
CB NE1
CB CE2
CB CE3
CG HE1
CG HE3
CG CZ2
CG CZ3
CD1 CE3
CD1 CZ2
HD1 CD2
HD1 HE1
HD1 CE2
CD2 HE1
CD2 HZ2
CD2 HZ3
CD2 CH2
NE1 CE3
NE1 HZ2
NE1 CH2
HE1 CZ2
CE2 HE3
CE2 CZ3
CE2 OI
CE3 CZ2
CE3 OI
HE3 HZ3
HE3 CH2
CZ2 HZ3
HZ2 CZ3
HZ2 OI
HZ3 OI
[angles]
; ai aj ak gromos type
-C N H ga_32
-C N CA ga_31
H N CA ga_18
N CA CB ga_13
N CA C ga_13
CB CA C ga_13
CA CB CG ga_15
CB CG CD1 ga_37
CB CG CD2 ga_37
CD1 CG CD2 ga_7
CG CD1 HD1 ga_36
CG CD1 NE1 ga_7
HD1 CD1 NE1 ga_36
CG CD2 CE2 ga_7
CG CD2 CE3 ga_39
CE2 CD2 CE3 ga_27
CD1 NE1 HE1 ga_36
CD1 NE1 CE2 ga_7
HE1 NE1 CE2 ga_36
CD2 CE2 NE1 ga_7
CD2 CE2 CZ2 ga_27
NE1 CE2 CZ2 ga_39
CD2 CE3 HE3 ga_25
CD2 CE3 CZ3 ga_27
HE3 CE3 CZ3 ga_25
CE2 CZ2 HZ2 ga_25
CE2 CZ2 CH2 ga_27
HZ2 CZ2 CH2 ga_25
CE3 CZ3 HZ3 ga_25
CE3 CZ3 CH2 ga_27
HZ3 CZ3 CH2 ga_25
CZ2 CH2 CZ3 ga_27
CZ2 CH2 OI ga_27
CZ3 CH2 OI ga_27
CH2 OI HI ga_12
CA C O ga_30
CA C +N ga_19
O C +N ga_33
[impropers]
; ai aj ak al gromos type
N -C CA H gi_1
CA N C CB gi_2
CG CD1 CD2 CB gi_1
CG CD1 NE1 CE2 gi_1
CG CD2 CE2 NE1 gi_1
CD1 CG CD2 CE2 gi_1
CD1 CG NE1 HD1 gi_1
CD1 NE1 CE2 CD2 gi_1
CD2 CG CD1 NE1 gi_1
CD2 CE2 CE3 CG gi_1
CD2 CE2 CZ2 CH2 gi_1
CD2 CE3 CZ3 CH2 gi_1
NE1 CD1 CE2 HE1 gi_1
CE2 CD2 CE3 CZ3 gi_1
CE2 CD2 CZ2 NE1 gi_1
CE2 CZ2 CH2 CZ3 gi_1
CE3 CD2 CE2 CZ2 gi_1
CE3 CD2 CZ3 HE3 gi_1
CE3 CZ3 CH2 CZ2 gi_1
CZ2 CE2 CH2 HZ2 gi_1
CZ3 CE3 CH2 HZ3 gi_1
CH2 CZ2 CZ3 OI gi_1
C CA +N O gi_1
[dihedrals]
; ai aj ak al gromos type
-CA -C N CA gd_14
-C N CA C gd_44
-C N CA C gd_43
N CA CB CG gd_34
N CA C +N gd_45
N CA C +N gd_42
CA CB CG CD2 gd_40
CZ2 CH2 OI HI gd_11
; 5-hydroxytryptophan
[W5H]
[atoms]
N N -0.31000 0
H H 0.31000 0
CA CH1 0.00000 1
CB CH2 0.00000 1
CG C -0.21000 2
CD1 C -0.14000 2
HD1 HC 0.14000 2
CD2 C 0.00000 2
NE1 NR -0.10000 2
HE1 H 0.31000 2
CE2 C 0.00000 2
CE3 C -0.14000 3
HE3 HC 0.14000 3
CZ2 C -0.14000 4
HZ2 HC 0.14000 4
CZ3 C 0.20300 5 ; from the hydroxyl group of TYR
OH3 OA -0.61100 5 ; from the hydroxyl group of TYR
HH3 H 0.40800 5 ; from the hydroxyl group of TYR

```

```

CH2 C -0.14000 6
HH2 HC 0.14000 6
C C 0.450 7
O O -0.450 7
[ bonds ]
N H gb_2
N CA gb_21
CA CB gb_27
CA C gb_27
CB CG gb_27
CG CD1 gb_10
CG CD2 gb_16
CD1 HD1 gb_3
CD1 NE1 gb_10
CD2 CE2 gb_16
CD2 CE3 gb_16
NE1 HE1 gb_2
NE1 CE2 gb_10
CE2 CZ2 gb_16
CE3 HE3 gb_3
CE3 CZ3 gb_16
CZ2 HZ2 gb_3
CZ2 CH2 gb_16
CZ3 CH2 gb_16
CZ3 OH3 gb_13
CH2 HH2 gb_3
OH3 HH3 gb_1
C O gb_5
C +N gb_10
[ exclusions ]
; ai aj
CB HD1
CB NE1
CB CE2
CB CE3
CG HE1
CG HE3
CG CZ2
CG CZ3
CD1 CE3
CD1 CZ2
HD1 CD2
HD1 HE1
HD1 CE2
CD2 HE1
CD2 HZ2
CD2 OH3
CD2 CH2
NE1 CE3
NE1 HZ2
NE1 CH2
HE1 CZ2
CE2 HE3
CE2 CZ3
CE2 HH2
CE3 CZ2
CE3 HH2
HE3 OH3
HE3 CH2
CZ2 OH3
HZ2 CZ3
HZ2 HH2
OH3 HH2
[ angles ]
; ai aj ak gromos type
-C N H ga_32
-C N CA ga_31
H N CA ga_18
N CA CB ga_13
N CA C ga_13
CB CA C ga_13
CA CB CG ga_15
CB CG CD1 ga_37
CB CG CD2 ga_37
CD1 CG CD2 ga_7
CG CD1 HD1 ga_36
CG CD1 NE1 ga_7
HD1 CD1 NE1 ga_36
CG CD2 CE2 ga_7
CG CD2 CE3 ga_39
CE2 CD2 CE3 ga_27
CD1 NE1 HE1 ga_36
CD1 NE1 CE2 ga_7
HE1 NE1 CE2 ga_36
CD2 CE2 NE1 ga_7
CD2 CE2 CZ2 ga_27
NE1 CE2 CZ2 ga_39
CD2 CE3 HE3 ga_25
CD2 CE3 CZ3 ga_27
HE3 CE3 CZ3 ga_25
CE2 CZ2 HZ2 ga_25
CE2 CZ2 CH2 ga_27
HZ2 CZ2 CH2 ga_25
CE3 CZ3 CH2 ga_27
CE3 CZ3 OH3 ga_12
CZ2 CH2 CZ3 ga_27
CZ2 CH2 HH2 ga_25
CZ3 CH2 HH2 ga_25
CA C O ga_30
CA C +N ga_19
O C +N ga_33
[ impropers ]
; ai aj ak al gromos type
N -C CA H gi_1
CA N C CB gi_2
CG CD1 CD2 CB gi_1
CG CD1 NE1 CE2 gi_1
CG CD2 CE2 NE1 gi_1
CD1 CG CD2 CE2 gi_1
CD1 CG NE1 HD1 gi_1
CD1 NE1 CE2 CD2 gi_1
CD2 CG CD1 NE1 gi_1
CD2 CE2 CE3 CG gi_1
CD2 CE2 CZ2 CH2 gi_1
CD2 CE3 CZ3 CH2 gi_1
NE1 CD1 CE2 HE1 gi_1
CE2 CD2 CE3 CZ3 gi_1
CE2 CD2 CZ2 NE1 gi_1
CE2 CZ2 CH2 CZ3 gi_1
CE3 CD2 CE2 CZ2 gi_1
CE3 CD2 CZ3 HE3 gi_1
CE3 CZ3 CH2 CZ2 gi_1
CZ2 CE2 CH2 HZ2 gi_1
CZ3 CE3 CH2 OH3 gi_1
CH2 CZ2 CZ3 HH2 gi_1
C CA +N O gi_1
[ dihedrals ]
; ai aj ak al gromos type
-C A -C N CA gd_14
-C N CA C gd_44
-C N CA C gd_43
N CA CB CG gd_34
N CA C +N gd_45
N CA C +N gd_42
CA CB CG CD2 gd_40
CE3 CZ3 OH3 HH3 gd_11
; 4-hydroxytryptophan
[ W4H ]
[ atoms ]
N N -0.31000 0
H H 0.31000 0
CA CH1 0.00000 1
CB CH2 0.00000 1
CG C -0.21000 2
CD1 C -0.14000 2
HD1 HC 0.14000 2
CD2 C 0.00000 2
NE1 NR -0.10000 2
HE1 H 0.31000 2
CE2 C 0.00000 2
CE3 C 0.20300 3 ; from the hydroxyl group of TYR
OZ4 OA -0.61100 3 ; from the hydroxyl group of TYR
HZ4 H 0.40800 3 ; from the hydroxyl group of TYR
CZ2 C -0.14000 4
HZ2 HC 0.14000 4
CZ3 C -0.14000 5
HZ3 HC 0.14000 5
CH2 C -0.14000 6
HH2 HC 0.14000 6
C C 0.450 7
O O -0.450 7
[ bonds ]
N H gb_2
N CA gb_21
CA CB gb_27
CA C gb_27
CB CG gb_27
CG CD1 gb_10
CG CD2 gb_16
CD1 HD1 gb_3
CD1 NE1 gb_10
CD2 CE2 gb_16
CD2 CE3 gb_16
NE1 HE1 gb_2
NE1 CE2 gb_10
CE2 CZ2 gb_16
CE3 HE3 gb_3
CE3 CZ3 gb_16
CZ2 HZ2 gb_3
CZ2 CH2 gb_16
CZ3 CH2 gb_16
CZ3 OH3 gb_13
CH2 HH2 gb_3
OH3 HH3 gb_1
C O gb_5
C +N gb_10

```

```

CH2 HH2 gb_3
C O gb_5
C +N gb_10
[exclusions ]
; ai aj
CB HD1
CB NE1
CB CE2
CB CE3
CG HE1
CG CZ2
CG CZ3
CG OZ4
CD1 CE3
CD1 CZ2
HD1 CD2
HD1 HE1
HD1 CE2
CD2 HE1
CD2 HZ2
CD2 HZ3
CD2 CH2
NE1 CE3
NE1 HZ2
NE1 CH2
HE1 CZ2
CE2 CZ3
CE2 OZ4
CE2 HH2
CE3 CZ2
CE3 HH2
CZ2 HZ3
HZ2 CZ3
HZ2 HH2
HZ3 OZ4
HZ3 HH2
OZ4 CH2
[angles ]
; ai aj ak gromos type
-C N H ga_32
-C N CA ga_31
H N CA ga_18
N CA CB ga_13
N CA C ga_13
CB CA C ga_13
CA CB CG ga_15
CB CG CD1 ga_37
CB CG CD2 ga_37
CD1 CG CD2 ga_7
CG CD1 HD1 ga_36
CG CD1 NE1 ga_7
HD1 CD1 NE1 ga_36
CG CD2 CE2 ga_7
CG CD2 CE3 ga_39
CE2 CD2 CE3 ga_27
CD1 NE1 HE1 ga_36
CD1 NE1 CE2 ga_7
HE1 NE1 CE2 ga_36
CD2 CE2 NE1 ga_7
CD2 CE2 CZ2 ga_27
NE1 CE2 CZ2 ga_39
CD2 CE3 CZ3 ga_27
CD2 CE3 OZ4 ga_27
CZ3 CE3 OZ4 ga_27
CE2 CZ2 HZ2 ga_25
CE2 CZ2 CH2 ga_27
HZ2 CZ2 CH2 ga_25
CE3 CZ3 HZ3 ga_25
CE3 CZ3 CH2 ga_27
HZ3 CZ3 CH2 ga_25
CE3 OZ4 HZ4 ga_12
CZ2 CH2 CZ3 ga_27
CZ3 CH2 HH2 ga_25
CA C O ga_30
CA C +N ga_19
O C +N ga_33
[impropers ]
; ai aj ak al gromos type
N -C CA H gi_1
CA N C CB gi_2
CG CD1 CD2 CB gi_1
CG CD1 NE1 CE2 gi_1
CG CD2 CE2 NE1 gi_1
CD1 CG CD2 CE2 gi_1
CD1 CG NE1 HD1 gi_1
CD1 NE1 CE2 CD2 gi_1
CD2 CG CD1 NE1 gi_1
CD2 CE2 CE3 CG gi_1
CD2 CE2 CZ2 CH2 gi_1
CD2 CE3 CZ3 CH2 gi_1
NE1 CD1 CE2 HE1 gi_1
CE2 CD2 CE3 CZ3 gi_1
CE2 CD2 CZ2 NE1 gi_1
-C N CA C gd_14
-C N CA C gd_44
-C N CA C gd_43
N CA CB CG gd_34
N CA C +N gd_45
N CA C +N gd_42
CA CB CG CD2 gd_40
CD2 CE3 OZ4 HZ4 gd_11
; 2-hydroxytryptophan
[W2H]
[atoms ]
N N -0.31000 0
H H 0.31000 0
CA CH1 0.00000 1
CB CH2 0.00000 1
CG C -0.21000 2
CD1 C 0.20300 2 ; from the hydroxyl group of TYR
OE4 OA -0.61100 2 ; from the hydroxyl group of TYR
HE4 H 0.40800 2 ; from the hydroxyl group of TYR
CD2 C 0.00000 2
NE1 NR -0.10000 2
HE1 H 0.31000 2
CE2 C 0.00000 2
CE3 C -0.14000 3
HE3 HC 0.14000 3
CZ2 C -0.14000 4
HZ2 HC 0.14000 4
CZ3 C -0.14000 5
HZ3 HC 0.14000 5
CH2 C -0.14000 6
HH2 HC 0.14000 6
C C 0.450 7
O O -0.450 7
[bonds ]
N H gb_2
N CA gb_21
CA CB gb_27
CA C gb_27
CB CG gb_27
CG CD1 gb_10
CG CD2 gb_16
CD1 OE4 gb_13
CD1 NE1 gb_10
CD2 CE2 gb_16
CD2 CE3 gb_16
NE1 HE1 gb_2
NE1 CE2 gb_10
CE2 CZ2 gb_16
CE3 HE3 gb_3
CE3 CZ3 gb_16
OE4 HE4 gb_1
CZ2 HZ2 gb_3
CZ2 CH2 gb_16
CZ3 HZ3 gb_3
CZ3 CH2 gb_16
CH2 HH2 gb_3
C O gb_5
C +N gb_10
[exclusions ]
; ai aj
CB NE1
CB CE2
CB CE3
CB OE4
CG HE1
CG HE3
CG CZ2
CG CZ3
CD1 CE3
CD1 CZ2
CD2 HE1
CD2 OE4
CD2 HZ2
CD2 HZ3
CD2 CH2
NE1 CE3
NE1 HE4
NE1 HZ2
NE1 CH2
HE1 OE4
HE1 CZ2

```

```

CE2 HE3
CE2 OE4
CE2 CZ3
CE2 HH2
CE3 CZ2
CE3 HH2
HE3 HZ3
HE3 CH2
CZ2 HZ3
HZ2 CZ3
HZ2 HH2
HZ3 HH2
[angles]
; ai aj ak gromos type
-C N H ga_32
-C N CA ga_31
H N CA ga_18
N CA CB ga_13
N CA C ga_13
CB CA C ga_13
CA CB CG ga_15
CB CG CD1 ga_37
CB CG CD2 ga_37
CD1 CG CD2 ga_7
CG CD1 NE1 ga_7
CG CD1 OE4 ga_37
NE1 CD1 OE4 ga_37
CG CD2 CE2 ga_7
CG CD2 CE3 ga_39
CE2 CD2 CE3 ga_27
CD1 NE1 HE1 ga_36
CD1 NE1 CE2 ga_7
HE1 NE1 CE2 ga_36
CD2 CE2 NE1 ga_7
CD2 CE2 CZ2 ga_27
NE1 CE2 CZ2 ga_39
CD2 CE3 HE3 ga_25
CD2 CE3 CZ3 ga_27
HE3 CE3 CZ3 ga_25
CD1 OE4 HE4 ga_12
CE2 CZ2 HZ2 ga_25
CE2 CZ2 CH2 ga_27
HZ2 CZ2 CH2 ga_25
CE3 CZ3 HZ3 ga_25
CE3 CZ3 CH2 ga_27
HZ3 CZ3 CH2 ga_25
CZ2 CH2 CZ3 ga_27
CZ2 CH2 HH2 ga_25
CZ3 CH2 HH2 ga_25
CA C O ga_30
CA C +N ga_19
O C +N ga_33
[impropers]
; ai aj ak al gromos type
N -C CA H gi_1
CA N C CB gi_2
CG CD1 CD2 CB gi_1
CG CD1 NE1 CE2 gi_1
CG CD2 CE2 NE1 gi_1
CD1 CG CD2 CE2 gi_1
CD1 CG NE1 OE4 gi_1
CD1 NE1 CE2 CD2 gi_1
CD2 CG CD1 NE1 gi_1
CD2 CE2 CE3 CG gi_1
CD2 CE2 CZ2 CH2 gi_1
CD2 CE3 CZ3 CH2 gi_1
NE1 CD1 CE2 HE1 gi_1
CE2 CD2 CE3 CZ3 gi_1
CE2 CD2 CZ2 NE1 gi_1
CE2 CZ2 CH2 CZ3 gi_1
CE3 CD2 CE2 CZ2 gi_1
CE3 CD2 CZ3 HE3 gi_1
CE3 CZ3 CH2 CZ2 gi_1
CZ2 CE2 CH2 HZ2 gi_1
CZ3 CE3 CH2 HZ3 gi_1
CH2 CZ2 CZ3 HH2 gi_1
C CA +N O gi_1
[dihedrals]
; ai aj ak al gromos type
-CA -C N CA gd_14
-C N CA C gd_44
-C N CA C gd_43
N CA CB CG gd_34
N CA C +N gd_45
N CA C +N gd_42
CA CB CG CD2 gd_40
CG CD1 OE4 HE4 gd_11
; 3-hydroxyleucine (R)
[L3H]
[atoms]
N N -0.31000 0
H H 0.31000 0
CA CH1 0.00000 1
CB CH1 0.26600 2; from the hydroxyl group of THR
OG1 OA -0.67400 2; from the hydroxyl group of THR
HG1 H 0.40800 2; from the hydroxyl group of THR
CG2 CH1 0.00000 3
CD1 CH3 0.00000 3
CD2 CH3 0.00000 3
C C 0.450 4
O O -0.450 4
[bonds]
N H gb_2
N CA gb_21
CA CB gb_27
CA C gb_27
CB OG1 gb_18
CB CG2 gb_27
OG1 HG1 gb_1
CG2 CD1 gb_27
CG2 CD2 gb_27
C O gb_5
C +N gb_10
[angles]
; ai aj ak gromos type
-C N H ga_32
-C N CA ga_31
H N CA ga_18
N CA CB ga_13
N CA C ga_13
CB CA C ga_13
CA CB OG1 ga_13
CA CB CG2 ga_13
OG1 CB CG2 ga_13
CB OG1 HG1 ga_12
CB CG2 CD1 ga_15
CB CG2 CD2 ga_15
CD1 CG2 CD2 ga_15
CA C O ga_30
CA C +N ga_19
O C +N ga_33
[impropers]
; ai aj ak al gromos type
N -C CA H gi_1
CA N C CB gi_2
CB OG1 CG2 CA gi_2
CB CD1 CD2 CG2 gi_2
C CA +N O gi_1
[dihedrals]
; ai aj ak al gromos type
-CA -C N CA gd_14
-C N CA C gd_44
-C N CA C gd_43
N CA CB CG2 gd_34
N CA C +N gd_45
N CA C +N gd_42
CA CB CG2 CD1 gd_34
CA CB OG1 HG1 gd_23
; 3-hydroxyleucine (S)
[LH3]
[atoms]
N N -0.31000 0
H H 0.31000 0
CA CH1 0.00000 1
CB CH1 0.26600 2; from the hydroxyl group of THR
OG1 OA -0.67400 2; from the hydroxyl group of THR
HG1 H 0.40800 2; from the hydroxyl group of THR
CG2 CH1 0.00000 3
CD1 CH3 0.00000 3
CD2 CH3 0.00000 3
C C 0.450 4
O O -0.450 4
[bonds]
N H gb_2
N CA gb_21
CA CB gb_27
CA C gb_27
CB OG1 gb_18
CB CG2 gb_27
OG1 HG1 gb_1
CG2 CD1 gb_27
CG2 CD2 gb_27
C O gb_5
C +N gb_10
[angles]
; ai aj ak gromos type
-C N H ga_32
-C N CA ga_31
H N CA ga_18
N CA CB ga_13
N CA C ga_13
CB CA C ga_13
CA CB OG1 ga_13
CA CB CG2 ga_13

```

```

OG1 CB CG2 ga_13
CB OG1 HG1 ga_12
CB CG2 CD1 ga_15
CB CG2 CD2 ga_15
CD1 CG2 CD2 ga_15
CA C O ga_30
CA C +N ga_19
O C +N ga_33
[impropers]
; ai aj ak al gromos type
N -C CA H gi_1
CA N C CB gi_2
CB CG2 OG1 CA gi_2
CB CD1 CD2 CG2 gi_2
C CA +N O gi_1
[dihedrals]
; ai aj ak al gromos type
-C -C N CA gd_14
-C N CA C gd_44
-C N CA C gd_43
N CA CB CG2 gd_34
N CA C +N gd_45
N CA C +N gd_42
CA CB CG2 CD1 gd_34
CA CB OG1 HG1 gd_23

; 4-hydroxyleucine
[L4H]
[atoms]
N N -0.31000 0
H H 0.31000 0
CA CH1 0.00000 1
CB CH2 0.00000 1
CG CH3 0.26600 2; from the hydroxyl group of THR
OD3 OA -0.67400 2; from the hydroxyl group of THR
HD3 H 0.40800 2; from the hydroxyl group of THR
CD1 CH3 0.00000 3
CD2 CH3 0.00000 4
C C 0.450 5
O O -0.450 5
[bonds]
N H gb_2
N CA gb_21
CA CB gb_27
CA C gb_27
CB CG gb_27
CG CD1 gb_27
CG CD2 gb_27
CG OD3 gb_18
OD3 HD3 gb_1
C O gb_5
C +N gb_10
[angles]
; ai aj ak al gromos type
-C N H ga_32
-C N CA ga_31
H N CA ga_18
N CA CB ga_13
N CA C ga_13
CB CA C ga_13
CA CB CG ga_15
CB CG CD1 ga_15
CB CG CD2 ga_15
CD1 CG CD2 ga_15
CG CD2 OE ga_13
CD2 OE HE ga_12
CA C O ga_30
CA C +N ga_19
O C +N ga_33
[impropers]
; ai aj ak al gromos type
N -C CA H gi_1
CA N C CB gi_2
CB CD1 CD2 CG gi_2
C CA +N O gi_1
[dihedrals]
; ai aj ak al gromos type
-C -C N CA gd_14
-C N CA C gd_44
-C N CA C gd_43
N CA CB CG gd_34
N CA C +N gd_45
N CA C +N gd_42
CA CB CG CD2 gd_34
CB CG CD2 OE gd_34
CG CD2 OE HE gd_23

; 5-hydroxyleucine (S)
[LH5]
[atoms]
N N -0.31000 0
H H 0.31000 0
CA CH1 0.00000 1
CB CH2 0.00000 1
CG CH3 0.00000 2
CD1 CH3 0.00000 2
CD2 CH2 0.26600 3; from the hydroxyl group of THR
OE OA -0.67400 3; from the hydroxyl group of THR
HE H 0.40800 3; from the hydroxyl group of THR
C C 0.450 4
O O -0.450 4
[bonds]
N H gb_2
N CA gb_21
CA CB gb_27
CA C gb_27
CB CG gb_27
CG CD1 gb_27
CG CD2 gb_27
CD2 OE gb_18
OE HE gb_1
C O gb_5
C +N gb_10
[angles]
; ai aj ak al gromos type
-C N H ga_32
-C N CA ga_31
H N CA ga_18
N CA CB ga_13
N CA C ga_13
CB CA C ga_13
CA CB CG ga_15
CB CG CD1 ga_15
CB CG CD2 ga_15
CD1 CG CD2 ga_15
CG CD2 OE ga_13
CD2 OE HE ga_12
CA C O ga_30
CA C +N ga_19
O C +N ga_33
[impropers]
; ai aj ak al gromos type
N -C CA H gi_1
CA N C CB gi_2
CB CD1 CD2 CG gi_2
C CA +N O gi_1
[dihedrals]
; ai aj ak al gromos type
-C -C N CA gd_14
-C N CA C gd_44
-C N CA C gd_43
N CA CB CG gd_34
N CA C +N gd_45
N CA C +N gd_42
CA CB CG OD3 gd_34
CB CG OD3 HD3 gd_23

; 5-hydroxyleucine (R)
[L5H]
[atoms]
N N -0.31000 0
H H 0.31000 0
CA CH1 0.00000 1

```

```

CG CD2 OE ga_13
CD2 OE HE ga_12
CA C O ga_30
CA C +N ga_19
O C +N ga_33
[impropers]
; ai aj ak al gromos type
N -C CA H gi_1
CA N C CB gi_2
CB CD2 CD1 CG gi_2
C CA +N O gi_1
[dihedrals]
; ai aj ak al gromos type
-CA -C N CA gd_14
-C N CA C gd_44
-C N CA C gd_43
N CA CB CG gd_34
N CA C +N gd_45
N CA C +N gd_42
CA CB CG CD2 gd_34
CB CG CD2 OE gd_34
CG CD2 OE HE gd_23

;3-hydroxyvaline
[V3H]
[atoms]
N N -0.31000 0
H H 0.31000 0
CA CH1 0.00000 1
CB CH0 0.26600 2; from the hydroxyl group of THR
OG3 OA -0.67400 2; from the hydroxyl group of THR
HG3 H 0.40800 2; from the hydroxyl group of THR
CG1 CH3 0.00000 3
CG2 CH3 0.00000 4
C C 0.450 5
O O -0.450 5
[bonds]
N H gb_2
N CA gb_21
CA CB gb_27
CA C gb_27
CB CG1 gb_27
CB CG2 gb_27
CB OG3 gb_18
OG3 HG3 gb_1
C O gb_5
C +N gb_10
[angles]
; ai aj ak al gromos type
-C N H ga_32
-C N CA ga_31
H N CA ga_18
N CA CB ga_13
N CA C ga_13
CB CA C ga_13
CA CB CG1 ga_13
CA CB CG2 ga_13
CA CB OG3 ga_13
CG1 CB CG2 ga_13
CG1 CB OG3 ga_13
CG2 CB OG3 ga_13
CB OG3 HG3 ga_12
CA C O ga_30
CA C +N ga_19
O C +N ga_33
[impropers]
; ai aj ak al gromos type
N -C CA H gi_1
CA N C CB gi_2
C CA +N O gi_1
[dihedrals]
; ai aj ak al gromos type
-CA -C N CA gd_14
-C N CA C gd_44
-C N CA C gd_43
N CA CB SG gd_34
N CA C +N gd_45
N CA C +N gd_42
CA CB SG OD gd_26
CB SG OD HD gd_23

;5-hydroxyproline (R)
[PH5]
[atoms]
N N 0.00000 0
CA CH1 0.00000 1
CB CH2R 0.00000 1
CG CH2R 0.00000 2
CD CH1 0.26600 3; from the hydroxyl group of THR
OE OA -0.67400 3; from the hydroxyl group of THR
HE H 0.40800 3; from the hydroxyl group of THR
C C 0.450 4
O O -0.450 4
[bonds]
N CA gb_21
N CD gb_21
CA CB gb_27
CA C gb_27
CB CG gb_27
CG CD gb_27
CD OE gb_18
OE HE gb_1
C O gb_5
C +N gb_10
[exclusions]
; ai aj
N HE
[angles]
; ai aj ak al gromos type
-C N CA ga_31
-C N CD ga_31
CA N CD ga_21
N CA CB ga_13
N CA C ga_13
CB CA C ga_13
CA CB CG ga_13
CB CG CD ga_13
N CD CG ga_13
N CD OE ga_13
CG CD OE ga_13
CD OE HE ga_12
CA C O ga_30
CA C +N ga_19
O C +N ga_33
[impropers]
; ai aj ak al gromos type
N -C CA CD gi_1
CA N C CB gi_2
C CA +N O gi_1
CD CG N OE gi_2
[dihedrals]
; ai aj ak al gromos type
-CA -C N CA gd_14
-C N CA C gd_44
-C N CA C gd_43

```



```

CA N CD CG gd_39
N CA CB CG gd_34
N CA C +N gd_45
N CA C +N gd_42
CA CB CG CD gd_34
CB CG CD N gd_34
CG CD OE HE gd_23

; 5-hydroxyproline (S)
[PSH]
[atoms]
N N 0.00000 0
CA CH1 0.00000 1
CB CH2R 0.00000 1
CG CH2R 0.00000 2
CD CH1 0.26600 3 ; from the hydroxyl group of THR
OE OA -0.67400 3 ; from the hydroxyl group of THR
HE H 0.40800 3 ; from the hydroxyl group of THR
C C 0.450 4
O O -0.450 4
[bonds]
N CA gb_21
N CD gb_21
CA CB gb_27
CA C gb_27
CB CG gb_27
CG CD gb_27
CD OE gb_18
OE HE gb_1
C O gb_5
C +N gb_10
[exclusions]
; ai aj
N HE
[angles]
; ai aj ak gromos type
-C N CA ga_31
-C N CD ga_31
CA N CD ga_21
N CA CB ga_13
N CA C ga_13
CB CA C ga_13
CA CB CG ga_13
CB CG CD ga_13
N CD CG ga_13
N CD OE ga_13
CG CD OE ga_13
CD OE HE ga_12
CA C O ga_30
CA C +N ga_19
O C +N ga_33
[impropers]
; ai aj ak al gromos type
N -C CA CD gi_1
CA N C CB gi_2
C CA +N O gi_1
CD N CG OE gi_2
[dihedrals]
; ai aj ak al gromos type
-C -C N CA gd_14
-C N CA C gd_44
-C N CA C gd_43
CA N CD CG gd_39
N CA CB CG gd_34
N CA C +N gd_45
N CA C +N gd_42
CA CB CG CD gd_34
CB CG CD N gd_34
CG CD OE HE gd_23

; glutamic semialdehyde
[GSA]
[atoms]
N N -0.31000 0
H H 0.31000 0
CA CH1 0.00000 1
CB CH2 0.00000 1
CG CH2 0.00000 1
CD C 0.35000 2 ; by analogy to the aldehyde group reported by Dolenc et al.
DOI: 10.1093/nar/gki195
HD HC 0.10000 2 ; by analogy to the aldehyde group reported by Dolenc et al. DOI: 10.1093/nar/gki195
OE O -0.45000 2 ; from the carbonyl group (of e.g., GLN)
C C 0.450 3
O O -0.450 3
[bonds]
N H gb_2
N CA gb_21
CA CB gb_27
CA C gb_27
CB CG gb_27
CG CD gb_27
CD HD gb_3

CD OE gb_5
C O gb_5
C +N gb_10
[angles]
; ai aj ak gromos type
-C N H ga_32
-C N CA ga_31
H N CA ga_18
N CA CB ga_13
N CA C ga_13
CB CA C ga_13
CA CB CG ga_15
CB CG CD ga_15
CG CD HD ga_25
CG CD OE ga_27
HD CD OE ga_25
CA C O ga_30
CA C +N ga_19
O C +N ga_33
[impropers]
; ai aj ak al gromos type
N -C CA H gi_1
CA N C CB gi_2
C CA +N O gi_1
CD OE CG HD gi_1
[dihedrals]
; ai aj ak al gromos type
-C -C N CA gd_14
-C N CA C gd_44
-C N CA C gd_43
N CA CB CG gd_34
N CA C +N gd_45
N CA C +N gd_42
CA CB CG CD gd_34
CB CG CD OE gd_40

; 2-amino-3-ketobutyric acid
[TOX]
[atoms]
N N -0.31000 0
H H 0.31000 0
CA CH1 0.00000 1
CB C 0.45000 2 ; from the carbonyl group (of e.g., GLN)
OG1 O -0.45000 2 ; from the carbonyl group (of e.g., GLN)
CG2 CH3 0.00000 3
C C 0.450 4
O O -0.450 4
[bonds]
N H gb_2
N CA gb_21
CA CB gb_27
CA C gb_27
CB OG1 gb_5
CB CG2 gb_27
C O gb_5
C +N gb_10
[angles]
; ai aj ak gromos type
-C N H ga_32
-C N CA ga_31
H N CA ga_18
N CA CB ga_13
N CA C ga_13
CB CA C ga_13
CA CB OG1 ga_27
CA CB CG2 ga_27
OG1 CB CG2 ga_27
CA C O ga_30
CA C +N ga_19
O C +N ga_33
[impropers]
; ai aj ak al gromos type
N -C CA H gi_1
CA N C CB gi_2
CB OG1 CG2 CA gi_1
C CA +N O gi_1
[dihedrals]
; ai aj ak al gromos type
-C -C N CA gd_14
-C N CA C gd_44
-C N CA C gd_43
N CA CB OG1 gd_40
N CA C +N gd_45
N CA C +N gd_42

; pyroglutamic acid
[PGA]
[atoms]
N N 0.00000 0
CA CH1 0.00000 1
CB CH2R 0.00000 1
CG CH2R 0.00000 2
CD C 0.45000 3 ; from the carbonyl group (of e.g., GLN)

```

```

OE O -0.45000 3 ; from the carbonyl group (of e.g., GLN)
C C 0.450 4
O O -0.450 4
[ bonds ]
N CA gb_21
N CD gb_10
CA CB gb_27
CA C gb_27
CB CG gb_27
CG CD gb_27
CD OE gb_5
C O gb_5
C +N gb_10
[ angles ]
; ai aj ak gromos type
-C N CA ga_31
-C N CD ga_31
CA N CD ga_21
N CA CB ga_13
N CA C ga_13
CB CA C ga_13
CA CB CG ga_13
CB CG CD ga_13
N CD CG ga_19
N CD OE ga_33
CG CD OE ga_30
CA C O ga_30
CA C +N ga_19
O C +N ga_33
[ impropers ]
; ai aj ak al gromos type
N -C CA CD gi_1
CA N C CB gi_2
C CA +N O gi_1
CD CG N OE gi_1
[ dihedrals ]
; ai aj ak al gromos type
-CA -C N CA gd_14
-C N CA C gd_44
-C N CA C gd_43
CA N CD CG gd_14
N CA CB CG gd_34
N CA C +N gd_45
N CA C +N gd_42
CA CB CG CD gd_34
CB CG CD N gd_40

; 2-oxo-histidine
[H2X]
[ atoms ]
N N -0.31000 0
H H 0.31000 0
CA CH1 0.00000 1
CB CH2 0.00000 1
CG C 0.00000 2
ND1 NR -0.31000 3
HD1 H 0.31000 3
CD2 C -0.14000 4 ; to add up to 0 net charge
HD2 HC 0.14000 4
NE2 NR -0.31000 5
HE2 H 0.31000 5
CE1 C 0.45000 6 ; from the carbonyl group (of e.g., GLN)
OZ O -0.45000 6 ; from the carbonyl group (of e.g., GLN)
C C 0.450 7
O O -0.450 7
[ bonds ]
N H gb_2
N CA gb_21
CA CB gb_27
CA C gb_27
CB CG gb_27
CG ND1 gb_10
CG CD2 gb_10
ND1 CE1 gb_10
ND1 HD1 gb_2
CD2 HD2 gb_3
CD2 NE2 gb_10
NE2 HE2 gb_2
CE1 NE2 gb_10
CE1 OZ gb_5
C O gb_5
C +N gb_10
[ exclusions ]
; ai aj
CB HD1
CB HD2
CB CE1
CB NE2
CG HE2
CG OZ
ND1 HD2
ND1 HE2
HD1 CD2

HD1 NE2
HD1 OZ
CD2 OZ
HD2 CE1
HD2 HE2
HE2 OZ
[ angles ]
; ai aj ak gromos type
-C N H ga_32
-C N CA ga_31
H N CA ga_18
N CA CB ga_13
N CA C ga_13
CB CA C ga_13
CA CB CG ga_15
CB CG ND1 ga_37
CB CG CD2 ga_37
ND1 CG CD2 ga_7
CG ND1 HD1 ga_36
CG ND1 CE1 ga_7
HD1 ND1 CE1 ga_36
CG CD2 HD2 ga_36
CG CD2 NE2 ga_7
HD2 CD2 NE2 ga_36
ND1 CE1 NE2 ga_7
ND1 CE1 OZ ga_37
NE2 CE1 OZ ga_37
CD2 NE2 CE1 ga_7
CD2 NE2 HE2 ga_36
CE1 NE2 HE2 ga_36
CA C O ga_30
CA C +N ga_19
O C +N ga_33
[ impropers ]
; ai aj ak al gromos type
N -C CA H gi_1
CA N C CB gi_2
CG ND1 CD2 CB gi_1
CG ND1 CE1 NE2 gi_1
CG CD2 NE2 CE1 gi_1
ND1 CG CD2 NE2 gi_1
ND1 CE1 NE2 CD2 gi_1
ND1 CG CE1 HD1 gi_1
CD2 CG ND1 CE1 gi_1
CD2 CG NE2 HD2 gi_1
CE1 ND1 NE2 OZ gi_1
NE2 CD2 CE1 HE2 gi_1
C CA +N O gi_1
[ dihedrals ]
; ai aj ak al gromos type
-CA -C N CA gd_14
-C N CA C gd_44
-C N CA C gd_43
N CA CB CG gd_34
N CA C +N gd_45
N CA C +N gd_42
CA CB CG ND1 gd_40

; methionine sulfoxide (R)
[ MSX ]
[ atoms ]
N N -0.31000 0
H H 0.31000 0
CA CH1 0.00000 1
CB CH2 0.00000 1
CG CH2 0.24100 2
SD S -0.03200 2 ; to add up to 0 net charge
CE1 CH3 0.24100 2
OE2 O -0.45000 2 ; from the carbonyl group (of e.g., GLN)
C C 0.450 3
O O -0.450 3
[ bonds ]
N H gb_2
N CA gb_21
CA CB gb_27
CA C gb_27
CB CG gb_27
CG SD gb_32
SD CE1 gb_32
SD OE2 gb_25
C O gb_5
C +N gb_10
[ angles ]
; ai aj ak gromos type
-C N H ga_32
-C N CA ga_31
H N CA ga_18
N CA CB ga_13
N CA C ga_13
CB CA C ga_13
CA CB CG ga_15
CB CG SD ga_16
CG SD CE1 ga_4

```

```

CG SD OE2 ga_6
CE1 SD OE2 ga_6
CA C O ga_30
CA C +N ga_19
O C +N ga_33
[impropers]
; ai aj ak al gromos type
N -C CA H gi_1
CA N C CB gi_2
C CA +N O gi_1
SD OE2 CE1 CG gi_2
[dihedrals]
; ai aj ak al gromos type
-C -C N CA gd_14
-C N CA C gd_44
-C N CA C gd_43
N CA CB CG gd_34
N CA C +N gd_45
N CA C +N gd_42
CA CB CG SD gd_34
CB CG SD CE1 gd_26

; methionine sulfoxide (S)
[MXS]
[atoms]
N N -0.31000 0
H H 0.31000 0
CA CH1 0.00000 1
CB CH2 0.00000 1
CG CH2 0.24100 2
SD S -0.03200 2; to add up to 0 net charge
CE1 CH3 0.24100 2
OE2 O -0.45000 2; from the carbonyl group (of e.g., GLN)
C C 0.450 3
O O -0.450 3
[bonds]
N H gb_2
N CA gb_21
CA CB gb_27
CA C gb_27
CB CG gb_27
CG SD gb_32
SD CE1 gb_32
SD OE2 gb_25
C O gb_5
C +N gb_10
[angles]
; ai aj ak gromos type
-C N H ga_32
-C N CA ga_31
H N CA ga_18
N CA CB ga_13
N CA C ga_13
CB CA C ga_13
CA CB CG ga_15
CB CG SD ga_16
CG SD CE1 ga_13
CG SD OE2 ga_13
CG SD OE3 ga_13
CE1 SD OE2 ga_13
CE1 SD OE3 ga_13
OE2 SD OE3 ga_13
CA C O ga_30
CA C +N ga_19
O C +N ga_33
[impropers]
; ai aj ak al gromos type
N -C CA H gi_1
CA N C CB gi_2
C CA +N O gi_1
[dihedrals]
; ai aj ak al gromos type
-C -C N CA gd_14
-C N CA C gd_44
-C N CA C gd_43
N CA CB CG gd_34
N CA C +N gd_45
N CA C +N gd_42
CA CB CG SD gd_34
CB CG SD CE gd_26

; cysteine sulfinic acid
[CSA]
[atoms]
N N -0.31000 0
H H 0.31000 0
CA CH1 0.00000 1
CB CH2 0.15000 2; from the carbon atom attached to the phosphate group of
nucleotides (e.g., ATP)
SG S 0.12000 2; to add up to -1 net charge
OD1 OM -0.63500 2; from the phosphate group of nucleotides (e.g., ATP)
OD2 OM -0.63500 2; from the phosphate group of nucleotides (e.g., ATP)
C C 0.450 3
O O -0.450 3
[bonds]
N H gb_2
N CA gb_21
CA CB gb_27
CA C gb_27
CB SG gb_32
SG OD1 gb_25
SG OD2 gb_25
C O gb_5
C +N gb_10
[angles]
; ai aj ak gromos type
-C N H ga_32
-C N CA ga_31
H N CA ga_18
N CA CB ga_13
N CA C ga_13
CB CA C ga_13
CA CB SG ga_16
CB SG OD1 ga_6
CB SG OD2 ga_6
OD1 SG OD2 ga_6
CA C O ga_30
CA C +N ga_19
O C +N ga_33
[impropers]
; ai aj ak al gromos type
N -C CA H gi_1
CA N C CB gi_2
C CA +N O gi_1
SG CB OD1 OD2 gi_2
[dihedrals]
; ai aj ak al gromos type

```

```

-CA -C N CA gd_14
-C N CA C gd_44
-C N CA C gd_43
N CA CB SG gd_34
N CA C +N gd_45
N CA C +N gd_42
CA CB SG OD1 gd_26

; cysteine acid
[CSE]
[atoms]
N N -0.31000 0
H H 0.31000 0
CA CH1 0.00000 1
CB CH2 0.15000 2; from the carbon atom attached to the phosphate group of
nucleotides (e.g., ATP)
SG S 0.75500 2; to add up to -1 net charge
OD1 OM -0.63500 2; from the phosphate group of nucleotides (e.g., ATP)
OD2 OM -0.63500 2; from the phosphate group of nucleotides (e.g., ATP)
OD3 OM -0.63500 2; from the phosphate group of nucleotides (e.g., ATP)
C C 0.450 3
O O -0.450 3
[bonds]
N H gb_2
N CA gb_21
CA CB gb_27
CA C gb_27
CB SG gb_32
SG OD1 gb_25
SG OD2 gb_25
SG OD3 gb_25
C O gb_5
C +N gb_10
[angles]
; ai aj ak gromos type
-C N H ga_32
-C N CA ga_31
H N CA ga_18
N CA CB ga_13
N CA C ga_13
CB CA C ga_13
CA CB SG ga_16
CB SG OD1 ga_13
OD1 SG OD2 ga_13
CB SG OD2 ga_13
CB SG OD3 ga_13
OD1 SG OD3 ga_13
OD2 SG OD3 ga_13
CA C O ga_30
CA C +N ga_19
O C +N ga_33
[impropers]
; ai aj ak al gromos type
N -C CA H gi_1
CA N C CB gi_2
C CA +N O gi_1
[dihedrals]
; ai aj ak al gromos type
-CA -C N CA gd_14
-C N CA C gd_44
-C N CA C gd_43
N CA CB SG gd_34
N CA C +N gd_45
N CA C +N gd_42
CA CB SG OD1 gd_26

; 3-nitrotyrosine (-1)
[YNI]
[atoms]
N N -0.31000 0
H H 0.31000 0
CA CH1 0.00000 1
CB CH2 0.00000 1
CG C 0.00000 1
CD1 C -0.14000 2
HD1 HC 0.14000 2
CD2 C -0.14000 3
HD2 HC 0.14000 3
CE1 C 0.10000 4; to add up to -1 net charge
NZ1 NR 0.05500 4; to add up to -1 net charge
OH1 O -0.36000 4; from the phosphate group of nucleotides (e.g., ATP)
OH2 O -0.36000 4; from the phosphate group of nucleotides (e.g., ATP)
CZ2 C 0.20000 4; to add up to -1 net charge
OH3 OM -0.63500 4; from the carboxyl group (of e.g., GLU)
CE2 C -0.14000 5
HE2 HC 0.14000 5
C C 0.450 6
O O -0.450 6
[bonds]
N H gb_2
N CA gb_21
CA CB gb_27
CA C gb_27
CB SG gb_32
SG OD1 gb_25
SG OD2 gb_25
SG OD3 gb_25
C O gb_5
C +N gb_10
[angles]
; ai aj ak gromos type
-C N H ga_32
-C N CA ga_31
H N CA ga_18
N CA CB ga_13
N CA C ga_13
CB CA C ga_13
CA CB SG ga_16
CB SG OD1 ga_13
OD1 SG OD2 ga_13
CB SG OD2 ga_13
CB SG OD3 ga_13
OD1 SG OD3 ga_13
OD2 SG OD3 ga_13
CA C O ga_30
CA C +N ga_19
O C +N ga_33
[impropers]
; ai aj ak al gromos type
N -C CA H gi_1
CA N C CB gi_2
CG CD1 CD2 CB gi_1
CG CD1 CE1 CZ2 gi_1
CG CD2 CE2 CZ2 gi_1
CD1 CG CD2 CE2 gi_1
CD1 CG CE1 HD1 gi_1
CD1 CE1 CZ2 CE2 gi_1
CD2 CG CD1 CE1 gi_1
CD2 CG CE2 HD2 gi_1
CD2 CE2 CZ2 CE1 gi_1
CE1 CD1 CZ2 NZ1 gi_1
HE2 CD2 CZ2 CE2 gi_1
NZ1 OH1 OH2 CE1 gi_1
CZ2 CE1 CE2 OH3 gi_1
C CA +N O gi_1
[dihedrals]
CB CG gb_27
CG CD1 gb_16
CG CD2 gb_16
CD1 HD1 gb_3
CD1 CE1 gb_16
CD2 HD2 gb_3
CD2 CE2 gb_16
CE1 NZ1 gb_12
CE1 CZ2 gb_16
CE2 HE2 gb_3
CE2 CZ2 gb_16
NZ1 OH1 gb_6
NZ1 OH2 gb_6
CZ2 OH3 gb_13
OH3 HH3 gb_1
C O gb_5
C +N gb_10
[exclusions]
; ai aj
CB HD1
CB HD2
CB CE1
CB CE2
CG HE2
CG NZ1
CG CZ2
CD1 HD2
CD1 CE2
CD1 OH3
HD1 CD2
HD1 NZ1
HD1 CZ2
CD2 CE1
CD2 OH3
HD2 HE2
HD2 CZ2
CE1 HE2
HE2 OH3
NZ1 CE2
NZ1 OH3
[angles]
; ai aj ak gromos type
-C N H ga_32
-C N CA ga_31
H N CA ga_18
N CA CB ga_13
N CA C ga_13
CB CA C ga_13
CA CB SG ga_16
CA CB CG ga_15
CB CG CD1 ga_27
CB CG CD2 ga_27
CD1 CG CD2 ga_27
CG CD1 HD1 ga_25
CG CD1 CE1 ga_27
HD1 CD1 CE1 ga_25
CG CD2 HD2 ga_25
CG CD2 CE2 ga_27
HD2 CD2 CE2 ga_25
CD1 CE1 NZ1 ga_27
CD1 CE1 CZ2 ga_27
NZ1 CE1 CZ2 ga_27
CD2 CE2 HE2 ga_25
CD2 CE2 CZ2 ga_27
HE2 CE2 CZ2 ga_25
CE1 NZ1 OH1 ga_27
CE1 NZ1 OH2 ga_27
OH1 NZ1 OH2 ga_27
CE1 CZ2 CE2 ga_27
CE1 CZ2 OH3 ga_27
CE2 CZ2 OH3 ga_27
CZ2 OH3 HH3 ga_12
CA C O ga_30
CA C +N ga_19
O C +N ga_33
[impropers]
; ai aj ak al gromos type
N -C CA H gi_1
CA N C CB gi_2
CG CD1 CD2 CB gi_1
CG CD1 CE1 CZ2 gi_1
CG CD2 CE2 CZ2 gi_1
CD1 CG CD2 CE2 gi_1
CD1 CG CE1 HD1 gi_1
CD1 CE1 CZ2 CE2 gi_1
CD2 CG CD1 CE1 gi_1
CD2 CG CE2 HD2 gi_1
CD2 CE2 CZ2 CE1 gi_1
CE1 CD1 CZ2 NZ1 gi_1
HE2 CD2 CZ2 CE2 gi_1
NZ1 OH1 OH2 CE1 gi_1
CZ2 CE1 CE2 OH3 gi_1
C CA +N O gi_1
[dihedrals]

```

```

; ai aj ak al gromos type
-CA -C N CA gd_14
-C N CA C gd_44
-C N CA C gd_43
N CA CB CG gd_34
N CA C +N gd_45
N CA C +N gd_42
CA CB CG CD1 gd_40
CD1 CE1 NZ1 OH1 gd_14
CE1 CZ2 OH3 HH3 gd_11

; 3-nitrotyrosine (0)
[ YNN ]
[ atoms ]
N N -0.31000 0
H H 0.31000 0
CA CH1 0.00000 1
CB CH2 0.00000 1
CG C 0.00000 1
CD1 C -0.14000 2
HD1 HC 0.14000 2
CD2 C -0.14000 3
HD2 HC 0.14000 3
CE1 C 0.10000 4 ; newly developed parameters tp match the experimental
HFE
NZ1 NR 0.30000 4 ; newly developed parameters tp match the experimental
HFE
OH1 O -0.20000 4 ; newly developed parameters tp match the experimental
HFE
OH2 O -0.20000 4 ; newly developed parameters tp match the experimental
HFE
CE2 C -0.14000 5
HE2 HC 0.14000 5
CZ2 C 0.05000 6 ; newly developed parameters tp match the experimental
HFE
OH3 OA -0.36000 6 ; newly developed parameters tp match the experimental
HFE
HH3 H 0.31000 6 ; newly developed parameters tp match the experimental
HFE
C C 0.450 7
O O -0.450 7
[ bonds ]
N H gb_2
N CA gb_21
CA CB gb_27
CA C gb_27
CB CG gb_27
CG CD1 gb_16
CG CD2 gb_16
CD1 HD1 gb_3
CD1 CE1 gb_16
CD2 HD2 gb_3
CD2 CE2 gb_16
CE1 NZ1 gb_12
CE1 CZ2 gb_16
CE2 HE2 gb_3
CE2 CZ2 gb_16
NZ1 OH1 gb_6
NZ1 OH2 gb_6
CZ2 OH3 gb_13
OH3 HH3 gb_1
C O gb_5
C +N gb_10
[ exclusions ]
; ai aj
CB HD1
CB HD2
CB CE1
CB CE2
CG HE2
CG NZ1
CG CZ2
CD1 HD2
CD1 CE2
CD1 OH3
HD1 CD2
HD1 NZ1
HD1 CZ2
CD2 CE1
CD2 OH3
HD2 HE2
HD2 CZ2
CE1 HE2
HE2 OH3
NZ1 CE2
NZ1 OH3
[ angles ]
; ai aj ak gromos type
-C N H ga_32
-C N CA ga_31
H N CA ga_18
N CA CB ga_13
N CA C ga_13
CB CA C ga_13
CA CB CG ga_15
CB CG CD1 ga_27
CB CG CD2 ga_27
CD1 CG CD2 ga_27
CG CD1 HD1 ga_25
CG CD1 CE1 ga_27
HD1 CD1 CE1 ga_25
CG CD2 HD2 ga_25
CG CD2 CE2 ga_27
HD2 CD2 CE2 ga_25
CD1 CE1 NZ1 ga_27
CD1 CE1 CZ2 ga_27
NZ1 CE1 CZ2 ga_27
CD2 CE2 HE2 ga_25
CD2 CE2 CZ2 ga_27
HE2 CE2 CZ2 ga_25
CE1 NZ1 OH1 ga_27
CE1 NZ1 OH2 ga_27
OH1 NZ1 OH2 ga_27
CE1 CZ2 CE2 ga_27
CE1 CZ2 OH3 ga_27
CE2 CZ2 OH3 ga_27
CZ2 OH3 HH3 ga_12
CA C O ga_30
CA C +N ga_19
O C +N ga_33
[ impropers ]
; ai aj ak al gromos type
N -C CA H gi_1
CA N C CB gi_2
CG CD1 CD2 CB gi_1
CG CD1 CE1 CZ2 gi_1
CG CD2 CE2 CZ2 gi_1
CD1 CG CD2 CE2 gi_1
CD1 CG CE1 HD1 gi_1
CD1 CE1 CZ2 CE2 gi_1
CD2 CG CD1 CE1 gi_1
CD2 CG CE2 HD2 gi_1
CD2 CE2 CZ2 CE1 gi_1
CE1 CD1 CZ2 NZ1 gi_1
HE2 CD2 CZ2 CE2 gi_1
NZ1 OH1 OH2 CE1 gi_1
CZ2 CE1 CE2 OH3 gi_1
C CA +N O gi_1
[ dihedrals ]
; ai aj ak al gromos type
-CA -C N CA gd_14
-C N CA C gd_44
-C N CA C gd_43
N CA CB CG gd_34
N CA C +N gd_45
N CA C +N gd_42
CA CB CG CD1 gd_40
CD1 CE1 NZ1 OH1 gd_14
CE1 CZ2 OH3 HH3 gd_11

; 3-nitrotyrosine (0)
[ YNB ]
[ atoms ]
N N -0.31000 0
H H 0.31000 0
CA CH1 0.00000 1
CB CH2 0.00000 1
CG C 0.00000 1
CD1 C -0.14000 2
HD1 HC 0.14000 2
CD2 C -0.14000 3
HD2 HC 0.14000 3
CE1 C 0.10000 4 ; to add up to 0 net charge
NZ1 NR 0.62000 4 ; to add up to 0 net charge
OH1 O -0.36000 4 ; from the phosphate group of nucleotides (e.g., ATP)
OH2 O -0.36000 4 ; from the phosphate group of nucleotides (e.g., ATP)
CE2 C -0.14000 5
HE2 HC 0.14000 5
CZ2 C 0.20300 6
OH3 OA -0.61100 6
HH3 H 0.40800 6
C C 0.450 7
O O -0.450 7
[ bonds ]
N H gb_2
N CA gb_21
CA CB gb_27
CA C gb_27
CB CG gb_27
CG CD1 gb_16
CG CD2 gb_16
CD1 HD1 gb_3
CD1 CE1 gb_16
CD2 HD2 gb_3
CD2 CE2 gb_16
CE1 NZ1 gb_12
CE1 CZ2 gb_16
CE2 CE2 gb_16
CE1 NZ1 gb_12
[ angles ]
; ai aj ak gromos type
-C N H ga_32
-C N CA ga_31
H N CA ga_18
N CA CB ga_13
N CA C ga_13

```

```

CE1 C22 gb_16
CE2 HE2 gb_3
CE2 C22 gb_16
NZ1 OH1 gb_6
NZ1 OH2 gb_6
C22 OH3 gb_13
OH3 HH3 gb_1
  C O gb_5
  C +N gb_10
[exclusions]
; ai aj
CB HD1
CB HD2
CB CE1
CB CE2
CG HE2
CG NZ1
CG C22
CD1 HD2
CD1 CE2
CD1 OH3
HD1 CD2
HD1 NZ1
HD1 C22
CD2 CE1
CD2 OH3
HD2 HE2
HD2 C22
CE1 HE2
HE2 OH3
NZ1 CE2
NZ1 OH3
[angles]
; ai aj ak gromos type
-C N H ga_32
-C N CA ga_31
H N CA ga_18
N CA CB ga_13
N CA C ga_13
CB CA C ga_13
CA CB CG ga_15
CB CG CD1 ga_27
CB CG CD2 ga_27
CD1 CG CD2 ga_27
CG CD1 HD1 ga_25
CG CD1 CE1 ga_27
HD1 CD1 CE1 ga_25
CG CD2 HD2 ga_25
CG CD2 CE2 ga_27
HD2 CD2 CE2 ga_25
CD1 CE1 NZ1 ga_27
CD1 CE1 C22 ga_27
NZ1 CE1 C22 ga_27
CD2 CE2 HE2 ga_25
CD2 CE2 C22 ga_27
HE2 CE2 C22 ga_25
CE1 NZ1 OH1 ga_27
CE1 NZ1 OH2 ga_27
OH1 NZ1 OH2 ga_27
CE1 C22 CE2 ga_27
CE1 C22 OH3 ga_27
CE2 C22 OH3 ga_27
C22 OH3 HH3 ga_12
CA C O ga_30
CA C +N ga_19
O C +N ga_33
[impropers]
; ai aj ak al gromos type
N -C CA H gi_1
CA N C CB gi_2
CG CD1 CD2 CB gi_1
CG CD1 CE1 C22 gi_1
CG CD2 CE2 C22 gi_1
CD1 CG CD2 CE2 gi_1
CD1 CG CE1 HD1 gi_1
CD1 CE1 C22 CE2 gi_1
CD2 CG CD1 CE1 gi_1
CD2 CG CE2 HD2 gi_1
CD2 CE2 C22 CE1 gi_1
CE1 CD1 C22 NZ1 gi_1
HE2 CD2 C22 CE2 gi_1
NZ1 OH1 OH2 CE1 gi_1
C22 CE1 CE2 OH3 gi_1
  C CA +N O gi_1
[dihedrals]
; ai aj ak al gromos type
-CA -C N CA gd_14
-C N CA C gd_44
-C N CA C gd_43
N CA CB CG gd_34
N CA C +N gd_45
N CA C +N gd_42
CA CB CG CD1 gd_40
CD1 CE1 NZ1 OH1 gd_14
CE1 C22 OH3 HH3 gd_11
; 6-nitrotryptophan
[WNI]
[atoms]
  N N -0.31000 0
  H H 0.31000 0
CA CH1 0.00000 1
CB CH2 0.00000 1
CG C -0.21000 2
CD1 C -0.14000 2
HD1 HC 0.14000 2
CD2 C 0.00000 2
NE1 NR -0.10000 2
HE1 H 0.31000 2
CE2 C 0.00000 2
CE3 C -0.14000 3
HE3 HC 0.14000 3
C22 C -0.14000 4
HZ2 HC 0.14000 4
CZ3 C -0.14000 5
HZ3 HC 0.14000 5
CH2 C 0.10000 6 ; to add up to 0 net charge
NT NR 0.62000 6 ; to add up to 0 net charge
OI1 O -0.36000 6 ; from the phosphate group of nucleotides (e.g., ATP)
OI2 O -0.36000 6 ; from the phosphate group of nucleotides (e.g., ATP)
  C C 0.450 7
  O O -0.450 7
[bonds]
  N H gb_2
  N CA gb_21
  CA CB gb_27
  CA C gb_27
  CB CG gb_27
  CG CD1 gb_10
  CG CD2 gb_16
  CD1 HD1 gb_3
  CD1 NE1 gb_10
  CD2 CE2 gb_16
  CD2 CE3 gb_16
  NE1 HE1 gb_2
  NE1 CE2 gb_10
  CE2 C22 gb_16
  CE3 HE3 gb_3
  CE3 CZ3 gb_16
  C22 HZ2 gb_3
  C22 CH2 gb_16
  CZ3 HZ3 gb_3
  CZ3 CH2 gb_16
  CH2 NT gb_12
  NT OI1 gb_6
  NT OI2 gb_6
  C O gb_5
  C +N gb_10
[exclusions]
; ai aj
CB HD1
CB NE1
CB CE2
CB CE3
CG HE1
CG HE3
CG C22
CG CZ3
CD1 CE3
CD1 C22
HD1 CD2
HD1 HE1
HD1 CE2
CD2 HE1
CD2 HZ2
CD2 HZ3
CD2 CH2
NE1 CE3
NE1 HZ2
NE1 CH2
HE1 C22
CE2 HE3
CE2 CZ3
CE2 NT
CE3 C22
CE3 NT
HE3 HZ3
HE3 CH2
C22 HZ3
HZ2 CZ3
HZ2 NT
HZ3 NT
[angles]
; ai aj ak gromos type
-C N H ga_32
-C N CA ga_31

```

```

H N CA ga_18
N CA CB ga_13
N CA C ga_13
CB CA C ga_13
CA CB CG ga_15
CB CG CD1 ga_37
CB CG CD2 ga_37
CD1 CG CD2 ga_7
CG CD1 HD1 ga_36
CG CD1 NE1 ga_7
HD1 CD1 NE1 ga_36
CG CD2 CE2 ga_7
CG CD2 CE3 ga_39
CE2 CD2 CE3 ga_27
CD1 NE1 HE1 ga_36
CD1 NE1 CE2 ga_7
HE1 NE1 CE2 ga_36
CD2 CE2 NE1 ga_7
CD2 CE2 CZ2 ga_27
NE1 CE2 CZ2 ga_39
CD2 CE3 HE3 ga_25
CD2 CE3 CZ3 ga_27
HE3 CE3 CZ3 ga_25
CE2 CZ2 HZ2 ga_25
CE2 CZ2 CH2 ga_27
HZ2 CZ2 CH2 ga_25
CE3 CZ3 HZ3 ga_25
CE3 CZ3 CH2 ga_27
HZ3 CZ3 CH2 ga_25
CZ2 CH2 CZ3 ga_27
CZ2 CH2 NT ga_27
CZ3 CH2 NT ga_27
CH2 NT O11 ga_27
CH2 NT O12 ga_27
O11 NT O12 ga_27
CA C O ga_30
CA C +N ga_19
O C +N ga_33
[impropers]
; ai aj ak al gromos type
N -C CA H gi_1
CA N C CB gi_2
CG CD1 CD2 CB gi_1
CG CD1 NE1 CE2 gi_1
CG CD2 CE2 NE1 gi_1
CD1 CG CD2 CE2 gi_1
CD1 CG NE1 HD1 gi_1
CD1 NE1 CE2 CD2 gi_1
CD2 CG CD1 NE1 gi_1
CD2 CE2 CE3 CG gi_1
CD2 CE2 CZ2 CH2 gi_1
CD2 CE3 CZ3 CH2 gi_1
NE1 CD1 CE2 HE1 gi_1
CE2 CD2 CE3 CZ3 gi_1
CE2 CD2 CZ2 NE1 gi_1
CE2 CZ2 CH2 CZ3 gi_1
CE3 CD2 CE2 CZ2 gi_1
CE3 CD2 CZ3 HE3 gi_1
CE3 CZ3 CH2 CZ2 gi_1
CZ2 CE2 CH2 HZ2 gi_1
CZ3 CE3 CH2 HZ3 gi_1
CH2 CZ2 CZ3 NT gi_1
NT O11 O12 CH2 gi_1
C CA +N O gi_1
[dihedrals]
; ai aj ak al gromos type
-C -C N CA gd_14
-C N CA C gd_44
-C N CA C gd_43
N CA CB CG gd_34
N CA C +N gd_45
N CA C +N gd_42
CA CB CG CD2 gd_40
CZ2 CH2 NT O11 gd_14

; kynurenine
[WKY]
[atoms]
N N -0.31000 0
H H 0.31000 0
CA CH1 0.00000 1
CB CH2 0.00000 1
CG C 0.45000 2
OD1 O -0.45000 2
CD2 C 0.00000 3
CE1 C 0.00000 3
NZ1 NT -0.88000 4; from ARGN
HZ11 H 0.44000 4; from ARGN
HZ12 H 0.44000 4; from ARGN
CE2 C -0.14000 5
HE2 HC 0.14000 5
CZ2 C -0.14000 6
HZ2 HC 0.14000 6
CZ3 C -0.14000 7
HZ3 HC 0.14000 7
CH C -0.14000 8
HH HC 0.14000 8
C C 0.450 9
O O -0.450 9
[bonds]
N H gb_2
N CA gb_21
CA CB gb_27
CA C gb_27
CB CG gb_27
CG OD1 gb_5
CG CD2 gb_23
CD2 CE1 gb_16
CD2 CE2 gb_16
CE1 NZ1 gb_9
CE1 CZ2 gb_16
CE2 HE2 gb_3
CE2 CZ3 gb_16
NZ1 HZ11 gb_2
NZ1 HZ12 gb_2
CZ2 HZ2 gb_3
CZ2 CH gb_16
CZ3 HZ3 gb_3
CZ3 CH gb_16
CH HH gb_3
C O gb_5
C +N gb_10
[exclusions]
; ai aj
CB CE1
CB CE2
CG NZ1
CG HE2
CG CZ2
CG CZ3
CD2 HZ11
CD2 HZ12
CD2 HZ2
CD2 HZ3
CD2 CH
CE1 HE2
CE1 CZ3
CE1 HH
CE2 CZ2
CE2 HH
HE2 HZ3
HE2 CH
NZ1 CE2
NZ1 HZ2
NZ1 CH
HZ11 CZ2
HZ12 CZ2
CZ2 HZ3
HZ2 CZ3
HZ2 HH
HZ3 HH
[angles]
; ai aj ak gromos type
-C N H ga_32
-C N CA ga_31
H N CA ga_18
N CA CB ga_13
N CA C ga_13
CB CA C ga_13
CA CB CG ga_15
CB CG OD1 ga_27
CB CG CD2 ga_27
OD1 CG CD2 ga_27
CG CD2 CE1 ga_27
CG CD2 CE2 ga_27
CE1 CD2 CE2 ga_27
CD2 CE1 NZ1 ga_27
CD2 CE1 CZ2 ga_27
NZ1 CE1 CZ2 ga_27
CD2 CE2 HE2 ga_25
CD2 CE2 CZ3 ga_27
HE2 CE2 CZ3 ga_25
CE1 NZ1 HZ11 ga_23
CE1 NZ1 HZ12 ga_23
HZ11 NZ1 HZ12 ga_24
CE1 CZ2 HZ2 ga_25
CE1 CZ2 CH ga_27
HZ2 CZ2 CH ga_25
CE2 CZ3 HZ3 ga_25
CE2 CZ3 CH ga_27
HZ3 CZ3 CH ga_25
CZ2 CH CZ3 ga_27
CZ2 CH HH ga_25
CZ3 CH HH ga_25
CA C O ga_30
CA C +N ga_19

```

```

O C +N ga_33
[ impropers ]
; ai aj ak al gromos type
N -C CA H gi_1
CA N C CB gi_2
CG CD2 OD1 CB gi_1
CD2 CE1 CE2 CG gi_1
CD2 CE1 CZ2 CH gi_1
CD2 CE2 CZ3 CH gi_1
CE1 CD2 CE2 CZ3 gi_1
CE1 CD2 CZ2 NZ1 gi_1
CE1 CZ2 CH CZ3 gi_1
CE2 CD2 CE1 CZ2 gi_1
CE2 CD2 CZ3 HE2 gi_1
CE2 CZ3 CH CZ2 gi_1
NZ1 HZ11 HZ12 CE1 gi_1
HZ2 CE1 CH CZ2 gi_1
HZ3 CE2 CH CZ3 gi_1
CH CZ2 CZ3 HH gi_1
C CA +N O gi_1
[ dihedrals ]
; ai aj ak al gromos type
-CA -C N CA gd_14
-C N CA C gd_44
-C N CA C gd_43
N CA CB CG gd_34
N CA C +N gd_45
N CA C +N gd_42
CA CB CG CD2 gd_40
CB CG CD2 CE1 gd_10
CD2 CE1 NZ1 HZ11 gd_14

; 3-hydroxykynurenine
[WKH]
[ atoms ]
N N -0.31000 0
H H 0.31000 0
CA CH1 0.00000 1
CB CH2 0.00000 1
CG C 0.45000 2
OD1 O -0.45000 2
CD2 C 0.00000 3
CE1 C 0.00000 3
NZ1 NT -0.88000 4 ; from ARGN
HZ11 H 0.44000 4 ; from ARGN
HZ12 H 0.44000 4 ; from ARGN
CE2 C -0.14000 5
HE2 HC 0.14000 5
CZ2 C 0.20300 6 ; from the hydroxyl group of TYR
OH1 OA -0.61100 6 ; from the hydroxyl group of TYR
HH1 H 0.40800 6 ; from the hydroxyl group of TYR
CZ3 C -0.14000 7
HZ3 HC 0.14000 7
CH2 C -0.14000 8
HH2 HC 0.14000 8
C C 0.450 9
O O -0.450 9
[ bonds ]
N H gb_2
N CA gb_21
CA CB gb_27
CA C gb_27
CB CG gb_27
CG OD1 gb_5
CG CD2 gb_23
CD2 CE1 gb_16
CD2 CE2 gb_16
CE1 NZ1 gb_9
CE1 CZ2 gb_16
CE2 HE2 gb_3
CE2 CZ3 gb_16
NZ1 HZ11 gb_2
NZ1 HZ12 gb_2
CZ2 OH1 gb_13
CZ2 CH2 gb_16
CZ3 HZ3 gb_3
CZ3 CH2 gb_16
OH1 HH1 gb_1
CH2 HH2 gb_3
C O gb_5
C +N gb_10
[ exclusions ]
; ai aj
CB CE1
CB CE2
CG HE2
CG NZ1
CG CZ2
CG CZ3
CD2 HZ11
CD2 HZ12
CD2 HZ3
CD2 OH1
CD2 CH2
CE1 HE2
CE1 CZ3
CE1 HH1
CE1 HH2
CE2 CZ2
CE2 HH2
HE2 HZ3
HE2 CH2
NZ1 CE2
NZ1 OH1
NZ1 HH1
NZ1 CH2
HZ11 CZ2
HZ11 OH1
HZ12 CZ2
HZ12 OH1
CZ2 HZ3
HZ3 HH2
OH1 CZ3
OH1 HH2
HH1 CH2
[ angles ]
; ai aj ak gromos type
-C N H ga_32
-C N CA ga_31
H N CA ga_18
N CA CB ga_13
N CA C ga_13
CB CA C ga_13
CA CB CG ga_15
CB CG OD1 ga_27
CB CG CD2 ga_27
OD1 CG CD2 ga_27
CG CD2 CE1 ga_27
CG CD2 CE2 ga_27
CE1 CD2 CE2 ga_27
CD2 CE1 NZ1 ga_27
CD2 CE1 CZ2 ga_27
NZ1 CE1 CZ2 ga_27
CD2 CE2 HE2 ga_25
CD2 CE2 CZ3 ga_27
HE2 CE2 CZ3 ga_25
CE1 NZ1 HZ11 ga_23
CE1 NZ1 HZ12 ga_23
HZ11 NZ1 HZ12 ga_24
CE1 CZ2 OH1 ga_27
CE1 CZ2 CH2 ga_27
OH1 CZ2 CH2 ga_27
CE2 CZ3 HZ3 ga_25
CE2 CZ3 CH2 ga_27
HZ3 CZ3 CH2 ga_25
CZ2 OH1 HH1 ga_12
CZ2 CH2 CZ3 ga_27
CZ2 CH2 HH2 ga_25
CZ3 CH2 HH2 ga_25
CA C O ga_30
CA C +N ga_19
O C +N ga_33
[ impropers ]
; ai aj ak al gromos type
N -C CA H gi_1
CA N C CB gi_2
CG CD2 OD1 CB gi_1
CD2 CE1 CE2 CG gi_1
CD2 CE1 CZ2 CH2 gi_1
CD2 CE2 CZ3 CH2 gi_1
CE1 CD2 CE2 CZ3 gi_1
CE1 CD2 CZ2 NZ1 gi_1
CE1 CZ2 CH2 CZ3 gi_1
CE2 CD2 CE1 CZ2 gi_1
CE2 CD2 CZ3 HE2 gi_1
CE2 CZ3 CH2 CZ2 gi_1
NZ1 HZ11 HZ12 CE1 gi_1
OH1 CE1 CH2 CZ2 gi_1
HZ3 CE2 CH2 CZ3 gi_1
CH2 CZ2 CZ3 HH2 gi_1
C CA +N O gi_1
[ dihedrals ]
; ai aj ak al gromos type
-CA -C N CA gd_14
-C N CA C gd_44
-C N CA C gd_43
N CA CB CG gd_34
N CA C +N gd_45
N CA C +N gd_42
CA CB CG CD2 gd_40
CB CG CD2 CE1 gd_10
CD2 CE1 NZ1 HZ11 gd_14
CE1 CZ2 OH1 HH1 gd_11

; formyl-kynurenine
[WKF]

```



```

[ atoms ]
N N -0.31000 0
H H 0.31000 0
CA CH1 0.00000 1
CB CH2 0.00000 1
CG C 0.45000 2
OD1 O -0.45000 2
CD2 C 0.00000 3
CE1 C 0.00000 3
NZ1 N -0.15000 4 ; by analogy to ASN/GLN and the peptide bond
HZ1 H 0.31000 4 ; from the hydrogen of the peptide bond
CH1 C 0.19000 4 ; by analogy to ASN/GLN, the peptide bond and the
aldehyde group reported by Dolenc et al. DOI: 10.1093/nar/gki195
HH1 HC 0.10000 4 ; by analogy to the aldehyde group reported by Dolenc et
al. DOI: 10.1093/nar/gki195
OI O -0.45000 4 ; from the carbonyl group (of e.g., GLN)
CE2 C -0.14000 5
HE2 HC 0.14000 5
CZ2 C -0.14000 6
HZ2 HC 0.14000 6
CZ3 C -0.14000 7
HZ3 HC 0.14000 7
CH2 C -0.14000 8
HH2 HC 0.14000 8
C C 0.450 9
O O -0.450 9
[ bonds ]
N H gb_2
N CA gb_21
CA CB gb_27
CA C gb_27
CB CG gb_27
CG OD1 gb_5
CG CD2 gb_23
CD2 CE1 gb_16
CD2 CE2 gb_16
CE1 NZ1 gb_9
CE1 CZ2 gb_16
CE2 HE2 gb_3
CE2 CZ3 gb_16
NZ1 HZ1 gb_2
NZ1 CH1 gb_10
CZ2 HZ2 gb_3
CZ2 CH2 gb_16
CZ3 HZ3 gb_3
CZ3 CH2 gb_16
CH1 HH1 gb_3
CH1 OI gb_5
CH2 HH2 gb_3
C O gb_5
C +N gb_10
[ exclusions ]
; ai aj
CB CE1
CB CE2
CG NZ1
CG HE2
CG CZ2
CG CZ3
CD2 HZ1
CD2 HZ2
CD2 HZ3
CD2 CH2
CE1 HE2
CE1 CZ3
CE1 HH2
CE2 CZ2
CE2 HH2
HE2 HZ3
HE2 CH2
NZ1 CE2
NZ1 HZ2
NZ1 CH2
HZ1 CZ2
CZ2 HZ3
HZ2 CZ3
HZ2 HH2
HZ3 HH2
[ angles ]
; ai aj ak gromos type
-C N H ga_32
-C N CA ga_31
H N CA ga_18
N CA CB ga_13
N CA C ga_13
CB CA C ga_13
CA CB CG ga_15
CB CG OD1 ga_27
CB CG CD2 ga_27
OD1 CG CD2 ga_27
CG CD2 CE1 ga_27
CG CD2 CE2 ga_27
CE1 CD2 CE2 ga_27
CD2 CE1 NZ1 ga_27
CD2 CE1 CZ2 ga_27
NZ1 CE1 CZ2 ga_27
CE1 CZ2 HZ2 ga_25
HZ2 CZ2 CH2 ga_25
CE2 CZ3 HZ3 ga_25
CE2 CZ3 CH2 ga_27
HZ3 CZ3 CH2 ga_25
NZ1 CH1 HH1 ga_19
NZ1 CH1 OI ga_33
HH1 CH1 OI ga_30
CZ2 CH2 CZ3 ga_27
CZ2 CH2 HH2 ga_25
CZ3 CH2 HH2 ga_25
CA C O ga_30
CA C +N ga_19
O C +N ga_33
[ impropers ]
; ai aj ak al gromos type
N -C CA H gi_1
CA N C CB gi_2
CG CD2 OD1 CB gi_1
CD2 CE1 CE2 CG gi_1
CD2 CE1 CZ2 CH2 gi_1
CD2 CE2 CZ3 CH2 gi_1
CE1 CD2 CE2 CZ3 gi_1
CE1 CD2 CZ2 NZ1 gi_1
CE1 CZ2 CH2 CZ3 gi_1
CE2 CD2 CE1 CZ2 gi_1
CE2 CD2 CZ3 HE2 gi_1
CE2 CZ3 CH2 CZ2 gi_1
NZ1 CH1 CE1 HZ1 gi_1
HZ2 CE1 CH2 CZ2 gi_1
HZ3 CE2 CH2 CZ3 gi_1
CH1 OI NZ1 HH1 gi_1
CH2 CZ2 CZ3 HH2 gi_1
C CA +N O gi_1
[ dihedrals ]
; ai aj ak al gromos type
-C -C N CA gd_14
-C N CA C gd_44
-C N CA C gd_43
N CA CB CG gd_34
N CA C +N gd_45
N CA C +N gd_42
CA CB CG CD2 gd_40
CB CG CD2 CE1 gd_10
CD2 CE1 NZ1 CH1 gd_14
CE1 NZ1 CH1 OI gd_14
; chlorotyrosine
[ YCH ]
[ atoms ]
N N -0.31000 0
H H 0.31000 0
CA CH1 0.00000 1
CB CH2 0.00000 1
CG C 0.00000 1
CD1 C -0.14000 2
HD1 HC 0.14000 2
CD2 C -0.14000 3
HD2 HC 0.14000 3
CE1 C 0.08700 4 ; from CHCL3
CLZ1 CL -0.08700 4 ; from CHCL3
CE2 C -0.14000 5
HE2 HC 0.14000 5
CZ2 C 0.20300 6
OH OA -0.61100 6
HH H 0.40800 6
C C 0.450 7
O O -0.450 7
[ bonds ]
N H gb_2
N CA gb_21
CA CB gb_27
CA C gb_27
CB CG gb_27
CG CD1 gb_16
CG CD2 gb_16
CD1 HD1 gb_3
CD1 CE1 gb_16
CD2 HD2 gb_3
CD2 CE2 gb_16
CE1 CLZ1 gb_40
CE1 CZ2 gb_16
CE2 HE2 gb_3

```

```

CE2 CZ2 gb_16
CZ2 OH gb_13
OH HH gb_1
C O gb_5
C +N gb_10
[ exclusions ]
; ai aj
CB HD1
CB HD2
CB CE1
CB CE2
CG HE2
CG CLZ1
CG CZ2
CD1 HD2
CD1 CE2
CD1 OH
HD1 CD2
HD1 CLZ1
HD1 CZ2
CD2 CE1
CD2 OH
HD2 HE2
HD2 CZ2
CE1 HE2
HE2 OH
CLZ1 CE2
CLZ1 OH
[ angles ]
; ai aj ak gromos type
-C N H ga_32
-C N CA ga_31
H N CA ga_18
N CA CB ga_13
N CA C ga_13
CB CA C ga_13
CA CB CG ga_15
CB CG CD1 ga_27
CB CG CD2 ga_27
CD1 CG CD2 ga_27
CG CD1 HD1 ga_25
CG CD1 CE1 ga_27
HD1 CD1 CE1 ga_25
CG CD2 HD2 ga_25
CG CD2 CE2 ga_27
HD2 CD2 CE2 ga_25
CD1 CE1 CLZ1 ga_27
CD1 CE1 CZ2 ga_27
CLZ1 CE1 CZ2 ga_27
CD2 CE2 HE2 ga_25
CD2 CE2 CZ2 ga_27
HE2 CE2 CZ2 ga_25
CE1 CZ2 CE2 ga_27
CE1 CZ2 OH ga_27
CE2 CZ2 OH ga_27
CZ2 OH HH ga_12
CA C O ga_30
CA C +N ga_19
O C +N ga_33
[ impropers ]
; ai aj ak al gromos type
N -C CA H gi_1
CA N C CB gi_2
CG CD1 CD2 CB gi_1
CG CD1 CE1 CZ2 gi_1
CG CD2 CE2 CZ2 gi_1
CD1 CG CD2 CE2 gi_1
CD1 CG CE1 HD1 gi_1
CD1 CE1 CZ2 CE2 gi_1
CD2 CG CD1 CE1 gi_1
CD2 CG CE2 HD2 gi_1
CD2 CE2 CZ2 CE1 gi_1
CLZ1 CD1 CZ2 CE1 gi_1
HE2 CD2 CZ2 CE2 gi_1
CZ2 CE1 CE2 OH gi_1
C CA +N O gi_1
[ dihedrals ]
; ai aj ak al gromos type
-C A -C N CA gd_14
-C N CA C gd_44
-C N CA C gd_43
N CA CB CG gd_34
N CA C +N gd_45
N CA C +N gd_42
CA CB CG CD gd_34
CB CG CD CE gd_34
CG CD CE NZ gd_34
CD CE NZ CH gd_39
CE NZ CH NI2 gd_14
NZ CH NI2 HI21 gd_14
; carboxyllysine (-1)
[ KCA ]
[ atoms ]
N N -0.31000 0
H H 0.31000 0
CA CH1 0.00000 1
CB CH2 0.00000 1
CG CH2 0.00000 2
CD CH2 0.00000 2
CE CH2 0.00000 3
NZ N -0.31000 4 ; from the peptide bond
HZ H 0.31000 4 ; from the peptide bond
CH C 0.27000 5 ; from the carboxyl group (of e.g., GLU)
OI1 OM -0.63500 5 ; from the carboxyl group (of e.g., GLU)
OI2 OM -0.63500 5 ; from the carboxyl group (of e.g., GLU)
C C 0.450 6

```

```

O O -0.450 6
[ bonds ]
N H gb_2
N CA gb_21
CA CB gb_27
CA C gb_27
CB CG gb_27
CG CD gb_27
CD CE gb_27
CE NZ gb_21
NZ HZ gb_2
NZ CH gb_10
CH OI1 gb_6
CH OI2 gb_6
C O gb_5
C +N gb_10
[ angles ]
; ai aj ak gromos type
-C N H ga_32
-C N CA ga_31
H N CA ga_18
N CA CB ga_13
N CA C ga_13
CB CA C ga_13
CA CB CG ga_15
CB CG CD ga_15
CG CD CE ga_15
CD CE NZ ga_15
CE NZ HZ ga_18
CE NZ CH ga_31
HZ NZ CH ga_32
NZ CH OI1 ga_22
NZ CH OI2 ga_22
OI1 CH OI2 ga_38
CA C O ga_30
CA C +N ga_19
O C +N ga_33
[ impropers ]
; ai aj ak al gromos type
N -C CA H gi_1
CA N C CB gi_2
C CA +N O gi_1
NZ CH CE HZ gi_1
CH OI2 OI1 NZ gi_1
[ dihedrals ]
; ai aj ak al gromos type
-C -C N CA gd_14
-C N CA C gd_44
-C N CA C gd_43
N CA CB CG gd_34
N CA C +N gd_45
N CA C +N gd_42
CA CB CG CD gd_34
CB CG CD CE gd_34
CG CD CE NZ gd_34
CD CE NZ CH gd_39
CE NZ CH OI2 gd_14
NZ CH OI2 HI2 gd_12
; S-carbamoyl-cysteine
[ CAM ]
[ atoms ]
N N -0.31000 0
H H 0.31000 0
CA CH1 0.00000 1
CB CH2 0.00000 2
SG S 0.00000 2
CD C 0.29000 3; from ASN/GLN
OE1 O -0.45000 3; from ASN/GLN
NE2 NT -0.72000 3; from ASN/GLN
HE21 H 0.44000 3; from ASN/GLN
HE22 H 0.44000 3; from ASN/GLN
C C 0.450 4
O O -0.450 4
[ bonds ]
N H gb_2
N CA gb_21
CA CB gb_27
CA C gb_27
CB SG gb_32
SG CD gb_32
CD OE1 gb_5
CD NE2 gb_9
NE2 HE21 gb_2
NE2 HE22 gb_2
C O gb_5
C +N gb_10
[ angles ]
; ai aj ak gromos type
-C N H ga_32
-C N CA ga_31
H N CA ga_18
N CA CB ga_13
N CA C ga_13
CB CA C ga_13
CA CB SG ga_16
CB SG CD ga_4
SG CD OE1 ga_30
SG CD NE2 ga_19
OE1 CD NE2 ga_33
CD NE2 HE21 ga_23
CD NE2 HE22 ga_23
HE21 NE2 HE22 ga_24
CA C O ga_30
CA C +N ga_19
O C +N ga_33
[ impropers ]
; ai aj ak al gromos type
N -C CA H gi_1
[ atoms ]
N N -0.31000 0
H H 0.31000 0
CA CH1 0.00000 1
CB CH2 0.00000 1
CG CH2 0.00000 2
CD CH2 0.00000 2
CE CH2 0.00000 3
NZ N -0.31000 4; from the peptide bond
HZ H 0.31000 4; from the peptide bond
CH C 0.33000 5; from the carboxyl group (of e.g., GLUH)
OI1 O -0.45000 5; from the carboxyl group (of e.g., GLUH)
OI2 OA -0.28800 5; from the carboxyl group (of e.g., GLUH)
HI2 H 0.40800 5; from the carboxyl group (of e.g., GLUH)
C C 0.450 6
O O -0.450 6
[ bonds ]
N H gb_2
N CA gb_21
CA CB gb_27
CA C gb_27
CB CG gb_27
CG CD gb_27
CD CE gb_27
CE NZ gb_21
NZ HZ gb_2
NZ CH gb_10
CH OI1 gb_5
CH OI2 gb_13
OI2 HI2 gb_1
C O gb_5
C +N gb_10
[ angles ]
; ai aj ak gromos type
N -C CA H gi_1

```

```

CA N C CB gi_2
CD OE1 NE2 SG gi_1
NE2 HE21 HE22 CD gi_1
C CA +N O gi_1
[ dihedrals ]
; ai aj ak al gromos type
-CA -C N CA gd_14
-C N CA C gd_44
-C N CA C gd_43
N CA CB SG gd_34
CA CB SG CD gd_26
CB SG CD NE2 gd_40
SG CD NE2 HE21 gd_14
N CA C +N gd_45
N CA C +N gd_42

; norleucine
[LNO]
[ atoms ]
N N -0.31000 0
H H 0.31000 0
CA CH1 0.00000 1
CB CH2 0.00000 1; from aliphatic carbon atoms
CG CH2 0.00000 1; from aliphatic carbon atoms
CD CH2 0.00000 2; from aliphatic carbon atoms
CE CH3 0.00000 2; from aliphatic carbon atoms
C C 0.450 3
O O -0.450 3
[ bonds ]
N H gb_2
N CA gb_21
CA CB gb_27
CA C gb_27
CB CG gb_27
CG CD gb_27
CD CE gb_27
C O gb_5
C +N gb_10
[ angles ]
; ai aj ak gromos type
-C N H ga_32
-C N CA ga_31
H N CA ga_18
N CA CB ga_13
N CA C ga_13
CB CA C ga_13
CA CB CG ga_15
CB CG CD ga_15
CG CD CE ga_15
CA C O ga_30
CA C +N ga_19
O C +N ga_33
[ impropers ]
; ai aj ak al gromos type
N -C CA H gi_1
CA N C CB gi_2
C CA +N O gi_1
[ dihedrals ]
; ai aj ak al gromos type
-CA -C N CA gd_14
-C N CA C gd_44
-C N CA C gd_43
N CA CB CG gd_34
N CA C +N gd_45
N CA C +N gd_42
CA CB CG CD gd_34
CB CG CD CE gd_34

; pyruvic acid (N-terminal modification)
[PYA]
[ atoms ]
CA C 0.45000 0; from the carbonyl group (of e.g., GLN)
OB2 O -0.45000 0; from the carbonyl group (of e.g., GLN)
CB1 CH3 0.00000 1; from aliphatic carbon atoms
C C 0.450 2
O O -0.450 2
[ bonds ]
CA CB1 gb_27
CA OB2 gb_5
CA C gb_23 ; shorter bond type to account for double bond effect
C O gb_5
C +N gb_10
[ angles ]
; ai aj ak gromos type
CB1 CA OB2 ga_27
CB1 CA C ga_27
OB2 CA C ga_27
CA C O ga_30
CA C +N ga_19
O C +N ga_33
[ impropers ]
; ai aj ak al gromos type
CA OB2 C CB1 gi_1

C CA +N O gi_1
[ dihedrals ]
; ai aj ak al gromos type
CB1 CA C +N gd_14

; aminoacids.n.tdb file (N-terminal parameters)
; N-methyl-AA (0)
[ 1NM ]
[ replace ]
N NT 14.0067 -0.88
; from dimethylamine reported by Oostenbrink et al. DOI:
10.1002/cphc.200400542
CA CH1 13.019 0.220 0
; from dimethylamine reported by Oostenbrink et al. DOI:
10.1002/cphc.200400542
[ add ]
1 1 H1 N CA C
H 1.008 0.440
; from dimethylamine reported by Oostenbrink et al. DOI:
10.1002/cphc.200400542
1 4 CN1 N CA C
CH3 15.035 0.220
; from dimethylamine reported by Oostenbrink et al. DOI:
10.1002/cphc.200400542
[ delete ]
H
[ bonds ]
N H1 gb_2
N CN1 gb_21
[ angles ]
CN1 N H1 ga_11
CA N H1 ga_11
CA N CN1 ga_13
[ dihedrals ]
CN1 N CA C gd_29

; N-methyl-glycine (0)
[ GLY-1NM ]
[ replace ]
N NT 14.0067 -0.88
; from dimethylamine reported by Oostenbrink et al. DOI:
10.1002/cphc.200400542
CA CH2 14.027 0.220 0
; from dimethylamine reported by Oostenbrink et al. DOI:
10.1002/cphc.200400542
[ add ]
1 1 H1 N CA C
H 1.008 0.440
; from dimethylamine reported by Oostenbrink et al. DOI:
10.1002/cphc.200400542
1 4 CN1 N CA C
CH3 15.035 0.220
; from dimethylamine reported by Oostenbrink et al. DOI:
10.1002/cphc.200400542
[ delete ]
H
[ bonds ]
N H1 gb_2
N CN1 gb_21
[ angles ]
CN1 N H1 ga_11
CA N H1 ga_11
CA N CN1 ga_13
[ dihedrals ]
CN1 N CA C gd_29

; N-methyl-proline (0)
[ PRO-1NM ]
[ replace ]
N NT 14.0067 -0.63
; from trimethylamine reported by Oostenbrink et al. DOI:
10.1002/cphc.200400542
CA CH1 13.019 0.210 0
; from trimethylamine reported by Oostenbrink et al. DOI:
10.1002/cphc.200400542
CD CH2 14.027 0.210 0
; from trimethylamine reported by Oostenbrink et al. DOI:
10.1002/cphc.200400542
[ add ]
1 4 CN1 N CA C
CH3 15.035 0.210
; from trimethylamine reported by Oostenbrink et al. DOI:
10.1002/cphc.200400542
[ bonds ]
N CN1 gb_21
[ angles ]
CA N CN1 ga_13
CD N CN1 ga_13
[ dihedrals ]
CN1 N CA C gd_29

```

```

; N-methyl-AA (+1)
[ 1NM+ ]
[ replace ]
N          NL          14.0067    0.104
          ; to add up to +1 net charge
CA          CH1          13.019    0.200    0
          ; derived by analogy to methyl groups of amines reported by
Oostenbrink et al. DOI: 10.1002/cphc.200400542
[ add ]
2          4          H          N          CA          C
          H          1.008    0.248
1          1          CN1         N          CA          C
          CH3         15.035    0.200
          ; derived by analogy to methyl groups of amines reported by
Oostenbrink et al. DOI: 10.1002/cphc.200400542
[ delete ]
H
[ bonds ]
N          H1          gb_2
N          H2          gb_2
N          CN1         gb_21
[ angles ]
H1         N          H2          ga_10
H2         N          CN1         ga_11
CN1        N          H1          ga_11
CA         N          H1          ga_11
CA         N          H2          ga_11
CA         N          CN1         ga_13
[ dihedrals ]
CN1        N          CA          C          gd_29

; N-methyl-glycine (+1)
[ GLY-1NM+ ]
[ replace ]
N          NL          14.0067 0.104          ; to add up to +1 net
charge
CA          CH2         14.027 0.200          0          ; derived by analogy to
methyl groups of amines reported by Oostenbrink et al. DOI:
10.1002/cphc.200400542
[ add ]
2          4          H          N          CA          C
          H          1.008 0.248
1          1          CN1         N          CA          C
          CH3         15.035 0.200          ; derived by analogy to
methyl groups of amines reported by Oostenbrink et al. DOI:
10.1002/cphc.200400542
[ delete ]
H
[ bonds ]
N          H1          gb_2
N          H2          gb_2
N          CN1         gb_21
[ angles ]
H1         N          H2          ga_10
H2         N          CN1         ga_11
CN1        N          H1          ga_11
CA         N          H1          ga_11
CA         N          H2          ga_11
CA         N          CN1         ga_13
[ dihedrals ]
CN1        N          CA          C          gd_29

; N-methyl-proline (+1)
[ PRO-1NM+ ]
[ replace ]
N          NL          14.0067 0.152          ; to add up to +1 net
charge
CA          CH1         13.019 0.200          0          ; derived by analogy to
methyl groups of amines reported by Oostenbrink et al. DOI:
10.1002/cphc.200400542
CD          CH2         14.027 0.200          0          ; derived by analogy to
methyl groups of amines reported by Oostenbrink et al. DOI:
10.1002/cphc.200400542
[ add ]
1          4          H          N          CA          C
          H          1.008 0.248
1          1          CN1         N          CA          C
          CH3         15.035 0.200          ; derived by analogy to
methyl groups of amines reported by Oostenbrink et al. DOI:
10.1002/cphc.200400542
[ bonds ]
N          H          gb_2
N          CN1         gb_21
[ angles ]
H          N          CD          ga_11
CD         N          CN1         ga_13
CN1        N          H          ga_11
CA         N          H          ga_11
CA         N          CD          ga_13
CA         N          CN1         ga_13
[ dihedrals ]
CN1        N          CA          C          gd_29

; N,N-dimethyl-AA (0)
[ 2NM ]
[ replace ]
N          NT          14.0067    -0.63
          ; from trimethylamine reported by Oostenbrink et al. DOI:
10.1002/cphc.200400542
CA          CH1          13.019    0.210    0
          ; from trimethylamine reported by Oostenbrink et al. DOI:
10.1002/cphc.200400542
[ add ]
2          4          CN         N          CA          C
          CH3         15.035    0.210
          ; from trimethylamine reported by Oostenbrink et al. DOI:
10.1002/cphc.200400542
[ delete ]
H
[ bonds ]
N          CN1         gb_21
N          CN2         gb_21
[ angles ]
CN1        N          CN2         ga_13
CA         N          CN2         ga_13
CA         N          CN1         ga_13
[ dihedrals ]
CN1        N          CA          C          gd_29

; N,N-dimethyl-glycine (0)
[ GLY-2NM ]
[ replace ]
N          NT          14.0067 -0.63          ; from trimethylamine
reported by Oostenbrink et al. DOI: 10.1002/cphc.200400542
CA          CH2         14.027 0.210          0          ; from trimethylamine
reported by Oostenbrink et al. DOI: 10.1002/cphc.200400542
[ add ]
2          4          CN         N          CA          C
          CH3         15.035 0.210          ; from trimethylamine
reported by Oostenbrink et al. DOI: 10.1002/cphc.200400542
[ delete ]
H
[ bonds ]
N          CN1         gb_21
N          CN2         gb_21
[ angles ]
CN1        N          CN2         ga_13
CA         N          CN2         ga_13
CA         N          CN1         ga_13
[ dihedrals ]
CN1        N          CA          C          gd_29

; N,N-dimethyl-AA (+1)
[ 2NM+ ]
[ replace ]
N          NL          14.0067    0.152
          ; to add up to +1 net charge
CA          CH1          13.019    0.200    0
          ; derived by analogy to methyl groups of amines reported by
Oostenbrink et al. DOI: 10.1002/cphc.200400542
[ add ]
1          1          H1          N          CA          C
          H          1.008    0.248
2          4          CN         N          CA          C
          CH3         15.035    0.200
          ; derived by analogy to methyl groups of amines reported by
Oostenbrink et al. DOI: 10.1002/cphc.200400542
[ delete ]
H
[ bonds ]
N          H1          gb_2
N          CN1         gb_21
N          CN2         gb_21
[ angles ]
CN1        N          H1          ga_11
CN1        N          CN2         ga_13
CN2        N          H1          ga_11
CA         N          H1          ga_11
CA         N          CN2         ga_13
CA         N          CN1         ga_13
[ dihedrals ]
CN1        N          CA          C          gd_29

; N,N-dimethyl-glycine (+1)
[ GLY-2NM+ ]
[ replace ]
N          NL          14.0067 0.152          ; to add up to +1 net
charge
CA          CH2         14.027 0.200          0          ; derived by analogy to
methyl groups of amines reported by Oostenbrink et al. DOI:
10.1002/cphc.200400542
[ add ]
1          1          H1          N          CA          C
          H          1.008 0.248
2          4          CN         N          CA          C
          CH3         15.035 0.200

```

CH3 15.035 0.200 ; derived by analogy to methyl groups of amines reported by Oostenbrink et al. DOI: 10.1002/cphc.200400542

[ delete ]  
H  
[ bonds ]  
N H1 gb\_2  
N CN1 gb\_21  
N CN2 gb\_21  
[ angles ]  
CN1 N H1 ga\_11  
CN1 N CN2 ga\_13  
CN2 N H1 ga\_11  
CA N H1 ga\_11  
CA N CN2 ga\_13  
CA N CN1 ga\_13  
[ dihedrals ]  
CN1 N CA C gd\_29

; N,N-dimethyl-proline (+1)  
[ PRO-2NM+ ]  
[ replace ]  
N NL 14.0067 0.200 ; to add up to +1 net charge  
CA CH1 13.019 0.200 0 ; derived by analogy to methyl groups of amines reported by Oostenbrink et al. DOI: 10.1002/cphc.200400542  
CD CH2 14.027 0.200 0 ; derived by analogy to methyl groups of amines reported by Oostenbrink et al. DOI: 10.1002/cphc.200400542  
[ add ]  
2 4 CN N CA C  
CH3 15.035 0.200 ; derived by analogy to methyl groups of amines reported by Oostenbrink et al. DOI: 10.1002/cphc.200400542  
[ bonds ]  
N CN1 gb\_21  
N CN2 gb\_21  
[ angles ]  
CN1 N CD ga\_13  
CN1 N CN2 ga\_13  
CN2 N CD ga\_13  
CA N CN2 ga\_13  
CA N CN1 ga\_13  
[ dihedrals ]  
CN1 N CA C gd\_29

; N,N,N-trimethyl-AA (+1)  
[ 3NM+ ]  
[ replace ]  
N NL 14.0067 0.200 ; to add up to +1 net charge  
CA CH1 13.019 0.200 0 ; derived by analogy to methyl groups of amines reported by Oostenbrink et al. DOI: 10.1002/cphc.200400542  
[ add ]  
3 4 CN N CA C  
CH3 15.035 0.200 ; derived by analogy to methyl groups of amines reported by Oostenbrink et al. DOI: 10.1002/cphc.200400542  
[ delete ]  
H  
[ bonds ]  
N CN1 gb\_21  
N CN2 gb\_21  
N CN3 gb\_21  
[ angles ]  
CN1 N CN3 ga\_13  
CN1 N CN2 ga\_13  
CN2 N CN3 ga\_13  
CA N CN3 ga\_13  
CA N CN2 ga\_13  
CA N CN1 ga\_13  
[ dihedrals ]  
CN1 N CA C gd\_29

; N,N,N-trimethyl-glycine (+1)  
[ GLY-3NM+ ]  
[ replace ]  
N NL 14.0067 0.200 ; to add up to +1 net charge  
CA CH2 14.027 0.200 0 ; derived by analogy to methyl groups of amines reported by Oostenbrink et al. DOI: 10.1002/cphc.200400542  
[ add ]  
3 4 CN N CA C  
CH3 15.035 0.200 ; derived by analogy to methyl groups of amines reported by Oostenbrink et al. DOI: 10.1002/cphc.200400542  
[ delete ]  
H  
[ bonds ]  
N CN1 gb\_21

N CN2 gb\_21  
N CN3 gb\_21  
[ angles ]  
CN1 N CN3 ga\_13  
CN1 N CN2 ga\_13  
CN2 N CN3 ga\_13  
CA N CN3 ga\_13  
CA N CN2 ga\_13  
CA N CN1 ga\_13  
[ dihedrals ]  
CN1 N CA C gd\_29

; N-acetyl-AA  
[ NAC ]  
[ replace ]  
N N 14.0067 -0.15  
; by analogy to ASN/GLN and the peptide bond  
[ add ]  
1 2 H N C CA  
H 1.008 0.3100  
; from the hydrogen of the peptide bond  
1 1 CN1 N C CA  
C 12.011 0.1900  
; by analogy to ASN/GLN, the peptide bond and the aldehyde group reported by Dolenc et al. DOI: 10.1093/nar/gki195  
1 2 ON2 N CA C  
O 15.9994 -0.4500  
; from the carbonyl group (of e.g., GLN)  
1 2 CN2 N C CA  
CH3 15.035 0.1000  
; by analogy to the aldehyde group reported by Dolenc et al. DOI: 10.1093/nar/gki195  
[ bonds ]  
N H gb\_2  
N CN1 gb\_10  
CN1 ON2 gb\_5  
CN1 CN2 gb\_27  
[ angles ]  
CA N H ga\_18  
CN1 N H ga\_32  
CN1 N CA ga\_31  
N CN1 ON2 ga\_33  
N CN1 CN2 ga\_19  
CN2 CN1 ON2 ga\_30  
[ impropers ]  
N CN1 CA H gi\_1  
CN1 CN2 N ON2 gi\_1  
[ dihedrals ]  
CN2 CN1 N CA gd\_14  
CN1 N CA C gd\_39

; N-acetyl-proline  
[ PRO-NAC ]  
[ add ]  
1 1 CN1 N C CA  
C 12.011 0.3500  
; by analogy to the aldehyde group reported by Dolenc et al. DOI: 10.1093/nar/gki195  
1 2 ON2 N CA C  
O 15.9994 -0.4500  
; from the carbonyl group (of e.g., GLN)  
1 2 CN2 N C CA  
CH3 15.035 0.1000  
; by analogy to the aldehyde group reported by Dolenc et al. DOI: 10.1093/nar/gki195  
[ bonds ]  
N CN1 gb\_10  
CN1 ON2 gb\_5  
CN1 CN2 gb\_27  
[ angles ]  
CN1 N CD ga\_31  
CN1 N CA ga\_31  
N CN1 ON2 ga\_33  
N CN1 CN2 ga\_19  
CN2 CN1 ON2 ga\_30  
[ impropers ]  
N CN1 CA CD gi\_1  
CN1 CN2 N ON2 gi\_1  
[ dihedrals ]  
CN2 CN1 N CA gd\_14  
CN1 N CA C gd\_39

; pyroglutamic acid  
[ PGA-NH ]  
[ replace ]  
N N 14.0067 -0.31  
[ add ]  
1 1 H N CA CD  
H 1.008 0.31  
[ bonds ]  
N H gb\_2  
[ angles ]  
CA N H ga\_31

```

CD      N      H      ga_31      O      15.9994      -0.45
[ impropers ]      ; from the ester group reported by Chandrasekhar et al. DOI:
N      CA      CD      H      gi_1      10.1081/smts-120030764
[ dihedrals ]      1      2      CC2      O      C      CA
CD      N      CA      C      gd_39      CH3      15.035      0.266
; from the ester group reported by Chandrasekhar et al. DOI:
; N-formylmethionine      10.1081/smts-120030764
[ MET-FOR ]      [ bonds ]
[ replace ]      C      O      gb_13
N      N      14.0067      -0.15      C      OC1      gb_5
; by analogy to ASN/GLN and the peptide bond      O      CC2      gb_18
[ add ]      [ angles ]
1      2      H      N      C      CA      O      C      OC1      ga_33
H      1.008      0.31      C      O      CC2      ga_22
; from the hydrogen of the peptide bond      CA      C      O      ga_19
1      1      CN1      N      C      CA      CA      C      OC1      ga_30
C      12.011      0.1900
; by analogy to ASN/GLN, the peptide bond and the aldehyde group
reported by Dolenc et al. DOI: 10.1093/nar/gki195
1      2      ON2      N      CA      C      [ impropers ]
O      15.9994      -0.4500      C      CA      OC1      O      gi_1
; from the carbonyl group (of e.g., GLN)      [ dihedrals ]
1      2      HC1      N      C      CA      N      CA      C      O      gd_40
H      1.008      0.1      CA      CA      CA      C      O      CC2      gd_12
; by analogy to the aldehyde group reported by Dolenc et al. DOI:
10.1093/nar/gki195
[ bonds ]
N      H      gb_2
N      CN1      gb_10
CN1      ON2      gb_5
CN1      HC1      gb_3
[ angles ]
CA      N      H      ga_18
CA      N      CN1      ga_31
H      N      CN1      ga_32
N      CN1      ON2      ga_33
N      CN1      HC1      ga_19
ON2      CN1      HC1      ga_30
[ impropers ]
N      CN1      CA      H      gi_1
CN1      N      ON2      HC1      gi_1
[ dihedrals ]
ON2      CN1      N      CA      gd_14
CN1      N      CA      C      gd_39
; aminoacids.c.tdb file (C-terminal parameters)
; AA-amide
[ AMD ]
[ replace ]
C      C      12.011      0.29
; from ASN/GLN
[ add ]
1      1      NC1      C      N      O
NT      14.00670      -0.7200      ; from
ASN/GLN
1      1      HC11      C      CA      N
H      1.008      0.4400
; from ASN/GLN
1      2      HC12      C      CA      N
H      1.008      0.4400
; from ASN/GLN
[ bonds ]
C      NC1      gb_9
NC1      HC11      gb_2
NC1      HC12      gb_2
[ angles ]
O      C      NC1      ga_33
CA      C      O      ga_30
CA      C      NC1      ga_19
C      NC1      HC11      ga_23
C      NC1      HC12      ga_23
HC11      NC1      HC12      ga_24
[ impropers ]
C      CA      O      NC1      gi_1
NC1      C      HC11      HC12      gi_1
[ dihedrals ]
N      CA      C      NC1      gd_40
CA      C      NC1      HC11      gd_14
; AA-methyl ester
[ CME ]
[ replace ]
C      C      12.011      0.253
; from the ester group reported by Chandrasekhar et al. DOI:
10.1081/smts-120030764
O      OE      15.9994      -0.069
; from the ester group reported by Chandrasekhar et al. DOI:
10.1081/smts-120030764
[ add ]
1      2      OC1      C      CA      N

```

1	1	HE1	CE1	ND1	NE2	EME 1	1						
; 3-phosphohistidine (-1)													
H31	4					1	1	H	N	-C	CA		
1	1	H	N	-C	CA	DMA	1						
1	1	HD2	CD2	CG	NE2	1	1	H	N	-C	CA		
1	1	HE1	CE1	ND1	NE2	; 5-methylcysteine							
1	2	HZ3	OZ3	PE3	ND1	CYM	1						
; 3-phosphohistidine (-2)													
H32	3					1	1	H	N	-C	CA		
1	1	H	N	-C	CA	; N6-acetyllysine							
1	1	HD2	CD2	CG	NE2	KAC	2						
1	1	HE1	CE1	ND1	NE2	1	1	H	N	-C	CA		
; N6-methyllysine (0)													
KMN	2					1	1	HZ	NZ	CE	CH		
1	1	H	N	-C	CA	; 3-hydroxyproline (R)							
1	2	HZ	NZ	CE	CD	PH3	1						
; N6-methyllysine (+1)													
KMC	2					1	2	HG1	OG1	CB	CA		
1	1	H	N	-C	CA	; 3-hydroxyproline (S)							
2	4	HZ	NZ	CE	CD	P3H	1						
; N6,N6-dimethyllysine (0)													
K2M	1					1	2	HG1	OG1	CB	CA		
1	1	H	N	-C	CA	; 4-hydroxyproline (S)							
; N6,N6-dimethyllysine (+1)													
K2C	2					HY2	1						
1	1	H	N	-C	CA	1	2	HD1	OD1	CG	CB		
1	2	HZ	NZ	CE	CD	; 3,4-dihydroxyproline							
; N6,N6,N6-trimethyllysine													
K3C	1					PHH	2						
1	1	H	N	-C	CA	1	2	HG1	OG1	CB	CA		
1	2	HZ	NZ	CE	CD	1	2	HD1	OD1	CG2	CB		
; omega-N-methylarginine (0)													
RMN	3					; 5-hydroxylysine (0,R)							
1	1	H	N	-C	CA	KH5	3						
1	1	HE	NE	CD	CZ	1	1	H	N	-C	CA		
2	3	HH2	NH2	CZ	NE	1	2	HE1	OE1	CD	CB		
; omega-N-methylarginine (+1)													
RMC	4					2	4	HZ	NZ	CE2	CD		
1	1	H	N	-C	CA	; 5-hydroxylysine (0,S)							
1	1	HE	NE	CD	CZ	K5H	3						
2	3	HH2	NH2	CZ	NE	1	1	H	N	-C	CA		
; symmetric-dimethylarginine (0)													
RSM	3					1	2	HE1	OE1	CD	CB		
1	1	H	N	-C	CA	3	4	HZ	NZ	CE2	CD		
1	1	HE	NE	CD	CZ	; 5-hydroxylysine (+1,R)							
1	1	HH2	NH2	CT2	CZ	KPH	3						
; symmetric-dimethylarginine (+1)													
RMS	4					1	1	H	N	-C	CA		
1	1	H	N	-C	CA	1	2	HE1	OE1	CD	CB		
1	1	HE	NE	CD	CZ	1	2	HE1	OE1	CD	CB		
2	3	HH1	NH1	CZ	NE	3	4	HZ	NZ	CE2	CD		
1	1	HH2	NH2	CT	CZ	; 5-hydroxylysine (+1,S)							
; asymmetric-dimethylarginine (0)													
RAM	3					KHP	3						
1	1	H	N	-C	CA	1	1	H	N	-C	CA		
1	1	HE	NE	CD	CZ	1	2	HE1	OE1	CD	CB		
1	1	HH2	NH2	CT2	CZ	3	4	HZ	NZ	CE2	CD		
; asymmetric-dimethylarginine (+1)													
RMA	3					; 3,4-dihydroxyphenylalanine							
1	1	H	N	-C	CA	HTY	6						
1	1	HE	NE	CD	CZ	1	1	H	N	-C	CA		
2	3	HH1	NH1	CZ	NE	1	1	HD1	CD1	CG	CE1		
1	1	HH2	NH2	CT2	CZ	1	1	HD2	CD2	CG	CE2		
; 1-methylhistidine (0)													
H1M	3					1	2	HZ1	OZ1	CE1	CD1		
1	1	H	N	-C	CA	1	1	HE2	CE2	CD2	CZ2		
1	1	HD2	CD2	CG	NE2	1	2	HH	OH	CZ2	CE1		
1	1	HE1	CE1	ND1	NE2	; 7-hydroxytryptophan							
; 1-methylhistidine (+1)													
H1C	4					W7H	7						
1	1	H	N	-C	CA	1	1	H	N	-C	CA		
1	1	HD1	ND1	CG	CE1	1	1	HD1	CD1	CG	NE1		
1	1	HD2	CD2	CG	NE2	1	1	HE1	NE1	CD1	CE2		
1	1	HE1	CE1	ND1	NE2	1	1	HE3	CE3	CD2	CZ3		
; 3-methylhistidine (0)													
H3M	3					1	1	HZ3	CZ3	CE3	CH3		
1	1	H	N	-C	CA	1	1	HH3	CH3	CZ3	CZ2		
1	1	HD2	CD2	CG	NE2	1	2	HH2	OH2	CZ2	CE2		
1	1	HE1	CE1	ND1	NE2	; 3-hydroxyaspartate (-1,R)							
; 3-methylhistidine (+1)													
H3C	4					DH3	2						
1	1	H	N	-C	CA	1	1	H	N	-C	CA		
1	1	HD2	CD2	CG	NE2	1	2	HG1	OG1	CB	CA		
1	1	HE1	CE1	ND1	NE2	; 3-hydroxyaspartate (-1,S)							
; N5-methylglutamine													
QME	2					D3H	2						
1	1	H	N	-C	CA	1	1	H	N	-C	CA		
1	1	HD2	CD2	CG	NE2	1	2	HG1	OG1	CB	CA		
1	1	HE1	CE1	ND1	NE2	1	2	HD2	OD2	CG2	CB		
1	1	HE2	NE2	CE1	CD2	; 3-hydroxyaspartate (0,R)							
; N4-methylasparagine													
NME	2					DN3	3						
1	1	H	N	-C	CA	1	1	H	N	-C	CA		
1	1	HE2	NE2	CZ	CD	1	2	HG1	OG1	CB	CA		
; glutamate methyl ester													
ECA	1					1	2	HD2	OD2	CG2	CB		
1	1	H	N	-C	CA	; 3-hydroxyaspartate (0,S)							
1	1	HD2	CD2	CG	NE2	D3N	3						
1	1	HE1	CE1	ND1	NE2	1	1	H	N	-C	CA		
; 4-carboxyglutamate (-2)													
1	1	H	N	-C	CA	1	2	HG1	OG1	CB	CA		
1	1	HD2	ND2	CE	CG	2	3	HD2	ND2	CG2	CB		
; glutamate methyl ester													
1	1	H	N	-C	CA	; 3-hydroxyasparagine (R)							
1	1	HD2	CD2	CG	NE2	N3H	3						
1	1	HE1	CE1	ND1	NE2	1	1	H	N	-C	CA		
1	1	HE2	NE2	CE1	CD2	1	2	HG1	OG1	CB	CA		
; 3-hydroxyasparagine (S)													
NH3	3					2	3	HD2	ND2	CG2	CB		
1	1	H	N	-C	CA	; 3-hydroxyasparagine (S)							
1	1	HE2	NE2	CZ	CD	1	1	H	N	-C	CA		
1	1	HE2	NE2	CZ	CD	1	2	HG1	OG1	CB	CA		
2	3	HD2	ND2	CG2	CB	2	3	HD2	ND2	CG2	CB		
; 4-carboxyglutamate (-2)													
ECA	1					; 4-carboxyglutamate (-2)							
1	1	H	N	-C	CA	ECA	1						
1	1	H	N	-C	CA	1	1	H	N	-C	CA		



; 4-carboxylglutamate (-1)						1	1	HZ3	CZ3	CE3	CH2
ECN	2					1	1	HH2	CH2	CZ3	CZ2
1	1	H	N	-C	CA	1	1	HZ2	CZ2	CE2	CH2
; sulfotyrosine						; 2-hydroxytryptophan					
YSU	5					W2H	7				
1	1	H	N	-C	CA	1	1	H	N	-C	CA
1	1	HD1	CD1	CG	CE1	1	2	HE4	OE4	CD1	CG
1	1	HD2	CD2	CG	CE2	1	1	HE1	NE1	CD1	CE2
1	1	HE1	CE1	CD1	CZ	1	1	HE3	CE3	CD2	CZ3
1	1	HE2	CE2	CD2	CZ	1	1	HZ3	CZ3	CE3	CH2
; dehydroalanine						; 3-hydroxytryptophan					
SDH	1					L3H	2				
1	1	H	N	-C	CA	1	1	H	N	-C	CA
; 2,3-didehydrobutyryne						; 3-hydroxytryptophan (S)					
TDH	1					LH3	2				
1	1	H	N	-C	CA	1	2	HG1	OG1	CB	CA
; 6-bromotryptophan						; 4-hydroxytryptophan					
WBR	6					L4H	2				
1	1	H	N	-C	CA	1	1	H	N	-C	CA
1	1	HD1	CD1	CG	NE1	1	2	HG1	OG1	CB	CA
1	1	HE1	NE1	CD1	CE2	; 5-hydroxytryptophan (R)					
1	1	HE3	CE3	CD2	CZ3	L5H	2				
1	1	HZ3	CZ3	CE3	CH2	1	1	H	N	-C	CA
1	1	HZ2	CZ2	CE2	CH2	1	2	HD3	OD3	CG	CB
; 5-nitrosocysteine						; 3-hydroxytryptophan (S)					
CSN	1					LH5	2				
1	1	H	N	-C	CA	1	1	H	N	-C	CA
; citrulline						; 5-hydroxytryptophan (S)					
RCI	3					LH5	2				
1	1	H	N	-C	CA	1	1	H	N	-C	CA
1	1	HE	NE	CD	CZ	1	2	HE	OE	CD2	CG
2	3	HH2	NH2	CZ	NE	; 3-hydroxyvaline					
; allysine (amino adipic semialdehyde)						; 5-hydroxytryptophan (S)					
KAL	2					V3H	2				
1	1	H	N	-C	CA	1	1	H	N	-C	CA
1	1	HE	CE	OZ	CD	1	2	HG3	OG3	CB	CA
; N-acetylglucosamine (N4-linked to ASN)						; cysteine sulfenic acid					
NNG	6					CYH	2				
1	1	H	N	-C	CA	1	1	H	N	-C	CA
1	1	HD2	ND2	CG	C1	1	2	HD	OD	SG	CB
1	1	HN2	N2	C7	C2	; 5-hydroxyproline (R)					
1	2	HO3	O3	C3	C2	PH5	1				
1	2	HO4	O4	C4	C3	1	2	HE	OE	CD	CG
1	2	HO6	O6	C6	C5	; 5-hydroxyproline (S)					
; 2,3-dihydroxyphenylalanine						; 2-amino-3-ketobutyric acid					
F23	6					P5H	1				
1	1	H	N	-C	CA	1	2	HE	OE	CD	CG
1	2	HE3	OE3	CD1	CG	; glutamic semialdehyde					
1	1	HD2	CD2	CG	CE2	GSA	2				
1	2	HZ1	OZ1	CE1	CD1	1	1	H	N	-C	CA
1	1	HE2	CE2	CD2	CZ2	1	1	HD	CD	OE	CG
1	1	HZ2	CZ2	CE1	CE2	; 2-oxo-histidine					
; 2-hydroxyphenylalanine						; 2-amino-3-ketobutyric acid					
F2H	6					TOX	1				
1	1	H	N	-C	CA	1	1	H	N	-C	CA
1	2	HE3	OE3	CD1	CG	; methionine sulfoxide (R)					
1	1	HD2	CD2	CG	CE2	MSX	1				
1	1	HE1	CE1	CD1	CZ	1	1	H	N	-C	CA
1	1	HE2	CE2	CD2	CZ	; methionine sulfoxide (S)					
1	1	HZ	CZ	CE1	CE2	MXS	1				
; 3-hydroxyphenylalanine						; methionine sulfone					
F3H	6					MES	1				
1	1	H	N	-C	CA	1	1	H	N	-C	CA
1	1	HD1	CD1	CG	CE1	; cysteine sulfinic acid					
1	1	HD2	CD2	CG	CE2	CSA	1				
1	2	HZ1	OZ1	CE1	CD1	1	1	H	N	-C	CA
1	1	HE2	CE2	CD2	CZ2	; cysteic acid					
1	1	HZ2	CZ2	CE1	CE2	CSE	1				
; 6-hydroxytryptophan						; 3-nitrotyrosine (-1)					
W6H	7					YNI	4				
1	1	H	N	-C	CA	1	1	H	N	-C	CA
1	1	HD1	CD1	CG	NE1	1	1	HD1	CD1	CG	CE1
1	1	HE1	NE1	CD1	CE2	1	1	HD2	CD2	CG	CE2
1	1	HE3	CE3	CD2	CZ3	1	1	HE2	CE2	CD2	CZ2
1	1	HZ3	CZ3	CE3	CH2	; 3-nitrotyrosine (0)					
1	2	HI	OI	CH2	CZ2	YNN	5				
1	1	HZ2	CZ2	CE2	CH2	1	1	H	N	-C	CA
; 5-hydroxytryptophan						; 3-nitrotyrosine (0)					
W5H	7					YNB	5				
1	1	H	N	-C	CA	1	1	H	N	-C	CA
1	1	HD1	CD1	CG	NE1	1	1	HD1	CD1	CG	CE1
1	1	HE1	NE1	CD1	CE2	1	1	HD2	CD2	CG	CE2
1	1	HE3	CE3	CD2	CZ3	1	1	HE2	CE2	CD2	CZ2
1	2	HH3	OH3	CZ3	CE2	1	2	HH3	OH3	CZ2	CE1
1	1	HH2	CH2	CZ3	CZ2	; 4-hydroxytryptophan					
1	1	HZ2	CZ2	CE2	CH2	W4H	7				
; 4-hydroxytryptophan						; 4-hydroxytryptophan					
W4H	7					1	1	H	N	-C	CA
1	1	H	N	-C	CA	1	1	HD1	CD1	CG	CE1
1	1	HD1	CD1	CG	NE1	1	1	HD2	CD2	CG	CE2
1	1	HE1	NE1	CD1	CE2	1	1	HE2	CE2	CD2	CZ2
1	2	HZ4	OZ4	CE3	CD2	1	1	HE2	CE2	CD2	CZ2

1	2	HH3	OH3	CZ2	CE1	1	1	HD1	CD1	CG	CE1
; 6-nitrotryptophan											
WNI	6					1	1	HD2	CD2	CG	CE2
1	1	H	N	-C	CA	1	1	HE2	CE2	CD2	CZ2
1	1	HD1	CD1	CG	NE1	1	2	HH	OH	CZ2	CE1
1	1	HE1	NE1	CD1	CE2	; homocitrulline					
1	1	HE3	CE3	CD2	CZ3	KAM	3				
1	1	HZ3	CZ3	CE3	CH2	1	1	H	N	-C	CA
1	1	HZ2	CZ2	CE2	CH2	1	1	HZ	NZ	CH	CE
; kynurenine											
WKY	6					2	4	HI2	NI2	CH	NZ
1	1	H	N	-C	CA	; carboxyllysine (-1)					
1	1	HE2	CE2	CD2	CZ3	KCA	2				
2	3	HZ1	NZ1	CE1	CD2	1	1	H	N	-C	CA
1	1	HZ2	CZ2	CE1	CH	1	1	HZ	NZ	CH	CE
1	1	HZ3	CZ3	CE2	CH	; carboxyllysine (0)					
1	1	HH	CH	CZ2	CZ3	KCN	3				
; 3-hydroxykynurenine											
WKH	6					1	1	H	N	-C	CA
1	1	H	N	-C	CA	1	1	H	N	-C	CA
1	1	HE2	CE2	CD2	CZ3	1	1	HZ	NZ	CH	CE
2	3	HZ1	NZ1	CE1	CD2	; S-carbamoyl-cysteine					
1	1	HZ3	CZ3	CE2	CH2	CAM	2				
1	2	HH1	OH1	CZ2	CE1	1	1	H	N	-C	CA
1	1	HH2	CH2	CZ2	CZ3	2	3	HE2	NE2	CD	SG
; formyl-kynurenine											
WKF	7					; norleucine					
1	1	H	N	-C	CA	LNO	1				
1	1	HE2	CE2	CD2	CZ3	1	1	H	N	-C	CA
1	1	HZ1	NZ1	CE1	CH1	; chlorotyrosine					
1	1	HZ2	CZ2	CE1	CH2	YCH	5				
1	1	HZ3	CZ3	CE2	CH2	1	1	H	N	-C	CA
1	1	HH1	CH1	NZ1	OI						
1	1	HH2	CH2	CZ2	CZ3						

**Dataset S3. UniProt entries of post-translationally modified proteins.** The dataset is excluded from the thesis due to its size, but it is available online as a part of the publication.

## Chapter II

# Vienna-PTM web server: a toolkit for MD simulations of protein post-translational modifications

Margreitter, C.,\* Petrov, D.\* & Zagrovic, B. (2013). *Nucleic Acids Res.* **41** (Web Server issue), W422-6.

\*The authors contribute equally to this work.

CM, DP and BZ conceived and designed the study. CM, DP and BZ designed and CM and DP created the back-end module, while CM, DP and BZ designed and CM created the front-end module of the web server. CM, DP and BZ wrote the paper.

**ABSTRACT**

Post-translational modifications (PTMs) play a key role in numerous cellular processes by directly affecting structure, dynamics and interaction networks of target proteins. Despite their importance, our understanding of protein PTMs at the atomistic level is still largely incomplete. Molecular dynamics (MD) simulations, which provide high-resolution insight into biomolecular function and underlying mechanisms, are in principle ideally suited to tackle this problem. However, because of the challenges associated with the development of novel MD parameters and a general lack of suitable computational tools for incorporating PTMs in target protein structures, MD simulations of post-translationally modified proteins have historically lagged significantly behind the studies of unmodified proteins. Here we present Vienna-PTM web server (<http://vienna-ptm.univie.ac.at>), a platform for automated introduction of PTMs of choice to protein 3D structures (PDB files) in a user-friendly visual environment. With 256 different enzymatic and non-enzymatic PTMs available, the server performs geometrically realistic introduction of modifications at sites of interests, as well as subsequent energy minimization. Finally, the server makes available force field parameters and input files needed to run MD simulations of modified proteins within the framework of the widely used GROMOS 54A7 and 45A3 force fields and GROMACS simulation package.

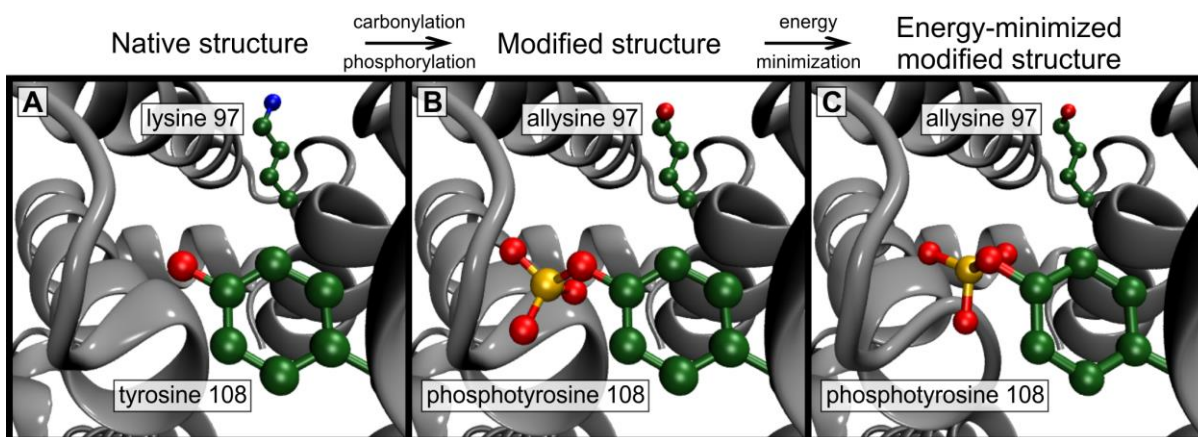
## INTRODUCTION

Post-translational modifications (PTMs) of proteins, such as phosphorylation, acetylation, methylation, carboxylation or hydroxylation, play a key role in a variety of different cellular processes.<sup>1,2</sup> For example, PTMs have been shown to be important in regulating enzyme activity, ensuring proper localization of biomolecules,<sup>3,4</sup> modifying protein stability<sup>5,6</sup> or directing chromatin remodeling.<sup>6,7</sup> What is more, non-enzymatic PTMs, such as carbonylation or oxidation, frequently arise as a consequence of oxidative stress and are considered to be a ubiquitous mode of non-specific protein damage<sup>8,9</sup> involved in age-related disorders including neurodegenerative diseases, cancer and diabetes. Importantly, amino acids often undergo a significant change in their physico-chemical properties on modification, resulting sometimes in a dramatic alteration of the structure of the affected protein, its dynamics and the way it interacts with the environment.<sup>1,10-13</sup> Of the 20 canonical amino acids, 17 can be modified, thus creating a vast source of proteome diversification. The paramount importance of such modifications is underscored by the fact that ~5% of the human genome encodes enzymes related to PTMs.<sup>1</sup> However, despite their extreme biological relevance, our atomistic-level understanding of PTMs and their effect on protein structure, dynamics and interaction networks is still rudimentary.

Molecular dynamics (MD) computer simulations using semi-empirical atomistic force fields are a powerful way to study biomolecules at a single-molecule level with atomistic spatial resolution and femtosecond temporal resolution.<sup>14,15</sup> In particular, MD simulations allow one to study properties and processes that are not directly accessible through experiment and frequently play an important role in interpreting time- and ensemble-averaged experimental results.<sup>15,16</sup> What is more, the power of MD simulations in particular and computational modeling approaches in general is expected to only increase in the future because of growing computational capabilities and ever-improving models. Despite this inherent potential, simulation studies of PTMs have typically lagged behind both wet-laboratory research and simulation studies of unmodified proteins, focusing even in best cases only on a few modification types for a small subset of proteins.<sup>9,10,12,17-22</sup> (G. A. Khoury, J. P. Thompson and C. A. Floudas, unpublished results). The reasons for this are 2-fold. First, there are currently no computational tools allowing one to quickly and accurately modify

protein structures with PTMs of choice, a necessary prerequisite for any MD simulations of PTMs. Second, there are no self-consistent, comprehensive force field parameters for treating the large majority of protein PTMs in MD simulations. Although there exist several automated or semi-automated tools for generating MD parameters for novel groups, such as ParamChem or SwissParam for CHARMM,<sup>23-26</sup> q4md-forcefieldtools for AMBER/GLYCAM<sup>27,28</sup> or ATB for GROMOS<sup>29</sup> force fields, none of them focuses exclusively on PTMs or provides human-curated and validated PTM parameters.

This article focuses on the first of the aforementioned challenges by presenting Vienna-PTM web server (<http://vienna-ptm.univie.ac.at>), a web-based platform for introducing PTMs of choice in Protein Data Bank (PDB) structures<sup>30</sup> and GROMACS<sup>31,32</sup> structure files quickly and in a realistic fashion. Practically, adding PTMs to a structure of choice entails altering the chemical composition of select residues including deletion of unnecessary atoms, geometrically and energetically realistic addition of new atoms, renumbering of atomic indices and residue renaming. In particular, addition of new atoms to a structure can take considerable effort, as the appropriate atomic coordinates have to be determined for each individual modified amino acid and any inconsistency with force field definitions may lead to severe problems. To assist with this, Vienna-PTM web server provides an automated protein structure modification procedure including 256 chemically distinct PTM reactions whereby users are able to give their instructions through an intuitive graphical interface, limiting errors to a minimum (the workflow of the server is illustrated in Figure 1). The required time from the initial PDB structure to the energy-minimized altered structure of choice can thus be reduced to several seconds. Finally, as a repository of newly developed PTM parameters (D. Petrov, C. Margreitter, M. Grandits, C. Oostenbrink and B. Zagrovic, under review) for two widely used and extensively tested MD force fields (GROMOS 45A3<sup>34</sup> and 54A7<sup>35,36</sup>), the server also directly addresses the second challenge aforementioned. In particular, in addition to modified PDB files, the output of the server includes all relevant structure and topology files needed to run MD simulations of modified proteins using GROMACS biomolecular simulation package and one of the aforementioned two force fields.



**Figure 1. Vienna-PTM web server workflow.** The server introduces one or more PMTs of choice to a user-supplied PDB structure followed by optional energy minimization. In the example, carbonylation and phosphorylation modifications are added to two select residues in human serum albumine (PDB code: 1N5U<sup>33</sup>).

## MATERIALS AND METHODS

### Vienna-PTM web server: input data and overall workflow

The input data that are passed to the server consists of (i) a protein X-ray or nuclear magnetic resonance structure in the form of a code-specified or manually uploaded PDB file together with processing options, such as MD force field and energy-minimization specification, and (ii) a choice of residues to be modified together with desired modifications. On upload of a protein structure in Step 1, the server redirects users to a page with the sequence from the uploaded PDB file interactively displayed either as ‘pearls on a string’ (Figure 2, graphical interface, JavaScript required) or a list (text-based interface) with available modifications for each residue given in drop-down menus. Depending on the interface type, selected modifications are either collected in a hidden text field or forwarded separately. In the graphical interface, a modified residue is visually labeled with a modification mark (Figure 2). When a job is submitted, the server adds, deletes, renames and renumbers atoms to apply the selected PTM(s), followed by an optional energy minimization/geometry optimization. To maximize input coverage, all statements in the input PDB file except ATOM lines are ignored in the main modification step. This also means that already modified proteins may be uploaded again. Non-canonical residues in the input PDB file are represented as an exclamation mark and cannot be modified. Finally, if one uses

a nuclear magnetic resonance structure with multiple model structures as input, the server modifies just the first model and includes it in the modified PDB file. In addition, a notification is issued on the results page informing the user of this fact. Detailed instructions can be obtained on server webpage (<http://vienna-ptm.univie.ac.at/about.php>), whereas support requests and reports of problems can be communicated in a user board (<http://vienna-ptm.univie.ac.at/wbb>).

The image shows the Vienna-PTM web interface. At the top, there is a banner with a protein ribbon structure and a ball-and-stick model of a modification. The text reads "...extending your possibilities..." and "Vienna-PTM a toolkit for MD simulations of protein post-translational modifications". Below the banner is a navigation menu with links: HOME, ABOUT, DOWNLOAD, LITERATURE, BOARD.

The main content area is titled "Chain: A" and displays a sequence editor. The sequence is shown in two rows of colored circles representing amino acids, numbered 41 to 76. The first row contains: M (41), L (42), S (43), D (44), E (45), D (46), F (47), K (48), A (49), V (50), F (51), G (52), M (53), T (54), R (55), S (56), A (57), F (58). The second row contains: A (59), N (60), L (61), P (62), L (63), W (64), K (65), Q (66), Q (67), N (68), L (69), K (70), K (71), E (72), K (73), G (74), L (75), F (76). Above the sequence, there are labels for modifications: "Hyd" above residue 43, "Pho" above residue 46, and "Deh" above residue 54. A bracket under residues 49-51 (A, V, F) is labeled "3-hydroxyvaline remove modification". A "Process" button is located at the bottom of the interface.

**Figure 2. Data input.** Modifications of choice are specified via a user-friendly graphical interface (depicted) or an optional text-based interface.

Writing configuration files, calling back-end modules and checking status of current jobs (every few seconds) are carried out by back-end processing scripts. The back-end module provides parameters for each particular modification and force field combination. New atoms are added using relative pre-minimized coordinates for the modified side chain in a coordinate system whose axes are defined taking the last remaining bond, the reference point and the last dihedral orientation into account to avoid unfavorable side-chain conformations. The modification step itself takes ~9 s on average, with minimization up to 3 min for largest systems. On the final result page, job-related information, such as the log file, is displayed to the user together with download links.



## Output

The final output of the server includes (i) a three-letter-code sequence of the modified protein, (ii) a PTM-containing PDB file (visualized on the webpage using Jmol<sup>37</sup>), (iii) GROMACS MD simulation input files and force field parameters for simulating the modified protein, including the GROMACS structure file (.gro) and topology file (.top) and (iv) modification and energy minimization log files. In the output PDB file, the modified residues are treated the same as canonical ones, meaning that they are added in the ATOM instead of the HETATM section of the resulting PDB file. Moreover, the original HETATM entries are also included in the output and renumbered properly, together with chain information and MODEL/ENDMDL statements. Depending on user's specifications, the original header information, including REMARK and COMPND fields, is also included in the output file. Note that if energy minimization is not chosen during initialization, a modified PDB file is produced without the associated GROMACS files. Finally, one should emphasize that the server only provides files needed to prepare and run MD simulations, but not computational resources to do so.

## Features of the web server

### *Handling of input files*

Input files can be either uploaded from a local hard drive or specified by a PDB ID. In the latter case, the PDB file is automatically downloaded from <http://www.pdb.org>. On user's request on the initialization page, header information may be copied (not parsed) to the output PDB file. Depending on a modification, some information given in the original header may not be consistent with the modified structure; therefore, this option should be used with caution.

### *Available modifications*

The server currently covers 256 distinct PTM reactions, including phosphorylation, methylation, acetylation, hydroxylation, carboxylation, carbonylation, nitration, deamidation and many others or 110 non-redundant post-translationally modified amino acids and protein termini. The difference between these two figures arises from the fact that a number of PTM reactions result in the same final modification. The complete list of all

available modifications and the associated chemical structures are given in Supplementary Materials, whereas the details of the parameter development and the results of the validation procedure are further discussed in reference (D. Petrov, C. Margreitter, M. Grandits, C. Oostenbrink and B. Zagrovic, under review). In principle, the number of modifications that can be applied simultaneously is limited only by the size of the protein. However, if a large number of simultaneous modifications are requested in combination with energy minimization, the time limit for a particular job may be exceeded in rare cases. If this occurs, the final output contains an unminimized structure. Finally, in all output files, the newly introduced modified residues are represented using a three-letter residue code to match PDB file format definitions (version considered: 3.20).

### *Energy minimization*

All modified residues have been pre-energy-minimized using the GROMOS 45A3<sup>34</sup> and 54A7<sup>35,36</sup> force fields before being incorporated into the target protein. To optimize the geometry and energy of the entire modified protein, energy minimization may be requested during the initialization step. In such cases, an initial test is performed to check whether the uploaded file is suitable as input for minimization. A negative outcome leads automatically to deactivation of minimization. The reasons for failure can be inclusion of non-standard residues or unique ligands, missing atoms or residues, non-standard formatting of PDB file and others. It is the responsibility of the user to provide a suitable PDB file for energy minimization. Note, however, that the initial coordinates of newly added atoms have been pre-minimized, thus ensuring meaningful initial coordinates even if minimization of the whole molecule is disabled or fails. Energy minimization uses GROMACS routines to perform steepest gradient minimization: 1500 minimization steps are performed *in vacuo* with a maximum force convergence threshold of 1.0 kJ/mol/nm. A cut-off range of 1.4 nm is used for both the van-der-Waals and Coulomb interactions. The .mdp files used for minimization are available for download in the 'DOWNLOAD' section of the server (<http://viennaptm.univie.ac.at/download.php>).

## Security

Job files cannot be downloaded or deleted (both uploaded and rendered) without the correct passphrase, which is generated automatically. This key is provided implicitly in links and, in case this is specified, sent to the user by email. Note that no email will be sent in case the job gets aborted. Once the job has been deleted, there is no way to recover data.

## Technical details

Vienna-PTM runs on a dedicated web server with sufficient storage capacity for ~18 000 jobs. At the moment, eight jobs can run in parallel. The job limit is due to the fact that both the server and the modification programs are executed on the same physical machine. The server software is Apache2. The front end is written using MySQL, PHP5, JavaScript, CSS and Jmol plugin,<sup>37</sup> whereas the back end is written in C++ (OO). GROMACS version 4.5.5 is used for energy minimization.

## CONCLUSIONS

Vienna-PTM is a freely available tool, which allows rapid and reliable addition of a wide variety of PTMs to protein side chains and termini. The workflow of the server results in an output PDB file, which can be downloaded and used for simulation studies or visualization purposes. By also including molecular dynamics parameters for modified amino acids and relevant input files, Vienna-PTM web server also provides a comprehensive platform to support all key steps in setting up MD simulations of post-translationally modified proteins. The parameters are currently available for GROMOS force fields 45a3<sup>34</sup> and 54a7<sup>35,36</sup> and are provided in GROMACS file formats both for versions <4.5.x and ≥4.5.x.<sup>31,32</sup> Addition of new modification types and even completely new force fields to the server is logistically straightforward because of its flexible structure. Although MD parameters for several different PTMs have been developed and used before,<sup>9,10,12,17-22</sup> (G. A. Khoury, J. P. Thompson and C. A. Floudas, unpublished results) Vienna-PTM is to the best of our knowledge the first publicly available repository containing human-curated and validated parameters for an almost complete set of biologically relevant modifications.

The Vienna-PTM server was launched in June 2012 for testing purposes and is expected to have high visibility in MD and PTM research communities. The focus in web design was on

compatibility, preferably almost independent of the user's operating system and browser settings. In conjunction with extensive beta-testing (altogether, ~3000 test jobs have been performed by the authors and another 1000 by external beta-testers), this ensures maximal stability and user-friendliness. From direct MD simulations to biomolecular structure refinement to computational free-energy estimation and drug design, Vienna-PTM web server greatly expands the range of MD methodology to a large class of biomolecular systems of paramount importance. It is our hope that this advance will further catalyze the usage of analytical, quantitative methods of structural biophysics and chemistry, as embodied in the MD method, in addressing questions concerning realistic, PTM-dominated cell biology.

## **FUNDING**

Austrian Science Fund FWF [START grant Y 514-B11 to B.Z.] (in part) and European Research Council Starting Independent grant [279408 to B.Z.]. Funding for open access charge: European Research Council Starting Independent grant [279408 to B.Z.].

## **ACKNOWLEDGEMENTS**

The authors thank members of the Laboratory of Computational Biophysics at Max F. Perutz Laboratories for useful input and critical reading of the manuscript. They especially thank Alexander Zech for his help in graphics design and all beta-testers for testing the server.

## REFERENCES

1. Walsh, C. T., Garneau-Tsodikova, S. & Gatto, G. J., Jr. Protein posttranslational modifications: the chemistry of proteome diversifications. *Angew. Chem. Int. Ed.* **44**, 7342-7372 (2005).
2. Walsh, C. T. Posttranslational modification of proteins: expanding nature's inventory. Roberts and Company Publishers, Englewood, Colorado, 2006.
3. Seger, R. & Krebs, E. G. The MAPK signaling cascade. *FASEB J.* **9**, 726-735 (1995).
4. Arozarena, I., Calvo, F. & Crespo, P. Ras, an actor on many stages: Posttranslational modifications, localization, and site-specified events. *Genes Cancer* **2**, 182-194 (2011).
5. Feng, L., Lin, T., Uranishi, H., Gu, W. & Xu, Y. Functional analysis of the roles of posttranslational modifications at the p53 C terminus in regulating p53 stability and activity. *Mol. Cell. Biol.* **25**, 5389-5395 (2005).
6. Latham, J. A. & Dent, S. Y. Cross-regulation of histone modifications. *Nat. Struct. Mol. Biol.* **14**, 1017-1024 (2007).
7. Paik, W. K., Paik, D. C. & Kim, S. Historical review: the field of protein methylation. *Trends Biochem. Sci.* **32**, 146-152 (2007).
8. Nystrom, T. Role of oxidative carbonylation in protein quality control and senescence. *Embo J.* **24**, 1311-1317 (2005).
9. Petrov, D. & Zagrovic, B. Microscopic analysis of protein oxidative damage: Effect of carbonylation on structure, dynamics, and aggregability of villin headpiece. *J. Am. Chem. Soc.* **133**, 7016-7024 (2011).
10. Polyansky, A. A. & Zagrovic, B. Protein electrostatic properties predefining the level of surface hydrophobicity change upon phosphorylation. *J Phys Chem Lett* **3**, 973-976 (2012).
11. Polyansky, A. A., Kuzmanic, A., Hlevnjak, M. & Zagrovic, B. On the contribution of linear correlations to quasi-harmonic conformational entropy in proteins. *J Chem Theory Comput* **8**, 3820-3829 (2012).
12. Potoyan, D. A. & Papoian, G. A. Regulation of the H4 tail binding and folding landscapes via lys-16 acetylation. *Proc. Natl. Acad. Sci. U.S.A.* **109**, 17857-17862 (2012).
13. Terman, J. R. & Kashina, A. Post-translational modification and regulation of actin. *Curr. Opin. Cell Biol.* (2012).
14. Karplus, M. & McCammon, J. A. Molecular dynamics simulations of biomolecules. *Nat. Struct. Biol.* **9**, 646-652 (2002).
15. van Gunsteren, W. F. *et al.* Biomolecular modeling: goals, problems, perspectives. *Angew. Chem. Int. Ed.* **45**, 4064-4092 (2006).
16. Kruschel, D. & Zagrovic, B. Conformational averaging in structural biology: Issues, challenges and computational solutions. *Mol Biosyst* **5**, 1606-1616 (2009).
17. Chen, H. F. Molecular dynamics simulation of phosphorylated KID post-translational modification. *PLoS ONE* **4**, e6516 (2009).
18. Grauffel, C., Stote, R. H. & Dejaegere, A. Force field parameters for the simulation of modified histone tails. *J Comput Chem* **31**, 2434-2451 (2010).
19. Seeliger, D. *et al.* Quantitative assessment of protein interaction with methyl-lysine analogues by hybrid computational and experimental approaches. *ACS Chem. Biol.* **7**, 150-154 (2012).
20. Olausson, B. E. *et al.* Molecular dynamics simulations reveal specific interactions of post-translational palmitoyl modifications with rhodopsin in membranes. *J. Am. Chem. Soc.* **134**, 4324-4331 (2012).
21. Steinbrecher, T., Latzer, J. & Case, D. A. Revised AMBER parameters for bioorganic phosphates. *J Chem Theory Comput* **8**, 4405-4412 (2012).

22. Marlowe, A. E., Singh, A. & Yingling, Y. G. The effect of point mutations on structure and mechanical properties of collagen-like fibril: A molecular dynamics study. *Mater Sci Eng C Mater Biol Appl* **32**, 2583 - 2588 (2012).
23. Vanommeslaeghe, K. & MacKerell Jr., A. D. Automation of the CHARMM General Force Field (CGenFF) I: bond perception and atom typing. *J. Chem. Inf. Model* **52**, 3144 - 3154 (2012).
24. Vanommeslaeghe, K. & MacKerell Jr., A. D. Automation of the CHARMM General Force Field (CGenFF) II: Assignment of bonded parameters and partial atomic charges. *J. Chem. Inf. Model* **52**, 3155 - 3168 (2012).
25. Yesselman, J. D., Price, D. J., Knight, J. L. & Brooks, C. L. MATCH: An atom-typing toolset for molecular mechanics force fields. *J. Comput. Chem.* **33**, 189 - 202 (2012).
26. Zoete, V., Cuendet, M. A., Grosdidier, A. & Michielin, O. SwissParam, a fast force field generation tool for small organic molecules. *J. Comput. Chem.* **32**, 2359 - 2368 (2011).
27. Vanquelef, E. *et al.* RED Server: a web service for deriving RESP and ESP charges and building force field libraries for new molecules and molecular fragments. *Nucleic Acids Res.* **39**, W511-W517 (2011).
28. Dupradeau, F.-Y. *et al.* The R.ED. tools: advances in RESP and ESP charge derivation and force field library building. *Phys Chem Chem Phys* **12**, 7821-7839 (2010).
29. Malde, A. K. *et al.* An Automated force field Topology Builder (ATB) and repository: version 1.0. *J Chem Theory Comput* **7**, 4026 - 4037 (2011).
30. Berman, H. M. *et al.* The Protein Data Bank. *Nucleic Acids Res.* **28**, 235-242 (2000).
31. Hess, B., Kutzner, C., Van Der Spoel, D. & Lindahl, E. GROMACS 4: algorithms for highly efficient, load-balanced, and scalable molecular simulation. *J Chem Theory Comput* **4**, 435-447 (2008).
32. Van Der Spoel, D. *et al.* GROMACS: fast, flexible, and free. *J Comput Chem* **26**, 1701-1718 (2005).
33. Wardell, M. *et al.* The atomic structure of human methemalbumin at 1.9 Å. *Biochem. Biophys. Res. Commun.* **291**, 813-819 (2002).
34. Oostenbrink, C., Villa, A., Mark, A. E. & van Gunsteren, W. F. A biomolecular force field based on the free enthalpy of hydration and solvation: the GROMOS force-field parameter sets 53A5 and 53A6. *J Comput Chem* **25**, 1656-1676 (2004).
35. Schuler, L. D., Daura, X. & van Gunsteren, W. F. An improved GROMOS96 force field for aliphatic hydrocarbons in the condensed phase. *J Comput Chem* **22**, 1205-1218 (2001).
36. Schmid, N. *et al.* Definition and testing of the GROMOS force-field versions 54A7 and 54B7. *Eur. Biophys. J.* **40**, 843-856 (2011).
37. Steinbeck, C. *et al.* The Chemistry Development Kit (CDK): An open-source Java library for chemo- and bioinformatics. *J. Chem. Inf. Comput. Sci.* **43**, 493-500 (2003).

## Appendices to Chapter II

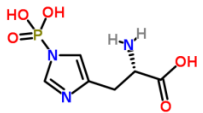
**Table 1. Post-translational modifications available in Vienna-PTM with PTM index number (column 1), chemical moiety index number (column 2), amino acids they target given using the canonical 3-letter code (AA, column 3), PTM 3-letter code (column 4), chemical names (column 5) and structures (column 6). If two protonation states are possible, the one with higher occupancy at the physiological pH is highlighted in bold. \* no prolines included.**

### ENZYMATIC

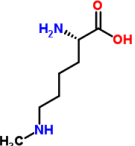
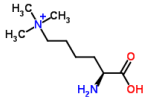
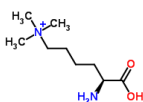
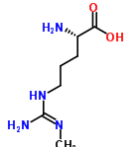
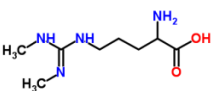
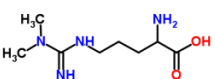
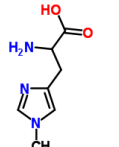
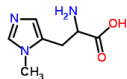

# PTM	AA	code	chemical	structure
-------	----	------	----------	-----------

#### Phosphorylation

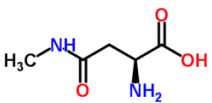
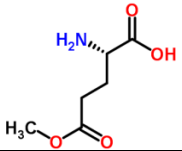
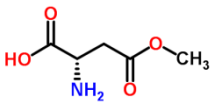
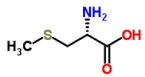
1	1	SER	S1P	phosphoserine (-1)	
2	2		<b>S2P</b>	phosphoserine (-2)	
3	3	THR	T1P	phosphothreonine (-1)	
4	4		<b>T2P</b>	phosphothreonine (-2)	
5	5	TYR	Y1P	phosphotyrosine (-1)	
6	6		<b>Y2P</b>	phosphotyrosine (-2)	
7	7	ASP	D1P	phosphoaspartate (-1)	
8	8		<b>D2P</b>	phosphoaspartate (-2)	
9	9	LYS	K1P	phospholysine (-1)	
10	10		<b>K2P</b>	phospholysine (-2)	
11	11	ARG	R1P	phosphoarginine (0)	
12	12		<b>R2P</b>	phosphoarginine (-1)	
13	13	HIS	H11	1-phosphohistidine (-1)	
14	14		<b>H12</b>	1-phosphohistidine (-2)	

15	15	HIS	H31	3-phosphohistidine (-1)	
16	16		<b>H32</b>	3-phosphohistidine (-2)	

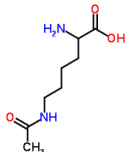
### Methylation

17	17	LYS	KMN	methyllysine (0)	
18	18		<b>KMC</b>	N6-methyllysine (+1)	
19	19	LYS	K2M	N6,N6-dimethyllysine (0)	
20	20		<b>K2C</b>	N6,N6-dimethyllysine (+1)	
21	21	LYS	K3C	N6,N6,N6-trimethyllysine	
22	22	ARG	RMN	omega-N-methylarginine (0)	
23	23		<b>RMC</b>	omega-N-methylarginine (+1)	
24	24	ARG	RSM	symmetric-dimethylarginine (0)	
25	25		<b>RMS</b>	symmetric-dimethylarginine (+1)	
26	26	ARG	RAM	asymmetric-dimethylarginine (0)	
27	27		<b>RMA</b>	asymmetric-dimethylarginine (+1)	
28	28	HIS	<b>H1M</b>	1-methylhistidine (0)	
29	29		H1C	1-methylhistidine (+1)	
30	30	HIS	<b>H3M</b>	3-methylhistidine (0)	
31	31		H3C	3-methylhistidine (+1)	
32	32	GLN	QME	N5-methylglutamine	

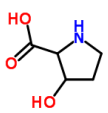
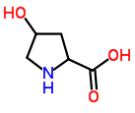
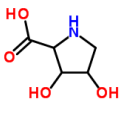
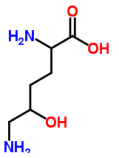


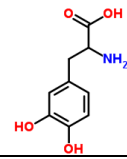
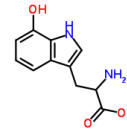
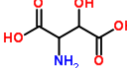
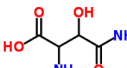
33	33	ASN	NME	N4-methylasparagine	
34	34	GLU	EME	glutamate methyl ester	
35	35	ASP	DME	aspartate methyl ester	
36	36	CYS	CYM	S-methylcysteine	

**Acetylation**

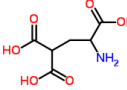
37	37	LYS	KAC	N-acetyllysine	
----	----	-----	-----	----------------	--

**Hydroxylation**

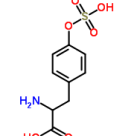
38	38	PRO	PH3	3-hydroxyproline (R)	
39	39		P3H	3-hydroxyproline (S)	
40	40	PRO	HYP	4-hydroxyproline (R)	
41	41		HY2	4-hydroxyproline (S)	
42	42	PRO	PHH	3,4-dihydroxyproline	
43	43	LYS	KH6	5-hydroxylysine (0,R)	
44	44		K6H	5-hydroxylysine (0,S)	
45	45		<b>KPH</b>	5-hydroxylysine (+1,R)	
46	46		<b>KHP</b>	5-hydroxylysine (+1,S)	

47	47	TYR	HTY	3,4-dihydroxyphenylalanine	
48	48	TRP	W7H	7-hydroxytryptophan	
49	49	ASP	DH3	3-hydroxyaspartate (-1,R)	
50	50		D3H	3-hydroxyaspartate (-1,S)	
51	51		DN3	3-hydroxyaspartate (0,R)	
52	52		D3N	3-hydroxyaspartate (0,S)	
53	53	ASN	N3H	3-hydroxyasparagine (R)	
54	54		NH3	3-hydroxyasparagine (S)	



**Carboxylation**

55	55	GLU	ECA	4-carboxyglutamate (-2)	
56	56		ECN	4-carboxyglutamate (-1)	

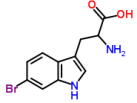
**Sulfation**

57	57	TYR	YSU	sulfotyrosine	
----	----	-----	-----	---------------	---

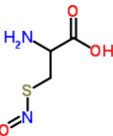
**Dehydration**

58	58	SER	SDH	dehydroalanine	
59	59	THR	TDH	2,3-didehydrobutyrate	

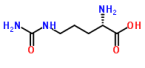
**Bromidation**

60	60	TRP	WBR	6-bromotryptophan	
----	----	-----	-----	-------------------	---

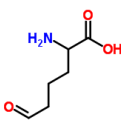
**S-nitrosylation**

61	61	CYS	CSN	S-nitrosocysteine	
----	----	-----	-----	-------------------	---

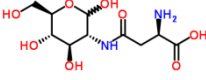
**Citrullination**

62	62	ARG	RCI	citrulline	
----	----	-----	-----	------------	---

**Allysine formation (the same as carbonylation)**

63	63	LYS	KAL	allysine (amino adipic semialdehyde)	
----	----	-----	-----	--------------------------------------	---

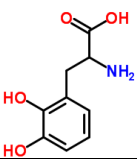
**Glycosylation**

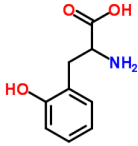
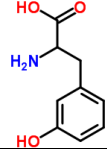
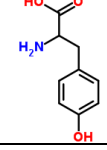
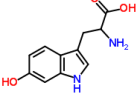
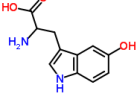

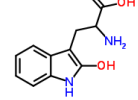
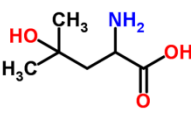
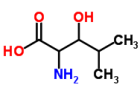
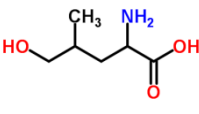

64	64	ASN	NNG	N-acetylglucosamine	
----	----	-----	-----	---------------------	---


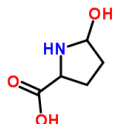
**NONENZYMATIC**

# PTM	AA	Code	chemical	structure
-------	----	------	----------	-----------

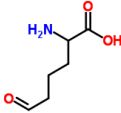
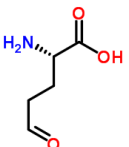

**Hydroxylation**

65	65	PHE	F23	2,3-dihydroxyphenylalanine	
----	----	-----	-----	----------------------------	---

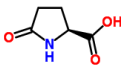
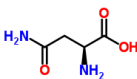
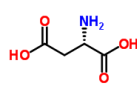
66	66	PHE	F2H	2-hydroxyphenylalanine	
67	67	PHE	F3H	3-hydroxyphenylalanine	
68	68	PHE	TYR	tyrosine	
69	69	TRP	W6H	6-hydroxytryptophan	
70	70	TRP	W5H	5-hydroxytryptophan	
71	71	TRP	W4H	4-hydroxytryptophan	
72	72	TRP	W2H	2-hydroxytryptophan	
73	73	LEU	L3H	3-hydroxyleucine (R)	
74	74		LH3	3-hydroxyleucine (S)	
75	75	LEU	L4H	4-hydroxyleucine	
76	76	LEU	L5H	5-hydroxyleucine (R)	
77	77		LH5	5-hydroxyleucine (S)	
78	78	VAL	V3H	3-hydroxyvaline	

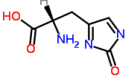
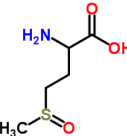
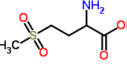
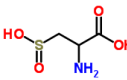
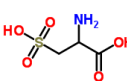
79	79	CYS	CYH	cysteine sulfenic acid	
80	80	PRO	PH5	5-hydroxyproline (R)	
81	81		P5H	5-hydroxyproline (S)	

**Carbonylation**

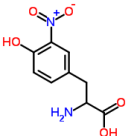
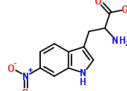
63	63	LYS	KAL	allysine (aminoadipic semialdehyde)	
82	82	PRO	GSA	glutamic semialdehyde	
83		ARG			
84	83	THR	TOX	2-amino-3-ketobutyric acid	

**Oxidation**

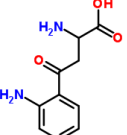
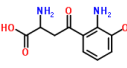
85	84	PRO	PGA	pyroglutamic acid	
86	85	HIS	ASN	asparagine	
87	86	HIS	<b>ASP</b>	aspartic acid (-1)	

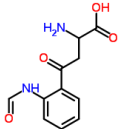
88	87	HIS	H2X	2-oxo-histidine	
89	88	MET	MSX	methionine sulfoxide (R)	
90	89		MXS	methionine sulfoxide (S)	
91	90	MET	MES	methionine sulfone	
92	91	CYS	CSA	cysteine sulfinic acid	
93	92	CYS	CSE	cysteic acid	

### Nitration

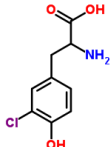
94	93	TYR	YNI	3-nitrotyrosine (-1)	
95	94		YNN	3-nitrotyrosine (0)	
96	95	TRP	WNI	6-nitrotryptophan	

### Kynurenine formation

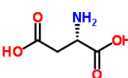
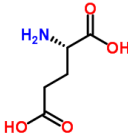
97	96	TRP	WKY	kynurenine	
98	97	TRP	WKH	3-hydroxykynurenine	

99	98	TRP	WKF	formyl-kynurenine	
----	----	-----	-----	-------------------	---

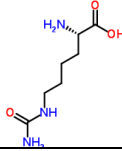
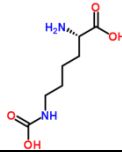
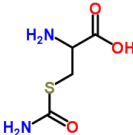
**Chlorination**

100	99	TYR	YCH	chlorotyrosine	
-----	----	-----	-----	----------------	---

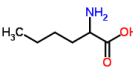
**Deamidation**

101	86	ASN	<b>ASP</b>	aspartic acid (-1)	
102	100	GLN	<b>GLU</b>	glutamic acid (-1)	

**Carbamylation**

103	101	LYS	KAM	homocitrulline	
104	102	LYS	<b>KCA</b>	carboxyllysine (+1)	
105	103		KCN	carboxyllysine (0)	
106	104	CYS	CAM	S-carbamoyl-cysteine	

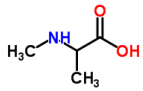
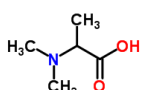
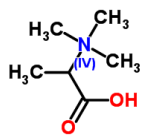
**Norleucine**

107	105	LEU	LNO	norleucine	
108		LYS			
109		MET			

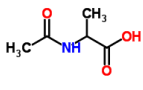
## N-TERMINAL

# PTM	AA	Code	chemical	structure
-------	----	------	----------	-----------

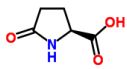
## Methylation

110-129	106	all	1NM	N-methyl-AA (0)	
130-149	107		1NM+	N-methyl-AA (+1)	
150-168	108	all*	2NM	N,N-dimethyl-AA (0)	
169-188	109		2NM+	N,N-dimethyl-AA (+1)	
189-207	110	all*	3NM+	N,N,N-trimethyl-AA	

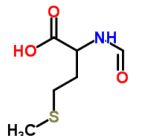
## Acetylation

208-227	111	all	NAC	N-acetyl-AA	
---------	-----	-----	-----	-------------	---

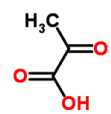
## Pyrrolidone formation

228	84	GLN	PGA	pyroglutamic acid	
229		GLU			

## Formylation

230	112	MET	FOR	N-formylmethionine	
-----	-----	-----	-----	--------------------	---

## Pyruvate formation


231	113	SER	PYA	pyruvic acid	
232		CYS			
233		VAL			



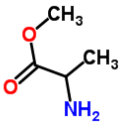
## C-TERMINAL

# PTM	AA	Code	chemical	structure
-------	----	------	----------	-----------

## Amidation

234-253	114	all	AMD	AA-amide	
---------	-----	-----	-----	----------	---

## Methylation

254	115	CYS	CME	AA-methyl ester	
255		LEU			
256		LYS			



## Chapter III

# Microscopic analysis of protein oxidative damage: effect of carbonylation on structure, dynamics, and aggregability of villin headpiece

Petrov, D. & Zagrovic, B. (2011). *J. Am. Chem. Soc.* **133** (18), 7016-7024.

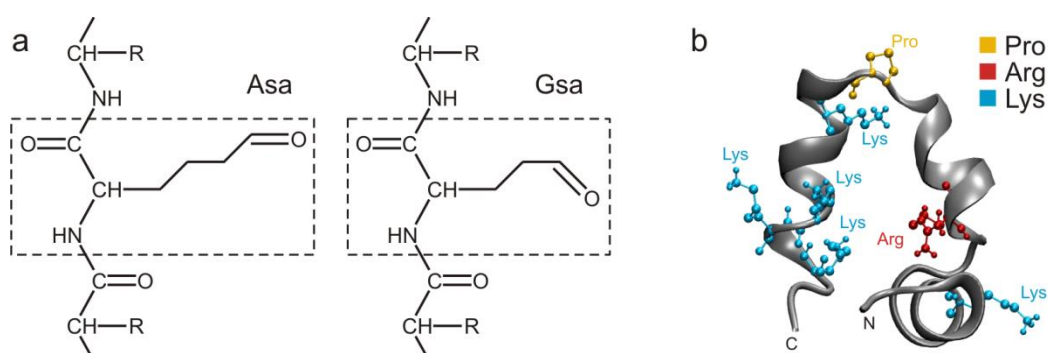
DP and BZ conceived and designed the study. DP collected and DP and BZ analyzed the data.  
DP and BZ wrote the paper.

**ABSTRACT**

One of the most important irreversible oxidative modifications of proteins is carbonylation, the process of introducing a carbonyl group in reaction with reactive oxygen species. Notably, carbonylation increases with the age of cells and is associated with the formation of intracellular protein aggregates and the pathogenesis of age-related disorders such as neurodegenerative diseases and cancer. However, it is still largely unclear how carbonylation affects protein structure, dynamics, and aggregability at the atomic level. Here, we use classical molecular dynamics simulations to study structure and dynamics of the carbonylated headpiece domain of villin, a key actin-organizing protein. We perform an exhaustive set of molecular dynamics simulations of a native villin headpiece together with every possible combination of carbonylated versions of its seven lysine, arginine, and proline residues, quantitatively the most important carbonylatable amino acids. Surprisingly, our results suggest that high levels of carbonylation, far above those associated with cell death *in vivo*, may be required to destabilize and unfold protein structure through the disruption of specific stabilizing elements, such as salt bridges or proline kinks, or tampering with the hydrophobic effect. On the other hand, by using thermodynamic integration and molecular hydrophobicity potential approaches, we quantitatively show that carbonylation of hydrophilic lysine and arginine residues is equivalent to introducing hydrophobic, charge-neutral mutations in their place, and, by comparison with experimental results, we demonstrate that this by itself significantly increases the intrinsic aggregation propensity of both structured, native proteins and their unfolded states. Finally, our results provide a foundation for a novel experimental strategy to study the effects of carbonylation on protein structure, dynamics, and aggregability using site-directed mutagenesis.

## INTRODUCTION

Proteins are frequently modified by different reactions involving reactive oxygen species (ROS), including metal-catalyzed carbonylation, oxidation of aromatic and sulfur-containing amino acid residues, oxidation of the protein backbone, or even protein fragmentation due to backbone breakage.<sup>1-3</sup> One of the most important mechanisms of oxidative damage to proteins is metal-catalyzed carbonylation, where ROS are created in a Fenton-type reaction involving transition metals such as iron or copper.<sup>4</sup> Quantitatively the most important products of carbonylation of amino acids are amino adipic semialdehyde (Asa), derived from lysine, and glutamic semialdehyde (Gsa), derived from arginine and proline residues (Figure 1a).<sup>5,6</sup> Albeit to a much lower extent, carbonyl groups can also be introduced in proteins by direct carbonylation of threonine residues, a secondary reaction with aldehydes produced during lipid peroxidation, or a secondary reaction with carbonyl derivatives generated in reaction of reducing sugars.<sup>1,2</sup>



**Figure 1.** (a) Chemical structures of Asa, derived by carbonylation of Lys, and Gsa, derived by carbonylation of Arg and Pro. (b) Villin structure. The seven quantitatively most important carbonylatable sites are colored as follows: Pro, yellow; Arg, red; Lys, blue.

As compared to other modifications induced by ROS, carbonylation is relatively difficult to induce, but once proteins get carbonylated, the change is permanent due to the irreversible nature of the reaction.<sup>7,8</sup> For this reason, protein carbonyl content is by far the most widely used marker of protein oxidation.<sup>9</sup> The cellular carbonylation level increases with age, with the concentration of carbonylated proteins rising exponentially during the last third of the life span in a wide range of organisms.<sup>3,10</sup> Furthermore, carbonylation is associated with age-related disorders such as neurodegenerative diseases, cancer, and diabetes, but it should be emphasized that it is still unclear whether carbonylation is a direct cause of aging or just a

consequence and a useful reporter on aging.<sup>4</sup> Importantly, the presence of highly carbonylated protein aggregates has been observed in many of these diseases, but so far no clear causal relationship between carbonylation and aggregation has been established.<sup>11,12</sup> Finally, the extreme robustness to ionizing radiation and UV light of some extremophile bacteria such as *Deinococcus radiodurans* has been shown to depend on efficient protection of the proteome against basal and radiation-induced protein carbonylation.<sup>13</sup>

The basal level of carbonylation in cells is approximately 2 nmol of carbonyl per milligram of protein, while the level that appears to correlate with cell and organism death is approximately 6 nmol of carbonyl per milligram of protein, corresponding to about one carbonylated residue per 4000 amino acids on average.<sup>3,10,13</sup> Although these average numbers are actually relatively low, it has been speculated that cellular aging is a direct consequence of the loss of structural stability, unfolding, and exposure of hydrophobic residues of select proteins upon carbonylation.<sup>11</sup> However, to the best of our knowledge, only a few high-resolution studies of structural stability of proteins in the face of oxidative stress have been carried out, and not one focusing explicitly on carbonylation. Most studies focused on the gross functional and structural consequences of oxidation, but with typically very little atomistic details.<sup>14-20</sup> A common denominator of most of these studies is that oxidation of amino acids leads to local disruption of tertiary structure of proteins with a concomitant exposure of hydrophobic amino acids and subsequent aggregation.

Here, we use molecular dynamics (MD)<sup>21</sup> simulation to model the carbonylated villin headpiece molecule. Villin is a tissue-specific actin-binding protein involved in different functions such as cell motility, definition of morphology, and cell death,<sup>22</sup> and it carries out these functions by bundling, nucleating, capping, and severing actin filaments.<sup>23</sup> Our interest in villin was motivated by two principal rationales. First, oxidative stress in non-muscle mammalian cells is known to cause major changes in cellular morphology and structure of the actin cytoskeleton.<sup>24,25</sup> Second, the 36-residue C-terminal headpiece domain of villin is one of the most widely studied and best understood proteins when it comes to folding mechanism and stability.<sup>26-33</sup> Here, we study atomistic-level changes in structure and dynamics of the villin headpiece at different carbonylation levels. In addition to specific effects, such as the disruption of a key salt bridge and a proline kink or alteration of the

hydrophobic effect, we ask what overall level of carbonylation can be tolerated without major effects on the molecule's structural and dynamical integrity. Finally, we ask how does carbonylation affects the intrinsic aggregability of the molecule by altering the basic physicochemical properties of the affected amino acids.

## MATERIALS AND METHODS

We have used MD to study the stability of the carbonylated villin headpiece domain (sequence: **ML**SDEDF**KAV**FGM**TR**SAFAN**LPL**WK**Q**Q**N**L**K**KE**K**GL**F**). The seven bolded letters mark the quantitatively most important carbonylatable amino acids (K, R, and P) in villin headpiece (Figure 1b). The simulations were run using the Gromacs 3.3.3 biomolecular simulation package. United-atom GROMOS 45A3 force field,<sup>34,35</sup> SPC explicit water,<sup>36</sup> and a 2 fs integration step were used. For electrostatics calculations, reaction field was employed with a cutoff of  $r_c = 1.4$  nm and the dielectric constant of  $\epsilon_{rf} = 65$ . An NMR structure of the villin headpiece domain (PDB code 1VII) was used as the starting structure.<sup>26</sup> After steepest descent minimization was performed in vacuum (500 steps) and subsequently in water (1500 steps), the system was equilibrated by gradually increasing the temperature (from 100 to 300 K) over 100 ps with gradually decreasing position restraints (from 25 000 to 5000 kJ mol<sup>-1</sup> nm<sup>-2</sup>) at constant volume and temperature, and finally additionally equilibrated for 20 ps at constant pressure and temperature of 1 bar and 300 K. The temperature and pressure in all production simulations were kept at 300 K and 1 bar using a Berendsen thermostat ( $\tau_T = 0.05$  ps) and barostat ( $\tau_p = 1$  ps and compressibility =  $4.5 \times 10^{-5}$  bar<sup>-1</sup>).<sup>37</sup>

Since the villin headpiece domain has seven potential carbonylation sites belonging to the quantitatively most important carbonylatable residues K, R, and P (see sequence above), the total number of all possible carbonylation combinations of these residues is  $2^7 = 128$ . Altogether, 136 independent 110-ns-long trajectories were generated for a total of 14.96  $\mu$ s of simulation time (five copies of the native and completely carbonylated villin headpiece plus one copy of every other combination:  $5 + 5 + 126 = 136$ ). Coordinates were output every 100 ps, and for the analysis of equilibrium properties, only the last 25 ns of each trajectory was used. Carbonylation modifications were introduced before energy minimization by changing the villin headpiece coordinate file and introducing parameters for the two carbonylated amino acids, Asa and Gsa, in the force field. Details of

parametrization for Asa and Gsa are given in the Supporting Information (SI). For analysis, the simulations were divided into four sets: (1) simulations in set K include different levels of carbonylation of Lys residues, (2) those in set KR include Arg15 carbonylation together with different levels of Lys carbonylation, (3) those in set KP include carbonylation of Pro22 together with different levels of Lys carbonylation, and (4) those in set KRP include simultaneous Arg15 and Pro22 carbonylation with different levels of Lys carbonylation. The trajectories were analyzed primarily using Gromacs tools,<sup>38</sup> including calculation of root-mean-square deviation (rmsd), solvent-accessible surface area (SASA), molecular volume, and distances between groups of atoms, except for (1) secondary structure analysis, where DSSP<sup>39</sup> was used, (2) conformational entropy calculations, where quasiharmonic approximation for calculating entropy was used as described in refs 40 and 41, and (3) characterization of hydrophobic properties of protein surface, where the molecular hydrophobicity potential (MHP) calculation was employed, as described by Efremov *et al.*<sup>42</sup> Throughout the paper, atom-positional rmsd after rotational-translational fitting was calculated with respect to the native NMR villin headpiece structure (PDB code 1VII, residues 43-74; the two residues at each end of the peptide were excluded in calculation as they tend to be dynamic). The PDB structure 1VII starts with the residue 41 and ends with the residue 76, since the complete villin headpiece is 76 residues long, while the reported structure captures just the 36-residues-long C-terminal domain. We used 1-36 numbering here, using backbone atoms for alignment and all atoms for rmsd calculation, if not stated otherwise. Exposure of residues to water was estimated by calculating solvent accessibility fraction, calculated as a fraction of SASA calculated for a given side chain in the context of the villin headpiece structure as compared with the SASA of the same side chain when completely exposed to solvent. Distance between given residues was calculated as the distance between centers of masses of their side chains.

We used the formula proposed by Chiti *et al.*<sup>43</sup> to calculate the change in aggregability upon carbonylation (for structurally destabilized proteins):

$$\ln(v_{mut}/v_{wt}) = A\Delta Hydr + B(\Delta\Delta G_{coil\ \alpha} + \Delta\Delta G_{\beta\ coil}) + C\Delta Charge \quad (1)$$

where  $v_{mut}$  and  $v_{wt}$  are rates of forming aggregates,  $\Delta Hydr$  is the change in hydrophobicity according to the hydrophobicity scale based on water-to-octanol partition,<sup>43</sup>  $\Delta\Delta G_{coil-\alpha} +$

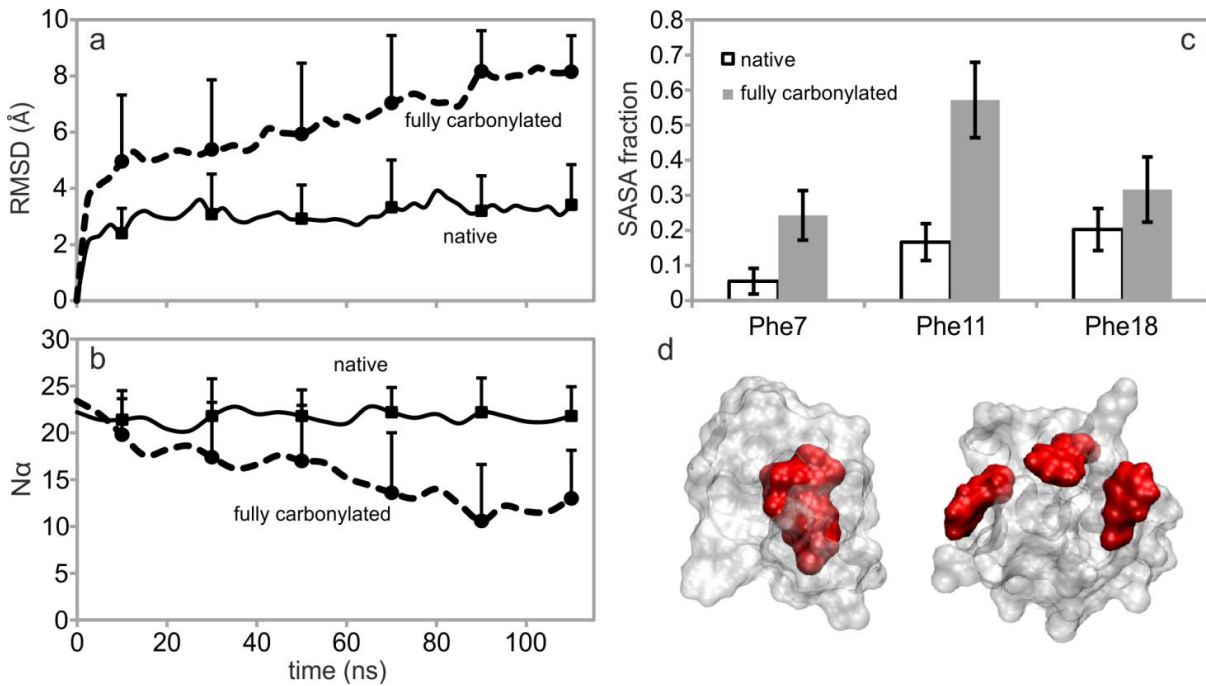


$\Delta\Delta G_{\beta\text{-coil}}$  is the change in propensity to form an  $\alpha$ -helix over a  $\beta$ -sheet,  $\Delta\text{Charge}$  is the change in the absolute value of protein net charge, and  $A = 0.633$ ,  $B = 0.198$ , and  $C = -0.491$  are fitted constants. We used only the first term and the last term, with water/octanol partitioning hydrophobicity values for Asa and Gsa obtained from the MHP calculation described by Efremov *et al.*<sup>42</sup> and the correlation given in Figure 5a (below), but also provided upper and lower bounds derived from the standard deviation of  $\alpha$ -helix and  $\beta$ -sheet propensities over the 27 protein studied by Chiti *et al.*<sup>43</sup> We used the “Zygggregator”<sup>44</sup> model to study the carbonylation-induced change in intrinsic aggregability directly from the native state of the villin headpiece. For this calculation, Asa and Gsa residues were replaced by amino acids that most closely match them in terms of charge and MHP, i.e., Leu and Val, respectively. We could not use Asa and Gsa directly, as not all parameters (such as  $\alpha$  and  $\beta$  propensities) needed for prediction are available at this point.

## RESULTS

### Effect of Carbonylation on Protein Structural and Dynamical Integrity

The structure of the villin headpiece domain is principally stabilized by (1) three phenylalanines buried in the core of the protein, keeping its  $\alpha$ -helices together,<sup>32</sup> and (2) a salt bridge between Asp4 and Arg15 residues.<sup>33</sup> Simultaneous carbonylation of all seven major carbonylatable residues in the protein results in the loss of approximately 40% of its  $\alpha$ -helical secondary structure and most of its tertiary structure in approximately 100 ns (Figure 2a,b). While the simulated native protein keeps its  $\alpha$ -helical content and tertiary structure largely intact over the same period, the carbonylated protein unfolds and starts exploring the accessible areas of the Ramachandran map more freely. Unfolding of the protein upon carbonylation occurs simultaneously with the disintegration of its Phe core (Phe7, Phe11, and Phe18) (Figure 2c,d). Interestingly, the solvent exposure of the Phe core increases multiple-fold as a consequence of carbonylation (Figure 2c), while the total SASA of the protein remains the same although the core residues become exposed to the surface.

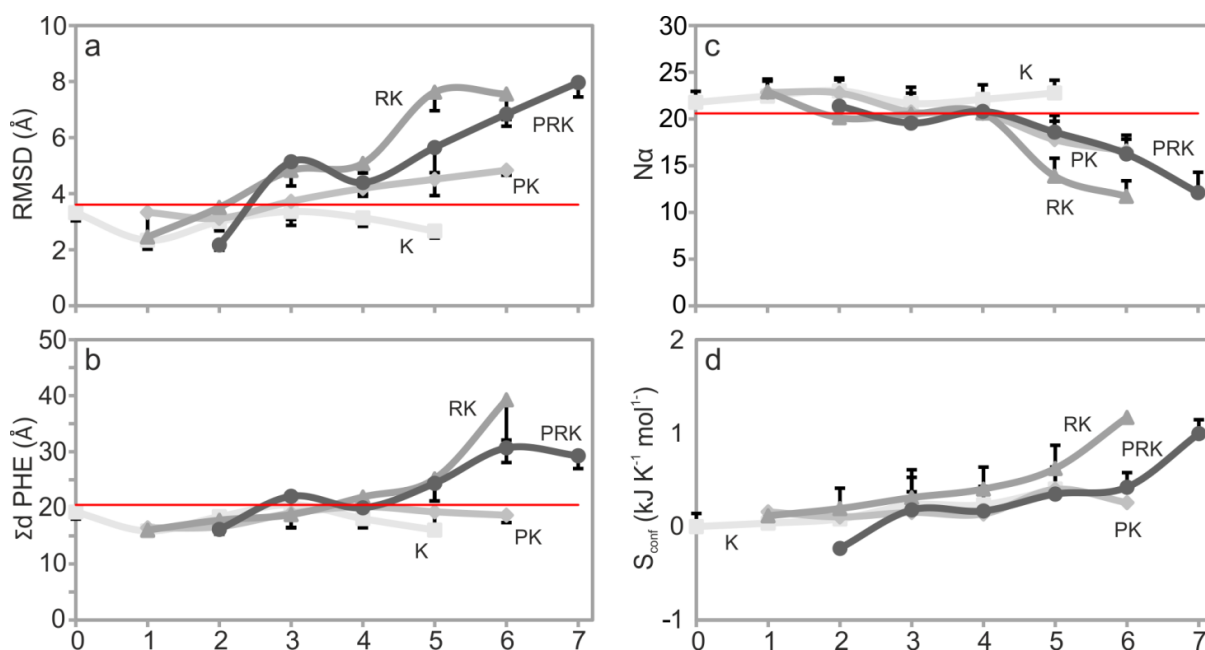


**Figure 2.** Complete carbonylation leads to unfolding of the villin headpiece. (a) All-atom rmsd from the native villin headpiece structure 1VII (residues 43-74) as a function of time. (b) The number of residues in R-helical conformation as a function of time. In both plots the solid line represents native villin headpiece while the dashed line represents fully carbonylated villin headpiece simulations. (c) Total SASA of the three core Phe residues normalized by the total SASA of fully solvent-exposed Phe. Empty bars represent native villin headpiece while gray bars represent fully carbonylated villin headpiece simulations. All curves and bars in panels a-c were obtained as averages over five independent native/fully carbonylated simulations and are shown with standard deviations. (d) A representative structure of native (left) and completely carbonylated (right) villin headpiece showing the surface of the three core phenylalanines in red and the rest of the protein in white.

**Table 1. Types of trajectories studied.** Each set contains a given carbonylation event plus every possible combination of carbonylating the 0-5 Lys residues in the villin headpiece. Set K includes five simulations of the native villin headpiece, i.e., a combination with no Lys residues carbonylated. Similarly, set KRP contains five simulations of the completely carbonylated villin headpiece, i.e., a combination with all five Lys residues carbonylated.

SET	# TRAJ.	CARB. RES.	EVALUATED EFFECTS
K	36	0-5 Lys	$\Delta$ hydrophobicity
KR	32	0-5 Lys + Arg	salt bridge disruption + $\Delta$ hydrophobicity
KP	32	0-5 Lys + Pro	proline kink disruption + $\Delta$ hydrophobicity
KRP	36	0-5 Lys + Arg + Pro	all three effects combined

What happens if just a subset of different carbonylatable residues in villin headpiece are carbonylated, and how does this depend on the type and position of the residues affected? To address this, we have divided our simulations into four distinct sets which were analyzed separately (Table 1). The four sets were organized in such a way to probe different structural effects of carbonylation: surface hydrophobicity change, Asp4-Arg15 salt bridge removal, proline kink removal, or a combination thereof. Interestingly, the structure remains intact when it comes to tertiary fold (as measured by rmsd from the native structure), core compactness (as measured by the sum of distances between the centers of mass of core phenylalanines,  $\Sigma dPHE$ ), and secondary structure (as measured by the number of  $\alpha$ -helical residues) for all single and double carbonylation hits, regardless of their type or location (Figure 3a-c).

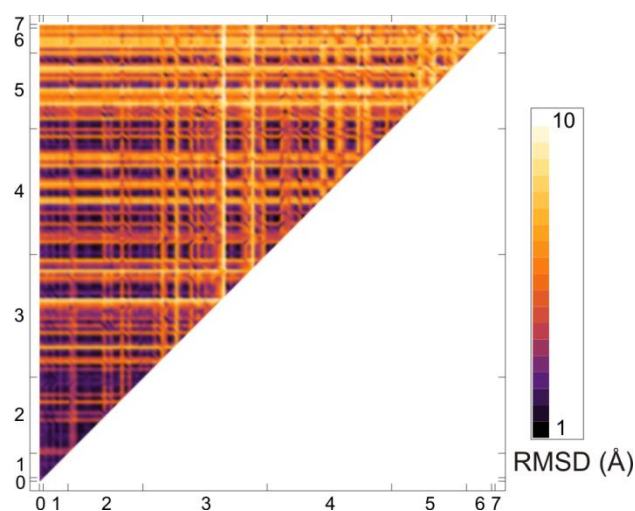


**Figure 3.** Structural stability of the villin headpiece as a function of carbonylation level: (a) rmsd from the native villin headpiece structure 1VII, (b) sum of the distances between the three core phenylalanines, (c) number of residues in  $\alpha$ -helical conformation, and (d) quasi-harmonic conformational entropy normalized by number of atoms, relative to that of native villin headpiece, all shown as a function of the number of carbonylated residues. Each line is obtained from a different subset of simulations: the lightest lines, set K; dark gray lines, set KR; light gray lines, set KP; the darkest lines, set KRP. All points in the plots were calculated as averages over the last 25 ns in each simulation and all simulations in a given subset with the same number of carbonylated residues and are shown with standard deviations. Red lines represent averages of given observables over the five native simulations, increased by the standard deviations, and were used as a criterion for determining whether a given structure is folded or unfolded.

Moreover, the structural features remain largely unchanged with regard to all structural measures, even with all five lysine residues carbonylated (K set) (Figure 3a-c). This is striking as Asa, the product of carbonylation of Lys residues, is significantly less hydrophilic than Lys itself (i.e., its hydration free energy is more positive, SI Figure S1), which could lead to a significant disruption of the stabilizing hydrophobic effect. Our thermodynamic integration (TI) calculations suggest that  $\Delta G_{\text{hydr}}$  between them exceeds  $10 \text{ kJ mol}^{-1}$  in uncharged form and  $230 \text{ kJ mol}^{-1}$  in charged form (SI Figure S1), with the carbonylation of Arg having a similar effect.

For all three structural measures of foldedness (rmsd, core compactness, and  $\alpha$ -helicity), an ensemble of structures with a given number of carbonylated residues (regardless of their type or position) was defined to be unfolded if the average value of the measure in question, reduced by its standard deviation, was greater than its average over the five native trajectories, increased by its respective standard deviation (e.g., if  $\overline{\text{rmsd}^{\text{carb}}} - \sigma_{\text{rmsd}^{\text{carb}}} > \overline{\text{rmsd}^{\text{nat}}} - \sigma_{\text{rmsd}^{\text{nat}}}$ ). According to this definition, significant unfolding (i.e., if  $\overline{\text{rmsd}^{\text{carb}}} - \sigma_{\text{rmsd}^{\text{carb}}} > 3.6 \text{ \AA}$ ,  $\overline{\Sigma dPhe^{\text{carb}}} - \sigma_{\Sigma dPhe^{\text{carb}}} > 20.5 \text{ \AA}$ , and  $\overline{N\alpha^{\text{carb}}} - \sigma_{N\alpha^{\text{carb}}} < 20.6$ ) was observed for (1) simulations in the KR set with Arg15 and at least four Lys residues carbonylated according to  $\alpha$ -helicity and core compactness, and in simulations with Arg15 and at least two Lys residues carbonylated according to rmsd; (2) simulations in the KP set with Pro22 and at least four Lys residues carbonylated according to  $\alpha$ -helicity, and simulations with Pro22 and at least three Lys residues carbonylated according to rmsd; and (3) simulations in the KRP set with Arg15, Pro22, and at least three Lys residues carbonylated according to  $\alpha$ -helicity and core compactness, and in simulations with Arg15, Pro22, and at least one Lys residue carbonylated according to rmsd. When it comes to conformational entropy, our results suggest that there is a sizable increase in conformational entropy after complete carbonylation (approximately  $1 \text{ J K}^{-1} \text{ mol}^{-1}$  per atom). While this increase is consistent with unfolding of the protein, its absolute magnitude could be affected by the sampling employed. On the whole, our results suggest that globular proteins like villin headpiece likely remain structurally stable upon carbonylation, unless the carbonylation level is high. Moreover, these results suggest that the type and the position of the affected residues do make a difference in terms of the extent of structural damage

caused. These findings are further corroborated by the analysis of the average pairwise rmsd between different simulated trajectories exhibiting varying levels and types of carbonylation (Figure 4). According to this analysis, ensembles with five or more carbonylated residues are by-and-large non-native-like, and furthermore their unfolded ensembles are largely mutually different when it comes to structure.



**Figure 4.** Pairwise rmsd density plot. Each point represents the results of comparison of two ensembles of structures from a given pair of simulations of given combinations of carbonylated residues (linear average of the distribution of all-against-all rmsd evaluations for the two ensembles). Altogether 128 combinations were analyzed, and both x and y axis range from 0 to 7 (number of carbonylated residues), where 0 represents the native ensemble and 7 represents the fully carbonylated ensemble. Backbone atoms were used for alignment and rmsd calculations.

In order to estimate to what extent carbonylation of different residues affects protein stability, we used a simple, two-state model with the difference in free energy between the folded and the unfolded states of villin headpiece represented as  $\Delta G_{f-u}$ . We assumed that carbonylation of each residue acts independently and that carbonylation of each Lys residue has the same thermodynamic effect. Using these assumptions, the total change in the free energy of stabilization of villin headpiece upon carbonylation,  $\Delta\Delta G_{carb}$ , can be expressed as

$$\Delta\Delta G_{carb} = n_K\Delta\Delta G_K + n_R\Delta\Delta G_R + n_P\Delta\Delta G_P \quad (2)$$

where  $\Delta\Delta G_K$ ,  $\Delta\Delta G_R$ , and  $\Delta\Delta G_P$  are free energy changes upon carbonylation of individual Lys, Arg, and Pro residues, respectively, and  $n_K$ ,  $n_R$ , and  $n_P$  are the numbers of carbonylated Lys, Arg, and Pro residues, respectively. According to this,

$$\Delta\Delta G_{carb} > \Delta G_{f-u} \quad (3)$$

when the villin headpiece unfolds, and

$$\Delta\Delta G_{carb} < \Delta G_{f-u} \quad (4)$$

when the molecule remains in the native conformation upon carbonylation. We used our simulated data and traces given in Figure 3a-c, together with the definition of foldedness given above, to determine whether a given ensemble of structures is folded or unfolded. For example, one inequality, derived using core compactness as a reporter of the state of the villin headpiece (folded or unfolded), is

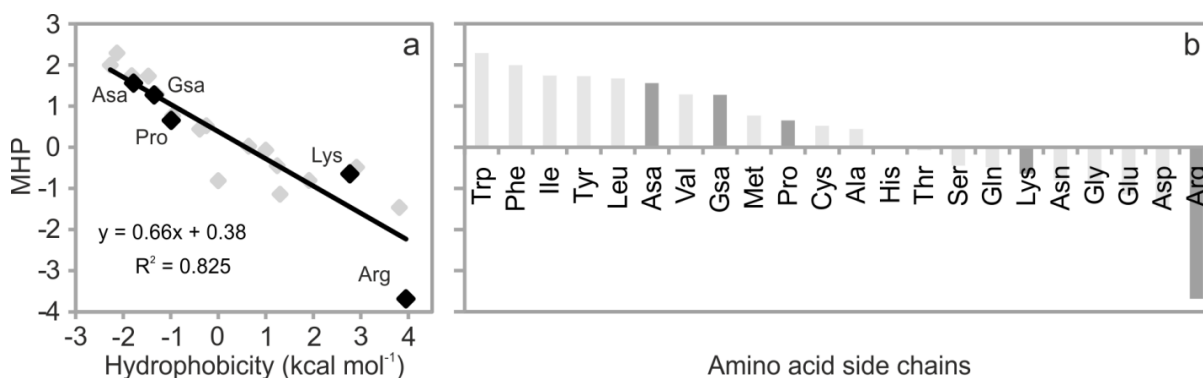
$$5\Delta\Delta G_K + \Delta\Delta G_P < \Delta G_{f-u} \quad (5)$$

Using the same approach, we derived 19 additional inequalities using rmsd, core compactness, and  $\alpha$ -helicity criteria (see SI for details). This system of inequalities has no unique solution, partly because different structural measures that were used are not necessarily mutually consistent when it comes to the definition of foldedness. However, it was possible to find an approximate solution using numerical approaches (see SI for details). Average values over 1136 variations of  $\Delta\Delta G_K$ ,  $\Delta\Delta G_R$ , and  $\Delta\Delta G_P$  values that fulfilled the maximal 16 out of 20 inequalities are  $\Delta\Delta G_K = 0.13\Delta G_{f-u}$ ,  $\Delta\Delta G_R = 0.54\Delta G_{f-u}$  and  $\Delta\Delta G_P = 0.13\Delta G_{f-u}$ . In other words, carbonylation of Arg15 has by far the largest effect on the protein's stability, while the effect of carbonylating Lys and Pro residues is markedly smaller.

### Effect of Carbonylation on Protein Aggregability

Since hydrophobicity is one of the most dominant properties that determines aggregability, we have compared the hydrophobicity (related to aggregability) of native Lys, Arg, and Pro residues and their carbonylated counterparts, Asa and Gsa, using the MHP approach<sup>42</sup> (Figure 5). MHP values correlate well with octanol/water partition factors for amino acid side-chain analogues (Figure 5a), a widely used measure of amino acid hydrophobicity. In agreement with our TI result discussed above, the intrinsic hydrophobicity of Lys and Arg residues increases dramatically upon carbonylation. In terms of MHP weights, converting Lys to Asa or Arg to Gsa is similar to mutating them to highly hydrophobic leucine and valine, respectively (Figure 5b). In fact, the similarity between Asa and Leu, and Gsa and Val, respectively, extends to other basic physicochemical properties as well (SI Table S1). The

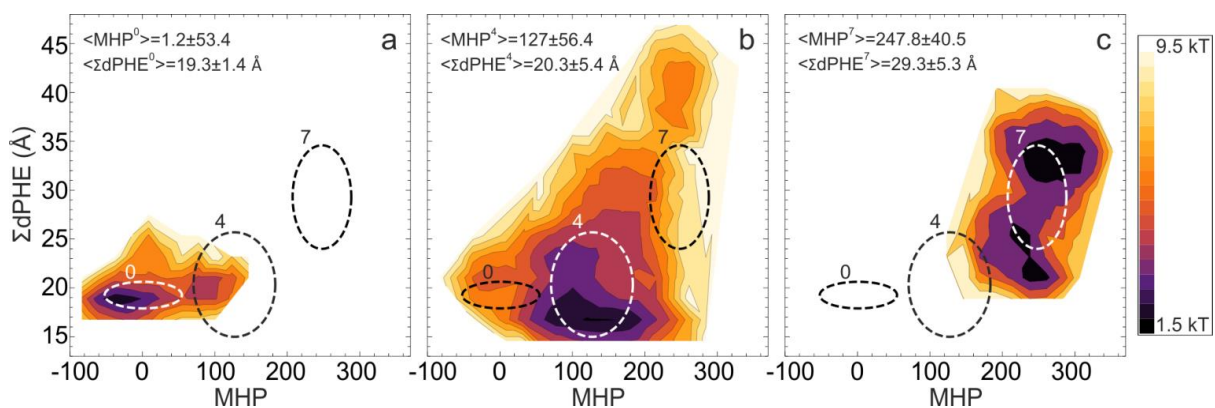
effect of carbonylating Pro to Gsa is less dramatic, albeit still resulting in a net increase in hydrophobicity (Figure 5b). In addition to increasing hydrophobicity, carbonylation also results in charge neutralization when it comes to Lys and Arg residues, and both of these effects potentially increase the intrinsic aggregability of the affected proteins.<sup>43-45</sup>



**Figure 5.** Molecular hydrophobicity potential (MHP) values of native and carbonylated residues. (a) Comparison of the calculated MHP values with the hydrophobicity scale based on free energy of partitioning between aqueous phase and octanol.<sup>43</sup> Large black diamonds represent carbonylatable and carbonylated residues Lys, Arg, Pro, Asa, and Gsa, while small gray diamonds represent standard amino acid residues. The regression line (calculated without Asa and Gsa residues) with  $R^2 = 0.825$  shows that the calculated values correlate well with hydrophobicity scale for standard amino acid residues. (b) Calculated MHP values for all native and carbonylated residues (black bars, carbonylatable and carbonylated residues; gray bars, other native residues).

To analyze this more closely, we have used the MHP approach to characterize the hydrophobicity of a protein surface and compare it with the degree of the protein's structural integrity. In particular, we have studied the projections of the free energy surface for native and fully carbonylated forms of villin headpiece, as well as for an intermediate including all combinations with four carbonylated residues, using MHP, phenylalanine core compactness, and rmsd from the experimental NMR structure as order parameters (Figure 6 and SI Figure S2). Note that free energy projections using MHP as an order parameter were first used by Polyansky and Zagrovic in the context of protein phosphorylation (manuscript in preparation). These free energy maps clearly demonstrate that surface hydrophobicity and the fraction of partially unfolded, aggregation-prone structures increase as the level of carbonylation increases. However, this analysis also shows that compact and structurally native-like, yet significantly hydrophobic structures are present to a high degree in ensembles with moderate levels of carbonylation (Figure 6b). This is a direct consequence of

the fact that Asa and Gsa are significantly more hydrophobic compared with Lys and Arg, respectively, which at moderate levels of carbonylation may not be enough to unfold the molecules but is enough to increase their surface hydrophobicity. On the other hand, only unfolded structures with high surface hydrophobicity are populated in the fully carbonylated ensemble (Figure 6c and SI Figure S2). Taken together, these results suggest that carbonylation increases surface hydrophobicity through unfolding, but it does so also just by itself by modifying the physicochemical properties of the affected residues, which consequently may lead to an increase in aggregability.



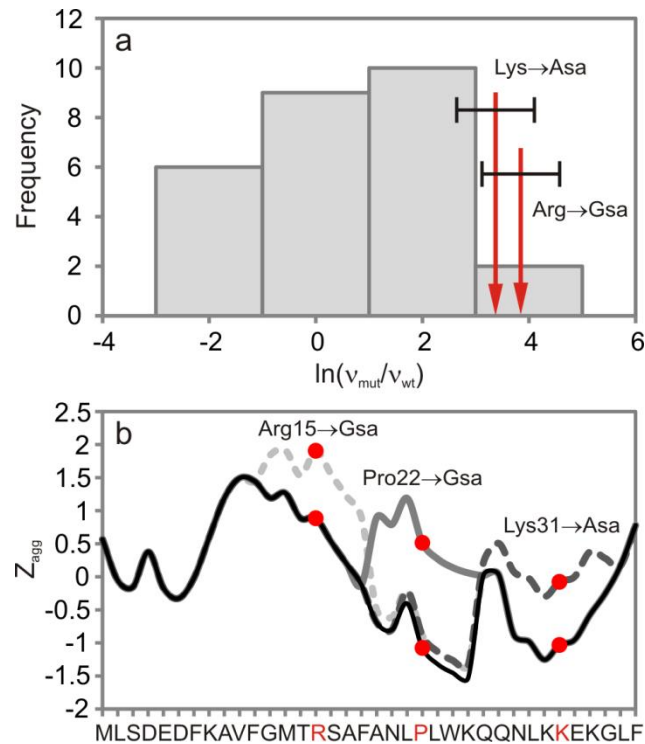
**Figure 6.** Two-dimensional projections of the free-energy surface as a function of MHP and hydrophobic core compactness (as captured by the sum of the distances between the three core phenylalanines) as calculated for (a) the native ensemble (five simulations), (b) the ensemble containing all combinations with four carbonylation events (35 simulations), and (c) the fully carbonylated ensemble (five simulations). Only the last 25 ns of each simulation were used to calculate the free-energy maps. The ellipses are centered at the average values of MHP and  $\Sigma d\text{Phe}$  for the three populations, with the major and minor semiaxes equal to the standard deviations of the distributions. The relative free energies were calculated as  $F = -kT \ln P$ , where  $P$  is the probability of occurrence of a given state, as seen in our simulations.

To put this on a quantitative footing, we have used the model of Chiti *et al.*<sup>43</sup> to estimate the expected change in the aggregation rate of an unstructured protein as a consequence of a single point “mutation” induced by carbonylation (i.e., Lys to Asa or Arg to Gsa conversion). Changes in aggregability for these two “mutations” are  $\ln(v_{\text{mut}}/v_{\text{wt}}) = 3.37 \pm 0.73$  (Lys to Asa) and  $\ln(v_{\text{mut}}/v_{\text{wt}}) = 3.85 \pm 0.73$  (Arg to Gsa), i.e., more than a 30- to 40-fold increase in the aggregation rate for a single carbonylation event, with the error bounds capturing the expected effects of the change in the intrinsic  $\alpha$ -helix and  $\beta$ -sheet propensity, not modeled here. Note that this model is sequence-independent and that these changes in aggregability



are applicable not just to the villin headpiece but rather to any given positively charged protein. Carbonylation increases aggregability of negatively charged proteins as well, but to a somewhat lower extent ( $\ln(v_{\text{mut}}/v_{\text{wt}}) = 2.39 \pm 0.73$  for Lys to Asa, and  $\ln(v_{\text{mut}}/v_{\text{wt}}) = 2.87 \pm 0.73$  for Arg to Gsa), which is still extremely significant. In Figure 7a, we compare this change in aggregability with the predicted change in aggregation rate for 27 different point mutations in seven different unstructured peptides or intrinsically disordered proteins causing diabetes and different neurodegenerative diseases (amylin, two prion peptides,  $\alpha$ -synuclein, amyloid  $\beta$ -peptide, tau protein, and a model protein) examined by Chiti *et al.*<sup>43</sup> Note that the latter predictions correlate well with experimental measurements (Pearson  $r = 0.85$ ). Strikingly, the effect of carbonylation of a single Lys or Arg residue is comparable in magnitude with the most drastic aggregation-inducing mutations in these proteins, with only 2 out of 27 such mutations having a greater effect on protein aggregability than either one of these carbonylation induced conversions.

Finally, to probe the effect of carbonylation on protein aggregability directly from the native state, we have used the model of Vendruscolo *et al.*,<sup>44</sup> replacing Asa and Gsa with amino acids that most closely match them in terms of charge and MHP hydrophobicity, i.e., Leu and Val, respectively. These approximations notwithstanding, it appears that carbonylation of a single residue indeed significantly increases intrinsic aggregability of villin headpiece even in the absence of any major unfolding (Figure 7b). For example, the carbonylation of Pro22 increases its Zagg score, i.e., the aggregability of the region around this residue, from an unfavorable -1 to a highly favorable 0.5. In this model, the Zagg score reflects the combined effect of the intrinsic aggregation propensity of a given sequence and its tendency to be structurally unstable in the native state. Our analysis (Figure 7b and SI Figure S3), showing a dramatic increase in Zagg upon carbonylation throughout the villin sequence, suggests that both of these factors change significantly upon carbonylation in the direction that favors aggregation.



**Figure 7.** Aggregability versus carbonylation. (a) Distribution of changes in aggregability upon 27 single-point mutations in six known proteins causing amyloidogenic disease and in one model protein. Red arrows represent the estimation of aggregability change upon Lys (left arrow,  $\ln(v_{mut}/v_{wt}) = 3.37 \pm 0.73$ ) and Arg (right arrow,  $\ln(v_{mut}/v_{wt}) = 3.85 \pm 0.73$ ) carbonylation, calculated using eq 5. The error bars show standard deviation around zero calculated for the change in  $\alpha$ -helix and  $\beta$ -sheet propensities for all proteins used by Chiti *et al.*<sup>43</sup> (b) Site-specific intrinsic aggregation propensity,  $Z_{agg}$ , for the native (solid black line) and three carbonylated villin headpiece molecules (only single carbonylation hits: Arg15 to Gsa, the lightest gray dotted line; Pro22 to Gsa, dark gray solid line; and Lys31 to Asa, the darkest gray dashed line).

## DISCUSSION

This study presents the first-ever computer simulation effort to analyze the effects of carbonylation on protein structure. We have shown that the structure of the completely carbonylated villin headpiece domain unfolds in the course of simulated trajectories. Further analysis showed that extent of destabilization is site-specific, and that the disruption of both specific stabilizing elements (salt bridges and proline kinks) together with surface hydrophobicity change upon carbonylation of a large number of residues is required for protein unfolding. Note, however, that the effect of surface hydrophobicity change cannot be disentangled from other specific effects: for example, the carbonylation event, which disrupts salt-bridge formation, invariably also changes the hydrophobicity of the involved

residue. Carbonylation of the proline residue is the only case where such a binary effect is avoided, as the native and the carbonylated forms of the residue exhibit similar levels of hydrophobicity.

The level of carbonylation at which the villin headpiece, a marginally stable protein,<sup>46</sup> unfolds in our simulations (ca. 14% of all residues) is  $\sim 3$  orders of magnitude greater than the average level of carbonylation which correlates with cellular senescence and death in vivo (ca. 0.025% of all residues).<sup>3,10,13</sup> This suggests that typical cellular levels of carbonylation are not likely to disrupt protein structure, which is not in contradiction with experimental studies.<sup>16,18</sup> If carbonylation does not induce major structural destabilization of a typical protein and thus lead to aggregation, as widely assumed,<sup>17,47</sup> how does it then promote the formation of cytotoxic aggregates? First, several studies suggest that some proteins are more susceptible to carbonylation than others,<sup>9,48-50</sup> which may result in a situation where these proteins are completely carbonylated, while the majority of other proteins are still intact, in agreement with our results. Second, newly synthesized proteins in an old organism might be misfolded or unfolded due to, for example, accumulated DNA mutations and would therefore be more susceptible to carbonylation, as has been shown by Dukan *et al.*<sup>51</sup> Finally, modifications of specific, functionally important residues may abolish the function of a protein without destabilizing its structure.

We propose two novel possibilities to explain this. First, our results suggest that carbonylation just by itself may increase protein aggregability of unstructured polypeptides (Figure 7a). In this scenario, protein unfolding arises because of either carbonylation or some other environmental factors, but importantly, carbonylation makes the unfolded molecule additionally aggregation-prone. Second, our results suggest that carbonylation may increase protein aggregability even in the absence of major unfolding (Figure 7b). From lysozyme to superoxide dismutase to prolactin, there are numerous examples of proteins which undergo amyloid formation under native conditions and without any major unfolding, simply as a consequence of local thermal fluctuations.<sup>52</sup> Increasing the local propensity to aggregate through carbonylation may speed this process up.

Using TI and MHP approaches, we have shown that the products of carbonylation of Lys and Arg residues are significantly more hydrophobic than these amino acids. Such an increase in

hydrophobicity, together with a concomitant charge removal, significantly increases the intrinsic aggregability of proteins.<sup>43-45</sup> On the other hand, the aggregation propensity of proline residues is decreased by precluding  $\beta$ -sheet formation, and their mutations are known to lead to protein aggregation.<sup>53</sup> Finally, recent findings that the three quantitatively most important carbonylatable residues (Arg, Lys, and Pro) in many proteins actually serve as key gatekeepers that flank aggregation-prone regions of proteins and prevent aggregation further support our suggestions.<sup>54</sup>

In general, the list of amyloidogenic, deposition diseases shows a strong overlap with the list of diseases in which high levels of protein carbonylation are detected, including Alzheimer's disease, Parkinson's disease, diabetes, rheumatoid arthritis, dementia with Lewy bodies, familial amyotrophic lateral sclerosis, and others.<sup>7,9,52,55</sup> Because of the complex pathophysiology of these diseases, the causal link between carbonylation and aggregation is not simple and is still to be fully explored. In fact, not all aggregation-prone proteins associated with these diseases are at the same time highly carbonylatable and vice versa. However, there are a number of important examples where this is precisely so. For example, ubiquitin C-terminal hydrolase L1 (UCH-L1), which features critically in sporadic variants of Alzheimer's and Parkinson's diseases, forms aggregates but is also highly carbonylatable.<sup>7,56</sup> Superoxide dismutase 1 in familial amyotrophic lateral sclerosis,<sup>7,52</sup> human  $\beta$ 2-microglobulin in end-stage renal failure,<sup>52,57</sup> and  $\beta$ -actin and  $\alpha/\beta$ -tubulin in multiple sclerosis<sup>58</sup> are further examples of such proteins. Importantly, our results provide a novel explanation that links aggregation and carbonylation in these systems, even at relatively low levels of carbonylation typically seen *in vivo*. One way to test this connection experimentally would be to use Lys to Leu, Arg to Val, and Pro to Val point mutations for high-resolution, site-specific studies of the structural and functional consequences of carbonylation, as these mutations, according to our results, quantitatively match the effects of hydrophobicity increase and charge removal in the course of carbonylation. Such studies, hand in hand with further computational analyses, may provide an atomistic picture behind protein carbonylation and its cellular consequences, protein aggregation, and cell senescence.

## ASSOCIATED CONTENT

**Supporting information.** Figures showing TI, MHP vs rmsd free energy surfaces, and Zagg results; table of physicochemical properties of Asa, Gsa, Leu, and Val; parametrization of Asa and Gsa residues; and details of TI calculation.

## ACKNOWLEDGEMENTS

This work was supported in part by the National Foundation of Science, Higher Education and Technological Development of Croatia (EMBO Installation grant to B.Z.), the Unity through Knowledge Fund (UKF 1A grant to B.Z.), and the Austrian Science Fund FWF (START grant Y 514-B11 to B.Z.). We thank A. Polyansky for help with MHP calculations, R. Zubac for help with entropy calculations, R. Santos for help with graphical representation of villin headpiece, and the members of the Laboratory of Computational Biophysics at MFPL for useful advice and assistance.

## REFERENCES

1. Stadtman, E. R. Protein oxidation and aging. *Science* **257**, 1220-1224 (1992).
2. Berlett, B. S. & Stadtman, E. R. Protein oxidation in aging, disease, and oxidative stress. *J. Biol. Chem.* **272**, 20313-20316 (1997).
3. Levine, R. L. & Stadtman, E. R. Oxidative modification of proteins during aging. *Exp. Gerontol.* **36**, 1495-1502 (2001).
4. Nystrom, T. Role of oxidative carbonylation in protein quality control and senescence. *EMBO J.* **24**, 1311-1317 (2005).
5. Requena, J. R., Levine, R. L. & Stadtman, E. R. Recent advances in the analysis of oxidized proteins. *Amino Acids* **25**, 221-226 (2003).
6. Maisonneuve, E. *et al.* Rules governing selective protein carbonylation. *PLoS ONE* **4**, e7269 (2009).
7. Dalle-Donne, I., Giustarini, D., Colombo, R., Rossi, R. & Milzani, A. Protein carbonylation in human diseases. *Trends Mol. Med.* **9**, 169-176 (2003).
8. Dalle-Donne, I., Rossi, R., Colombo, R., Giustarini, D. & Milzani, A. Biomarkers of oxidative damage in human disease. *Clin. Chem.* **52**, 601-623 (2006).
9. Dalle-Donne, I. *et al.* Protein carbonylation, cellular dysfunction, and disease progression. *J. Cell. Mol. Med.* **10**, 389-406 (2006).
10. Levine, R. L. Carbonyl modified proteins in cellular regulation, aging, and disease. *Free Radic. Biol. Med.* **32**, 790-796 (2002).
11. Grune, T., Jung, T., Merker, K. & Davies, K. J. Decreased proteolysis caused by protein aggregates, inclusion bodies, plaques, lipofuscin, ceroid, and 'aggresomes' during oxidative stress, aging, and disease. *Int. J. Biochem. Cell Biol.* **36**, 2519-2530 (2004).
12. Davies, K. J. Degradation of oxidized proteins by the 20S proteasome. *Biochimie* **83**, 301-310 (2001).
13. Krisko, A. & Radman, M. Protein damage and death by radiation in *Escherichia coli* and *Deinococcus radiodurans*. *Proc. Natl. Acad. Sci. U.S.A.* **107**, 14373-14377 (2010).
14. Davies, K. J. A. & Delsignore, M. E. Protein damage and degradation by oxygen radicals. III. Modification of secondary and tertiary structure. *J. Biol. Chem.* **262**, 9908-9913 (1987).
15. Gardner, P. R., Nguyen, D. D. H. & White, C. W. Aconitase is a sensitive and critical target of oxygen poisoning in cultured-mammalian-cells and in rat lungs. *Proc. Natl. Acad. Sci. U.S.A.* **91**, 12248-12252 (1994).
16. Lasch, P. *et al.* Hydrogen peroxide-induced structural alterations of RNase A. *J. Biol. Chem.* **276**, 9492-9502 (2001).
17. Bota, D. A. & Davies, K. J. A. Lon protease preferentially degrades oxidized mitochondrial aconitase by an ATP-stimulated mechanism. *Nat. Cell Biol.* **4**, 674-680 (2002).
18. Li, D. W. & Bruschweiler, R. All-atom contact model for understanding protein dynamics from crystallographic B-factors. *Biophys. J.* **96**, 3074-3081 (2009).
19. Perez, V. I. *et al.* Protein stability and resistance to oxidative stress are determinants of longevity in the longest-living rodent, the naked mole-rat. *Proc. Natl. Acad. Sci. U.S.A.* **106**, 3059-3064 (2009).
20. Wu, W., Wu, X. J. & Hu, Y. F. Structural modification of soy protein by the lipid peroxidation product acrolein. *Lebensm. Wiss. Technol.* **43**, 133-140 (2010).
21. van Gunsteren, W. F. *et al.* Biomolecular modeling: Goals, problems, perspectives. *Angew. Chem. Int. Ed.* **45**, 4064-4092 (2006).
22. Khurana, S. & George, S. P. Regulation of cell structure and function by actin-binding proteins: villin's perspective. *FEBS Lett.* **582**, 2128-2139 (2008).

23. Friederich, E., Vancompernelle, K., Louvard, D. & Vandekerckhove, J. Villin function in the organization of the actin cytoskeleton. Correlation of in vivo effects to its biochemical activities in vitro. *J. Biol. Chem.* **274**, 26751-26760 (1999).
24. Dalle-Donne, I. *et al.* Actin carbonylation: from a simple marker of protein oxidation to relevant signs of severe functional impairment. *Free Radic. Biol. Med.* **31**, 1075-1083 (2001).
25. Dalle-Donne, I., Rossi, R., Milzani, A., Di Simplicio, P. & Colombo, R. The actin cytoskeleton response to oxidants: from small heat shock protein phosphorylation to changes in the redox state of actin itself. *Free Radic. Biol. Med.* **31**, 1624-1632 (2001).
26. McKnight, C. J., Matsudaira, P. T. & Kim, P. S. NMR structure of the 35-residue villin headpiece subdomain. *Nat. Struct. Biol.* **4**, 180-184 (1997).
27. Duan, Y. & Kollman, P. A. Pathways to a protein folding intermediate observed in a 1-microsecond simulation in aqueous solution. *Science* **282**, 740-744 (1998).
28. Zagrovic, B., Snow, C. D., Shirts, M. R. & Pande, V. S. Simulation of folding of a small alpha-helical protein in atomistic detail using worldwide-distributed computing. *J. Mol. Biol.* **323**, 927-937 (2002).
29. Zagrovic, B., Snow, C. D., Khaliq, S., Shirts, M. R. & Pande, V. S. Native-like mean structure in the unfolded ensemble of small proteins. *J. Biol. Chem.* **323**, 153-164 (2002).
30. Meng, J. *et al.* High-resolution crystal structures of villin headpiece and mutants with reduced F-actin binding activity. *Biochemistry* **44**, 11963-11973 (2005).
31. Lei, H., Wu, C., Liu, H. & Duan, Y. Folding free-energy landscape of villin headpiece subdomain from molecular dynamics simulations. *Proc. Natl. Acad. Sci. U.S.A.* **104**, 4925-4930 (2007).
32. Cornilescu, G. *et al.* Solution structure of a small protein containing a fluorinated side chain in the core. *Protein Sci.* **16**, 14-19 (2007).
33. Gronwald, W., Hohm, T. & Hoffmann, D. Evolutionary Pareto-optimization of stably folding peptides. *BMC Bioinformatics* **9**, 109 (2008).
34. Schuler, L. D., Walde, P., Luisi, P. L. & van Gunsteren, W. F. Molecular dynamics simulation of n-dodecyl phosphate aggregate structures. *Eur. Biophys. J.* **30**, 330-343 (2001).
35. Schuler, L., Daura, X. & van Gunsteren, W. An improved GROMOS96 force field for aliphatic hydrocarbons in the condensed phase. *J. Comput. Chem.* **22**, 1205-1218 (2001).
36. Berendsen, H. J. C., Postma, J. P. M., van Gunsteren, W. F. & Hermans, J. in *Intermolecular Forces* (ed B. Pullman) 331-342 (Reidel, Dordrecht, 1981).
37. Berendsen, H. J. C., Postma, J. P. M., van Gunsteren, W. F., Dinola, A. & Haak, J. R. Molecular-dynamics with coupling to an external bath. *J Chem Phys* **81**, 3684-3690 (1984).
38. Lindahl, E., Hess, B. & van der Spoel, D. GROMACS 3.0: a package for molecular simulation and trajectory analysis. *J Mol Model* **7**, 306-317 (2001).
39. Kabsch, W. & Sander, C. Dictionary of protein secondary structure: pattern recognition of hydrogen-bonded and geometrical features. *Biopolymers* **22**, 2577-2637 (1983).
40. Andricioaei, I. & Karplus, M. On the calculation of entropy from covariance matrices of the atomic fluctuations. *J Chem Phys* **115**, 6289-6292 (2001).
41. Levy, R. M., Srinivasan, A. R., Olson, W. K. & McCammon, J. A. Quasi-harmonic method for studying very low-frequency modes in proteins. *Biopolymers* **23**, 1099-1112 (1984).
42. Efremov, R. G. *et al.* Molecular lipophilicity in protein modeling and drug design. *Curr. Med. Chem.* **14**, 393-415 (2007).
43. Chiti, F., Stefani, M., Taddei, N., Ramponi, G. & Dobson, C. M. Rationalization of the effects of mutations on peptide and protein aggregation rates. *Nature* **424**, 805-808 (2003).

44. Tartaglia, G. G. *et al.* Prediction of aggregation-prone regions in structured proteins. *J. Mol. Biol.* **380**, 425-436 (2008).
45. Dobson, C. M. Protein folding and misfolding. *Nature* **426**, 884-890 (2003).
46. Godoy-Ruiz, R. *et al.* Estimating free-energy barrier heights for an ultrafast folding protein from calorimetric and kinetic data. *J Phys Chem B* **112**, 5938-5949 (2008).
47. Pan, J. C., Yu, Z. H., Hui, E. F. & Zhou, H. M. Conformational change and inactivation of arginine kinase from shrimp *Fenneropenaeus chinensis* in oxidized dithiothreitol solutions. *Biochem. Cell Biol.* **82**, 361-367 (2004).
48. Das, N., Levine, R. L., Orr, W. C. & Sohal, R. S. Selectivity of protein oxidative damage during aging in *Drosophila melanogaster*. *Biochem. J* **360**, 209-216 (2001).
49. Jana, C. K., Das, N. & Sohal, R. S. Specificity of age-related carbonylation of plasma proteins in the mouse and rat. *Arch. Biochem. Biophys.* **397**, 433-439 (2002).
50. Choi, J. *et al.* Oxidative modifications and aggregation of Cu,Zn-superoxide dismutase associated with Alzheimer and Parkinson diseases. *J. Biol. Chem.* **280**, 11648-11655 (2005).
51. Dukan, S. *et al.* Protein oxidation in response to increased transcriptional or translational errors. *Proc. Natl. Acad. Sci. U.S.A.* **97**, 5746-5749 (2000).
52. Chiti, F. & Dobson, C. M. Amyloid formation by globular proteins under native conditions. *Nat. Chem. Biol.* **5**, 15-22 (2009).
53. Williams, A. D. *et al.* Mapping abeta amyloid fibril secondary structure using scanning proline mutagenesis. *J. Biol. Chem.* **335**, 833-842 (2004).
54. Rousseau, F., Serrano, L. & Schymkowitz, J. W. How evolutionary pressure against protein aggregation shaped chaperone specificity. *J. Biol. Chem.* **355**, 1037-1047 (2006).
55. Chiti, F. & Dobson, C. M. Protein misfolding, functional amyloid, and human disease. *Annu. Rev. Biochem.* **75**, 333-366 (2006).
56. Choi, J. *et al.* Oxidative modifications and down-regulation of ubiquitin carboxyl-terminal hydrolase L1 associated with idiopathic Parkinson's and Alzheimer's diseases. *J. Biol. Chem.* **279**, 13256-13264 (2004).
57. Michelis, R., Sela, S. & Kristal, B. Intravenous iron-gluconate during haemodialysis modifies plasma beta(2)-microglobulin properties and levels. *Nephrol. Dial. Transplant.* **20**, 1963-1969 (2005).
58. Bizzozero, O. A. in *Handbook of neurochemistry and molecular neurobiology. Brain and spinal cord trauma*, 3rd ed., Banik, N. L., Ray, S. K., Lajtha, A., eds.; Chapter 23, Springer: New York ; London, 2009



## Appendices to Chapter III

### Parameterization of Asa and Gsa residues

Lysine residues were changed into Asa by removing the hydrogen atoms (HZ1, HZ2 and HZ3) bonded to the nitrogen atom NZ in the side chain, and by replacing the nitrogen atom (NZ) with oxygen; arginine residue was changed into Gsa by removing all side chain atoms, except the three carbon atoms (CB, CG and CD) and the nitrogen atom NE, which was replaced with an oxygen atom; finally the proline residue was changed into Gsa the same way like arginine by replacing the hydrogen atom HD2 bound to CD carbon atom with oxygen. The double bond between carbon and oxygen atoms, and the potential energy term for an angle between a triplet of one oxygen and two carbon atoms in the GROMOS 45A3 force field<sup>1</sup> are described always using the same parameters regardless of the type of carbon or oxygen atoms (e.g., the carboxyl group in the backbone). In order to be internally consistent, we used the same bond parameters in the description of the bond between the atoms CD and oxygen in Asa and the atoms CG and oxygen in Gsa, and the same angle parameters in the description of the angle between the last two carbon atoms and oxygen atom both in Asa and Gsa. All other bonded parameters in Asa and Gsa residues were the same as in lysine and arginine residues, respectively. GROMOS 45A3 building block files for Asa and Gsa are given at the end of the Supporting Information.

### Thermodynamic integration:

We used thermodynamic integration (TI)<sup>2</sup> for the calculation of hydration free energies for all amino-acid side-chain analogues and two carbonylated amino-acid side-chain analogues in order to estimate the difference in hydration free-energy between Lys and Asa; and Arg and Gsa. Hydration free energies of neutral and charged forms of native and carbonylated amino-acid side-chain analogues with the CB atom  $CH_n$  replaced by  $CH_{n+1}$ , were calculated using TI. Since only hydration free energies of neutral forms of amino-acid side-chain analogues are experimentally measurable, we used them for direct comparison between calculated and experimental values.

The equilibration and free energy calculations in water were carried out using the same conditions as described above for protein simulations, while calculations *in vacuo* were

carried out at 300 K (Berendsen thermostat and  $\tau_T = 0.05$  ps were used) without periodical boundary condition, using the simple cut-off method for calculating electrostatics with a cutoff of  $r_c=1.4$  nm. Non-bonded interactions of side chains were scaled down to zero in a stepwise manner using a coupling parameter  $\lambda$ . Free energy changes upon removal of non-bonded interactions were calculated as integrals of the averages of the derivatives of the total system Hamiltonian with respect to  $\lambda$ , between the boundaries  $\lambda=0$  and  $\lambda=1$ ,

$$\Delta G = \int_0^1 \langle \frac{\partial H}{\partial \lambda} \rangle_{\lambda} d\lambda. \quad (1)$$

After initially 26 evenly spaced  $\lambda$ -points were sampled, changes in slope at each point of the  $\langle \frac{\partial H}{\partial \lambda} \rangle_{\lambda}$  versus  $\lambda$  graph were calculated. The number of additional  $\lambda$ -points placed between two given neighbor  $\lambda$ -points in the second step was proportional to the sum of slope changes at these points, for a total of 26 additional  $\lambda$ -points. The slope changes for the first and the last  $\lambda$ -point were considered to be the same as the slope changes in the second and the penultimate  $\lambda$ -point respectively. Trapezoidal integration was used to evaluate the integral in equation (1) using 52  $\lambda$ -points. Sampling of 50 ps of equilibration and 200 ps of data collection at each point were used. In order to avoid singularities in the non-bonded interaction a soft-core interaction was used

$$V_{sc}(r) = (1 - \lambda)V^A(r_A) + \lambda V^B(r_B), \quad (2)$$

$$r_A = (\alpha \sigma_A^6 \lambda^p + r^6)^{\frac{1}{6}}, \quad (3)$$

$$r_B = (\alpha \sigma_B^6 (1 - \lambda^p) + r^6)^{\frac{1}{6}}, \quad (4)$$

where  $\sigma_A$  and  $\sigma_B$  are van der Waals parameters and  $\alpha = 1.51$  and  $p = 1.3^4$ . The hydration free energy was calculated by subtracting the free energy change when side chain was simulated *in vacuo* from the free energy change when side chain was simulated in water.

### Fractional contribution of different specific factors to villin headpiece destabilization upon carbonylation

To find how much different specific factors contribute to destabilization of villin headpiece, using our simulated results, we have derived a set of 20 inequalities.

Inequalities based on RMSD:

$$5\Delta G_K < \Delta \Delta G_{f-u}, \quad (5)$$

$$\Delta G_K + \Delta G_R < \Delta \Delta G_{f-u}, \quad (6)$$

$$2\Delta G_K + \Delta G_R > \Delta \Delta G_{f-u}, \quad (7)$$

$$2\Delta G_K + \Delta G_P < \Delta \Delta G_{f-u}, \quad (8)$$

$$3\Delta G_K + \Delta G_P > \Delta \Delta G_{f-u}, \quad (9)$$

$$\Delta G_R + \Delta G_P < \Delta \Delta G_{f-u}, \quad (10)$$

$$\Delta G_K + \Delta G_R + \Delta G_P > \Delta \Delta G_{f-u}. \quad (11)$$

Inequalities based on core compactness:

$$5\Delta G_K < \Delta \Delta G_{f-u}, \quad (12)$$

$$3\Delta G_K + \Delta G_R < \Delta \Delta G_{f-u}, \quad (13)$$

$$4\Delta G_K + \Delta G_R > \Delta \Delta G_{f-u}, \quad (14)$$

$$5\Delta G_K + \Delta G_P < \Delta \Delta G_{f-u}, \quad (15)$$

$$2\Delta G_K + \Delta G_R + \Delta G_P < \Delta \Delta G_{f-u}, \quad (16)$$

$$3\Delta G_K + \Delta G_R + \Delta G_P > \Delta \Delta G_{f-u}. \quad (17)$$

Inequalities based on core  $\alpha$ -helicity:

$$5\Delta G_K < \Delta \Delta G_{f-u}, \quad (18)$$

$$3\Delta G_K + \Delta G_R < \Delta \Delta G_{f-u}, \quad (19)$$

$$4\Delta G_K + \Delta G_R > \Delta \Delta G_{f-u}, \quad (20)$$

$$3\Delta G_K + \Delta G_P < \Delta \Delta G_{f-u}, \quad (21)$$

$$4\Delta G_K + \Delta G_P > \Delta \Delta G_{f-u}, \quad (22)$$

$$2\Delta G_K + \Delta G_R + \Delta G_P < \Delta \Delta G_{f-u}, \quad (23)$$

$$3\Delta G_K + \Delta G_R + \Delta G_P > \Delta \Delta G_{f-u}. \quad (24)$$

To find a solution to this set of inequalities numerically, we discretized the space of values for  $\Delta \Delta G_K$ ,  $\Delta \Delta G_R$  and  $\Delta \Delta G_P$  to integer percentage of  $\Delta G_{f-u}$  and counted the number of fulfilled inequalities for a given set of discrete values of  $\Delta \Delta G_K$ ,  $\Delta \Delta G_R$  and  $\Delta \Delta G_P$ , among all 1030301 variations for  $0 \leq \Delta \Delta G_K \leq 100$ ,  $0 \leq \Delta \Delta G_R \leq 100$  and  $0 \leq \Delta \Delta G_P \leq 100$  in steps of  $0.01\Delta G_{f-u}$ . The number of fulfilled inequalities ranged from 6 to 16.

## Asa and Gsa GROMOS 45A3 parameters

ffG45a3.rtp file:

[ ASA ]

[ atoms ]

```

N N -0.28000 0
H H 0.28000 0
CA CH1 0.00000 1
CB CH2 0.00000 1
CG CH2 0.00000 1
CD CH2 0.00000 1
CE CH1 0.38000 2
OE1 O -0.38000 2
C C 0.380 3
O O -0.380 3

```

[ bonds ]

```

N H gb_2
N CA gb_20
CA C gb_26
C O gb_4
C +N gb_9
CA CB gb_26
CB CG gb_26
CG CD gb_26
CD CE gb_26
CE OE1 gb_4

```

[ angles ]

; ai aj ak gromos type

```

-C N H ga_31
H N CA ga_17
-C N CA ga_30
N CA C ga_12
CA C +N ga_18
CA C O ga_29
O C +N ga_32
N CA CB ga_12
C CA CB ga_12
CA CB CG ga_14
CB CG CD ga_14
CG CD CE ga_14

```

CD CE OE1 ga\_29

[ impropers ]

; ai aj ak al gromos type

```

N -C CA H gi_1
C CA +N O gi_1
CA N C CB gi_2

```

[ dihedrals ]

; ai aj ak al gromos type

```

-C A -C N CA gd_4
-C N CA C gd_19
N CA C +N gd_20
N CA CB CG gd_17
CA CB CG CD gd_17
CB CG CD CE gd_17
CG CD CE OE1 gd_20

```

[ GSA ]

[ atoms ]

```

N N -0.28000 0
H H 0.28000 0
CA CH1 0.00000 1
CB CH2 0.00000 1
CG CH2 0.00000 1
CD CH1 0.38000 2
OE1 O -0.38000 2
C C 0.380 3
O O -0.380 3

```

[ bonds ]

```

N H gb_2
N CA gb_20
CA C gb_26
C O gb_4
C +N gb_9
CA CB gb_26
CB CG gb_26
CG CD gb_26
CD OE1 gb_4

```

```

[ angles ]
; ai aj ak gromos type
-C N H ga_31
H N CA ga_17
-C N CA ga_30
N CA C ga_12
CA C +N ga_18
CA C O ga_29
O C +N ga_32
N CA CB ga_12
C CA CB ga_12
CA CB CG ga_14
CB CG CD ga_14
CG CD OE1 ga_29
[ impropers ]
; ai aj ak al gromos type
N -C CA H gi_1

```

```

C CA +N O gi_1
CA N C CB gi_2
[ dihedrals ]
; ai aj ak al gromos type
-CA -C N CA gd_4
-C N CA C gd_19
N CA C +N gd_20
N CA CB CG gd_17
CA CB CG CD gd_17
CB CG CD OE1 gd_20

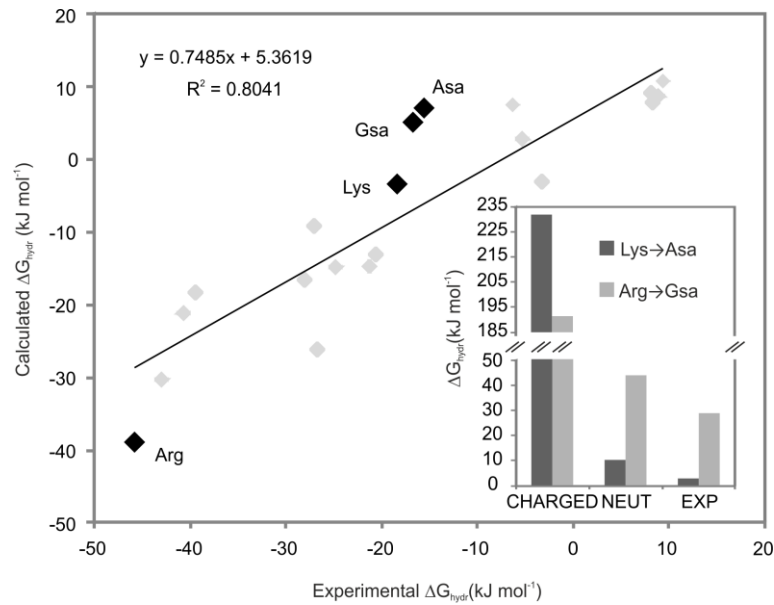
```

ffG45a3.hdb file:

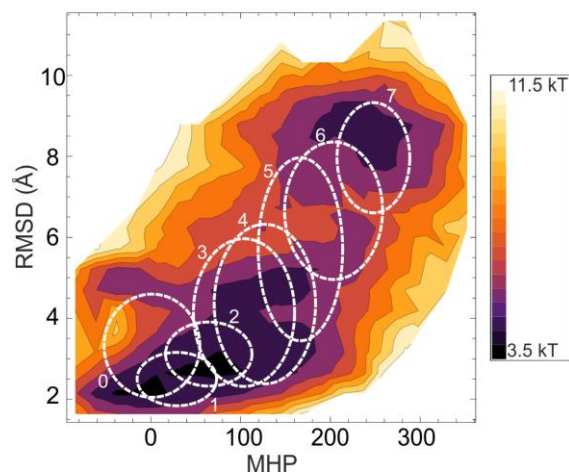
```

ASA 1
1 1 H N -C CA
GSA 1
1 1 H N -C CA

```

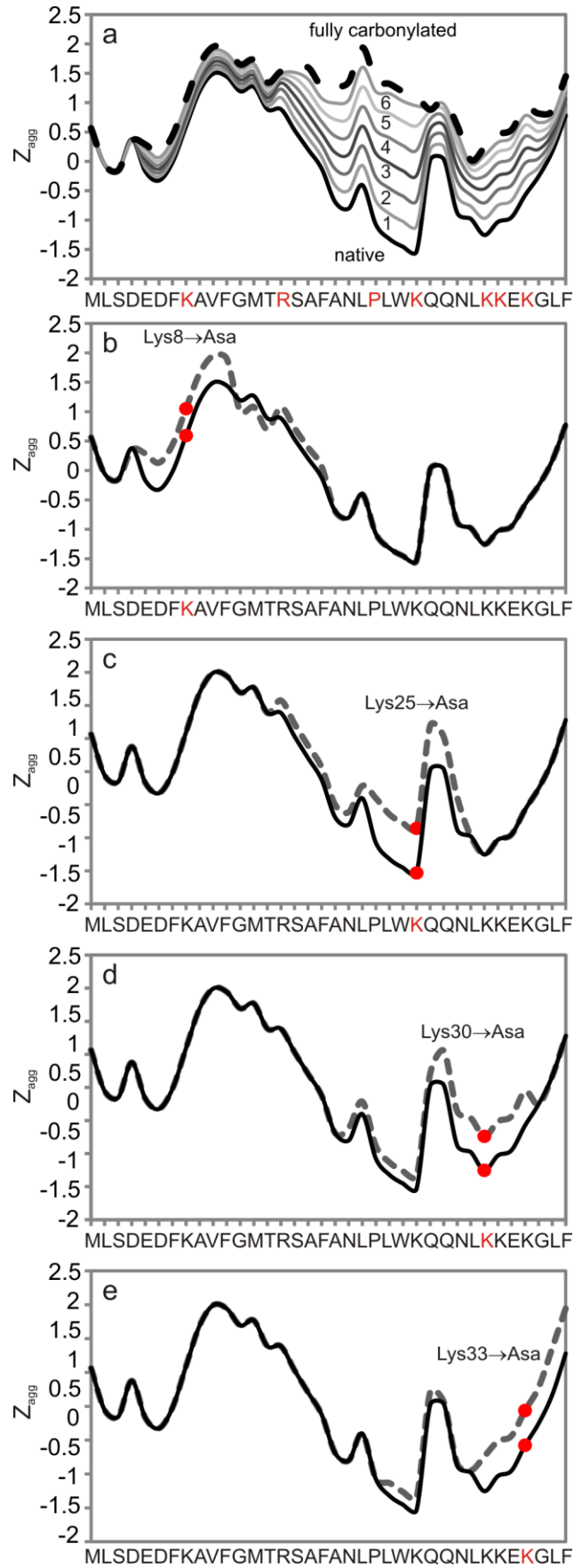


**Figure S1.** Hydration free energies of native and carbonylated side-chains analogues. Comparison of experimental and calculated hydration free energies using thermodynamic integration. Large black diamonds represent carbonylatable side chains Lys, Arg in neutral forms and their carbonylated side chains, amino adipic semialdehyde (Asa) and glutamic semialdehyde (Gsa), while small gray diamonds represent all other side chains. The regression line with  $R^2=0.804$  shows that experimental and calculated values are well correlated. Inset - differences ( $\Delta\Delta G_{hydr}$ ) between hydration free energies of Asa and Lys; and Gsa and Arg from experiment and simulation. Note that the difference in hydrophobicity is significantly greater than estimated by thermodynamic integration simulation because lysine and arginine residues at biologically relevant pH are usually in charged forms, which are much more hydrophilic than their neutral forms used here.



**Figure S2.** Two dimensional projection of the free-energy landscape as a function of MHP and RMSD from the experimental NMR structure for the last 25 ns of all the simulations. Since ensembles with different number of carbonylated residues contain structures from different number of simulations (e.g., native ensemble contains structures from 5 simulations while 5-carbonylations ensemble contains structures from 21 simulations), the fractions of total population are rescaled in such a way so that the total sums of the fractions for each

ensemble are equal. The relative free energy values were calculated as the negative logarithm of the rescaled fractions. The ellipses are centered at the average values of MHP and RMSD with the major and minor semi-axes equal to the standard deviations of the distributions.





**Figure S3.** Site-specific intrinsic aggregation propensity, Zagg, for: (a) The native (solid black line), fully carbonylated (dashed black line) villin headpiece and averages over all combinations of villin headpiece with 1, 2, 3, 4, 5 and 6 carbonylated residues (thin solid gray lines); comparison between villin headpiece in the native state and with one carbonylated residue: (b) native - solid black line, Lys8 to Asa - dashed gray line; (c) native - solid black line, Lys25 to Asa - dashed gray line; (d) native - solid black line, Lys30 to Asa - dashed gray line; and (e) native - solid black line, Lys33 to Asa - dashed gray line.

**Table S1.** Comparison of basic physico-chemical properties of Asa, Gsa, Leu and Val. Solvent accessible surface area (SASA) and molecular volume were calculated using Gromacs tools.<sup>5</sup>

Properties	Asa	Leu	Gsa	Val
Chemical formula	C <sub>4</sub> H <sub>8</sub> O	C <sub>4</sub> H <sub>10</sub>	C <sub>3</sub> H <sub>6</sub> O	C <sub>3</sub> H <sub>8</sub>
MHP	1.56	1.67	1.27	1.28
Mw (g mol <sup>-1</sup> )	72.11	58.12	58.08	44.1
SASA (nm <sup>2</sup> )	1.9	1.8	1.7	1.6
Volume (nm <sup>3</sup> )	0.23	0.21	0.19	0.18
Charge	0	0	0	0

## REFERENCES

- Schuler, L., Daura, X. & van Gunsteren, W. An improved GROMOS96 force field for aliphatic hydrocarbons in the condensed phase. *J. Comput. Chem.* **22**, 1205-1218 (2001).
- Beveridge, D. L. & DiCapua, F. M. Free energy via molecular simulation: applications to chemical and biomolecular systems. *Annu. Rev. Biophys. Biophys. Chem.* **18**, 431-492 (1989).
- Beutler, T. C., Mark, A. E., Vanschaik, R. C., Gerber, P. R. & van Gunsteren, W. F. Avoiding singularities and numerical instabilities in free-energy calculations based on molecular simulations. *Chem. Phys. Lett.* **222**, 529-539 (1994).
- van der Spoel, D. *et al.* Gromacs User Manual version 3.3. [www.gromacs.org](http://www.gromacs.org) 2005.
- Lindahl, E., Hess, B. & van der Spoel, D. GROMACS 3.0: a package for molecular simulation and trajectory analysis. *J. Mol. Model.* **7**, 306-317 (2001).



## Chapter IV

Are current atomistic force fields accurate enough  
to study proteins in crowded environments?

Petrov, D. & Zagrovic, B. Manuscript currently being processed for *Proc. Natl. Acad. Sci. U.S.A.*

DP and BZ conceived and designed the study. DP collected and DP and BZ analyzed the data.  
DP and BZ wrote the manuscript.

**ABSTRACT**

High concentration of macromolecules in the crowded cellular interior influences different thermodynamic and kinetic properties of proteins, including structural stabilities, intermolecular binding affinities and enzymatic rates. Moreover, various structural biology methods, such as NMR or different spectroscopies, typically involve samples with relatively high protein concentration. Due to large sampling requirements, however, the accuracy of classical molecular dynamics (MD) simulations in capturing protein behavior at physiologically or experimentally relevant concentrations still remains largely untested. Here, we use MD simulations to study native (aggregation-resistant) and oxidatively damaged (aggregation-prone) forms of villin headpiece at 6 mM and 9.2 mM protein concentration. We perform an exhaustive set of simulations using different force fields, electrostatics treatments and solution ionic strengths. Surprisingly, the two villin headpiece variants exhibit similar aggregation behavior, although their estimated aggregation propensities differ markedly. Importantly, regardless of the simulation protocol applied, native villin headpiece consistently aggregates even under conditions at which it is experimentally known to be fully soluble. We demonstrate that aggregation of native molecules, the same as that of carbonylated molecules, is accompanied by a dramatic decrease in total potential energy, with not only hydrophobic, but also polar residues and backbone contributing substantially. Strikingly, the same effect is observed for six major atomistic force fields examined, suggesting that they artificially promote protein aggregation likely due to the overestimation of protein-protein interactions originally intended to stabilize protein 3D structures. Overall, our results suggest that current MD force fields may strongly affect the picture of protein behavior in biologically relevant crowded environments.

## INTRODUCTION

Cell interior is comprised of various macromolecules occupying even up to 40% of the total cytoplasmic volume, with proteins being the most abundant class of molecules.<sup>1,2</sup> Importantly, such densely packed environment can drastically affect thermodynamic and kinetic properties of proteins.<sup>3,4</sup> Moreover, as a consequence of high intracellular concentration, proteins can form cytotoxic aggregates that have been linked with numerous pathologies.<sup>5,6</sup> Additionally, most solution-based biophysical experimental methods, such as NMR or different spectroscopies, involve samples with relatively high protein concentration. Volume-exclusion and confinement effects in the context of crowding have been qualitatively well-understood by statistical mechanical theories and computer simulations.<sup>4,7</sup> What is more, Brownian dynamics and coarse-grained simulations have provided a detailed description of multipart mixtures of biomolecules and have sometimes even matched real systems in their complexity.<sup>8-10</sup> Nevertheless, although highly successful, such approaches still fall short of capturing the fully atomistic, dynamic picture of high-concentration macromolecular systems. To this end, molecular dynamics (MD) simulations, a high-resolution computational biology tool,<sup>11</sup> have recently been employed to model in detail different aspects of crowding when it comes to protein structure, dynamics and interactions as well as solvent behavior.<sup>12-14</sup> Moreover, MD simulations have been applied to explore early events in the formation of protein aggregates, focusing predominantly on short peptides with high aggregation propensity and their association.<sup>15-20</sup> However, arguably due to high computational expenses, control tests to show that non-aggregating polypeptides do not aggregate are rarely performed, with only a few attempts in this direction. For example, Gsponer *et al.* and Tsai *et al.* have shown that control mutant peptides aggregate into structures with reduced amyloid character as compared to aggregation-prone peptides.<sup>15,18</sup> However, to the best of our knowledge, not a single study so far has provided clear evidence of a known non-aggregating peptide as a negative control.

Here, we use classical MD simulations to study the behavior of the 36-residue villin headpiece mini-protein<sup>21-23</sup> at atomistic resolution in the presence of multiple copies of the same molecule in the simulation box. In contrast to other MD simulation studies of protein-protein interactions or aggregation that mainly focus on highly interacting or aggregation-

prone polypeptides, our choice of the model system was primarily motivated by the fact that villin headpiece does not self-associate or aggregate at low and moderate protein concentrations. For example, this well-studied actin-binding polypeptide remains soluble at protein concentration of 1-2 mM, as shown by infrared spectroscopy.<sup>24,25</sup> Additionally, Fourier transform infrared spectra of the peptide indicate no aggregation at 6 mM when suspended in a 50 mM sodium acetate buffer with a possibility of aggregate or dimer formation only at a higher protein concentration of ~18 mM.<sup>23</sup> Similarly, circular dichroism experiments suggest that there is no significant aggregation of villin headpiece at the concentration of 9.2 mM, although in this case the data was collected at -40 °C in glycerol/water solution.<sup>22</sup> Finally, NMR spectra of villin headpiece can successfully be recorded even at the concentration of 32 mM, although with changes in chemical shifts of surface residues as a consequence of increased protein-protein interactions upon crowding.<sup>26</sup> Here, it should also be mentioned that villin headpiece adopts a completely  $\alpha$ -helical fold,<sup>21</sup> a secondary structure element known to prevent aggregation, as opposed to  $\beta$ -sheets that promote it.

Increased levels of protein aggregation have been repeatedly related to protein oxidative damage with highly oxidized proteins being a frequent component of potentially cytotoxic aggregates.<sup>27-29</sup> In a recent study, we have shown that metal-catalyzed carbonylation, arguably one of the most important types of irreversible oxidative modifications, drastically increases intrinsic aggregability of villin headpiece by directly affecting its hydrophobicity, net charge and secondary structure,<sup>30</sup> protein properties shown to strongly influence aggregation propensity.<sup>31</sup> In particular, using the formalism proposed by Chiti *et al.*<sup>31</sup>, we have shown that a single carbonylation event can increase the aggregation rate of villin headpiece by more than an order of magnitude even in the absence of unfolding, and have additionally corroborated this finding using Zyggregator<sup>32</sup> predictor. Additionally, simultaneous damage to lysine, arginine and proline residues, i.e., the main targets of protein carbonylation, causes unfolding of the protein with concomitant solvent-exposure of its hydrophobic core and backbone,<sup>30</sup> which is believed to be one of the main mechanisms of protein aggregation.<sup>5,29</sup> Therefore, the carbonylated villin with 7 affected residues is expected to have a significantly elevated propensity to self-associate as compared to the native variant. Accordingly, here we study two different villin headpiece

systems: 1) native, properly folded protein resistant to aggregation, and 2) carbonylated, completely unfolded and aggregation-prone protein. The principal question that we ask is what drives the formation of villin headpiece self-aggregates in MD simulations and, in the process, we explore the limitations of current atomistic force fields in describing biologically and experimentally realistic protein solutions.

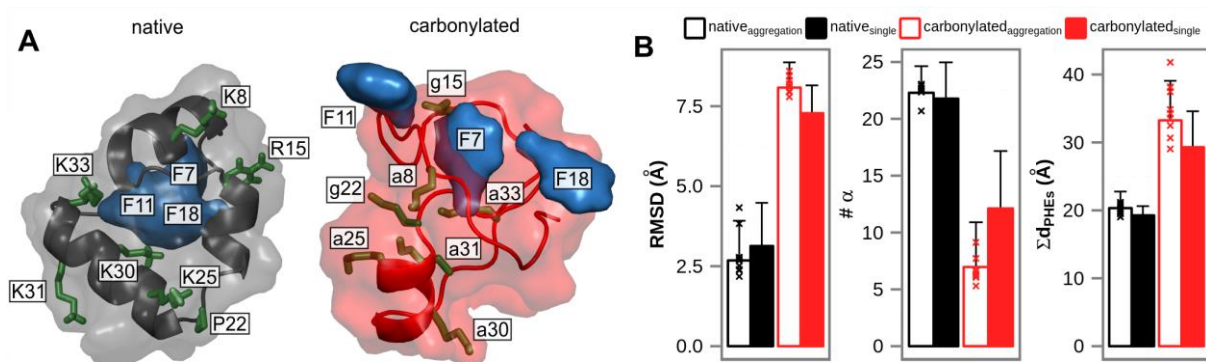
## RESULTS

We have examined the behavior of native and carbonylated villin headpiece at biologically relevant protein concentrations of 6 mM and 9.2 mM, using MD simulations with 4 or 8 chemically identical villin headpiece copies in the simulation box, respectively, at different sodium chloride concentrations (0 to 0.8 M). Furthermore, to account for potential inaccuracies in the physical description of the system, we have employed two different force fields (GROMOS45a3,<sup>33</sup> GROMOS54a7<sup>34</sup>) to generate MD trajectories and four additional force fields to analyze them (AMBER94,<sup>35</sup> AMBER99SB-ILDN,<sup>36</sup> CHARMM27-CMAP<sup>37</sup> and OPLS-AAL<sup>38</sup>) together with two types of electrostatics treatment (particle mesh Ewald<sup>39</sup> and reaction-field<sup>40</sup>). In total, we have applied 10 different simulation protocols to generate 5.2  $\mu$ s of explicit solvent MD trajectories. Such extensive sampling is essential given the complexity of the systems comprised of multiple polypeptides at finite protein concentration. In order to characterize thermodynamic properties of native (depicted in black throughout) and carbonylated (depicted in red throughout) systems, in several instances we have calculated averages over the entire simulated time (50 ns, 100 ns or 200 ns depending on the simulation protocol applied) and over all simulation setups (unless stated otherwise) in order to enhance the coverage of the phase space of studied systems or simply for illustration purposes. Note, however, that we exclude data obtained from MD simulations at 9.2 mM protein concentration (only 1 out of 10 simulation setups) from the analysis if the property in question is either extensive or concentration dependent (see Methods for more details).

### Structural analysis of native and carbonylated villin

Villin headpiece is a 3-helix bundle protein with a tightly packed hydrophobic core comprised of three phenylalanine residues (Fig. 1A).<sup>21</sup> To structurally characterize the

simulated proteins, we have used: 1) atom-positional root-mean-square deviation (RMSD) from the native villin headpiece structure,<sup>21</sup> 2) the number of residues in  $\alpha$ -helical conformation ( $\#\alpha$ ), and 3) the sum of distances between the centers of mass of core phenylalanines ( $\Sigma d_{\text{PHEs}}$ ). In Figure 1B, we present aggregate averages of these three measures over all simulated conditions, with the average values for individual simulation protocols given in Table S1. Overall, native polypeptides remain folded at infinite dilution as previously shown by us<sup>30</sup> and demonstrated here by averages of all three independent measures of foldedness (Figure 1B, single simulations):  $\langle \text{RMSD} \rangle = 2.7 \pm 1.2 \text{ \AA}$ ,  $\langle \#\alpha \rangle = 22.3 \pm 2.3$  and  $\langle \Sigma d_{\text{PHEs}} \rangle = 20.3 \pm 2.4 \text{ \AA}$ . On the other hand, carbonylated molecules at infinite dilution populate the unfolded state,<sup>30</sup> with an increase in the average RMSD ( $\langle \text{RMSD} \rangle = 8.1 \pm 0.8 \text{ \AA}$ ) and the sum of the distances between the solvent-exposed core phenylalanines ( $\langle \Sigma d_{\text{PHEs}} \rangle = 33.3 \pm 5.8 \text{ \AA}$ ) and a significant decrease in the  $\alpha$ -helical content ( $\langle \#\alpha \rangle = 7.0 \pm 3.9$ ) (Figure 1B, single simulations). Importantly, both native and carbonylated villin headpiece, simulated with multiple copies in the simulation box, closely resemble the structural properties of the equivalent polypeptides at infinite dilution (Figure 1B, aggregation simulations). Note that initial configurations for aggregation simulations were chosen randomly from the equilibrium ensemble of the last 25 ns (also used for the analysis) of previously simulated 110-ns-long, infinite dilution trajectories,<sup>30</sup> thus ensuring that the two sets of simulations are comparable.



**Figure 1.** Structural characterization of villin headpiece in the folded native and the unstructured carbonylated state. A) Typical structures of native and carbonylated villin showing the core phenylalanines in blue and carbonylated residues in green; B) three measures of villin foldedness averaged over all simulated trajectories and given with standard deviations (data for infinite dilution taken from ref<sup>30</sup>). The averages were calculated



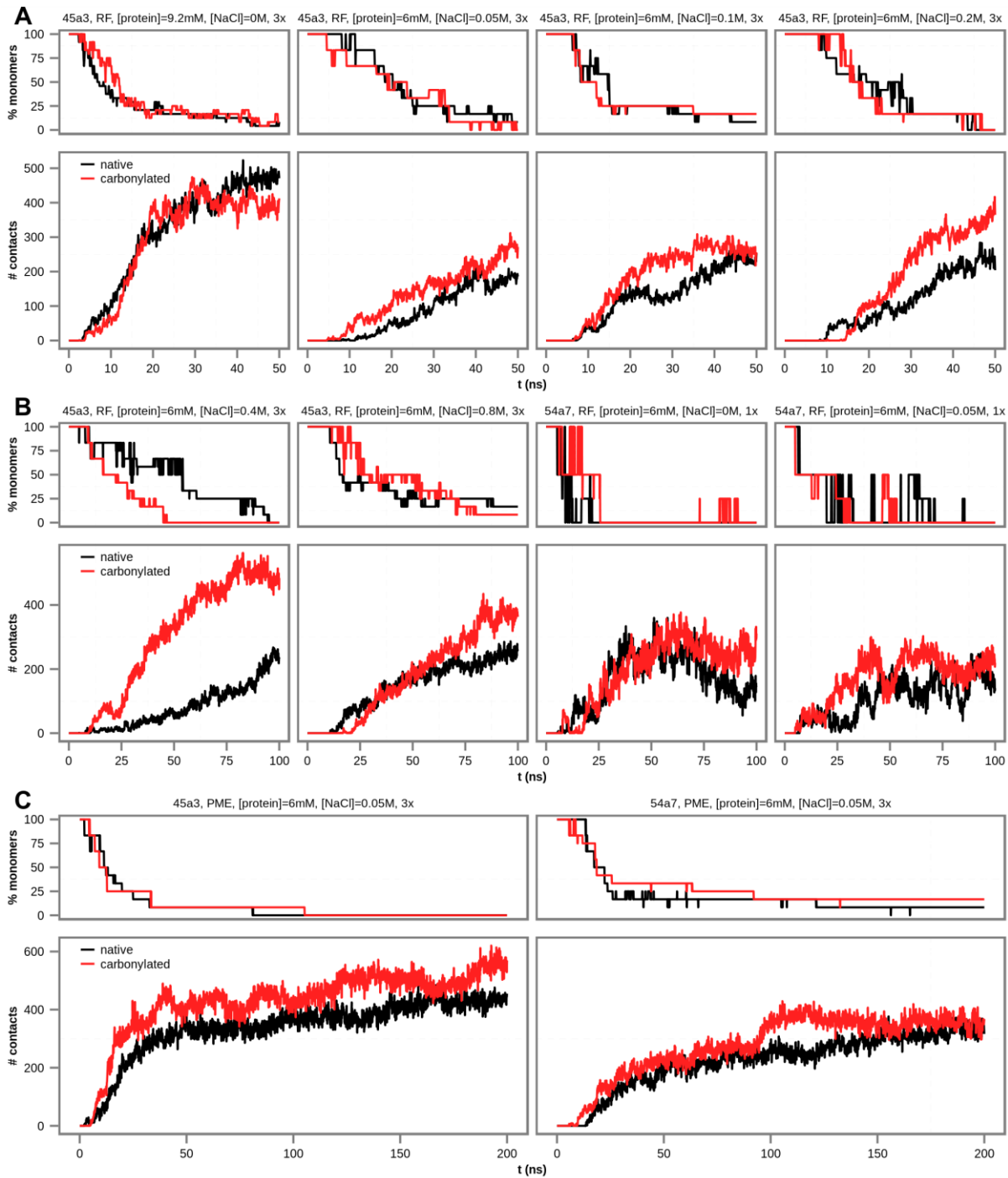
over the entire simulated time for finite protein-concentration systems, whereas only the last 25 ns of simulated time were used for infinite dilution systems.

### **Analysis of the aggregation process and villin headpiece aggregates**

As predicted, carbonylated villin headpiece molecules, initially placed to maximize their intermolecular distances, start to associate after only a few nanoseconds of free diffusion, leading to an exponential decrease in the number of free monomers in solution, together with a rapid increase in the number of intermolecular atomic contacts at all conditions examined (Figure 2, see Methods for more details). Namely, configurations in which the number of free monomers reaches 0 are observed in 23 out of 26 simulated trajectories with aggregates comprised of at least 75% of all monomers observed in every single trajectory (Figure 2). Surprisingly, in contradiction with experimental findings,<sup>13,14</sup> analysis of the native villin headpiece system shows that the fraction of free monomers decreases and the number of inter-protein atomic contacts increases with simulated time in the same manner as for carbonylated villin headpiece (Figure 2). Altogether, 10 different simulation setups have been examined (Table S1) using different force fields, types of electrostatics treatment and ionic strength, and strikingly, all fail to keep native villin headpiece monodisperse and reproduce experimental observations.

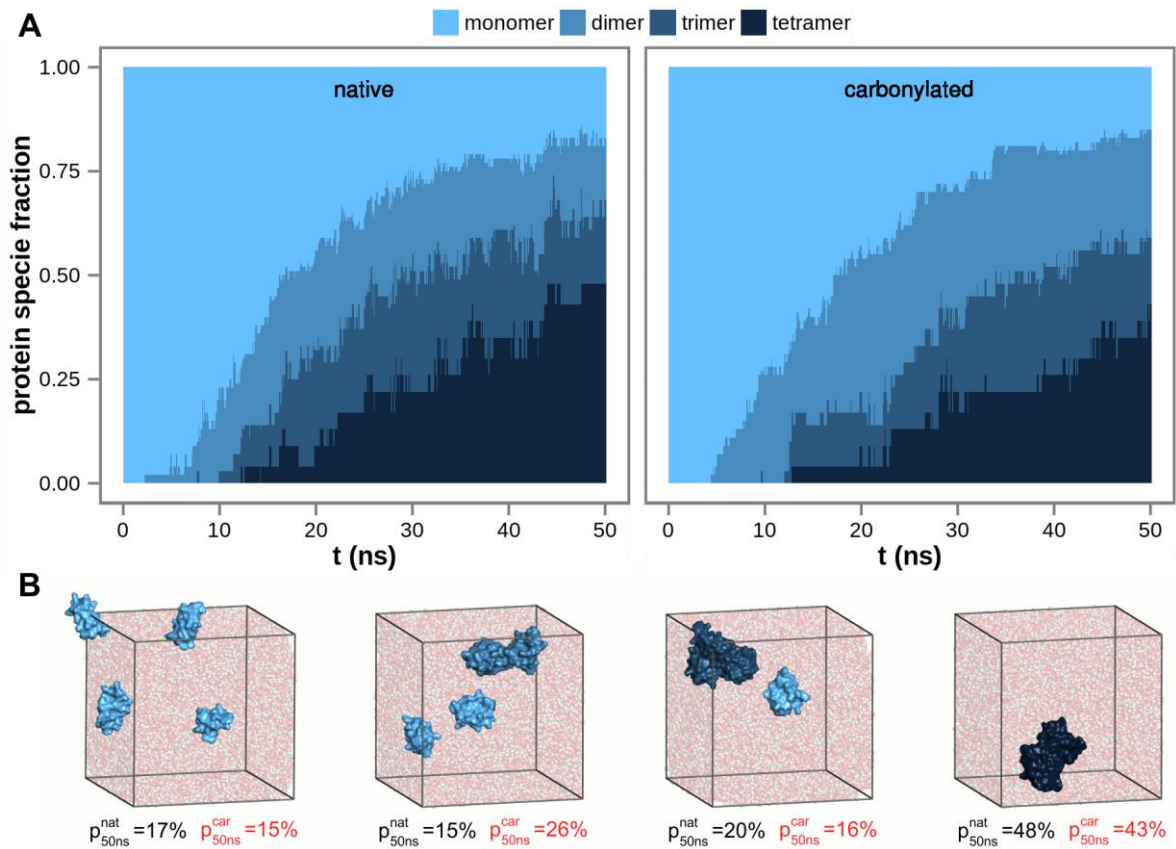
To further characterize the aggregation process of the studied systems, we have analyzed the kinetics of protein-protein association and dissociation. The average dissociation time of native molecules from aggregates is approximately 45 ns, which is significantly longer than the average time required for their association of approximately 17 ns. Similarly, the average timescales of protein dissociation and association for the carbonylated system are approximately 50 ns and 19 ns, respectively. Importantly, approximately 65% of native and 70% of carbonylated complexes that have formed never dissociate during the simulated time, including all those with life-times longer than 55 ns (SI Figure S1). This fact clearly indicates that the actual life-times of villin headpiece in the aggregated state may be much longer than the average values obtained from simulations, which are limited by sampling. On the other hand, longer simulations would not significantly influence the estimated association times, since only less than 5% of proteins in both systems remain free in solution in the course of simulations. This, in turn, suggests that even much lower protein

concentration would likely not prevent native villin headpiece from aggregating, but only increase the search time needed for proteins to find each other by free diffusion.



**Figure 2.** Aggregation of native and carbonylated villin headpiece under various simulation conditions monitored by the percentage of free monomers in solution and the number of intermolecular atomic contacts as a function of time, averaged over independent simulations performed at the same conditions. Altogether, 10 simulations setups were examined and are grouped here according to length: A) 50-ns-long, B) 100-ns-long,

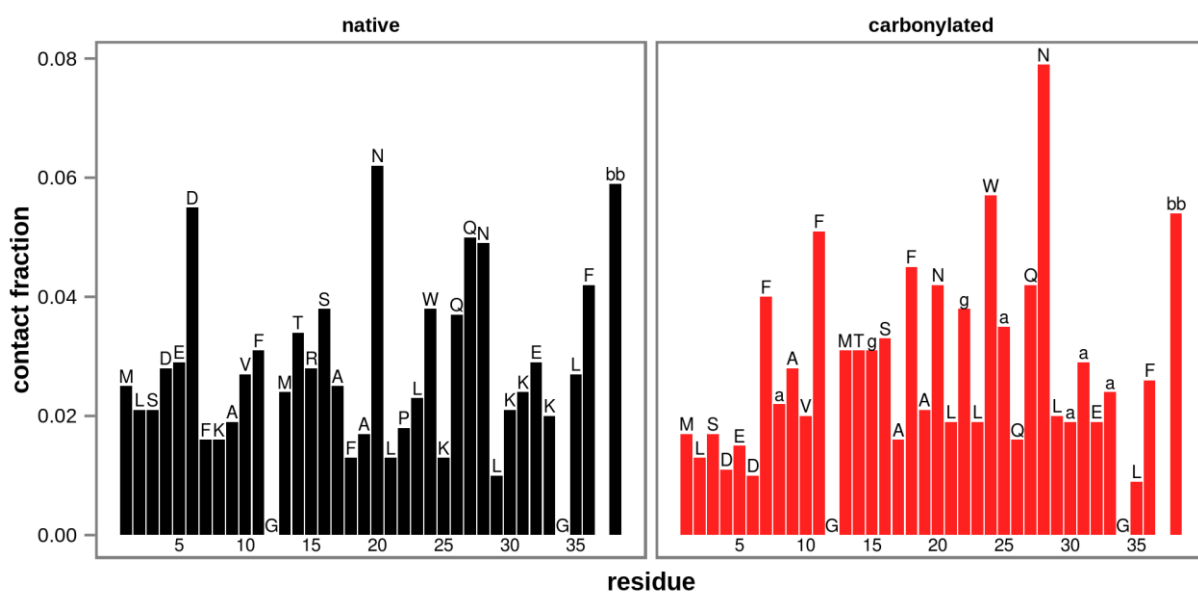
and C) 200-ns-long simulations. Exact simulation setup is given above each plot including number of replicate trajectories used to generate the curves (1x or 3x).



**Figure 3.** A) Average, aggregate progression of villin headpiece self-association as a function of time calculated over all simulated trajectories. B) Snapshots from simulated trajectories depicting a typical sequence of formation of villin headpiece self-aggregates from free monomers. Fraction of monomers, dimers, trimers and tetramers in the ensembles at 50 ns are given explicitly.

In both studied systems, starting from free monomers, peptide dimers begin to form first, followed by the formation of trimers and tetramers, leading to the maximum number of tetrameric aggregates after approximately 50 ns of simulated time. Overall, tetrameric aggregates are the most abundant and free monomers the least abundant species in our simulations, representing on average approximately 45% and 15% of the total protein content at 50 ns in native simulations, respectively (Figure 3). Furthermore, in order to identify specific residues involved in villin headpiece self-association, we have calculated the fraction of intermolecular atomic contacts formed by each residue (side chains only) over all native and carbonylated simulations, normalized by solvent-accessibility to account for surface exposure, i.e., the probability to interact. Surprisingly, while association of

hydrophobic residues is believed to be a key element in protein aggregation, our analysis reveals that interactions in both native and carbonylated aggregates are dominated by either backbone or glutamine and asparagine residues (Figure 4). In addition to these hydrophilic moieties, carbonylated aggregates are also characterized by contacts involving hydrophobic ring-containing phenylalanines and tryptophans (Figure 4). Finally, we have also analyzed the average contact maps for both native and carbonylated systems (Figure S2), which demonstrate that the N-terminal residues form fewer intermolecular contacts than the rest of the molecule in both studied systems. Additionally, the region between residues 15 and 25 of the native contact map is depleted in contacts, whereas the carbonylated map displays a more even distribution of contacts. However, no system-specific pattern among the residues exhibiting many intermolecular contacts has been observed.

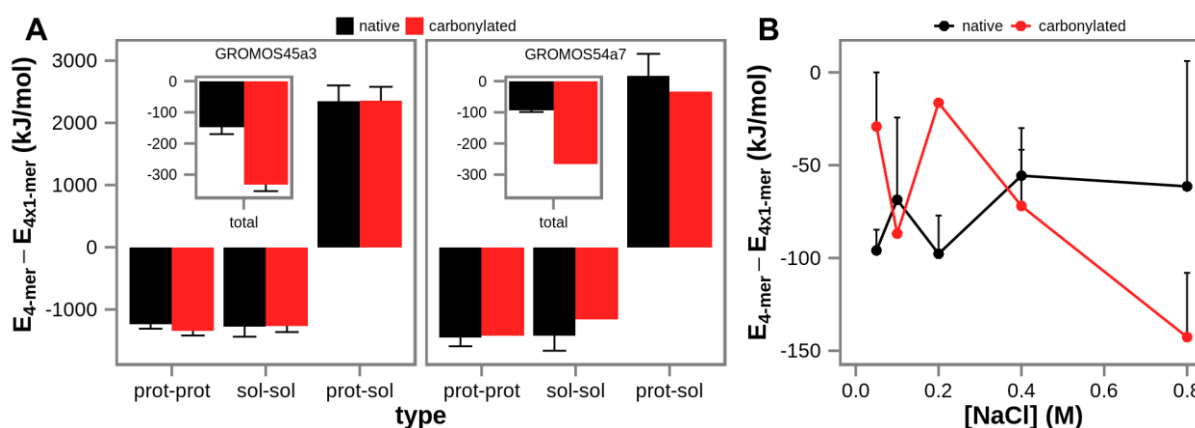


**Figure 4.** Sequence-wise peptide-peptide interaction propensity estimated by the number of inter-peptide atomic contacts normalized by solvent-accessibility, i.e., surface-exposure per amino acid (side chains only), with the peptide backbone treated as a separate residue, with the values obtained by averaging over all simulated trajectories (*bb* – backbone, *a* – aminoadipic semialdehyde, *g* – glutamic semialdehyde, while natural amino acids are indicated using standard 1-letter code).

### What drives villin headpiece aggregation in MD simulations?

To address this, we have explored the role of enthalpic contributions in the aggregation of the studied systems, including solvent-solvent, protein-solvent and protein-protein

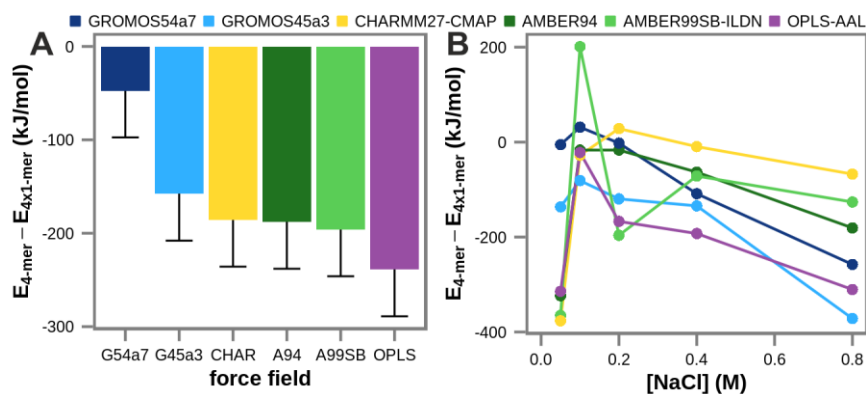
interactions, by calculating the average of the difference in potential energy between fully aggregated (tetrameric) and non-aggregated (monomeric) states. Expectedly, solvent-solvent and protein-protein interactions provide favorable contribution, while protein-solvent interactions provide unfavorable contribution to the total enthalpy of aggregation, as seen in the case of simulations with the most extensive sampling (200 ns), the PME electrostatics treatment and 0.05 M salt concentration (Figure 5A). However, the total potential energy of the same systems is significantly lower in the aggregated state (by approximately 150 kJ/mol and 330 kJ/mol for the native and the carbonylated system simulated by GROMOS45a3 force field, respectively, and approximately 100 kJ/mol and 270 kJ/mol for the native and the carbonylated system simulated by GROMOS54a7 force field, respectively, Figure 5A), suggesting that self-association may be an enthalpically driven process. Further analysis of the simulations obtained using RF electrostatics treatment (the GROMOS 45a3 parameter set only) shows that the aggregated states are also favored for every salt concentration examined (Figure 5B).



**Figure 5.** The difference in potential energy between aggregated (tetramers) and non-aggregated (free monomers) states of native and carbonylated villin headpiece calculated directly from simulated data. A) Average difference in total potential energy (inset, the y-axis the same as in the main figure), and contributions from solvent-solvent, protein-protein and protein-solvent interactions over: 1) simulations obtained using the GROMOS 45a3 parameter set, PME electrostatics treatment and 0.05 M salt concentration (left panel), and 2) simulations obtained using the GROMOS 54a7 parameter set, PME electrostatics treatment and 0.05 M salt concentration (right panel). B) Average difference in total potential energy over simulations obtained using GROMOS 45a3 and RF electrostatics treatment at different salt concentrations.

To study other force fields in addition to GROMOS 45a3 and 54a7, we have re-evaluated the potential energy of the simulated trajectories by using 6 widely used MD force fields

(GROMOS45a3,<sup>33</sup> GROMOS54a7,<sup>34</sup> AMBER94,<sup>35</sup> AMBER99SB-ILDN,<sup>36</sup> CHARMM27-CMAP<sup>37</sup> and OPLS-AAL<sup>38</sup>), and two electrostatic treatment methods treatments (RF and PME), on energy-minimized snapshot configurations, where the force field used for energy minimization was also used to re-evaluate the potential energy. Note that we have only re-evaluated potential energies for native systems since parameters for carbonylated residues are only available for the GROMOS force field. Remarkably, regardless of the type of electrostatics treatment, all of the evaluated force fields show the same trend in favoring tetrameric aggregated over non-aggregated conformers of native villin headpiece (Figure 6 and S3), with the extent of such bias ranging from approximately -50 kJ/mol to -240 kJ/mol (PME calculations) for GROMOS54a7 and OPLS-AAL force fields, respectively. Importantly, in order to decrease the uncertainty in estimation, we have averaged the re-evaluated differences in potential energy between the tetrameric and monomeric configurations for each force field over all trajectories no matter which simulation condition they came from (Figure 6A and S3A).



**Figure 6.** Difference in total potential energy between aggregated (tetramers) and non-aggregated (free monomers) conformations of native villin headpiece calculated from re-evaluated energies using PME electrostatics treatment and 6 widely used MD force fields on energy-minimized configurations taken from simulation. A) averages over all simulations with the estimated standard errors (50 kJ/mol) shown using one-sided error bars. B) averages over simulations at different salt concentrations.

Under the assumption that the entropic contribution to the free energy of association is comparable for all different force fields, this result suggests that utilizing any of these force fields would most likely lead to aggregation of native villin headpiece in MD simulations, and therefore be at odds with experimental observations. The fact that the two GROMOS force fields, which were used to generate configurations, exhibit the lowest preference towards

the aggregated state when compared to other evaluated force fields further supports this claim (Figure 6). Parenthetically, the primary strategy in parameterizing the GROMOS 54a7 force field was to reproduce experimental hydration free energies of amino-acid side-chain analogs, a property closely related to solubility in water, while the other force fields examined here significantly underestimate this property.<sup>41,42</sup>

## DISCUSSION

This study explores the behavior of the villin headpiece domain in its native and carbonylated forms at experimentally and biologically relevant protein concentrations in MD simulations. We have shown that native and carbonylated villin headpiece molecules remain folded and unfolded throughout the simulated trajectories, respectively, as previously seen in simulations at infinite dilution (Figure 1). Even though 4 individual native villin molecules unfolded in the course of simulated trajectories, this is to be expected in the ensemble of more than 100 polypeptides simulated herein, since the villin headpiece is only a marginally stable protein.<sup>43</sup> By probing various simulation conditions, we have observed that native and carbonylated molecules aggregate in a very similar fashion, despite the fact that they display markedly different aggregation propensities. This finding is even more remarkable given the fact that we have focused on conditions experimentally known to render villin headpiece soluble. Even though villin headpiece can begin to aggregate at protein concentration of 6 mM after a period of a few days,<sup>23</sup> it is highly unlikely that this is related to the nanosecond-time-scale aggregation observed here. Overall, our choice of the “borderline” concentrations at which villin headpiece remains soluble was based on three principal rationales: 1) we wanted to minimize the computational costs by minimizing the size of the simulation box (even at this protein concentrations each simulated system contains more than 100,000 atoms) and consequently the search time needed for peptides to find each other by free diffusion, 2) we wanted to maximize the likelihood of observing the difference in aggregation between the native, supposedly aggregation-resistant, and the carbonylated, aggregation-prone systems, and 3) 6 mM (90% of simulation protocols) and 9.2 mM (10% of protocols) concentrations of villin headpiece correspond to the protein mass fraction of approximately 3-4%, which is experimentally relevant, but also significantly lower than what one observes in typical crowded cellular environments. Likely, any

aggregation that was observed here would only be potentiated at higher concentrations. However, in order to address the possibility that aggregation of the native system is induced by the “borderline” villin headpiece concentrations used in this study, we have analyzed the kinetics of protein-protein association and dissociation. This analysis has revealed that a large number of protein-protein complexes never dissociate in the course of simulated trajectories, and that the average protein dissociation time is markedly longer than the average association time (Figure S1), suggesting that aggregation in MD simulations would occur even at lower concentrations than applied here.

Furthermore, in order to characterize the nature of villin headpiece intermolecular interactions, we have identified the residues involved in the formation of protein-protein atomic contacts. Surprisingly, this analysis shows that interactions in villin headpiece aggregates are mainly dominated by polar glutamines and asparagines as well as hydrophobic ring-containing phenylalanines and tryptophans (Figure 4). Although the two former hydrophilic amide-containing amino acids are generally considered to be aggregation reducing,<sup>31,44</sup> they have been repeatedly linked to protein aggregation and deposition disorders, most notably in poly-Q diseases.<sup>5,18,45</sup> In addition to this, the high occurrence of peptide backbone atoms among villin headpiece intermolecular contacts (Figure 4) supports the hypothesis that poly-peptide chains have a general tendency to aggregate due to an intrinsic aggregability of the protein backbone.<sup>46</sup> This is further corroborated by recent findings that poly-glycine and poly-alanine chains aggregate readily.<sup>47</sup>

Finally, to investigate what drives villin headpiece aggregation in MD simulations, we have analyzed how the potential energy of the system, and different contribution thereof, change upon aggregation. Expectedly, villin headpiece self-association is accompanied by a decrease in protein-protein and solvent-solvent, and an increase in protein-solvent short-range potential energy. However, the total potential energy drastically decreases upon aggregation, suggesting that the utilized force fields (the GROMOS 45a3 and 54a7 parameter sets) favor aggregated conformers (Figure 5), in contradiction with experimental findings. Strikingly, by re-evaluating the potential energy of the aggregated and non-aggregated conformers using 6 widely-used atomistic force fields (GROMOS45a3,<sup>33</sup>



GROMOS54a7,<sup>34</sup> AMBER94,<sup>35</sup> AMBER99SB-ILDN,<sup>36</sup> CHARMM27-CMAP<sup>37</sup> and OPLS-AAL<sup>38</sup>), we have shown that all of them favor the aggregated states of native villin headpiece (Figure 6). However, one should emphasize that this result has been obtained by averaging over conformers originally obtained by differently defined Hamiltonians and using a limited number of energy minimized configurations, significantly increasing the error in the estimated potential energy differences. These shortcomings notwithstanding, the calculated differences in the total potential energy come with an error of approximately 200 kJ/mol for each simulation and 50 kJ/mol for the aggregate average difference (Figure 6), as estimated using the root-mean-square errors from the potential energies derived directly from simulations, calculated for the same force field as used in the simulation.

Taken together, our results suggest that typical classical MD force fields bias protein aggregation by overestimating protein-protein and solvent-solvent as opposed to protein-solvent interactions. Additionally, the demonstrated imbalance between these three components of total potential energy displayed by the force fields may be partly a consequence of the widely-used force field validation approaches, aimed mostly at reproducing tertiary and secondary structures of well-characterized proteins. Simply put, strengthening of protein-protein and weakening of protein-solvent interactions leads to stabilization of protein structure, one of the principal targets of most parameterization strategies. This, if true, suggests that realistic polypeptides may display more dynamics and unstructuredness than generally observed in MD-simulation studies. Interestingly, a recent study exploring the limitations of MD simulations by employing a state-of-the-art designated supercomputer to perform a 200- $\mu$ s-long simulation of an intrinsically unfolded protein revealed that the modeled protein appears to be more compact and collapsed than observed by NMR,<sup>48</sup> further supporting this speculation. Importantly, these potential flaws of current force fields may have strong implications when it comes to the accuracy of MD models in describing protein dynamics and interactions in biologically relevant crowded environment. Finally, recent validation studies of force fields show that they improve over time, but are still not able to reproduce all relevant experimental data.<sup>49,50</sup> Such validations and synergy between experimental methods and MD simulations should in the years to come bring improvements in computational models and physical descriptions of biomolecular systems of interest as well as provide a better understanding of biologically

important processes such as protein folding, protein-ligand binding and protein aggregation in the context of experimentally or biologically realistic conditions. We hope that the results presented herein will provide an additional source of motivation in this direction.

## METHODS

### Molecular dynamics simulations setup

We have used classical MD simulations to study the behavior of villin headpiece with multiple copies of the molecule in the simulation box. Two systems were examined: 1) native villin headpiece (sequence: **MLSDEDFKAVFGMTR****SAFANLPLWKQ****QNLKKEKGLF**), and 2) its carbonylated form. The seven letters in bold mark the most important carbonylatable amino acids (K, R and P) in villin headpiece, which were all modified into their carbonylated versions in the carbonylated form of the molecule. Upon carbonylation, lysine is converted into aminoadipic-semialdehyde, while arginine and proline are converted into glutamic-semialdehyde, for which force field parameters were taken from refs<sup>30,51</sup>. In total, 10 simulation protocols were applied (Table S1), varying in protein (6 mM and 9.2 mM) and salt (0 M, 0.05 M, 0.1 M, 0.2 M, 0.4 M and 0.8 M) concentration, force field (GROMOS 45a3<sup>33</sup> and 54a7<sup>34</sup> parameter sets), electrostatics treatment (RF - reaction-field<sup>40</sup> and PME - particle mesh Ewald<sup>39</sup>), the number of protein molecules in a simulated box (4 and 8), simulation time (50 ns, 100 ns and 200 ns), and the number of independent simulations (1 and 3). All MD simulations were carried out using GROMACS biomolecular simulation package,<sup>52</sup> keeping the system at 300 K and 1 bar using a Berendsen thermostat ( $\tau_T = 0.05$  ps) and barostat ( $\tau_p = 1$  ps and compressibility =  $4.5 \times 10^{-5}$  bar<sup>-1</sup>).<sup>53</sup> A cutoff of 1.4 nm and the dielectric constant of 65 were used for RF, and the Fourier spacing of 0.1 nm for PME calculations. Starting from either native or carbonylated free monomers (4 and 8 for 6 mM and 9.2 mM protein concentration, respectively) maximally separated in a simulation box, polypeptides were allowed to diffuse freely and interact with each other and the solvent. The initial configurations were prepared by placing villin headpiece molecules in a cubic simulation box, with the size defined by the protein concentration, i.e., sides of approximately 10.4 nm (6 mM) and 11.3 nm (9.2 mM), for a total number of atoms exceeding 100,000 in all cases. Villin headpiece monomers were randomly selected from the

ensemble of the last 25 ns of five 110-ns-long independent simulated trajectories of both the peptide in the native and carbonylated form from ref<sup>30</sup>, only taking into account structures with atom-positional root-mean-square deviation (RMSD) from the native villin headpiece structure<sup>21</sup> in the range of the average ensemble plus or minus one standard deviation. After filling the simulation box with SPC water molecules<sup>54</sup> and sodium chloride at a given concentration, and steepest descent energy minimization (1500 steps), the system was equilibrated by gradually increasing the temperature (from 100 to 300 K) over 100 ps with gradually decreasing position restraints (from 25 000 to 5000 kJ mol<sup>-1</sup> nm<sup>-2</sup>) at constant volume and temperature, and finally additionally equilibrated for 20 ps at constant pressure and temperature of 1 bar and 300 K. Atom coordinates and velocities were saved every 50,000 integration steps, i.e., 100 ps.

### Potential energy re-evaluation

To examine the performance of 6 widely used MD force fields (GROMOS45a3,<sup>33</sup> GROMOS54a7,<sup>34</sup> AMBER94,<sup>35</sup> AMBER99SB-ILDN,<sup>36</sup> CHARMM27-CMAP<sup>37</sup> and OPLS-AAL<sup>38</sup>) in the context of villin headpiece aggregation, the trajectories of the native villin headpiece simulated using GROMOS 45a3 and 54a7 force fields were re-evaluated as follows: first, utilizing a given force field, each saved configuration was energy minimized by steepest descent in 1500 steps, and second, the total potential energy was calculated for the minimized configurations using the same force field as in the energy minimization step, together with contributions from short-range non-bonded solvent-solvent, protein-protein and protein-solvent interactions evaluated for all atom pairs within a cutoff distance of 1.4 nm. Electrostatic contribution to the potential energy was calculated using RF and PME methods with the same parameters as used in the simulation setups. The water TIP3P<sup>55</sup> model was used to re-evaluate potential energies of AMBER94,<sup>35</sup> AMBER99SB-ILDN,<sup>36</sup> CHARMM27-CMAP<sup>37</sup> and OPLS-AAL<sup>38</sup> force fields.

### Analysis of the simulated data and figure preparation

GROMACS,<sup>52</sup> DSSP,<sup>56</sup> PYMOL<sup>57</sup> and ggplot2<sup>58</sup> (from R) tools were used to analyze the collected trajectories and to generate the figures. Backbone atoms were used for rotational-translational fitting and calculation of atom-positional RMSD with respect to the NMR villin

headpiece structure (first model).<sup>21</sup> The number of inter-peptide atomic contacts and villin headpiece association and dissociation kinetics were evaluated by defining atomic contacts to be present any time two atoms from different villin headpiece molecules come within 0.4 nm from each other, and a peptide-peptide complex to be present any time a pair of villin headpiece molecules remain continuously in atomic contact in the course of at least 1 ns. The site-specific intermolecular interaction propensity along the villin headpiece sequence was estimated by calculating the fraction of the number of intermolecular atomic contacts (heavy atoms only) per residue (normalized at each time-point by the solvent-accessibility of a residue in question) in each simulation, and subsequently averaged over all simulated trajectories (either native or carbonylated). The solvent-accessibility, i.e., the surface-exposure of a given residue was calculated as the fraction of the solvent-accessible surface area (SASA) of the residue in the total SASA of the peptide. Note that only amino-acid side chains were used, while the backbone atoms were considered as a separate collective residue. Finally, the differences in potential energy between aggregated and non-aggregated villin headpiece conformers were calculated as the difference between the average potential energy of aggregated (all-tetramer) snapshots and the average potential energy of non-aggregated (free monomers) snapshots from each simulated trajectory, averaged over different simulation sets. In particular, energy differences evaluated directly from simulations were averaged over different simulation conditions, whereas those calculated from re-evaluated energies were averaged over all simulated systems (excluding simulations at 9.2 mM protein concentration for these cases). Only simulated trajectories with more than 20 snapshots of both aggregated and non-aggregated states were taken into account. Note that villin headpiece systems with protein concentration of 9.2 mM (1 out of 10 simulated setups) were excluded from calculation of average properties if the property in question was either extensive or concentration dependent, including evaluations of villin headpiece association/dissociation kinetics, time-dependent formation of higher order villin headpiece complexes (e.g., dimers) and potential energy.

## ACKNOWLEDGEMENTS

This work was supported in part by the Austrian Science Fund FWF (START grant Y 514-B11 to BZ, <http://www.fwf.ac.at/>) and European Research Council (ERC Starting Independent

grant 279408 to BZ, <http://erc.europa.eu/>). We thank members of the Laboratory of Computational Biophysics at MFPL for useful advice and assistance.

## REFERENCES

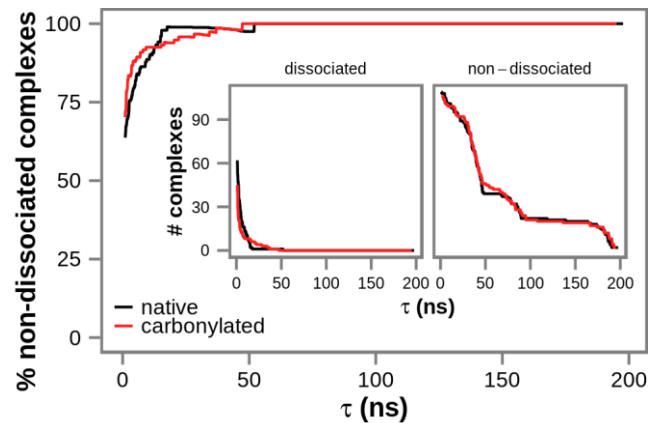
1. Ellis, R. J. Macromolecular crowding: Obvious but underappreciated. *Trends Biochem. Sci.* **26**, 597-604 (2001).
2. Ellis, R. J. & Minton, A. P. Cell biology - Join the crowd. *Nature* **425**, 27-28 (2003).
3. Zhou, H. X., Rivas, G. N. & Minton, A. P. in *Annual Review of Biophysics* Vol. 37 *Annual Review of Biophysics* 375-397 (2008).
4. Elcock, A. H. Models of macromolecular crowding effects and the need for quantitative comparisons with experiment. *Curr. Opin. Struct. Biol.* **20**, 196-206 (2010).
5. Ross, C. A. & Poirier, M. A. Protein aggregation and neurodegenerative disease. *Nat. Med.* **10**, S10-S17 (2004).
6. Chiti, F. & Dobson, C. M. Amyloid formation by globular proteins under native conditions. *Nat. Chem. Biol.* **5**, 15-22 (2009).
7. Minton, A. P. Models for excluded volume interaction between an unfolded protein and rigid macromolecular cosolutes: Macromolecular crowding and protein stability revisited. *Biophys. J.* **88**, 971-985 (2005).
8. Periole, X., Huber, T., Marrink, S. J. & Sakmar, T. P. G protein-coupled receptors self-assemble in dynamics simulations of model bilayers. *J. Am. Chem. Soc.* **129**, 10126-10132 (2007).
9. Scott, K. A. *et al.* Coarse-grained MD simulations of membrane protein-bilayer self-assembly. *Structure* **16**, 621-630 (2008).
10. McGuffee, S. R. & Elcock, A. H. Diffusion, crowding & protein stability in a dynamic molecular model of the bacterial cytoplasm. *PLoS Comp. Biol.* **6** (2010).
11. van Gunsteren, W. F. *et al.* Biomolecular modeling: Goals, problems, perspectives. *Angew. Chem. Int. Ed.* **45**, 4064-4092 (2006).
12. England, J. L., Lucent, D. & Pande, V. S. A role for confined water in chaperonin function. *J. Am. Chem. Soc.* **130**, 11838-11839 (2008).
13. Feig, M. & Sugita, Y. Variable interactions between protein crowders and biomolecular solutes are important in understanding cellular crowding. *J Phys Chem B* **116**, 599-605 (2012).
14. Harada, R., Sugita, Y. & Feig, M. Protein crowding affects hydration structure and dynamics. *J. Am. Chem. Soc.* **134**, 4842-4849 (2012).
15. Gsponer, J., Haberthur, U. & Caflisch, A. The role of side-chain interactions in the early steps of aggregation: Molecular dynamics simulations of an amyloid-forming peptide from the yeast prion Sup35. *Proc. Natl. Acad. Sci. U.S.A.* **100**, 5154-5159 (2003).
16. Hwang, W., Zhang, S. G., Kamm, R. D. & Karplus, M. Kinetic control of dimer structure formation in amyloid fibrillogenesis. *Proc. Natl. Acad. Sci. U.S.A.* **101**, 12916-12921 (2004).
17. Nguyen, H. D. & Hall, C. K. Molecular dynamics simulations of spontaneous fibril formation by random-coil peptides. *Proc. Natl. Acad. Sci. U.S.A.* **101**, 16180-16185 (2004).
18. Tsai, H. H. *et al.* Energy landscape of amyloidogenic peptide oligomerization by parallel-tempering molecular dynamics simulation: Significant role of Asn ladder. *Proc. Natl. Acad. Sci. U.S.A.* **102**, 8174-8179 (2005).
19. Ma, B. & Nussinov, R. Simulations as analytical tools to understand protein aggregation and predict amyloid conformation. *Curr. Opin. Chem. Biol.* **10**, 445-452 (2006).
20. Agrawal, N. J. *et al.* Aggregation in protein-based biotherapeutics: Computational studies and tools to identify aggregation-prone regions. *J. Pharm. Sci.* **100**, 5081-5095 (2011).

21. McKnight, C. J., Matsudaira, P. T. & Kim, P. S. NMR structure of the 35-residue villin headpiece subdomain. *Nat. Struct. Biol.* **4**, 180-184 (1997).
22. Havlin, R. H. & Tycko, R. Probing site-specific conformational distributions in protein folding with solid-state NMR. *Proc. Natl. Acad. Sci. U.S.A.* **102**, 3284-3289 (2005).
23. Chung, J. K., Thielges, M. C. & Fayer, M. D. Dynamics of the folded and unfolded villin headpiece (HP35) measured with ultrafast 2D IR vibrational echo spectroscopy. *Proc. Natl. Acad. Sci. U.S.A.* **108**, 3578-3583 (2011).
24. Brewer, S. H. *et al.* Effect of modulating unfolded state structure on the folding kinetics of the villin headpiece subdomain. *Proc. Natl. Acad. Sci. U.S.A.* **102**, 16662-16667 (2005).
25. Bunagan, M. R., Gao, J., Kelly, J. W. & Gai, F. Probing the folding transition state structure of the villin headpiece subdomain via side chain and backbone mutagenesis. *J. Am. Chem. Soc.* **131**, 7470-7476 (2009).
26. Harada, R., Tochio, N., Kigawa, T., Sugita, Y. & Feig, M. Reduced native state stability in crowded cellular environment due to protein-protein interactions. *J. Am. Chem. Soc.* **135**, 3696-3701 (2013).
27. Levine, R. L. & Stadtman, E. R. Oxidative modification of proteins during aging. *Exp. Gerontol.* **36**, 1495-1502 (2001).
28. Dalle-Donne, I., Rossi, R., Colombo, R., Giustarini, D. & Milzani, A. Biomarkers of oxidative damage in human disease. *Clin. Chem.* **52**, 601-623 (2006).
29. Chiti, F. & Dobson, C. M. Protein misfolding, functional amyloid, and human disease. *Annu. Rev. Biochem.* **75**, 333-366 (2006).
30. Petrov, D. & Zagrovic, B. Microscopic analysis of protein oxidative damage: Effect of carbonylation on structure, dynamics, and aggregability of villin headpiece. *J. Am. Chem. Soc.* **133**, 7016-7024 (2011).
31. Chiti, F., Stefani, M., Taddei, N., Ramponi, G. & Dobson, C. M. Rationalization of the effects of mutations on peptide and protein aggregation rates. *Nature* **424**, 805-808 (2003).
32. Tartaglia, G. G. *et al.* Prediction of aggregation-prone regions in structured proteins. *J. Mol. Biol.* **380**, 425-436 (2008).
33. Schuler, L., Daura, X. & van Gunsteren, W. An improved GROMOS96 force field for aliphatic hydrocarbons in the condensed phase. *J. Comput. Chem.* **22**, 1205-1218 (2001).
34. Schmid, N. *et al.* Definition and testing of the GROMOS force-field versions 54A7 and 54B7. *Eur. Biophys. J.* **40**, 843-856 (2011).
35. Cornell, W. D. *et al.* A 2nd generation force-field for the simulation of proteins, nucleic-acids, and organic-molecules. *J. Am. Chem. Soc.* **117**, 5179-5197 (1995).
36. Lindorff-Larsen, K. *et al.* Improved side-chain torsion potentials for the Amber ff99SB protein force field. *Proteins* **78**, 1950-1958 (2010).
37. Chen, J. H., Im, W. P. & Brooks, C. L. Balancing solvation and intramolecular interactions: Toward a consistent generalized born force field. *J. Am. Chem. Soc.* **128**, 3728-3736 (2006).
38. Kaminski, G. A., Friesner, R. A., Tirado-Rives, J. & Jorgensen, W. L. Evaluation and reparametrization of the OPLS-AA force field for proteins via comparison with accurate quantum chemical calculations on peptides. *J Phys Chem B* **105**, 6474-6487 (2001).
39. Essmann, U. *et al.* A smooth particle mesh Ewald method. *J Chem Phys* **103**, 8577-8593 (1995).
40. Tironi, I. G., Sperb, R., Smith, P. E. & van Gunsteren, W. F. A generalized reaction field method for molecular-dynamics simulations. *J Chem Phys* **102**, 5451-5459 (1995).
41. Shirts, M. R., Pitner, J. W., Swope, W. C. & Pande, V. S. Extremely precise free energy calculations of amino acid side chain analogs: Comparison of common molecular mechanics force fields for proteins. *J Chem Phys* **119**, 5740-5761 (2003).

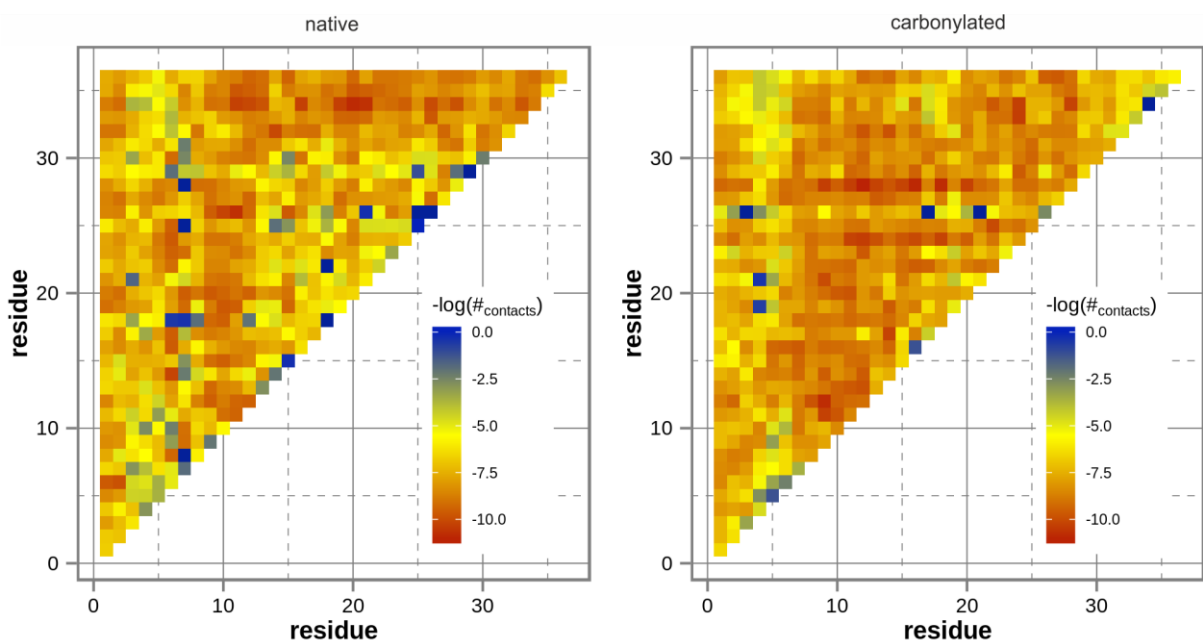
42. Oostenbrink, C., Villa, A., Mark, A. E. & van Gunsteren, W. F. A biomolecular force field based on the free enthalpy of hydration and solvation: the GROMOS force-field parameter sets 53A5 and 53A6. *J. Comput. Chem.* **25**, 1656-1676 (2004).
43. Godoy-Ruiz, R. *et al.* Estimating free-energy barrier heights for an ultrafast folding protein from calorimetric and kinetic data. *J Phys Chem B* **112**, 5938-5949 (2008).
44. Pawar, A. P. *et al.* Prediction of "aggregation-prone" and "aggregation-susceptible" regions in proteins associated with neurodegenerative diseases. *J. Mol. Biol.* **350**, 379-392 (2005).
45. Nelson, R. *et al.* Structure of the cross-beta spine of amyloid-like fibrils. *Nature* **435**, 773-778 (2005).
46. Gsponer, J. & Vendruscolo, M. Theoretical approaches to protein aggregation. *Protein Pept. Lett.* **13**, 287-293 (2006).
47. Lorusso, M., Pepe, A., Ibris, N. & Bochicchio, B. Molecular and supramolecular studies on polyglycine and poly-L-proline. *Soft Matter* **7**, 6327-6336 (2011).
48. Lindorff-Larsen, K., Trbovic, N., Maragakis, P., Piana, S. & Shaw, D. E. Structure and dynamics of an unfolded protein examined by molecular dynamics simulation. *J. Am. Chem. Soc.* **134**, 3787-3791 (2012).
49. Best, R. B., Buchete, N.-V. & Hummer, G. Are current molecular dynamics force fields too helical? *Biophys. J.* **95**, 4494-4494 (2008).
50. Lindorff-Larsen, K. *et al.* Systematic validation of protein force fields against experimental data. *PLoS ONE* **7** (2012).
51. Petrov, D., Margreitter, C., Grandits, M., Oostenbrink, C. & Zagrovic, B. A systematic framework for molecular dynamics simulations of protein post-translational modifications. *PLoS Comp. Biol.* **9**, e1003154 (2013).
52. Hess, B., Kutzner, C., van der Spoel, D. & Lindahl, E. GROMACS 4: algorithms for highly efficient, load-balanced, and scalable molecular simulation. *J. Chem. Theory. Comput.* **4**, 435-447 (2008).
53. Berendsen, H. J. C., Postma, J. P. M., van Gunsteren, W. F., Dinola, A. & Haak, J. R. Molecular-dynamics with coupling to an external bath. *J Chem Phys* **81**, 3684-3690 (1984).
54. Berendsen, H. J. C., Postma, J. P. M., van Gunsteren, W. F. & Hermans, J. Interaction models for water in relation to protein hydration. Reidel, Dordrecht, 1981.
55. Jorgensen, W. L., Chandrasekhar, J., Madura, J. D., Impey, R. W. & Klein, M. L. Comparison of simple potential functions for simulating liquid water. *J Chem Phys* **79**, 926-935 (1983).
56. Kabsch, W. & Sander, C. Dictionary of protein secondary structure: pattern recognition of hydrogen-bonded and geometrical features. *Biopolymers* **22**, 2577-2637 (1983).
57. Schrodinger, LLC. *The PyMOL Molecular Graphics System, Version 1.3r1* (2010).
58. Wickham, H. *ggplot2: elegant graphics for data analysis*. Springer, New York, 2009.



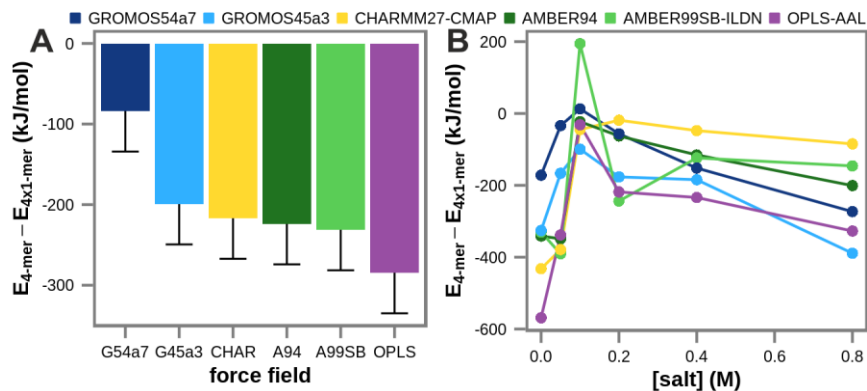
## Appendices to Chapter IV



**Figure S1.** Dissociation kinetics of villin complexes in native and carbonylated forms. Main panel - the percentage of peptide-peptide complexes that never dissociate in the course of simulated trajectories shown as a function of complex life-time. Inset – inverse of the cumulative distribution of the number of villin headpiece intermolecular complexes as a function of complex life-time, i.e., the function that at each value of  $\tau$  (complex life-time) gives the number of complexes with a longer life-times than the given  $\tau$ -value, shown for complexes that dissociate (left) and never dissociate (right) over simulated time.



**Figure S2.** Sequence-wise contact map of intermolecular atomic contacts for native and carbonylated villin headpiece estimated by the number of intermolecular atomic contacts normalized by solvent-accessibility, i.e., surface-exposure per amino acid. The color code of the heat map corresponds to the negative logarithm of the number of contacts for each pair of residues, additionally rescaled in such a way that 0 represents the pair of residues with the smallest number of contacts.



**Figure S3.** The difference in total potential energy between aggregated (tetramers) and non-aggregated (free monomers) states of native villin headpiece calculated from the re-evaluated energies using RF electrostatics treatment and 6 widely used MD force fields on energy-minimized configurations, where the force field used for re-evaluation of the potential energy was also used for energy-minimization. The averages over all simulations are shown with the estimated standard errors (50 kJ/mol) depicted by one-sided error bars.

**TABLE S1.** Simulation conditions and setups together with the averages and standard deviations of three measures of foldedness: atom-positional root-mean-square deviation (RMSD) from the native villin headpiece structure,<sup>1</sup> number of residues in  $\alpha$ -helical conformation (#  $\alpha$ ) and the sum of distances between the centers of mass of core phenylalanines ( $\Sigma$ dPHEs). The last two rows highlighted in gray are the aggregate averages over all 10 simulated systems at finite protein concentration and the averages over the infinitely diluted systems (data taken from ref<sup>2</sup>), together with their respective standard deviations. The averages for the finite protein-concentration systems were calculated over the entire simulated time, whereas for the infinitely diluted systems the last 25 ns of the simulated trajectories were used. Each simulation setup was used to model both native and carbonylated villin and accordingly, the averages and standard deviations are shown for native (left) and carbonylated (right) systems.

## REFERENCES

1. McKnight, C. J., Matsudaira, P. T. & Kim, P. S. NMR structure of the 35-residue villin headpiece subdomain. *Nat. Struct. Biol.* **4**, 180-184 (1997).
2. Petrov, D. & Zagrovic, B. Microscopic analysis of protein oxidative damage: Effect of carbonylation on structure, dynamics, and aggregability of villin headpiece. *J. Am. Chem. Soc.* **133**, 7016-7024 (2011).

#	[protein] (mM)	N peptides	[salt] (M)	force field	electrostatics	t (ns)	N simulations	RMSD (Å)	# alpha	dPHE
1	9.2	8	0	GROMOS45a3	RF	50	3	2.7 ± 1.1   8.2 ± 0.8	22.6 ± 1.9   6.3 ± 3.8	19.9 ± 1.7   34.9 ± 2.3
2	6	4	0.05	GROMOS45a3	RF	50	3	2.4 ± 0.8   8.5 ± 0.7	22.9 ± 1.5   5.3 ± 2.0	20.3 ± 1.7   38.2 ± 3.4
3	6	4	0.1	GROMOS45a3	RF	50	3	2.8 ± 1.8   8.4 ± 0.6	22.6 ± 1.9   6.2 ± 3.2	19.5 ± 1.0   37.5 ± 3.6
4	6	4	0.2	GROMOS45a3	RF	50	3	2.2 ± 0.5   8.1 ± 0.6	23.0 ± 1.4   6.6 ± 3.0	20.7 ± 1.6   33.5 ± 6.0
5	6	4	0.4	GROMOS45a3	RF	100	3	2.5 ± 0.8   8.3 ± 0.6	22.7 ± 1.8   6.7 ± 2.7	19.5 ± 1.9   38.1 ± 6.0
6	6	4	0.8	GROMOS45a3	RF	100	3	2.7 ± 1.3   8.1 ± 0.6	22.4 ± 2.0   6.1 ± 3.0	19.5 ± 1.3   32.5 ± 4.5
7	6	4	0	GROMOS54a7	RF	100	1	3.8 ± 3.0   8.6 ± 1.0	22.6 ± 2.1   7.7 ± 2.3	19.9 ± 1.2   41.8 ± 10.2
8	6	4	0.05	GROMOS54a7	RF	100	1	4.3 ± 2.5   8.0 ± 0.6	22.4 ± 2.4   6.6 ± 4.6	19.0 ± 1.0   34.3 ± 3.4
9	6	4	0.05	GROMOS45a3	PME	200	3	2.8 ± 0.8   7.9 ± 0.8	20.7 ± 3.2   6.4 ± 3.7	20.9 ± 3.2   29.0 ± 3.7
10	6	4	0.05	GROMOS54a7	PME	200	3	2.4 ± 0.5   7.8 ± 0.9	23.1 ± 1.5   9.1 ± 5.0	21.2 ± 2.9   30.7 ± 4.0
<b>aggregate average</b>										
Ref <sup>2</sup>	0	0	0	GROMOS45a3	RF	110	5	3.1 ± 1.4   7.3 ± 0.9	21.8 ± 3.2   12.1 ± 5.1	19.3 ± 1.4   29.3 ± 5.3



## Chapter V

# Effect of oxidative damage on the stability and dimerization of superoxide dismutase 1

Petrov, D., Daura, X. & Zagrovic, B. Further results (in preparation to be submitted to *PLoS Comput. Biol.*)

DP and BZ conceived and designed the study. DP collected and DP, XD and BZ analyzed the data. DP, XD and BZ wrote the manuscript.

**ABSTRACT**

Superoxide dismutase 1 (SOD1), a homo-dimeric metalloenzyme, is one of the key antioxidative agents in human cells. It has been linked to amyotrophic lateral sclerosis (ALS), a devastating, late-onset neurodegenerative disorder, with more than 150 ALS-related mutations identified in the SOD1 gene. Additionally, oxidatively damaged and aggregated species of the enzyme have been reported in ALS patients and animal models. However, the molecular mechanisms and possible implications of oxidative stress in the process of SOD1-mediated ALS development still remain elusive. Here, we use classical molecular dynamics (MD) simulations together with thermodynamic integration to study the effects of different oxidative modifications on SOD1 folding and dimerization free energies. In particular, we focus on lysine, arginine and proline carbonylation and cysteine oxidation, two of the most prominent modification types induced by oxidative stress, and examine residues at the homo-dimer interface. Our results show that oxidative damage to SOD1 can drastically destabilize both its homo-dimer and monomer structures, supporting the hypothesis that age-related increase in oxidative stress may be the main trigger of ALS, with the mutations in SOD1 gene being only an additional factor in the development of the disease. Finally, we propose and discuss further objectives of this ongoing project, including examination of ALS-related mutations in SOD1, exploration of binding free energies of metal ions bound to SOD1 and optimization of free energy calculation methods based on MD simulations.

## INTRODUCTION

Reactive oxygen species (ROS) participate in a large number of different chemical reactions with proteins leading to modified amino-acid side chains and backbone or even cross-linked and fragmented proteins.<sup>1</sup> Importantly, such oxidative modifications have been associated with aging and age-related disorders such as neurodegenerative diseases, cancer or diabetes.<sup>2,3</sup> Additionally, highly oxidized proteins have been found in potentially cytotoxic protein aggregates and amyloid fibrils.<sup>4,5</sup> Furthermore, recent evidence has indicated that carbonylation, arguably the most studied irreversible oxidative modification, increases protein aggregation propensity and can therefore trigger the formation of insoluble protein inclusions.<sup>6</sup> However, a direct causal relationship between oxidative stress on the one hand and protein aggregation, aging and development of late onset diseases on the other has not been established.<sup>7</sup> An important and widely studied system for exploring this relationship has been Cu/Zn superoxide dismutase (SOD1).<sup>8,9</sup> In particular, this enzyme has been found to associate with 20% of cases of familial amyotrophic lateral sclerosis (fALS), an age-related neurodegenerative disease, with more than 150 different mutations in the SOD1 gene having been linked with fALS.<sup>8,10,11</sup> Moreover, the presence of SOD1 in protein inclusions in motor neurons and astrocytes of fALS patients<sup>12-14</sup> and animal models<sup>15,16</sup> has been observed and documented in detail. Interestingly, SOD1, which breaks down free superoxide radicals as one of the key antioxidant enzymes in human cells, is by the nature of its function as well as its cellular localization exposed to higher levels of oxidative stress than most other proteins. However, the molecular cause and potential implications of oxidative stress in the development of fALS still remain elusive.

Under native conditions SOD1 forms a stable homo-dimer, which is thought to prevent its aggregation and subsequent cytotoxicity,<sup>17</sup> and binds zinc and copper ions, which are important for its dismutase activity as well as its tertiary and quaternary structure formation and stability.<sup>18-20</sup> The two main mechanisms that have been proposed to explain the toxicity of SOD1 mutants are: 1) reduced dismutase activity or increased peroxidase activity leading to an overall increase in oxidative damage of cellular proteins, and 2) formation of insoluble aggregates through a decrease in the stability of SOD1 monomers and/or SOD1 dimer destabilization. Concerning the latter, it has been suggested that it is possibly due to a

decrease in binding affinities of copper and zinc ions with a concomitant increase in their cellular levels, which by itself is thought to be neurotoxic.<sup>8,18</sup>

Here, we use molecular dynamics (MD) simulations<sup>21,22</sup> to investigate whether and under what circumstances direct oxidative damage of the SOD1 enzyme could trigger cytotoxicity. In particular, we explore how different oxidative modifications at the homo-dimer interface affect dimer stability, and further ask how these modifications modulate the stability of free monomers in solution. Importantly, while significant efforts have been directed at experimentally characterizing the thermodynamic properties of SOD1 wild-type and FALS mutants,<sup>23,24</sup> a systematic investigation of oxidatively modified SOD1, i.e., of oxidation “mutants”, has so far not been performed. With the continued advance of computer power, this problem has become tractable by different theoretical and computational approaches. On the one hand, various efficient semi-empirical methods, utilizing force-field- and knowledge-based scoring functions to predict protein stability upon mutation, have been developed.<sup>25-27</sup> Although validation against experimental data has shown that such methods in general reproduce correct trends, they, however, often fail in providing a precise quantitative measure of stability.<sup>28</sup> On the other hand, two recent studies have employed perturbation techniques in combination with classical MD, a rigorous, physically based and arguably more accurate approach, to estimate changes in folding free energies upon mutation. In particular, Seeliger and de Groot<sup>29</sup> have successfully calculated thermodynamic stability differences for 109 mutations in the microbial ribonuclease barnase, achieving a remarkable accuracy, with a Pearson correlation coefficient of  $R = 0.86$  against experimental data and an average absolute error of only 3.31 kJ/mol, using non-equilibrium fast-growth thermodynamic integration simulations. Furthermore, Lin *et al.*<sup>30</sup> have performed one-step perturbation calculations to explore the effects of four different side-chain substitutions in a hepta- $\beta$ -peptide on the folding equilibrium, obtaining results in agreement with experimentally available NMR and circular dichroism data.

Here, in light of these computer-simulation studies, we use the thermodynamic integration (TI) method<sup>31</sup>, one of the most widely used and most thoroughly tested thermodynamic techniques available,<sup>32-34</sup> in combination with equilibrium MD simulations to estimate changes in free energy of SOD1 homo-dimer formation and its monomer folding. While



computationally extremely expensive, TI is in principle capable of yielding free energy differences at the limit of accuracy of the force field used.<sup>35-37</sup> We test convergence of the free-energy calculations using block averaging. Finally, we discuss further plans and directions of this study.

## METHODS

### Molecular dynamics simulations and free energy calculations

We have used the thermodynamic integration approach<sup>31</sup> to calculate the impact of different types of oxidative modifications on the stability of SOD1 dimer and monomer. Alchemical modifications from native residues of interest to their oxidized forms, in the context of the folded SOD1 homo-dimer and monomer or its unfolded state (modeled by a GGXGG pentapeptide, where X stands for the affected residue), were performed by smoothly modifying the force field parameters from those defining the initial to those defining the end state. These processes were coupled to a parameter  $\lambda$ , ranging from  $\lambda=0$  to  $\lambda=1$ , with the end points representing the native and the modified residue, respectively. Starting from a fully stretched pentapeptide or a 3D structure of SOD1 (PDB code 3KH4<sup>38</sup>, using the chains A and B for dimer and the chain A for monomer simulations), each system was solvated in a cubic box filled with explicit SPC<sup>39</sup> water molecules, energy minimized and subsequently equilibrated in three independent copies by gradually increasing the temperature (from 100 to 300 K) over 100 ps and decreasing position restraints (from 25,000 to 5,000 kJ mol<sup>-1</sup> nm<sup>-2</sup>) at constant volume and temperature. Additional equilibration for 20 ps at constant pressure (1 bar) and temperature (300 K) was performed subsequently. Starting from each equilibrated system, three independent, 500-ps-long MD simulations were run at each of 21 equally spaced  $\lambda$ -points, with 2 additional  $\lambda$ -points near both ends of the  $\lambda$  range, for a total of 112.5 ns simulation time per system. The change in free energy of an alchemical modification was then calculated as the integral of the ensemble average of the derivative of the system Hamiltonian with respect to  $\lambda$ , between the boundaries  $\lambda=0$  and  $\lambda=1$ . The integrals were evaluated by the generalized Simpson's rule for non-equidistant nodes using averages over the nine independent simulations at each  $\lambda$ -point, including only the last 150 ps of each 500-ns-long simulation. The change upon

oxidative modification in the stability of SOD1 homo-dimer ( $\Delta\Delta G_{mono\rightarrow dim}^{nat\rightarrow oxi}$ ) and monomer ( $\Delta\Delta G_{unf\rightarrow mono}^{nat\rightarrow oxi}$ ) were calculated according to the thermodynamic cycle in Figure 1 as follows:

$$\Delta\Delta G_{mono\rightarrow dim}^{nat\rightarrow oxi} = \Delta G_{mono\rightarrow dim}^{oxi} - \Delta G_{mono\rightarrow dim}^{nat} = \Delta G_{dim}^{nat\rightarrow oxi} - 2\Delta G_{mono}^{nat\rightarrow oxi} \quad (1)$$

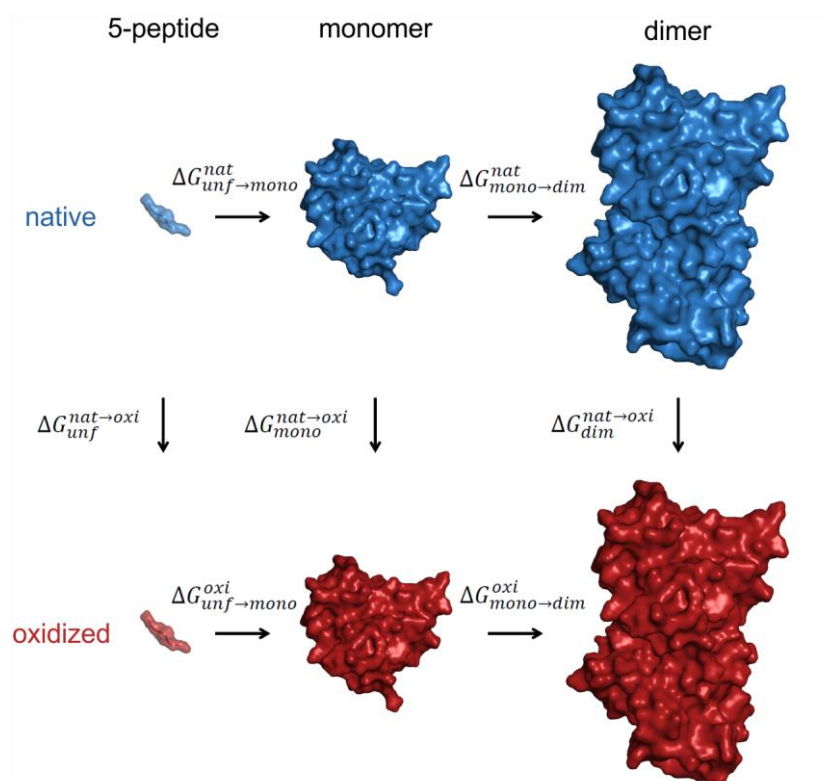
and

$$\Delta\Delta G_{unf\rightarrow mono}^{nat\rightarrow oxi} = \Delta G_{unf\rightarrow mono}^{oxi} - \Delta G_{unf\rightarrow mono}^{nat} = \Delta G_{mono}^{nat\rightarrow oxi} - \Delta G_{unf}^{nat\rightarrow oxi}. \quad (2)$$

Here,  $\Delta G_{mono\rightarrow dim}^{oxi}$  and  $\Delta G_{mono\rightarrow dim}^{nat}$  are free energies of dimer formation of the oxidatively modified and native SOD1 homo-dimer, respectively, while  $\Delta G_{unf\rightarrow mono}^{oxi}$  and  $\Delta G_{unf\rightarrow mono}^{nat}$  are the folding free energies of the oxidatively modified and native SOD1 monomer, respectively. Finally,  $\Delta G_{dim}^{nat\rightarrow oxi}$ ,  $\Delta G_{mono}^{nat\rightarrow oxi}$  and  $\Delta G_{unf}^{nat\rightarrow oxi}$  are free energy changes upon alchemical modification in the context of the folded SOD1 homo-dimer and monomer, and its unfolded state, respectively. Statistical errors were estimated using block averaging and standard propagation of error.<sup>40</sup> MD simulations were run using the GROMACS 4.0.7 biomolecular simulation package,<sup>41</sup> with the GROMOS force field 54A7 parameter set,<sup>42,43</sup> a reaction field electrostatic scheme with a cutoff  $r_c = 1.4$  nm and dielectric constant  $\epsilon_{rf} = 65$  and Berendsen thermostat and barostat keeping the temperature at 300 K ( $\tau_T = 0.05$  ps) and pressure at 1 bar ( $\tau_p = 1$  ps and compressibility =  $4.5 \times 10^{-5}$  bar<sup>-1</sup>).<sup>44</sup> A soft-core formalism<sup>45</sup> was used to avoid singularities in the potential energy function when removing the non-bonded interactions of atoms, with parameters  $sc-\alpha = 0.7$  and  $sc-power = 1$ , except for threonine carbonylation for which  $sc-\alpha = 1.51$  and  $sc-power = 2$  were used.

Using the above free energy calculation protocol, the effect of oxidative modifications of nine residues at the homo-dimer interface (THR2, LYS3, CYS6, LYS9, THR54, PRO62, CYS111, ARG115 and THR116) was explored. These particular residues were chosen because they were expected to affect the homo-dimer stability more strongly than others. Namely, out of 46 interfacial residues (defined to be all residues in an SOD1 monomer that are within 8 Å from any atom in the second monomer in an SOD1 dimer), we focused on carbonylation of threonines, lysines, arginines and prolines, and oxidation of cysteines to cysteic acids, two of the most frequent types of oxidative modification found in nature. Furthermore, these

modifications lead to a major change in local hydrophobicity as explained in more detail in Chapter I and ref<sup>46</sup>. Parameters of the modified residues were taken from Chapter I.



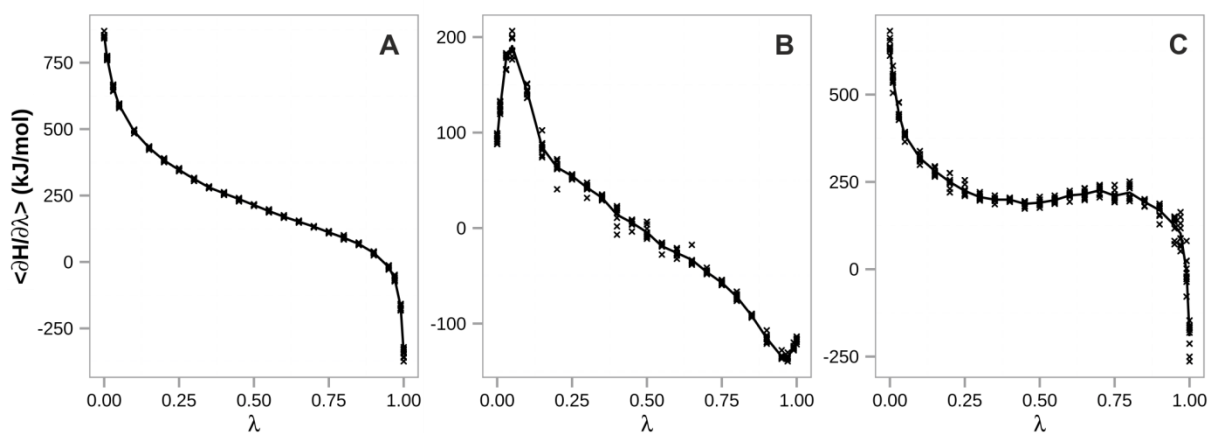
**Figure 1. Thermodynamic cycle.** Since free energy is a state function, sum of free energy changes between states that form a thermodynamic cycle add up to zero. This property allows one to assess the relative free energy difference between the native and oxidized SOD1 dimer/monomer stability, a quantity rather difficult to calculate directly, by evaluating changes in the free energy of an alchemical modification from a native residue of interest to its oxidized form ( $\Delta G_{dim}^{nat\rightarrow oxi}$  for an alchemical modification in the dimer,  $\Delta G_{mono}^{nat\rightarrow oxi}$  for an alchemical modification in the monomer and  $\Delta G_{unf}^{nat\rightarrow oxi}$  for an alchemical modification in the pentapeptide, i.e., unfolded state), according to the above thermodynamic cycle and Equations 1 and 2.

## RESULTS AND DISCUSSION

### How do oxidative modifications affect SOD1 homo-dimer and monomer stability?

To address this question, we have applied advanced free energy calculations based on MD simulations, focusing on the following residues at the SOD1 homo-dimer interface: THR2, LYS3, CYS6, LYS9, THR54, PRO62, CYS111, ARG115 and THR116. In particular, we have used the TI method<sup>31</sup> to calculate free energy changes upon alchemical switching from native to oxidatively modified residues, an approach recently applied to successfully estimate the

effect of point mutations on protein stability.<sup>29</sup> However, in contrast to the aforementioned study in which fast, non-equilibrium free energy calculations were performed, we have employed a widely used equilibrium simulation approach, using thermodynamically reversible paths for the calculations. One of the reasons for opting for this more traditional approach has been the recently observed and studied convergence problems of non-equilibrium free energy calculations.<sup>47</sup> Before discussing the specific effects of individual oxidative modifications studied here, we would first like to discuss the important issues of sampling and convergence in our simulations.



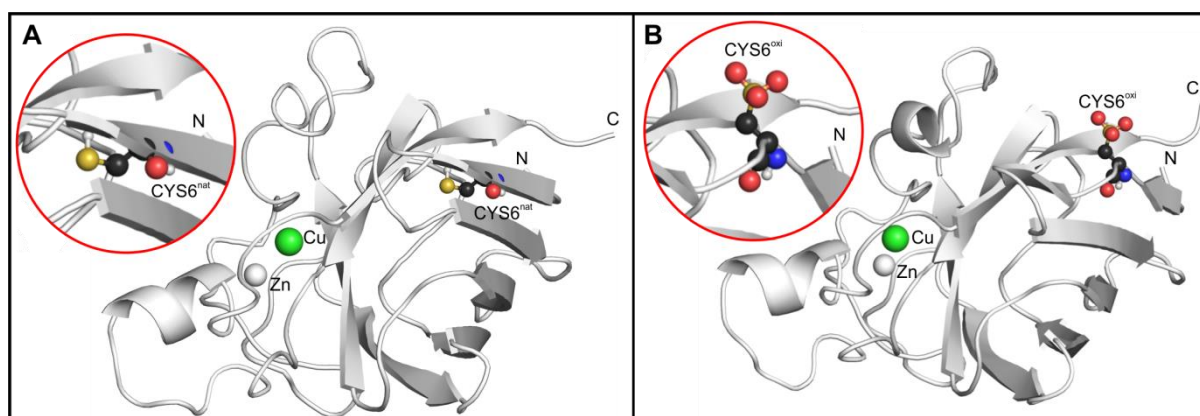
**Figure 2. Typical  $\langle \partial H / \partial \lambda \rangle$  curves.** Ensemble average derivative of the system Hamiltonian with respect to  $\lambda$  shown as a function of  $\lambda$ : A – LYS9, B – THR54 and C – ARG115. Multiple points at given  $\lambda$  come from independent simulations, with the average curves shown in solid lines.

In general, insufficient sampling is one of the major limitations of the MD method, especially in free energy calculations applied to complex systems with rough free energy landscapes. Thus, we have used block averaging (see Methods for details) to estimate the errors of the ensemble average derivative of the system Hamiltonian with respect to  $\lambda$  ( $\langle \partial H / \partial \lambda \rangle$ ). The analysis of the distribution of errors at individual  $\lambda$ -points shows that approximately 90% of errors are smaller than 10 kJ/mol, with the average over all SOD1 dimer and monomer simulations of 5.2 kJ/mol, which is comparable to  $2RT \approx 5$  kJ/mol at room temperature. Additionally, smooth  $\langle \partial H / \partial \lambda \rangle$  versus  $\lambda$  curves (Figure 2) allow for an adequate numerical estimation of the calculated integrals, i.e., free energy differences, with all errors of the calculated integrals smaller than 4 kJ/mol. Importantly, this suggests that our free energy

calculations are reasonably converged, and this is likely due to the extensive sampling performed (a total of 112.5 ns for each alchemical perturbation).

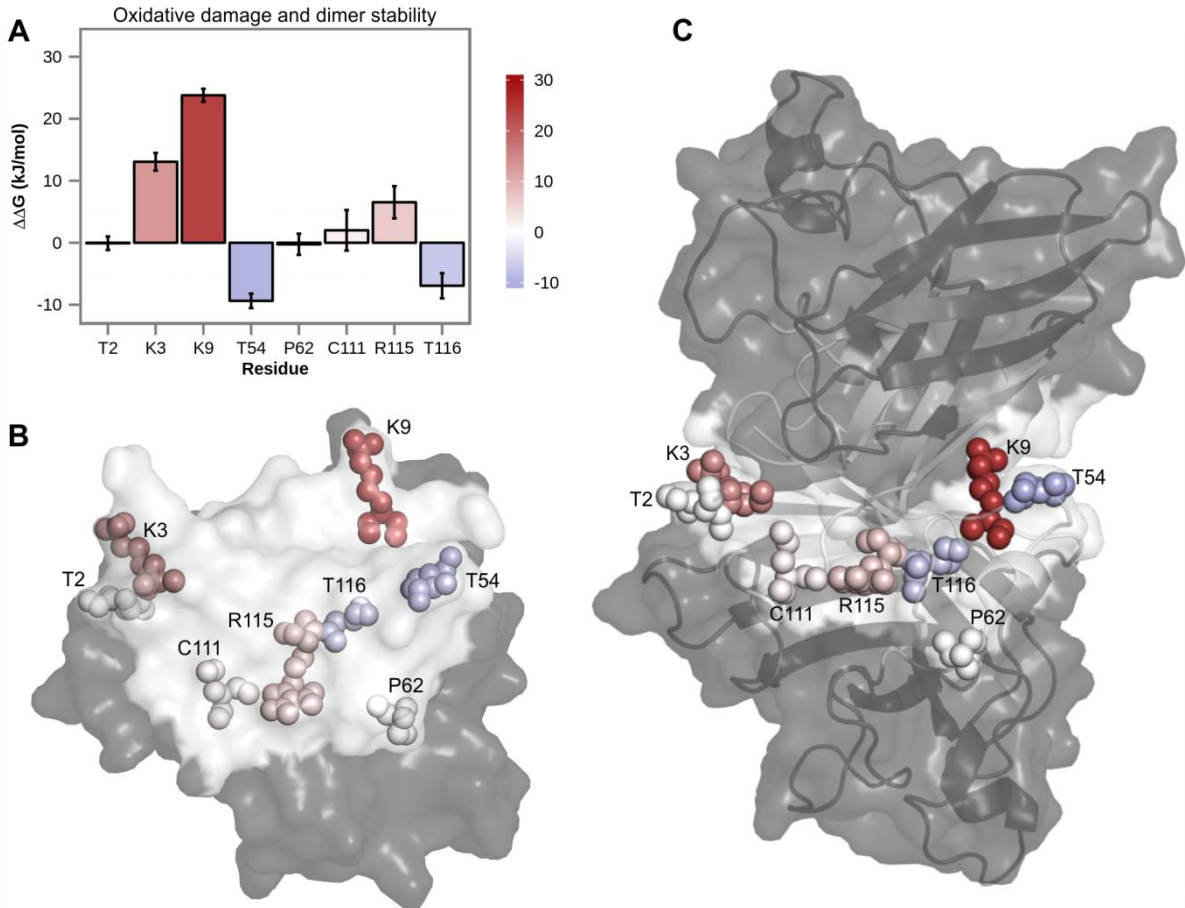
Small error bars of the calculated free energy changes, i.e., indicators of convergence, must be distinguished from accuracy of the obtained results. In addition to convergence, the latter depends primarily on the degree of systematic error of the employed method. In particular, alchemical modifications involving net charge perturbation are a sizeable source of systematic error in free energy calculations, introducing a significant reduction in accuracy. However, since the change in stability is defined as the difference between free energy changes in two separate legs of the thermodynamic cycle (Figure 1), the inclusion of the same alchemical perturbation and presumably the same systematic error would cancel out by subtraction. As reported by Seeliger and de Groot<sup>29</sup>, this would then provide acceptable accuracy with more than 50% of their calculated values within 1 kcal/mol (< 4.18 kJ/mol) of the experimental data. Importantly, corrections to free energies of charging can be applied *ex post* to obtain more accurate and reliable results.<sup>48,49</sup>

Notably, more than 20% of the errors from simulations probing oxidative modification of CYS6 residue are greater than 20 kJ/mol, with the average of 14 kJ/mol, clearly showing that the convergence has not been reached for this system. Additional inspection of the simulated trajectories revealed that the affected residue (CYS6) flips upon modification, concomitantly causing partial unfolding of the  $\beta$ -strand formed by the native residue (Figure 3). For this reason, we have excluded CYS6 from further analysis.



**Figure 3. Local unfolding as a consequence of oxidative damage of CYS6.** While the affected residue is buried in its native form (A), it flips to protein surface and becomes solvent exposed upon oxidative modification, additionally destabilizing local  $\beta$ -sheet structure (B). Inset: a close-up picture of the affected residue.

How do oxidative modifications affect homo-dimer and monomer stability of SOD1? The stability of the SOD1 homo-dimer is markedly decreased by carbonylation of LYS9 residue ( $\Delta\Delta G_{mono \rightarrow dim}^{nat \rightarrow oxi} = 23.8 \pm 1.1$  kJ/mol, Figure 4).



**Figure 4. Impact on the SOD1 dimer stability on oxidative damage of residues at the homo-dimer interface.** A) changes in free energy of the homo-dimer formation with the error bars calculated by block averaging and standard propagation of error. Location of the studied interface residues and effects of their oxidative modifications on the SOD1 dimer in the context of: B) one of the monomers (view at the interface) and C) SOD1 dimer. Color code for free energy changes: blue – stabilization, white - no effect and red – destabilization; color code for protein structure: white – interface and grey – rest of the protein.

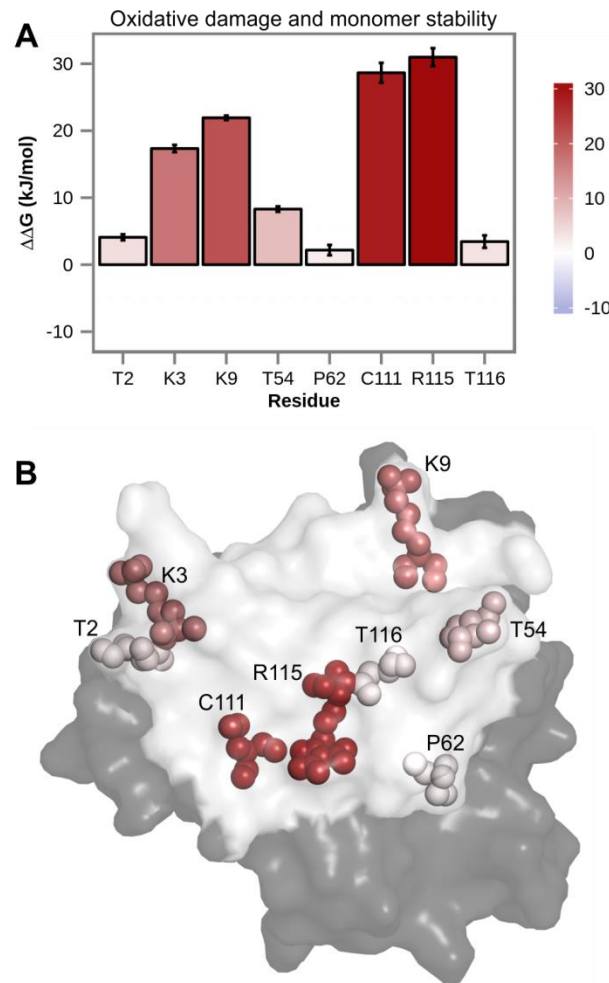
This is striking when compared to the stability of the dimer itself, which was estimated to be approximately -50 kJ/mol,<sup>23</sup> and to the experimentally measured destabilization effects of some ALS-causing mutations with  $\Delta\Delta G_{mono \rightarrow dim}^{nat \rightarrow mut}$  smaller than 5 kJ/mol.<sup>23</sup> Furthermore, oxidatively damaged LYS3 and ARG115 residues exhibit notable destabilization as well, although smaller in extent when compared to LYS9 ( $13.1 \pm 1.4$  kJ/mol and  $6.5 \pm 2.6$  kJ/mol, respectively, Figure 4). On the other hand, threonine carbonylation events stabilize the

homo-dimer by  $-9.4 \pm 1.2$  kJ/mol (THR54) and  $-6.9 \pm 2.0$  kJ/mol (THR116). It must be noted, however, that threonines are significantly less prone to carbonylation compared to other carbonylatable amino acids. Lastly, oxidative modifications of THR2, PRO62 and CYS111 show no effect, with the changes in the free energy of the dimer formation smaller than the calculated errors (Figure 4).

When it comes to the folding free energy of the SOD1 monomer, oxidative damage of ARG115, CYS111, LYS9 and LYS3 residues significantly affect monomer stability, decreasing it by  $31.0 \pm 1.3$  kJ/mol,  $28.7 \pm 1.5$  kJ/mol,  $21.9 \pm 0.3$  kJ/mol and  $17.3 \pm 0.5$  kJ/mol, respectively (Figure 5). Although such drastic destabilization effects correspond to an increase in the ratio between the unfolded and folded states of SOD1 by about four orders of magnitude, it is highly unlikely that these oxidative modifications are able to cause complete unfolding of the monomer, given that SOD1 is a hyperstable protein.<sup>50</sup> However, they might induce partial local unfolding, as observed for CYS6 (Figure 3), potentially leading to the formation of insoluble aggregates and consequently cytotoxicity, a mechanism already identified for SOD1 and other well-structured polypeptides involved in protein deposition disorders.<sup>51</sup> In contrast, carbonylation modifications of the remainder of the studied residues only marginally alter monomer stability, with all of them having destabilizing effects (Figure 5).

Taken all together, the results show that a majority of oxidative modifications, regardless of the type of modification and nature of the targeted residue, destabilize both the SOD1 homo-dimer and monomer, with a greater absolute impact on monomer stability. This, in turn, supports the idea that age-related increase in oxidative stress might lead to cytotoxicity through impaired dimerization and increased aggregation propensity of SOD1, consequently leading to ALS. Moreover, this suggests, as speculated before,<sup>17</sup> that increased level of oxidative damage of SOD1, triggered by age, may be a key element in ALS development, with fALS-linked SOD1 mutations being only an additional factor making the protein more susceptible to gain cytotoxic properties and increasing the probability of an early onset of the disease. Importantly, different lines of evidence support these speculations: 1) fALS is a late-onset disease, suggesting that other cause(s) in addition to the reported SOD1 mutations may be required for disease development, 2) as repeatedly shown, SOD1 is involved in sporadic ALS as well,<sup>52</sup> 3) increased oxidative stress induces

SOD1 aggregation both *in vitro* and *in vivo*,<sup>17,53</sup> 4) oxidative modifications increase protein aggregation propensity and this is particularly true for carbonylation, which can drastically promote aggregability even at low concentrations,<sup>6</sup> and 5) one of the predominant determinants of longevity appears to be resistance of proteome integrity and protein stability to oxidative stress, as recently shown.<sup>54,55</sup>



**Figure 5. Impact on the SOD1 monomer stability of oxidative damage of residues at the homo-dimer interface.** A) changes in free energy of the folding free energy of with the error bars calculated by block averaging and propagation of error. B) Location of the studied interface residues and effects of their oxidative modifications on the SOD1 monomer (view at the interface). *Color code for free energy changes:* blue – stabilization, white - no effect and red – destabilization; *color code for protein structure:* white – interface and grey – rest of the protein.

Finally, even though 5 of the 9 studied modifications involve net charge perturbation, thus potentially weakening the quantitative aspect of the estimated changes in SOD1 monomer and dimer stability, we strongly believe that the calculated data support the qualitative



interpretations given, considering that 1) we use multiple-fold longer simulation time per alchemical modification than in related studies,<sup>29,30,56</sup> arguably achieving better convergence and accuracy, 2) the majority of the estimated changes in free energy point in the direction of destabilization, with a sizeable fraction showing drastic effects and the most extreme examples in excess of 10RT at room temperature, and 3) since lysine and arginine carbonylation is a charge-removing and cysteine oxidation is a charge-introducing modification, one would in principle expect opposite impact on the calculated SOD1 stability (if affected by a systematic error), yet they both exhibit significant destabilization effects.

### FURTHER PLANS

In order to test the presented hypotheses and speculations in this chapter, we plan to analyze effects of other oxidizable residues of SOD1 on its homo-dimer and monomer stability. Moreover, we plan to explore if oxidative stress can lead to cytotoxicity through a decrease in the binding affinities to Zn and Cu ions. Additionally, we aim to compare the effects of fALS-related SOD1 point mutations with those of oxidative modifications, particularly those of the mutated residues. To address such a broad range (both in number and type) of mutations and modifications, an efficient and accurate automated protocol for free energy calculations upon alchemical perturbations is essential. In particular, improvements in the protocol that was applied herein could be achieved through: 1) separation of perturbations in electrostatics and van der Waals interactions, 2) calculations of charging corrections in free energy, 3) reducing the number of independent simulations, the number of  $\lambda$  points and/or the length of independent simulations by a more judicious choice of  $\lambda$  points, 4) quantitative estimation of the phase space overlap of MD simulations at neighboring  $\lambda$  points, and 5) resorting to alternative MD-based approaches for free energy calculation.<sup>34,48,49,57,58</sup> Importantly, as a control, we plan to calculate and compare free energy differences with available experimental data,<sup>29</sup> prior to applying calculations to SOD1 systems of interest. Furthermore, we have already developed an automated tool for introduction of alchemical modifications (GROMACS topology format), based on the VF algorithm for graph isomorphism matching.<sup>59</sup> However, extensive testing and debugging is still required to ensure desirable reliability and efficiency of the algorithm. Notably, these efforts might potentially result in a significant advance when it comes to the methodology

for free energy estimation, which may be applicable in different contexts ranging from estimation of protein stability to binding affinity calculations to rational drug development.<sup>29,60,61</sup>

## **ACKNOWLEDGEMENTS**

This work was supported in part by the Austrian Science Fund FWF (START grant Y 514-B11 to BZ, <http://www.fwf.ac.at/>), European Research Council (ERC Starting Independent grant 279408 to BZ, <http://erc.europa.eu/>) and the HPC-EUROPA2 project with the support of the European Commission - Capacities Area - Research Infrastructures (project number: 1036 to DP, <http://www.hpc-europa.eu/>). We thank members of the Laboratory of Computational Biophysics at MFPL for useful advice and assistance.

## REFERENCES

1. Levine, R. L. & Stadtman, E. R. Oxidative modification of proteins during aging. *Exp. Gerontol.* **36**, 1495-1502 (2001).
2. Nystrom, T. Role of oxidative carbonylation in protein quality control and senescence. *EMBO J.* **24**, 1311-1317 (2005).
3. Dalle-Donne, I., Rossi, R., Colombo, R., Giustarini, D. & Milzani, A. Biomarkers of oxidative damage in human disease. *Clin. Chem.* **52**, 601-623 (2006).
4. Davies, K. J. Degradation of oxidized proteins by the 20S proteasome. *Biochimie* **83**, 301-310 (2001).
5. Grune, T., Jung, T., Merker, K. & Davies, K. J. Decreased proteolysis caused by protein aggregates, inclusion bodies, plaques, lipofuscin, ceroid, and 'aggresomes' during oxidative stress, aging, and disease. *Int. J. Biochem. Cell Biol.* **36**, 2519-2530 (2004).
6. Petrov, D. & Zagrovic, B. Microscopic analysis of protein oxidative damage: Effect of carbonylation on structure, dynamics, and aggregability of villin headpiece. *J. Am. Chem. Soc.* **133**, 7016-7024 (2011).
7. Andersen, J. K. Oxidative stress in neurodegeneration: cause or consequence? *Nat. Med.* **10**, S18-S25 (2004).
8. Hand, C. K. & Rouleau, G. A. Familial amyotrophic lateral sclerosis. *Muscle Nerve* **25**, 135-159 (2002).
9. Barber, S. C. & Shaw, P. J. Oxidative stress in ALS: Key role in motor neuron injury and therapeutic target. *Free Radic. Biol. Med.* **48**, 629-641 (2010).
10. Ince, P. G. *et al.* Molecular pathology and genetic advances in amyotrophic lateral sclerosis: an emerging molecular pathway and the significance of glial pathology. *Acta Neuropathol.* **122**, 657-671 (2011).
11. Abel, O., Powell, J. F., Andersen, P. M. & Al-Chalabi, A. ALSod: A user-friendly online bioinformatics tool for amyotrophic lateral sclerosis genetics. *Hum. Mutat.* **33**, 1345-1351 (2012).
12. Kato, S. *et al.* New consensus research on neuropathological aspects of familial amyotrophic lateral sclerosis with superoxide dismutase 1 (SOD1) gene mutations: Inclusions containing SOD1 in neurons and astrocytes. *Amyotroph. Lateral Scler.* **1**, 163-184 (2000).
13. Liu, H.-N. *et al.* Lack of evidence of monomer/misfolded superoxide dismutase-1 in sporadic amyotrophic lateral sclerosis. *Ann. Neurol.* **66**, 75-80 (2009).
14. Forsberg, K., Andersen, P. M., Marklund, S. L. & Brannstrom, T. Glial nuclear aggregates of superoxide dismutase-1 are regularly present in patients with amyotrophic lateral sclerosis. *Acta Neuropathol.* **121**, 623-634 (2011).
15. Bruijn, L. I. *et al.* Aggregation and motor neuron toxicity of an ALS-linked SOD1 mutant independent from wild-type SOD1. *Science* **281**, 1851-1854 (1998).
16. Johnston, J. A., Dalton, M. J., Gurney, M. E. & Kopito, R. R. Formation of high molecular weight complexes of mutant Cu,Zn-superoxide dismutase in a mouse model for familial amyotrophic lateral sclerosis. *Proc. Natl. Acad. Sci. U.S.A.* **97**, 12571-12576 (2000).
17. Rakhit, R. *et al.* Monomeric Cu,Zn-superoxide dismutase is a common misfolding intermediate in the oxidation models of sporadic and familial amyotrophic lateral sclerosis. *J. Biol. Chem.* **279**, 15499-15504 (2004).
18. Valentine, J. S., Doucette, P. A. & Potter, S. Z. Copper-zinc superoxide dismutase and amyotrophic lateral sclerosis. *Annu. Rev. Biochem.* **74**, 563-593 (2005).
19. Banci, L. *et al.* Metal-free superoxide dismutase forms soluble oligomers under physiological conditions: A possible general mechanism for familial ALS. *Proc. Natl. Acad. Sci. U.S.A.* **104**, 11263-11267 (2007).

20. Kurahashi, T., Miyazaki, A., Suwan, S. & Isobe, M. Extensive investigations on oxidized amino acid residues in H<sub>2</sub>O<sub>2</sub>-treated Cu,Zn-SOD protein with LC-ESI-Q-TOF-MS, MS/MS for the determination of the copper-binding site. *J. Am. Chem. Soc.* **123**, 9268-9278 (2001).
21. van Gunsteren, W. F. *et al.* Biomolecular modeling: Goals, problems, perspectives. *Angew. Chem. Int. Ed.* **45**, 4064-4092 (2006).
22. Best, R. B. Atomistic molecular simulations of protein folding. *Curr. Opin. Struct. Biol.* **22**, 52-61 (2012).
23. Vassall, K. A., Stathopoulos, P. B., Rumfeldt, J. A. O., Lepock, J. R. & Meiering, E. M. Equilibrium thermodynamic analysis of amyotrophic lateral sclerosis-associated mutant apo Cu,Zn superoxide dismutases. *Biochemistry* **45**, 7366-7379 (2006).
24. Rumfeldt, J. A. O., Stathopoulos, P. B., Chakrabarty, A., Lepock, J. R. & Meiering, E. M. Mechanism and thermodynamics of guanidinium chloride-induced denaturation of ALS-associated mutant Cu,Zn superoxide dismutases. *J. Mol. Biol.* **355**, 106-123 (2006).
25. Rohl, C. A., Strauss, C. E. M., Misura, K. M. S. & Baker, D. Protein structure prediction using rosetta. *Methods Enzymol.* **383**, 66-93 (2004).
26. Capriotti, E., Fariselli, P. & Casadio, R. I-Mutant2.0: predicting stability changes upon mutation from the protein sequence or structure. *Nucleic Acids Res.* **33**, W306-W310 (2005).
27. Benedix, A., Becker, C. M., de Groot, B. L., Caflisch, A. & Boeckmann, R. A. Predicting free energy changes using structural ensembles. *Nat. Methods* **6**, 3-4 (2009).
28. Potapov, V., Cohen, M. & Schreiber, G. Assessing computational methods for predicting protein stability upon mutation: good on average but not in the details. *Protein Eng. Des. Sel.* **22**, 553-560 (2009).
29. Seeliger, D. & de Groot, B. L. Protein thermostability calculations using alchemical free energy simulations. *Biophys. J.* **98**, 2309-2316 (2010).
30. Lin, Z., Kornfeld, J., Maechler, M. & van Gunsteren, W. F. Prediction of folding equilibria of differently substituted peptides using one-step perturbation. *J. Am. Chem. Soc.* **132**, 7276-7278 (2010).
31. Beveridge, D. L. & DiCapua, F. M. Free energy via molecular simulation: applications to chemical and biomolecular systems. *Annu. Rev. Biophys. Biophys. Chem.* **18**, 431-492 (1989).
32. Straatsma, T. P. & McCammon, J. A. Computational alchemy. *Annu. Rev. Phys. Chem.* **43**, 407-435 (1992).
33. Peter, C., Oostenbrink, C., van Dorp, A. & van Gunsteren, W. F. Estimating entropies from molecular dynamics simulations. *J Chem Phys* **120**, 2652-2661 (2004).
34. de Ruiter, A. & Oostenbrink, C. Free energy calculations of protein-ligand interactions. *Curr. Opin. Chem. Biol.* **15**, 547-552 (2011).
35. Shirts, M. R. & Pande, V. S. Comparison of efficiency and bias of free energies computed by exponential averaging, the Bennett acceptance ratio, and thermodynamic integration. *J Chem Phys* **122** (2005).
36. Bruckner, S. & Boresch, S. Efficiency of alchemical free energy simulations. I. A practical comparison of the exponential formula, thermodynamic integration, and Bennett's acceptance ratio method. *J. Comput. Chem.* **32**, 1303-1319 (2011).
37. Bruckner, S. & Boresch, S. Efficiency of alchemical free energy simulations. II. Improvements for thermodynamic integration. *J. Comput. Chem.* **32**, 1320-1333 (2011).
38. Gazdag, E. M. *et al.* Purification and crystallization of human Cu/Zn superoxide dismutase recombinantly produced in the protozoan *Leishmania tarentolae*. *Acta Crystallogr. Sect. F Struct. Biol. Cryst. Commun.* **66**, 871-877 (2010).

39. Berendsen, H. J. C., Postma, J. P. M., van Gunsteren, W. F. & Hermans, J. Interaction models for water in relation to protein hydration. Reidel, Dordrecht, 1981.
40. Boned, R., van Gunsteren, W. E. & Daura, X. Estimating the temperature dependence of peptide folding entropies and free enthalpies from total energies in molecular dynamics simulations. *Chemistry* **14**, 5039-5046 (2008).
41. Hess, B., Kutzner, C., van der Spoel, D. & Lindahl, E. GROMACS 4: Algorithms for highly efficient, load-balanced, and scalable molecular simulation. *J. Chem. Theory. Comput.* **4**, 435-447 (2008).
42. Oostenbrink, C., Villa, A., Mark, A. E. & van Gunsteren, W. F. A biomolecular force field based on the free enthalpy of hydration and solvation: the GROMOS force-field parameter sets 53A5 and 53A6. *J. Comput. Chem.* **25**, 1656-1676 (2004).
43. Schmid, N. *et al.* Definition and testing of the GROMOS force-field versions 54A7 and 54B7. *Eur. Biophys. J.* **40**, 843-856 (2011).
44. Berendsen, H. J. C., Postma, J. P. M., van Gunsteren, W. F., Dinola, A. & Haak, J. R. Molecular-dynamics with coupling to an external bath. *J Chem Phys* **81**, 3684-3690 (1984).
45. Beutler, T. C., Mark, A. E., Vanschaik, R. C., Gerber, P. R. & van Gunsteren, W. F. Avoiding singularities and numerical instabilities in free-energy calculations based on molecular simulations. *Chem. Phys. Lett.* **222**, 529-539 (1994).
46. Berlett, B. S. & Stadtman, E. R. Protein oxidation in aging, disease, and oxidative stress. *J. Biol. Chem.* **272**, 20313-20316 (1997).
47. Daura, X., Affentranger, R. & Mark, A. E. On the relative merits of equilibrium and non-equilibrium simulations for the estimation of free-energy differences. *Chemphyschem* **11**, 3734-3743 (2010).
48. Kastenholz, M. A. & Huenenberger, P. H. Computation of methodology-independent ionic solvation free energies from molecular simulations. II. The hydration free energy of the sodium cation. *J Chem Phys* **124** (2006).
49. Hunenberger, P. & Reif, M. in *Single-ion solvation: Experimental and theoretical approaches to elusive thermodynamic quantities* RSC Theoretical and Computational Chemistry Series (ed Jonathan Hirst) 1-664 (Royal Society of Chemistry, London, 2011).
50. Forman, H. J. & Fridovic, I. Stability of bovine superoxide dismutase - effects of metals. *J. Biol. Chem.* **248**, 2645-2649 (1973).
51. Chiti, F. & Dobson, C. M. Amyloid formation by globular proteins under native conditions. *Nat. Chem. Biol.* **5**, 15-22 (2009).
52. Gagliardi, S. *et al.* SOD1 mRNA expression in sporadic amyotrophic lateral sclerosis. *Neurobiol. Dis.* **39**, 198-203 (2010).
53. Oeda, T. *et al.* Oxidative stress causes abnormal accumulation of familial amyotrophic lateral sclerosis-related mutant SOD1 in transgenic *Caenorhabditis elegans*. *Hum. Mol. Genet.* **10**, 2013-2023 (2001).
54. Perez, V. I. *et al.* Protein stability and resistance to oxidative stress are determinants of longevity in the longest-living rodent, the naked mole-rat. *Proc. Natl. Acad. Sci. U.S.A.* **106**, 3059-3064 (2009).
55. Krisko, A. & Radman, M. Protein damage and death by radiation in *Escherichia coli* and *Deinococcus radiodurans*. *Proc. Natl. Acad. Sci. U.S.A.* **107**, 14373-14377 (2010).
56. Lin, Z. & van Gunsteren, W. F. Combination of Enveloping Distribution Sampling (EDS) of a Soft-Core Reference-State Hamiltonian with One-Step Perturbation to Predict the Effect of Side Chain Substitution on the Relative Stability of Right- and Left-Helical Folds of beta-Peptides. *J. Chem. Theory. Comput.* **9**, 126-134 (2013).

57. Wu, D. & Kofke, D. A. Phase-space overlap measures. I. Fail-safe bias detection in free energies calculated by molecular simulation. *J Chem Phys* **123** (2005).
58. Wu, D. & Kofke, D. A. Phase-space overlap measures. II. Design and implementation of staging methods for free-energy calculations. *J Chem Phys* **123** (2005).
59. Cordella, L. P., Foggia, P., Sansone, C. & Vento, M. Subgraph transformations for the inexact matching of attributed relational graphs. *Graph Based Representations in Pattern Recognition* **12**, 43-52 (1998).
60. Chodera, J. D. *et al.* Alchemical free energy methods for drug discovery: Progress and challenges. *Curr. Opin. Struct. Biol.* **21**, 150-160 (2011).
61. de Ruiter, A. & Oostenbrink, C. Efficient and accurate free energy calculations on trypsin inhibitors. *J. Chem. Theory. Comput.* **8**, 3686-3695 (2012).

Concluding discussion

From enzymatic activation to transcription and translation regulation to disease development and aging, post-translational modifications (PTMs) of proteins play an essential role in various biological processes.<sup>1-3</sup> However, despite the great importance of understanding atomistic-level effects of PTMs, molecular dynamics (MD) simulations,<sup>4</sup> a premier high-resolution computational biology tool, has been limited to unmodified, native proteins due to a surprising deficiency of suitable tools and systematically developed parameters for treating modified proteins. To fill this gap, we have obtained novel force field parameters for more than 250 different types of enzymatic and non-enzymatic PTMs occurring at amino-acid side chains and protein termini as presented in **Chapter I**. These parameters have been generated in the context of the GROMOS force field (45a3<sup>5</sup> and 54a7<sup>6,7</sup> parameter sets), chosen primarily because of its wide-spread usage, accuracy in reproducing experimental data and general transferability of parameters between chemically similar groups in different compounds.<sup>6</sup> Importantly, such parameterization strategy has yielded a remarkable, near chemical-accuracy matching of calculated and experimentally measured hydration free energies (RMSE = 4.2 kJ/mol over the validation set comprised of small molecules), a thermodynamic property closely related to hydrophobicity and originally used to develop the GROMOS 53a6 force field in 2004,<sup>6</sup> lending support for the general validity of the reported parameters and soundness of the parameterization philosophy underlying the GROMOS force field. However, further verification is expected to be carried out at a community-wide level through simulations of post-translationally modified proteins and direct comparison with relevant experimental data. Additionally, this study has aimed at systematic parameterization of a large majority of known PTMs, providing human curated, fully-consistent set of parameters, which has to be contrasted with typical MD studies focusing on a single modification using different procedures and force fields,<sup>8-10</sup> and available tools for automated generation of force field parameters (e.g., the AMBER<sup>11</sup> feature *antechamber* and online tools SwissParam<sup>12</sup>, PRODRG<sup>13</sup>, ATB<sup>14</sup> and *q4md-forcefieldtools*<sup>15</sup>), directed at small chemicals rather than protein PTMs. Moreover, the reported parameters have been used to quantitatively show that most PTMs significantly alter physico-chemical properties (e.g., hydrophobicity) of target amino acids, a mechanism shown to have broad biological implications.<sup>16,17</sup>



In an accompanying study presented in **Chapter II**, we have developed the Vienna-PTM web server designated to automated incorporation of PTMs into protein 3D structures and supplying the associated force field parameters described in Chapter I. Notably, in addition to reliability and compatibility with different operating systems and web browsers, the emphasis of servers' design has been primarily put on flexible structure allowing for easy and straightforward introduction of new features, tools and modification types or even completely new force fields. Therefore, even though the server currently provides exclusively GROMOS force field parameters of protein PTMs in GROMOS<sup>18</sup> and GROMACS<sup>19</sup> formats, our hope is that the implemented service will expand to other widely-used force fields (e.g., AMBER,<sup>20</sup> CHARMM<sup>21</sup> and OPLS<sup>22</sup>) and simulation packages (e.g., AMBER<sup>11</sup>, CHARMM<sup>23</sup> and NAMD<sup>24</sup>) as well as modifications of other biologically important molecules such as nucleic acids and phospholipids.<sup>25,26</sup> Collectively, the developed PTM parameters together with the Vienna-PTM server provide a comprehensive and user-friendly platform for preparing, running and analyzing MD simulations of modified proteins.

While enzymatic PTMs regulate a large number of cellular processes, non-enzymatic, oxidative damage to proteins is associated with aging and age-related disorders, including neurodegenerative diseases, cancer and diabetes.<sup>3,27-29</sup> Additionally, potentially cytotoxic aggregates comprised of highly oxidized proteins have consistently been reported in these pathologies.<sup>30,31</sup> However, a direct causal relationship between oxidative stress on the one hand and protein aggregation, aging and development of late onset diseases on the other has not been established. In order to examine this relationship, we study the effects of non-enzymatic oxidative modifications on protein structure, dynamics and aggregation propensity. In particular, in **Chapter III** we focus on metal-catalyzed carbonylation, one of the most important and the most studied non-enzymatic PTMs,<sup>32</sup> and examine how it affects the villin headpiece domain, a structurally well characterized polypeptide.<sup>33,34</sup> Using MD simulations, we have modeled all possible variants with Lys, Arg and Pro residues carbonylated. This microscopic, site-specific analysis reveals that disruption of specific structural elements (e.g., a salt bridge) together with high overall levels of carbonylation, i.e., approximately three orders of magnitude above those related to cellular death,<sup>3</sup> are required to unfold villin headpiece, only a marginally stable protein.<sup>35</sup> Surprisingly, even though it is widely assumed that carbonylation leads to cytotoxicity through destabilization

of protein structure,<sup>32</sup> this result, additionally corroborated with experimental evidence,<sup>36,37</sup> suggests that protein structure most likely remains intact at typical cellular levels of carbonylation. On the other hand, we show that local changes in physico-chemical properties upon single carbonylation event, i.e., *point mutation* to a charge-neutral and more hydrophobic residue when compared to the cognate amino acid, drastically increase protein aggregation propensity. Importantly, these findings potentially provide a direct link between biologically relevant conditions and cytotoxicity induced by formation of insoluble protein inclusions.

To investigate this further, we have simulated aggregation of the villin headpiece domain in its native and carbonylated forms as described in **Chapter IV**. As expected, carbonylated, aggregation-prone version of the peptide self-associate to dimers and higher order oligomers, however, the carbonylated residues play only a small role in this process. Surprisingly, in addition to hydrophobic ring-containing residues, i.e., phenylalanine and tryptophan, polar asparagines and glutamines as well as hydrophilic backbone are predominantly involved in the formation of inter-peptide contacts, supporting the hypothesis that aggregability is an intrinsic property of polypeptide chains.<sup>38</sup> Importantly, the native villin displays the same aggregation mechanism and behavior as the carbonylated form, accompanied by a drastic decrease in the potential energy of the system, despite the fact that the applied simulation conditions correspond to those, which are experimentally known to render villin soluble.<sup>13,14</sup> Strikingly, we demonstrate that such aggregation-biasing imbalance between protein-protein, protein-solvent and solvent-solvent interactions is also shared by six widely used force fields, namely: GROMOS45a3,<sup>5</sup> GROMOS54a7,<sup>7</sup> AMBER94,<sup>39</sup> AMBER99SB-ILDN,<sup>20</sup> CHARMM27-CMAP,<sup>21</sup> and OPLS-AAL.<sup>22</sup> One may speculate that the favoring of protein-protein over protein-solvent interactions by current force fields is an artifact of a commonly accepted verification procedure, in which the ability of a given force field to reproduce experimentally obtained secondary and tertiary protein structure is tested. This could also be related to the finding that most force fields exhibit a tendency to describe amino acids as being more hydrophobic than they actually are.<sup>40</sup> This, in turn, implies that MD simulations potentially underestimate protein dynamics and unstructuredness, as indeed shown in a recent study of an intrinsically disordered protein.<sup>41</sup> Importantly, this suggests that current force fields in general might have limited accuracy

when it comes to describing protein dynamics and behavior in biologically relevant crowded environments.

In conditions of increased oxidative stress, carbonylated proteins are most likely affected by other oxidative modifications as well, since they are more readily introduced when compared to carbonylation modifications.<sup>42</sup> However, one should emphasize that as an irreversible reaction, carbonylation permanently damages target residues, and is for this reason arguably one of the most widely-used biomarkers of protein damage, oxidative stress and aging.<sup>32,43</sup> In Chapters III and IV, the villin headpiece domain has been used as a model system primarily due to its small size, fast folding kinetics and well-characterized folding mechanism.<sup>13,14</sup> Even though this actin-binding peptide is not directly linked to aging and oxidative stress, actin cytoskeleton morphology and structure are known to get compromised upon oxidative damage.<sup>44,45</sup> In order to extend the scope of our study, in **Chapter V** we have explored different types of non-enzymatic oxidative PTMs and their potential cytotoxicity as mediated through damage to superoxide dismutase 1 (SOD1), a key antioxidant protein in humans which, by the nature of its function, is exposed to higher levels of oxidative stress than most other proteins. Importantly, this homo-dimeric metalloenzyme has been repeatedly linked to familial amyotrophic lateral sclerosis (fALS), a devastating, late-onset neurodegenerative disease, with more than 150 fALS-related mutations in the SOD1 gene.<sup>46-48</sup> Additionally, aggregated SOD1 has been reported in motor neurons and astrocytes of fALS patients<sup>49-51</sup> and animal models.<sup>52,53</sup> However, the exact molecular mechanism of cytotoxicity triggered by SOD1 remains elusive. As a first step towards better understanding of the microscopic effects of oxidative damage to SOD1, we have employed classical MD simulations in combination with the thermodynamic integration method<sup>54</sup> to estimate changes in the free energy of SOD1 folding and dimerization. In particular, we have focused on nine residues at the homo-dimer interface, which are affected by presumably the most prominent non-enzymatic oxidative PTMs. Our results show that most of the studied oxidative modifications destabilize both homo-dimer and monomer structures, the mechanisms that have been shown to increase aggregation propensity of SOD1 protein.<sup>55,56</sup> Markedly, the extent of destabilization observed herein is significantly greater than that experimentally determined for fALS-related mutations,<sup>57</sup> even up to 10-fold in the most extreme cases. This suggests that, as speculated before,<sup>55</sup> age-

related increase in oxidative damage to SOD1 may play a key role in ALS development, with the reported SOD1 mutations being only an additional factor in promoting early onset of the disease. Although in this study we provide only calculated estimates of the changes in stability without experimental verification, two recent studies applying similar methods involving alchemical perturbations have successfully accessed effects of side-chain substitutions on the thermodynamic stability of microbial ribonuclease barnase and a hepta- $\beta$ -peptide,<sup>58,59</sup> obtaining results in a good agreement with experimental measurements. Notably, we have performed significantly longer simulations than in these related studies,<sup>58,59</sup> arguably achieving better convergence and accuracy. However, such extensive sampling comes at a price of high computational requirements, which further engenders the need for an improved and more efficient protocol in order to further investigate the relationship between oxidative stress and SOD1-mediated cytotoxicity. In particular, such improvements would be needed in order to analyze the effects of additional oxidizable residues as well as fALS-related mutations (including oxidatively-modified versions of mutated residues) on the stability of SOD1 homo-dimer and monomer, and binding affinities to Zn and Cu ions which are important for the dismutase activity as well as the tertiary and quaternary structure formation and stability of SOD1.<sup>60-62</sup> In particular, by using more advanced approaches for sampling and free energy evaluation (e.g., local elevation method<sup>63</sup> and Bennett acceptance ratio<sup>64</sup>) and quantitative estimation of the phase space overlap between states along the perturbation path, or methods for calculating free energy corrections of charging a part of the system,<sup>65-70</sup> one should in principle decrease the computational costs without affecting, if not even enhancing, the accuracy. Additionally, an efficient and reliable tool for automated introduction of alchemical modifications is essential for treating a wide range of modifications and mutations, as required to systematically address biologically relevant variants of SOD1. We have already made a significant progress in developing an automated dual topology builder (GROMACS format) based on the VF algorithm for graph isomorphism matching,<sup>71</sup> designed to find the greatest overlap between two given compounds, i.e., the largest common substructure, and create an arguably optimal alchemical perturbation path between the two compounds. Importantly, in addition to the analysis of the discussed SOD1 systems, such a powerful tool can be utilized in various contexts involving alchemical free energy calculations.<sup>72</sup> We plan

to: firstly, introduce this tool as an additional feature to the Vienna-PTM server to provide dual topologies of modified and cognate amino acids, and secondly, to calculate relative changes in physico-chemical properties (e.g., hydration free energy and solvation free energy in non-polar solvents) of canonical amino acids upon different PTMs. Furthermore, the range of applicability of this tool extends to research areas involving calculation of binding free energies, including protein ligand binding affinities, screening procedures for a large number of candidate compounds and rational drug design.<sup>69,72,73</sup>

Lastly, driven by the extreme biological importance of more than 400 existing PTMs, and how they have surprisingly been largely neglected by the MD community, this thesis is primarily aimed at providing a systematic, comprehensive and user-friendly toolkit designed for computational modeling of post-translationally modified proteins. From direct MD simulations to biomolecular structure refinement to computational free energy estimation and drug design, the developed force field parameters in combination with the Vienna-PTM server greatly expand the range of MD methodology to a large class of biomolecular systems of paramount importance. It is our hope that this advance will play a catalytic role in bringing together realistic cell biology, dominated by PTMs, and the quantitative, reductionist power of structural biology and chemistry, as embodied in the MD method, and help shed light on a broad spectrum of important biological questions. By using these tools, we have explored potential molecular mechanisms of aging and development of age-related diseases in the context of oxidatively damaged proteins. By probing atomic-level dynamics and gaining high-resolution insight into effects of oxidative modifications on protein structure, dynamics and interactions, we have: linked microscopic determinants of protein structure stability and aggregation to aging through oxidative stress, made and provided experimentally testable predictions, and tested limitations of current models to describe biologically relevant crowded environments. We believe that such computational studies, in synergy with experimental efforts, will improve our microscopic-level understanding of oxidative stress, disease development and aging and possibly lead to novel and more successful therapeutic strategies.

## REFERENCES

1. Walsh, C. T., Garneau-Tsodikova, S. & Gatto, G. J., Jr. Protein posttranslational modifications: the chemistry of proteome diversifications. *Angew. Chem. Int. Ed.* **44**, 7342-7372 (2005).
2. Lothrop, A. P., Torres, M. P. & Fuchs, S. M. Deciphering post-translational modification codes. *FEBS Lett.* **587**, 1247-1257 (2013).
3. Levine, R. L. & Stadtman, E. R. Oxidative modification of proteins during aging. *Exp. Gerontol.* **36**, 1495-1502 (2001).
4. van Gunsteren, W. F. *et al.* Biomolecular modeling: Goals, problems, perspectives. *Angew. Chem. Int. Ed.* **45**, 4064-4092 (2006).
5. Schuler, L., Daura, X. & van Gunsteren, W. An improved GROMOS96 force field for aliphatic hydrocarbons in the condensed phase. *J. Comput. Chem.* **22**, 1205-1218 (2001).
6. Oostenbrink, C., Villa, A., Mark, A. E. & van Gunsteren, W. F. A biomolecular force field based on the free enthalpy of hydration and solvation: the GROMOS force-field parameter sets 53A5 and 53A6. *J. Comput. Chem.* **25**, 1656-1676 (2004).
7. Schmid, N. *et al.* Definition and testing of the GROMOS force-field versions 54A7 and 54B7. *Eur. Biophys. J.* **40**, 843-856 (2011).
8. Petrov, D. & Zagrovic, B. Microscopic analysis of protein oxidative damage: Effect of carbonylation on structure, dynamics, and aggregability of villin headpiece. *J. Am. Chem. Soc.* **133**, 7016-7024 (2011).
9. Seeliger, D. *et al.* Quantitative assessment of protein interaction with methyl-lysine analogues by hybrid computational and experimental approaches. *ACS Chem. Biol.* **7**, 150-154 (2012).
10. Potoyan, D. A. & Papoian, G. A. Regulation of the H4 tail binding and folding landscapes via Lys-16 acetylation. *Proc. Natl. Acad. Sci. U.S.A.* **109**, 17857-17862 (2012).
11. Case, D. A. *et al.* AMBER 12. University of California, San Francisco, 2012.
12. Zoete, V., Cuendet, M. A., Grosdidier, A. & Michielin, O. SwissParam: A fast force field generation tool for small organic molecules. *J. Comput. Chem.* **32**, 2359-2368 (2011).
13. Schuttelkopf, A. W. & van Aalten, D. M. F. PRODRG: a tool for high-throughput crystallography of protein-ligand complexes. *Acta Crystallogr. Sect. D. Biol. Crystallogr.* **60**, 1355-1363 (2004).
14. Malde, A. K. *et al.* An Automated Force Field Topology Builder (ATB) and Repository: Version 1.0. *J. Chem. Theory. Comput.* **7**, 4026-4037 (2011).
15. Vanquelef, E. *et al.* RED Server: a web service for deriving RESP and ESP charges and building force field libraries for new molecules and molecular fragments. *Nucleic Acids Res.* **39**, W511-W517 (2011).
16. Huq, M. D. M., Tsai, N. P., Khan, S. A. & Wei, L. N. Lysine trimethylation of retinoic acid receptor- $\alpha$  - A novel means to regulate receptor function. *Mol. Cell. Proteomics* **6**, 677-688 (2007).
17. Hlevnjak, M., Zitkovic, G. & Zagrovic, B. Hydrophilicity matching - A potential prerequisite for the formation of protein-protein complexes in the cell. *PLoS ONE* **5(6)** (2010).
18. Schmid, N., Christ, C. D., Christen, M., Eichenberger, A. P. & van Gunsteren, W. F. Architecture, implementation and parallelisation of the GROMOS software for biomolecular simulation. *Comput. Phys. Commun.* **183**, 890-903 (2012).
19. Pronk, S. *et al.* GROMACS 4.5: a high-throughput and highly parallel open source molecular simulation toolkit. *Bioinformatics* **29**, 845-854 (2013).
20. Lindorff-Larsen, K. *et al.* Improved side-chain torsion potentials for the Amber ff99SB protein force field. *Proteins* **78**, 1950-1958 (2010).
21. Chen, J. H., Im, W. P. & Brooks, C. L. Balancing solvation and intramolecular interactions: Toward a consistent generalized born force field. *J. Am. Chem. Soc.* **128**, 3728-3736 (2006).

22. Kaminski, G. A., Friesner, R. A., Tirado-Rives, J. & Jorgensen, W. L. Evaluation and reparametrization of the OPLS-AA force field for proteins via comparison with accurate quantum chemical calculations on peptides. *J Phys Chem B* **105**, 6474-6487 (2001).
23. Brooks, B. R. *et al.* CHARMM: The Biomolecular Simulation Program. *J. Comput. Chem.* **30**, 1545-1614 (2009).
24. Phillips, J. C. *et al.* Scalable molecular dynamics with NAMD. *J. Comput. Chem.* **26**, 1781-1802 (2005).
25. Fu, Y. & He, C. A. Nucleic acid modifications with epigenetic significance. *Curr. Opin. Chem. Biol.* **16**, 516-524 (2012).
26. Nyska, A. & Kohen, R. Oxidation of biological systems: Oxidative stress phenomena, antioxidants, redox reactions, and methods for their quantification. *Toxicol. Pathol.* **30**, 620-650 (2002).
27. Berlett, B. S. & Stadtman, E. R. Protein oxidation in aging, disease, and oxidative stress. *J. Biol. Chem.* **272**, 20313-20316 (1997).
28. Sohal, R. S. Role of oxidative stress and protein oxidation in the aging process. *Free Radic. Biol. Med.* **33**, 37-44 (2002).
29. Garcia-Garcia, A. *et al.* Biomarkers of Protein Oxidation in Human Disease. *Curr. Mol. Med.* **12**, 681-697 (2012).
30. Ross, C. A. & Poirier, M. A. Protein aggregation and neurodegenerative disease. *Nat. Med.* **10**, S10-S17 (2004).
31. Chiti, F. & Dobson, C. M. Protein misfolding, functional amyloid, and human disease. *Annu. Rev. Biochem.* **75**, 333-366 (2006).
32. Nystrom, T. Role of oxidative carbonylation in protein quality control and senescence. *EMBO J.* **24**, 1311-1317 (2005).
33. Zagrovic, B., Snow, C. D., Shirts, M. R. & Pande, V. S. Simulation of folding of a small alpha-helical protein in atomistic detail using worldwide-distributed computing. *J. Mol. Biol.* **323**, 927-937 (2002).
34. Lei, H., Wu, C., Liu, H. & Duan, Y. Folding free-energy landscape of villin headpiece subdomain from molecular dynamics simulations. *Proc. Natl. Acad. Sci. U.S.A.* **104**, 4925-4930 (2007).
35. Godoy-Ruiz, R. *et al.* Estimating free-energy barrier heights for an ultrafast folding protein from calorimetric and kinetic data. *J Phys Chem B* **112**, 5938-5949 (2008).
36. Lasch, P. *et al.* Hydrogen peroxide-induced structural alterations of RNase A. *J. Biol. Chem.* **276**, 9492-9502 (2001).
37. Le, H. T. *et al.* Impact of hydrogen peroxide on the activity, structure, and conformational stability of the oxidized protein repair enzyme methionine sulfoxide reductase A. *J. Mol. Biol.* **393**, 58-66 (2009).
38. Gsponer, J. & Vendruscolo, M. Theoretical approaches to protein aggregation. *Protein Pept. Lett.* **13**, 287-293 (2006).
39. Cornell, W. D. *et al.* A 2nd generation force-field for the simulation of proteins, nucleic-acids, and organic-molecules. *J. Am. Chem. Soc.* **117**, 5179-5197 (1995).
40. Shirts, M. R., Pitner, J. W., Swope, W. C. & Pande, V. S. Extremely precise free energy calculations of amino acid side chain analogs: Comparison of common molecular mechanics force fields for proteins. *J Chem Phys* **119**, 5740-5761 (2003).
41. Lindorff-Larsen, K., Trbovic, N., Maragakis, P., Piana, S. & Shaw, D. E. Structure and dynamics of an unfolded protein examined by molecular dynamics simulation. *J. Am. Chem. Soc.* **134**, 3787-3791 (2012).
42. Stadtman, E. R. Protein oxidation and aging. *Science* **257**, 1220-1224 (1992).
43. Dalle-Donne, I., Giustarini, D., Colombo, R., Rossi, R. & Milzani, A. Protein carbonylation in human diseases. *Trends Mol. Med.* **9**, 169-176 (2003).

44. Dalle-Donne, I. *et al.* Actin carbonylation: from a simple marker of protein oxidation to relevant signs of severe functional impairment. *Free Radic. Biol. Med.* **31**, 1075-1083 (2001).
45. Dalle-Donne, I., Rossi, R., Milzani, A., Di Simplico, P. & Colombo, R. The actin cytoskeleton response to oxidants: from small heat shock protein phosphorylation to changes in the redox state of actin itself. *Free Radic. Biol. Med.* **31**, 1624-1632 (2001).
46. Hand, C. K. & Rouleau, G. A. Familial amyotrophic lateral sclerosis. *Muscle Nerve* **25**, 135-159 (2002).
47. Ince, P. G. *et al.* Molecular pathology and genetic advances in amyotrophic lateral sclerosis: an emerging molecular pathway and the significance of glial pathology. *Acta Neuropathol.* **122**, 657-671 (2011).
48. Abel, O., Powell, J. F., Andersen, P. M. & Al-Chalabi, A. ALSod: A user-friendly online bioinformatics tool for amyotrophic lateral sclerosis genetics. *Hum. Mutat.* **33**, 1345-1351 (2012).
49. Kato, S. *et al.* New consensus research on neuropathological aspects of familial amyotrophic lateral sclerosis with superoxide dismutase 1 (SOD1) gene mutations: Inclusions containing SOD1 in neurons and astrocytes. *Amyotroph. Lateral Scler.* **1**, 163-184 (2000).
50. Liu, H.-N. *et al.* Lack of evidence of monomer/misfolded superoxide dismutase-1 in sporadic amyotrophic lateral sclerosis. *Ann. Neurol.* **66**, 75-80 (2009).
51. Forsberg, K., Andersen, P. M., Marklund, S. L. & Brannstrom, T. Glial nuclear aggregates of superoxide dismutase-1 are regularly present in patients with amyotrophic lateral sclerosis. *Acta Neuropathol.* **121**, 623-634 (2011).
52. Bruijn, L. I. *et al.* Aggregation and motor neuron toxicity of an ALS-linked SOD1 mutant independent from wild-type SOD1. *Science* **281**, 1851-1854 (1998).
53. Johnston, J. A., Dalton, M. J., Gurney, M. E. & Kopito, R. R. Formation of high molecular weight complexes of mutant Cu,Zn-superoxide dismutase in a mouse model for familial amyotrophic lateral sclerosis. *Proc. Natl. Acad. Sci. U.S.A.* **97**, 12571-12576 (2000).
54. Beveridge, D. L. & DiCapua, F. M. Free energy via molecular simulation: applications to chemical and biomolecular systems. *Annu. Rev. Biophys. Biophys. Chem.* **18**, 431-492 (1989).
55. Rakhit, R. *et al.* Monomeric Cu,Zn-superoxide dismutase is a common misfolding intermediate in the oxidation models of sporadic and familial amyotrophic lateral sclerosis. *J. Biol. Chem.* **279**, 15499-15504 (2004).
56. Chiti, F. & Dobson, C. M. Amyloid formation by globular proteins under native conditions. *Nat. Chem. Biol.* **5**, 15-22 (2009).
57. Vassall, K. A., Stathopoulos, P. B., Rumpfheldt, J. A. O., Lepock, J. R. & Meiering, E. M. Equilibrium thermodynamic analysis of amyotrophic lateral sclerosis-associated mutant apo Cu,Zn superoxide dismutases. *Biochemistry* **45**, 7366-7379 (2006).
58. Lin, Z., Kornfeld, J., Maechler, M. & van Gunsteren, W. F. Prediction of folding equilibria of differently substituted peptides using one-step perturbation. *J. Am. Chem. Soc.* **132**, 7276-7278 (2010).
59. Seeliger, D. & de Groot, B. L. Protein thermostability calculations using alchemical free energy simulations. *Biophys. J.* **98**, 2309-2316 (2010).
60. Valentine, J. S., Doucette, P. A. & Potter, S. Z. Copper-zinc superoxide dismutase and amyotrophic lateral sclerosis. *Annu. Rev. Biochem.* **74**, 563-593 (2005).
61. Banci, L. *et al.* Metal-free superoxide dismutase forms soluble oligomers under physiological conditions: A possible general mechanism for familial ALS. *Proc. Natl. Acad. Sci. U.S.A.* **104**, 11263-11267 (2007).



62. Kurahashi, T., Miyazaki, A., Suwan, S. & Isobe, M. Extensive investigations on oxidized amino acid residues in H<sub>2</sub>O<sub>2</sub>-treated Cu,Zn-SOD protein with LC-ESI-Q-TOF-MS, MS/MS for the determination of the copper-binding site. *J. Am. Chem. Soc.* **123**, 9268-9278 (2001).
63. Huber, T., Torda, A. E. & van Gunsteren, W. F. Local elevation - A method for improving the searching properties of molecular-dynamics simulation. *J. Comput. Aided Mol. Des.* **8**, 695-708 (1994).
64. Bennett, C. H. Efficient estimation of free-energy differences from Monte-Carlo data. *J Comput Phys* **22**, 245-268 (1976).
65. Wu, D. & Kofke, D. A. Phase-space overlap measures. I. Fail-safe bias detection in free energies calculated by molecular simulation. *J Chem Phys* **123** (2005).
66. Wu, D. & Kofke, D. A. Phase-space overlap measures. II. Design and implementation of staging methods for free-energy calculations. *J Chem Phys* **123** (2005).
67. Kastenholz, M. A. & Huenenberger, P. H. Computation of methodology-independent ionic solvation free energies from molecular simulations. II. The hydration free energy of the sodium cation. *J Chem Phys* **124** (2006).
68. Hunenberger, P. & Reif, M. in *Single-ion solvation: Experimental and theoretical approaches to elusive thermodynamic quantities RSC Theoretical and Computational Chemistry Series* (ed Jonathan Hirst) 1-664 (Royal Society of Chemistry, London, 2011).
69. de Ruiter, A. & Oostenbrink, C. Free energy calculations of protein-ligand interactions. *Curr. Opin. Chem. Biol.* **15**, 547-552 (2011).
70. Garate, J. A. & Oostenbrink, C. Free-energy differences between states with different conformational ensembles. *J. Comput. Chem.* **34**, 1398-1408 (2013).
71. Cordella, L. P., Foggia, P., Sansone, C. & Vento, M. Subgraph transformations for the inexact matching of attributed relational graphs. *Graph Based Representations in Pattern Recognition* **12**, 43-52 (1998).
72. Chodera, J. D. *et al.* Alchemical free energy methods for drug discovery: Progress and challenges. *Curr. Opin. Struct. Biol.* **21**, 150-160 (2011).
73. Shirts, M. R., Mobley, D. L. & Chodera, J. D. in *Annual Reports in Computational Chemistry, Vol 3 Vol. 3 Annual Reports in Computational Chemistry* (eds D. C. Spellmeyer & R. A. Wheeler) 41-59 (2007).



## Acknowledgments

In the end, I would like to express my gratitude to kind people who have helped and supported me along this exciting journey.

First and foremost, I would like to thank my supervisor **Bojan Zagrovic** for giving me the opportunity to join his group. I am deeply grateful for the vision, guidance, immense knowledge, necessary help and advice that you have provided. Most of all, your thoughtful approach to science and the courage to ask the unexpected, almost eccentric, questions have been an enormous source of ideas and inspiration for my work. Simply put, in my humble attempt to match your impressive message-conveying ability as the master of analogies, you have been a compass navigating me through rough waters of research.

I would like to show my greatest appreciation to **Chris Oostenbrink** by assigning my partial gratitude as follows: 0.7 on the wizard-like chemistry knowledge and intuition as the main contribution to our interaction, 0.2 on the old-schoolness to account for the hand-edited manuscript and 0.1 on the great and fruitful collaboration to add up to 1 net gratitude. I would also like to offer my special thanks to **Christian** for a great deal of help, work and contribution to this thesis, especially for stoically accepting web-design suggestions, and **Melanie** for countless comments on the Vienna-PTM Board (you should earn some additional experience points though).

I have greatly benefited from spending two months in Barcelona, receiving generous support and insightful comments and suggestions from my host **Xavier Daura**. In addition, *muchas gracias* goes to people from the institute for making my visit a joyful experience, especially to **Txino** for letting me steal his coffee and sugar and all his help, and to **Alicia** and **Montse** for helping me integrate with the locals and showing me the best bar in Cerdanyola.

I am indebted to the **members** of the Laboratory of Computational Biology (including the coffee machine). It has been a great pleasure and a privilege to work in such relaxed and creative environment. I would like to thank you all for enlightening discussions, kind assistance and valuable criticism, as well as friendly atmosphere. In particular, I would like to mention **Antonija**, for all the great moments that we have shared (back from high-school

days to date), for revealing the secrets of online shopping to me and for imposing on me good-quality TV-shows and books (I have almost finished reading Calvin and Hobbes), and even a guitar that unleashed a long-forgotten artist in me; and **Mario**, for being such a great colleague, a flat mate (that *kulen* you always bring is just fabulous) and a friend above all.

I appreciate the feedback, constructive discussion and suggestions offered by the members of my thesis committee: **Stefan Boresch**, **Robert Konrat** and **Egon Ogris**.

I also thank **Nico** for granting me (a person who has never touched a pipette beforehand) permission to use his laboratory equipment and helping me with protein purification. Unfortunately, these experiments have not been included in the thesis.

I owe a very important debt to **Davor Juretic**, who has been an encouraging and supportive supervisor, in whose group I have made my very first scientific steps at the University of Split. I would also like to mention **Dinko** for endless coffee breaks and discussions at Mediterranean Institute for Life Sciences that have sparked a few ideas incorporated in this thesis.

Surely, without the help from the administration **team** at Max F. Perutz Laboratories, this thesis would have never been submitted, and most probably I would have gotten deported from Austria due to the expiration of my residence permit.

For bringing the essentials to the life of us, poor students (Zwickel, lamb and tons of fun), a well-deserved thank you goes to **O'Connor's Old Oak**, a place that has been a good second home to me and my **friends** to whom I owe a massive *cheers*: a magnificent couple **Ana** and **Maja**, always ready to slack off and join for a pint of milk and beer, respectively; **Vanja**, an honorary organizer of unforgettable adventures, from trips to Mexico to cycling down the Danube to Bratislava; and a number of others that have been sharing laughs and good times with me on a daily basis. In addition, I am particularly grateful to my **mates** from Split, who make a tremendous effort to stay in touch with me and throw at least 2 welcome and 3 farewell parties each time I go back home.

Lastly, I owe my heartfelt gratitude to my **family**, who I endlessly love: my mother **Vesna**, ever caring and loving, the only person able to diligently prepare a life-time supply of the very best food, stuffing up my freezer beyond the laws of physics, bending the space to fill

yet another portion of her magic; my father **Rato**, who has taught me that finding the right answer begins always with asking the right question and whose infectious curiosity rolled me down the path of research and science; and my brother **Vedran**, whose first and foremost wish at the age of 5 was to get an older brother (I hope I managed to match the expectations), who has been watching after me ever since as a patient ‘younger’ brother, tolerant of my mischief.



## Curriculum vitae

### PERSONAL DATA

---

Date and place of birth	7th April 1986, Split, Croatia
Current address	Muhrengasse 35/6, 1100 Vienna Austria
Phone	+43 681 20366574
Email	drazen.petrov@univie.ac.at

### EDUCATION

---

Oct 2010 - present	<b>University of Vienna, Vienna, Austria</b> Molecular Biology Doctoral Programme (transfer from Split)
Oct 2009 - Oct 2010	<b>University of Split, Faculty of Sciences, Split, Croatia</b> Biophysics Doctoral Programme (transfer to Vienna)
Oct 2004 - Jan 2009	<b>University of Split, Faculty of Sciences, Split, Croatia</b> MSc in Physics Thesis: "Dynamics of antimicrobial peptide Adepantin in interaction with membranes"

### WORK EXPERIENCE

---

Apr 2010 - present	<b>Max F. Perutz Laboratories GmbH, Vienna, Austria</b> Effects of post-translational modifications on protein structure, dynamics and aggregability Supervision: Bojan Zagrovic, PhD
Mar 2009 - Mar 2010	<b>University of Split, Faculty of Sciences, Split, Croatia</b> Signal peptide and propeptide sequences analysis in host defense peptides Supervision: Davor Juretic, PhD
Nov 2008 - Mar 2010	<b>Mediterranean Institute for Life Sciences, Split, Croatia</b> Protein dynamics and stability upon carbonylation damage Supervision: Bojan Zagrovic, PhD

### SKILLS

---

Molecular dynamics simulations	GROMACS simulation package
Programing	Python, Perl, R, PyMOL, HTML, PHP, JavaScript, css

SCHOLARSHIPS AND AWARDS

---

- 2012     **HPC-Europa2 Transnational Access program**  
Collaborative research visits using High Performance Computing grant
- 2009     **University of Split, Faculty of Sciences, Split, Croatia**  
Award for the best graduated student of the year
- 2007     **University of Split, Faculty of Sciences, Split, Croatia**  
Rector's award
- 2004     **Croatian Ministry of Science, Technology and Sports**  
Scholarship for talented students

PUBLICATIONS

---

- Petrov D, Zagrovic B (2013) Are current atomistic force fields accurate enough to study proteins in crowded environments? (in preparation)
- Petrov D, Juretic D (2013) Identification of novel antimicrobial peptides using conserved signal peptide and propeptide sequences. (in preparation)
- Petrov D, Margreitter C, Grandits M, Oostenbrink C, Zagrovic B (2013) A systematic framework for molecular dynamics simulations of protein post-translational modifications. *PLoS Comput. Biol.* **9**(7):e1003154.
- Petrov D, Margreitter C, Zagrovic B (2013) Vienna-PTM web server: a toolkit for MD simulations of protein post-translational modifications. *Nucleic Acids Res.* **41**(Web Server issue):W422-6.
- Petrov D & Zagrovic B (2011) Microscopic analysis of protein oxidative damage: effect of carbonylation on structure, dynamics, and aggregability of villin headpiece. *J. Am. Chem. Soc.* **133**(18):7016-24.
- Juretic D, Vukicevic D, Petrov D, Novkovic M, Bojovic V, Lucic B, Ilic N, Tossi A (2011) Knowledge-based computational methods for identifying or designing novel, non-homologous antimicrobial peptides. *Eur Biophys J.* **40**(4):371-85.

CONFERENCES AND WORKSHOPS

---

- 2012     Functional Dynamics of Biomolecules - computational and experimental approaches, Lugano, Switzerland
- 2012     High Performance Computing in Computational Chemistry and Molecular Biology: Challenges and Solutions provided by ScalaLife project, Lausanne, Switzerland
- 2012     **Careers in Science – Insights from Structural Biologists, Vienna, Austria** - talk presentation
- 2011     **6<sup>th</sup> Christmas Biophysics Workshop, Varazdin, Croatia** - talk presentation
- 2011     3rd EMBO meeting, Vienna, Austria - poster presentation



- 2010    **Regional Biophysics Conference, Primosten, Croatia** - organization of the conference and poster presentation
- 2010    1<sup>st</sup> Prague Protein Spring, Prague, Czech Republic - poster presentation
- 2009    3rd Adriatic Meeting on Computational Solutions in Life Sciences, Primosten, Croatia - poster presentation
- 2009    FEBS Practical Course in Computational Biology, hands-on training in numerical simulation of diffusional processes, Split, Croatia
- 2009    7th European Biophysics Congress, Genoa, Italy - poster presentation
- 2008    23rd International Conference of Physics Students, Krakow, Poland - poster presentation
- 2006    21st International Conference of Physics Students, Bucharest, Romania - poster presentation

#### LANGUAGES

---

- Croatian (native)
- English (fluent)
- Italian (basic)
- German (basic)